

NOVEL EARLY AND LATE TRANSITION METAL COMPLEXES FOR THE SYNTHESIS OF FUNCTIONAL VINYL-INSERTION AND METATHESIS POLYMERIZATION-DERIVED BLOCK- COPOLYMERS

Von der Fakultät Chemie der Universität Stuttgart
zur Erlangung der Würde eines
Doktors der Naturwissenschaften (Dr. rer. nat.) genehmigte Abhandlung

vorgelegt von
Gurram Venkata Narayana, M.Sc.
aus Andhra Pradesh/ Indien

Erstberichter	:	Prof. Dr. Michael R. Buchmeiser
Mitberichter	:	Prof. Dr. Sabine Ludwigs
Zusätzlicher Prüfer	:	Prof. Dr.-Ing. Elias Klemm
Tag der mündlichen Prüfung	:	07/03/2012

Institut für Polymerchemie
der Universität Stuttgart

2012

Dedicated to My Family

Acknowledgements

First of all I would like to express my deepest thanks to my advisor Prof. Dr. Michael R. Buchmeiser for giving me an opportunity to work and study in his well-established research group. It has been an honour in my life to work in his group and I am very grateful for his motivation, encouragement, valuable advices and generous support during my Ph.D programme.

Special thanks to Dr. Dongren Wang and Jan Pigorsch for their support to build the polymerization reactor and high temperature NMR measurements. I would also like to thank Dr. Wolfgang Frey for the X-ray analysis of the metal complexes and Dr. Michael Schweizer (ITCF, Denkendorf) for the DSC measurements of polymers.

I would like to thank all my former colleagues at the IOM, Leipzig and present colleagues at the Institute of Polymer Chemie, University of Stuttgart for their help during my Ph.D. Especially, I would like to mention my dearest friends Dr. Rajendar Bandari, Dr. Sudhendran Mavila, Dr. Sankaran Anantharaman, Dr. Arunoday Singh and Anjan Kumar for their kind help and suggestions during the time I spent in Germany. I like to thank my close friends in India, especially Kiran Kumar, Krishna, Suresh, PVB Swamy, Dr. Rambabu, Dr. Raji reddy and Dr. Ravi Kumar.

My deepest gratitude goes to my father, mother, my brother, my sister-in-law, my grand mother and my relatives for their love and continuous support in my life. Last but not least, I would like to express my heartiest thanks to my wife Gurram Radha for her kind support during my Ph.D, without her help and encouragement this dissertation would not have been completed.

Curriculum Vitae

Personal Details

Family name : Gurram
Given name : Venkata Narayana
Nationality : Indian
Sex : Male
Date of Birth : 26th April 1975

Present Address

Allmandring-I, H. No: 12B/17,
Stuttgart, D-70569,
Germany.
Tel (m): +49-176-70202477

Email: gurram.venkata@ipoc.uni-stuttgart.de

Permanent Address

S/o Gurram Venkateswarlu,
Dendukur(Post), Madhira (Mandal),
Khammam(Dist), Andhra pradesh,
India- 507203.

gurramvenkat2002@gmail.com

Education

Ph.D

❖ **From Jan 2010- Mar 2012** Ph.D in Polymer Chemistry, Institute of Polymer Chemistry, University of Stuttgart, Germany. **Supervisor:** Prof. Michael R. Buchmeiser.

❖ **From May 2008- Dec 2009** Ph.D in Polymer Chemistry at the Leibniz-Institute of Surface Modification (IOM), University of Leipzig, Leipzig, Germany. **Supervisor:** Prof. Michael R. Buchmeiser.

Thesis title: "Synthesis of Novel Early and Late Transition Metal Complexes for the Synthesis of Functional Vinyl-insertion and Metathesis Polymerization-Derived Block-Copolymers".

Master of Sciences (M.Sc)

❖ **From 1996-98** M.Sc (Organic Chemistry) from Osmania University, Hyderabad, India.

Career Summary

❖ **GVK Biosciences Pvt. Ltd** **Nov 2003 - Apr 2008**

As a Sr. Research Associate at GVK Biosciences, Hyderabad, India. This is a custom research organization (CRO), to deliver the research and development services to the leading pharmaceutical companies in the World.

❖ **Suven Life Sciences Ltd.** **Dec 2000 - Oct 2003**

As a **Chemist** in **Suven Life sciences**, Suryapet, India. This is a process research and development unit to transfer the technology from R&D to pilot plants.

List of Publications

1. Pseudo-Halide and Nitrate Derivatives of Grubbs and Grubbs-Hoveyda Initiators: Some Structural Features Related to the Alternating Ring-Opening Metathesis Copolymerization of Norborn-2-ene with Cyclic Olefins. M.R. Buchmeiser, I. Ahmad, **V.N. Gurram**, P.S. Kumar, *Macromolecules*, **2011**, 44, 4098-4106.
2. Tandem Catalysts for Olefin Polymerization. S.Camadanli, Y. Zou, **V.N. Gurram**, M.R. Buchmeiser, *Stuttgarter Kunststoff-Kolloquium 1V1*, 1-6, ISBN 978-3-00034152-6 (2011).
3. Catalysts for the Simultaneous Ring-Opening Metathesis and Vinyl Insertion Copolymerization of Ethylene with Cyclic Olefins. S. Camadanli, Y. Zou, **V.N.Gurram**, D.Wang, M.R. Buchmeiser, *Polym.Preprints (Div. Polym. Chem, Am. Chem. Soc)* **2011**, 52, 217.
4. Group-IV Dimethylsilylenbisamido Complexes Bearing the 6-(2-(Diethylboryl) phenyl) pyrid-2-yl Motif: Synthesis and Use in Tandem Ring-Opening Metathesis/Vinyl-Insertion Copolymerization of Cyclic Olefins with Ethylene. Y. Zou, D. Wang, K. Wurst, C. Kühnel, I. Reinhardt, U. Decker, **V.N. Gurram**, S. Camadanli, M.R. Buchmeiser, *Chem. Eur. J.*, **2011**, 17, 13832-13846.
5. Bis(diamido)silylene Zirconium (IV) and Non-bridged Half-Titanocene (IV) Complexes; Synthesis and Use in Olefin Polymerization, **V.N. Gurram**, D.Wang, W. Frey, M.R. Buchmeiser, (*manuscript in preparation*).

Posters and International Conferences attended

1. Macromolecular Colloquium, Feb 25th- 28th 2009, Freiburg, Germany.
2. ISOM XVIII- 18th International Symposium on Olefin Metathesis and Related Chemistry, Aug 02-07, 2009, Leipzig, Germany.
3. ISOM XIV- 19th International Symposium on Olefin Metathesis and Related Chemistry, July 10-15, 2011, Rennes, France.
4. Pseudo-Halide and Nitrate Derivatives of Grubbs and Grubbs-Hoveyda Initiators: Some Structural Features Related to the Alternating Ring-Opening Metathesis Copolymerization of Norborn-2-ene with Cyclic Olefins; **V. N. Gurram**, A. Irshad, P. Santosh Kumar, Michael R. Buchmeiser, *The 19th International Symposium on Olefin Metathesis and Related Chemistry (ISOM XIV)* July 10-15, 2011, Rennes, France.

Table of Contents

List abbreviations.....	i	
Zusammenfassung.....	v	
Abstract.....	viii	
Aim of the Thesis.....	xi	
1.0	General introduction	
1.1	Historical development of polyolefins.....	1
1.2	Ziegler-Natta catalysis.....	3
1.3	Metallocenes.....	5
1.4	Chain termination.....	6
1.5	Ring opening metathesis polymerization.....	9
1.5.1	Schrock-type initiators and reactivity.....	11
1.5.2	Grubbs-type initiators and reactivity.....	12
1.6	Vinyl Insertion Polymerization.....	16
1.7	Relationship between Vinyl Insertion Polymerization (VIP) and Ring Opening Metathesis Polymerization (ROMP).....	17
1.8	References.....	19
2.0	Pseudo-Halide and Nitrate Derivatives of Grubbs- and Grubbs-Hoveyda Initiators: Structural Features Related to the Alternating Ring Opening Metathesis Copolymerization of Norborn-2-ene with Cyclic Olefins	
2.1	Introduction.....	25
2.2	Results and discussion	
2.2.1	Synthesis of initiators.....	26
2.2.2	Homopolmerization of norborn-2-ene (NBE).....	27
2.2.3	Alternating copolymerization of NBE with CPE.....	28
2.2.4	Cis/trans Ratio of the poly(NBE) homopolymer blocks in poly(NBE)- <i>alt</i> - poly(CPE).....	32
2.2.5	Influence of the NBE: CPE ratio on the extent of alternating copolymerization.....	34
2.2.6	Alternating copolymerization of NBE with <i>cis</i> -cyclooctene (COE).....	36
2.3	Summary.....	41

2.4	Polymerization procedure	
2.4.1	Typical copolymerization procedure.....	41
2.4.2	Typical homopolymerization procedure.....	41
2.5	References.....	42
3.0	Bis(diamido)silylene Zirconium (IV) and Non-bridged Half-Titanocene (IV) Complexes; Synthesis and use in Olefin Polymerization	
3.1	Introduction.....	47
3.2	Results and Discussion	
3.2.1	Synthesis of ligands and precatalysts.....	49
3.2.2	Synthesis of model compounds.....	59
3.2.3	Synthesis of ethyl- and phenyl- bridged ligands.....	61
3.2.4	Unsuccessful synthesis of metal complexes.....	62
3.3	Homopolymerizations	
3.3.1	Homopolymerization of ethylene.....	65
3.3.2	Homopolymerization of styrene.....	69
3.4	Copolymerizations	
3.4.1	Copolymerization of ethylene with cyclopentene (CPE).....	72
3.4.2	Copolymerization of ethylene with norborn-2-ene (NBE) using the Zr- based precatalysts 13 and 17	75
3.4.3	Copolymerization of ethylene with norborn-2-ene (NBE) using Ti-based precatalysts 22 , 23 , 24 , 26 and 27	83
3.4.4	Copolymerization of ethylene with cis-cyclooctene (COE).....	86
3.5	¹³ C NMR spectroscopic analysis of the E-NBE copolymers	
3.5.1.	Microstructure of the Zr-based complexes 13 and 17 derived E-NBE copolymers.....	88
3.5.2.	Microstructure of the Ti-based complexes 22 , 23 , 24 , 26 and 27 derived E- NBE copolymers	91
3.6	Conclusion.....	93
3.7	References.....	94
4.0	Experimental data.....	99
5.0	Appendix.....	117

List of Abbreviations

Å	Angstrom
ADMET	Acyclic diene metathesis polymerization
Ad	Adamantyl
Bn	Benzyl
Bu	Butyl
CM	Cross-metathesis
CGC	Constrained geometry complexes
CHE	Cyclohexene
CHP	Cycloheptene
COE	<i>cis</i> -Cyclooctene
CPE	Cyclopentene
COCs	Cyclic olefin copolymers
Cp	Cyclopentadienyl
DCPD	Dicyclopentadiene
DMF	<i>N,N</i> -Dimethylformamide
DMSO	Dimethylsulfoxide
DSC	Differential Scanning Calorimetry
°C	Degree Celcius
DCM	Dichloromethane
<i>et.al</i>	and others
Et	Ethyl
E	Ethylene
EVE	Ethyl vinyl ether
eq.	Equation
Flu	Fluorenyl
GC-MS	Gas chromatography –mass spectrometry
GPC	Gel permeation chromatography
h	Hour
HDPE	High density polyethylene
HR-MS	High resolution mass spectra
HT-GPC	High temperature gel permeation chromatography
Ind	Indenyl
iPP	Isotactic polypropylene

iPr	Isopropyl
J	Coupling constants in Hertz
k_i	Rate of initiation
k_p	Rate of propagation
LAH	Lithium aluminum hydride
LDPE	Low density polyethylene
LLDPE	Linear low density polyethylene
LUMO	Lowest unoccupied molecular orbital
MAO	Methyl aluminoxane
MDPE	Medium density polyethylene
Me	Methyl
MeOH	Methanol
mg	Milligram
m	Multiplet
M_n	Number-average molecular weight
M_w	Weight-average molecular weight
mol.	Mole
MWD	Molecular weight distribution
NBE	Norborn-2-ene
NMR	Nuclear magnetic resonance
PA	Phenylacetylene
PCy ₃	Tricyclohexylphosphine
PDI	Polydispersity index
PE	Polyethylene
PP	Polypropylene
PPh ₃	Triphenyl phosphine
ppm	parts per million
Ph	Phenyl
RCM	Ring closing metathesis
ROM	Ring opening metathesis
ROMP	Ring opening metathesis polymerization
SPS	Solvent purification system
t	Triplet
<i>tert.</i>	Tertiary
TEA	Triethylamine

THF	Tetrahydrofuran
TIBA	Triisobutylaluminum
TLC	Thin layer chromatography
T_g	Glass transition temperature
T_m	Melting temperature
VLDPE	Very low density polyethylene
VIP	Vinyl insertion polymerization
Z.N	Ziegler-Natta

Zusammenfassung

Polyolefine bilden eine überaus wichtige Materialklasse mit einer großen Bandbreite an Anwendungen und werden industriell in großem Maßstab hergestellt. Ein beachtlicher Anteil dieser Polyolefine wird durch katalytische (Co-)Polymerisation von 1-Olefinen mittels Übergangsmetallen produziert.

Das erste Kapitel dieser Arbeit befasst sich mit einer allgemeinen Einführung in das Gebiet der Polyolefine und der geschichtlichen Entwicklung der Ziegler-Natta-Katalyse und damit auch der homogenen Katalyse. Des Weiteren sollen ihre Anwendungen in der Polymerchemie skizziert werden. Darüber hinaus soll die Chemie der Grubbs- und Schrock-Katalysatoren und ihre Reaktivität in der Metathese beschrieben werden und insbesondere die Zusammenhänge zwischen Ziegler-Natta und Metathese sollen näher beleuchtet werden.

Im zweiten Kapitel werden Synthese und Reaktivität einer Reihe neuartiger Ru-Alkylidene erläutert, bei denen beide Chloridliganden durch Pseudohalogen- oder Nitrat-Liganden ersetzt wurden, also 0 (**1b**), $[\text{Ru}(\text{CF}_3\text{SO}_3)_2(\text{IMesH}_2)(\text{C}_5\text{H}_5\text{N})(\text{CHC}_6\text{H}_5)]$ (**1c**), $[\text{Ru}(\text{NCO})(\text{CF}_3\text{SO}_3)(\text{IMesH}_2)(\text{C}_5\text{H}_5\text{N})(\text{CHC}_6\text{H}_5)]$ (**1d**), $[\text{Ru}(\text{CF}_3\text{SO}_3)(\text{CF}_3\text{CO}_2)(\text{IMesH}_2)(\text{C}_5\text{H}_5\text{N})(\text{CHC}_6\text{H}_5)]$ (**1e**), $[\text{Ru}(\text{NCS})_2(\text{IMesH}_2)(\text{C}_5\text{H}_5\text{N})(\text{CHC}_6\text{H}_5)]$ (**1f**), $[\text{Ru}(\text{NO}_3)_2(\text{IMesH}_2)(\text{CH-2-(2-PrO)-C}_6\text{H}_4)]$ (**2d**) und $[\text{Ru}((\text{CF}_2)_3(\text{CO}_2)_2)(\text{IMesH}_2)(\text{CH-2-(2-PrO)-C}_6\text{H}_4)]$ (**2f**), (IMesH₂=1,3-Dimesitylimidazolin-2-yliden). Diese neuen Initiatoren sowie die der allgemeinen Zusammensetzung $[\text{RuX}_2(\text{L})_n(\text{NHC})(\text{CHPh})]$ bzw. $[\text{RuX}_2(\text{NHC})(\text{CH-2-(2-PrO)-C}_6\text{H}_4)]$ (X=Cl, C₆F₅COO; NHC=IMesH₂, 1,3-Dimesitylpyrimidin-2-yliden, 1,3-Dimesityldiazepin-2-yliden, 1-Mesityl-3-(2-phenylethyl)imidazolin-2-yliden, 1-Mesityl-3-adamantylimidiazolin-2-yliden; L=PCy₃, Pyridin, n=1, 2) wurden in Bezug auf ihre Neigung zur alternierenden Copolymerisation von Norborn-2-en (NBE) mit Cyclopenten (CPE) und *cis*-Cycloocten (COE) hin untersucht. Alternierende Copolymere der Art Poly(NBE-*alt*-CPE)_n und Poly(NBE-*alt*-COE)_n mit bis zu 55 und 40% alternierenden Diaden wurden erhalten. Außerdem stellte sich Ru(CF₃COO)₂(1,3-dimesityl-4,5,6,7-tetrahydro-1,3-diazepin-2-yliden)(=CH-2-(2-PrO)C₆H₄) (**4b**) als hocheffizienter Initiator für die Homopolymerisation von Cyclopenten (CPE) heraus und ermöglichte die Synthese von Poly(CPE) mit hohen Molmassen. Einige grundlegende Auswirkungen der Art des Pseudohalogenliganden auf den Grad der Alternierung bei der Copolymerisation von NBE mit CPE oder COE werden vorgestellt werden. Abschließend wird noch die Auswirkung der Ringgröße des N-heterocyclischen Carbens auf die Konfiguration der Doppelbindungen im Polymer angesprochen. Im dritten Kapitel werden neuartige Zr^{IV}-Komplexe des Typus (Me₂Si((NR)(6-(2-(diethylboryl)phenyl)pyrid-2-yl)))ZrCl₂·THF; R= ^tBu (**13**), Adamantyl (**17**)) und Ti^{IV}-

basierte Metallocenkomplexe, und zwar Bis((N(6-(2-(diethylboryl)phenyl)pyrid-2-yl)Me)TiCl₂; (**24**)) sowie nicht-verbrückte Halb-Titanocenverbindungen der Art Cp'TiCl₂(N(6-(2-(diethylboryl)phenyl)pyrid-2-yl)R); R=Me (**22**, **23**), Si(CH₃)₃ (**26**, **27**), Cp'=Cp (**22** und **26**), Cp* (**23** und **27**) besprochen. Zusätzlich wird noch die Chemie der Aminoboran-freien Modelkomplexe Cp'TiCl₂(N-(biphenyl-3-yl)R); R= SiMe₃ (**30**, **31**), Me (**33**, **34**), (Cp'=Cp (**30**, **34**), Cp* (**31**, **33**)) erörtert (Abbildung 2). Diese Zr- und Ti-Komplexe wurden durch ¹H- und ¹³C-NMR-Spektroskopien und durch Elementaranalysen charakterisiert. Die Molekularstruktur der Verbindungen **22**, **23**, **27** und **34** wurde durch Röntgenstrukturanalyse bestimmt. Nach Aktivierung mit MAO zeigen die Komplexe **13**, **17**, **22**, **23**, **26** und **27** für die Homopolymerisation von Ethylen (E) Aktivitäten von bis zu 3000 kg-PE /mol-M'h, wobei hauptsächlich lineares Polyethylen (PE) (HDPE) mit molaren Massen zwischen 100 000 und 4 x 10⁶ g/mol gebildet wird. Überraschenderweise zeigt Komplex **13** bei der Copolymerisation von Ethylen (E) mit CPE eine hohe katalytische Aktivität (30 000 kg-PE /mol-Zr'h), wobei Poly(E)-*co*-poly(CPE)_{VIP} produziert wird, das 3-4 mol-% CPE durch Vinyladditionspolymerisation aufweist. Die Komplexe **13**, **17**, **22**, **23**, **26** und **27** ergeben bei der Copolymerisation von E mit NBE vorwiegend Poly(E)-*co*-poly(NBE)_{VIP} durch Vinyladditionspolymerisation mit eingebauten NBE-Anteilen von bis zu 36%, wie durch ¹³C-NMR-Messungen bewiesen werden konnte. Interessanterweise ergibt sich bei niedrigem Druck (2 bar) von Ethylen und hohen NBE-Konzentrationen für den Komplex 23/MAO, reversibel hergestellt durch ROMP- und VIP-abgeleitete Co-Polymere von NBE mit E, die Bildung von poly(NBE)_{ROMP}-*co*-poly(NBE)_{VIP}-*co*-poly(E). Diese bestimmte Co-Polymerbildung kann durch einen reversiblen α -H-Elimination-/ α -H-Additions-Prozess während der Polymerisation erklärt werden und wird eindeutig der Rolle des 6-[2-(diethylboryl)phenyl]pyrid-2-yl-Ligandenrestes in diesem Komplex zugeordnet. Die katalytische Aktivität Zr-basierter Komplexe für die Copolymerisation von E mit NBE war niedriger als für die Homopolymerisation von E. Die E-NBE Copolymere die durch die Zr^{IV}-basierten und die nicht-verbrückten Halb-Titanocen-Komplexe erhalten wurden, besaßen alternierende *it* E-NBE Abschnitte und *st* E-NBE Abschnitte neben isolierten NBE-Sequenzen. Durch einen hohen Anteil an NN-Diaden im NBE-Copolymer (>10 mol-%) tauchten mehrere kleinere Signale bei 21.2, 31.0, 33.5 und 41.1 ppm auf. Der Einbau von NBE in die resultierenden Copolymere wurde stark durch den eingestellten Druck von E beeinflusst, vor allem bei niedrigen Drücken (1 oder 2 bar E) war der NBE-Gehalt im Copolymer hoch. Auch die NBE-Konzentration wirkte sich auf die katalytische Aktivität und die zahlenmittlere Molmasse der Copolymere aus. Mit wachsender NBE-Konzentration sank die katalytische Aktivität. In ähnlicher Weise erhöhte sich die zahlenmittlere Molmasse im

resultierenden E-NBE-Copolymer. Copolymere mit niedrigem NBE-Anteil (<10 mol-%) besaßen nur alternierende *st* E-NBE-Sequenzen neben isolierten NBE-Abschnitten ohne jegliche alternierenden *it* E-NBE-Sequenzen und NBE Diaden. Copolymere mit hohem NBE-Anteil (>10 mol-%) besaßen sowohl *it* und *st* E-NBE-Sequenzen als auch isolierte NBE-Abschnitte mit einigen schwachen Resonanzen von NBE Diaden.

Zusätzlich wurde noch die Homopolymerisation von Styrol mit den nicht-verbrückten Halb-Titanocen Komplexen **26** und **27**, die den 6-[2-(Diethylboryl)phenyl]-pyrid-2-yl-Baustein enthielten, und den Aminoboran-freien nicht-verbrückten Halb-Titanocen-Komplexen **31** und **32** unter verschiedenen Bedingungen in der Anwesenheit von MAO als Cokatalysator untersucht. Die Ergebnisse zeigten, dass die katalytischen Aktivitäten bei Erhöhung der Polymerisationstemperatur wuchsen. Komplexe, die den 6-[2-(Diethylboryl)phenyl]-pyrid-2-yl-Baustein beinhalteten, zeigten niedrigere Aktivitäten (bis zu 1100 kg_{s,PS}/mol_{Katalysator}·h) im Vergleich zu den Aminoboran-freien nicht-verbrückten Halb-Titanocen-Komplexen (bis zu 3500 kg_{s,PS}/mol_{Katalysator}·h), und all diese Verbindungen führten hauptsächlich zu syndiotaktischem Polystyrol mit zahlenmittleren Molmassen im Bereich zwischen 29 000 und 1,4 x 10⁵ g/mol.

Abstract

Polyolefins form a highly important class of materials with a wide range of applications and are produced industrially on a large scale. A significant fraction of polyolefins are produced via the catalytic (co-)polymerization of 1-olefins using transition metal catalysts.

The first chapter of this thesis deals with a general introduction to polyolefins and the historical development of Ziegler-Natta catalysis as well as with homogeneous catalysis. Furthermore, their applications in the field of polymer chemistry are outlined. Also, the chemistry of Grubbs- and Schrock-type catalysts and their reactivity in metathesis and the intercorrelation between Ziegler-Natta and metathesis chemistry is described.

The second chapter deals with the synthesis and reactivity of a series of novel Ru-alkylidene-based initiators, in which both chloride ligands were replaced by pseudo-halides or by nitrate, i.e. $[\text{Ru}(\text{NCO})_2(\text{IMesH}_2)(\text{C}_5\text{H}_5\text{N})(\text{CHC}_6\text{H}_5)]$ (**1b**), $[\text{Ru}(\text{CF}_3\text{SO}_3)_2(\text{IMesH}_2)(\text{C}_5\text{H}_5\text{N})(\text{CHC}_6\text{H}_5)]$ (**1c**), $[\text{Ru}(\text{NCO})(\text{CF}_3\text{SO}_3)(\text{IMesH}_2)(\text{C}_5\text{H}_5\text{N})(\text{CHC}_6\text{H}_5)]$ (**1d**), $[\text{Ru}(\text{CF}_3\text{SO}_3)(\text{CF}_3\text{CO}_2)(\text{IMesH}_2)(\text{C}_5\text{H}_5\text{N})(\text{CHC}_6\text{H}_5)]$ (**1e**), $[\text{Ru}(\text{NCS})_2(\text{IMesH}_2)(\text{C}_5\text{H}_5\text{N})(\text{CHC}_6\text{H}_5)]$ (**1f**), $[\text{Ru}(\text{NO}_3)_2(\text{IMesH}_2)(\text{CH-2-(2-PrO)-C}_6\text{H}_4)]$ (**2d**) and $[\text{Ru}((\text{CF}_2)_3(\text{CO}_2)_2)(\text{IMesH}_2)(\text{CH-2-(2-PrO)-C}_6\text{H}_4)]$ (**2f**), (IMesH₂=1,3-dimesitylimidazol-2-ylidene). The novel initiators and those of the general formula $[\text{RuX}_2(\text{L})_n(\text{NHC})(\text{CHPh})]$ and $[\text{RuX}_2(\text{NHC})(\text{CH-2-(2-PrO)-C}_6\text{H}_4)]$ (X=Cl, C₆F₅COO; NHC=IMesH₂, 1,3-dimesitylpyrimidin-2-ylidene, 1,3-dimesityldiazepin-2-ylidene, 1-mesityl-3-(2-phenylethyl)imidazol-2-ylidene, 1-mesityl-3-adamantylimidiazolin-2-ylidene; L=PCy₃, pyridine, n=1, 2) were investigated for their propensity to copolymerize norborn-2-ene (NBE) with cyclopentene (CPE) and *cis*-cyclooctene (COE), respectively, in an alternating way. Alternating copolymers, that is, poly(NBE-*alt*-CPE)_n and poly(NBE-*alt*-COE)_n containing up to 55 and 40% alternating diads, respectively, were obtained. Moreover, Ru(CF₃COO)₂(1,3-dimesityl-4,5,6,7-tetrahydro-1,3-diazepin-2-ylidene)(=CH-2-(2-PrO)C₆H₄) (**4b**) turned out to be a highly efficient initiator for the homopolymerization of cyclopentene (CPE), allowing for the synthesis of high-molecular weight poly(CPE). Some fundamental effects of the nature of the pseudo-halide ligand on the extent of alternating copolymerization of NBE with CPE or COE are presented. Finally, the effects of the ring-size of the *N*-heterocyclic carbene on the configuration of the double bonds in the final polymer are addressed.

The 3rd chapter deals with novel Zr^{IV}-complexes of the type (Me₂Si((NR)(6-(2-(diethylboryl)phenyl)pyrid-2-yl)))ZrCl₂·THF; R= ^tBu (**13**), adamantyl (**17**)) and Ti^{IV}-based

metallocene-type complexes i.e. bis((N(6-(2-(diethylboryl)phenyl)pyrid-2-yl)Me)TiCl₂ (**24**) and non-bridged half-titanocene complexes of the type Cp'TiCl₂(N(6-(2-(diethylboryl)phenyl)pyrid-2-yl)R); R=Me (**22**, **23**), Si(CH₃)₃ (**26**, **27**), Cp'=Cp (**22** and **26**), Cp* (**23** and **27**) as well as with the chemistry of the aminoborane-free model complexes Cp'TiCl₂(N-(biphenyl-3-yl)R); R= SiMe₃ (**30**, **31**), Me (**33**, **34**), (Cp'=Cp (**30**, **34**), Cp* (**31**, **33**)); (Figure 2). These Zr- and Ti-complexes were characterized by ¹H and ¹³C NMR spectroscopy and elemental analysis. The molecular structures of complexes **22**, **23**, **27** and **34** were determined by single-crystal X-ray diffraction. Upon activation with MAO, complexes **13**, **17**, **22**, **23**, **26** and **27** show activities up to 3000 kg-PE /mol-M'h in the homopolymerization of ethylene (E), producing mainly linear poly(ethylene) (PE) (HDPE) with molecular weights in the range of 100,000 < M_n < 4 x 10⁶ g mol⁻¹. Surprisingly, in the copolymerization of ethylene (E) with CPE, complex **13** exhibits high catalytic activity (30,000 kg-PE /mol-Zr'h), producing poly(E)-*co*-poly(CPE)_{VIP} with 3-4 mol-% of vinyl addition polymer incorporated CPE. In the copolymerization of E with NBE, complexes **13**, **17**, **22**, **23**, **26** and **27** mainly produced vinyl addition copolymerization-derived poly(E)-*co*-poly(NBE)_{VIP} with incorporated NBE-fractions of up to 36 mol-% as evidenced by ¹³C NMR analysis. Interestingly, at low E pressures (2 bar) and higher NBE concentrations, complex **23/MAO** produced reversible ROMP- and VIP-derived copolymers of NBE with E, resulting in the formation of poly(NBE)_{ROMP}-*co*-poly(NBE)_{VIP}-*co*-poly(E). This particular copolymer formation can be explained by a reversible α-H elimination/ α-H addition process during the polymerization and is attributed to the unique role of the 6-[2-(diethylboryl)phenyl]pyrid-2-yl ligand moiety in this complex. The catalytic activity of Zr-based complexes for the copolymerization E with NBE was lower than that for E homopolymerization. The Zr^{IV}-based and non-bridged half-titanocenes complexes derived E-NBE copolymers possessed alternating *it* E-NBE sequences and *st* E-NBE sequences along with isolated NBE sequences. Several minor signals at 21.2, 31.0, 33.5 and 41.1 ppm appeared, due to the result of NN diads in high content of NBE (>10 mol-%) copolymers. The incorporation of NBE in the resulting copolymers was highly influenced by the E pressure, mainly at low pressures (1 or 2 bar E) the NBE content was high in the resulting copolymers. The influence of the NBE feed also exhibits impact on both the catalytic activity and NBE incorporation as well as on the number-average molecular weights of the resulting copolymers. While increasing the NBE feed, the catalytic activity decreased. Similarly, the number-average molecular weight increased in the resulting E-NBE copolymer. Copolymers with low NBE incorporation (<10 mol-%) possessed only alternating *st* E-NBE sequences along with isolated NBE sequences without any alternating *it* E-NBE sequences and NBE diads. Copolymers with a high NBE

content (>10 mol-%) possessed both alternating *it* and *st* E-NBE sequences as well as isolated NBE sequences with some minor NBE diads resonances.

In addition, the homopolymerization of styrene was investigated using the non-bridged half-titanocene complexes **26** and **27** containing the 6-[2-(diethylboryl)phenyl]-pyrid-2-yl motif, as well as the aminoborane-free non-bridged half-titanocene complexes **30** and **31** at various conditions in the presence of MAO as co-catalyst. The study revealed that catalytic activities increased upon increasing the polymerization temperatures. Complexes bearing the 6-[2-(diethylboryl)phenyl]-pyrid-2-yl motif exhibited lower activities (up to 1100 kg_{.sPS}/mol_{catalyst}·h) when compared with aminoborane-free non-bridged half-titanocene complexes (up to 3500 kg_{.sPS}/mol_{catalyst}·h) and all these complexes mainly produced syndiotactic poly(styrene) with number-average molecular weights in the range of 29,000 < M_n < 1.4 x 10⁵ g/mol.

Aim of the Thesis

The first aspect of my research was related to the alternating ring-opening metathesis copolymerization of norborn-2-ene (NBE) with cyclopentene (CPE) and *cis*-cyclooctene (COE), respectively, using various modified Grubbs- and Grubbs-Hoveyda-type initiators. The degree of copolymerization was quantified by ^{13}C NMR and correlated with the structural features of the initiators used. For these purposes, various metathesis catalysts, i.e. **1a-1g**, **2a-2g**, **3a-3d**, **4a**, **4b**, **5a**, **5b**, **6** (Figure 1) were prepared and investigated for their copolymerization propensity. ^[1]The obtained results are discussed in Chapter 2.

Another aspect of my thesis includes the synthesis of well-defined group IV organometallic precatalysts for the simultaneous vinyl insertion/ ring-opening metathesis copolymerization of cyclic olefins with 1-olefins. These organometallic complexes bear an auxiliary amine- and borane- containing ligand, which is capable of reversibly switching between ROMP and VIP by abstracting a proton from the cationic species and re-adding a proton to the metal alkylidene. In other words, α -H elimination/ α -H addition can be induced thereby allowing for metathesis and Ziegler-Natta type polymerization to take place within the same polymer chain. This α -elimination process is temperature-dependent. The derived polymers hold both saturated (VIP) and unsaturated (ROMP) units within one single polymer chain and had high molecular weights and narrow molecular weight distribution. The focus of this work was thus on the synthesis of designed ligands and the corresponding group IV organometallic complexes **13**, **17**, **22**, **23**, **24**, **26**, **27**, **30**, **31**, **33** and **34** (Figure 2) and their applications in simultaneous vinyl insertion and ring-opening metathesis co-polymerization of cyclic olefins with 1-olefins. The obtained results are discussed in Chapter 3. The synthetic protocol of all ligands and group IV organometallic complexes and their characterization (^1H NMR, ^{13}C NMR, HRMS, and elemental analysis) are shown in the experimental part of chapter 4. Single-crystal X-ray analyses of selected organometallic complexes are summarized in the appendix.

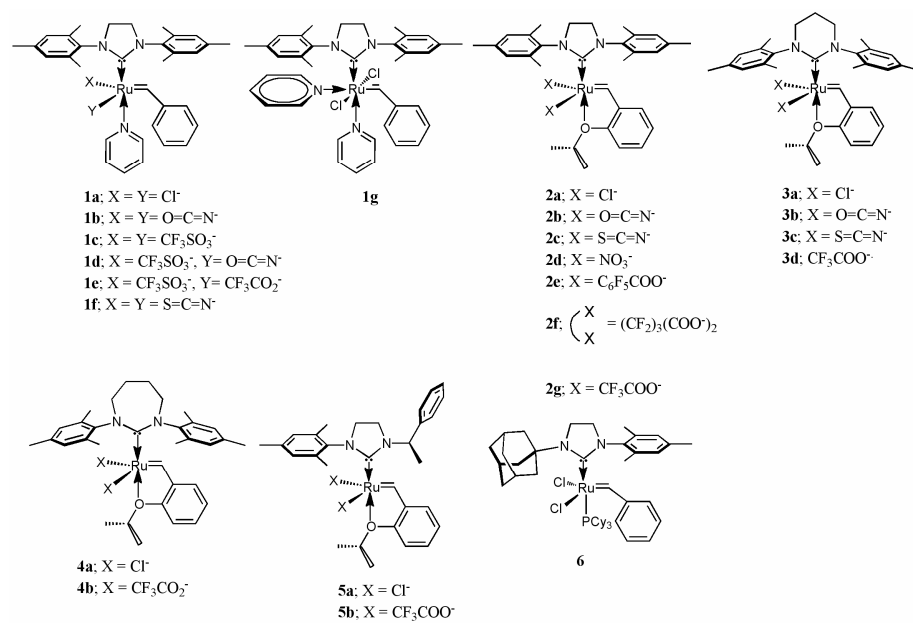


Figure 1. Structure of initiators **1a-1g**, **2a-2g**, **3a-3d**, **4a**, **4b**, **5a**, **5b** and **6**.

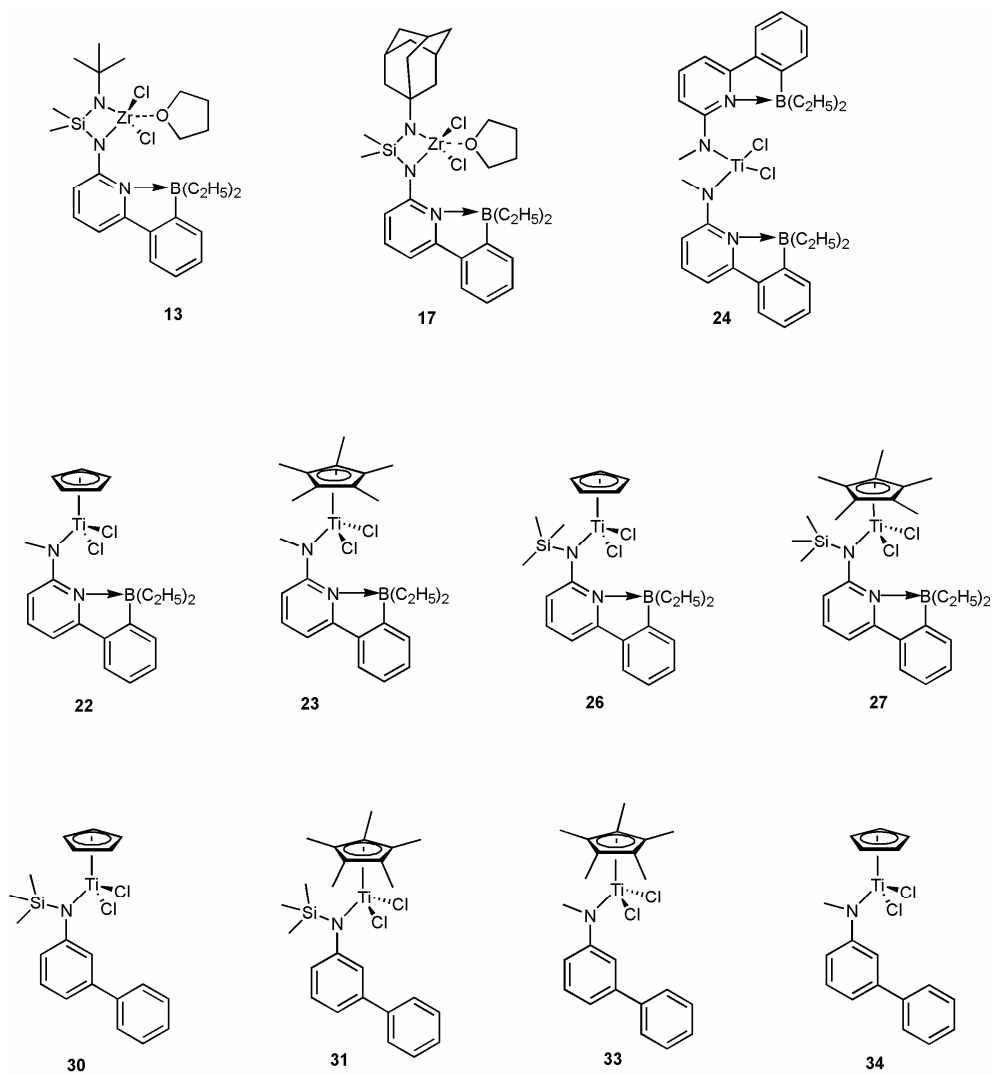


Figure 2. Structure of precatalysts **13**, **17**, **22**, **23**, **24**, **26**, **27**, **30**, **31**, **33** and **34**.

CHAPTER 1
General Introduction

I. Introduction: Background

1.1. Historical Development of Polyolefins

Polyolefins form a highly important class of materials with a wide range of applications and are produced industrially on a large scale. A significant fraction of polyolefins are produced via the catalytic (co-)polymerization of 1-olefins using transition metal catalysts. Olefin-based polymers such as PE, PP and ethylene/1-olefin copolymers are widely used as synthetic commodity polymers world wide due to their versatility, flexibility and strength. They possess a combination of properties including flexibility, strength, lightness, stability, impermeability and processability. PE and poly PP are also well suited for recycling and re-use. PE, PP and poly(ethylene)-*co*-poly(vinyl acetate) are among the most important commercial polymers. PE is classified according to its density as very low density polyethylene (VLDPE), low density polyethylene (LDPE), linear low density polyethylene (LLDPE), medium density polyethylene (MDPE), and high density polyethylene (HDPE).

Table 1.1. Classification and applications of polyolefin products.

Name	Abbr.	Density (g/cm ³)	Use
High Density Polyethylene	HDPE	>0.941	Plastic lumber, fuel tanks, furniture, storage sheds, chemical & heat resistant piping & containers
Medium Density Polyethylene	MDPE	0.926- 0.940	Containers with good shock and drop resistance, gas pipes, shrink film, packaging films
Linear Low Density Polyethylene	LLDPE	0,915- 0.920	Industrial containers, trash cans, automotive parts, packaging materials under FDA regulations
Low Density Polyethylene	LDPE	0.910- 0.940	Trays & general purpose containers, computer parts, plastic bags, playground equipment
Very Low Density Polyethylene	VLDPE	0.880- 0.915	Blown films, molded parts, industrial & general rubber, stretch wrap
Polypropylene	PP	0.855- 0.946	Packaging, textile fibers, ropes, thermal clothing, reusable containers
poly(ethylene)- <i>co</i> -poly(vinyl acetate)	EVA	0.93	Biomedical applications for time release medications, foam padding for sport equipment.

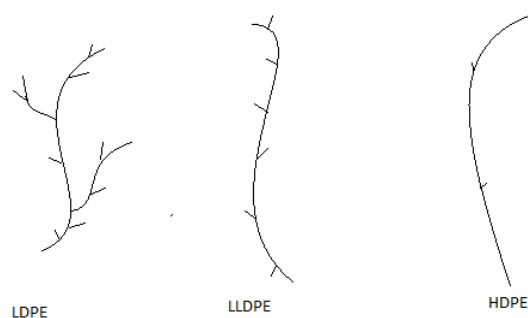


Figure 1.1. Structure of different PE.

The first industrial PE synthesis was invented by Eric Fawcett and Reginald Gibson from ICI chemicals in 1933. Ethylene was polymerized under high pressure (500-1200 atm) and high temperatures (200-400°C) to produce a white waxy material. This reaction was initiated by trace contamination of oxygen.^[2] Robert Bank's and John Hogan's synthesis of the PE at low pressure and temperature led to the discovery of the Phillips catalyst (chromium trioxide on silica) in 1951 at Phillips petroleum. This type of catalyst was patented in 1958.^[3] In 1953, Karl Ziegler discovered a heterogeneous catalyst system based on titanium halides that allowed for producing HDPE upon activation with organoaluminium co-catalysts such as $\text{Al}(\text{C}_2\text{H}_5)_2\text{Cl}$ by coordination polymerization at low temperature and pressure. In 1954, G. Natta *et.al* synthesized rubber-like PP using $\text{TiCl}_4/\text{Al}(\text{C}_2\text{H}_5)_2$. The polymers obtained contained different kinds of polymers, from which an insoluble polymer was isolated from boiling heptane, showing a melting point $>160^\circ\text{C}$. Later, in 1955 G. Natta proved the existence of isotactic polypropylene, which was prepared by supported CrO_3 catalysts. Another important milestone was achieved by Natta. He showed that the stereospecificity of the polymerization was connected to the regularity of the surface of the heterogeneous catalyst. For this purpose, crystalline TiCl_3 was prepared by reduction of TiCl_4 with hydrogen and treated with trialkylaluminum or dialkylaluminum chloride in a hydrocarbon solvent. By this approach, the percentage of *i*PP was drastically enhanced from 40% to around 90% of the produced polymer. The use of a Lewis base in the polymerization further increased the *i*PP content up to 95%. In view of catalytic activity, a major improvement was achieved by supporting TiCl_4 on activated MgCl_2 ^[4] or other magnesium compounds.^{[5, 6] [7-9]}

Polyolefin consumption significantly increased each year and is expected to almost double by 2017. The graph below illustrates polyolefin consumption (Figure 1.2).

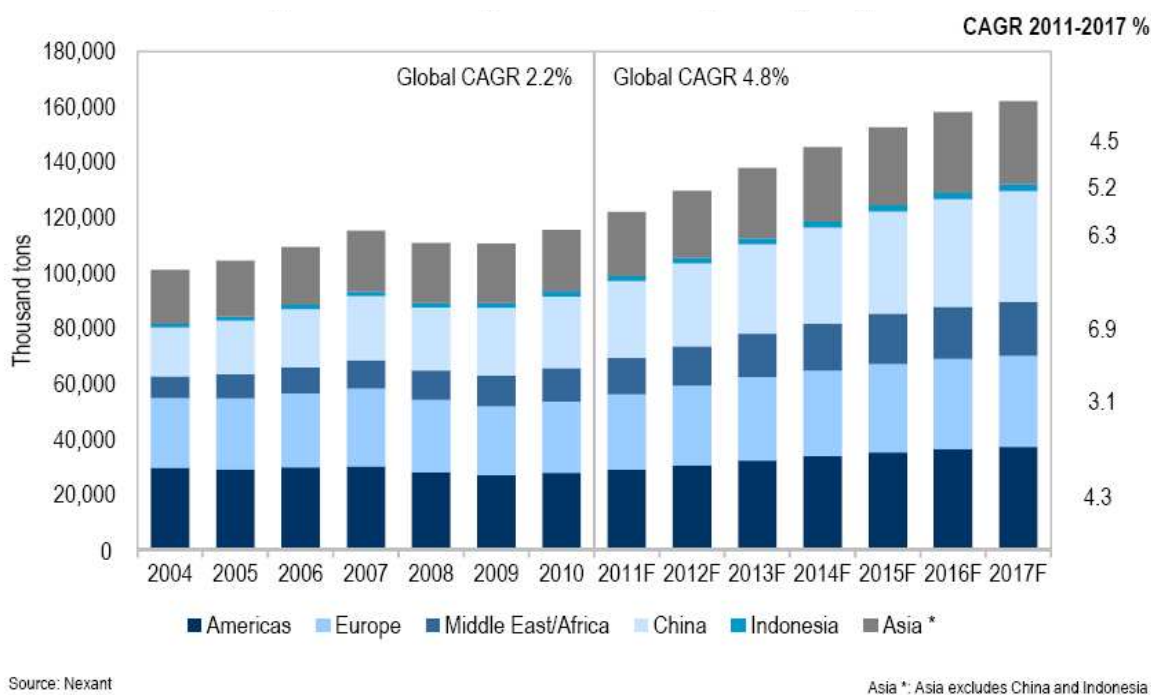


Figure 1.2. Polyolefin consumption by region.

1.2. Ziegler-Natta Catalysis

Coordination polymerization originated in the mid-1950s with the pioneering work of Karl Ziegler in Germany and Giulio Natta in Italy. While Ziegler discovered in the early 1950s that a combination of aluminum alkyls with certain transition metal compounds such as $TiCl_4$ or VCl_4 generated a complex that would polymerize ethylene at low temperatures and pressures producing PE with an essentially linear structure, referred to as high density polyethylene (HDPE), Natta's work led to the recognition that the catalytic complexes described by Ziegler were capable of polymerizing 1-alkenes to yield stereoregular polymers. These types of catalysts are known as Ziegler-Natta catalysts. For their pioneering work, Karl Ziegler and G. Natta jointly won the Nobel Prize for Chemistry in 1963. Research was subsequently extended aiming on polymers with a wide range of stereoregular structures including those derived from cycloalkenes. Many polymers are now manufactured on a commercial scale using Ziegler-Natta catalysts, the most prominent among them being stereoregular *i*PP of high molecular weight.^[5] The most important stereospecific structures of polymers are shown in Figure 1.3.

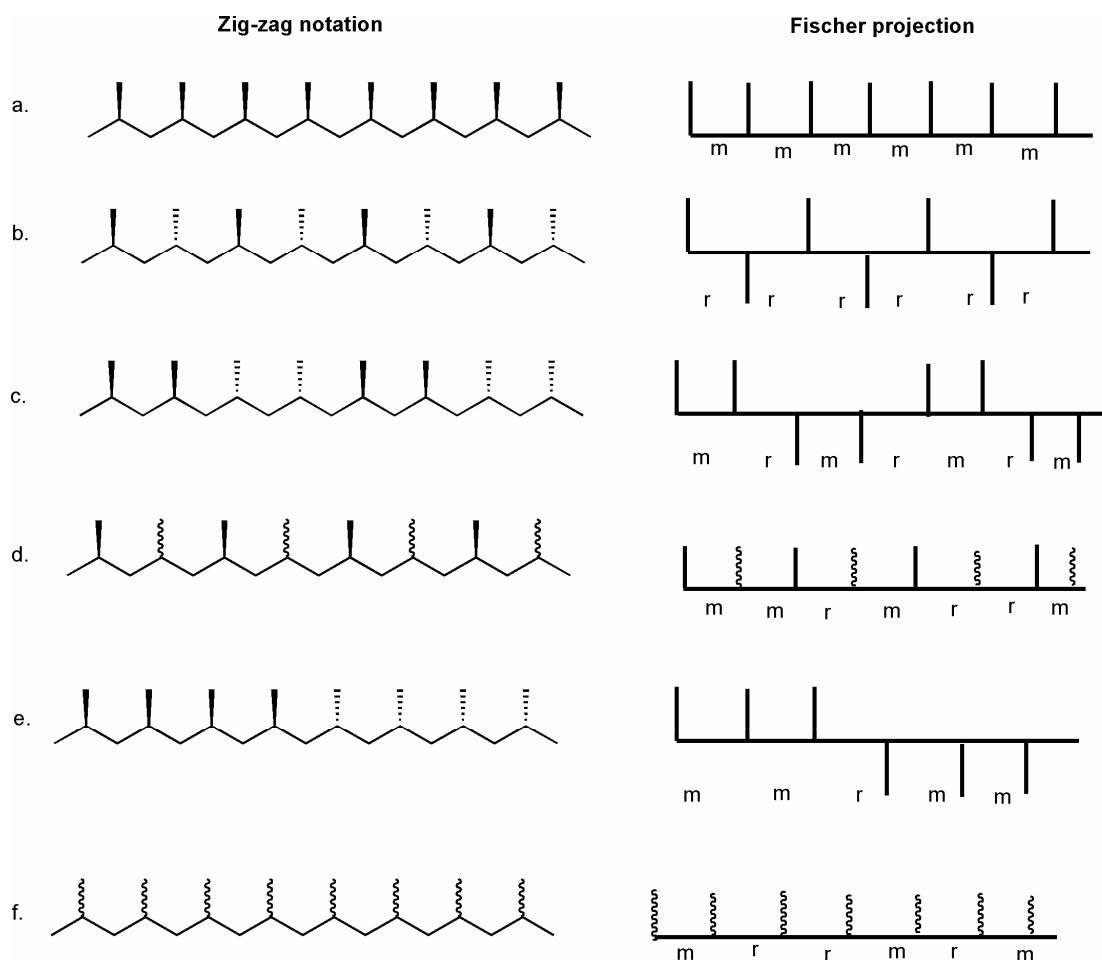


Figure 1.3. Stereoregular polymer structures: a) isotactic, b) syndiotactic, c) heterotactic, d) hemiisotactic, e) isotactic stereoblock, f) atactic. ^[10]

In the late 1970s in Germany, Kaminsky and Sinn discovered a new class of Ziegler-Natta catalysts based on metallocene/methylaluminoxane. ^[7-9, 11] This new generation of catalysts showed higher activity and the resulting polymers had higher molecular weights than those produced with commercially available Ziegler-Natta type catalysts.

A further step was the discovery of chiral *ansa*-metallocenes with well-defined active centers by Britzinger in 1982. This catalyst was used for the synthesis of highly *i*PP by Kaminsky, Britzinger in 1985^[5, 12, 13] Since then, the structure of the metallocenes has been modified worldwide in industrial and academic areas to provide a range of different catalyst structures that can be used to synthesize highly isotactic, syndiotactic or atactic polyolefins with different molecular weights and different degrees of tacticity.

1.3 Metallocenes

Metallocenes show high activity in 1-olefin polymerization. The advantage of these homogeneous polymerization catalysts is their well-defined single-site nature and their versatility and flexibility in synthesis, which leads to higher control over the specific polymer microstructure together with high molecular weights and narrow molecular weight distributions (MWD) as compared to multi-site heterogeneous catalysts.^[14, 15] This unique class of complexes can also be used to produce high-density polyethylene (HDPE), PP with various tacticities (atactic, isotactic, syndiotactic, etc.), and copolymers of ethylene with α -olefins, and for the synthesis of COCs.^[16]

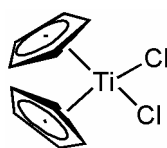


Figure 1.4. Structure of metallocenes exemplified by Dicyclopentadienyl Ti-dichloride.

Natta and co-workers reported in 1957 that dicyclopentadienyltitanium dichloride polymerized ethylene and produced polymers that had low molecular weights, also the catalytic activities were very low, and these catalytic systems was inactive for propylene polymerization when activated with trialkylaluminum.^[17] Natta also reported that in the polymerization of ethylene at 95°C, 40 atm in heptane solution for 20 hours, about 8.0 g of PE was produced in the presence of 0.6 g of an Ti-Al complex.^[17] Therefore, these catalytic systems show much lower activities than heterogeneous Ziegler-Natta catalysts (3000 g/mol·Ti·h).

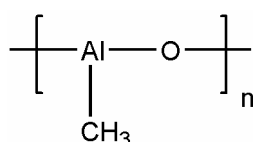
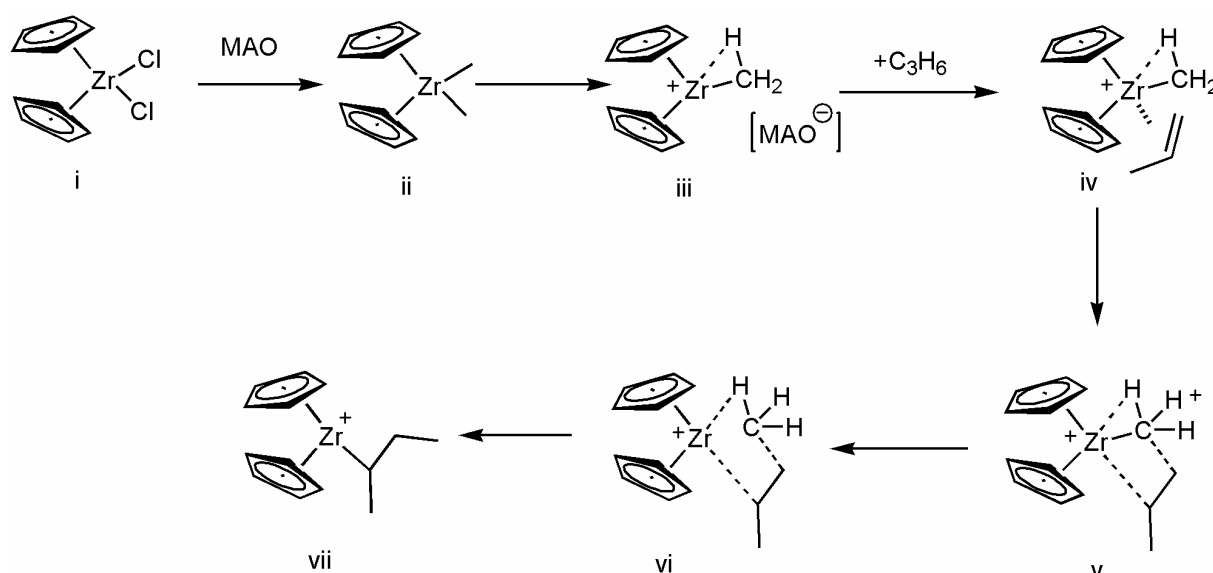


Figure 1.5. Structure of methylaluminoxane.

A major discovery by Natta^[17] that was confirmed by Breslow *et.al* was the complete inactivity of dicyclopentadienyltitanium dichloride in the polymerization of ethylene in the absence of a cocatalyst.^[18] Thus, the trialkyl aluminum species served as an important role as a co-catalyst. In 1980, Sinn and Kaminsky discovered that partially hydrolyzed trimethylaluminum, called methylalumoxane (MAO), employed as a co-catalyst, amazingly enhanced metallocene activity in polymerization.^{[11, 14, 19] [20]} The catalytic mechanism for 1-olefin polymerization is shown in Scheme 1.1. The dicyclopentadienylzirconium dichloride

(Cp_2ZrCl_2) is an 16-electron species complex and activated cationic group IV metallocene species are generally assumed to be 14 electron species and these active species are stabilized by α -agostic interactions. Initially, MAO alkylates the chloride ligands of metallocene and excess of MAO abstracts one of the methyl groups, which creates a cationic metal center and a weakly coordinated anion, which is the active species for olefin polymerization. The interaction between the metal and the hydrogen on the methyl group called an α -agostic interaction^[21]. Upon addition of monomer as propylene, a four-membered transition state forms (Scheme 1.1, v) and this strained four-membered ring allows for the breaking of the Zr-methyl bond, and forms a bond between Zr and the β carbon on the monomer. Again, a fourteen electron species is formed, which is active for repeating the polymerization cycle.^[16]

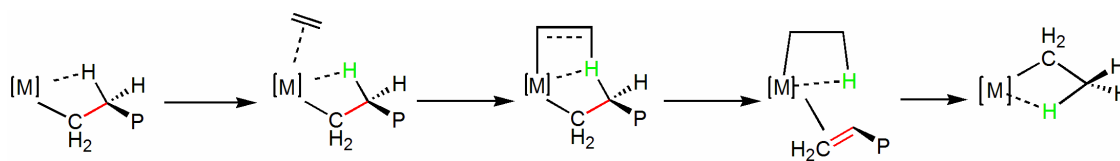


Scheme 1.1. Metallocene polymerization mechanism.^[16]

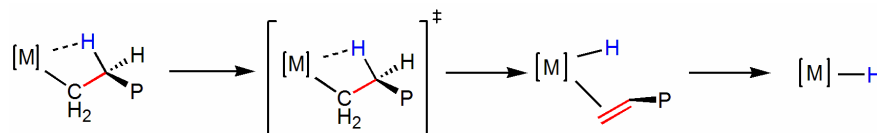
1.4 Chain Termination

An important chain-transfer reaction is the β -hydrogen transfer to a monomer (Scheme 1.2). This reaction produces vinyl groups at the terminated chain end and n -ethyl groups at the initiated chain end. An alternative chain-transfer reaction is a β -hydrogen transfer to the metal (Scheme 1.3). The same chain end groups derived from β -hydrogen transfer to the monomer are formed through this reaction. This is the dominant chain transfer mechanism under the usual experimental conditions. β -Hydrogen elimination (i.e., hydrogen transfer to the metal) can only compete in the limit of very small monomer concentrations or if monomer complexation is otherwise disfavored. The activation barrier for β -hydrogen transfer to the monomer is only weakly dependent on the character of the metal center and the auxiliary

ligand ^[22]. β -Hydrogen elimination is the main cause for low molecular weights of the produced polymers, in comparison with heterogeneous catalysts ^[23].

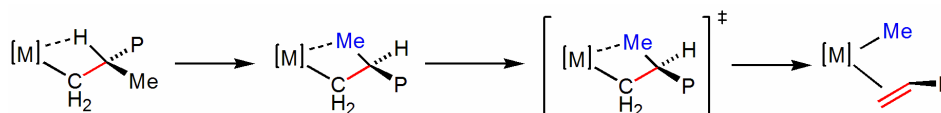


Scheme 1.2. β -Hydrogen transfer to monomer.^[22]



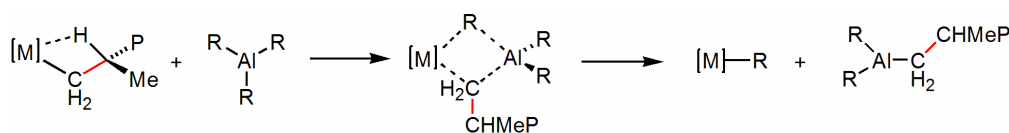
Scheme 1.3. β -Hydrogen elimination (hydrogen transfer to metal).

The third chain transfer reaction is a β -methyl transfer to the metal and the chain end structure of a vinyl group is formed through β -methyl elimination. β -methyl transfer is dominant during propene polymerization by sterically crowded systems. i.e. bis(η^5 -C₅Me₅) metallocens. It has been suggested that the reason for this is the orientation of the polymer. The migrating methyl group lies between the Cp-rings rather than eclipses the η^5 -C₅Me₅ rings, and can migrate the methyl group to the lowest unoccupied molecular orbital (LUMO) of the metal.^[16] ^[24] β -Methyl elimination becomes viable and is actually the most important in propylene polymerization when Cp*₂M^{IV}-type complexes (Cp* = pentamethyl cyclopentadienyl; M = Zr, Hf) are used as catalyst precursors.^[24-27]



Scheme 1.4. β -Methyl elimination mechanism.

The fourth chain transfer reaction is a chain transfer to Al³⁺. In the case of MAO, this chain transfer reaction occurs at lower polymerization temperature or lower propylene concentration. In the case of AlR₃ (without MAO), chain transfer to aluminum was determined by chain-end analysis of the resulting polypropylenes. The presence of isobutyl end groups was indicated by ¹³C NMR analysis.^[28, 29]



Scheme 1.5. Chain transfer to Al³⁺.^[28, 29]

Stereochemistry of the polymerization reaction depends on both the ligand set of a single-site catalyst, as well as growing polymer chain. During a chain-growth polymerization reaction and monomer enchainment, a polymer chain remains bound to the active metal center. Thus, last enchainment monomer unit stereogenic center will have influence on the stereochemistry of the incoming monomer addition. If this influence is significant, the mode of stereochemical control is referred to as “polymer chain-end control”. If the chirality of the ligand has a dominant influence on the stereochemistry of the resulting polymer chain, the mechanism is referred to as ‘enantiomorphic-site-control’.^[19] The effect of catalyst symmetry on polymer stereoselectivity can be seen in Figure 1.6.

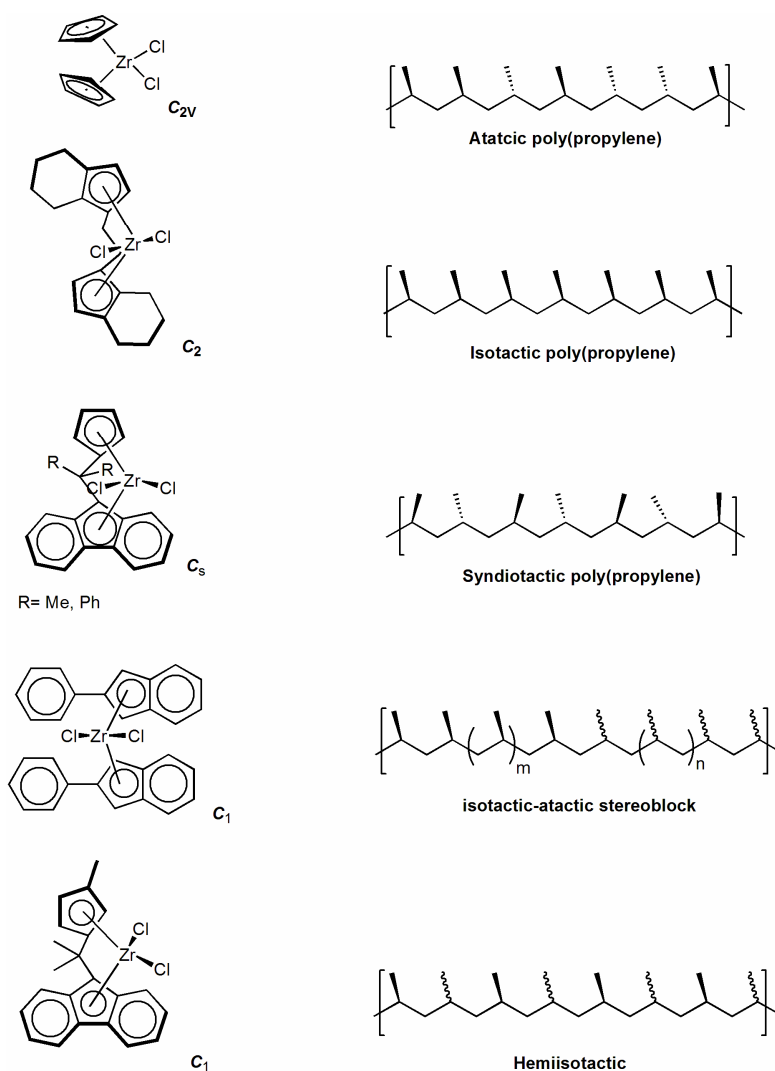
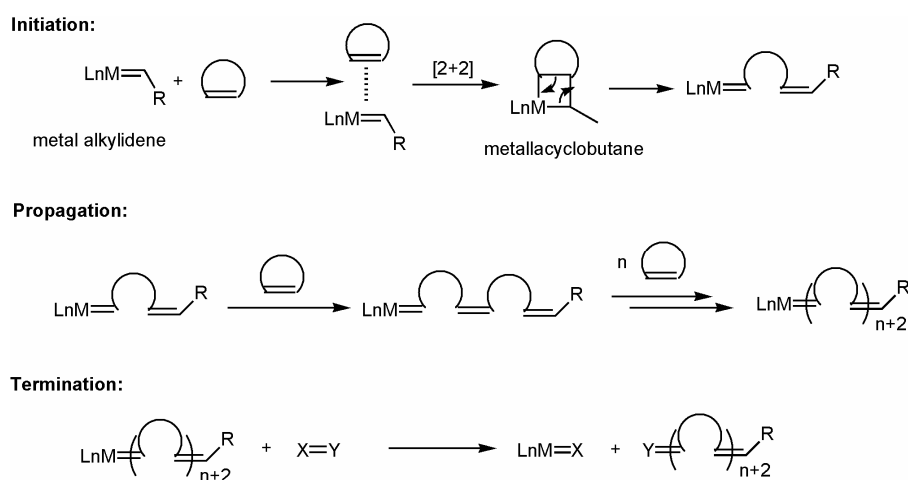


Figure 1.6. Catalyst symmetry effects on stereospecificity.^[19]

Polymer tacticity mainly depends on the symmetry of the catalytic system; catalysts such as Cp_2ZrCl_2 exhibiting C_{2v} symmetry, these complexes mainly produce atactic polymers. As for C_2 symmetric complexes, both racemic mixtures and enantiomerically pure complexes typically produce isotactic polymers. C_s symmetric metallocene catalysts typically produce syndiospecific polymers, Ewen *et.al* reported that a C_s symmetric catalyst such as isopropyl(cyclopentadienyl-1-fluorenyl)hafnium (IV) dichloride i.e. (*i*-PrCp-1-FluHfCl₂), is highly active for the syndiospecific polymerization of propylene.^[30] Stereoselectivities of C_1 (asymmetric) catalysts are unpredictable, and the derived polymers architecture from these catalysts have been reported to produce isotactic, atactic, hemiisotactic and isotactic-atactic stereoblock polymers, Ewen *et.al* reported that C_1 symmetric catalyst, such as $\text{Me}_2\text{C}(\text{3-MeCp})(\text{Flu})\text{ZrCl}_2$ polymerize propylene to hemiisotactic polypropylene. Interestingly, Waymouth and Coates reported that oscillating metallocene complex i.e. (2-phenylindenyl)₂ZrCl₂ produces isotactic and atactic stereoblock polypropylene.^[19, 31]

1.5 Ring Opening Metathesis Polymerization (ROMP)

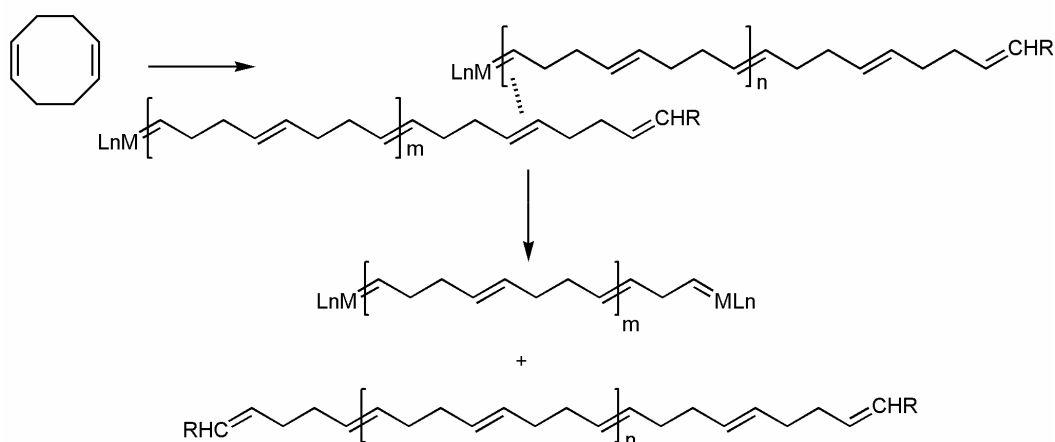
Ring-opening metathesis polymerization (ROMP)^[32] is a chain-growth polymerization process, in which monocyclic (CPE and COE) or bicyclic olefins (NBE) are converted to a polymer. ROMP has emerged as a powerful and broadly applicable method for synthesizing polymeric materials^[33-36]. The olefin metathesis polymerization mechanism is a metal-mediated one, in which a carbon-carbon double bond exchange process takes place between two olefins. The basic mechanism of ROMP is illustrated in Scheme 1.6. Among the large number of contributions, R.H. Grubbs, R.R. Schrock and Y. Chauvin were honored for their discovery by the award of the Noble Prize in Chemistry in 2005.^[37-39]



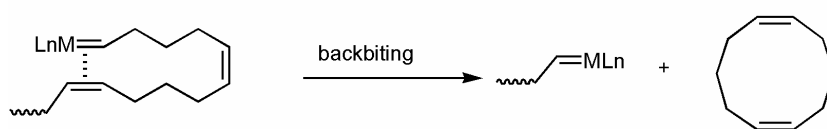
Scheme 1.6. General mechanism for ROMP.^[35]

The ability of a cycloalkene (CPE, NBE and COE) to undergo ROMP is primarily related to the difference in free energy between the ring and the corresponding open chain structure. The reaction is driven from the monomer to polymer by the release of ring strain associated with the cyclic olefin. The most common monomers used in ROMP are cyclic olefins which possess a considerable degree of strain (>5 kcal/mol) such as cyclobutene, cyclopentene, *cis*-cyclooctene and norborn-2-ene. Cyclohexene is one notable exception due to its low ring strain. Hence it does not undergo ROMP unless there is high ring strain in the molecule due to bridging, like in norbornene. Steric factors such as substituents close to the double bond are also important in determining the reactivity of a cyclic monomer. Finally, since the polymers have double bonds (i.e. one per repeat unit), there may be a chance for intramolecular chain-transfer reactions (i.e. back-biting) leading to cyclic oligomers and polymers. The back-biting process mainly depends on temperature, the solvent, monomer concentration and *cis/trans* configuration of the double bonds within the polymer chain as well as on the steric bulk of the monomer.^[40]

Intermolecular Chain Transfer:



Intramolecular Chain Transfer:



Scheme 1.7. Inter- and intra-chain transfer reactions in ROMP.^[35]

Effective catalysts for ROMP (and also for olefin metathesis) are metal alkylidene ($\text{LnM}=\text{CHR}$) complexes of molybdenum, tungsten, tantalum, rhenium and ruthenium. From these, two classes of alkylidene complexes are well-defined. i.e. Schrock-type molybdenum complexes and Grubbs-type ruthenium complexes.

1.5.1 Schrock-type initiators and reactivity

The synthesis of high oxidation state molybdenum alkylidenes was first reported by Schrock *et al.* These and the analogous tungsten systems are commonly noted as “Schrock-type catalysts”.^[41-43] These catalysts possess the general formula $M(\text{NAr}')(\text{OR}')_2(\text{CHR})$ where $M = \text{Mo}, \text{W}$; $\text{Ar}' = \text{Phenyl}$ or substituted phenyl, adamantyl; $\text{R} = \text{ethyl}, \text{phenyl}, \text{trimethylsilyl}, \text{t-butyl}$ and CMe_2Ph ; $\text{R}' = \text{CMe}_3, \text{CMe}_2\text{CF}_3, \text{CMe}(\text{CF}_3)_2, \text{aryl}$ etc. The structures of typical Schrock-type initiators are illustrated in Figure 1.7.

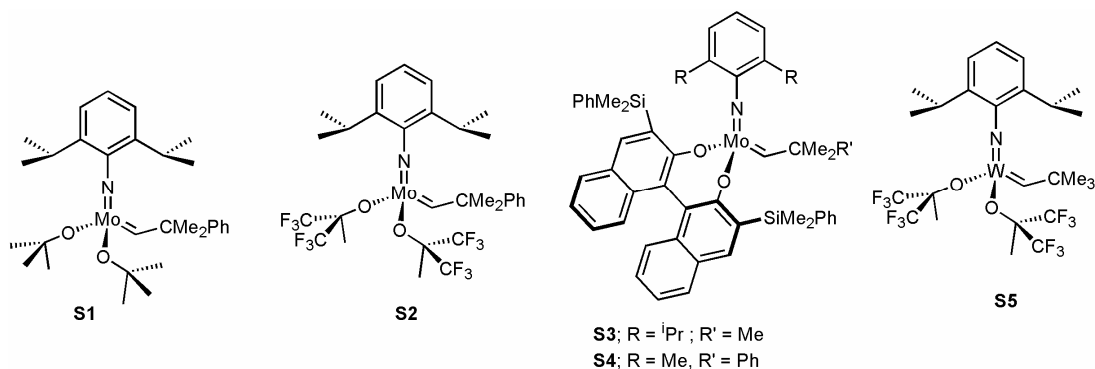
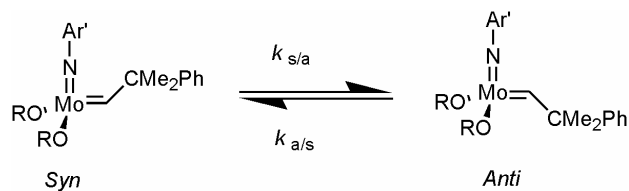


Figure 1.7. Schrock-type initiators (**S1**, **S2**, **S3**, **S4** and **S5**).

In the late 1980's Schrock *et al.* reported on the development of well-defined catalysts for ROMP.^[41-43] Molybdenum and tungsten carbene complexes have been reported to exhibit high activities for ROMP with good control over molecular weight and stereochemistry of the resulting polymers.^[19] However, for several reasons molybdenum complexes are much more preferred than the corresponding tungsten complexes. First molybdenum is much cheaper than tungsten; second, molybdenum complexes are synthesized more easily; and third molybdacyclobutane rings are less stable than tungstacyclobutanes and finally, molybdenum is more tolerant towards functionalities such as carbonyl groups.^[44]

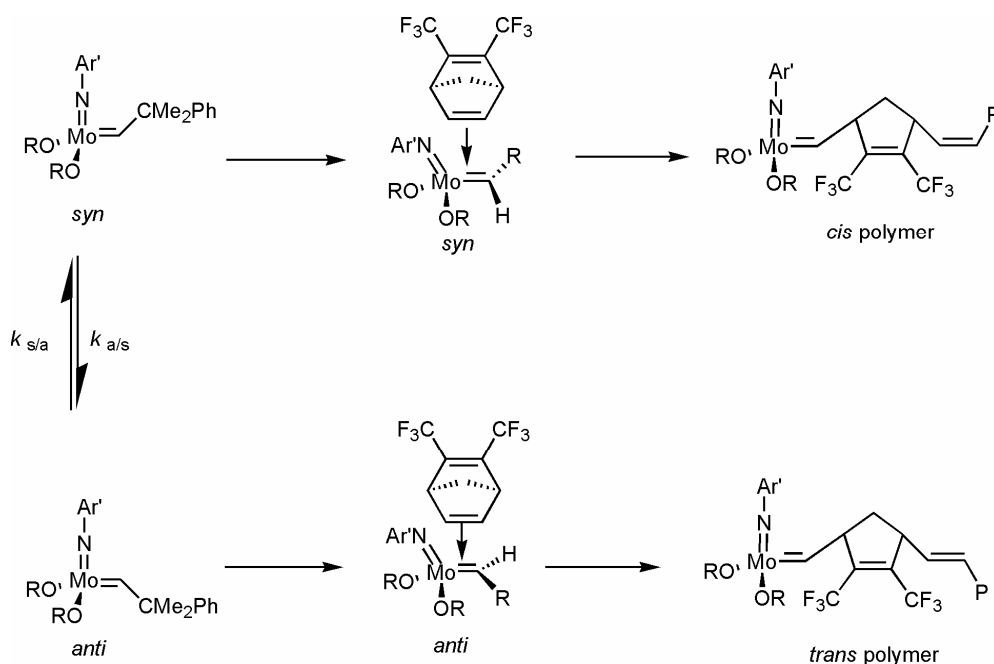
In an alkylidene complex, the electron withdrawing effect of an alkoxide is the most important factor for tuning the reactivity of the complex. Electron-withdrawing groups render the metal more electrophilic and the resulting complex will be a more active catalyst.^[44, 45] Schrock type initiators of the type $\text{Mo}(\text{NAr}')(\text{OR}')_2(\text{CHCMe}_2\text{R})$ possess a tetrahedral geometry. Addition of PMe_3 or quinuclidine to $\text{Mo}(\text{NAr}')(\text{OCMe}(\text{CF}_3)_2)_2(\text{CH-t-Bu})$, allows for identifying two isomers, i.e. *syn*- and *anti*-rotamers of the alkylidene ligand.^[46] The approach of the alkene via the C/N/O face of the alkylidene ligand is considered the main reaction pathway. $\text{Mo}(\text{NAr}')(\text{OR}')_2(\text{CHR})$ complexes, in which R = *tert*-butyl or CMe_2Ph point towards the imido-ligand are called the *syn*-rotamers, while those, in

which the R group points away from the imido-ligand are called *anti*-rotamers (Scheme 1.8). The rotamer ratio and reactivity is affected by the electronic nature of the alkoxide ligand, which was found to be responsible for the structure of final ROMP derived polymer.



Scheme 1.8. *Syn*- and *anti*-rotamers of Schrock catalysts. $k_{s/a}$ and $k_{a/s}$ are the rate constants of inter conversion from the *syn*- into the *anti*-rotamer and *vice versa*.^[47]

2,3-Bis(trifluoromethyl)bicyclo[2.2.1]hepta-2,5-diene was polymerized to give >98% *trans*-vinylenes^[48] in the resulting polymer using the molybdenum complex S1 (Figure. 1.7). In 1992 Gibson *et.al*^[49] reported that, 2,3-bis(trifluoromethyl)bicyclo[2.2.1]hepta-2,5-diene was polymerized to give >98% *cis*-vinylenes using the partially fluorinated complex S2 (Figure. 1.7).^[19]

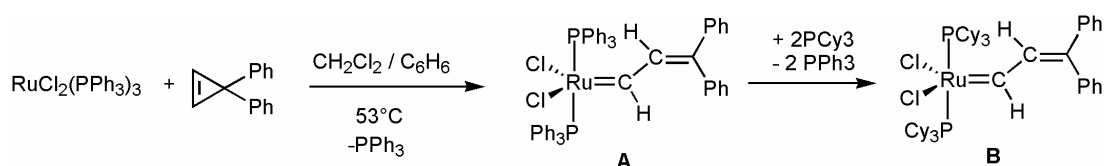


Scheme 1.9. Formation of *cis* and *trans*- poly(2,3-bis(trifluoromethyl)norbornadiene) from the *syn* and *anti* -rotamers of a Schrock catalyst.^[47]

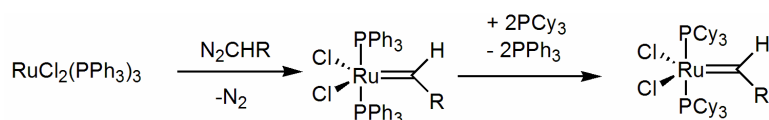
1.5.2 Grubbs-type initiators and reactivity

In 1992, Grubbs *et.al.* described the synthesis of the first well-defined ruthenium alkylidene complexes for olefin metathesis. Their air stability and functional group tolerance were their main advantages.^[50] The reaction of $\text{RuCl}_2(\text{PPh}_3)_3$ with 2,2-diphenylcyclopropene

in benzene or dichloromethane (DCM) yielded the desired carbene complex $\text{RuCl}_2(\text{PPh}_3)_2(\text{CH}=\text{CH}=\text{CPh}_2)$ (A). Exchange of the triphenylphosphane ligands with tricyclohexylphosphane yielded initiator B (Scheme 1.10). These systems are highly active in ROMP and RCM. In addition, these complexes show a remarkable stability towards functional groups and protic media. However, an alternative route to ruthenium alkylidenes was elaborated by Schwab *et.al* and Grubbs *et.al* to avoid the multistep synthesis of diphenylcyclopropene and low initiation rates of diphenylvinylalkylidenes. The synthetic protocol entailed the reaction of $\text{RuCl}_2(\text{PPh}_3)_3$ with an diazoalkane (Scheme 1.11).^[50]



Scheme 1.10. Synthesis of vinyl alkylidene complexes **A** and **B**.^[50]



R= Ph, Me, Et, etc.

Scheme 1.11. Synthesis of alkylidene complexes.^[50]

Via this route, the resulting compounds of the general formula $\text{RuCl}_2(\text{PR}_3)_2(\text{CHR}')$ (R=Ph, Cy and R'=Ph, Me, Et, etc.) become known as the 1st-generation Grubbs catalysts.^[51] A synthetic protocol consisting of the reaction of $\text{RuCl}_2(\text{PR}_3)_2(\text{CHR}')$ (R=Ph, Cy and R'=Ph, Me, Et, etc.) with 1,3-dimesityl-4,5-dihydroimidazolin-2-ylidene (IMesH₂), resulted in the formation of $\text{RuCl}_2(\text{PCy}_3)(\text{IMesH}_2)(\text{CHPh})$, known as the 2nd-generation Grubbs Catalyst. (Figure 1.8). Another breakthrough in catalyst activity was the development of Grubbs-type initiators with oxygen-chelated ruthenium alkylidenes known as 1st-generation Grubbs-Hoveyda type ($\text{RuCl}_2(\text{PCy}_3)(\text{CH}-2-(2\text{-PrO})-\text{C}_6\text{H}_4)$) and 2nd-generation Grubbs-Hoveyda ($\text{RuCl}_2(\text{IMesH}_2)(\text{CH}-2-(2\text{-PrO})-\text{C}_6\text{H}_4)$) catalysts^[52] (Figure 1.8).

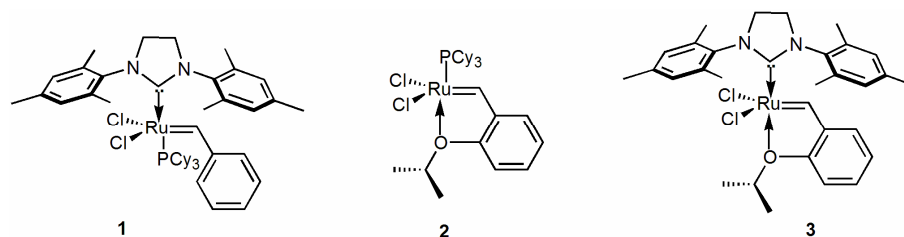
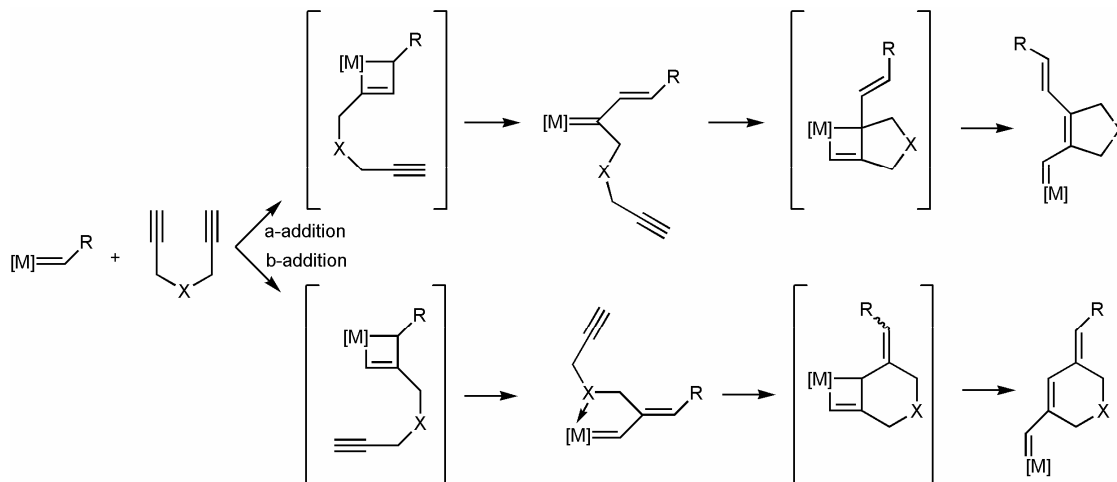


Figure 1.8. 2nd generation Grubbs catalyst (**1**), 1st generation Grubbs-Hoveyda catalyst (**2**), 2nd generation Grubbs-Hoveyda catalyst (**3**).^[52]

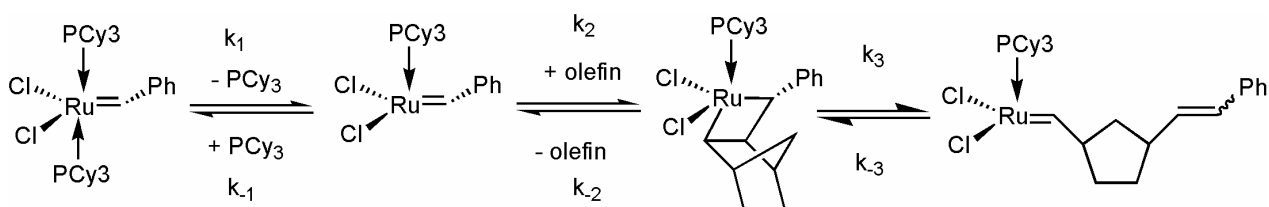
The introduction of “pseudo-halide” ligands has led to significant advances in reactivity and selectivity for the synthesis of organic molecules as well as macromolecular materials. Mol *et.al* reported that the exchanging of chloride ligands with carboxylates to get a Ru-alkylidene carboxylate dimer these complexes are active in acyclic alkene metathesis as well as in ring closing metathesis.^{[53] [54]} These anion-exchanged metathesis catalysts were defined as “pseudo-halide” derivatives. Buchmeiser *et.al* synthesized modified Grubbs-type and Grubbs-Hoveyda-type Ru-alkylidene based initiators^{[34] [55-59]}, in which both chlorides were replaced by pseudo-halides or nitrates i.e, [Ru(CF₃SO₂)₂(IMesH₂)(C₆H₅N)(CHC₆H₅)], [Ru(NCO)(CF₃SO₂)(IMesH₂)(C₆H₅N)(CHC₆H₅)], [Ru(CF₃CO₂)(CF₃SO₂)(IMesH₂)(C₆H₅N)(CHC₆H₅)], [Ru(NCS)₂(IMesH₂)(C₆H₅N)(CHC₆H₅)], [Ru(NO₃)₂(IMesH₂)(CH-2-(2-PrO)-C₆H₄)] and [Ru(CF₂)₃(CO₂)₂(IMesH₂)(CH-2-(2-PrO)-C₆H₄)] (IMesH₂=1,3-dimesitylimidazolin-2-ylidene). The novel initiators and those of the general formula [RuX₂(L)_n(NHC)(CHPh)] and [RuX₂(NHC)(CH-2-(2-PrO)-C₆H₄)] (X=Cl, CF₃COO, N=C=O, N=C=S, C₆F₅COO; NHC=IMesH₂, 1,3-dimesitylpyrimidin-2-ylidene, 1,3-dimesityldiazepin-2-ylidene, 1-mesityl-3-(2-phenylethyl)imidazolin-2-ylidene, 1-mesityl-3-adamantylimidiazolin-2-ylidene; L=PCy₃, pyridine, n=1, 2) were also synthesized. The Ru-alkylidene complexes containing mixed anionic ligands, such as [Ru(NCO)(CF₃SO₃)(IMesH₂)(C₅H₅N)(CHPh)], [Ru(CF₃SO₃)(CF₃CO₂)(IMesH₂)(C₅H₅N)(CHPh)], and [Ru(CF₃SO₃)(CF₃CO₂)(IMesH₂)(CH-2-(2-PrO)-C₆H₄)], did not show any ligand scrambling, most probably because of the high stability of the Ru-triflate bonds.^[1] Among the isocyanate- and thioisocyanate-derived 2nd generation Grubbs-Hoveyda-type Ru-alkylidene complexes, the isocyanate- derived Ru-alkylidene complexes were found to have excellent activity in the ROMP of *cis*-cycloocta-1,5-diene(COD) and as well as shows good catalytic activity in cross-metathesis(CM) reactions. Finally, isocyanate-derived Ru-alkylidene complexes were shown to display excellent activity in the regioselective cyclopolymerization of 1,6-heptadiynes.^[57] In view of the high activity of these ‘pseudo-halide’ derived Grubbs- and Grubbs-Hoveyda-type complexes,^[1, 55, 56, 58, 59] we investigated their propensity to cyclopolymerize 1, 6-heptadiynes. Cyclopolymerization derived polymers are attractive due to the conjugated double bonds in the polymer back bone and these polymers are normally highly soluble in organic solvents due to the 5- and 6-membered rings with pendant groups. The formation of these five- or six-membered rings depends on the mode of insertion of the monomer into the initiator. α -Insertion leads to the formation of 5-membered rings and the β -insertion results in the formation of six-membered rings.^[60] These highly conjugated polymers exhibit high

conductivity upon doping with doping agents such as I_2 or $NO^+BF_4^-$. While both polymers are conjugated, especially polymers based on five- membered repeat units i.e poly(cyclopent-1-ene-2-vinylene)s have higher conjugation lengths and display higher conductivity.^[55, 61]



Scheme 1.12. Formation of poly(ene)s based on five- and six-membered repeat units, X= NH^s or O.

The reactivity of Grubbs type ruthenium-based initiator is different when compared to Schrock-type initiators (molybdenum- or tungsten-based). The difference in reactivity of Grubbs-type catalysts varies by changing the different phosphane ligands^[62] or the nature of the alkylidene moieties^[50] or by replacing the halide anions by pseudo-halides.^[63-65] Two pathways were proposed for ROMP;^[66] one is an associative pathway, in which two phosphane groups attached to the metal form together with the monomer an 18-electron transition state and a dissociative pathway, in which only one phosphane group remains attached to the metal and forms together with the monomer an 16-electron transition complex. The existence of these pathways and of the mono- and diphosphane complexes were confirmed by quantum molecular dynamic simulation studies.^[67] Grubbs *et.al* studied the experimental data of complexes of the general formula $RuCl_2(PCy_3)_2(=CHPh)$ to identify the mechanism of olefin metathesis. Their results clearly indicate that a monophosphine complex is more reactive than the corresponding biphosphine complex as demonstrated by the addition of CuCl or CuCl₂ as phosphane scavenger. Thus, addition of CuCl resulted in significantly increased the catalytic activities,^{[67] [68]} at the same time the addition of an excess phosphane resulted in a decreased catalytic activity in both RCM and ROMP. The most accepted mechanism is a dissociate one and is shown in Scheme 1.13.



Scheme 1.13. Mechanism of ROMP for Grubbs type initiators.^[32]

The catalyst performance is, e.g. affected by the size and nature of the phosphane ligands; Gibson *et.al* ^[69] reported that small variations in the phosphane ligand had a larger impact on metathesis performance, for this reason they turned to smaller and less basic phosphane ligands such as $\text{PCy}_2\text{CH}_2\text{SiMe}_3$ as compared to the PCy_3 ligand, to synthesize the initiator $\text{RuCl}_2(\text{PCy}_2\text{CH}_2\text{SiMe}_3)(=\text{CHPh})$, which was found to have remarkable initiation characteristics for the ROMP of norborn-5-ene-2,3-dicarboximides and to allow for a good control of the molecular weights and molecular weight distributions. At the same time by varying the anionic ligands (Cl, Br, I) in the ruthenium complexes, their reactivity in olefin metathesis was investigated. These reactivity of the catalysts decreased while changing the anion from Cl to Br to I. In terms of initiation, the rate constant of initiation was increased from Cl to Br to I. The increase in initiation is due to the increasing steric bulk on ruthenium center while moving the anion from Cl to Br to I, thus promoting the dissociation of ligand.^[64]

1.6 Vinyl Insertion Polymerization (VIP)

Homopolymers of $\text{poly}(\text{NBE})_{\text{vinyl}}$, $\text{poly}(\text{CPE})_{\text{vinyl}}$, $\text{poly}(\text{COE})_{\text{vinyl}}$ consist of rings, which are formed via the addition polymerization of the cyclic olefin. These polymers generally exhibit higher melting points ($T_m > 400\text{ }^\circ\text{C}$) or high glass transition temperatures (T_g), which are nearly close to their decomposition temperature, they also possess very poor solubility in most organic solvents, which makes them difficult to process and of limited commercial interest.^[70] To overcome these difficulties, the introduction of a co-monomer such as ethylene or another α -olefin into the poly(cycloolefin) ($\text{poly}(\text{NBE})_{\text{vinyl}}$, $\text{poly}(\text{CPE})_{\text{vinyl}}$, $\text{poly}(\text{COE})_{\text{vinyl}}$) chains via the coordinative addition mechanism is a useful method because the resulting cyclic olefin copolymers (COCs) have lower rigidity. COCs are characterized by excellent transparency and outstanding thermal, optical and mechanical properties such as excellent heat resistance. COCs are soluble and can be melt-processed. Due to their high carbon and hydrogen ratio, these copolymers have a high refractive index, e.g., 1.53 for an ethylene-norbornene copolymer with 50 mol-% of NBE incorporation (TOPAS[®]).^[71] These features render those materials attractive for optical applications, e.g., for compact discs, lenses, optical fibers and films.

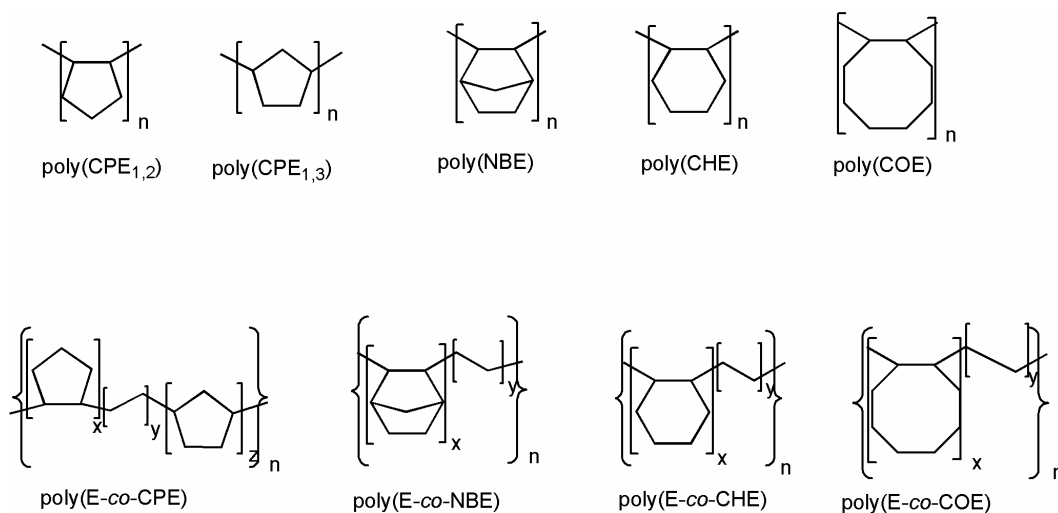
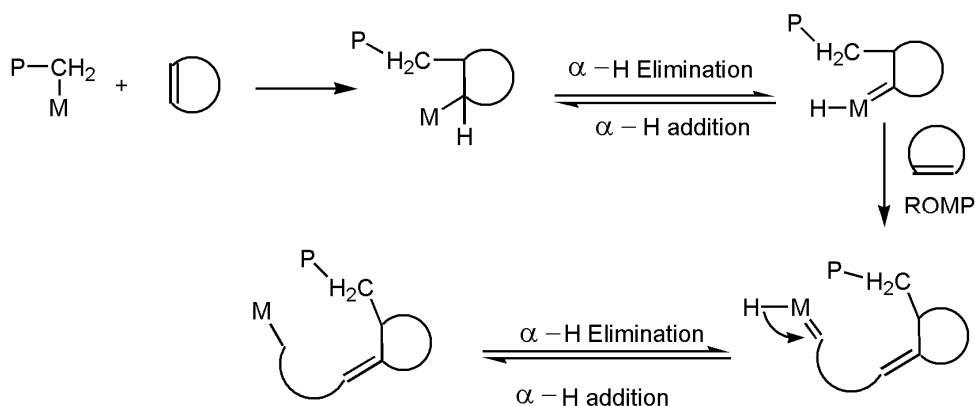


Figure 1.9. Homopolymers of monocyclic olefins and copolymers of cyclic olefins with ethylene.

1.7 Relationship between vinyl insertion polymerization (VIP) and ring opening metathesis polymerization (ROMP)

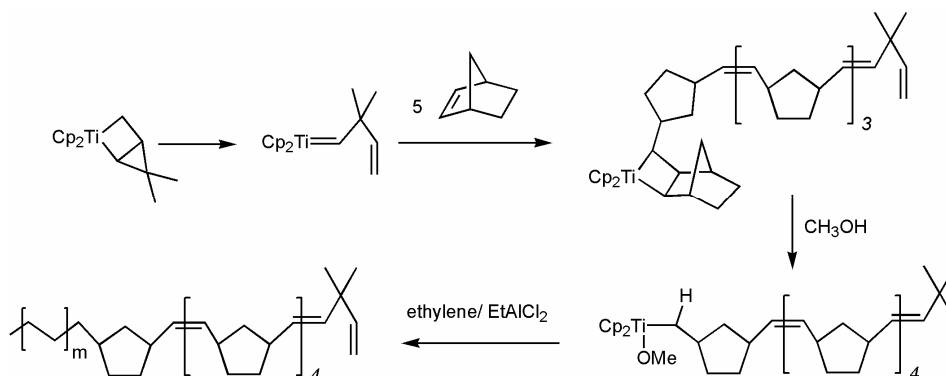
Simultaneous vinyl insertion and ring opening metathesis copolymerization of cyclic olefins with α -olefins is a fascinating field. In several cases it has been reported that cyclic olefin-derived polymers contained double bonds opened (ring-retained) and ring opened units, which indicates that the polymer contains both saturated and unsaturated units. For example, cyclobutene and derivatives of cyclobutene polymers contain both ring-retained and ring-opened units. This is the basic speculation for the possibility that both a Ziegler-Natta and ROMP-based mechanism are active within the same catalytic system. Evidence for this possibility comes from two patents where IR spectra showed that ethylene and cyclopentene could be co-polymerized to give unsaturated and saturated units within the same polymeric chain.^[72, 73] To account for this, Ivin proposed a mechanism for the possibility of VIP and ROMP in the same polymer chain based on α -H migration, which requires a switch between α -H addition and α -H elimination.^[74]

Later Farona *et.al* reported that the presence of both VIP- and ROMP-derived structures within the same polymer chain using Mo and Re based initiators^[74, 75], and they unambiguously labeled the characteristic signals for the quaternary carbon and methylene group in VIP and ROMP derived poly(NBE). The VIP and ROMP takes place within the same polymer chain and the underlying mechanism can be explained by a reversible α -H elimination/ α -H addition process.



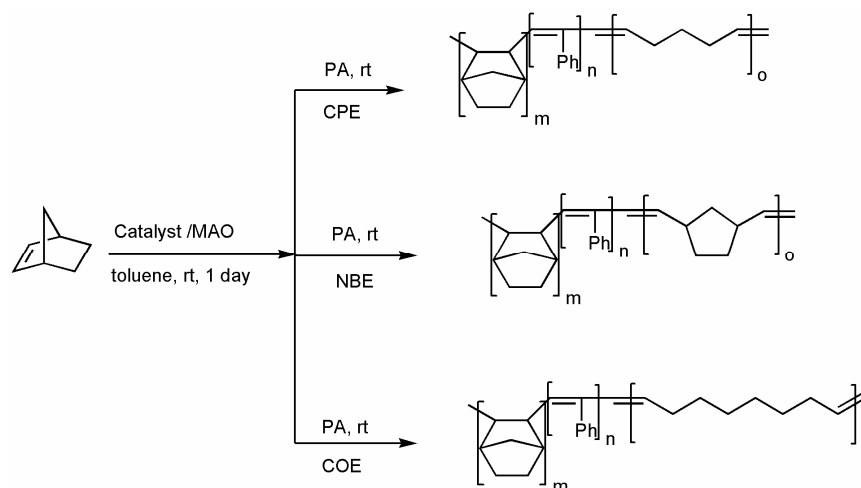
Scheme 1.14. Mechanism proposed by Ivin. ^[75] ^[74]

Grubbs *et.al* proved that it is possible to switch from ROMP to vinyl addition polymerization in one direction.^[76] A titanacyclobutane compound was active in the ROMP of NBE. After forming one block of ROMP-derived polymer, the metallocarbene was converted into a cationic species, which was active in the vinyl addition polymerization of ethylene (E). This process was carried out by addition of an alcohol followed by activation with Et_2AlCl . This resulted finally in an AB block copolymer i.e poly(NBE)_{ROMP}-*b*-poly(E).



Scheme 1.15. Single switch from ROMP to VIP.^[76]

Kaminsky *et.al* ^[77] reported that the controlled transformation from a vinyl addition polymerization to ROMP can be achieved by introducing a reactive transfer agent like phenyl acetylene (PA) during the polymerization. They succeeded in synthesizing poly(NBE)_{vinyl}-*b*-poly(NBE)_{ROMP}, poly(NBE)_{vinyl}-*b*-poly(CPE)_{ROMP} and poly(NBE)_{vinyl}-*b*-poly(COE)_{ROMP} (Scheme 1.16). However, these polymers were not fully characterized (¹³C NMR, GPC and DSC) due to poor solubility.



Scheme 1.16. Proposed structure of polymers by switching from VIP to ROMP using phenylacetylene (PA).^[77]

1.8 References:

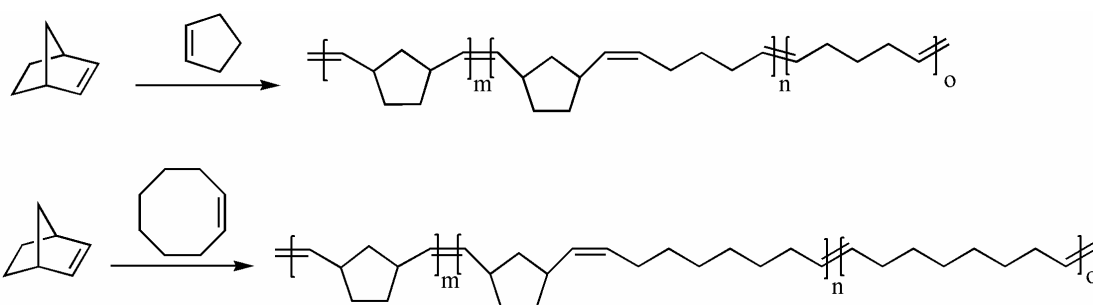
- [1] M. R. Buchmeiser, I. Ahmad, V. Gurrarn, P. S. Kumar, *Macromolecules* **2011**, *44*, 4098.
- [2] E. W. Fawcett, R. O. Gibson, M. W. Perrin, J. G. Paton, E. G. Williams, *Imperial Chemical Industries Ltd. GB 471590 (1937)*.
- [3] J. P. Hogan, R. L. Banks, *Polymerization of olefins; USA US 2825721; Philips Petroleum Co. 1958*.
- [4] U. Giunmi, A. Cussuru, P. Longi, R. Marrochi, *Belg. Pat. 785332 (1972), Montedison. S.p.A.*
- [5] P. Pino, R. Mülhaupt, *Angew. Chem.* **1980**, *92*, 869; *Angew. Chem. Int. Ed.* **1980**, *19*, 857.
- [6] K. Gardner, I. W. Parsons, R. N. Haward, *J. Polym. Sci.: Polym. Chem. Ed.* **1978**, *16*, 1683.
- [7] K. Ziegler, E. Holzkamp, H. Breil, H. Martin, *Angew. Chem.* **1955**, *67*, 541.
- [8] G. Natta, *Angew. Chem.* **1956**, *68*, 393.
- [9] G. Natta, *Angew. Chem.* **1964**, *76*, 553.
- [10] M. J. Miri, B. P. Pritchard, H. N. Cheng, *J. Mol. Model.* **2011**, *17*, 1767-1780 **2011**.
- [11] H. Sinn, W. Kaminsky, H.-J. Vollmer, R. Woldt, *Angew. Chem.* **1980**, *92*, 396; *Angew. Chem. Int. Ed.* **1980**, *19*, 390.
- [12] W. Kaminsky, K. Külper, H. H. Brintzinger, F. R. W. P. Wild, *Angew. Chem. Int. Ed.* **1985**, *24*, 507; *Angew. Chem.* **1985**, *97*, 507.

- [13] F. R. W. P. Wild, M. Wasiucionek, G. Huttner, H. H. Brintzinger, *J. Organomet. Chem.* **1985**, 288, 63.
- [14] A. L. McKnight, R. M. Waymouth, *Chem. Rev.* **1998**, 98, 2587.
- [15] G. G. Hlatky, *Chem. Rev.* **2000**, 100, 1347.
- [16] M. W. McKittrick, *Single-site Olefin Polymerization Catalysts via the Molecular Design of Porous Silica*; thesis, Georgia Institute of Technology **2005**.
- [17] G. Natta, P. Pino, G. Mazzanti, U. Giannini, *J. Am. Chem. Soc.* **1957**, 79, 2975.
- [18] D. S. Breslow, N. R. Newburg, *J. Am. Chem. Soc.* **1957**, 79, 5072.
- [19] G. W. Coates, *Chem. Rev.* **2000**, 100, 1223.
- [20] W. Kaminsky, R. Steiger, *Polyhedron* **1988**, 7, 2375.
- [21] L. Resconi, L. Cavallo, A. Fait, F. Piemontesi, *Chem. Rev.* **2000**, 100, 1253.
- [22] P. Margl, L. Deng, T. Ziegler, *J. Am. Chem. Soc.* **1998**, 121, 154.
- [23] L. Resconi, F. Piemontesi, G. Franciscano, L. Abis, T. Fiorani, *J. Am. Chem. Soc.* **1992**, 114, 1025.
- [24] M. Lin, G. J. Spivak, M. C. Baird, *Organometallics* **2002**, 21, 2350.
- [25] S. Hajela, J. E. Bercaw, *Organometallics* **1994**, 13, 1147.
- [26] Z. Guo, D. C. Swenson, R. F. Jordan, *Organometallics* **1994**, 13, 1424.
- [27] L. Resconi, F. Piemontesi, I. Camurati, D. Balboni, A. Sironi, M. Moret, H. Rychlicki, R. Ziegler, *Organometallics* **1996**, 15, 5046.
- [28] L. Resconi, S. Bossi, L. Abis, *Macromolecules* **1990**, 23, 4489.
- [29] N. Naga, K. Mizunuma, *Polymer* **1998**, 39, 5059.
- [30] J. A. Ewen, R. L. Jones, A. Razavi, J. D. Ferrara, *J. Am. Chem. Soc.* **1988**, 110, 6255.
- [31] G. W. Coates, R. M. Waymouth, *Science* **1995**, 267, 217.
- [32] P. Dubois, O. Coulembier, J.-M. Raquez, *Handbook of Ring-Opening Polymerization, Chapter 8*, Willey-VCH, Weinheim, **2009**.
- [33] U. Frenzel, O. Nuyken, *J. Poly. Sci. Part A: Poly. Chem.* **2002**, 40, 2895.
- [34] M. R. Buchmeiser, *Chem. Rev.* **2000**, 100, 1565.
- [35] C. W. Bielawski, R. H. Grubbs, *Prog. Polym. Sci.* **2007**, 32, 1.
- [36] T. M. Trnka, R. H. Grubbs, *Acc. Chem. Res.* **2000**, 34, 18.
- [37] Y. Chauvin, *Angew. Chem.* **2006**, 118, 3824; *Angew. Chem. Int. Ed.* **2006**, 45, 3740.
- [38] R. H. Grubbs, *Angew. Chem.* **2006**, 118, 3845; *Angew. Chem. Int. Ed.* **2006**, 45, 3760.
- [39] R. R. Schrock, *Angew. Chem.* **2006**, 118, 3832 ; *Angew. Chem. Int. Ed.* **2006**, 45, 3748.
- [40] M. R. Buchmeiser, *Adv. Polym. Sci.* **2005**, 89, 176.
- [41] R. R. Schrock, *Acc. Chem. Res.* **1990**, 23, 158.

- [42] R. R. Schrock, *Chem. Rev.* **2009**, *109*, 3211.
- [43] R. R. Schrock, *Chem. Rev.* **2002**, *102*, 145.
- [44] S. Richard R, *Tetrahedron* **1999**, *55*, 8141.
- [45] S. Richard R, *Polyhedron* **1995**, *14*, 3177.
- [46] R. R. Schrock, W. E. Crowe, G. C. Bazan, M. DiMare, M. B. O'Regan, M. H. Schofield, *Organometallics* **1991**, *10*, 1832.
- [47] M. R. Buchmeiser, *Handbook of Ring-Opening Polymerization*, (Eds.: P. Dubois, O. Coulembier, J.-M. Raquez) 1st ed., Wiley-VCH, Weinheim, **2009**, pp 197-219.
- [48] G. C. Bazan, E. Khosravi, R. R. Schrock, W. J. Feast, V. C. Gibson, M. B. O'Regan, J. K. Thomas, W. M. Davis, *J. Am. Chem. Soc.* **1990**, *112*, 8378.
- [49] W. J. Feast, V. C. Gibson, E. L. Marshall, *J. Chem. Soc., Chem. Commun.* **1992**, 1157.
- [50] P. Schwab, R. H. Grubbs, J. W. Ziller, *J. Am. Chem. Soc.* **1996**, *118*, 100.
- [51] P. Schwab, M. B. France, J. W. Ziller, R. H. Grubbs, *Angew. Chem.* **1995**, *107*, 2179-2181; *Angew. Chem. Int. Ed.* **1995**, *34*, 2039.
- [52] S. B. Garber, J. S. Kingsbury, B. L. Gray, A. H. Hoveyda, *J. Am. Chem. Soc.* **2000**, *122*, 8168.
- [53] W. Buchowicz, F. Ingold, J. C. Mol, M. Lutz, A. L. Spek, *Chem. Eur. J.* **2001**, *7*, 2842.
- [54] W. Buchowicz, J. C. Mol, M. Lutz, A. L. Spek, *J. Organomet. Chem.* **1999**, *588*, 205.
- [55] P. S. Kumar, K. Wurst, M. R. Buchmeiser, *J. Am. Chem. Soc.* **2008**, *131*, 387.
- [56] P. S. Kumar, K. Wurst, M. R. Buchmeiser, *Organometallics* **2009**, *28*, 1785.
- [57] P. S. Kumar, K. Wurst, M. R. Buchmeiser, *Chem. Asian. J.* **2009**, *4*, 1275.
- [58] J. O. Krause, O. Nuyken, K. Wurst, M. R. Buchmeiser, *Chem. Eur. J.* **2004**, *10*, 777.
- [59] J. O. Krause, O. Nuyken, M. R. Buchmeiser, *Chem. Eur. J.* **2004**, *10*, 2029.
- [60] H. H. Fox, R. R. Schrock, *Organometallics* **1992**, *11*, 2763.
- [61] J. O. Krause, D. Wang, U. Anders, R. Weberskirch, M. T. Zarka, O. Nuyken, C. Jäger, D. Haarer, M. R. Buchmeiser, *Macromol. Symp.* **2004**, *217*, 179.
- [62] M. I. E. Cucullu, C. Li, S. P. Nolan, S. T. Nguyen, R. H. Grubbs, *Organometallics* **1998**, *17*, 5565.
- [63] Z. Wu, S. T. Nguyen, R. H. Grubbs, J. W. Ziller, *J. Am. Chem. Soc.* **1995**, *117*, 5503.
- [64] M. S. Sanford, J. A. Love, R. H. Grubbs, *J. Am. Chem. Soc.* **2001**, *123*, 6543.
- [65] M. S. Sanford, M. Ulman, R. H. Grubbs, *J. Am. Chem. Soc.* **2001**, *123*, 749.
- [66] S. F. Vyboishchikov, M. Bühl, W. Thiel, *Chem. Eur. J.* **2002**, *8*, 3962.
- [67] O. M. Aagaard, R. J. Meier, F. Buda, *J. Am. Chem. Soc.* **1998**, *120*, 7174.
- [68] E. L. Dias, S. T. Nguyen, R. H. Grubbs, *J. Am. Chem. Soc.* **1997**, *119*, 3887.

- [69] D. A. Robson, V. C. Gibson, R. G. Davies, M. North, *Macromolecules* **1999**, *32*, 6371.
- [70] W. Kaminsky, *J. Chem. Soc., Dalton Trans.* **1998**, 1413.
- [71] W. Kaminsky, P.-D. Tran, R. Werner, *Macromol. Symp.* **2004**, *213*, 101.
- [72] G. Dall'Asta, G. Motroni, *J. Polym. Sci. Part A: Polym. Chem.* **1968**, *6*, 2405.
- [73] G. Dall'Asta, *J. Polym. Sci. Part A: Polym. Chem.* **1968**, *6*, 2397.
- [74] Maria A. Alonso, Kenneth E. Bower, Jay A. Johnston, M. F. Farona, *Polym. Bull.* **1988**, *19*, 211.
- [75] J. A. Johnston, M. Tokles, G. S. Hatvany, P. L. Rinaldi, M. F. Farona, *Macromolecules* **1991**, *24*, 5532.
- [76] I. Tritto, M. C. Sacchi, R. H. Grubbs, *J. Mol. Catal.* **1993**, *82*, 103.
- [77] R. Manivannan, G. Sundararajan, W. Kaminsky, *J. Mol. Cat. A* **2000**, *160*, 85.

**Pseudo-Halide and Nitrate Derivatives of Grubbs- and Grubbs-Hoveyda
Initiators: Structural Features Related to the Alternating Ring Opening
Metathesis Copolymerization of Norborn-2-ene with Cyclic Olefins**



The material covered in this chapter is part of a paper that appeared in
M. R. Buchmeiser, I. Ahmad, V. Gurram, P. S. Kumar, *Macromolecules* **2011**, *44*, 4098.

2.1 Introduction

During the last 20 years, remarkable progress in more efficient and selective metathesis catalysts has been achieved paving the way for various types of metathesis-based reactions in organic and polymer chemistry as well as in materials science.^[1] Both well-defined Schrock^[2-5] and Grubbs-type^[1, 6, 7] initiators match well the requirements for ring-opening metathesis polymerization (ROMP)^[8] and in many cases allow for truly living polymerizations. Significant efforts have been put into the development of even more efficient and active Ru-alkylidene metathesis catalysts. For these purposes, numerous variations in the *N*-heterocyclic carbene (NHC) as well as in the alkylidene (benzylidene) ligand have been reported. Our group developed modified Grubbs- and Grubbs-Hoveyda initiators by replacing the parent chloride ligands in complexes of the general formula $\text{RuCl}_2(\text{L})(\text{NHC})(\text{CHR})$ (NHC=IMesH₂, 1,3-dimesitylpyrimidin-2-ylidene, 1,3-dimesityldiazepin-2-ylidene, 1-mesityl-3-(2-phenylethyl)imidazolin-2-ylidene; L=PCy₃, pyridine; n=1, 2; R=Ph, 2-PrO-C₆H₄, (OMe)₃-C₆H₂, 2-PrO-5-NO₂-C₆H₃) by pseudo-halide ligands such as triflates, carboxylates, phenoxides, isocyanates and isothiocyanates.^[9-15]

Here, we report on a library of novel Ru-alkylidenes by replacing the chloride ligand by electron withdrawing pseudo halide ligands such as isocyanates (OCN⁻), isothiocyanates (SCN⁻), perfluorocarboxylates (e.g., CF₃CO₂⁻, {(CF₂)₃(CO₂)₂}⁻), nitrate and trifluoromethanesulfonates (CF₃SO₃⁻) (Figure 2.1).^[12, 14, 15] In some cases we were able to prepare the mono(pyridine)-based “3rd-generation Grubbs-type” versions instead of the synthetically more easily accessible 2-PrO-benzylidene (Hoveyda-type) versions of these initiators. In total, 23 modified Grubbs- and Grubbs-Hoveyda-type initiators were investigated for their propensity to promote the alternating copolymerization^[16-24] of NBE with cyclopentene (CPE) and COE, respectively. Since both the selectivity and reactivity of Grubbs- or Grubbs-Hoveyda-type initiators is governed by the nature of the *N*-heterocyclic carbene (NHC), of the alkylidene and the anionic (pseudo) halide ligands, one goal of this investigation was therefore to identify the influence of each of these ligands on the extent of alternating copolymerization.

2.2 Result and Discussion

2.2.1 Synthesis of Initiators

Initiators **1a-g**, **2a-d**, **3a-c**, **4a-b**, **5a-b**, and **6** (Figure 2.1) were prepared according to reported procedures. [10-12, 14, 15, 25-30]

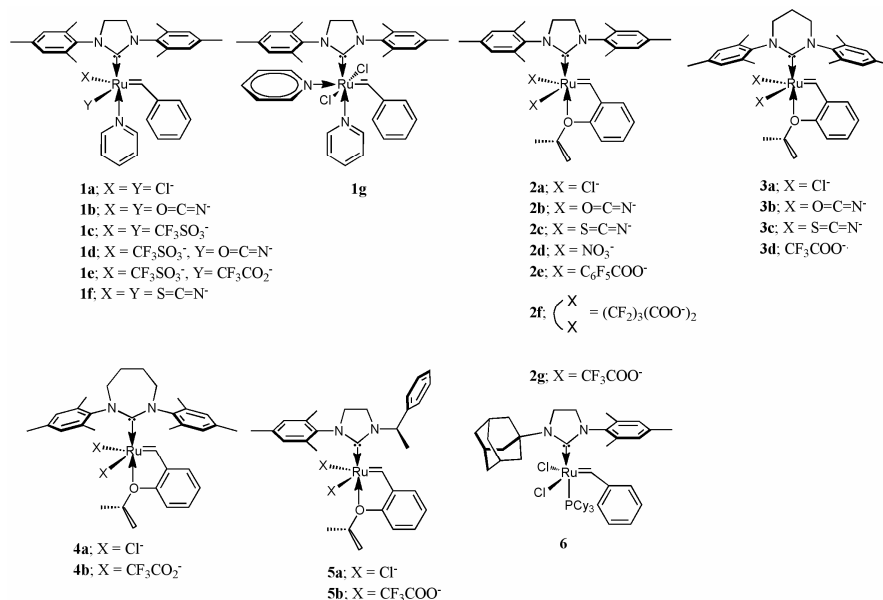


Figure 2.1. Structure of initiators **1a-g**, **2a-g**, **3a-d**, **4a-b**, **5a-b**, **6**.

The complexes [Ru(N=C=O)₂(IMesH₂)(=CH-2-(2-PrO)-C₆H₄)] (**2b**) and [Ru(N=C=S)₂(IMesH₂)(=CH-2-(2-PrO)-C₆H₄)] (**2c**) [15] were prepared from the 2nd generation Grubbs-Hoveyda initiator RuCl₂(IMesH₂)(=CH-2-(2-PrO)-C₆H₄) by exchanging the chloride anions with two equivalents of silver isocyanate and silver thiocyanate, respectively. The resulting complexes **2b** and **2c** were isolated as dark green and dark yellow green solids in 80% and 75% yields, respectively, and were characterized by ¹H NMR, showing an upfield shift of the Ru-alkylidene proton signal at δ=16.37 ppm (**2b**) and δ=16.4 ppm (**2c**) as compared to the alkylidene proton signal (16.56 ppm) of the parent Grubbs-Hoveyda. [27]

[Ru(NO₃)₂(IMesH₂)(CH-2-(2-PrO)-C₆H₄)] **2d** was prepared from RuCl₂(IMesH₂)(CH-2-(2-PrO)-C₆H₄) and 2 equiv. of AgNO₃ in THF and is to the best of our knowledge the first Ru-alkylidene-dinitrate complex. It was isolated as a brown solid in 84% yield. In the ¹H NMR spectrum, a significant downfield shift of the signal for the alkylidene proton (δ=18.63 ppm) as compared to the parent 2nd generation Grubbs-Hoveyda initiator (δ=16.56 ppm) [27] was observed, which is indicative for a stronger ionic character of the Ru-NO₃ bonds as compared to the Ru-Cl

bonds, ultimately resulting in a stronger polarization of the Ru-alkylidene bond. Complex $[\text{Ru}(\text{CF}_3\text{CO}_2)_2(\text{IMesH}_2)(\text{CH}_2\text{-2-(2-PrO)(C}_6\text{H}_4)]$ (**2g**)^[12] ^[10, 11] was prepared from $[\text{RuCl}_2(\text{IMesH}_2)(=\text{CH}_2\text{-2-(2-PrO)-C}_6\text{H}_4)]$ via reaction with two equiv. of CF_3COOAg and isolated as a red-brown solid in 86% yield. In the ^1H NMR spectrum, **2g** was characterized by a downfield shift of the alkylidene proton signal to $\delta=17.38$ ppm compared to the alkylidene proton signal of the parent second generation Grubbs-Hoveyda initiator ($\delta=16.56$ ppm).^[27] Complex $\text{RuCl}_2(1,3\text{-dimesityl-4,5,6,7-tetrahydro-1,3-diazepin-2-ylidene})(=\text{CH}_2\text{-2-(2-PrO)C}_6\text{H}_4)$ (**4a**), $\text{Ru}(\text{CF}_3\text{COO})_2(1,3\text{-dimesityl-4,5,6,7-tetrahydro-1,3-diazepin-2-ylidene})(=\text{CH}_2\text{-2-(2-PrO)C}_6\text{H}_4)$ (**4b**)^[14] ^[31] and $\text{RuCl}_2(1\text{-mesityl-3-}((1'R)\text{-1-phenylethyl})\text{-4,5-dihydro-imidazolin-2-ylidene})(=\text{CH}_2\text{-2-(2-PrO)C}_6\text{H}_4)$ (**5a**) and $\text{Ru}(\text{CF}_3\text{COO})_2(1\text{-mesityl-3-}((1'R)\text{-1-phenylethyl})\text{-4,5-dihydro-imidazolin-2-ylidene})(=\text{CH}_2\text{-2-(2-PrO)C}_6\text{H}_4)$ (**5b**) were synthesized according to published procedures.^[12, 18]

2.2.2 Homopolymerization of Norborn-2-ene (NBE)^a

Table 2.1. Homopolymerization of NBE by the action of initiators **2a**, **2g**, **3a**, **3d**, **5a** and **6**.

#	initiator	Isolated yield (%)	Cis/ trans ratio ^b	M_n (g/mol) ^c	PDI ^c
1	2a	60	35 / 65	550,000	1.2
2	2g	100	65 / 35	700,000	1.3
3	3a	72	65 / 35	650,000	1.3
4	3d	65	45 / 55	10,000	4.0
5	5a	73	60 / 40	600,000	1.6
6	6	60	10 / 90	300,000	1.6

[a] initiator: NBE = 1:1000, CH_2Cl_2 , M_n (*theor.*) = 94,150 g/mol; [b] Calculated from the ^1H NMR spectra, [c] determined by GPC.

Initiators **1a-e**, **2a-g**, **3a-d**, **4a, b**, **5a, b** and **6** are active for the ROMP of NBE.^[11, 14, 25, 26] Poly (NBE) was prepared using a ratio of 1: 1000 (initiator: NBE) and the number- average molecular weights (M_n) of the resulting polymer were in the range of 10,000-700,000 g/mol (M_n (*theor.*) =94,150 g/mol), polydispersity indices (PDIs) ranged from $1.2 < \text{PDI} < 4.1$. These data strongly suggest a non-living behavior of the initiators. The ROMP of NBE was completed in 60

s using 0.1 mol-% of initiator with respect to NBE at room temperature. Interestingly, the observed *cis*-content was around 50% in all cases, except with initiator **6**. Those, initiators that bore the unsymmetrical NHC ligand gave poly(NBE) with a high content of *trans*-configured double bonds (90%) in the resulting poly(NBE).

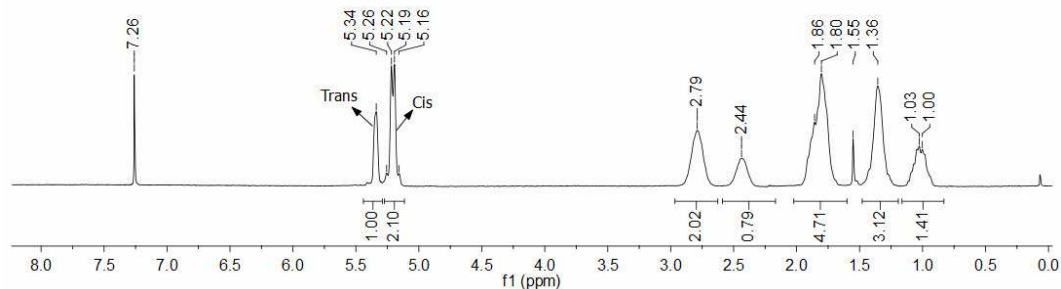


Figure 2.2. ^1H NMR spectrum of poly (NBE) in CDCl_3 prepared by the action of **3a** (Table 2.1, entry 3).

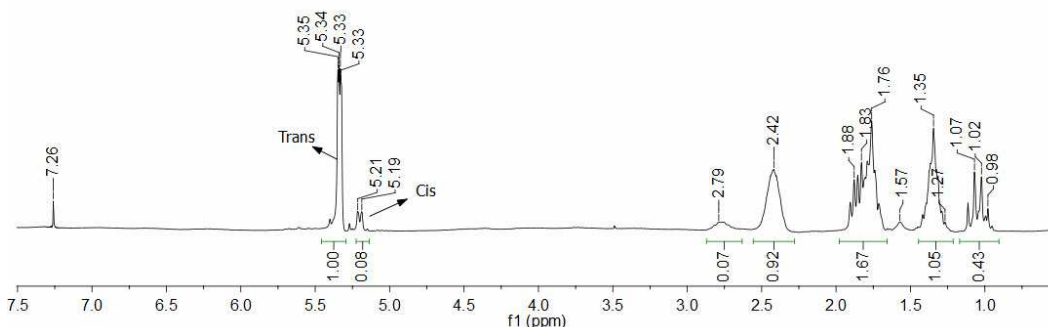


Figure 2.3. ^1H NMR spectrum of poly (NBE) in CDCl_3 prepared by the action of **6** (Table 2.1, entry 6).

2.2.3 Alternating Copolymerization of Norborn-2-ene (NBE) With Cyclopentene (CPE)

Initiators **1a-e**, **2b-e**, **3a-c**, **4a-b**, **5b**, and **6** were used in the copolymerization of NBE with CPE using a NBE:CPE ratio of 1:1. Due to its bicyclic nature, NBE is a by far more reactive monomer in ROMP than cyclopentene. Consequently, usually a considerable excess of CPE is used in the copolymerization with NBE in order to realize a substantial fraction of alternating diads in the corresponding copolymer.

Table 2.2. Alternating copolymerization of NBE and CPE by the action of initiators **1a-e**, **2b-d**, **3b-d**, **4a-b**, **5a-b** and **6**.

#	initiator	poly(NBE)		poly(CPE)		poly(NBE- <i>alt</i> -CPE) _n
		(%)	<i>cis/trans</i>	(%)	<i>cis/trans</i>	%
1	1a	78	50/50	7	30/70	15
2	1b	88	60/40	4	20/80	8
3	1c	91	60/40	2	n. a.	7
4	1d	84	60/40	5	30/70	10
5	1e	66	60/40	8	30/70	26
6	2a	65	40/60	20	15/85	15
7	2b	66	60/40	17	20/80	17
8	2c	90	60/40	3	30/70	7
9	2d	64	40/60	5	20/80	31
10	2e	57	70/30	11	20/80	32
11	2f	78	60/40	6	30/70	16
12	2g	48	40/60	22	30/70	30
13	3a	85	70/30	10	15/85	5
14	3b	86	50/50	5	20/80	9
15	3c	89	50/50	2	25/75	9
16	3d	50	60/40	13	15/85	37
17	4a	77	75/25	10	20/80	13
18	4b	50	70/30	10	20/80	40
19	5a	29	60/40	16	25/75	55
20	5b	59	60/40	24	20/80	17
21	6	91	30/70	0	-	9

^a Calculated from the ¹³C NMR spectra, initiator: NBE:CPE=1:1000:1000, CH₂Cl₂. n. a. not analyzed because of insufficient signal intensities and/or resolution.

Despite the low NBE:CPE ratio used here, the resulting copolymers contained up to 55% alternating diads (initiator **5a**, entry 19, Table 2.2), which is indicative for steric constraints in the NBE homopolymerization and which can be avoided by an alternating insertion of CPE. A

representative ^{13}C NMR of a copolymer prepared by the action of **3d**, **4b** and **5a** is shown in Figure 2.4, 2.5 and 2.6.

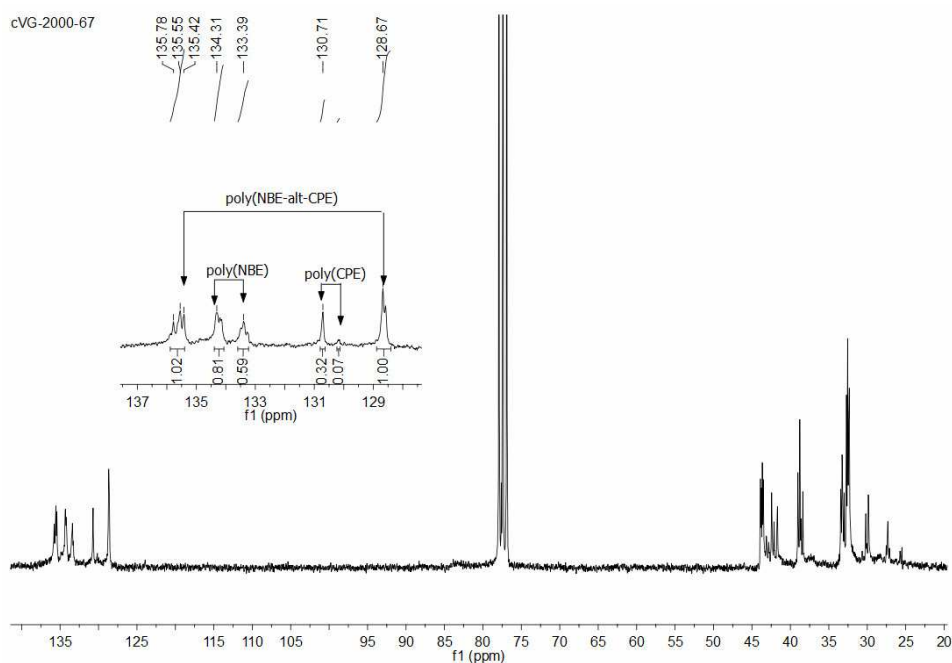


Figure 2.4. ^{13}C NMR spectrum (CDCl_3) of poly(NBE-*alt*-CPE) $_n$ prepared by the action of **3d** (Table 2.1, entry 16).

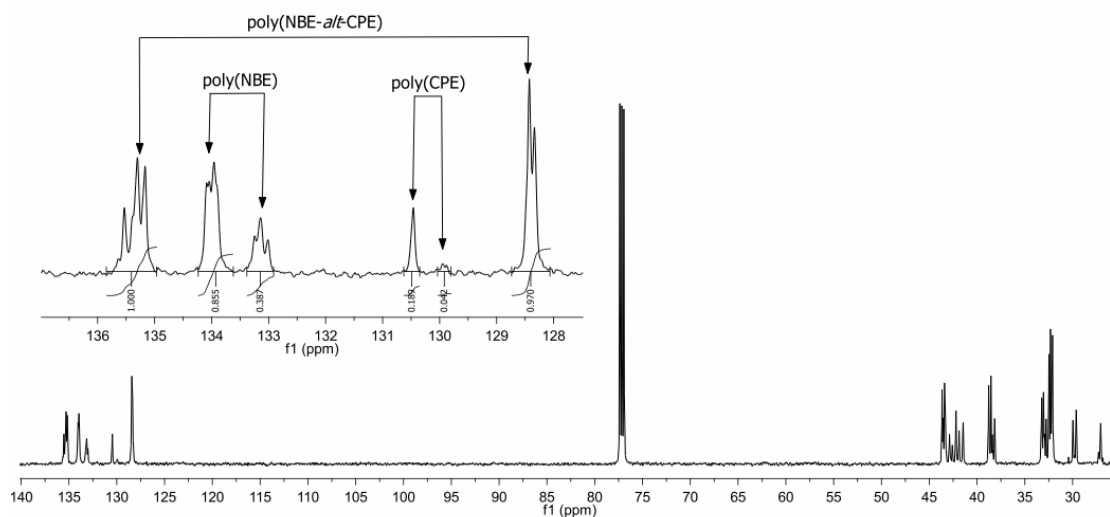


Figure 2.5. ^{13}C NMR spectrum (CDCl_3) of poly(NBE-*alt*-CPE) $_n$ prepared by the action of **4b** (Table 2.1, entry 18).

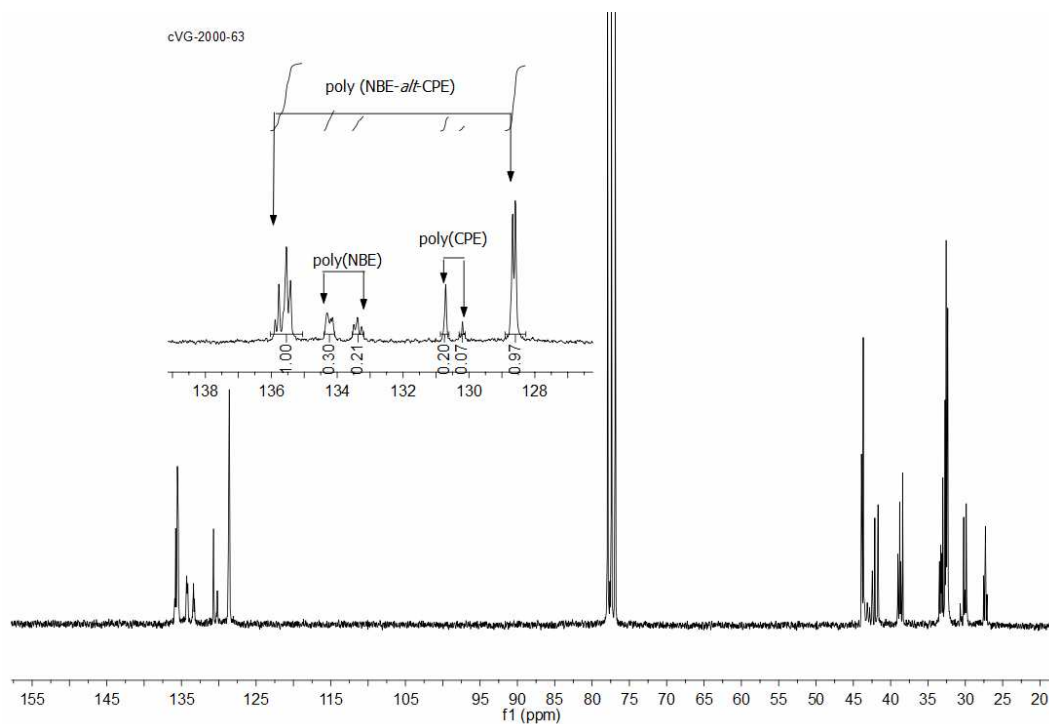


Figure 2.6. ^{13}C NMR spectrum (CDCl_3) of poly(NBE-*alt*-CPE) $_n$ prepared by the action of **5a** (Table 2.1, entry 19).

There, the signals for poly(NBE) at $\delta=133$ -134 ppm can be detected.^[23, 32] The signals around $\delta=130$ ppm stem from the poly(CPE) block. The signals around $\delta=135$ -136 and 128-129 ppm can be clearly attributed to the alternating copolymer. The first set of signals around $\delta=135$ -136 ppm is designated to the $\text{C}=\text{C}-\text{CH}_2$ carbon atoms and consists of eight different signals at 135.64, 135.55, 135.41, 135.33, 135.18, 135.05, 134.99, and 134.91 ppm, which can be attributed to the corresponding *ccc*, *tcc*, *ctc*, *cct*, *ttc*, *tct*, *ctt*, and *ttt* diads.^[21, 22] The less resolved signals around $\delta=128$ -129 ppm are assigned to the $\text{C}=\text{C}-\text{CH}_2$ carbon atoms and correspond to the same diads.

Using a 1:1 ratio of NBE:CPE, the highest content of alternating copolymer with 26-55% of alternating diads was observed with initiators **1e**, **2d**, **2e**, **2g**, **4b**, **3d** and **5a** (Table 2.2). Surprisingly, **4b** was found to be an efficient initiator for the homopolymerization of CPE.

Thus, 5000 molequiv. of CPE with respect to **4b** were quantitatively consumed within 30 s yielding poly(CPE) with an M_n of 125,000 g/mol and a PDI of 1.62 (σ_{cis} =17%) (Figure 2.7).

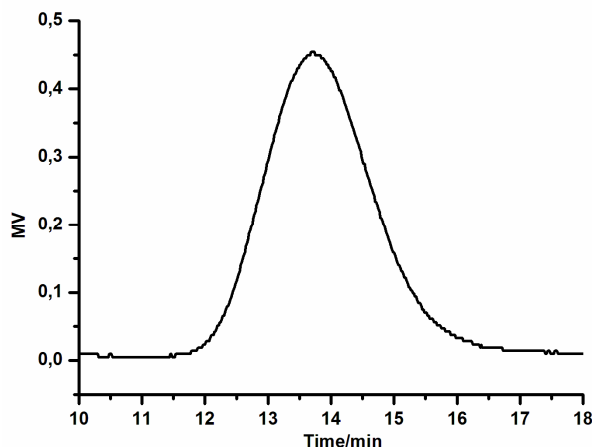


Figure 2.7. GPC of poly (CPE) in CHCl_3 derived from initiator **4b**.

An important finding that becomes evident is that the use of initiators in which both chlorides have been substituted by electron-withdrawing, potentially chelating ligands such as CF_3COO^- , CF_3SO_3^- , NO_3^- or $\text{C}_6\text{F}_5\text{COO}^-$ as found in **1e**, **2d**, **2e**, **2g**, **3d** and **4b** favors the formation of alternating copolymers. Exceptions are initiator **5a**, which represents an unsymmetrically substituted NHC, as well as **1c** bearing *two* CF_3SO_3^- -ligands. The mechanism of alternating copolymerization with Ru-carbenes bearing un-symmetrically substituted NHCs as realized in **5a** has already been proposed.^[18, 23, 33] The low copolymerization propensity of **1c** is not surprising, since bis(trifluoromethanesulfonate)-substituted metathesis initiators and catalysts often display a reactivity that differs significantly from the one of other anionic ligands and which rather stems from the special features of the CF_3SO_3^- group than from the excellent leaving group character of the ligand. Thus, bis(trifluoromethanesulfonate)-substituted Mo-alkylidenes are virtually inactive in ROMP, too.^[34] Unlike in Mo-based Schrock initiators,^[34] no correlation of the electron-withdrawing character of the X-ligand with the *cis/trans* ratio of the final polymer was found.

2.2.4 *Cis/trans* Ratios of the Poly(NBE) Homopolymer Blocks in Poly(NBE)-*alt*-poly(CPE)

In the ^1H and ^{13}C NMR spectra, the signals of the *cis*- and *trans*-double bonds of poly(NBE)-*alt*-poly(CPE) can be found at δ =5.38/5.28 and 135.4/128.4 ppm, respectively .

Because of overlapping signals, the *cis*-content of the alternating diads was hard to determine exactly, however, was estimated to lie in the range of $50 < \sigma_{cis} < 70\%$ throughout. Except for initiators **2a**, **3a**, **4a**, **4b** and **6**, a *cis:trans* ratio around 1:1 was observed for the poly(NBE) block. A comparison of initiators **1a**, **2a**, **3a**, **4a**, which differ in the size of the NHC (i.e. imidazolin-2-ylidene (**1a**, **2a**) vs. pyrimidin-2-ylidene (**3a**) or 1,3-diazepin-2-ylidene (**4a**)), reveals no differences in their propensity to produce alternating copolymers from NBE with CPE (Table 2.2). However, changing from the imidazolin-2-ylidene (**1a**) to the pyrimidin-2-ylidene (**3a**) and 1,3-diazepin-2-ylidene (**4a**) results in a strong *increase* of the *cis*-content in homo-poly(NBE) ($50/50 \rightarrow 70/30 \rightarrow 75/25$, Table 2.2). The high *cis*-content of the poly(NBE) homopolymer blocks apparently originates from NHCs based on tetrahydropyrimidin-2-ylidenes and diazepin-2-ylidenes. In these NHCs, the angle at the nitrogens defined by the mesityl group and the carbene are smaller than those in imidazolin-2-ylidenes, consequently, the two mesityl groups are located closer to the Ru-alkylidene than in **1a**. In due consequence, the steric interaction between the growing polymer chain (P) and the mesityl groups increases in case an intermediary ruthenacyclobutane *trans* to the NHC forms (structure B, Figure 2.8). As an alternative, a ruthenacyclobutane with side-on coordination and one Cl-ligand *trans* to the NHC can form (structure A, Figure 2.8). In order to reduce the steric interaction between the growing polymer chain and mesityl groups, a *cis*-configured ruthenacyclobutane is favored, which gives rise to *cis*-configured double bonds along the polymer chain (Figure 2.8).

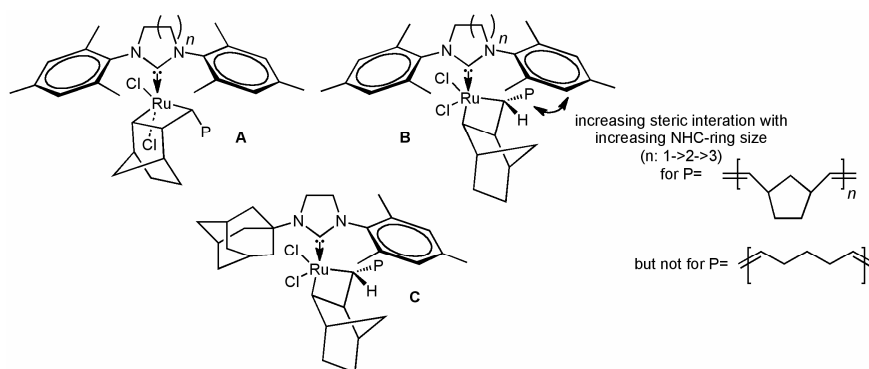


Figure 2.8. Different ruthenacyclobutanes and impact on the *cis/trans* configuration of the final polymer.

In contrast, the use of initiator **6** bearing an unsymmetrically substituted NHC results in the formation of poly (NBE) blocks with a high *trans*-content (70%). This particular feature of **6** is related to the restricted rotation of the NHC-ligand around the Ru-C₂-bond, thereby forcing the propagating alkylidene to remain at the same side as the mesityl ligand.^[25] There, a

ruthenacyclobutane *trans* to the NHC is energetically favored (structure C, Figure 2.8), resulting in a higher fraction of *trans*-configured double bonds in the polymer. As outlined for the alternating copolymerization of NBE with COE by the action of **5a**, poly(CPE) derived Ru-alkylidenes are sterically much less demanding than poly(NBE)-derived Ru-alkylidenes. Consequently, ruthenacyclobutanes *trans* to the NHC should dominate, giving rise to larger fractions of *trans*-configured double bonds in the poly (CPE) blocks. In fact, these poly (CPE) blocks were characterized by a *cis:trans* ratio around 20:80 throughout.

Despite the correlations outlined above one has to state that the influence of changes in both the NHC and the X-ligand on both the initiator's reactivity and the polymer structure are much less pronounced than, e.g., in Schrock-type carbenes. This is attributed to the nature of the Ru=C-bond, which is, as confirmed by numerous electrochemical measurements,^[1, 35] more a Ru(II)-carbene than a true Ru(IV) alkylidene, which is in stark contrast to high-oxidation state Schrock catalysts,^[3, 4, 36] which possess a pronounced metal-alkylidene character.

2.2.5 Influence of the NBE:CPE Ratio on the Extent of Alternating Copolymerization

To further explore the scope and limits of the alternating copolymerization of NBE with CPE, we focused on the most promising initiators, i.e. **2d**, **4b** and **6**, and used different NBE:CPE ratios. The results in terms of the percentage of alternating diads are summarized in Table 2.2. With **2d**, an increase in the NBE:CPE ratio from 1:1 to 1:5 resulted in an increase in the content of the alternating diads from 31 to 46%.

A further increase of the NBE:CPE ratio up to 1:50, however, resulted in a decrease in the content of alternating diads and, concomitantly, in a strong decrease in the formation of the poly(NBE) homopolymer block as well as in a significant increase in the formation of the poly(CPE) homopolymer block. Similar results were found for initiators **4b**. There a maximum of alternating diads of 40 % was found (Table 2.3).

Table 2.3. Alternating copolymerization of NBE and CPE by the action of initiators **2d**, **4b** and **6** using different monomer ratios (solvent=CH₂Cl₂), *T*=25°C, *t*=3 min).^a

initiator	I:NBE:CPE	poly(NBE)		poly(CPE)		poly(NBE- <i>alt</i> -CPE) _{<i>n</i>}
		(%)	<i>cis/trans</i>	(%)	<i>cis/trans</i>	(%)
2d	1:1000:1000	64	40/60	5	20/80	31
2d	1:1000:5000	28	30/70	26	30/70	46
2d	1:1000:7000	22	30/70	35	30/70	43
2d	1:1000:10000	11	30/70	50	30/70	39
2d	1:1000:50000	0	-	73	30/70	27
4b	1:1000:500	68	70/30	3	0/100	29
4b	1:1000:1000	50	70/30	10	20/80	40
4b	1:1000:2000	18	70/30	47	20/80	35
6	1:1000:1000	91	30/70	0	-	9
6	1:1000:3000	81	30/70	0	-	19
6	1:1000:4000	74	30/70	0	-	26
6	1:1000:10000	58	20/80	0	-	42
6	1:1000:20000	51	10/90	5	11/89	44
6	1:1000:30000	42	20/80	11	12/88	47
6	1:1000:40000	33	10/90	16	10/90	51
6	1:1000:50000	28	15/85	19	14/86	53
6	1:1000:60000	14	10/90	38	13/87	48

^a Calculated from the ¹³C NMR spectra.

These data clearly show that irrespective of the anionic ligand, the NHC and the NBE:CPE ratio used, the content of alternating diads was <53% throughout for initiators **2d** and **4b** and thus much smaller than in alternating copolymers prepared by the action of unsymmetrical NHC ligands.^[18, 23] To clarify the role of such unsymmetrical NHCs, we also investigated the scope and limitations of a Grubbs-type initiator bearing such an unsymmetrically substituted *N*-heterocyclic carbene (NHC), i.e. [RuCl₂(IAdMesH₂)(CHPh)(PCy)₃] (**6**) containing one (comparably small) mesityl and one (large) adamantly(Ad) group in the 1- and 3-position of the imidazolin-2-ylidene, respectively. Using different ratios of NBE:CPE (1:1 to 1:50), the percentage of alternating diads could in fact be increased from 9 to 53%.

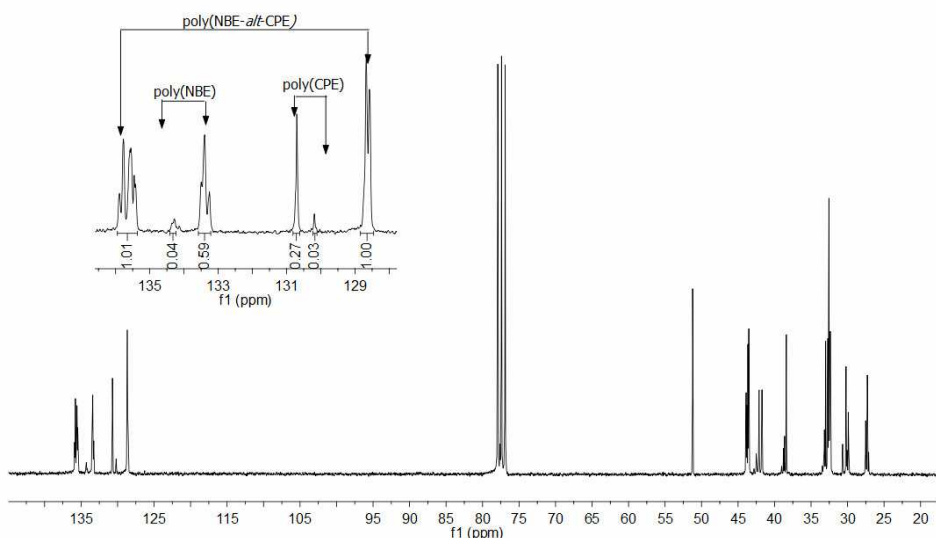


Figure 2.9. ^{13}C NMR of poly(NBE-*alt*-CPE) in CDCl_3 prepared by the action of **6**.
I: NBE: CPE (1:1000: 40,000).

2.2.6 Alternating Copolymerization of NBE with *cis*-Cyclooctene (COE)

We also looked into the copolymerization of NBE with COE, ^[16, 17, 24] again using a NBE:COE ratio of 1:1. The results are summarized in Table 2.4.

Table 2.4. Alternating copolymerization of NBE and COE by the action of initiators **1a-e**, **2b-e**, **3b-c**, **4a, b**, and **5b** and **6**.

#	initiator	poly(NBE)		poly(COE)		poly(NBE- <i>alt</i> -COE) _n
		(%)	<i>cis/trans</i>	(%)	<i>cis/trans</i>	
1	1a	42	60/40	48	20/80	10
2	1b	42	60/40	44	30/70	14
3	1c	100	60/40	0	-	0
4	1d	67	60/40	27	60/40	6
5	1e	79	40/60	13	30/70	8
6	2a	35	70/30	55	20/80	10
7	2b	39	40/60	44	20/80	17
8	2c	59	60/40	29	40/60	12
9	2d	70	40/60	18	50/50	12
10	2e	77	70/30	15	30/70	8

11	2g	47	40/60	45	25/75	8
12	3a	36	70/30	64	30/70	0
13	3b	42	60/40	50	20/80	8
14	3c	46	50/50	32	45/55	22
15	3d	100	50/50	0	-	0
16	4a	49	70/30	48	30/70	3
17	4b	99	80/20	1	-	0
18	5a	29	60/40	31	40/60	40
19	5b	53	60/40	38	40/60	9
20	6	88	20/80	8	10/90	4

^a Calculated from the ¹³C NMR spectra, initiator: NBE:COE=1:1000:1000, CH₂Cl₂.

Initiators **1c** and **4b** bearing CF₃SO₃⁻ and CF₃COO⁻ groups, respectively, produced only poly(NBE) under the given conditions. Among all initiators investigated, **5a** showed the highest content of 40% of alternating diads. This percentage of alternating units is lower than the one obtained in the copolymerization of NBE with CPE (Table 2.2).

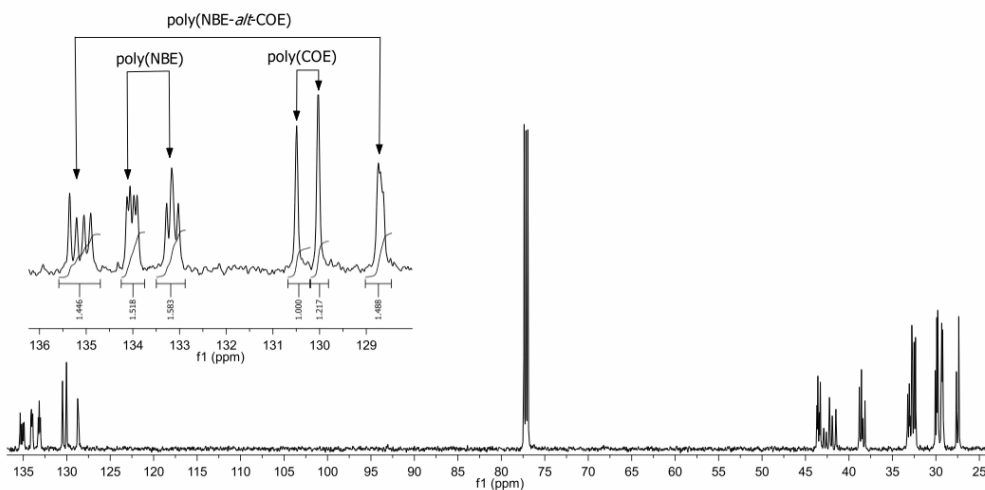


Figure 2.10. ¹³C NMR spectrum (CDCl₃) of poly(NBE-*alt*-COE)_n prepared by the action of **3c** I: NBE: COE (1:1000: 1000, Table 2.4, entry 14).

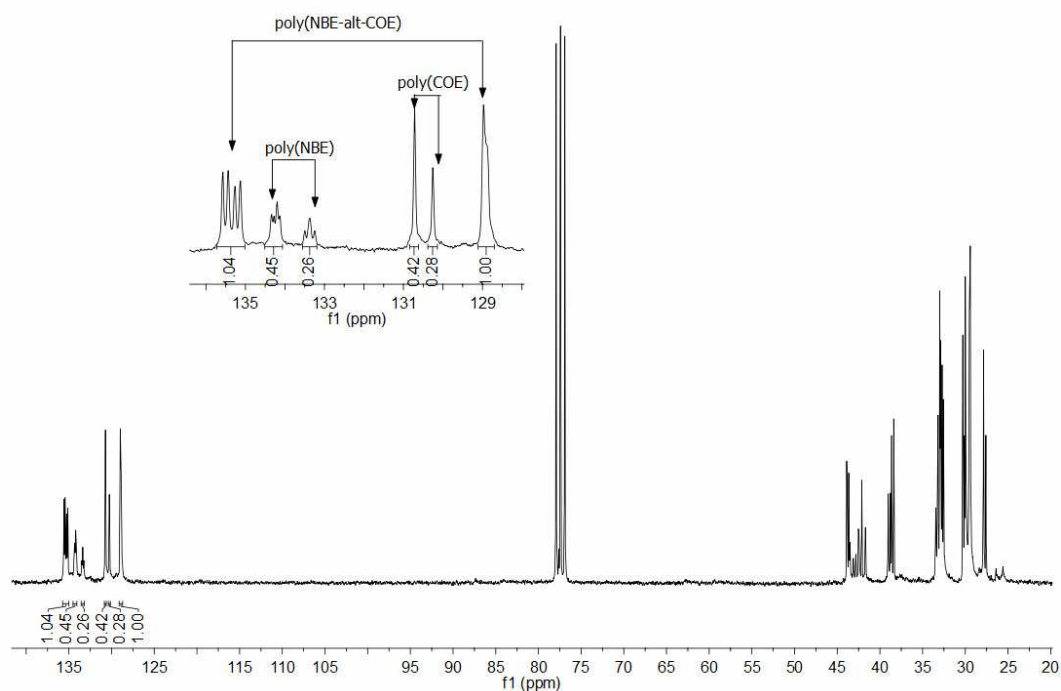


Figure 2.11. ^{13}C NMR of poly(NBE-*alt*-COE) in CDCl_3 prepared by the action of **5a**.
I: NBE: COE (1:1000: 1000, Table 2.4, entry 18).

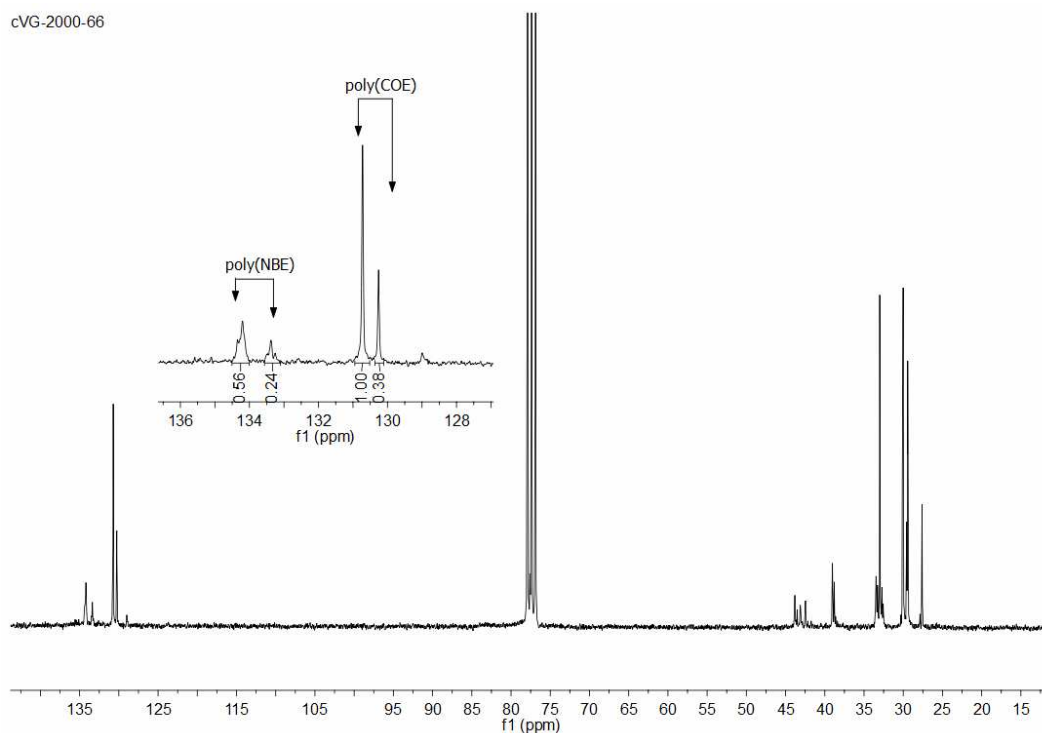


Figure 2.12. ^{13}C NMR of poly(NBE-*co*-COE) in CDCl_3 prepared by the action of **3a**.
I: NBE: COE (1:1000: 1000, Table 2.4, entry 12).

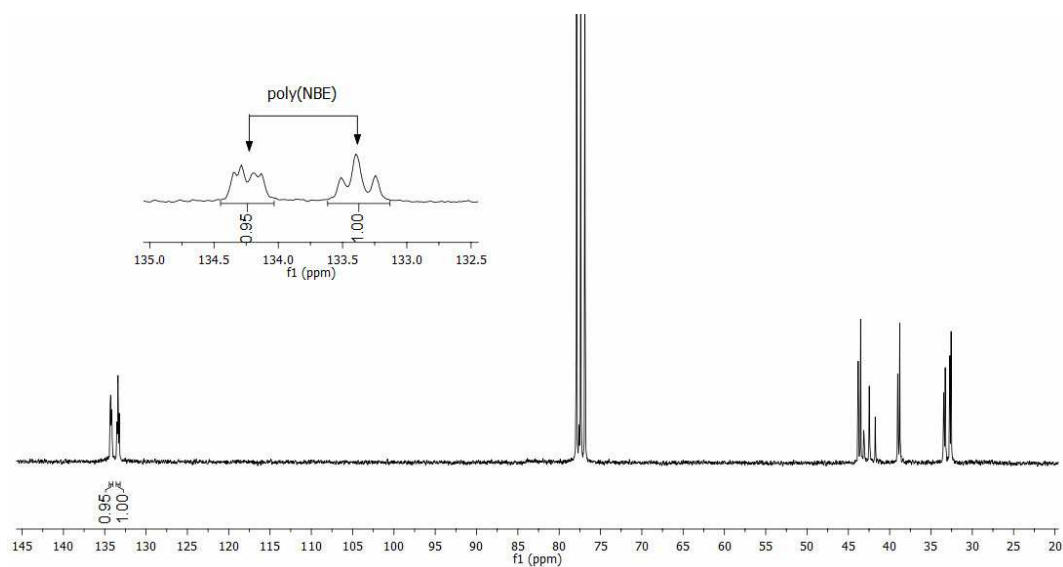


Figure 2.13. ^{13}C NMR of poly(NBE-*co*-COE) in CDCl_3 prepared by the action of **3d**.
I: NBE: COE (1:1000: 1000, Table 2.4, entry 15).

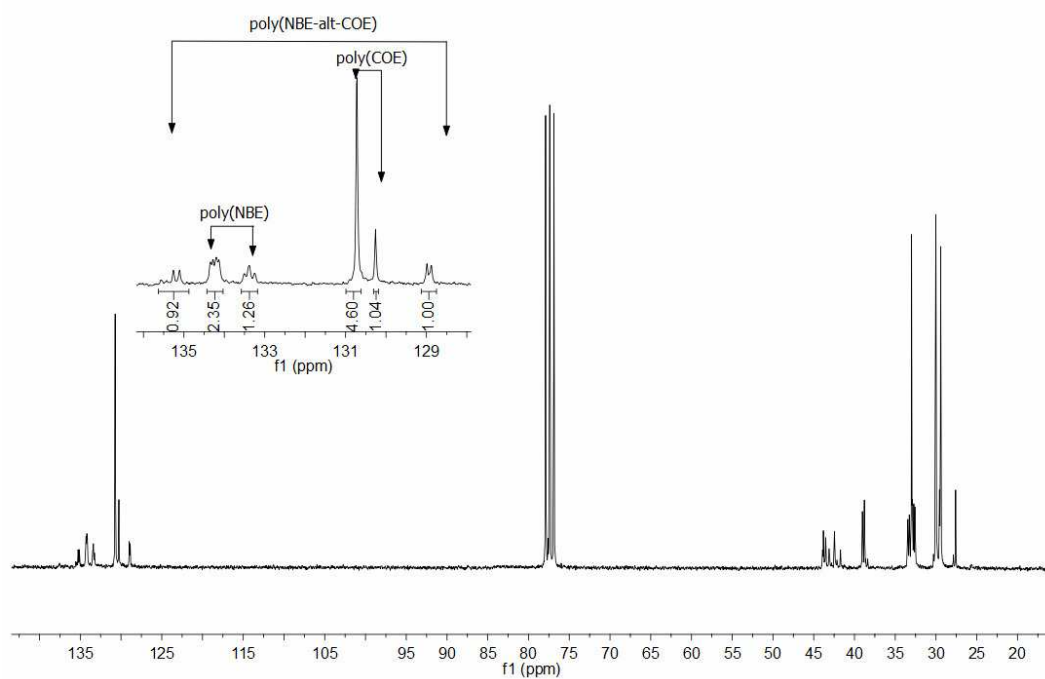


Figure 2.14. ^{13}C NMR of poly(NBE-*alt*-COE) in CDCl_3 prepared by the action of **2a**.
I: NBE: COE (1:1000: 1000, Table 2.4, entry 6).

cVG-2000-61

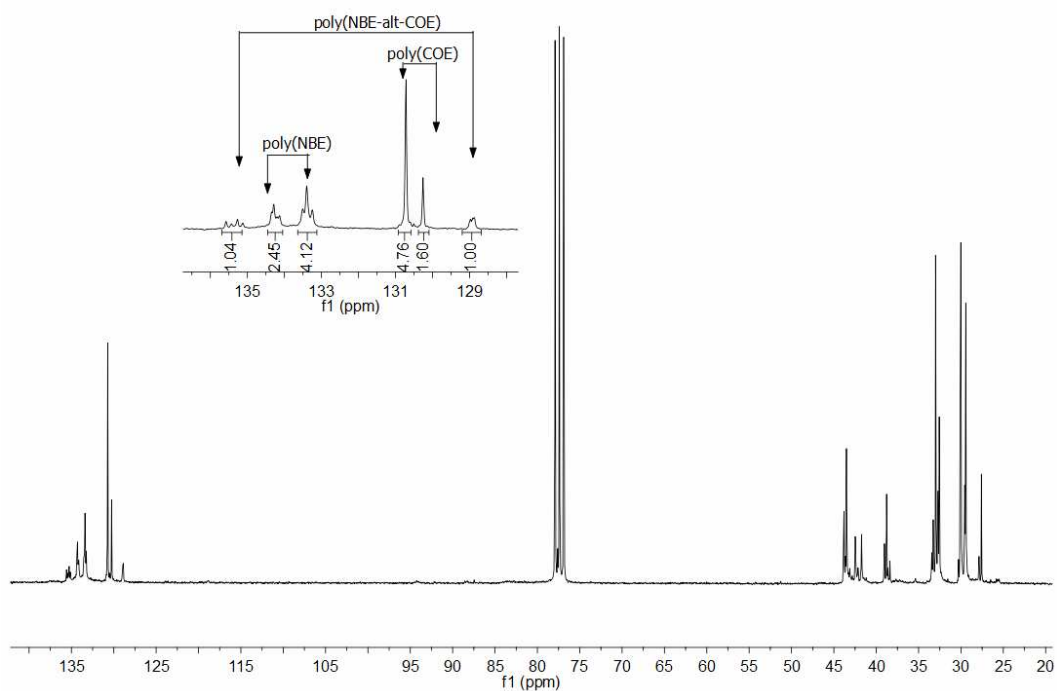


Figure 2.15. ^{13}C NMR of poly(NBE-*alt*-COE) in CDCl_3 prepared by the action of **2g**. I: NBE: COE (1:1000: 1000, Table 2.4, entry 11).

2.3 Summary

A series of modified 2nd-generation Grubbs- and Grubbs-Hoveyda-type metathesis initiators in which the chloride ligands were replaced by electron-withdrawing pseudo-halide ligands have been investigated for their ROMP activity vs. NBE as well as for their propensity to copolymerize NBE with cyclic olefins such as COE and CPE. Ru(CF₃COO)₂(1,3-dimesityl-1,3-diazepinidin-2-ylidene)(CH-2-(2-PrO)-C₆H₄) (**4b**) was identified as an unusually active initiator for the homopolymerization of cyclopentene. All initiators containing electron-withdrawing potentially chelating ligands showed high activity in the alternating copolymerization with NBE/CPE. In addition, in the copolymerization with CPE, an increase in the size of the NHC favors the formation of poly(NBE) blocks with a high *cis*-content.

2.4 Polymerization Procedure

2.4.1 Typical Copolymerization Procedure:

Initiator **5a** (2.0 mg, 0.0032 mmol), dissolved in 0.5 mL of CH₂Cl₂, was added to a solution of NBE (300 mg, 3.18 mmol) and CPE (218 mg, 3.18 mmol) in 2 mL of CH₂Cl₂. The reaction mixture was stirred for 2 min. Then the reaction was stopped by the addition of ethyl vinyl ether, and the polymer was precipitated by the drop-wise addition of the reaction mixture into methanol. The precipitated polymer was collected by filtration and washed with an excess methanol and dried *in vacuo*.

2.4.2 Typical Homopolymerization Procedure:

Initiator **2b** (2 mg, 0.0031 mmol), dissolved in 0.5 mL of CH₂Cl₂, was added to a solution of cyclopentene (210 mg, 3.08 mmol) in 1 mL of CH₂Cl₂. The reaction mixture was stirred for 5 h at 50°C. After 5 h, the reaction was stopped by the addition of ethyl vinyl ether and the polymer was precipitated by the drop-wise addition of the solution into methanol. The precipitated polymer was collected by filtration and washed with an excess methanol and dried *in vacuo*.

2.5 References

- [1] R. H. Grubbs, *Handbook of Metathesis*, 1st ed.; Wiley-VCH: Weinheim, **2003**, Vols. 1-3.
- [2] R. R. Schrock, *Ring-Opening Metathesis Polymerization*. In *Ring-Opening Polymerization*, 1st ed.; Brunelle, D.J., Ed.; Hanser: Munich **1993**, pp 129.
- [3] R. R. Schrock, *Chem. Rev.* **2001**, *102*, 145.
- [4] R. R. Schrock, *Chem. Rev.* **2009**, *109*, 3211.
- [5] R. R. Schrock, *The Discovery and Development of High-Oxidation State Mo and W Imido Alkylidene Complexes for Alkene Metathesis*, **2003**, 1st ed.; Wiley-VCH: Weinheim, Vol. 1, pp 8.
- [6] R. H. Grubbs, *Angew. Chem.* **2006**, *118*, 3845-3850; *Angew. Chem. Int. Ed.* **2006**, *45*, 3760 – 3765.
- [7] T. M. Trnka, R. H. Grubbs, *Acc. Chem. Res.* **2000**, *34*, 18.
- [8] M. R. Buchmeiser, *Ring-Opening Metathesis Polymerization*, 1st ed., Wiley-VCH: Weinheim; **2009**, pp 197
- [9] J. O. Krause, M. T. Zarka, U. Anders, R. Weberskirch, O. Nuyken, M. R. Buchmeiser, *Angew. Chem.* **2003**, *115*, 6147; *Angew. Chem. Int. Ed.* **2003**, *42*, 5965.
- [10] J. O. Krause, O. Nuyken, M. R. Buchmeiser, *Chem. Eur. J.* **2004**, *10*, 2029.
- [11] J. O. Krause, O. Nuyken, K. Wurst, M. R. Buchmeiser, *Chem. Eur. J.* **2004**, *10*, 777.
- [12] P. S. Kumar, K. Wurst, M. R. Buchmeiser, *J. Am. Chem. Soc.* **2008**, *131*, 387.
- [13] Y. S. Vygodskii, A. S. Shaplov, E. I. Lozinskaya, P. S. Vlasov, I. A. Malyshkina, N. D. Gavrilova, P. Santhosh Kumar, M. R. Buchmeiser, *Macromolecules* **2008**, *41*, 1919.
- [14] P. S. Kumar, K. Wurst, M. R. Buchmeiser, *Organometallics* **2009**, *28*, 1785.
- [15] P. S. Kumar, K. Wurst, M. R. Buchmeiser, *Chem. Asian. J.* **2009**, *4*, 1275.
- [16] M. Bornand, P. Chen, *Angew. Chem.* **2005**, *117*, 8123; *Angew. Chem. Int. Ed.* **2005**, *44*, 7909, 117.
- [17] S. Torker, A. Müller, P. Chen, *Angew. Chem.* **2010**, *122*, 3850; *Angew. Chem. Int. Ed.* **2010**, *49*, 3762, 122.
- [18] K. Vehlouw, D. Wang, M. R. Buchmeiser, S. Blechert, *Angew. Chem.* **2008**, *120*, 2655; *Angew. Chem. Int. Ed.* **2008**, *47*, 2615.
- [19] J. G. Hamilton, K. J. Ivin, J. J. Rooney, L. C. Waring, *Chem. Commun.* **1983**, 159.
- [20] M. Buchmeiser, R. R. Schrock, *Macromolecules* **1995**, *28*, 6642.
- [21] B. Al Samak, A. G. Carvill, J. J. Rooney, J. M. Thompson, *Chem. Commun.* **1997**, 2057.

- [22] V. Amir-Ebrahimi, J. J. Rooney, *J. Mol. Cat. A* **2004**, *208*, 115.
- [23] M. Lichtenheldt, D. Wang, K. Vehlow, I. Reinhardt, C. Kühnel, U. Decker, S. Blechert, M. R. Buchmeiser, *Chem. Eur. J.* **2009**, *15*, 9451.
- [24] M. Bornand, S. Torker, P. Chen, *Organometallics* **2007**, *26*, 3585.
- [25] M. B. Dinger, P. Nieczypor, J. C. Mol, *Organometallics* **2003**, *22*, 5291.
- [26] J. C. Conrad, K. D. Camm, D. E. Fogg, *Inorg. Chim. Acta* **2006**, *359*, 1967.
- [27] S. B. Garber, J. S. Kingsbury, B. L. Gray, A. H. Hoveyda, *J. Am. Chem. Soc.* **2000**, *122*, 8168.
- [28] M. S. Sanford, J. A. Love, R. H. Grubbs, *Organometallics* **2001**, *20*, 5314.
- [29] T.-L. Choi, R. H. Grubbs, *Angew. Chem.* **2003**, *115*, 1785; *Angew. Chem. Int. Ed.* **2003**, *42*, 1743.
- [30] R. Bandari, A. Prager-Duschke, C. Kühnel, U. Decker, B. Schlemmer, M. R. Buchmeiser, *Macromolecules* **2006**, *39*, 5222.
- [31] M. Iglesias, D. J. Beetstra, J. C. Knight, L.-L. Ooi, A. Stasch, S. Coles, L. Male, M. B. Hursthouse, K. J. Cavell, A. Dervisi, I. A. Fallis, *Organometallics* **2008**, *27*, 3279.
- [32] K. Vehlow, S. Gessler, S. Blechert, *Angew. Chem. Int. Ed.* **2007**, *46*, 8082; *Angew. Chem.* **2007**, *119*, 8228.
- [33] K. Vehlow, M. Lichtenheldt, D. Wang, S. Blechert, M. R. Buchmeiser, *Macromol. Symp.* **2010**, *296*, 44.
- [34] S. Richard R, *Polyhedron* **1995**, *14*, 3177.
- [35] T. K. Maishal, B. Mondal, V. G. Puranik, P. P. Wadgaonkar, G. K. Lahiri, A. Sarkar, *J. Organomet. Chem.* **2005**, *690*, 1018.
- [36] R. R. Schrock, *Chem. Commun.* **2005**, 2773.

Chapter 3

Bis(diamido)silylene Zirconium (IV) and Non-bridged Half-Titanocene (IV) Complexes; Synthesis and Use in Olefin Polymerization

Novel Zr^{IV}-complexes of the type (Me₂Si((NR)(6-(2-(diethylboryl)phenyl)pyridyl-2-yl))ZrCl₂·THF; R= ^tBu (**13**), adamantyl (**17**)) and the Ti^{IV}-based metallocene-type complex bis((N(6-(2-(diethylboryl)phenyl)-pyrid-2-yl)Me)TiCl₂ (**24**); and the non-bridged half-titanocene complexes of the type Cp'TiCl₂(N(6-(2-(diethylboryl)phenyl)-pyrid-2-yl)R); R=Me (**22**, **23**), Si(CH₃)₃ (**26**, **27**), Cp'=Cp (**22** and **26**), Cp* (**23** and **27**) as well as aminoborane-free model complexes Cp'TiCl₂(N-(biphenyl-3-yl)R); R= SiMe₃ (**30**, **31**), Me (**33**, **34**), (Cp'=Cp (**30**, **34**), Cp* (**31**, **33**)) have been synthesized. These Zr and Ti complexes were characterized by ¹H and ¹³C NMR spectroscopy and elemental analysis. The molecular structures of complexes **22**, **23**, **27** and **34** were determined by single-crystal X-ray diffraction analysis. In polymerization, upon activation of these complexes with MAO, complexes **13**, **17**, **22**, **23**, **26** and **27** showed activities up to 3000 kg-PE /mol-M·h in the homopolymerization of ethylene (E), producing mainly linear PE (HDPE) with molecular weights in the range of 100,000 < M_n < 4 × 10⁶ g mol⁻¹. Surprisingly, in the copolymerization of ethylene with CPE, complex **13** exhibits high catalytic activity (30,000 kg-PE /mol-Zr·h), producing poly(E)-*co*-poly(CPE)_{VIP} with 3-4 mol-% of vinyl addition polymer incorporated CPE. In the copolymerization of ethylene with NBE, complexes **13**, **17**, **22**, **23**, **26** and **27** mainly produced vinyl addition copolymerization derived poly(E)-*co*-poly(NBE)_{VIP} with incorporated NBE-fractions of up to 36 mol-% as evidenced by ¹³C NMR analysis.

3.1 Introduction

Olefin polymerization by homogeneous transition metal complexes is a mature field of polymer chemistry, especially when using early transition metals.^[1-6] During the past twenty years it has emerged that group IV transition metal complexes containing amide ligands are promising systems in olefin polymerization catalysis.^[2] In particular, a large number of metallocene complexes have been developed for the copolymerization of ethylene with cycloolefins.^[7, 8] Metallocene catalysts, particularly zirconium complexes, are effective catalyst systems for the copolymerization of ethylene with cycloolefins (NBE, CPE). The copolymerization of ethylene and norborn-2-ene has been investigated with various metallocene catalysts, and the resulting polymer turned out to be amorphous solids with high transparency.^[9-14] Kaminsky et.al^[15] reported that C_s symmetric catalyst systems, e.g ([Me₂C(Flu)(Cp)]ZrCl₂ or ([Ph₂C(Flu)(Cp)]ZrCl₂, are well suited for yielding amorphous copolymers with high activities and high glass transition temperatures (<180°) compared to C₂-symmetric catalyst systems e.g ([Me₂Si(Ind)₂]ZrCl₂, ([Ph₂Si(Ind)₂]ZrCl₂ under the same conditions.

Nomura *et.al* [16, 17] reported on non-bridged (anilido)(cyclopentadienyl)titanium(IV) complexes of the type $\text{Cp}^*\text{TiCl}_2[\text{N}(2,6\text{-Me}_2\text{C}_6\text{H}_3)(\text{R})]$ ($\text{Cp}^*=\text{C}_5\text{Me}_5$, $1,3\text{-Me}_2\text{C}_5\text{H}_3$, $(\text{C}_5\text{H}_5)\text{Cp}$; $\text{R}=\text{SiMe}_3$) for olefin polymerization, in which particularly $\text{Cp}^*\text{TiCl}_2[\text{N}(2,6\text{-Me}_2\text{C}_6\text{H}_3)(\text{SiMe}_3)]$ exhibited moderate activity (1080 Kg PE/molTi·h) in ethylene polymerization. However, the zirconium analogues $\text{Cp}^*\text{ZrCl}_2[\text{N}(2,6\text{-Me}_2\text{C}_6\text{H}_3)(\text{SiMe}_3)]$ showed lower activity (637 Kg PE/molTi·h) in ethylene homopolymerization. In the copolymerization of ethylene with NBE by various non-bridged (aryloxo)(cyclopentadienyl) TiCl_2 type complexes of the general formula $\text{Cp}^*\text{TiCl}_2(\text{OAr})$ { $\text{Cp}^*=\text{indenyl}$, C_5Me_5 , $t\text{-BuC}_5\text{H}_4$, $1,2,4\text{-Me}_3\text{C}_5\text{H}_2$; $\text{OAr}=\text{O-}2,6\text{-}i\text{-Pr C}_6\text{H}_3$ } the catalytic activity and incorporation of NBE was found to be highly dependent on the substituent on Cp^* . Especially indenyl-based Ti complexes showed high activity and efficient incorporation of NBE in poly(E)-*co*-poly(NBE). These complexes were also active in the copolymerization of ethylene with CPE, however, incorporation of CPE was less effective than the one of NBE.^[18]
[9]

We recently reported on $\text{Me}_2\text{Si}(\eta^5\text{-Me}_4\text{Cp})(6\text{-}(2\text{-}(\text{diethylboryl})\text{phenyl})\text{pyridine-}2\text{-amine})\text{TiCl}_2$,^[19] $\text{Me}_2\text{Si}(\text{DbppN})_2\text{ZrCl}_2(\text{THF})$ and $\text{Me}_2\text{Si}(\text{DbppN})_2\text{HfCl}_2(\text{THF})$, ($\text{DbppN}=6\text{-}(2\text{-}(\text{diethylboryl})\text{phenyl})\text{pyridine-}2\text{-amido}$) initiator systems, which were after activation with methylalumoxane (MAO) capable of forming both VIP- and ROMP-derived structures from a cyclic olefin and which were additionally capable of copolymerizing ethylene to yield narrowly distributed ($1.05 < \text{PDI} < 2.0$), high-molecular weight copolymers ($M_n \leq 1,500,000$ g/mol) containing multiple blocks of both ROMP- and VIP-derived structures within one single polymer chain.

In view of these results we were interested in the question which reactivity and $\alpha\text{-H}$ elimination propensity of Zr^{IV} - and Ti^{IV} -based bis(amido) precatalysts and Ti^{IV} -based half metallocenes precatalysts (Figure 3.1) would display. Consequently, such systems were prepared and investigated in the homopolymerization of ethylene (E) as well as in the copolymerization of E with both CPE and NBE. These Zr^{IV} -based bis(amido) precatalysts having C_s symmetric system (Figure 3.1), were not performing well in the reversible $\alpha\text{-H}$ elimination/ $\alpha\text{-H}$ addition process to switch from Ziegler-Natta polymerization to ROMP and *vice versa*. However, these complexes are well suited to synthesize mostly linear PE and as well as vinyl addition derived copolymers of poly(E)-*co*-poly(NBE)_{VIP} and poly(E)-*co*-poly(CPE)_{VIP} with high molecular weights.

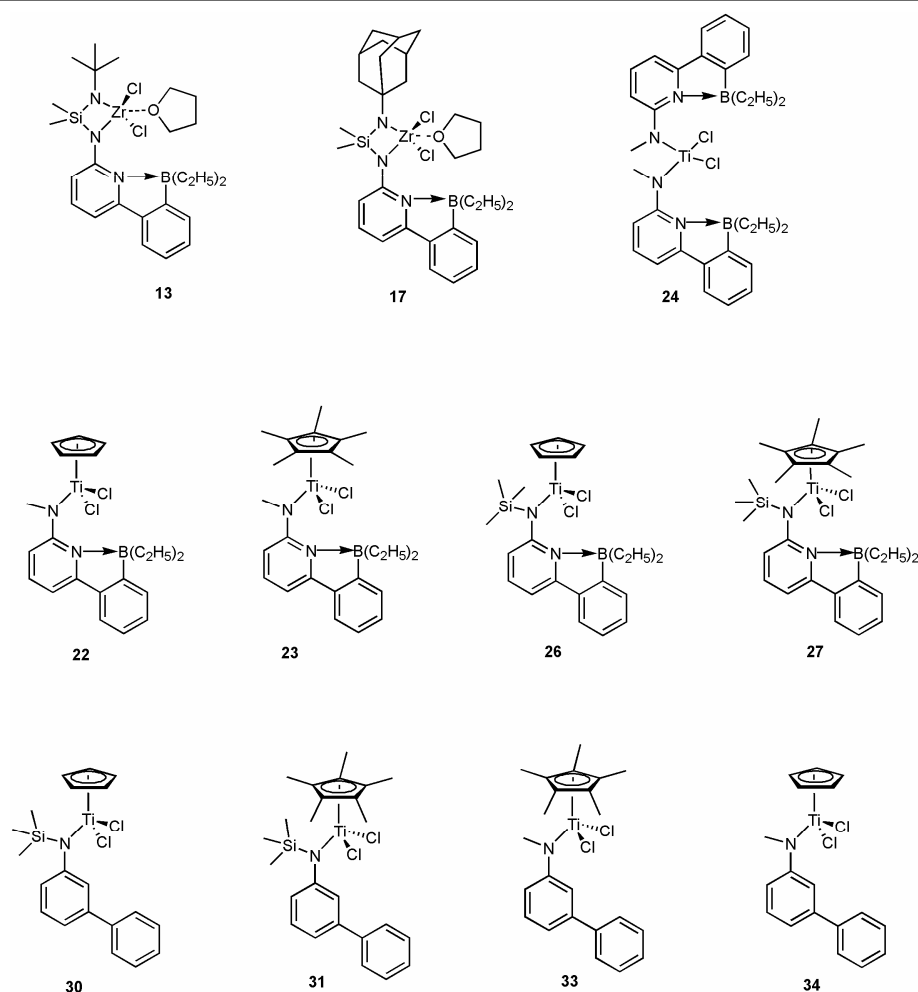


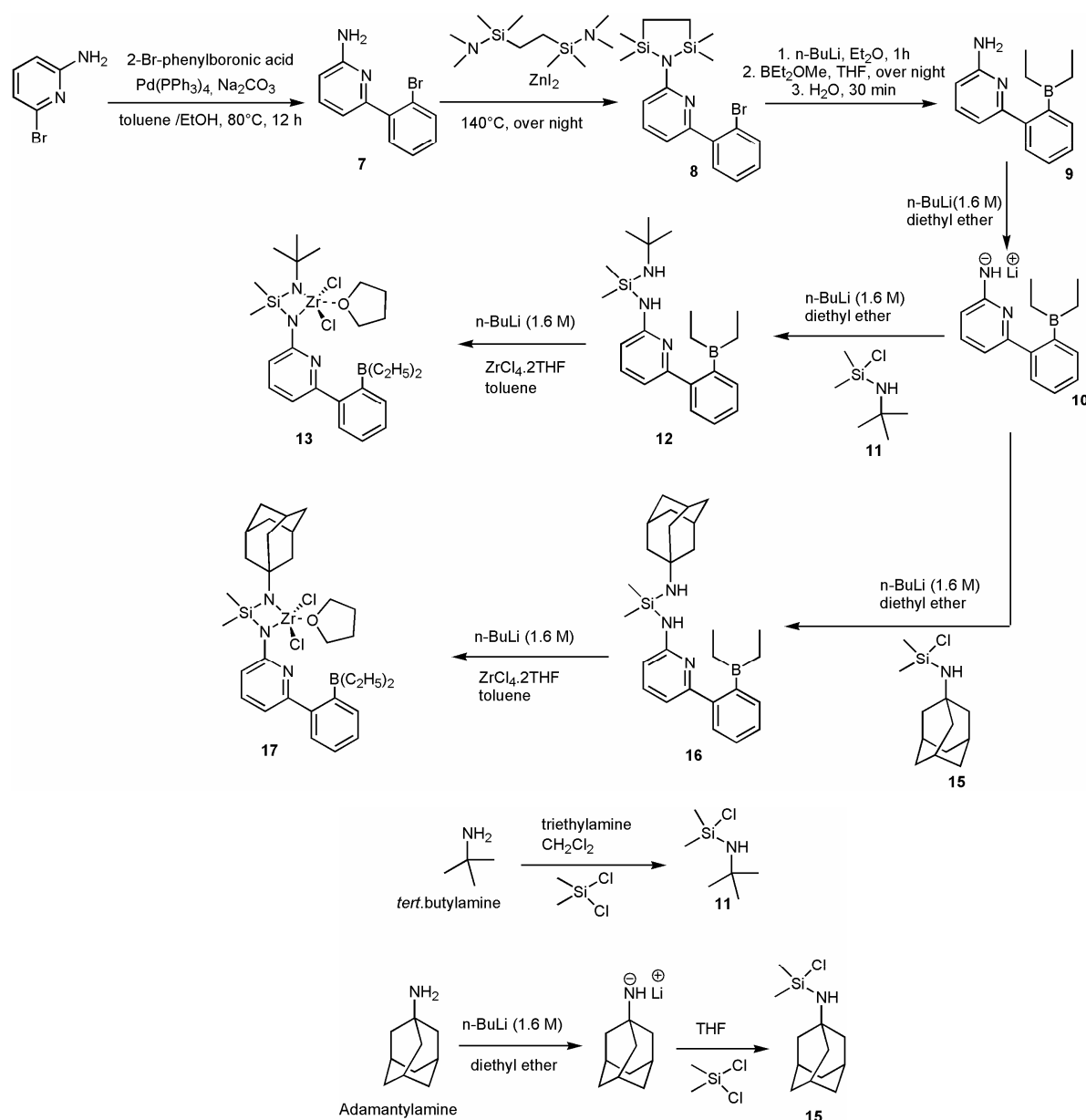
Figure 3.1. Structure of precatalysts 13, 17, 22, 23, 24, 26, 27, 30, 31, 33 and 34.

3.2 Results and Discussion

3.2.1 Synthesis of ligands and precatalysts

An efficient synthesis was developed for the synthesis of the aminoborane-containing ligand **9** (Scheme 3.1). It entailed the reaction of 2-Br-5-aminopyridine with 2-Br-phenylboronic acid to yield 2-(2-Br-phenyl)-5-aminopyridine (**7**). Compound **7** was then N-protected with 1,2 bis[(dimethylamino)dimethylsilyl]ethane to yield **8**. Compound **8** was deprotonated using *n*-BuLi and borylated with diethylmethoxyborane to yield **9**. In this entire sequence, the use of bis[(dimethylamino)dimethylsilyl]ethane turned out to be crucial for the high-yield synthesis of **9** and allowed for its synthesis in 51% overall yield. Subsequently, N-*tert*-butyl-chlorodimethylsilylamine (**11**) was synthesized by treating *tert*-butyl amine with dichlorodimethylsilane in the presence of a base such as triethylamine to yield **11** in 90% yield. Subsequently, deprotonation of **9** with *n*-BuLi and *in-situ* reaction with N-*tert*-butyl-chloro-dimethylsilylamine (**11**) yielded **12**. In a similar way, **10** was treated with N-adamantylchlorodimethylsilyl amine (**15**) to yield **16**. Finally, the Zr complexes **13** and **17**

were synthesized via the reaction of $(\text{Me}_2\text{Si}((\text{NHR})(6\text{-}(2\text{-}(\text{diethylboryl})\text{phenyl})\text{pyrid-2-yl})))$; $\text{R}=\textit{tert}$ -butyl (**12**), adamantyl (**16**)) with 2.0 equiv of $n\text{-BuLi}$ at -36°C , followed by treatment with $\text{ZrCl}_4\cdot 2\text{THF}$ in toluene. The desired Zr-complexes were isolated in approx. 70% yield and were characterized by ^1H NMR, ^{13}C NMR and elemental analysis. Particularly with complex **13**, ^1H NMR and ^{13}C NMR data as well as elemental analysis showed that no ligand scrambling occurred before crystallization (Figure 3.2). Before crystallization the elemental analysis calcd. for $\text{C}_{25}\text{H}_{40}\text{BCl}_2\text{N}_3\text{OSiZr}$: C 50.08; H 6.72; N 7.01; found C 50.37; H 7.08; N 7.34. These data clearly show that no ligand scrambling occurred before the crystallization process.



Scheme 3.1. Synthesis of compounds 7- 17.

Finally, the Zr complex **13** was crystallized from toluene and pentane (3:7), white needles were grown upon standing at -36°C inside a glove-box for 10 days. The molecular

structure of complex **13** was determined by single-crystal X-ray diffraction analysis and revealed that the Zr-complex **13** contained two bisamido ligands upon standing for a long time in a solvent thus forming complex **13a** (Scheme 3.2). The X-ray structure is shown in Figure 3.4. For comparison, the ^1H and ^{13}C NMR data of the Zr-based complex **13** (before crystallization) and complex **13a** (after crystallization) are shown in Figures 3.2 and 3.3. Similarly, all attempts to synthesize the corresponding Hf-based complexes from the Li-salt of compounds **12** and **16** with 1.0 equiv of HfCl_4 in different solvents such as toluene and diethyl ether lead to Hf-complexes containing two bisamido ligands (Scheme 3.3) as confirmed by ^1H NMR, ^{13}C NMR and elemental analysis. Also all attempts to synthesize the Ti-based complexes from the Li-salt of compounds **12** and **16** with $\text{TiCl}_4 \cdot 2\text{THF}$ in both toluene and diethyl ether were unsuccessful.

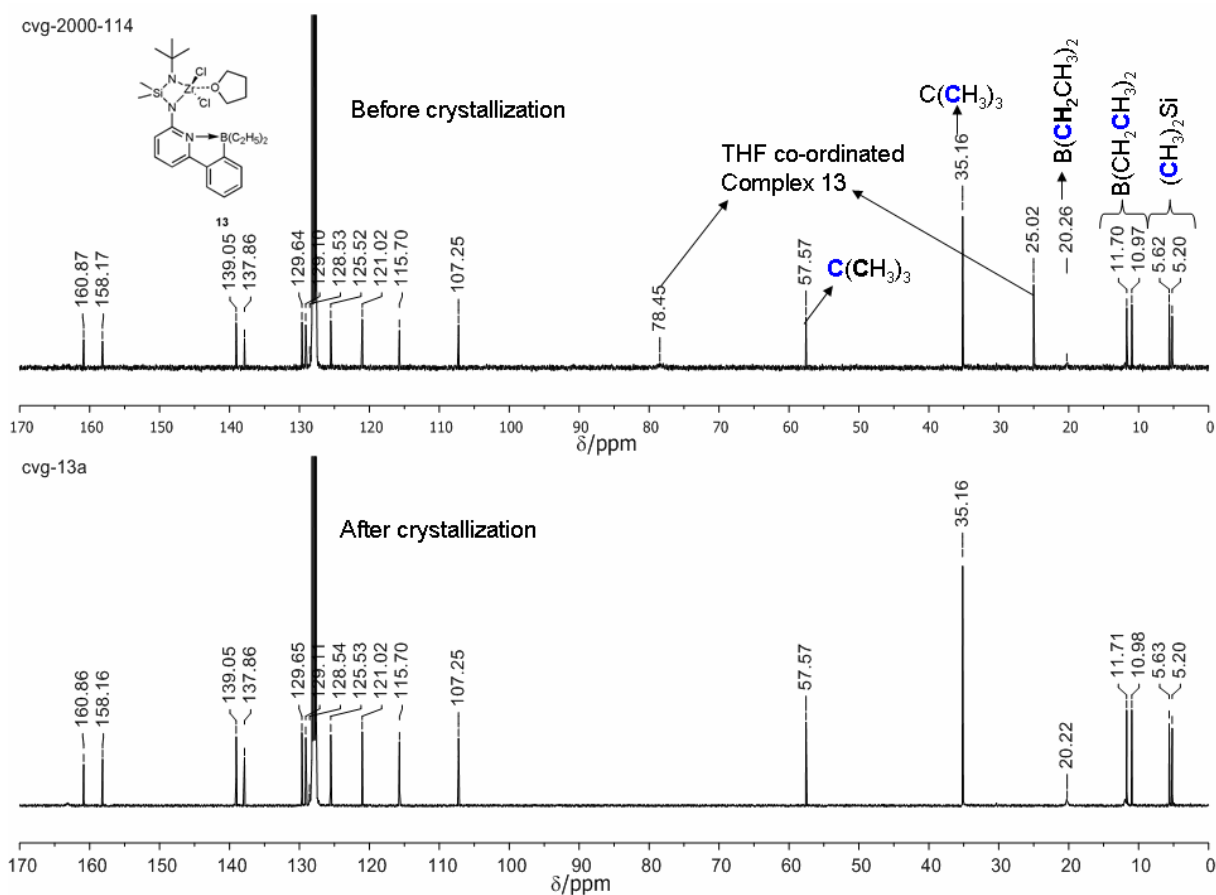


Figure 3.2. a) ^{13}C NMR of complex **13** before crystallization; b) ^{13}C NMR of complex **13** after crystallization in toluene and pentane (3:7).

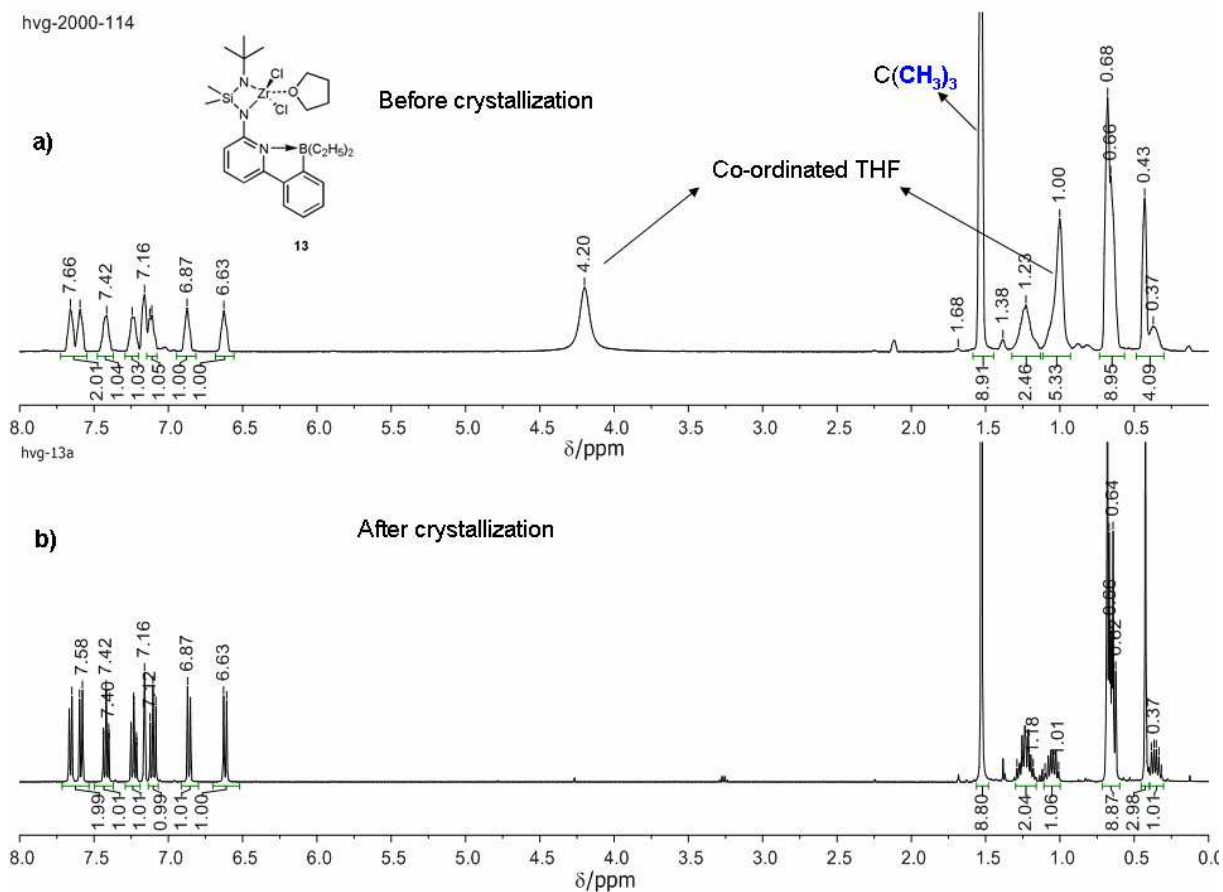
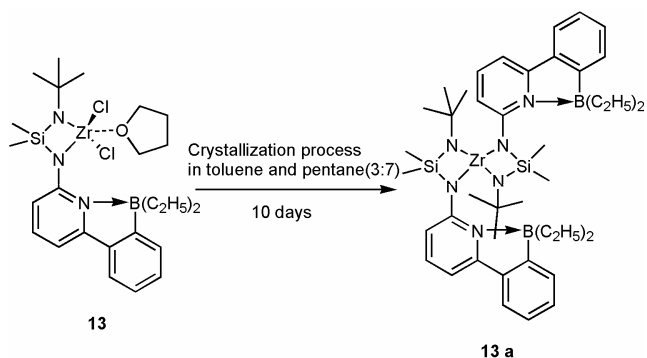


Figure 3.3. a) ^1H NMR of complex **13** before crystallization and b) after crystallization in toluene and pentane (3:7).



Scheme 3.2. Structure of Zr-based complex **13a**, which was formed during the crystallization of **13**.

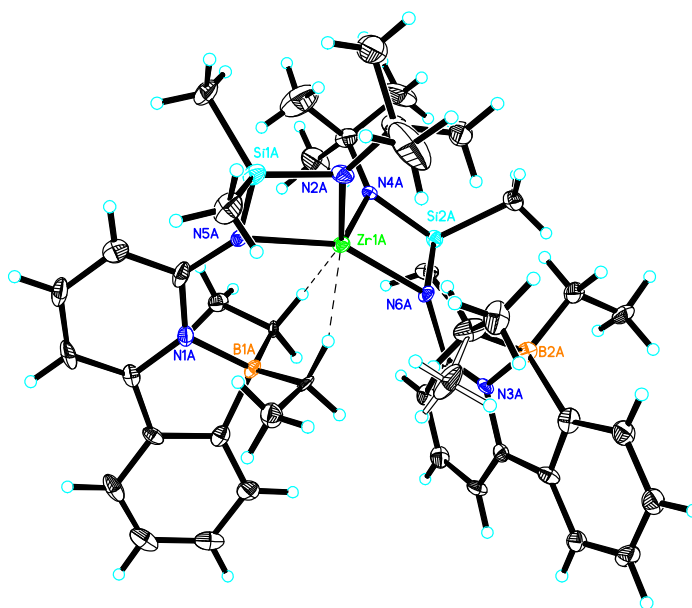
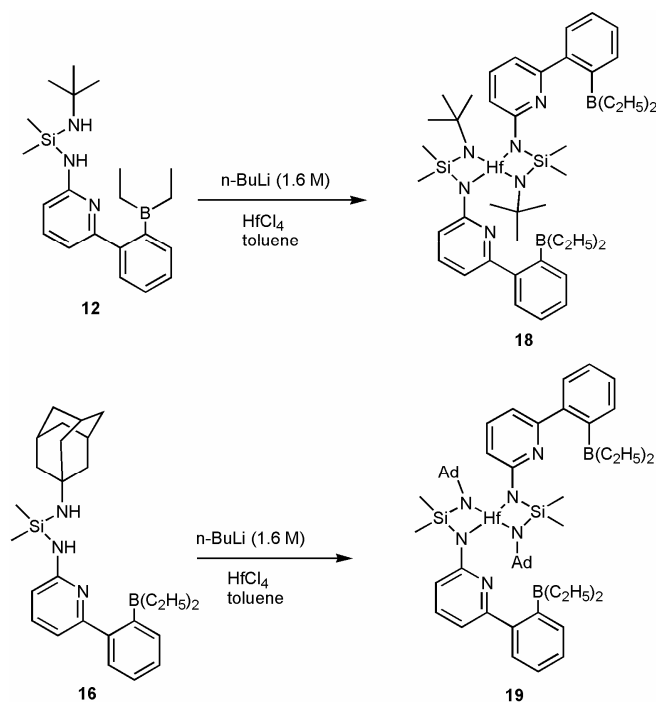


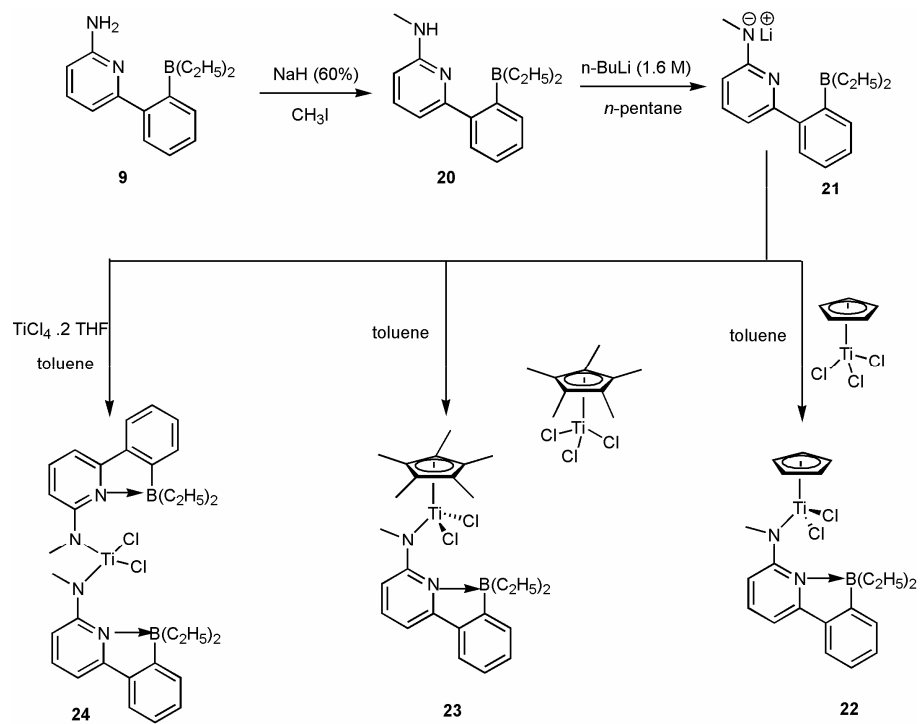
Figure 3.4. Molecular structure of complex **13 a**, containing two bisamido ligands.



Scheme 3.3. Synthesis of Hf-based complexes **18** and **19**.

The Ti-based complexes $\text{Cp}^*\text{TiCl}_2\{\text{N}[\text{6}-(2\text{-diethylborylphenyl})\text{pyrid-2-yl}]\text{-N-Me}\}$ ($\text{Cp}^* = \text{Cp}$ (**22**), Cp^* (**23**), and $\text{TiCl}_2\{\text{bis}(\text{N}[\text{6}-(2\text{-diethylborylphenyl})\text{pyrid-2-yl}]\text{-N-Me})\}$ (**24**) were synthesized in a three step procedure according to Scheme 3.4. In a first step, the ligand $\text{N}-(6-(2-(2\text{-diethylborylphenyl})\text{pyrid-2-yl}))\text{-N-methylamine}$ (**20**) was synthesized via the reaction of compound **9** with NaH (60 wt-% in mineral oil) in DMF at 0°C followed by treatment with CH_3I and was isolated in high yield (90%). The resulting compound **20** was

deprotonated using *n*-BuLi (1.6 M) in *n*-pentane and the corresponding Li salt (**21**) was isolated by filtration. Finally, the Li salt (**21**) was treated with Cp'TiCl₃ (Cp'=Cp and Cp*) in toluene at room temperature for 12 h and the corresponding Ti-complexes of **22** and **23** were isolated in moderate yields (50-55%). The Ti complex **24** was synthesized in an analogous manner using 0.5 mol eq. of TiCl₄·2THF in toluene.^[20] All complexes were characterized by ¹H NMR, ¹³C NMR and elemental analysis. Complex **22** and **23** were crystallized in a mixture of toluene and pentane (2:8) at -36°C inside a glove-box. After a few days, the red colored needle type crystals had grown from the solvent mixture and these crystals were subjected to single-crystal X-ray diffractometry. The molecular structures of complexes **22** and **23** are shown in Figure 3.5 and 3.6, selected bond lengths (Å) and bond angles (°) are summarized in Tables 3.1 and 3.2 respectively. Complex **22** crystallizes in monoclinic space group *P2(1)/n*, *a*= 10.9979(11), *b*= 16.1318(19), *c*=12.3324(11) pm, $\alpha=\gamma=90^\circ$, $\beta=106.79^\circ$, *Z*=4, complex **23** crystallizes in the triclinic space group *p-1*, *a*= 9.2538(4), *b*= 11.5135(5), *c*=12.7779(6) pm, $\alpha=77.233^\circ$, $\beta=81.007^\circ$, $\gamma=72.946^\circ$, *Z*=2 respectively. The structural analysis reveals that both complexes **22** and **23** have a tetrahedral geometry around the metal center and that the pyridine-nitrogen is coordinated to the diethylboryl group in the solid state. Bond lengths and bond angles were compared to those of previously reported Ti-complexes from Nomura *et.al*^[21] and Ying Mu *et.al.*^[22] The Ti-N distances in complex **22** (1.8891 Å) and complex **23** (1.9259 Å) are longer than the reported values (1.867 – 1.878 Å). In all these complexes, the Ti-N distance is shorter than the estimated value (2.02 Å) of a Ti-N single bond according to Pauling's radii. The average bond distance of the Ti-Cl in complexes **22** (2.267 Å) and complex **23** (2.2719 Å) are shorter than those reported for [CpTiCl₂{N(2,6-*i*Pr-C₆H₃)Me}] (2.275 Å), [Cp*TiCl₂{N(2,6-*i*Pr-C₆H₃)Me}] (2.285 Å), [Cp*TiCl₂{N(2,6-Me-C₆H₃)Me}] (2.281 Å)^[22] and longer than the reported value of [Cp*TiCl₂{N(Me)Cy}] (2.303 Å)^[21], which indicates that the bond distances are slightly changing by varying the anionic ligand. The N(1)-Ti(1)-Cl(1) bond angle is almost of the same length in both Ti-complexes **22** (106.22°) and **23** (106.26°), a slight difference was observed in the bond angles of N(1)-Ti(1)-Cl(2) in complexes **22** (100.95°) and **23** (99.61°). The bond angles of Cl(1)-Ti(1)-Cl(2) (103.71° in **22** and 101.22° in **23**) were slightly smaller when compared to [CpTiCl₂{N(2,6-*i*Pr-C₆H₃)Me}] (105.22°) and [Cp*TiCl₂{N(2,6-*i*Pr-C₆H₃)Me}] (104.91°), respectively.



Scheme 3.4. Synthesis of compounds 20-23 and 24.

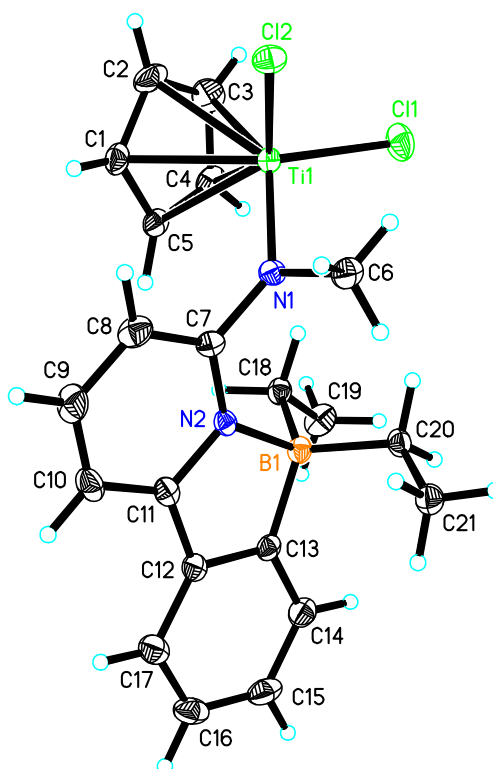


Figure 3.5. Molecular structure of complex 22.

Table 3.1. Selected bond lengths (Å) and bond angles (°) of complex **22**.^a

Bond length (Å)			
Ti (1) - N (1)	1.8891	Ti (1) - C (1)	2.355
Ti (1) - Cl (1)	2.2601	Ti (1) - C (2)	2.358
Ti (1) - Cl (2)	2.2739	Ti (1) - C (3)	2.337
N (1) - C (6)	1.490	Ti (1) - C (4)	2.334
N (1) - C (7)	1.413	Ti (1) - C (5)	2.3459
B (1) - N (2)	1.694	N (2) - C (7)	1.360
Bond angle (°)			
N(1)- Ti(1)- Cl(1)	106.22	C(7)- N(1)- Ti(1)	136.20
N(1)- Ti(1)- Cl(2)	100.95	C(6)- N(1)- Ti(1)	108.79
Cl(1)- Ti(1)- Cl(2)	103.71	C(7)- N(1)- C(6)	111.17

^a For detailed X-ray structural data information, please refer to the appendix.

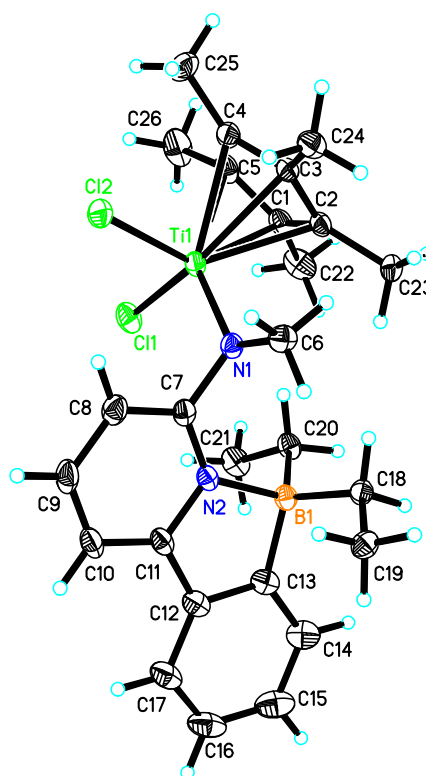
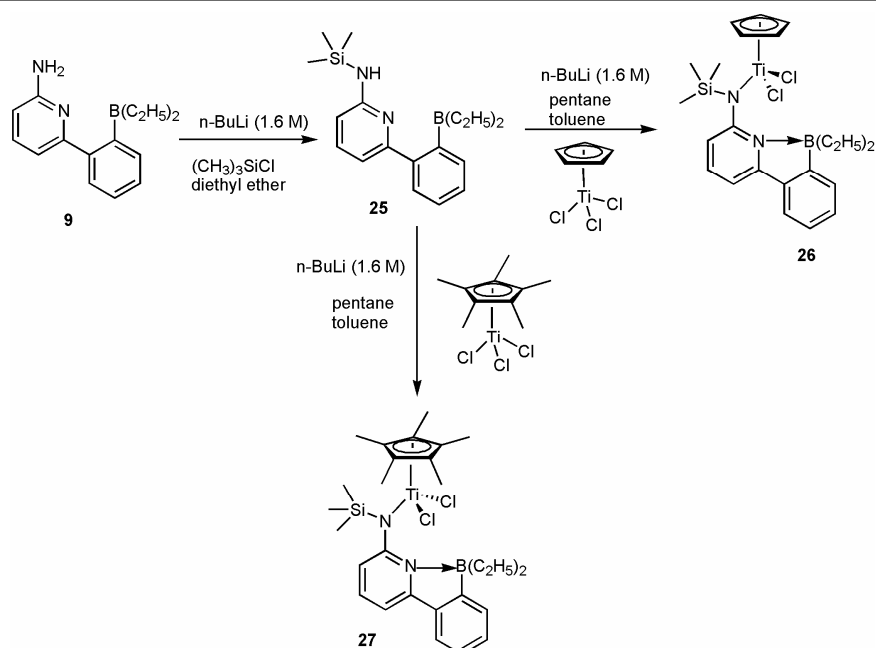
**Figure 3.6.** Molecular structure of complex **23**.

Table 3.2. Selected bond lengths (Å) and bond angles (°) of complex **23**.^a

Bond length (Å)			
Ti (1) - N (1)	1.9259	Ti (1) - C (3)	2.3724
Ti (1) - Cl (1)	2.2571	Ti (1) - C (4)	2.3795
Ti (1) - Cl (2)	2.2868	Ti (1) - C (5)	2.3874
N (1) - C (6)	1.4779	C (1) - C (22)	1.4991
N (1) - C (7)	1.4242	C (2) - C (23)	1.5015
B (1) - N (2)	1.6800	C (3) - C (24)	1.5005
Ti (1) - C (1)	2.3670	C (4) - C (25)	1.4935
Ti (1) - C (2)	2.3842	C (5) - C (26)	1.5034
Bond angle (°)			
N(1)- Ti(1)- Cl(1)	106.26	C(7)- N(1)- Ti(1)	117.28
N(1)- Ti(1)- Cl(2)	99.61	C(6)- N(1)- Ti(1)	126.24
Cl(1)- Ti(1)- Cl(2)	101.225	C(7)- N(1)- C(6)	109.85

^a For detailed X-ray structural data information, please refer to the appendix.

The Ti-based complexes Cp'TiCl₂(N-(6-(2-(diethylboryl)phenyl)pyrid-2-yl)SiMe₃); (Cp'=Cp (**26**), Cp* (**27**)) (Scheme 3.5) were synthesized in high yields (80%), by the reaction of CpTiCl₃ and Cp*TiCl₃, respectively, with the Li-salt of compound **25** in toluene. The isolated complexes **26** and **27** were characterized by ¹H NMR, ¹³C NMR and elemental analysis. Crystallization of these complexes from a mixture of toluene and pentane (2:8) allowed for growing red colored needle-type crystals from a concentrated solution of complex **27** upon standing several days at -36°C inside the glove-box. These crystals were found suitable for single-crystal X-ray diffraction analysis. The molecular structure of complex **27** is shown in Figure 3.7, selected bond lengths (Å) and bond angles (°) are summarized in Table 3.3. The X-ray data of complex **27** was compared to those of (1,3-Me₂C₅H₃)TiCl₂[N(2,6-Me₂C₆H₃)(SiMe₃)] reported by Nomura *et.al.*^[16] The X-ray structural analysis of complex **27** reveals a tetrahedral geometry around the metal centre with the aryl ligand almost perpendicular to the cyclopentadienyl ring in the Ti-N-Si plane. The bond distance (1.9319 Å) of Ti(1)-N(1) is slightly longer than the one (1.898 Å) in (1,3-Me₂C₅H₃)TiCl₂[N(2,6-Me₂C₆H₃)(SiMe₃)].^[16] The average bond distance (2.2684 Å) of Ti-Cl is shorter than the bond distance (2.2716 Å) of (1,3-Me₂C₅H₃)TiCl₂[N(2,6-Me₂C₆H₃)(SiMe₃)].^[16] Finally, attempts to synthesize the Zr- and Hf-based analogues of Cp'MCl₂(N-(6-(2-(diethylboryl)phenyl)pyrid-2-yl)SiMe₃); (Cp'=Cp, Cp* and M=Zr, Hf) via the reaction of Cp'TiCl₃ with LiN[6-(2-(diethylboryl)phenyl)pyrid-2-yl]SiMe₃ were not successful.



Scheme 3.5. Synthesis of compounds 25, 26 and 27.

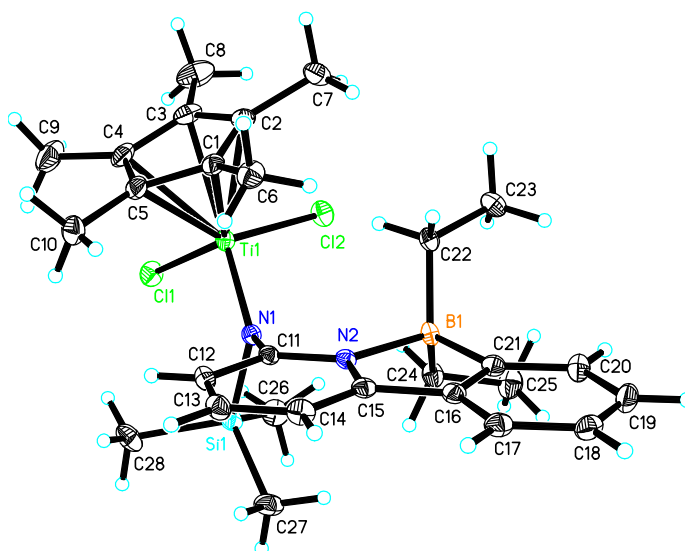


Figure 3.7. Molecular structure of complex 27.

Table 3.3. Selected bond lengths (Å) and bond angles ($^\circ$) of complex 27.^a

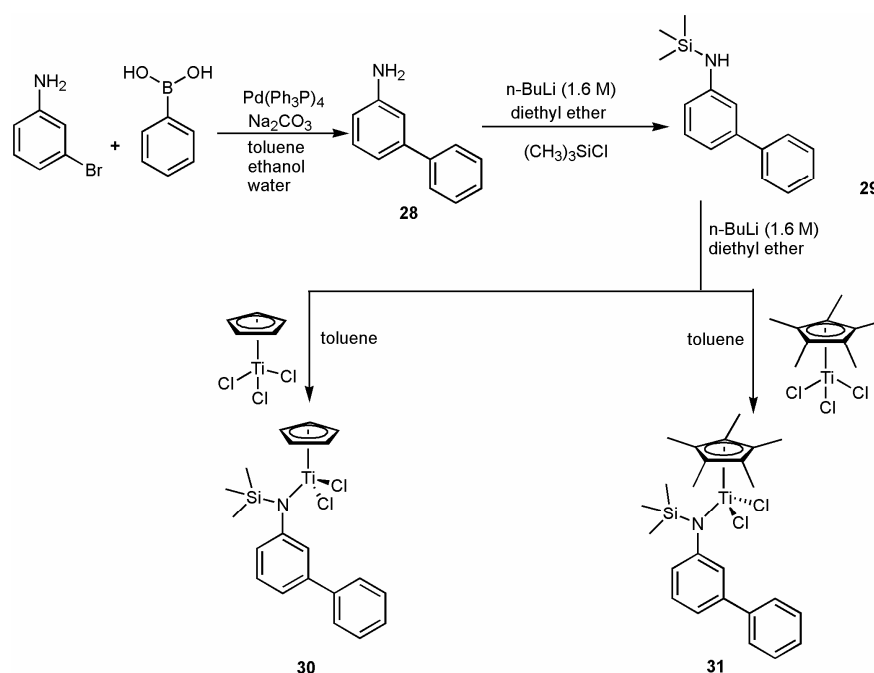
Bond length (Å)			
Ti (1) - N (1)	1.9319	Ti (1) - C (3)	2.3680
Ti (1) - Cl (1)	2.2715	Ti (1) - C (4)	2.3920
Ti (1) - Cl (2)	2.2653	Ti (1) - C (5)	2.4042
N (1) - Si (1)	1.8327	C (1) - C (6)	1.498
N (1) - C (11)	1.412	C (2) - C (7)	1.503
B (1) - N (2)	1.697	C (3) - C (8)	1.497
Ti (1) - C (1)	2.4124	C (4) - C (9)	1.488
Ti (1) - C (2)	2.3815	C (5) - C (10)	1.503

Bond angle (°)			
N(1)- Ti(1)- Cl(1)	104.02	C(11)- N(1)- Ti(1)	130.65
N(1)- Ti(1)- Cl(2)	104.77	Si(1)- N(1)- Ti(1)	118.84
Cl(1)- Ti(1)- Cl(2)	97.121	C(11)- N(1)- Si(1)	108.53

^a For detailed X-ray structure data information, please refer to the appendix.

3.2.2 Synthesis of model compounds

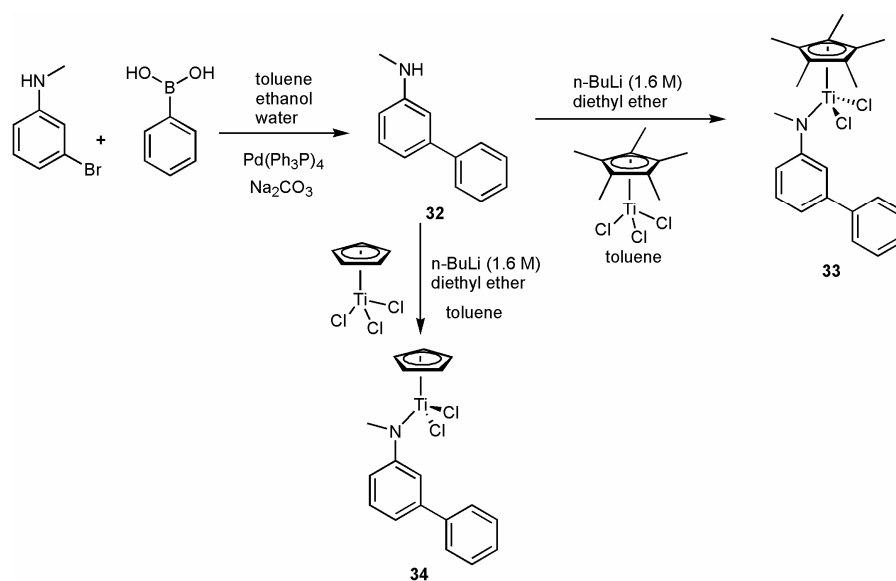
The synthesis of the aminoborane-free half-titanocene model complexes of the general formula $\text{Cp}'\text{TiCl}_2[\text{N}(\text{biphenyl-3-yl})\text{SiMe}_3]$; ($\text{Cp}'=\text{Cp}$ (**30**), Cp^* (**31**)) (Scheme 3.6) was accomplished in a three-step approach in high yields (75%). The first step entailed the palladium-catalyzed cross-coupling Suzuki reaction between 3-bromoaniline and phenylboronic acid in the presence of a base and yielded 3-phenylaniline (**28**). In the 2nd step compound **28** was deprotonated using *n*-BuLi and reacted with TMSCl to yield compound **29** in 75% yield. In the 3rd step, deprotonation of compound **29** with *n*-BuLi in diethyl ether and treatment with $\text{Cp}'\text{TiCl}_3$ in toluene resulted in the formation of $\text{Cp}'\text{TiCl}_2[\text{N}(\text{biphenyl-3-yl})\text{SiMe}_3]$; ($\text{Cp}'=\text{Cp}$ (**30**), Cp^* (**31**)). The isolated complexes were characterized by ¹H NMR, ¹³C NMR and elemental analysis.



Scheme 3.6. Synthesis of compounds **28-31**.

The aminoborane-free half-titanocene model complexes $\text{Cp}'\text{TiCl}_2[\text{N}(\text{biphenyl-3-yl})\text{Me}]$; ($\text{Cp}'=\text{Cp}^*$ (**33**), Cp (**34**)) were synthesized in a two-step procedure (Scheme 3.7). In a first step, the ligand *N*-methyl-3-phenylaniline (**32**) was synthesized by the palladium-catalyzed cross-coupling Suzuki reaction between 3-bromo-*N*-methylaniline and phenylboronic acid in the presence of a base in 90% yield. The resulting compound **32** was

deprotonated using *n*-BuLi (1.6 M) in diethyl ether and treated with Cp'TiCl₃ in toluene to yield Cp'TiCl₂[*N*-(biphenyl-3-yl)Me]; (Cp'=Cp (**34**), Cp* (**33**)). These complexes were characterized by ¹H NMR, ¹³C NMR and elemental analysis. Complex **34** crystallized in a mixture of toluene and pentane (2:8) at -36°C inside the glove-box. Yellow colored needle-type crystals were grown from the solvent mixture and these crystals were measured by single-crystal X-ray diffractometry. The molecular structure of complex **34** is shown in Figure 3.8, selected bond lengths (Å), bond angles (°) are summarized in Table 3.4. Complex **34** crystallizes in the orthorhombic space group, *a*= 13.2542(12), *b*= 11.6665(9), *c*=21.732(2) pm, $\alpha=\beta=\gamma=90^\circ$ and *Z*=8. The structural analysis revealed that complex **34** has a tetrahedral geometry around the metal center. The bond lengths (Å) and bond angles (°) were compared with the aminoborane group-containing complex type CpTiCl₂{N-[6-(2-Diethylborylphenyl)pyrid-2-yl]-N-Me} (**22**). The Ti-N bond length in complex **22** (1.8891 Å) is longer than the corresponding bond in complex **34** (1.8750 Å). In all these complexes, the Ti-N distance is shorter than the estimated value (2.02 Å) of the Ti-N single bond according to Pauling's radii. The average bond distance of the Ti-Cl bond in complex **22** (2.267 Å) is slightly shorter than the Ti-Cl bond distance in complex **34** (2.278 Å). The N(1)-Ti(1)-Cl(1) bond angle (106.22°) of complex **22** is larger than in complex **34** (103.02°). For N(1)-Ti(1)-Cl(2), the bond angle in complex **34** (107.34°) is substantially larger than in complex **22** (100.95°). The bond angle of Cl(1)-Ti(1)-Cl(2) in **22** (103.71°) is greater than the one in complex **34** (101.05°).



Scheme 3.7. Synthesis of compounds **32-34**.

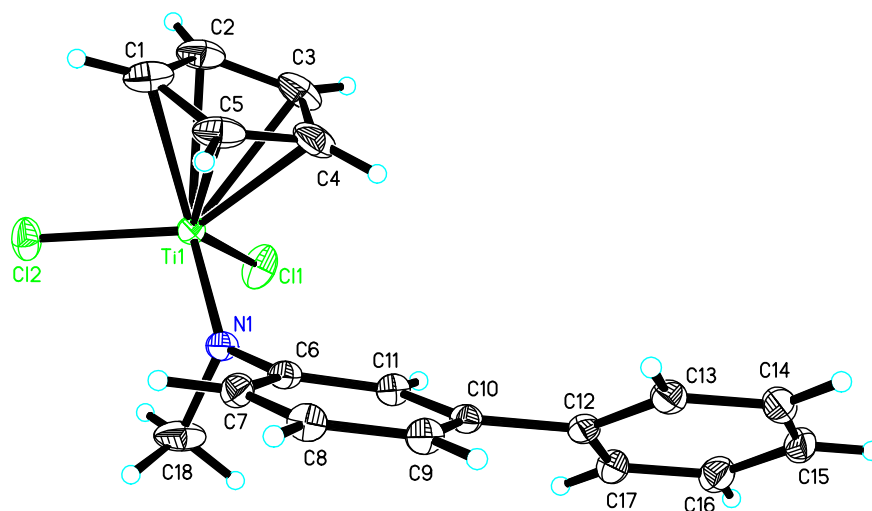


Figure 3.8. Molecular structure of complex **34**.

Table 3.4. Selected bond lengths (Å) and bond angles (°) of complex **34**.^a

Bond length (Å)			
Ti (1) - N (1)	1.8750	Ti (1) - C (1)	2.3505
Ti (1) - Cl (1)	2.2759	Ti (1) - C (2)	2.3446
Ti (1) - Cl (2)	2.2810	Ti (1) - C (3)	2.3489
N (1) - C (6)	1.4327	Ti (1) - C (4)	2.3400
N (1) - C (18)	1.4803	Ti (1) - C (5)	2.3384
Bond angle (°)			
N(1)- Ti(1)- Cl(1)	103.02	C(18)- N(1)- Ti(1)	109.19
N(1)- Ti(1)- Cl(2)	107.34	C(6)- N(1)- Ti(1)	138.24
Cl(1)- Ti(1)- Cl(2)	101.055	C(18)- N(1)- C(6)	112.27

^a For detailed X-ray structure data information, please refer to the appendix.

3.2.3 Synthesis of ethyl- and phenyl- bridged ligands

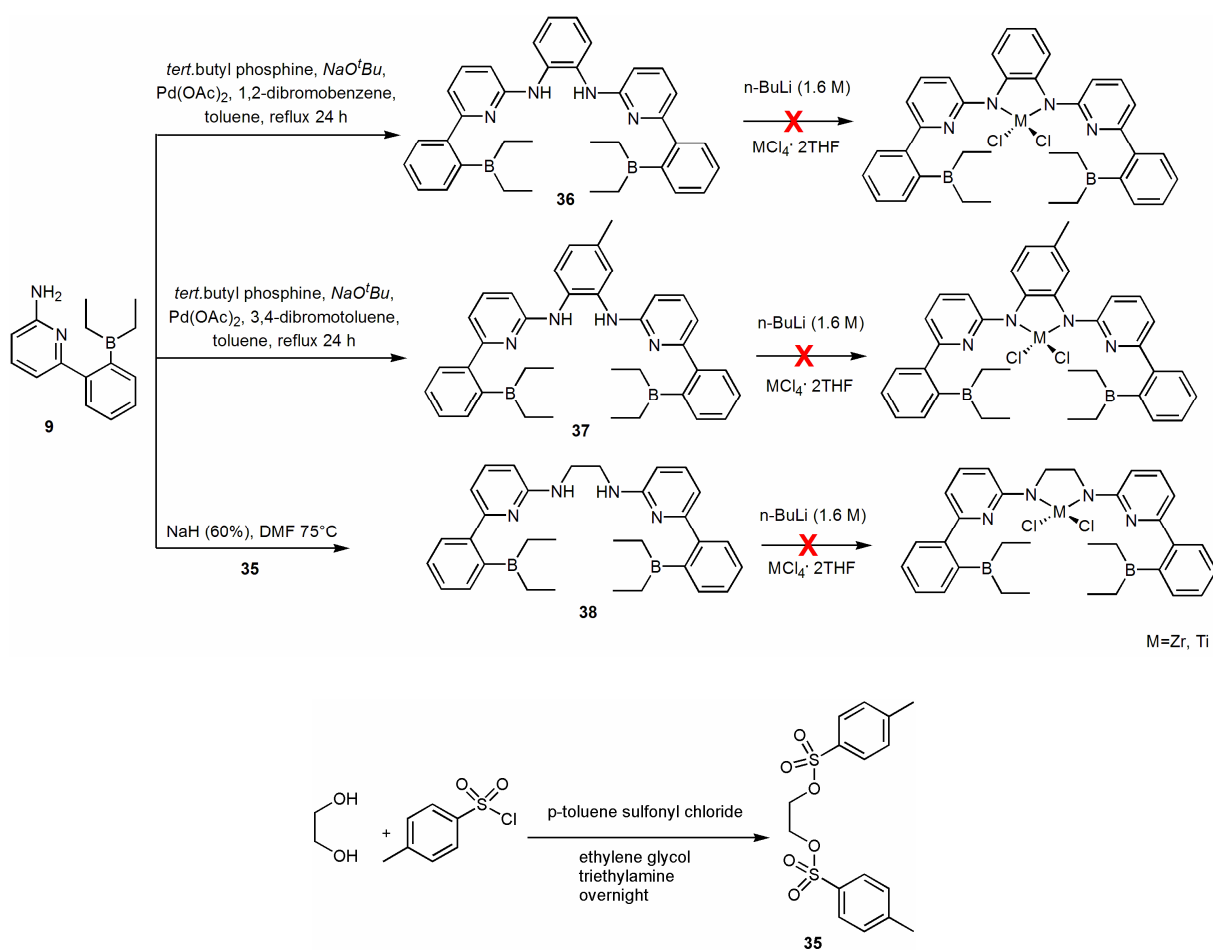
Ligands **36** and **37** were successfully synthesized in up to 70% yield using the standard protocol for the Buchwald-Hattwig cross-coupling of aryl halides and aryl amines in the presence of palladium acetate, tri-*tert*-butyl phosphine and a base such as sodium *tert*-butoxide. The symmetrical ligand **38** was synthesized in 55% yield using NaH (60 wt-% in mineral oil) as base to deprotonate **9** followed by the addition of **35** (Scheme 3.8). All ligands were characterized by ¹H NMR, ¹³C NMR and HRMS respectively.

Aiming on an enhancement of the bulkiness of the ligand by introducing *tert*-butyl and adamantyl groups, ligands **41** and **43** (Scheme 3.9) were successfully synthesized by reacting **9** with bromoacetyl bromide in the presence of base such as DMAP in DCM. Treatment of **39** with excess amine (*tert*-butyl and adamantyl amine) in DCM resulted **40** and **42**. Subsequent

reduction of the carbonyl group with LiAlH_4 in THF yielded ligands **41** and **43**, these compounds were characterized by ^1H NMR, ^{13}C NMR and GC-MS respectively.

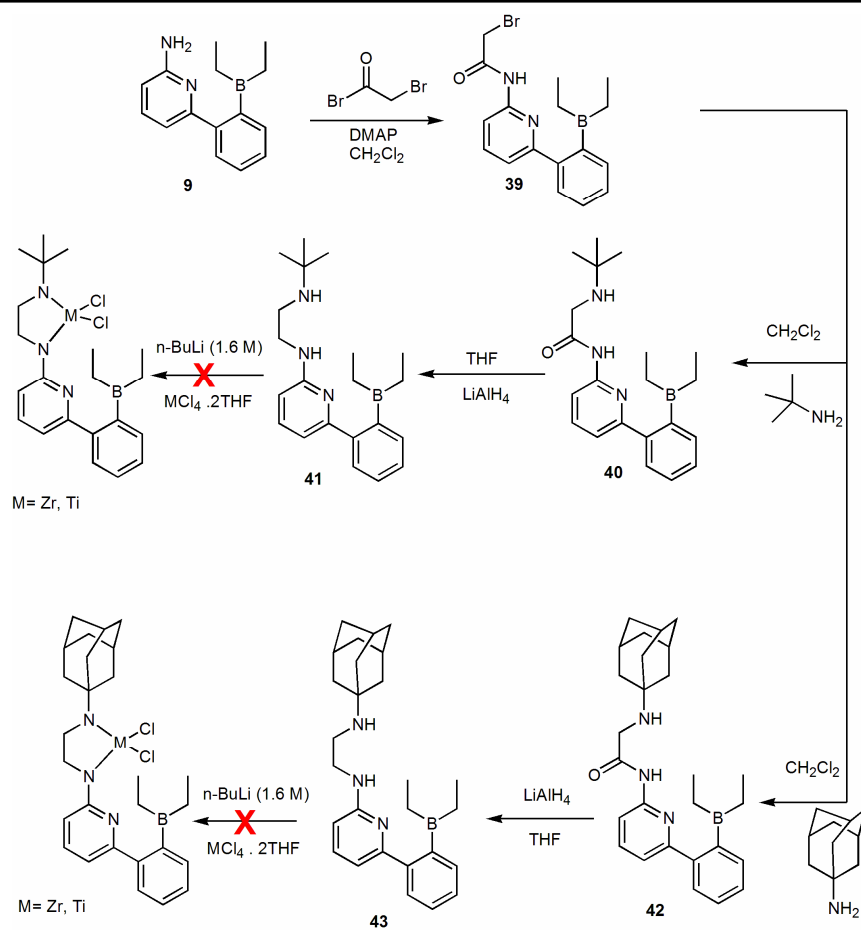
3.2.4 Unsuccessful synthesis of metal complexes

The attempted synthesis of the Zr- and Ti-based organometallic complexes prepared from **36**, **37** and **38** in diethyl ether using 2 equivalents of $n\text{-BuLi}$ to deprotonate the corresponding amine, followed by treatment with $\text{ZrCl}_4\cdot 2\text{THF}/\text{ZrCl}_4$ or $\text{TiCl}_4\cdot 2\text{THF}/\text{TiCl}_4$ in toluene at -36°C to room temperature and failed. An alternative approach that entailed the use of tetrakis(dimethylamido)zirconium (IV) and tetrakis(dimethylamido)titanium (IV) in toluene at various temperatures (70° to 130°C) was unsuccessful, too.



Scheme 3.8. Synthesis of compounds **35-38**.

An attempted synthesis of the Zr- and Ti-based organometallic complexes prepared from **41** and **43**, respectively, in diethyl ether using 2 equivalents of $n\text{-BuLi}$ to deprotonate the amine followed by treatment with $\text{ZrCl}_4\cdot 2\text{THF}/\text{ZrCl}_4$ or $\text{TiCl}_4\cdot 2\text{THF}/\text{TiCl}_4$ in toluene at -36°C to room temperature resulted in a black solution with formation of multiple products. In conclusion, the synthesis of both alkyl- and phenyl- bridged Zr- and Ti-based complexes containing the aminoborane moiety were unsuccessful.



Scheme 3.9. Synthesis of compounds 39-43.

Table 3.5. Crystallographic data of complexes **22**, **23** and **27**; Diffractometer: Bruker Kappa APEXII Duo; Structure solution: direct methods; Refinement: full matrix least squares.

	Complex No. 22	Complex No. 23	Complex No. 27
Empirical formula	C ₂₁ H ₂₅ BCl ₂ N ₂ Ti	C ₂₆ H ₃₅ BCl ₂ N ₂ Ti	C ₂₈ H ₄₁ BCl ₂ N ₂ SiTi
Formula weight	435.04	505.17	563.33
Temp.	100(2) K	100(2) K	100(2) K
Wavelength	0.71073 Å	0.71073 Å	0.71073 Å
Crystal system, space group	monoclinic, P2(1)/n	triclinic, p-1	monoclinic, P2(1)/c
Unit cell dimensions	a = 10.9979(11) Å alpha = 90 deg b = 16.1318(19) Å beta=106.79(6)deg c = 12.3324(11) Å gamma = 90 deg	a =9.2538(4) Å alpha=77.233(2)deg b =11.5135(5) Å beta=81.007(2) deg c =12.7779(6) Å gamma=72.946(2)deg	a =9.2509(4) Å alpha = 90 deg b =15.4881(6) Å beta = 98.239(3)deg c = 20.6554(10) Å gamma = 90 deg
Volume	2094.6(4) Å ³	1263.24(10) Å ³	2928.9(2) Å ³
Z, Calculated density	4, 1.380 Mg/m ³	2, 1.328 Mg/m ³	4, 1.277 Mg/m ³
Absorption coefficient	0.672 mm ⁻¹	0.567 mm ⁻¹	0.535 mm ⁻¹
F ₀₀₀	904	532	1192
Crystal size	0.22 x 0.19 x 0.08 mm	0.36 x 0.20 x 0.10 mm	0.22 x 0.16 x 0.14 mm
θ range for data collection	2.14 to 28.57 deg	1.64 to 28.49 deg	1.65 to 28.38 deg
Limiting indices	-14<=h<=14, -21<=k<=21, -14<=l<=16	-12<=h<=12, -15<=k<=15, -17<=l<=17	-12<=h<=12, -20<=k<=20, -27<=l<=24
Reflections collected /unique	19850 / 5240 [R(int) = 0.0584]	44991 / 6331 [R(int) = 0.0242]	51448 / 7311 [R(int) = 0.0452]
Completeness to theta	97.9 %	98.8 %	99.4 %
Max. and min. transmission	0.9482 and 0.8662	0.9444 and 0.8240	0.7454 and 0.7160
Refinement method	Full-matrix least-squares on F ²	Full-matrix least-squares on F ²	Full-matrix least-squares on F ²
Data / restraints / parameters	5240 / 0 / 247	6331 / 0 / 297	7311 / 0 / 326
Goodness of fit on F ²	1.047	1.039	1.049
Final R indices	R1 = 0.0418, wR2 = 0.0741	R1 = 0.0274, wR2 = 0.0712	R1 = 0.0355, wR2 = 0.0749
R indices (all data)	R1 = 0.0792, wR2 = 0.0804	R1 = 0.0360, wR2 = 0.0742	R1 = 0.0581, wR2 = 0.0798
Largest diff. peak and hole	0.403 and -0.291 e. Å ⁻³	0.362 and -0.257 e. Å ⁻³	0.392 and -0.391 e. Å ⁻³

3.3 Homopolymerization

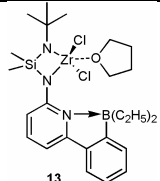
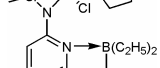
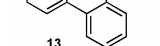
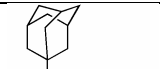
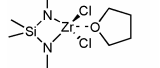
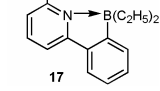
3.3.1 Homopolymerization of Ethylene

Group IV bisamido-complexes are known to present active precatalysts for olefin homo- and copolymerization.^[2, 23, 24] While non-bridged bisamido complexes showed comparably moderate activities (<20 kg of polymer/mol_{catalyst}·h·bar), the bridged analogues allow for activities of up to 350,000 kg/mol_{catalyst}·h, e.g., in the polymerization of 1-hexene,^[25, 26] however, typical values for PE and PP are in the range of 3.5-5300 and 7-320 kg/mol_{catalyst}·h·bar.^{[27] [28-30] [31, 32]} In all these polymerizations, both the polymerization kinetics and the activity are strongly influenced by the chelate ring size.^[30]

Homopolymerization of Ethylene (E) using Zr-(13 and 17) and Ti-based Precatalysts (22-24, 26 and 27)

The homopolymerization of E by the action of **13** and **17** was activated by methylaluminoxane (MAO) and produced highly linear PE with melting points in the range of 130< T_m <133°C (Table 3.6). Moderate activities up to 700 kg/mol_{catalyst}·h were observed. The molecular weights ranged from 325,000< M_n <4,000,000 g/mol.

Table 3.6. Results of E homopolymerization by the action of the Zr-based complexes **13** and **17** activated by MAO.

# ^a	Cat.	T (°C)	Productivity ^b	M_n (g/mol) ^c	PDI ^c	T_m (°C) ^d
1		50	212	1,800,000	9	133
2		65	215	1,000,000	11	130
3		90	700	900,000	8	132
4		50	350	325,000	11	133
5		65	480	n.d.	n.d.	133
6		90	550	4,000,000	7	132

^a Polymerization conditions: 500 mL autoclave, total volume of the reaction mixture: 250 mL, catalyst:MAO=1:2000, p=4 bar of E unless stated otherwise, toluene, $t=1$ h.; ^b kg/mol_{catalyst}·h.; ^c GPC data in 1,2,4-trichlorobenzene vs. PS; ^d measured by DSC; n.d.=not determined due to poor solubility.

Tables 3.6 and 3.7 summarize the results of E-homopolymerization with the Zr-based catalysts **13** and **17** and the Ti-based half-metallocene catalysts **22**, **23**, **24**, **26** and **27** at various temperatures i.e. 50, 65 and 90°C while keeping the E pressure constant at 4 bar. An increase in temperature resulted in an increase in activity and a constant E-uptake was observed over 60 minutes, especially in the case of catalysts **13** and **17**, which reflects that the catalyst was still active after this time. With increasing polymerization temperature the resulting polymer molecular weights dramatically decreased. This can be attributed to either an increasing β -H elimination reaction or an α -H elimination reaction followed by cross-metathesis with E.^{[33] [34]} The resulting poly(ethylene)'s T_m , molecular weights and molecular weight distributions (PDIs) were measured by DSC and GPC analysis, respectively. In most cases, broad molecular weight distributions were observed by GPC analysis (Table 3.6), GPC profiles of complex **13**-derived PE at various temperatures are shown in Figure 3.9.

The molecular weights of the resulting polymers were mainly dependent on the structure of the catalyst; a complex which contained bulky ligands produced high-molecular weight polymers. Complex **13** possesses a *tert*-butyl amido-type ligand, which is less bulky than the one in complex **17**, which contains an adamantyl amido-ligand. Variation of the molecular weights of polymers prepared from the Zr-based complexes **13** and **17** can be explained, by the bulky nature of the ligand around the metal centre.

In the homopolymerization of E with the Zr-based **13**, **17** and Ti-based complexes **22**, **24** and **26** mostly linear PE (HDPE) was obtained. High temperature ^{13}C NMR indicates that the obtained PE possessed virtually no branching evidenced in the high melting temperatures (T_m values 130 - 136°C) measured by DSC.^[35] ^{13}C NMRs of the resulting PE are shown in Figures 3.10, 3.11 and 3.12.

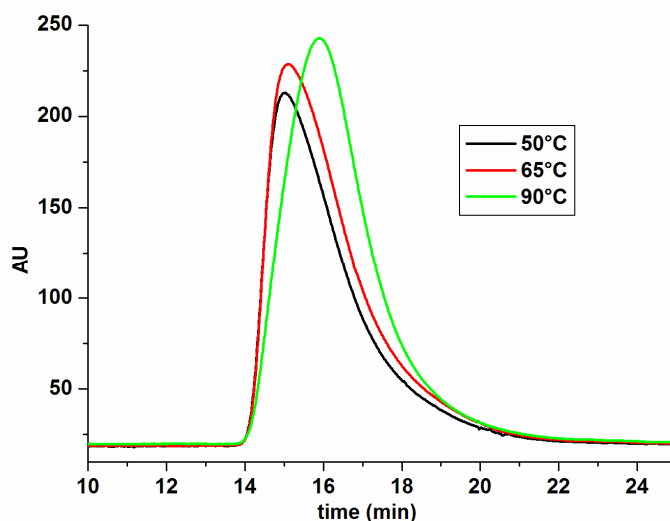

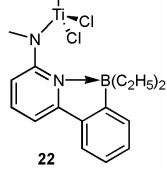
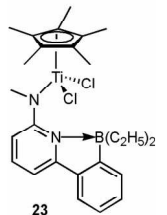
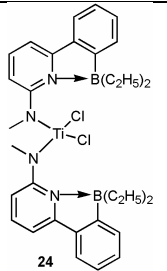
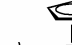
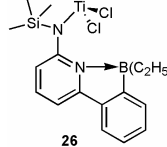


Figure 3.9. GPC graphs of complex **13**/MAO-derived PE at different polymerization temperatures (Table 3.6, entries 1-3).

Table 3.7. Results of E homopolymerization by the action of the Ti-based complexes **22**, **23**, **24**, **26** and **27** activated by MAO.

# ^a	Cat.	T (°C)	Productivity ^b	M _n (g/mol) ^c	PDI ^c	T _m (°C) ^d
1		50	50	1,800,000	1.65	132
2		65	75	900,000	2.7	133
3		90	22	800,000	2.1	130
4		50	50	3,000,000	17	115
5		65	65	n.d	n.d	130
6		90	65	1,500,000	6	132
7		50	1200	2,700,000	3.4	136
8		65	3000	700,000	4.7	134
9		90	3000	600,000	6	131
10		50	125	2,500,000	1.6	130
11		65	105	1,500,000	2.6	134
12		90	80	1,000,000	3.1	132

^a Polymerization conditions: 500 mL autoclave, total volume of the reaction mixture: 250 mL, catalyst:MAO=1:2000, p=4 bar of E unless stated otherwise, toluene, t=1 h; ^b kg/mol_{catalyst}·h; ^c GPC data in 1,2,4-trichlorobenzene vs PS; ^d measured by DSC; n.d.=not determined due to poor solubility.

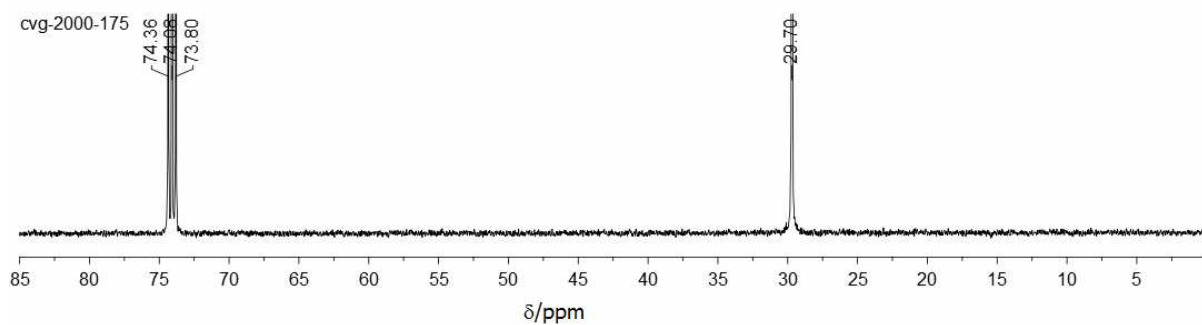


Figure 3.10. ¹³C NMR spectrum of PE produced by the action of **23/MAO** at 90° using 4 bar of E (Table 3.7, entry 6 in 1,1,2,2-[D₂]tetrachloroethane).

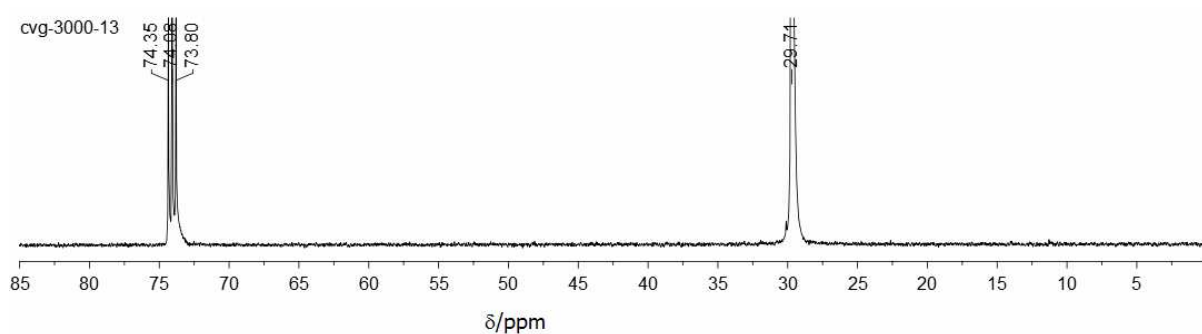


Figure 3.11. ¹³C NMR spectrum of PE produced by the action of **24/MAO** at 65°C using 4 bar of E (Table 3.7, entry 8 in 1,1,2,2-[D₂]tetrachloroethane).

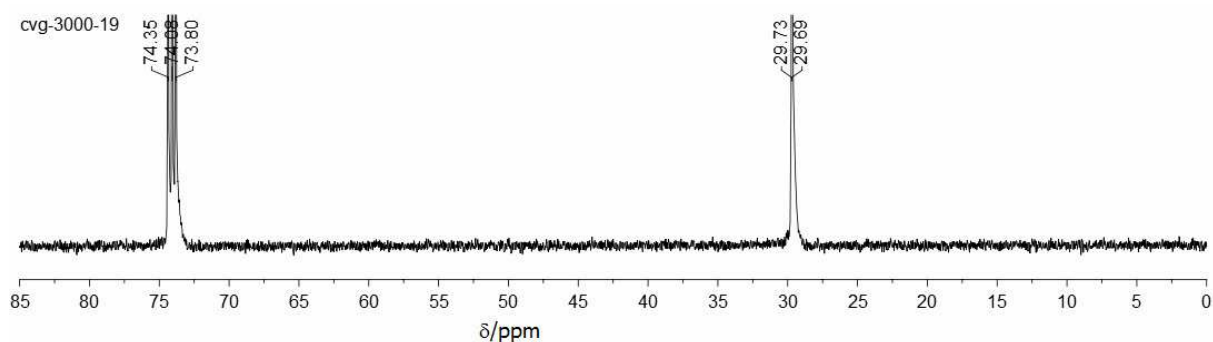


Figure 3.12. ¹³C NMR spectrum of PE produced by the action of **24/MAO** at 90°C using 4 bar of E (Table 3.7, entry 9 in 1,1,2,2-[D₂]tetrachloroethane).

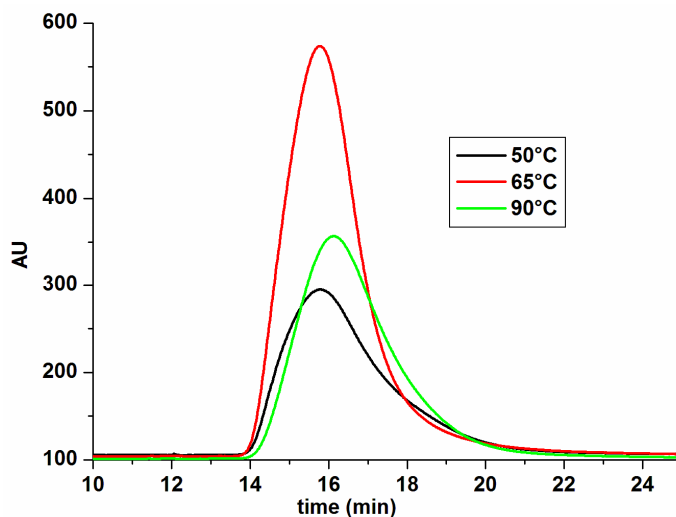


Figure 3.13. GPC graphs of complex **24**/MAO-derived PE at different polymerization temperatures (Table 3.7, entries 7-9).

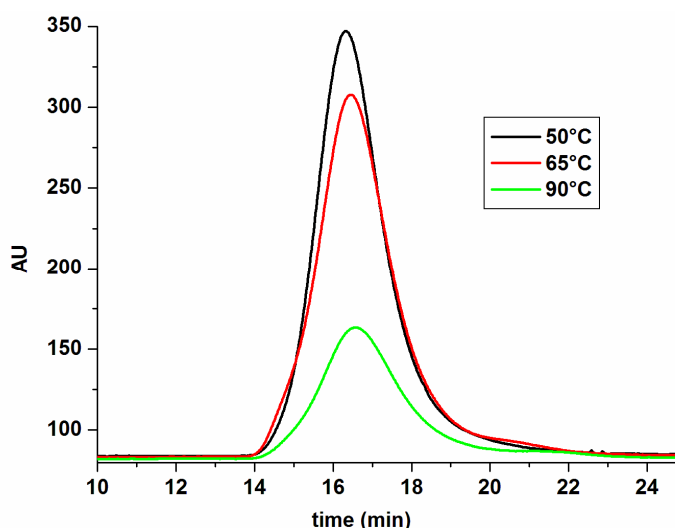


Figure 3.14. GPC graphs of complex **26**/MAO-derived PE at different polymerization temperatures (Table 3.7, entries 10-12).

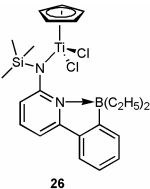
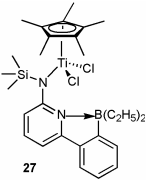
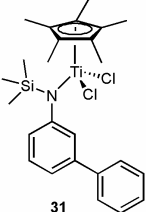
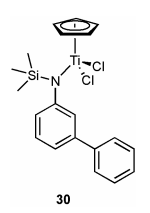
3.3.2 Homopolymerization of Styrene

The polymerization of styrene was first accomplished by Ishihara and co-workers^[36] with Ti-based half-metallocenes in the presence of MAO to yield syndiotactic polystyrene (*st*-PS). *st*-PS is a crystalline material with a high melting point (270°C) and good resistance to water and organic solvents at ambient temperature. Recent studies have identified mono(η^5 -cyclopentadienyl) complexes of group IV metals as efficient catalysts for styrene polymerization. While $[\text{Zr}(\eta^5\text{-C}_5\text{H}_5)]$ -based complexes are poorly syndioselective, the related Ti-complexes are effective in the stereocontrol of polystyrene.^[37-39]

In view of these results, we were interested to study the homopolymerization of styrene^[36, 37] by non-bridged half-titanocene^[40] complexes containing aminoborane moiety of the formula $\text{Cp}^*\text{TiCl}_2(\text{N}(6\text{-}(2\text{-(diethylboryl)phenyl)-pyrid-2-yl)R})$; $\text{R}=\text{Si}(\text{CH}_3)_3$ (**26**, **27**), $\text{Cp}'=\text{Cp}$ (**26**), Cp^* (**27**) and by the aminoborane-free model complexes of the general formula $\text{Cp}^*\text{TiCl}_2(\text{N}(\text{biphenyl-3-yl})\text{SiMe}_3)$; ($\text{Cp}'=\text{Cp}$ (**30**), Cp^* (**31**)) ($\text{Cp}=\text{cyclopentadienyl}$; $\text{Cp}^*=\text{pentamethylcyclopentadienyl}$) using MAO as co-catalyst at various temperatures and monomer concentrations. The results are summarized in Table 3.8. The catalytic activity increased with increasing polymerization temperature, while the resulting polymer number-average molecular weights decreased. The aminoborane-free model complexes **30/MAO** and **31/MAO** showed better performance in terms of catalytic activity than the **26/MAO** and **27/MAO** systems, respectively. All complexes produced a MAO mixture of atactic 'at' (around 10%, *at*-PS) and syndiotactic 'st' PS (around 90%, *st*-PS), from which the *st*-PS was isolated from boiling acetone via filtration. The number-average molecular weight of the resulting *st*-PS was affected by the nature of the Cp ligand; thus the introduction of methyl donor groups, which additionally exert a steric hindrance to the cyclopentadienyl ligand, was effective for obtaining high molecular weight *st*-PS. This could be due to a reduced propensity for α/β -H elimination reactions, so that the molecular weight of the resulting *st*-PS increases and leaving the polydispersity index in the range of $1.24 < \text{PDI} < 2.05$. The observed number-average molecular weights (M_n) of the resulting *st*-PS derived from non-bridged half-titanocenes increased in the order of $\text{Cp}^*\text{TiCl}_2(\text{N}(\text{biphenyl-3-yl})\text{SiMe}_3)$ (**31**) > $\text{Cp}^*\text{TiCl}_2(\text{N}(6\text{-}(2\text{-(diethylboryl)phenyl)-pyrid-2-yl})\text{Si}(\text{Me})_3)$ (**27**) > $\text{CpTiCl}_2(\text{N}(\text{biphenyl-3-yl})\text{SiMe}_3)$ (**30**) > $\text{CpTiCl}_2(\text{N}(6\text{-}(2\text{-(diethylboryl)phenyl)-pyrid-2-yl})\text{Si}(\text{Me})_3)$ (**26**).

The ^{13}C NMR of *st*-PS in $\text{C}_2\text{D}_2\text{Cl}_4$ reveals the typical signals of *st*-PS at $\delta=145.1$ (C_{ipso} of Ph), $\delta=127.8, 127.5$ (*o*- and *m*-CH of Ph), $\delta=125.5$ (*p*-CH of Ph), $\delta=43.4$ (CH) and 40.3 (CH_2) ppm (Figure 3.15).^[39] The presence of a sharp signal for the quaternary carbon of the phenyl ring at $\delta=145.1$ ppm revealed that the polymer was highly *st*-PS.

Table 3.8. Results of styrene homopolymerization by the action of **26**, **27**, **30** and **31**/MAO.

# ^a	Cat.	Cat : MAO : Styrene	T (°C)	Productivity ^a	M_n (g/ mol) ^b	PDI ^b
1		1: 1500 : 5000	50	300	97,000	1.51
2		1: 1500 : 5000	60	900	53,000	1.57
3		1: 1500 : 5000	75	1100	29,000	1.63
4	26	1: 1500 : 15000	50	500	160,000	1.52
5		1: 1500 : 15000	60	1000	105,000	1.30
6		1: 1500 : 15000	75	1100	84,000	1.66
7		1: 1500 : 5000	50	0	--	--
8	27	1: 1500 : 5000	60	115	445,000	1.37
9		1: 1500 : 5000	75	285	273,000	1.53
10		1: 1500 : 5000	50	550	559,000	1.59
11		1: 1500 : 5000	60	1200	1,065,000	1.45
12	31	1: 1500 : 5000	75	1600	1,400,000	1.38
13		1: 1500 : 15000	50	700	1,000,000	1.72
14		1: 1500 : 15000	60	3500	930,000	1.41
15		1: 1500 : 15000	75	5000	960,000	1.24
16		1: 1500 : 5000	50	720	97,000	1.76
17		1: 1500 : 5000	60	1100	65,000	1.56
18	30	1: 1500 : 5000	75	1360	36,000	2.0
19		1: 1500 : 15000	50	1700	188,000	1.58
20		1: 1500 : 15000	60	2638	83,000	2.1
21		1: 1500 : 15000	75	2978	30,000	1.94

^a Polymerization conditions: 50 mL of toluene, $t=15$ min; ^b kg_s-sPS/mol_{catalyst}h; ^c GPC data in 1,2,4-trichlorobenzene vs PS.

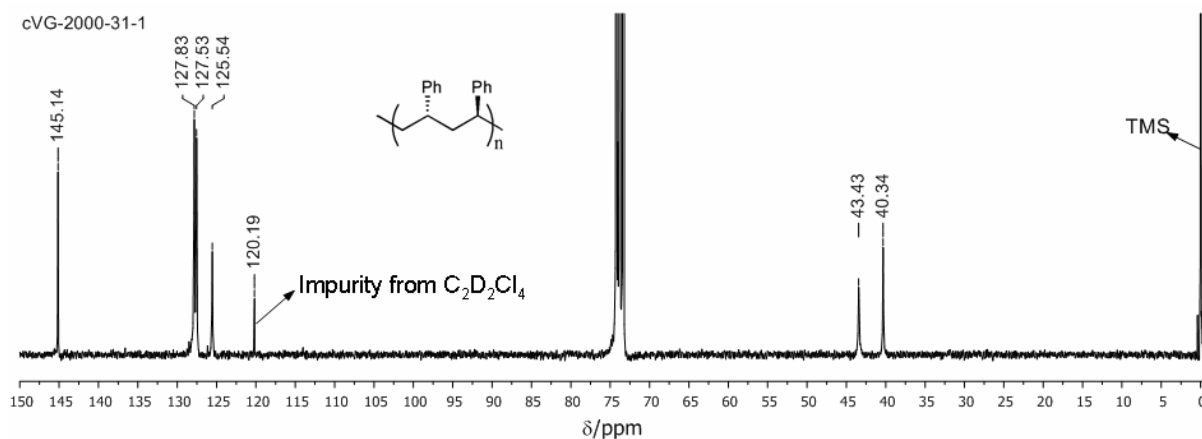


Figure 3.15. ^{13}C NMR of *st*-PS derived from the non-bridged half-titanocene complex **27**/MAO (in 1,1,2,2- $[\text{D}_2]$ tetrachloroethane)

3.4 Copolymerizations

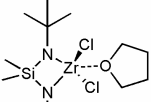
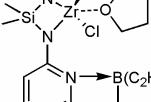
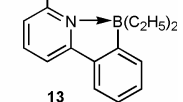
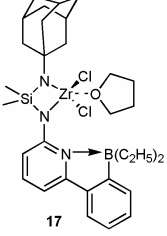
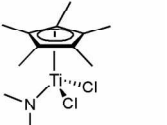
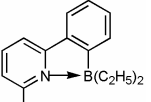
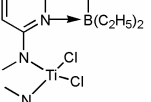
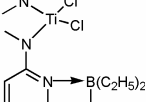
3.4.1 Copolymerization of E with cyclopentene (CPE)

The copolymerization of E with CPE was carried out with the Zr-complexes **13** and **17** at 50°C . Polymerization results are summarized in Table 3.9. One important effect was observed in the copolymerization of E with CPE in toluene at 50°C by the action of **13**/MAO using different concentrations of CPE. Thus, no CPE-incorporation was detected by NMR up to 20 vol.-% of CPE, at a further increase to 40 vol.-% of CPE in the reaction mixture a ≤ 4 mol-% incorporation of CPE was observed. One important note in this copolymerization is that during the polymerization the reaction temperature gradually increased from 50 to 95°C during the reaction time of 60 min. and a continuous ethylene uptake was observed until closing the E-valve. Due to this strongly exothermic event, the number-average molecular weight of the resulting polymer decreased. However, the activity increased from 2300 to 30,000 $\text{kg}_{\text{polymer}}/\text{mol}_{\text{catalyst}}\cdot\text{h}$ (Table 3.9, entries 1, 4) by increasing CPE concentration from 2 to 40 vol.-% in the reaction mixture. In this case, PE with number-average molecular weights between 50,000 and 900,000 g/mol (PDI in the range of 1.5 to 2.5) and $127^\circ < T_m < 134^\circ\text{C}$ was produced.

In the case of complex **24**, the copolymerization of E with CPE was carried out at 50 and 70°C with various CPE concentrations (10 vol.-% and 25 vol.-%) (Table 3.9, entries 8-11). The observed activities were in the range of 800-1100 $\text{Kg PE}/\text{mol}_{\text{catalyst}}\cdot\text{h}$, and catalyst activity decreased with increasing CPE concentration. The resulting polymer number-average molecular weights also decreased. Generally, the activity of the Ti-based complexes was low

compared to corresponding Zr-based complex **13** and the polymers derived from the Ti-based complexes were mostly linear PE without any noticeable incorporation of CPE.

Table 3.9. Results of E homopolymerization in the presence of CPE by the action of complexes **13**, **23** and **24** activated by MAO.

# ^a	Cat.	CPE (vol.-%)	T (°C)	Productivity ^b	M _n (g/mol) ^c	X ^d [mol %]	PDI ^c	T _m (°C) ^e
1		2	50	2300	900,000	0	2.3	132
2		5	50	12,000	600,000	0	1.56	134
3		20	50	9000	100,000	0	2.7	128
4	13	40	50	30,000	50,000	3.5	2.5	127
5		2	70	11,000	190,000	0	1.64	135
6		2	50	60	2,800,000	0	2.3	129
7	23	2	70	77	n.d	0	n.d	130
8		10	50	1000	2,500,000	0	3.3	132
9		25	50	800	400,000	< 0.3	2.5	130
10		10	70	1100	700,000	0	1.83	132
11	24	25	70	900	1,700,000	0	1.84	130

^a Polymerization conditions: 500 mL autoclave, total volume of the reaction mixture: 250 mL, p=4 bar of E unless stated otherwise, catalyst: MAO= 1: 2000; toluene, t=1 h; ^b kg/mol_{catalyst}·h; ^c GPC data in 1,2,4-trichlorobenzene vs. PS; ^d co-monomer content in the copolymer [mol-%] as estimated by ¹³C NMR spectroscopy; ^e measured by DSC; n.d.=not determined due to poor solubility.

Figure 3.16 illustrates the GPC-traces of the polymerizations of E in the presence of varying amount of CPE. The gradual increase in the CPE feed leads to a decrease in the

resulting polymer number-average molecular weight, suggesting that elimination reactions become more dominant.

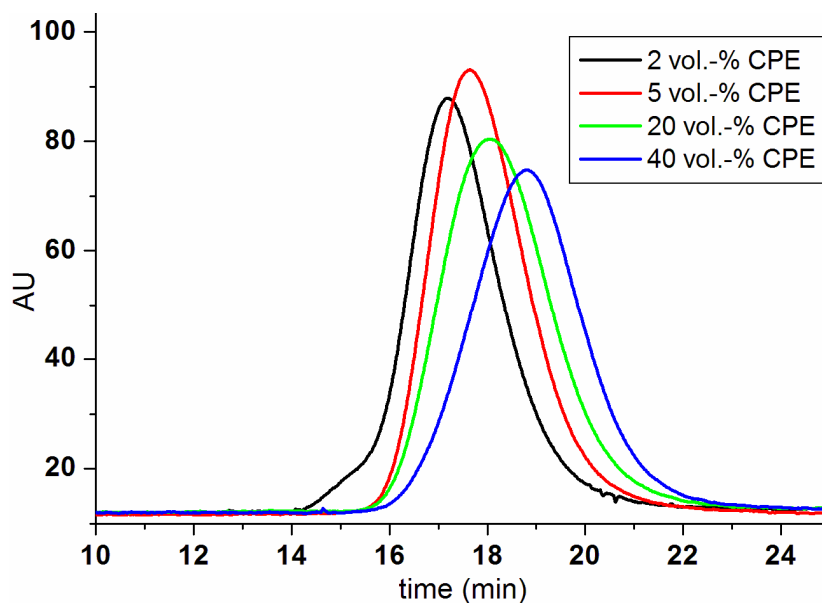


Figure 3.16. GPC graphs of complex **13**/MAO-derived PE in the presence of CPE at 50°C (Table 3.9, entries 1-4).

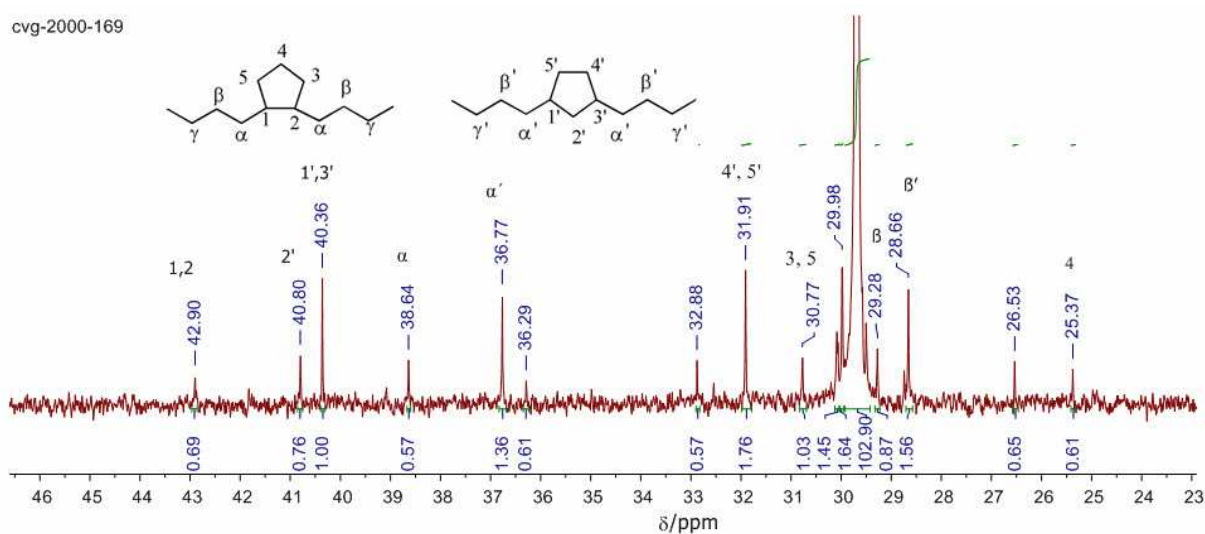


Figure 3.17. ^{13}C NMR of complex **13**/MAO-derived poly(E-*co*-CPE) using 40 vol.-% of CPE (Table 3.9, entry 4 in 1,1,2,2- $[\text{D}_2]$ tetrachloroethane).

Figure 3.17 shows the ^{13}C NMR spectrum of poly(E)-*co*-poly(CPE)_{vinyl} prepared in the presence of 40 vol.-% CPE (Table 3.9, entry 4). Approx. 4 mol-% of CPE incorporation can be detected by ^{13}C NMR. Apart from the signal for linear PE at $\delta=29.68$ ppm, the signals at $\delta=31.9$ ($\text{C}_{4',5'}$), 40.3 ($\text{C}_{1',3'}$) and 40.8 ($\text{C}_{2'}$) are typical for 1,3-incorporated CPE units that are

formed via 1,2-insertion of CPE followed by β -H elimination and subsequent reinsertion^[41-44] and the signals at $\delta=42.9$ ($C_{1,2}$), 30.7 ($C_{3,5}$) and $\delta=25.3$ (4) are assigned to isolated 1,2-incorporated CPE units in the E sequence.

The role of the aminoborane ligand in polymerization of E in the presence of CPE was investigated in a previous paper^[34] using the aminoborane-free model catalyst $\{\text{Me}_2\text{Si}(\text{N}(2\text{-}i\text{Pr-biphenyl-3-yl}))_2\}\text{ZrCl}_2\cdot\text{THF}$. With this precatalyst the polymerization of E in the presence of 60 vol.-% of CPE resulted PE activities of 25,000 $\text{kg/mol}_{\text{catalyst}}\cdot\text{h}$ are observed without any noticeable CPE incorporation (compared to 30,000 $\text{kg/mol}_{\text{catalyst}}\cdot\text{h}$ for **13/MAO** using 40 vol.-% of CPE, Table 3.9, entry 4). The activities of both the aminoborane-free Zr-based complex $\{\text{Me}_2\text{Si}(\text{N}(2\text{-}i\text{Pr-biphenyl-3-yl}))_2\}\text{ZrCl}_2\cdot\text{THF}$ and aminoborane-containing complex **13/MAO** can be enhanced up to a factor of 15 by increasing the CPE concentration from 2 to 40-60 vol.-% of CPE. Since CPE was hardly incorporated into the polymer chain (≤ 4 mol-%), it must preferably serve as a stabilizing ligand/chain transfer agent, reversibly coordinating to the cationic Zr-center. After β -H elimination, most probably from an E as the last inserted monomer, the terminal alkene is then replaced by CPE, which inserts into the Zr-H bond and starts a new polymer chain.^[34]

3.4.2 Copolymerization of E with norborn-2-ene (NBE) using the Zr-based precatalysts **13** and **17**

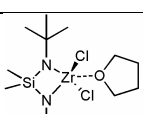
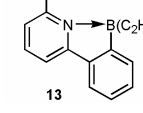
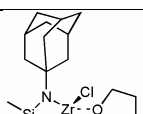
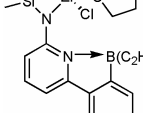
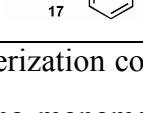
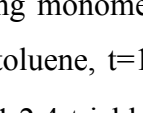
Recently, our group reported on group IV catalysts bearing the aminoborane motif, activated by MAO, which undergo α -H elimination/ α -H addition process, with both VIP and ROMP occurring within the same polymer chain at high concentration of the cyclic olefins allowing for the formation of $\text{poly}(\text{NBE})_{\text{ROMP-co-poly}}(\text{NBE})_{\text{VIP-co-poly}}(\text{E})$ as demonstrated for a $(\eta^5\text{-tetramethylcyclopentadienyl})\text{dimethylsilylamido-Ti}^{\text{IV}}$ and a Zr^{IV} -bisamido system.^[19, 34] To check for the propensity of other Zr^{IV} -bisamido systems and Ti-based half-metallocenes (Figure 3.1) bearing the same aminoborane motif to promote the formation of such copolymers, we used the Zr-based complexes **13** and **17** and the Ti-based complexes **22**, **23**, **24**, **26** and **27** containing Cp and Cp* ligands in the copolymerization of E with NBE.

It turned out that the Zr-based complexes **13** and **17** allowed for formation of vinyl insertion copolymerization-derived $\text{poly}(\text{E})\text{-co-poly}(\text{NBE})_{\text{VIP}}$ with activities between 7 and 2000 $\text{kg}_{\text{polymer}}/\text{mol}_{\text{cat}}\cdot\text{h}$ using both low and high NBE concentrations at various temperatures and pressures. The results are summarized in Tables 3.10 – 3.12.

Table 3.10 summarizes the results of copolymerization of E with NBE at various temperatures yielding $\text{poly}(\text{E})\text{-co-poly}(\text{NBE})_{\text{VIP}}$. In most cases an increase in polymerization

temperature resulted in an increase in catalytic activity, concomitantly, the NBE content in the resulting copolymer increased up to $T=90^{\circ}\text{C}$. However, a further increase in the polymerization temperature causes a decrease in catalytic activity and incorporation of NBE. In the ^{13}C NMR spectrum of poly(E)-*co*-poly(NBE)_{VIP} obtained by the action **13** and **17** (Figures 3.18 and 3.19), the signals characteristic for both alternating (E-N-E-N) and isolated (E-N-E-E-E-E) NBE sequences were observed and assigned as follows: $\delta=47.8$, 47.0 (2 signals, C₂/C₃), 42.0, 41.5 (2 signals, C₁/C₄), 32.8 (C₇), and 30.7-29.0 ppm (C₅/C₆, PE, all C₂D₂Cl₄). The copolymers contained mainly isolated NBE units with only few alternating (*st/it*-) E-NBE diads^[11, 13, 14, 45-47]. Signals assignable to NBE-NBE diads and NBE-NBE-NBE triads were absent. None of the copolymers showed signals for ROMP-derived poly(NBE)_{ROMP}, at various temperatures using 4 bar of E. As expected, an increase in polymerization temperature resulted in a decrease in the number-average molecular weight of the resulting polymer.

Table 3.10. Results of E-NBE copolymerization by the action of complexes **13**, **17**/MAO at various temperatures.

# ^a	Cat.	<i>T</i> (°C)	Productivity ^b	NBE content (mol-%) ^c	<i>M_n</i> (g/mol) ^d	PDI ^d	<i>T_m</i> (°C) ^e
1		50	30	1	1,300,000	3.5	123
2		70	180	3.5	550,000	2.9	99
3		90	240	20	540,000	2.2	73
4	13	110	110	2.7	350,000	3.3	124
5		50	165	4.2	1,400,000	2.0	119
6		70	275	7.7	800,000	1.76	96
7		90	165	8.9	400,000	2.3	124

^a Polymerization conditions: 500 mL autoclave, total volume of the reaction mixture: 250 mL (including monomer), $p=4$ bar of E unless stated otherwise, catalyst: MAO: NBE=1: 2000: 20000, toluene, $t=1$ h; ^b kg_{polymer}/mol_{catalyst}·h; ^c NBE content estimated by ^{13}C NMR; ^d GPC data in 1,2,4-trichlorobenzene vs. PS; ^e measured by DSC; n.d.=not determined due to poor solubility.

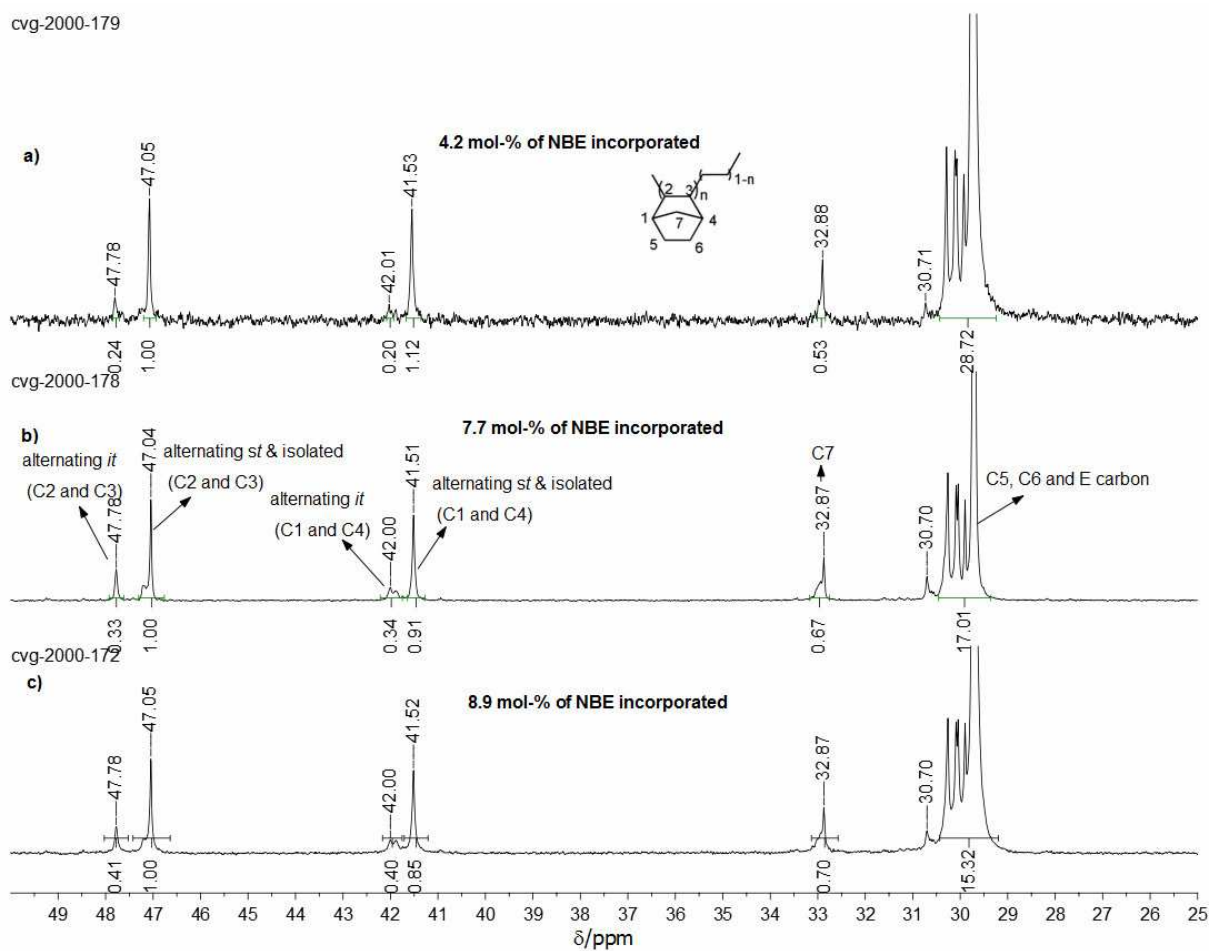


Figure 3.18. Complex 17/MAO-derived poly(E)-*co*-poly(NBE)_{VIP} (a) at 50°C; (b) at 70°C; (c) at 90°C (Table 3.10, entries 5, 6 and 7 in 1,1,2,2-[D₂]tetrachloroethane).

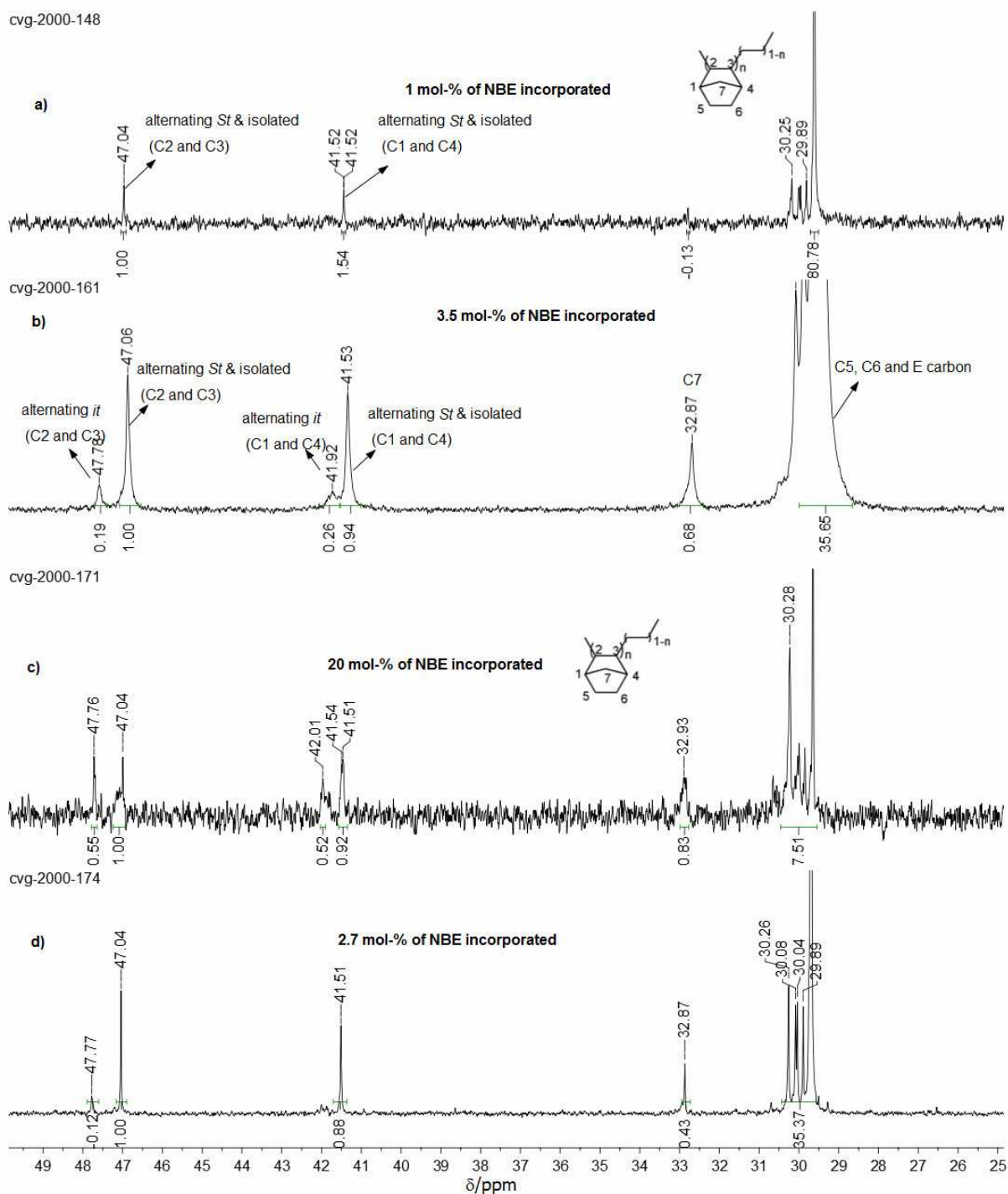


Figure 3.19. Complex 13/MAO derived poly(E)-*co*-poly(NBE)_{VIP} (a) at 50°; (b) at 70°; (c) at 90°C; (d) at 110° C (Table 3.10, entries 1, 2, 3 and 4 in 1,1,2,2-[D₂]tetrachloroethane).

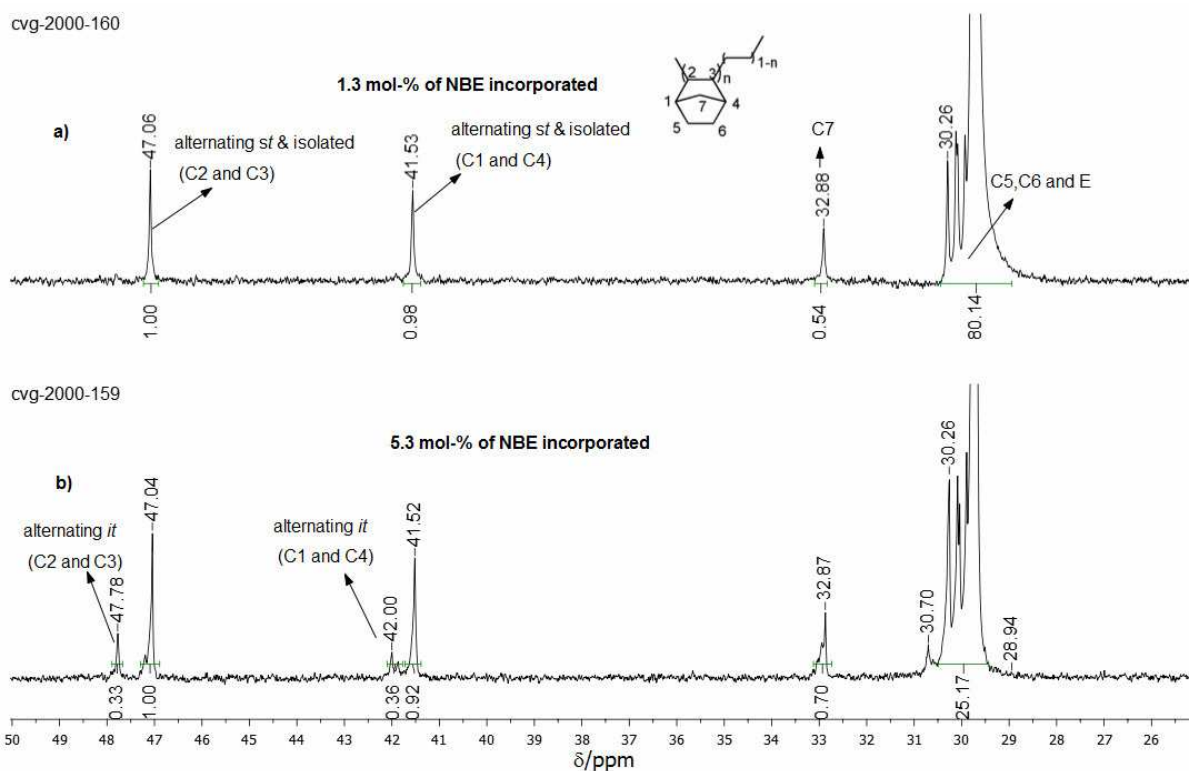
Table 3.11 summarizes the copolymerization of E with NBE at 70°C using different ratios of NBE with respect to the catalyst, resulting in the formation of poly(E)-*co*-poly(NBE)_{VIP}. The influence of the NBE concentration on the outcome of the copolymerization of E with NBE was investigated and these results clearly show first an increase and then a sharp decrease of catalytic activity and NBE incorporation in the resulting

polymer backbone, with increasing NBE concentration.^[45] The number-average molecular weights of the copolymers increased from 450,000 to 550,000 g/mol with increasing NBE concentration from 5000 equivalents to 60,000 equivalents with respect to catalyst and monomodal molecular weight distributions (PDIs) were obtained in the range of $2.4 < \text{PDI} < 3.0$, respectively.

Table 3.11. Results of E-NBE copolymerization by the action of **13/MAO** at different NBE concentrations.

# a	Cat.	Cat:MAO: NBE	Productivity ^b	NBE content (mol-%) ^c	M_n (g/mol) ^d	PDI ^d	T_m (°C) ^e
1		1: 2000: 5000	75	1.3	450,000	3.0	123
2		1: 2000: 10,000	330	5.3	500,000	2.4	115
3		1: 2000: 20,000	180	3.4	550,000	2.9	99
4		1: 2000: 60,000	90	< 2	n.d	n.d	--

^a Polymerization conditions: 500 mL autoclave, total volume of reaction mixture: 250 mL (including monomer), $T = 70^\circ\text{C}$, $p = 4$ bar of E unless stated otherwise, toluene, $t = 1$ h; ^b kg/mol_{catalyst}·h; ^c NBE content estimated by ¹³C NMR ^d GPC data in 1,2,4-trichlorobenzene vs. PS; ^e measured by DSC; n.d.=not determined due to poor solubility.



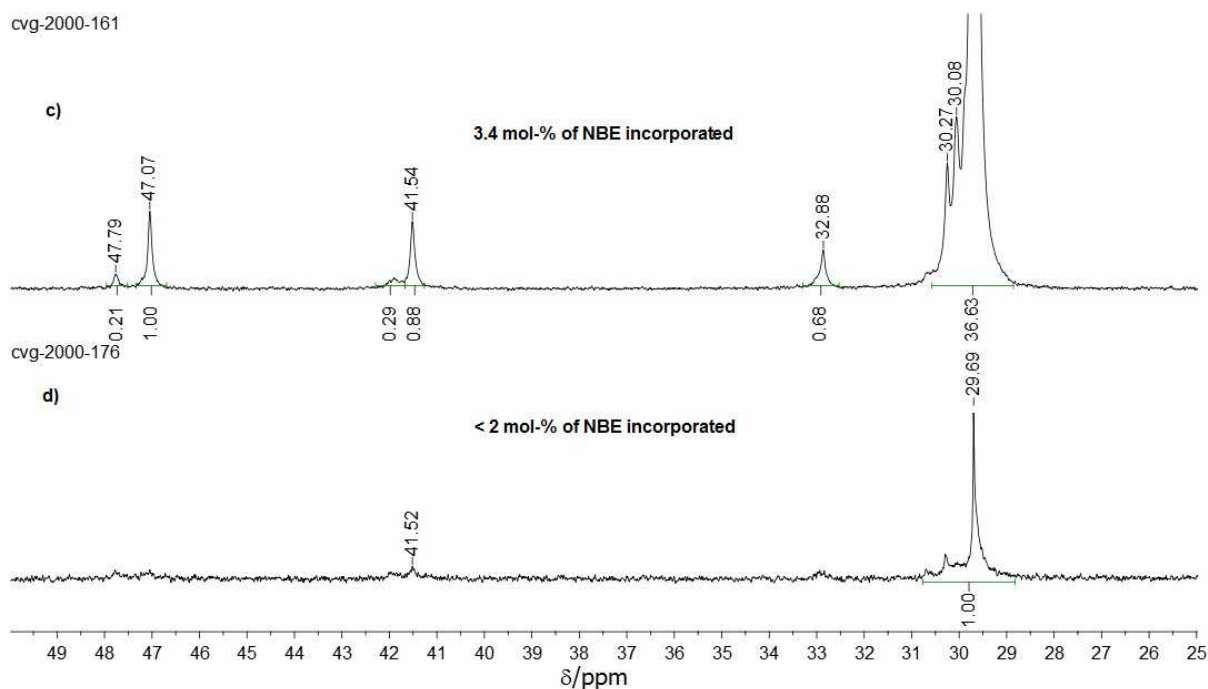
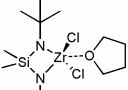
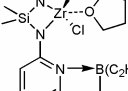
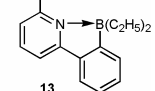
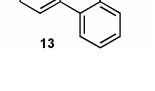
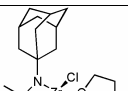
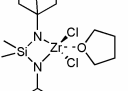
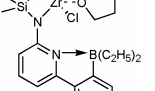
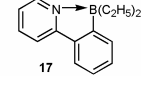


Figure 3.20. Complex **13**/MAO derived poly(E)-*co*-poly(NBE)_{VIP} using (a) cat: MAO: NBE (1: 2000: 5000); (b) cat: MAO: NBE (1: 2000: 10,000); (c) cat: MAO: NBE (1: 2000: 20,000); (d) cat: MAO: NBE (1: 2000: 60,000) (Table 3.11, entries 1, 2, 3 and 4 in 1,1,2,2-[D₂]tetrachloroethane).

Table 3.12 summarizes the copolymerization results of E with NBE at different pressures using the Zr-based complexes **13** and **17**. An increase in the E-pressure leads to an increase in catalytic activity and a reduced incorporation of NBE in the resulting copolymers. Complex **13**/MAO-derived poly(E)-*co*-poly(NBE)_{VIP} shows up to 36 mol-% of NBE incorporation at 70°C using 1 bar of E. Clearly, at a low E-pressure (1 bar), the incorporation of NBE is higher than at high pressure (p=4 bar). In fact, the observed 36 mol-% of NBE incorporation is so far the higher for all Zr- (**13** and **17**) and Ti- (**22**, **23**, **24**, **26** and **27**) derived poly(E)-*co*-poly(NBE)_{VIP}. In the copolymerization of E with NBE, complex **17** is less active as compared to complex **13**, also the incorporation of NBE was low and there was no significant difference in NBE incorporation at 1 and 2 bar of E at 70°C (Table 3.12, entries 6 and 7). Upon activation with MAO, both complexes **13** and **17** showed very low activity (Table 3.12, entries 4 and 9) at 30°C and 2 bar of E. Typical ¹³C NMR spectra are shown in Figures 3.21 and 3.22, respectively.

Table 3.12. Results of E-NBE copolymerization by the action of complexes **13/MAO** and **17/MAO** at various temperature and pressures.

# ^a	Cat	<i>T</i> (°C) / <i>p</i> (bar)	Productivity _b	NBE content (mol-%) ^c	<i>M_n</i> (g/mol) ^d	PDI ^d	<i>T_m</i> (°C) ^e
1 ^f		70/ 1	400	36	n.d	n.d	--
2 ^f		70, 2	1800		n.d	n.d	94
3 ^f		70/ 4	2000	6	300,000	1.69	95
4 ^f	13 	30/ 2	9.0	10	n.d	n.d	--
5 ^f		50/ 2	70	19.3	800,000	1.60	124
6		70/ 1	25	14.7	n.d	n.d	--
7		70/ 2	155	12.1	350,000	1.66	77
8		70/ 4	275	7.8	800,000	1.76	96
9	17 	30/ 2	7	n.d	n.d	n.d	--

^a Polymerization conditions: 500 mL autoclave, total volume of the reaction mixture: 250 mL (including monomer), toluene, *t*=1 h, catalyst: MAO: NBE=1: 2000: 20000; ^b kg/mol_{catalyst}·h; ^c NBE content estimated by ¹³C NMR; ^d GPC data in 1,2,4-trichlorobenzene vs. PS; ^e measured by DSC; ^f solvent, MAO, NBE and catalyst added together into the reactor and heated to desired temperature, then E pressure was applied; n.d.=not determined due to poor solubility.

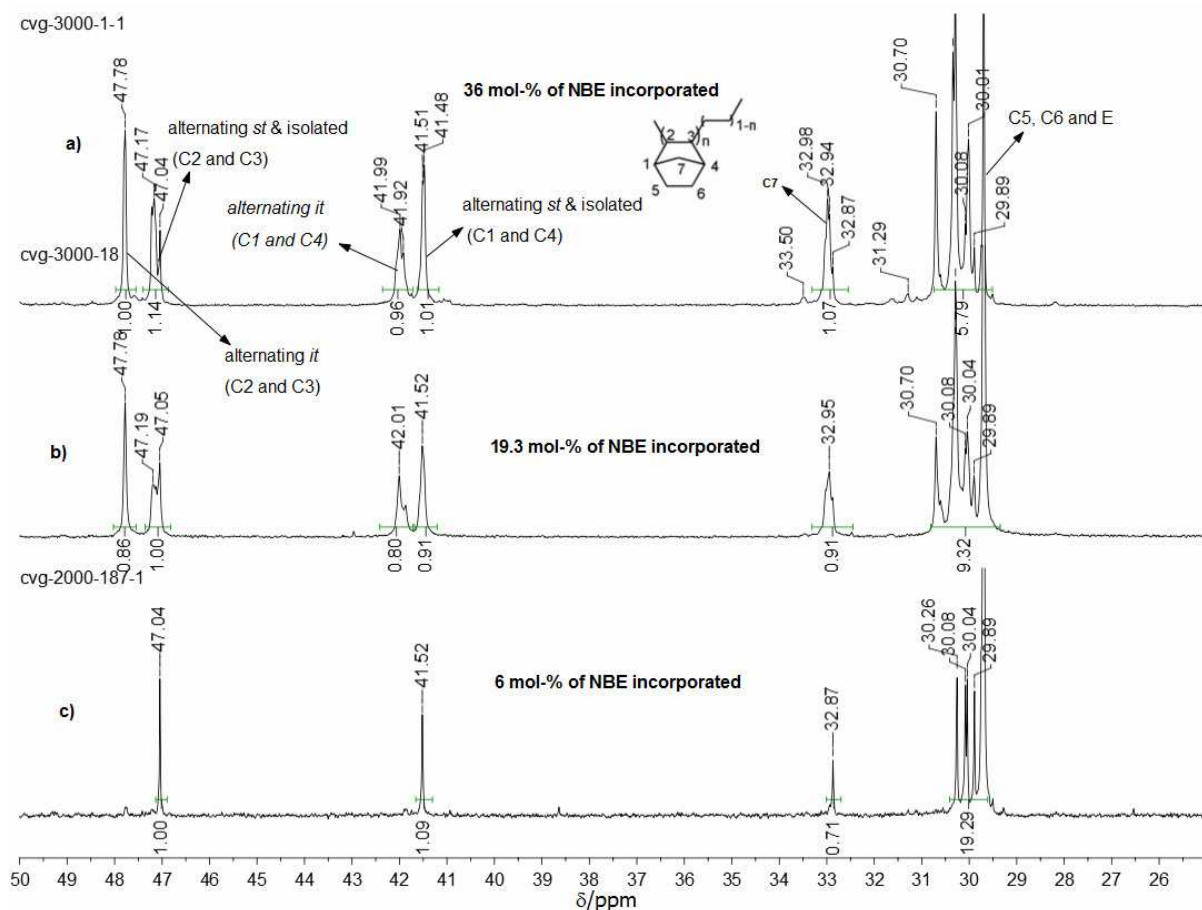


Figure 3.21. Complex **13**/MAO derived poly(E)-*co*-poly(NBE)_{VIP} at (a) 70°C using 1 bar of E; (b) 50°C using 2 bar of E; (c) 70°C using 4 bar of E, (Table 3.12, entries 1, 5 and 3 in 1,1,2,2-[D₂]tetrachloroethane).

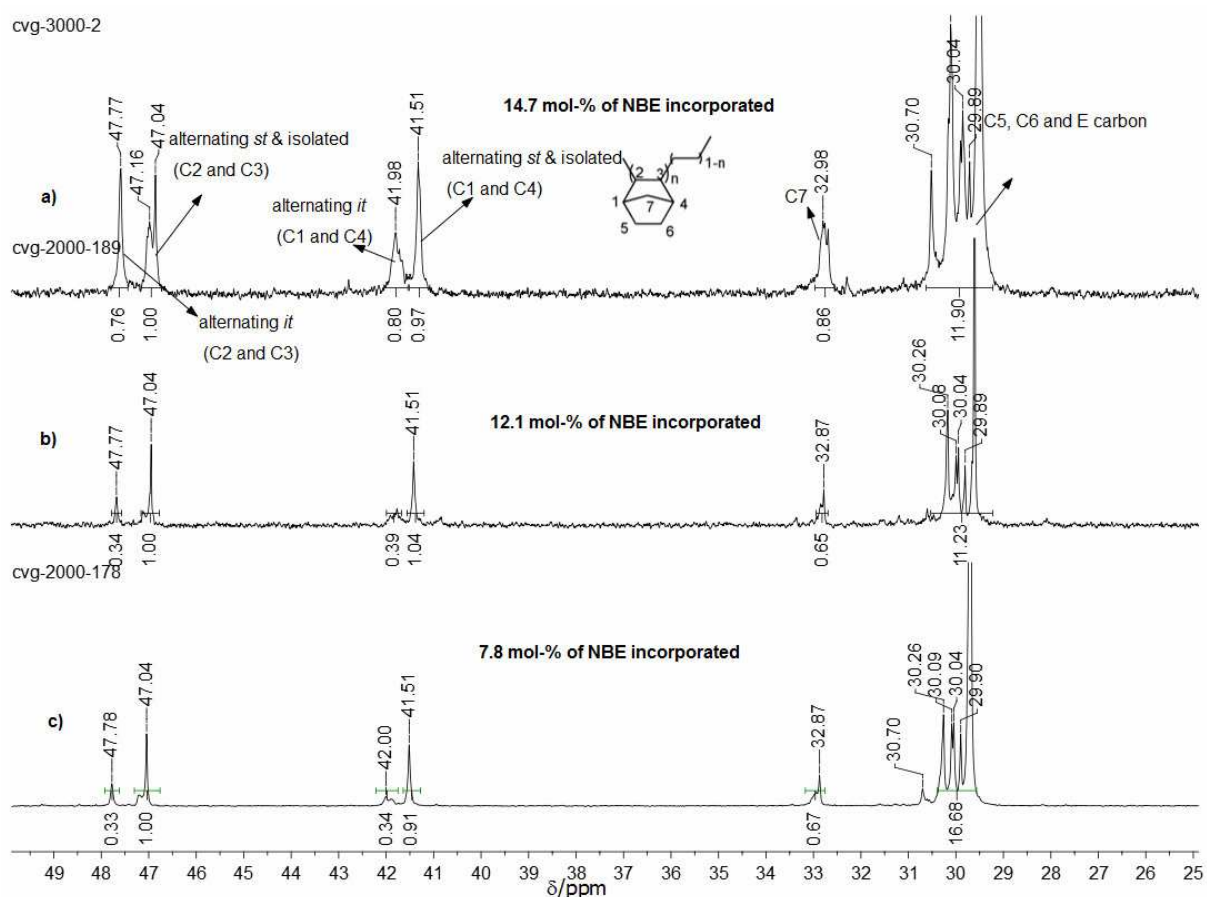


Figure 3.22. Complex **17**/MAO-derived poly(E)-*co*-poly(NBE)_{VIP} obtained at (a) 70°C using 1 bar of E; (b) 70°C using 2 bar of E; (c) 70°C using 4 bar of E (Table 3.12, entries 6, 7 and 8 in 1,1,2,2-[D₂]tetrachloroethane).

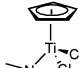
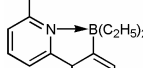
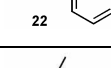
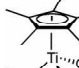
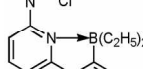
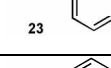
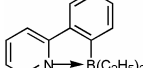
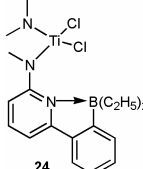
3.4.3 Copolymerization of E with NBE using the Ti-based complexes **22**, **23**, **24**, **26** and **27**

Various non-bridged half-titanocene complexes of the general formula Cp'TiCl₂(N(6-(2-(diethylboryl)phenyl)pyrid-2-yl)R); R=Me (**22**, **23**), Si(CH₃)₃ (**26**, **27**), Cp'=Cp (**22** and **26**), Cp* (**23** and **27**) and Ti-based metallocene-type TiCl₂ [(N(6-(2-(diethylboryl)phenyl)pyrid-2-yl)Me)]₂ (**24**) have been investigated towards their capabilities to copolymerize E with NBE. All these complexes are mainly producing poly(E)-*co*-poly(NBE)_{VIP} copolymers at high E pressure (4 bar) and various temperatures, with moderate activities (up to 500 Kg_{polymer}/mol.Ti·h) and an NBE incorporation up to 12.5 mol-% (Table 3.13). Interestingly, at low pressures (2 bar), complex **23**/MAO produced both ROMP- and VIP derived structures within the same polymer chain, thereby forming poly(NBE)_{ROMP}-*co*-poly(NBE)_{VIP}-*co*-poly(E)-type copolymers. Typical ¹H and ¹³C NMR spectra are shown in Figure 3.23. The structure of this particular copolymer can in fact be explained by a reversible α-H

elimination/ α -H addition process, where both VIP and ROMP occurred within the same polymer chain. The signal at $\delta=133.17$ corresponds to the ROMP-derived polymer olefinic signal, those at $\delta=47.78$ and 41.9 ppm correspond to the alternating *it* VIP-derived E-NBE diads and the signals at $\delta=47.04$ - 47.17 and 41.5 ppm correspond to the alternating *st* and isolated VIP-derived E-NBE sequences, while the signal at $\delta=32.9$ ppm stems from alternating E-NBE and isolated NBE sequences.^[11, 13, 14, 45] Finally, the signal at $\delta=29.7$ ppm can be attributed to PE sequences in ^{13}C NMR. The signal around $\delta=5.33$ and 5.50 ppm in the ^1H NMR correspond to the ROMP-derived *cis* and *trans* olefinic signals (Figure 3.23).

Table 3.13 illustrates that the catalytic activity of the Cp*-containing catalysts **23** and **27** was higher when compared to the Cp-containing catalysts **22** and **26**, and NBE incorporation increased with increasing polymerization temperature. Also, the resulting copolymers possessed lower number-average molecular weights. All Ti-based complexes showed efficient NBE incorporation up to 12.5 mol-% (Table 3.13, entry 12). The activity of complex **24** was much higher when compared to other half-titanocene complexes **22**, **23**, **26** and **27** and NBE incorporation increased with increasing temperature. Typical ^{13}C NMR spectra of complex **24**-derived poly(E)-*co*-poly(NBE)_{VIP} are shown in Figure 3.24.

Table 3.13. Results of E-NBE copolymerization by the action of Ti-based half-metalocene complexes **22**, **23**, **24**, **26** and **27**/MAO at various temperatures.

# ^a	Cat	T (°C)	Productivity ^b	NBE content (mol-%) ^c	M _n (g/mol) ^d	PDI ^d	T _m (°C) ^e
1		50	25	9.3	1,300,000	2.2	103
2		70	60	9.6	700,000	2.5	--
3		90	40	10.3	400,000	2.4	118
4		50	20	5.7	1,000,000	1.43	118
5		70	75	2.5	2,000,000	1.56	115
6		90	85		n.d	n.d	120
7		50	500	10.5	150,000	1.3	120
8		70	400	12.2	250,000	2.5	123

9		50	100	10	700,000	2.3	102
10		70	75	11.3	500,000	2.1	105
11		90	70		450,000	2.8	102
12		50	285	12.5	1,500,000	2.0	114
13		70	90	10.2	550,000	3.3	103

^a Polymerization conditions: 500 mL autoclave, total volume of the reaction mixture: 250 mL (including monomer), toluene, $t=1$ h, 4 bar of E unless stated otherwise, catalyst: MAO: NBE=1: 2000: 20000; ^b kg/mol_{catalyst}·h; ^c NBE-content estimated by ¹³C NMR; ^d GPC data in 1,2,4-trichlorobenzene vs. PS; ^e measured by DSC; n.d.=not determined due to poor solubility.

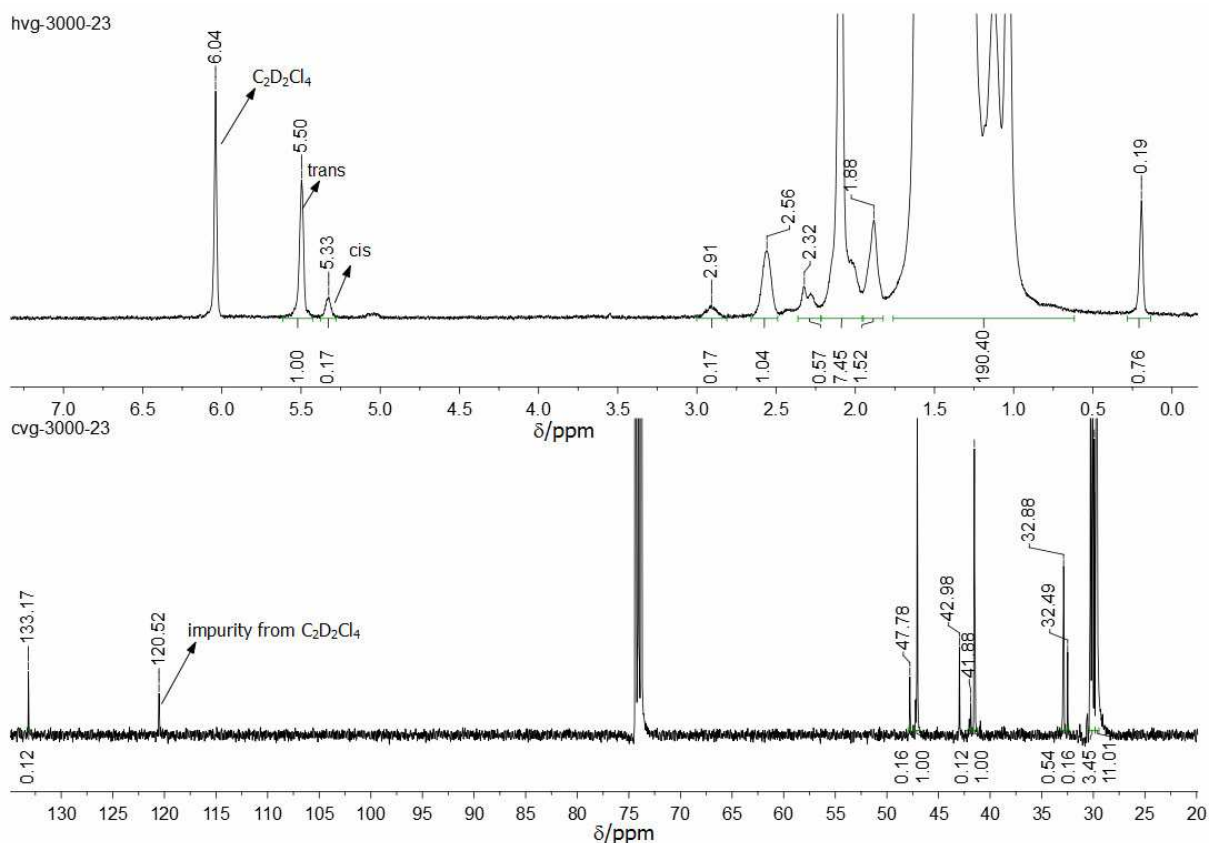


Figure 3.23. Complex **23**/MAO-derived ¹H NMR (top) and ¹³C NMR (bottom) of poly(NBE)_{ROMP}-*co*-poly(NBE)_{VIP}-*co*-poly(E) prepared at 50°C using 2 bar of E (in 1,1,2,2-[D₂]tetrachloroethane).

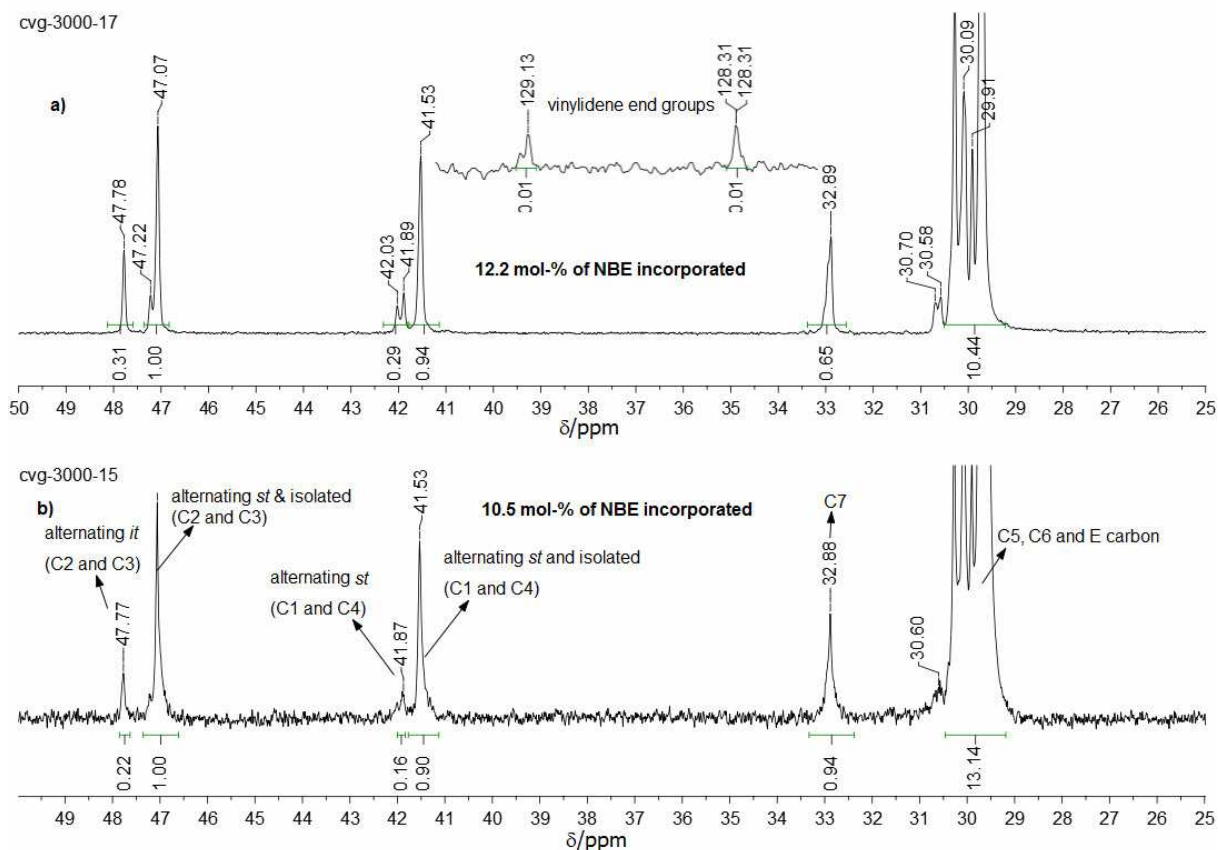
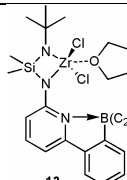
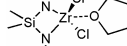
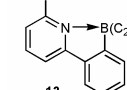
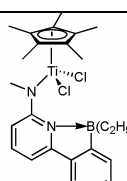


Figure 3.24. Complex **24**/MAO-derived ^{13}C NMR spectrum of poly(E)-*co*-poly(NBE)_{VIP} (a) at $T=70^\circ\text{C}$ using 4 bar of E; (b) at 50°C using 4 bar of E (Table 3.13, entries 7 and 8 in 1,1,2,2-[D₂]tetrachloroethane).

3.4.4 Copolymerization of E with *cis*-cyclooctene (COE)

The copolymerization of E with *cis*-cyclooctene was investigated with the use of the Zr-based complex **13** and the Ti-based complex **23** using different ratios of COE at 50 and 70°C . Mostly linear PE without any incorporated COE was obtained. The Zr-based complex activities were moderate (up to $500 \text{ Kg}_{\text{polymer}}/\text{molZrh}$), the ones of the Ti-based complexes very low (up to $8 \text{ Kg}_{\text{polymer}}/\text{molTih}$). In the polymerization of E in the presence of COE the catalytic activities are lower as compared to the ones in the polymerization of E in the presence of CPE ($30,000 \text{ kg}_{\text{polymer}}/\text{molZrh}$). A typical complex **13**-derived ^{13}C NMR spectrum of PE prepared in the presence of COE at 70°C is shown in Figure 3.25.

Table 3.14. Results of E-COE copolymerization by the action of **13**, **23**/MAO.

# ^a	Cat	Cat:MAO:COE	T (°C) / p (bar)	Productivity ^b	M _n (g/mol) ^c	PDI ^c	T _m (°C) ^d
1		1: 2000 :10,000	50/ 4	136	1,500,000	3.6	133
2		1: 2000 :30,000	50/ 4	140	350,000	5.8	131
3		1: 2000 :10,000	70/ 4	500	900,000	8.3	132
4	13	1: 2000 :30,000	70/ 4	475	700,000	4.5	130
5		1: 2000 :30,000	50/ 2	180			
6		1: 2000 :30,000	50/ 2	8	n.d	n.d	--

^a Polymerization conditions: 500 mL autoclave, total volume of the reaction mixture: 250 mL (including monomer), toluene, *t*=1 h; ^b kg_{polymer}/mol_{catalyst}·h; ^c GPC data in 1,2,4-trichlorobenzene vs. PS; ^d measured by DSC; n.d.=not determined due to poor solubility.

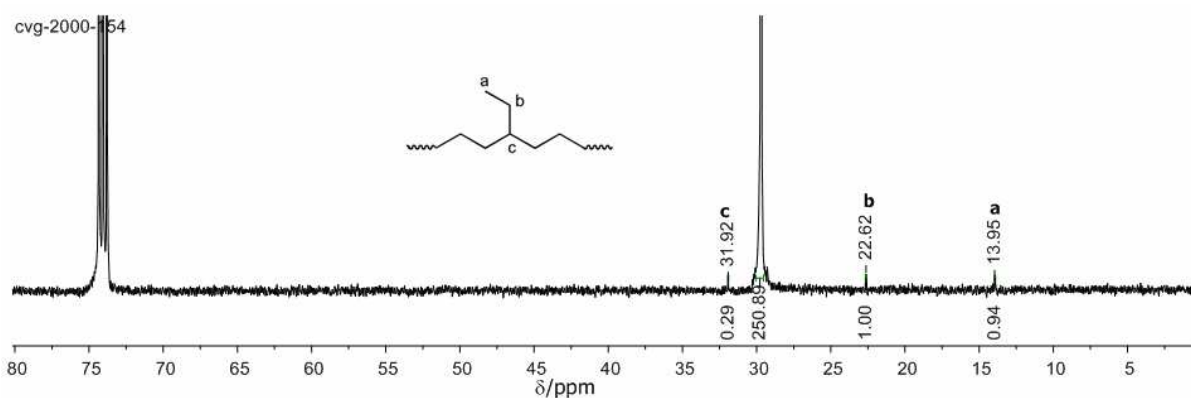


Figure 3.25. ¹³C NMR of PE prepared by the action of complex **13**/MAO in the presence of COE at 70°C using 4 bar of E (Table 3.14, entry 3 in 1,1,2,2-[D₂]tetrachloroethane).

3.5 ^{13}C NMR spectroscopic analysis of E-NBE copolymers

3.5.1 Microstructure of the Zr-based complexes 13, 17-derived E-NBE copolymers

^{13}C NMR studies on the microstructure of E-NBE copolymer have been carried out and the interpretation of signals exists in the literature.^[9, 11, 13, 14, 45, 46, 48, 49] The assignments of the chemical shifts for the different carbon atoms are listed in Table 3.14. The chemical shifts between 28 and 32 ppm, i.e. the ethene signals overlap with the C5 and C6 resonances of the NBE carbon atoms. The ^{13}C NMR of the E-NBE copolymer microstructure with higher norbornene contents reveals many resonances and looks more complex due to different monomer sequences and different lengths of NBE microblocks and different stereosequences in the E-N copolymers.

A copolymer chain in which every NBE unit is considered isolated from other NBE units in the polymer chain (EEEENEEE) is shown in Figure 3.26. Figure 3.27 illustrates the possible blocks in the copolymer chain, in which the NBE units are alternating (ENENE), diads (ENNE) and triads (ENNNE) regardless of the stereochemical differences (structures A, B and C) and the configuration of the C2, C3 carbons in NBE. These can either be R/S or S/R and the relationship to the alternating NBE unit will be either *meso* (alternating *it*) or *racemic* (alternating *st*). Generally, microstructure formation mainly depends on the structure of the catalyst.^[48, 50] (structures D and E)

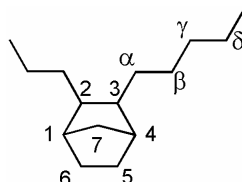


Figure 3.26. Isolated NBE unit in a E-NBE polymer chain.

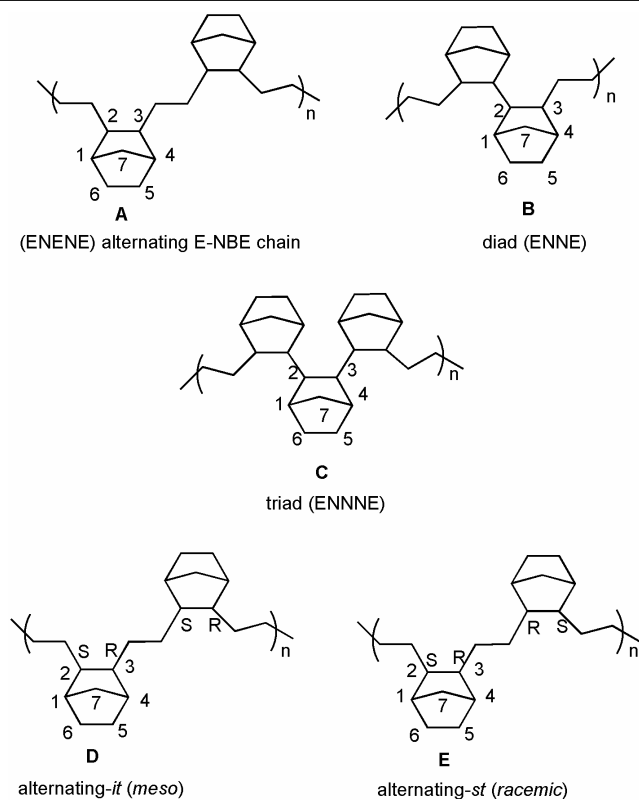


Figure 3.27. Possible blocks in E-N polymer chains.^[48]

Table 3.15. ^{13}C NMR assignments of the resonance in E-NBE copolymers.

^{13}C NMR chemical shifts (ppm)	assignment
28.0-32.0	C5, C6 and C_α , C_β , C_γ , C_δ
29.69	(EEEE) _n
32.8 – 33.5	C7
41.0 – 42.5	C1, C4
47.0 – 48.5	C2, C3

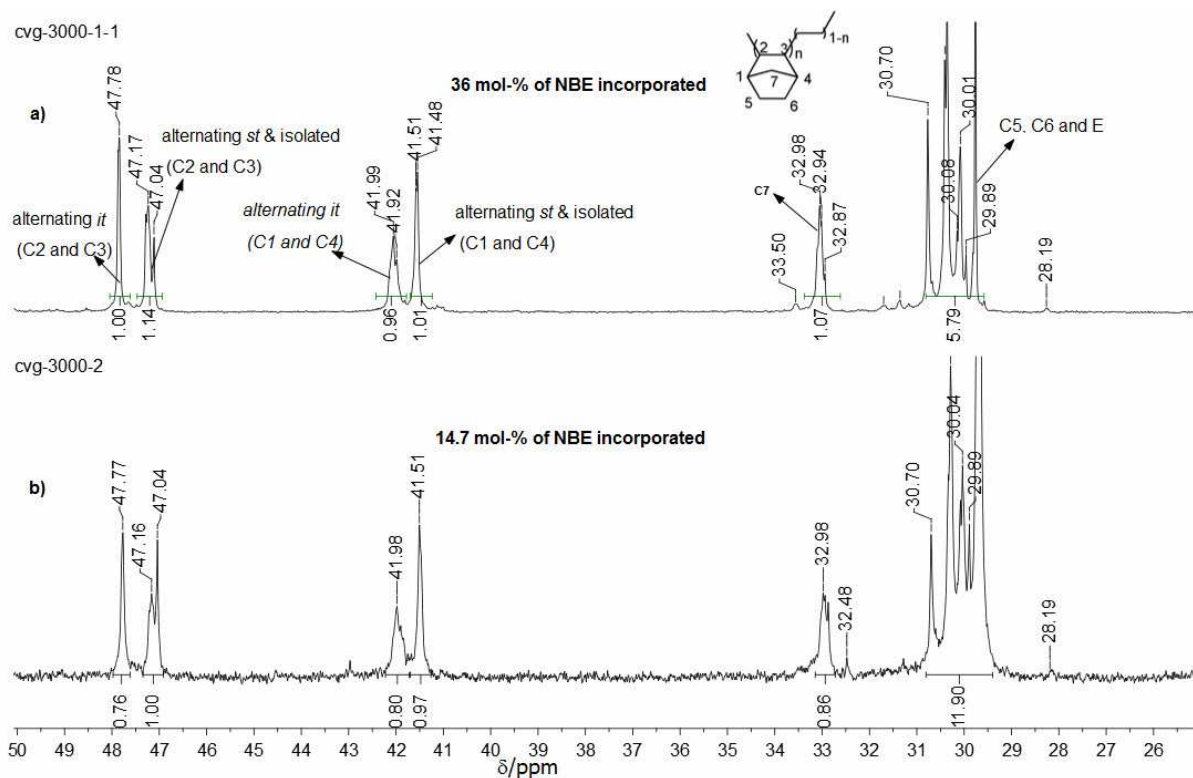


Figure 3.28. ^{13}C NMR of poly(E-*co*-NBE)_{VIP} produced by the action of (a) **13/MAO** at 70°C using 1 bar of E; (b) **17/MAO** at 70°C using 1 bar of E (Table 3.12, entries 1 and 6).

Figure 3.28 shows typical ^{13}C NMR spectra of poly(E-*co*-NBE)_{VIP} prepared by the action of **13** and **17/MAO** at 70°C using 1 bar of E. The obtained copolymers contained 36 and 14.7 mol-% of NBE, respectively. Analysis of the E-NBE copolymer spectra revealed that copolymers with high NBE incorporation were complex; moreover, in both spectra (a and b) mixtures of alternating *it* (C2/C3; 47.8 and C1/C4; 42.0 ppm) and *st* E-NBE sequences as well as isolated NBE sequences (C2/C3; 47.0 – 47.2 and C1/C4; 41.4 – 41.6 ppm) along with NBE diads were visible. The NBE diads resonances showed up at 28.2, 31.3, 33.5 and 41.3 ppm (Figure 3.28(a)). Complex **13/MAO** exhibited excellent NBE-incorporation when compared to **17/MAO**.

The E-pressure also shows a significant impact on NBE incorporation in the resulting E-NBE copolymers. Thus, the microstructure of the copolymers prepared by the action of **13** and **17/MAO** at 1 bar of E (Figure 3.28 a and b) is entirely different from the one obtained at 4 bar of E (Figure 3.29 a and b). Also, the incorporation of NBE dropped to around 6 mol-% using complex **13/MAO** at 4 bar of E mainly produced alternating *st* E-NBE sequences as well as isolated NBE sequences without any alternating *it* E-NBE sequences and NBE diads or triad sequences (Figure 3.29, a). Moreover, complex **17**-derived copolymers contain alternating *it* (47.8 and 42.0 ppm), *st* as well as isolated NBE sequences (47.0, 41.5 ppm).

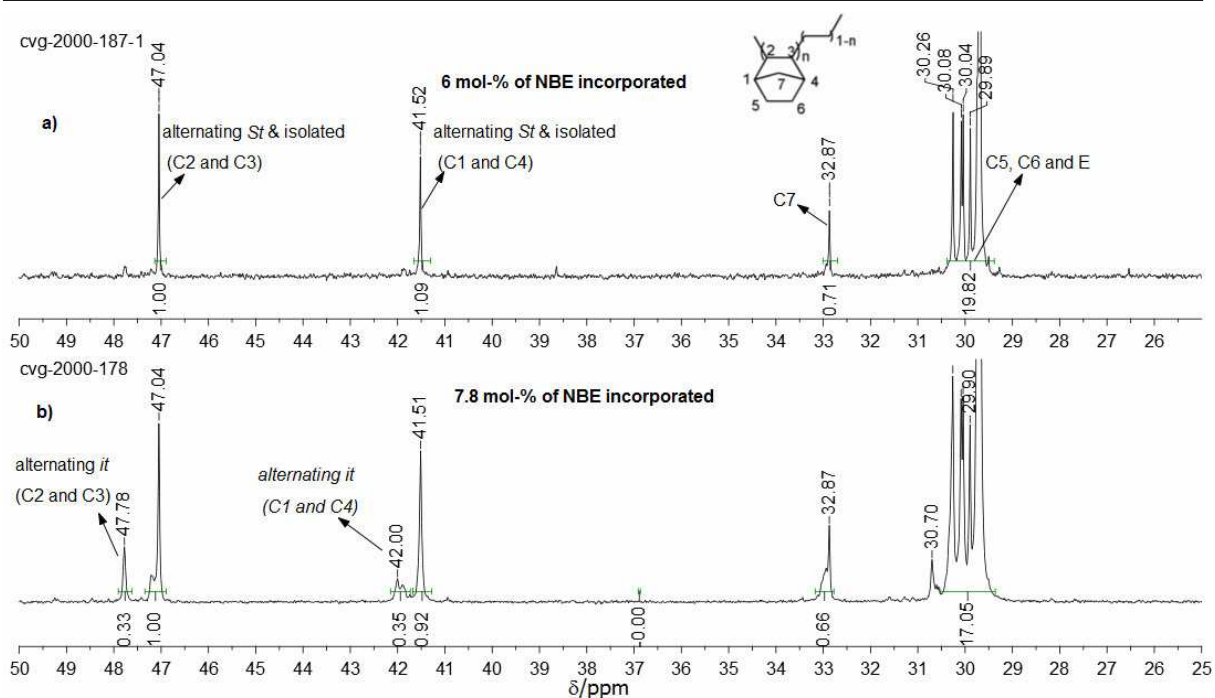


Figure 3.29. ^{13}C NMR of poly(E-co-NBE)_{VIP} produced by the action of (a) **13**/MAO at 70°C using 4 bar of E; (b) **17**/MAO at 70°C using 4 bar of E (Table 3.12, entries 3 and 8).

3.5.2 Microstructure of the Ti-based complexes **22**, **23**, **24**, **26** and **27**-derived E-NBE copolymers

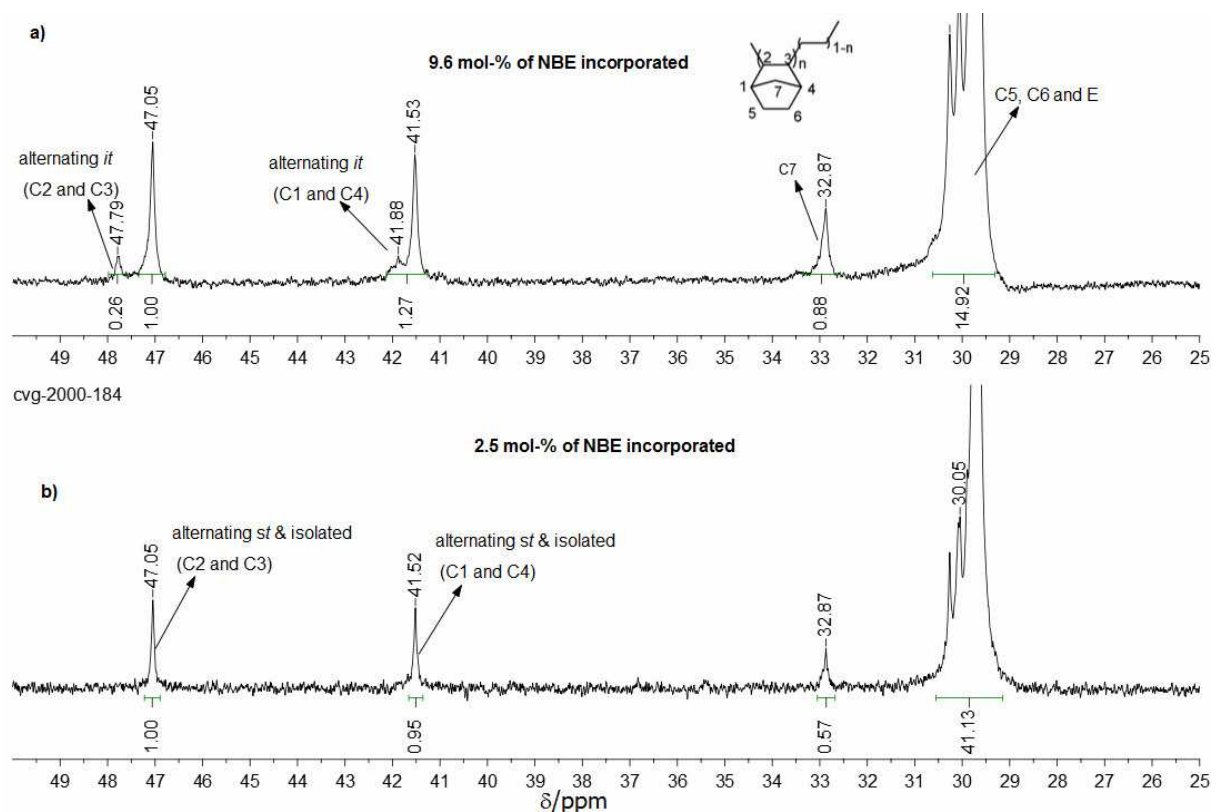


Figure 3.30. ^{13}C NMR of poly(E-co-NBE)_{VIP} produced by the action of (a) **22**/MAO; (b) **23**/MAO at 70°C using 4 bar of E (Table 3.13, entries 2 and 5).

Figure 3.30 shows a typical ¹³C NMR spectra of poly(E-co-NBE)_{VIP} prepared by the action of **22** (a, 9.6 mol-% of NBE) and **23/MAO** (b, 2.5 mol-% of NBE) systems. The chemical shifts of the observed signals along with the integral peak area were used for calculating the NBE-content of the resulting copolymer using the following equation:

$$\text{NBE (\%)} = 1/3(I_{C2, C3} + I_{C1, C4} + 2I_{C7}) / I_{CH2}$$

22/MAO derived spectra possess a mixture of alternating *it* (C2/C3 47.8 and C1/C4 41.9 ppm) and alternating *st* E-NBE sequences as well as isolated NBE sequences (47.0 and 41.5 ppm). On the other hand, resonances of the NBE diads were absent. Complex **23/MAO** mainly produced alternating *st* along with isolated NBE units in the resulting copolymer (47.0 and 41.5 ppm) without any NBE diads.

Figure 3.31 illustrates a typical ¹³C NMR spectrum of poly(E-co-NBE)_{VIP} prepared by the action of **26/MAO** (b, 11.3 mol-% of NBE) and **27/MAO** (a, 10.2 mol-% of NBE). Differences can be observed when comparing both **26**- and **27**-derived E-NBE copolymer. Although, both copolymers have nearly the same NBE content, spectrum **a**, which is derived from **27/MAO**, shows more isolated and alternating *st* E-NBE sequences without any NBE diads, while spectrum **b** which is derived from **26/MAO**, displays a mixture of alternating *it* and *st* E-NBE sequences and isolated NBE sequences along with NBE diads.

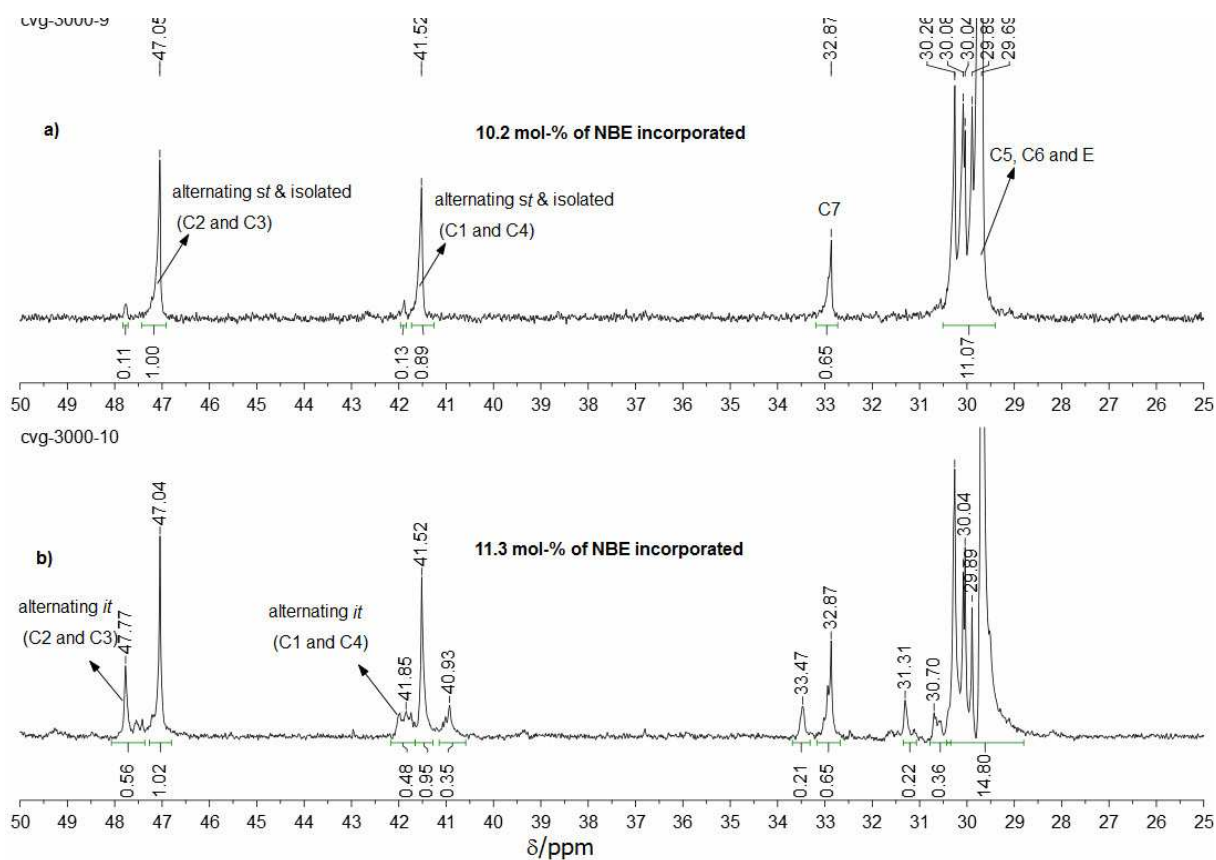


Figure 3.31. ¹³C NMR of poly(E-co-NBE)_{VIP} produced by the action of (a) **27/MAO**; (b) **26/MAO** at 70°C using 4 bar of E (Table 3.13, entries 10 and 13).

3.6 Conclusion

In summary, Zr^{IV}-dimethylsilylenebisamide complexes and non-bridged half-titanocene complexes bearing the aminoborane motif activated by MAO are capable of homopolymerizing of E. In copolymerization of E with CPE (up to 25 vol.-%) mainly linear PE (HDPE) without any noticeable incorporation of CPE is observed while higher concentrations (40 vol.-%) of CPE result in a CPE incorporation of up to 4 mol.-%. In the presence of CPE, the catalytic activity of the Zr^{IV}-based precatalyst **13/MAO** dramatically increased up to a factor of 15 (up to 30,000 kg_{polymer}/mol·Zr·h). In the copolymerization of E with NBE the Zr^{IV}-based and non-bridged half-titanocene complexes mainly produced poly(E-co-NBE)_{VIP} with moderate activities. As the NBE feed increased, the catalytic activity decreased and the resulting number-average molecular weights of the copolymers increased, while the incorporation of NBE in the copolymer increased. The ¹³C NMR spectra of the E-NBE copolymers indicate the presence of alternating *it* and *st* E-NBE sequences along with isolated NBE sequences. The presence of NN dyads and NNN triads was also detected with copolymers having a high NBE content (>10 mol.-%). The incorporation of NBE in the resulting copolymers was highly influenced by the E pressure, mainly at low pressures (1 or 2 bar E) the NBE content was high in the resulting copolymers. Non-bridged half-titanocenes were also effective in the homopolymerization of styrene in a syndiospecific manner resulting *st*-PS with moderate activities. Interestingly, the presence of an aminoborane group does not influence the copolymerization of E-NBE in terms of switching the mechanism from vinyl addition to ROMP and *vice versa* by reversible α -H elimination/ α -H addition process.

3.7 References

- [1] H. H. Brintzinger, D. Fischer, R. Mülhaupt, B. Rieger, R. M. Waymouth, *Angew. Chem. Int. Ed.* **1995**, *34*, 1143; *Angew. Chem.* **1995**, *107*, 1255.
- [2] G. J. P. Britovsek, V. C. Gibson, D. F. Wass, *Angew. Chem. Int. Ed.* **1999**, *38*, 428-447; *Angew. Chem.* **1999**, *111*, 448-468.
- [3] W. Kaminsky, *Macromol. Chem. Phys.* **1996**, *197*, 3907.
- [4] W. Kaminsky, M. Arndt, *Adv. Polym. Sci.* **1997**, *127*, 143.
- [5] A. L. McKnight, R. M. Waymouth, *Chem. Rev.* **1998**, *98*, 2587.
- [6] J. Suhm, J. Heinemann, C. Wörner, P. Müller, F. Stricker, J. Kressler, J. Okuda, R. Mülhaupt, *Macromol. Symp.* **1998**, *129*, 1.
- [7] S. Collins, W. M. Kelly, *Macromolecules* **1992**, *25*, 233.
- [8] W. Kaminsky, *J. Chem. Soc., Dalton Trans.* **1998**, 1413.
- [9] K. Nomura, M. Tsubota, M. Fujiki, *Macromolecules* **2003**, *36*, 3797.
- [10] A. L. McKnight, R. M. Waymouth, *Macromolecules* **1999**, *32*, 2816.
- [11] D. Ruchatz, G. Fink, *Macromolecules* **1998**, *31*, 4674.
- [12] T. Hasan, T. Ikeda, T. Shiono, *Macromolecules* **2004**, *37*, 8503.
- [13] D. Ruchatz, G. Fink, *Macromolecules* **1998**, *31*, 4681.
- [14] D. Ruchatz, G. Fink, *Macromolecules* **1998**, *31*, 4684.
- [15] W. Kaminsky, A. Noll, *Polym. Bull.* **1993**, *31*, 175.
- [16] K. Nomura, K. Fujii, *Organometallics* **2002**, *21*, 3042.
- [17] K. Nomura, J. Liu, S. Padmanabhan, B. Kitiyanan, *J. Mol. Catal. A* **2007**, *267*, 1.
- [18] W. Wang, T. Tanaka, M. Tsubota, M. Fujiki, S. Yamanaka, K. Nomura, *Adv. Synth. Cat.* **2005**, *347*, 433.
- [19] M. R. Buchmeiser, S. Camadanli, D. Wang, Y. Zou, U. Decker, C. Kühnel, I. Reinhardt, *Angew. Chem. Int. Ed.* **2011**, *50*, 3566; *Angew. Chem.* **2011**, *123*, 3628.
- [20] S. A. A. Shah, H. Dorn, A. Voigt, H. W. Roesky, E. Parisini, H.-G. Schmidt, M. Noltemeyer, *Organometallics* **1996**, *15*, 3176.
- [21] K. Nomura, K. Fujii, *Macromolecules* **2003**, *36*, 2633.
- [22] K. Liu, Q. Wu, W. Gao, Y. Mu, L. Ye, *Eur. J. Inorg. Chem.* **2011**, 1901.
- [23] R. R. Schrock, P. J. Bonitatebus, Y. Schrodi, *Organometallics* **2001**, *20*, 1056.
- [24] A. D. Horton, K. L. von Hebel, J. de With, *Macromol. Symp.* **2001**, *173*, 123.
- [25] J. D. Scollard, D. H. McConville, N. C. Payne, J. J. Vittal, *Macromolecules* **1996**, *29*, 5241.
- [26] J. D. Scollard, D. H. McConville, *J. Am. Chem. Soc.* **1996**, *118*, 10008.
- [27] R. Baumann, W. M. Davis, R. R. Schrock, *J. Am. Chem. Soc.* **1997**, *119*, 3830.

- [28] Y.-M. Jeon, S. J. Park, J. Heo, K. Kim, *Organometallics* **1998**, *17*, 3161.
- [29] C. H. Lee, Y.-H. La, J. W. Park, *Organometallics* **2000**, *19*, 344.
- [30] V. C. Gibson, B. S. Kimberley, A. J. P. White, D. J. Williams, P. Howard, *Chem. Commun.* **1998**, 313.
- [31] S. Tinkler, R. J. Deeth, D. J. Duncalf, A. McCamley, *Chem. Commun.* **1996**, 2623.
- [32] Y.-M. Jeon, J. Heo, W. M. Lee, T. Chang, K. Kim, *Organometallics* **1999**, *18*, 4107.
- [33] P. Margl, L. Deng, T. Ziegler, *J. Am. Chem. Soc.* **1998**, *121*, 154.
- [34] Y. Zou, D. Wang, K. Wurst, C. Kühnel, I. Reinhardt, U. Decker, V. Gurram, S. Camadanli, M. R. Buchmeiser, *Chem. Eur. J.* **2011**, *17*, 13832.
- [35] Y. Li, H. Gao, Q. Wu, *J. Polym. Sci. Part A: Polym. Chem.* **2008**, *46*, 93.
- [36] N. Ishihara, T. Seimiya, M. Kuramoto, M. Uoi, *Macromolecules* **1986**, *19*, 2464.
- [37] T. E. Ready, R. O. Day, J. C. W. Chien, M. D. Rausch, *Macromolecules* **1993**, *26*, 5822.
- [38] A. Zambelli, C. Pellecchia, L. Oliva, P. Longo, A. Grassi, *Makromol. Chem.* **1991**, *192*, 223.
- [39] D. J. Duncalf, H. J. Wade, C. Waterson, P. J. Derrick, D. M. Haddleton, A. McCamley, *Macromolecules* **1996**, *29*, 6399.
- [40] D. J. Byun, A. Fudo, A. Tanaka, M. Fujiki, K. Nomura, *Macromolecules* **2004**, *37*, 5520.
- [41] S. J. McLain, J. Feldman, E. F. McCord, K. H. Gardner, M. F. Teasley, E. B. Coughlin, K. J. Sweetman, L. K. Johnson, M. Brookhart, *Macromolecules* **1998**, *31*, 6705.
- [42] A. R. Lavoie, M. H. Ho, R. M. Waymouth, *Chem. Commun.* **2003**, 864.
- [43] N. Naga, Y. Imanishi, *Macromol. Chem. Phys.* **2002**, *203*, 159.
- [44] A. Jerschow, E. Ernst, W. Hermann, N. Mueller, *Macromolecules* **1995**, *28*, 7095.
- [45] D. Ruchatz, G. Fink, *Macromolecules* **1998**, *31*, 4669.
- [46] I. Tritto, L. Boggioni, M. C. Sacchi, P. Locatelli, *J. Mol. Catal. A: Chem.* **1998**, *133*, 139.
- [47] R. A. Wendt, G. Fink, *J. Mol. Catal. A: Chem.* **2003**, *203*, 101.
- [48] I. Tritto, C. Marestin, L. Boggioni, L. Zetta, A. Provasoli, D. R. Ferro, *Macromolecules* **2000**, *33*, 8931.
- [49] B. A. Harrington, D. J. Crowther, *J. Mol. Catal. A: Chem.* **1998**, *128*, 79.
- [50] A. Provasoli, D. R. Ferro, I. Tritto, L. Boggioni, *Macromolecules* **1999**, *32*, 6697.

CHAPTER 4

Experimental Data

4.0 Experimental Data

General Remarks

Except where noted, all manipulations were conducted in the absence of oxygen and water under an atmosphere of dinitrogen, either by the use of standard Schlenk techniques or within an MBraun glove box utilizing glassware that was oven-dried and evacuated while hot prior to use. The non-deuterated solvents (i.e. toluene, diethyl ether, pentane, THF and dichloromethane) were dried and deoxygenated by means of degassing with dinitrogen gas, followed by passage through a triple-column solvent purification of an MBraun SDS drying system. Deuterated NMR solvents were freeze-pump-thaw degassed. d_6 -benzene, d_8 -toluene and d_8 -tetrahydrofuran were dried and distilled from sodium/benzophenone, CD_2Cl_2 and $CDCl_3$ were dried and distilled from P_2O_5 . Methylaluminoxane (MAO) and triisobutylaluminum (1.1 M solution in toluene) were purchased from Aldrich. Trimethylaluminum was removed from commercial MAO (10 wt-% solution in toluene, Aldrich) via drying *in vacuo* (8 h, 70°C) and the obtained solid MAO was re-dissolved in toluene to make a 2.0 M solution, which was stored in the dry-box. Ethylene and propylene (Air Products) were dried by passing through columns filled with a Cu-based catalyst (BASF catalyst R3-11) and then through molecular sieves (3 Å) before use.

The monomers cyclopentene (95%, Fluka), cyclooctene (90%, Fluka), cyclohexene (99.5%, Fluka), 1-hexene (99%, Aldrich), 1,3-cyclohexadiene (96%, Acro's) and styrene (99.5%, Acro's) were dried over calcium hydride, vacuum transferred and stored in the glove box. Norborn-2-ene (99%, Aldrich) was used without any further purification. NMR data were obtained at 250.13 and 600.25 MHz for proton and 62.5 and 150.0 MHz for carbon in the indicated solvent at 25°C on a Bruker Spectrospin 250 and are listed in parts per million downfield from tetramethylsilane for proton and carbon. High-resolution mass spectra (ESI) were recorded on an APEX II FTICR mass spectrometer, Bruker Daltonics. Infrared spectra were recorded from 4000-400 cm^{-1} on a Perkin-Elmer 881 Spectrometer using ATR technology.

All homopolymerization reactions were performed in Schlenk tubes under an inert atmosphere. All copolymerization reactions of ethylene with cyclic olefins were performed in a Büchi-Uster pressure reactor (polyclave) equipped with a Huber thermostat (Unistat Tango Nuevo). The monomer feed of the gaseous monomer was kept constant with a Büchi pressflow bpc 6010 flow controller. The reaction was monitored by a bdsmc Büchi data system.

GC-MS investigations were carried out on a Shimadzu GCMS-QP2010S with an AOC-20i Autosampler using a SPB fused silica (Rxi-5MS) column (30 m × 0.25 mm × 0.25 μm film thickness). Molecular weights and molecular weight distributions were measured by high temperature gel chromatography (HT-GPC) on a Polymer Standards HT-GPC system with triple detection (refractive index, light-scattering at 15 and 90°, viscosimetry) using three consecutive Waters Styragel HR4 4.6 x 300 mm columns in 1,2,4-trichlorobenzene at 145°C. The flow rate was set to 1 mL/min. Narrow polystyrene standards in the range $162 < M_n < 6,035,000 \text{ g}\cdot\text{mol}^{-1}$ (Easi Vial-red, yellow and green) were purchased from Polymer Labs. DSC data were recorded by heating under a nitrogen atmosphere on a DSC7 Perkin-Elmer differential scanning calorimeter.

Catalysts **1a-1g**, **2c**, **2d**, **2e**, **2f** and **6** have been made by my former colleague I. Ahmad and compounds **7**, **8** and **9** were prepared according to the published procedure from *Angew. Chem. Int. Ed.* **2011**, 50, 3566-3571 and *Chem. Eur. J.* **2011**, 17, 13832-13846.

N-tert-butyl-chloro-dimethylsilylamine (11):

To a solution of dichlorodimethylsilane (17.6 g, 136.7 mmol) in *n*-pentane (50 mL) were added triethylamine (14.5 g, 143.5 mmol) and *tert*-butylamine (10 g, 136.7 mmol) simultaneously at 0-5°C, and the resulting reaction mixture was stirred at room temperature for 16 h, then filtered to remove the salts (triethylammonium hydrochloride) and the filtrate was transferred into a distillation apparatus to remove both triethylamine and pentane until a reflux temp. of 50°C was reached and remaining liquid was determined to be pure product (10 g, 44%). ¹H NMR (C₆D₆, 250 MHz): δ=0.29 (s, 6H, Si(CH₃)₂), 0.96 (br, 1H, NH), 1.08 (s, 9H, C(CH₃)₃) ppm. ¹³C NMR (C₆D₆, 250 MHz): δ=4.4, 33.1, 50.2 ppm. GC-MS: *m/z* calcd. for C₆H₁₆ClNSi: 165.07; found. 164.9 (M⁺); **Elemental anal.** calcd. for C₆H₁₆ClNSi: C 43.48; H 9.73; N 8.45; found C 43.26; H 9.85; N 8.63.

N-tert-butyl-N¹-(6-(2-(diethylboryl)phenyl)pyrid-2-yl) - 1, 1-dimethylsilanedi-amine (12):

A solution of *n*-BuLi (0.73 mL of 1.6 M in hexane, 0.69 mmol) was added to a solution of **9** (150 mg, 0.63 mmol) in diethyl ether (20 mL) at -37°C. The reaction mixture was warmed to room temperature for 2 h. Then, **11** (0.103 mg, 0.63 mmol) was dissolved in diethyl ether (10 mL) was added slowly to the reaction mixture and stirred at room temperature for 16 h. then the reaction mass was filtered over celite and the filtrate was removed *in vacuo* to obtain **12** (200 mg, 86%) as a white solid. ¹H NMR (C₆D₆, 250 MHz): δ= 0.21 (s, 6H, Si(CH₃)₂), 0.71 (br, 1H, *tert*-butyl-NH), 0.87-0.93 (t, 6H, *J*_{HH}=7.5 Hz, B(CH₂CH₃)₂), 1.11 (s, 9H, *tert*-butyl),

1.26-1.38 (m, 2H, B(CH₂CH₃)₂), 1.45-1.60 (m, 2H, B(CH₂CH₃)₂), 5.98 (br, 1H, Ar-NH), 6.67-6.71 (dd, 1H, $J_{\text{HH}}=0.75$ Hz, ArH), 6.88-6.91 (d, 1H, ArH), 7.13-7.19 (t, 1H, $J_{\text{HH}}=7.5$ Hz, ArH), 7.3-7.36 (ddd, 1H, $J_{\text{HH}}=1$ Hz, ArH), 7.48-7.54 (ddd, 1H, $J_{\text{HH}}=1$ Hz, ArH), 7.70-7.73 (d, 1H, $J_{\text{HH}}=7.5$ Hz, ArH), 7.90-7.93 (d, 1H, $J_{\text{HH}}=7.5$ Hz, ArH) ppm. ¹³C NMR (C₆D₆, 250 MHz): $\delta=1.4, 8.8, 14.1, 31.7, 48.3, 104.3, 106.9, 119.6, 124.1, 127.9, 128.7, 136.4, 138.1$ ppm. GC-MS: m/z calcd. for C₂₁H₃₄BN₃Si: 367.2, found. 338.2 [M-C₂H₅]⁺.

Synthesis of Zr-complex (13):

A solution of n-BuLi (1.6 M in hexane, 0.73 mL, 1.14 mmol) was added to a solution of **12** (200 mg, 0.544 mmol) in *n*-pentane (15 mL) at -37° C. A large amount of white precipitate formed during the addition. The reaction mixture was warmed to room temperature and stirred for 3 h. The resulting precipitate was collected on a frit, washed with cold *n*-pentane (10 mL) and dried *in vacuo* to give the pure Li salt of **12** (160 mg) which was used without any further analysis.

The Li salt of **12** (160 mg, 0.42 mmol) was dissolved in toluene (20 mL) and added to a solution of ZrCl₄·2THF (160 mg, 0.42 mmol) in toluene (15 mL) at -37°C and the resulting reaction mixture was allowed to stir at room temperature for 6 h. Then the mixture was filtered through celite and the solvent was removed under reduced pressure. *n*-Pentane was added to and the solution was stored in glove-box freezer for 24 h to precipitate the Zr-complex **13** (200 mg, 80%) as a white solid. ¹H NMR (C₆D₆, 250 MHz): $\delta=0.52$ (s, 3H, Si(CH₃)₂), 0.7-0.80 (m, 9H, Si(CH₃)₂, B(CH₂CH₃)₂), 1.05-1.14 (m, 4H, B(CH₂CH₃)₂), 1.29-1.40 (m, 4H, THF), 1.62 (s, 9H, *tert*-butyl), 4.29 (br, 4H, THF), 6.70-6.73 (d, 1H, $J_{\text{HH}}=7.5$ Hz, ArH), 6.95-6.98 (d, 1H, $J_{\text{HH}}=7.5$ Hz, ArH), 7.17-7.24 (t, 1H, $J_{\text{HH}}=7.5$ Hz, ArH), 7.30-7.37 (ddd, 1H, $J_{\text{HH}}=2.5$ Hz, ArH), 7.49-7.56 (ddd, 1H, $J_{\text{HH}}=0.75$ Hz, ArH), 6.67-6.70 (d, 1H, $J_{\text{HH}}=7.75$ Hz, ArH), 7.77-7.74 (d, 1H, $J_{\text{HH}}=7.25$ Hz, ArH) ppm. ¹³C NMR (C₆D₆, 250 MHz): $\delta=5.2, 5.6, 10.9, 11.7, 20.2, 25.0$ (THF), 35.16, 57.5, 78.0 (THF), 107.2, 115.7, 121.0, 125.5, 129.1, 129.6, 137.8, 139.0, 158.1, 160.8 ppm; **Elemental anal.** calcd. for C₂₅H₄₀BCl₂N₃OSiZr: C 50.08; H 6.72; N 7.01; found C 50.37; H 7.08; N 7.34.

Synthesis of N-adamantylchlorodimethylsilylamine (15):

A solution of n-BuLi (1.6 M in hexane 22 mL, 34.68 mmol) was slowly added to a solution of 1-adamantylamine (5.0 g, 33.05 mmol) in pentane (100 mL) at -60°C. A large amount of white precipitate formed during the addition. The reaction mixture was warmed to room temperature and stirred for 4 h. The resulting precipitate was collected on a frit, washed with

cold *n*-pentane (10 mL) and dried in *vacuo* to give pure lithium 1-adamantylamide (5.0 g, 99%), which was used for the next reaction without any analysis.

Dichlorodimethylsilane (10.25 g, 79.49 mmol) was stirred in THF (75 mL) and lithium-1-adamantylamide (5.0 g, 31.79 mmol) in THF (50 mL) was added slowly and the resulting reaction mixture was allowed to stir for 2.5 h at room temperature. Then, all volatiles were removed *in vacuo* and the residue was extracted with pentane and evaporated under reduced pressure to isolate the **15** as white solid (6.0 g, 75%). ¹H NMR (CDCl₃, 250 MHz): δ=0.44 (s, 6H, Si(CH₃)₂), 1.24 (br, 1H, NH), 1.59 (s, 6H, Ad-CH₂), 1.70 (s, 6H, Ad-CH₂), 2.02 (s, 3H, Ad-CH) ppm. ¹³C NMR (CDCl₃, 250 MHz): δ= 4.6, 29.8, 36.1, 46.5, 50.5 ppm. GC-MS: *m/z* calcd. for C₁₂H₂₂CINSi: 243.1; found.243.1 (M⁺); **Elemental anal.** calcd. for C₁₂H₂₂CINSi: C 59.11; H 9.09; N 5.74; found C 58.86; H 8.96; N 5.62.

N-adamantyl-N¹-(6-(2-(diethylboryl)phenyl)pyridin-2-yl)-1,1'-dimethylsilyldiamine (16):

A solution of *n*-BuLi (0.73 mL of 1.6 M in hexane, 1.14 mmol) was added to a solution of **9** (250 mg, 1.05 mmol) in diethyl ether (20 mL) at -37° C. The reaction mixture was warmed to room temperature for 2 h. Then, **15** (0.25 mg, 1.05 mmol) dissolved in diethyl ether (10 mL) was added slowly to the reaction mixture and the mixture was stirred at room temperature for 16 h. After filtration and evaporation of the solvent *in vacuo*, **16** (420 mg, 90%) was obtained as a white solid. ¹H NMR (C₆D₆, 250 MHz): δ= 0.29 (s, 6H, Si(CH₃)₂), 0.79 (br, 1H Ad-NH), 0.90-0.96 (t, 6H, *J*_{HH}=7.5 Hz, B(CH₂CH₃)₂), 1.28-1.43 (m, 2H, B(CH₂CH₃)₂), 1.48-1.57 (m, 2H, B(CH₂CH₃)₂), 1.57-1.6 (t, 6H, Ad-CH₂), 1.74 - 1.75 (d, 6H, *J*_{HH}=2.5 Hz, Ad-CH₂), 2.0 (m, 3H, Ad-CH), 6.05 (br, 1H, Ar-NH), 6.75 - 6.79 (d, 1H, *J*_{HH}=10 Hz, ArH), 6.92-6.95 (d, 1H, *J*_{HH}=7.5 Hz, ArH), 7.20-7.26 (t, 1H, *J*_{HH}=7.5 Hz, ArH), 7.33-7.39 (t, 1H, *J*_{HH}=7.5 Hz, ArH), 7.51-7.57 (t, 1H, *J*_{HH}=7.5 Hz, ArH), 7.72-7.75 (d, 1H, *J*_{HH}=7.5 Hz, ArH), 7.93-7.96 (d, 1H, *J*_{HH}=7.5 Hz, ArH) ppm. ¹³C NMR (C₆D₆, 250 MHz): δ=0.46, 10.3, 15.4, 30.1, 36.3, 46.9, 50.1, 105.7, 108.5, 121.0, 125.4, 129.3, 130.0, 137.9, 139.5, 156.2, 157.5 ppm.

Synthesis of Zr-compound 17:

A solution of *n*-BuLi (1.6 M in hexane, 1.28 mL, 2.0 mmol) was added to a solution of **16** (420 mg, 0.94 mmol) in *n*-pentane (40 mL) at -37°C. A large amount of white precipitate formed during the addition. The reaction mixture was warmed to room temperature and stirred for 12 h. The resulting precipitate was collected on a frit, washed with cold *n*-pentane (10 mL) and dried in *vacuo* to give the pure Li salt of **16** (350 mg), which was used without any analysis.

The Li salt of **16** (350 mg, 0.76 mmol) was dissolved in toluene (20 mL) and added to a solution of $\text{ZrCl}_4 \cdot 2\text{THF}$ (0.29 g, 0.76 mmol) in toluene (30 mL) at -37°C and the resulting reaction mixture was allowed to stir at room temperature for 16 h. Then the reaction mixture was filtered through celite and all volatiles were removed under reduced pressure. The crude product was dissolved in *n*-pentane (10 mL) from which **17** (280 mg, 45%) crystallized as an off-white solid. $^1\text{H NMR}$ (C_6D_6 , 250 MHz): δ = 0.62 (s, 3H, $\text{Si}(\underline{\text{C}}\text{H}_3)_2$), 0.78-0.83 (t, 6H, $J_{\text{HH}}=5$ Hz, $\text{B}(\underline{\text{C}}\text{H}_2\underline{\text{C}}\text{H}_3)_2$), 0.89 (s, 3H, $\text{Si}(\underline{\text{C}}\text{H}_3)_2$), 1.1 (br, THF), 1.3-1.46 (m, 4H, $\text{B}(\underline{\text{C}}\text{H}_2\underline{\text{C}}\text{H}_3)_2$), 1.67-1.91 (m, 6H, Ad- $\underline{\text{C}}\text{H}_2$), 2.28 (s, 3H, Ad- $\underline{\text{C}}\text{H}$), 2.37 (s, 6H, Ad- $\underline{\text{C}}\text{H}_2$), 4.30 (br, THF), 6.7-6.8 (d, 1H, $J_{\text{HH}}=10$ Hz, ArH), 6.97-7.00 (d, 1H, $J_{\text{HH}}=7.5$ Hz, ArH), 7.20-7.23 (d, 1H, $J_{\text{HH}}=7.5$ Hz, ArH), 7.32-7.39 (ddd, 1H, $J_{\text{HH}}=2.5$ Hz, ArH), 7.51-7.58 (ddd, 1H, $J_{\text{HH}}=2.5$ Hz, ArH), 7.70-7.73 (d, 1H, $J_{\text{HH}}=7.5$ Hz, ArH), 7.76-7.79 (d, 1H, $J_{\text{HH}}=7.5$ Hz, ArH) ppm. $^{13}\text{C NMR}$ (C_6D_6 , 250 MHz): δ =5.73, 6.32, 11.21, 11.79, 14.18 (pentane), 20.53, 22.62 (pentane), 25.08 (co-ordinated THF), 30.68, 34.32 (pentane), 36.63, 48.04, 58.89, 78.59 (co-ordinated THF), 107.27, 115.93, 121.07, 125.57, 129.12, 129.68, 137.95, 139.09, 158.17, 160.89 ppm; **Elemental anal.** calcd. for $\text{C}_{31}\text{H}_{46}\text{BCl}_2\text{N}_3\text{OSi Zr}$: C 54.94; H 6.84; N 6.20. found. C 55.39; H 7.39; N 5.88.

Synthesis of Hf- compound **18**:

A solution of *n*-BuLi (1.6 M in hexane, 0.73 mL, 1.14 mmol) was added to a solution of compound **12** (200 mg, 0.544 mmol) in *n*-pentane (15 mL) at -37°C . A large amount of white precipitate formed during the addition. The reaction mixture was warmed to room temperature and stirred for 3 h. The resulting precipitate was collected on a frit, washed with cold *n*-pentane (10 mL) and dried *in vacuo* to give the pure Li salt of **12** (160 mg), which was used without any further analysis.

Li salt of **12** (240 mg, 0.632 mmol) was dissolved in toluene (15 mL), this solution was added to a solution of HfCl_4 (202 mg, 0.632 mmol) in toluene (20 mL) at -37°C and the resulting reaction mixture was stirred at room temperature for 9 h. Then it was filtered under celite and all volatiles were removed under reduced pressure. *n*-Pentane was added and the solution was stored in a glove-box freezer for 24 h to precipitate **18** (200 mg, 51%) as a white solid. $^1\text{H NMR}$ (C_6D_6 , 250 MHz): δ =0.54 (s, 3H, $\text{Si}(\underline{\text{C}}\text{H}_3)_2$), 0.74-0.83 (m, 9H, $\text{Si}(\underline{\text{C}}\text{H}_3)_2$, $\text{B}(\underline{\text{C}}\text{H}_2\underline{\text{C}}\text{H}_3)_2$), 1.26-1.58 (m, 4H, $\text{B}(\underline{\text{C}}\text{H}_2\underline{\text{C}}\text{H}_3)_2$), 1.64 (s, 9H, tert-butyl), 6.73-6.76 (dd, 1H, $J_{\text{HH}}=0.75$ Hz, ArH), 6.94-6.98 (dd, 1H, $J_{\text{HH}}=0.5$ Hz, ArH), 7.19-7.25 (t, 1H, $J_{\text{HH}}=7.5$ Hz, ArH), 7.31-7.38 (ddd, 1H, $J_{\text{HH}}=1$ Hz, ArH), 7.50-7.56 (ddd, 1H, $J_{\text{HH}}=0.75$ Hz, ArH), 7.68-7.72 (d, 1H, $J_{\text{HH}}=7.75$ Hz, ArH), 7.76-7.78 (d, 1H, $J_{\text{HH}}=7.25$ Hz, ArH) ppm. $^{13}\text{C NMR}$ (C_6D_6 , 250 MHz): δ =5.4, 5.91, 11.3, 12.0, 12.5, 19.7, 35.9, 56.9, 107.7, 117.0, 121.3, 125.8, 129.4,

130.0, 138.10, 139.30, 158.4, 161.6 ppm; **Elemental anal.** calcd. for C₄₂H₆₄B₂HfN₆Si₂: C 55.48; H 7.09; N 9.24. found. C 55.45; H 7.20; N 9.19.

Synthesis of Hf-complex **19**:

A solution of *n*-BuLi (1.6 M in hexane, 0.73 mL, 1.14 mmol) was added to a solution of **16** (200 mg, 0.544 mmol) in *n*-pentane (15 mL) at -37° C. A large amount of white precipitate formed during the addition. The reaction mixture was warmed to room temperature and stirred for 3 h. The resulting precipitate was collected on a frit, washed with cold *n*-pentane (10 mL) and dried in *vacuo* to give the pure Li salt of **16** (160 mg), which was used without any further analysis.

The Li salt of **16** (400 mg, 0.87 mmol) was dissolved in toluene (20 mL) and added to a solution of HfCl₄ (280 mg, 0.87 mmol) in toluene (20 mL) and the resulting reaction mixture was stirred at room temperature for 9 h. Then it was filtered through celite and all volatiles were removed under reduced pressure. 20 mL of *n*-pentane were added to the crude and the solution was stored in a glove-box freezer for 24 h to precipitate the Hf-complex **19** (380 mg, 50%) as a white solid. ¹H NMR (C₆D₆, 250 MHz): δ=0.50 (s, 3H, Si(CH₃)₂), 0.67-0.79 (m, 9H, Si(CH₃)₂, -B(CH₂CH₃)₂), 1.28-1.79 (m, 10H, B(CH₂CH₃)₂, Ad-CH₂), 2.18 (s, 3H, Ad-CH), 2.25 (s, 6H, Ad-CH₂), 6.67-6.70 (d, 1H, *J*_{HH}=7.5 Hz, ArH), 6.84-6.87 (d, 1H, *J*_{HH}=7.5 Hz, ArH), 7.09-7.12 (d, 1H, *J*_{HH}=7.5 Hz, ArH), 7.21-7.27 (t, 1H, *J*_{HH}=7.5 Hz, ArH), 7.40-7.46 (t, 1H, *J*_{HH}=7.5 Hz, ArH), 7.58-7.61 (d, 1H, *J*_{HH}=7.5 Hz, ArH), 7.64-7.67 (d, 1H, *J*_{HH}=7.5 Hz, ArH) ppm. ¹³C NMR (C₆D₆, 250 MHz): δ=5.9, 6.6, 11.4, 12.0, 20.1, 31.0, 36.9, 48.8, 58.0, 107.7, 117.1, 121.3, 125.8, 129.40, 130.0, 138.2, 139.3, 158.4, 161.5 ppm. **Elemental anal.** calcd. for C₅₄H₇₆B₂HfN₆Si₂: C 60.87; H 7.19; N 7.89; found. C 60.79; H 7.80; N 7.15.

Synthesis of N-[6-(2-Diethylborylphenyl)pyrid-2-yl]-N-methylamine (**20**)

A solution of **9** (750 mg, 3.15 mmol) in dimethylformamide (20 mL) was cooled to 0-5°C and NaH (60 wt-% in mineral oil, 125 mg, 3.15 mmol) was added portion wise over 15 minutes and the resulting reaction mixture was stirred at 0-5°C for 2 h. After this time, CH₃I (0.894 mg, 6.3 mmol) in DMF (2 mL) was added. After 30 minutes, the reaction was quenched with ice, and the mixture was extracted with ethyl acetate (2 x 20 mL). The combined organic layers were washed with water (3 x 25 mL) and brine solution (20 mL) and then dried over Na₂SO₄. Finally, the solvent was removed under reduced pressure. The crude product was purified by column chromatography (60-120 silica gel) by eluting 2-3% ethyl acetate in petroleum ether, **20** (720 mg, 90%) was obtained as white solid. ¹H NMR (CDCl₃, 600 MHz): δ=0.34-0.36 (t, 6H, *J*_{HH}=6 Hz, B(CH₂CH₃)₂), 0.66-0.72 (m, 2H, B(CH₂CH₃)₂), 0.84-

0.90 (m, 2H, B(CH₂CH₃)₂), 3.01-3.02 (d, 3H, $J_{\text{HH}}=6$ Hz, N-CH₃), 5.76 (br, 1H, ArNH), 6.39-6.40 (d, 1H, $J_{\text{HH}}=6$ Hz, ArH), 7.17-7.18 (d, 1H, $J_{\text{HH}}=6$ Hz, ArH), 7.23-7.25 (t, 1H, $J_{\text{HH}}=6$ Hz, ArH), 7.35-7.38 (t, 1H, $J_{\text{HH}}=6$ Hz, ArH), 7.52-7.53 (d, 1H, $J_{\text{HH}}=6$ Hz, ArH), 7.7-7.72 (t, 2H, $J_{\text{HH}}=6$ Hz, ArH) ppm. ¹³C NMR (CDCl₃, 250 MHz): $\delta=9.9, 14.3, 29.7, 102.5, 104.8, 120.9, 125.1, 128.9, 129.5, 137.3, 140.4, 155.6, 157.0$ ppm. **Elemental anal.** calcd. for C₁₆H₂₁BN₂: C 76.21, H 8.39, N 11.11; found. C 76.23, H 8.33, N 11.10.

Synthesis of lithium N-(6-(2-(diethylboryl) phenyl) pyrid-2-yl)-N-methylamide (**21**):

A solution of *n*-BuLi (1.6 M in hexane, 2.72 mL, 4.36 mmol) was added to a solution of **20** (1.0 g, 3.96 mmol) in *n*-pentane (40 mL) at -37°C. A large amount of precipitate formed during the addition. The reaction mixture was warmed to room temperature for 3 h and the resulting precipitate was collected on a frit, washed with cold *n*-pentane (10 mL) and dried *in vacuo* to give the pure lithium salt of **21** (800 mg, 79%) as a yellow powder. ¹H NMR (C₆D₆, 600 MHz): $\delta= -0.38-0.32$ (m, 2H, B(CH₂CH₃)₂), 0.51-0.57 (m, 2H, B(CH₂CH₃)₂), 0.62-0.64 (t, 6H, $J_{\text{HH}}=6$ Hz, B(CH₂CH₃)₂), 2.68 (s, 3H, N-CH₃), 6.18 - 6.19 (d, 1H, $J_{\text{HH}}=6$ Hz, ArH), 6.50 - 6.51 (d, 1H, $J_{\text{HH}}=6$ Hz, ArH), 7.13-7.16 (t, 1H, ArH), 7.20-7.23 (ddd, 1H, $J_{\text{HH}}=0.6$ Hz, ArH), 7.36-7.38 (t, 1H, $J_{\text{HH}}=6$ Hz, ArH), 7.61-7.65 (m, 2H, ArH) ppm.

Synthesis of CpTiCl₂{N-[6-(2-diethylborylphenyl)pyrid-2-yl]-N-Me} (**22**):

To a solution of cyclopentadienyl titanium(IV) trichloride (85 mg, 0.387 mmol) in toluene (10 mL) was added **21** (100 mg, 0.387 mmol) in toluene (10 mL) at -37°C and the resulting reaction mixture was stirred at room temperature for 16 h. Then the mixture was filtered through celite and all volatiles were removed under reduced pressure. Crystallization from *n*-pentane allowed for isolating **22** (120 mg, 70%) as a red colored powder. ¹H NMR (C₆D₆, 250 MHz): $\delta= 0.75$ (br, 6H, B(CH₂CH₃)₂), 0.89-1.02 (m, 2H, B(CH₂CH₃)₂), 1.18-1.33 (m, 2H, B(CH₂CH₃)₂), 4.11 (s, 3H, N-CH₃), 5.86-5.89 (d, 1H, $J_{\text{HH}}=7.5$ Hz, ArH), 6.01 (s, 4H), 6.8-6.9 (ddd, 1H, $J_{\text{HH}}=1.75$ Hz, ArH), 7.02- 7.05(d, 1H, $J_{\text{HH}}=7.75$ Hz, ArH), 7.19-7.26 (ddd, 1H, $J_{\text{HH}}=1.25$ Hz, ArH), 7.35-7.41 (ddd, 1H, $J_{\text{HH}}=1$ Hz, ArH), 7.56-7.58 (d, 1H, $J_{\text{HH}}=5$ Hz, ArH), 7.75-7.78 (d, 1H, $J_{\text{HH}}=8.25$ Hz, ArH) ppm. ¹³C NMR (C₆D₆, 250 MHz): $\delta=10.8, 15.2, 50.7, 114.83, 118.4, 120.4, 121.5, 123.0, 125.4, 130.0, 130.8, 135.7, 140.9, 159.2, 168.2$ ppm. **Elemental anal.** calcd. for C₂₁H₂₅BCl₂N₂Ti: C 57.98, H 5.79, N 6.44; found C 58.35, H 5.88, N 6.41; Crystals suitable for single-crystal X-ray analysis were obtained via recrystallization from toluene/pentane.

Synthesis of Cp*TiCl₂{N-[6-(2-diethylborylphenyl)pyrid-2-yl]-N-Me} (23):

To a solution of pentamethylcyclopentadienyltitanium(IV) trichloride (0.112 g, 0.386 mmol) in toluene (20 mL) was added **21** (100 mg, 0.386 mmol) in toluene (20 mL) at -37°C and the resulting reaction mixture was allowed to stir at room temperature for 16 h. Then it was filtered through celite and all volatiles were removed under reduced pressure. Crystallisation from *n*-pentane allowed for isolating **23** (170 mg, 87%) as a red colored powder. ¹H NMR (C₆D₆, 250 MHz): δ=0.97- 1.03 (t, 6H, *J*_{HH}=1.75 Hz, B(CH₂CH₃)₂), 1.15-1.29 (m, 2H, B(CH₂CH₃)₂), 1.39-1.54 (m, 2H, B(CH₂CH₃)₂), 2.00 (s, 15H, cp*), 3.77 (s, 3H, N-CH₃), 7.06-7.20 (m, 3H, ArH), 7.316-7.381 (ddd, 1H, *J*_{HH}=1.25 Hz, ArH), 7.50-7.56 (ddd, 1H, *J*_{HH}=1 Hz, ArH), 7.67-7.70 (d, 1H, *J*_{HH}=7.75 Hz, ArH), 8.00-8.03 (d, 1H, *J*_{HH}=7.25 Hz, ArH) ppm. ¹³C NMR (C₆D₆, 250 MHz): δ=10.9, 13.6, 16.5, 49.0, 115.0, 120.9, 121.6, 125.5, 129.9, 130.7, 133.0, 136.4, 140.7, 159.5, 166.6 ppm. **Elemental anal.** calcd. for C₂₆H₃₅BCl₂N₂Ti: C 61.82, H 6.98, N 5.55, found. C 61.52, H 7.08, N 5.64; Crystals suitable for single-crystal X-ray analysis were obtained via re-crystallization from toluene/pentane.

Synthesis of TiCl₂{bis-(N-[6-(2-diethylborylphenyl)pyrid-2-yl]-N-Me)} (24):

To a solution of TiCl₄·2THF (454 mg, 1.36 mmol) in toluene (25 mL) was added **21** (700 mg, 2.72 mmol) at -37°C and the resulting reaction mass was stirred 16 h at room temperature. Then it was filtered through celite and all volatiles were removed under reduced pressure. Crystallization from *n*-pentane, and washing with cold diethyl ether (3 mL) allowed for obtaining **24** (500 mg, 30%) as a red colored powder. ¹H NMR (CDCl₃, 600 MHz): δ=0.43-0.46 (t, 12H, *J*_{HH}=6 Hz, B(CH₂CH₃)₂), 0.84 (br, 4H, B(CH₂CH₃)₂), 1.04 (br, 4H, B(CH₂CH₃)₂), 3.58 (s, 6H, N-CH₃), 7.29-7.31 (t, 2H, *J*_{HH}=6 Hz, ArH), 7.35-7.36 (d, 2H, *J*_{HH}=6 Hz, ArH), 7.42-7.45 (t, 2H, *J*_{HH}=6 Hz, ArH), 7.61-7.62 (d, 2H, *J*_{HH}=6 Hz, ArH), 7.83-7.84 (d, 2H, *J*_{HH}=6 Hz, ArH), 7.86-7.87 (d, 2H, *J*_{HH}=6 Hz, ArH), 8.03-8.05 (t, 2H, *J*_{HH}=6 Hz, ArH) ppm. ¹³C NMR (CDCl₃, 600 MHz): δ=10.5, 15.8, 42.3, 115.5, 119.8, 121.4, 125.4, 129.3, 130.3, 135.7, 141.6, 160.0, 162.6, 165.2 ppm.

Synthesis of N-[6-(2-Diethylborylphenyl)pyrid-2-yl]trimethylsilylamine (25)

A solution of **9** (250 mg, 1.05 mmol) in diethyl ether (20 mL) was cooled to -50°C and *n*-BuLi (1.6 M in hexane, 0.72 mL, 1.14 mmol) was added slowly. The resulting reaction mixture was stirred at same temperature for 2 h, then trimethylsilyl chloride (0.125 g, 1.15 mmol) was added and the mixture was stirred for another 3 h, filtered through celite and the diethyl ether was removed under reduced pressure, compound-**25** (270 mg, 85%) was isolated as a light yellow powder. ¹H NMR (C₆D₆, 250 MHz): δ=0.05 (s, 9H, Si(CH₃)₃), 0.77-0.81 (t,

6H, $J_{\text{HH}}=5$ Hz, B(CH₂CH₃)₂), 1.12-1.21 (m, 2H, B(CH₂CH₃)₂), 1.35-1.45 (m, 2H, B(CH₂CH₃)₂), 5.78 (br, 1H, Ar-NH), 6.08-6.10 (dd, 1H, $J_{\text{HH}}=2.5$ Hz, ArH), 6.77-6.79 (dd, 1H, $J_{\text{HH}}=2.5$ Hz, ArH), 6.95-6.99 (t, 1H, $J_{\text{HH}}=7.5$ Hz, ArH), 7.208-7.249 (ddd, 1H, $J_{\text{HH}}=0.75$ Hz, ArH), 7.388-7.427 (ddd, 1H, $J_{\text{HH}}=0.75$ Hz, ArH), 7.59-7.61 (d, 1H, $J_{\text{HH}}=7.5$ Hz, ArH), 7.79-7.81 (d, 1H, $J_{\text{HH}}=7.5$ Hz, ArH) ppm. ¹³C NMR (C₆D₆, 250 MHz): $\delta=0.01$, 11.0, 16.3, 106.6, 108.2, 121.9, 126.3, 130.2, 131.0, 138.5, 140.8, 157.1, 158.7 ppm. **GC-MS (EI, 70 ev)** calcd. for C₁₈H₂₇BN₂Si: m/z 310.20, found. 309.2 [M-H]⁺. **Elemental anal.** calcd. for C₁₈H₂₇BN₂Si: C 69.67, H 8.77, N 9.03; found. C 69.55, H 9.05, N 8.98.

Synthesis of CpTiCl₂(N-(6-(2-(diethylboryl)phenyl)pyrid-2-yl)SiMe₃) (26):

A solution of **25** (280 mg, 0.903 mmol) in diethyl ether (40 mL) was cooled to -37°C and n-BuLi (1.6 M in hexane, 0.4 mL, 0.937 mmol) was added slowly. The resulting reaction mixture was stirred at room temperature for 2 h, then the solvent was removed under reduced pressure to obtain the Li salt, it was re-dissolved in toluene (20 mL), the mixture was cooled to -37°C and slowly added to a toluene solution of trichloro(cyclopentadienyl)titanium (IV) (200 mg, 0.903 mmol). The mixture was stirred at room temperature for 12 h, then filtered through celite and the solvent was removed under reduced pressure. The crude product was washed with cold diethyl ether (2 mL) and dried to get **26** (200 mg, 45%) as a orange colored solid. ¹H NMR (C₆D₆, 250 MHz): $\delta=0.33$ (s, 9H, Si(CH₃)₃), 0.79 (br, 3H, B(CH₂CH₃)₂), 0.96 (br, 2H, B(CH₂CH₃)₂), 1.16 (br, 3H, B(CH₂CH₃)₂), 1.24 (br, 2H, B(CH₂CH₃)₂), 1.53 (br, 1H, cp), 6.17 (s, 4H, cp), 6.57-6.59 (d, 1H, $J_{\text{HH}}=7.5$ Hz, ArH), 6.99-7.03 (t, 1H, $J_{\text{HH}}=7.5$ Hz, ArH), 7.09-7.01 (d, 1H, $J_{\text{HH}}=7.5$ Hz, ArH), 7.19-7.22 (t, 1H, $J_{\text{HH}}=7.5$ Hz, ArH), 7.36-7.39 (t, 1H, $J_{\text{HH}}=7.5$ Hz, ArH), 7.58-7.60 (d, 1H, $J_{\text{HH}}=7.5$ Hz, ArH), 7.88-7.90 (d, 1H, $J_{\text{HH}}=7.5$ Hz, ArH) ppm. ¹³C NMR (C₆D₆, 250 MHz): $\delta=3.1$, 11.1, 11.7, 15.0, 113.5, 119.5, 121.4, 121.6, 125.1, 130.0, 130.3, 135.7, 139.6, 159.7, 165.6 ppm. **Elemental anal.** calcd. for C₂₃H₃₁BCl₂N₂SiTi : C 56.01, H 6.34, N 5.68; found. C 55.49, H 6.49, N 5.50.

Synthesis of Cp*TiCl₂(N-(6-(2-(diethylboryl)phenyl)pyrid-2-yl)SiMe₃) (27):

A solution of **25** (200 mg, 0.645 mmol) in diethyl ether (40 mL) was cooled to -37°C and n-BuLi (1.6 M in hexane, 0.44 mL, 0.937 mmol) was added slowly. The resulting reaction mixture was allowed to stir at room temperature for 2 h, then the solvent was removed under reduced pressure to obtain the Li salt. It was re-dissolved in toluene (20 mL) and slowly added to a toluene solution containing trichloro (pentamethylcyclopentadienyl) titanium (IV) (186 mg, 0.643 mmol) at -37°C. The mixture was warmed to room temperature and stirred for 12h. After this time, it was filtered through celite, then the solvent was evaporated under

reduced pressure and the remaining crude material was washed with cold diethyl ether (2 mL) and dried to obtain **27** (175 mg, 50%) as a red colored solid. $^1\text{H NMR}$ (C_6D_6 , 400 MHz): $\delta=0.34$ (s, 9H, $\text{Si}(\underline{\text{CH}_3})_3$), 1.14-1.5 (br, 10H, $\text{B}(\underline{\text{CH}_2\text{CH}_3})_2$), 1.74 (s, 15H, cp*), 6.66 (br, 1H, ArH), 6.93 (br, 1H, ArH), 7.06 (br, 1H, ArH), 7.16 (br, 1H, ArH), 7.32 (br, 1H, ArH), 7.57 (br, 1H, ArH), 7.90 (br, 1H, ArH) ppm. $^{13}\text{C NMR}$ (C_6D_6 , 400 MHz): $\delta=4.2$, 12.1, 13.5, 112.6, 120.6, 121.6, 124.9, 128.5, 129.9, 130.3, 133.8, 135.7, 138.5, 158.9, 166.6 ppm; Crystals suitable for single-crystal X-ray analysis were obtained via re-crystallization from toluene/pentane.

Synthesis of Biphenyl-3-yl-amine (**28**):

3-Bromo aniline (3.0 g, 17.44 mmol) and phenylboronic acid (2.34 g, 19.18 mmol) were dissolved in a mixture of toluene (45 mL) and ethanol (15 mL). To this reaction mixture was added Na_2CO_3 (4.49 g, 43.6 mmol), tetrakis(triphenylphosphine)palladium(0) (100 mg, 0.087 mmol) and water (10 mL) and the resulting reaction mixture was degassed with nitrogen and heated to reflux for 20 h. Then the solvent was removed under reduced pressure and the residue was diluted with water. The aq. layer was extracted with ethyl acetate (2 x 50 mL), and the combined organic layers were washed with water (50 mL) and brine solution (50 mL) and finally dried over Na_2SO_4 . All volatiles were removed under reduced pressure, and the resulting crude product was purified by column chromatography (60-120 silica) eluting with ethyl acetate in petroleum ether (2:8) to obtain **28** (2.5 g, 86%) as an oily product. $^1\text{H NMR}$ (CDCl_3 , 400 MHz): $\delta=3.75$ (br, 2H, Ar- NH_2), 6.72 (br, 1H, ArH), 6.95 (br, 1H, ArH), 7.04 (br, 1H, ArH), 7.28 (br, 1H, ArH), 7.38 (br, 1H, ArH), 7.46 (br, 2H, ArH), 7.61 (br, 2H, ArH) ppm. $^{13}\text{C NMR}$ (CDCl_3 , 400 MHz): $\delta=113.9$, 114.1, 117.70, 127.1, 127.2, 128.6, 129.7, 141.4, 142.5, 146.7 ppm. GC-MS: m/z calcd. for $\text{C}_{12}\text{H}_{11}\text{N}$: 169.1, found. 169.1 (M^+).

Synthesis of Biphen-3-yl-trimethylsilylamine (**29**):

A solution of biphenyl-3-ylamine (**28**) (1.0 g, 5.9 mmol) in diethyl ether (30 mL) was cooled to -60°C and $n\text{-BuLi}$ (1.6 M in hexane, 3.9 mL, 6.09 mmol) was added slowly. The resulting reaction mixture was stirred for 2 h at -60°C . Then trimethylsilyl chloride (1.28 g, 11.8 mmol) was added, the mixture was allowed to stir for 5 h at room temperature and then filtered. All volatiles were evaporated under reduced pressure to get **29** (1.2 g, 80%) as an off white solid. $^1\text{H NMR}$ (C_6D_6 , 400 MHz): $\delta=0.05$ (s, 9H, $\text{Si}(\underline{\text{CH}_3})_3$), 2.98 (br, 1H, Ar- $\underline{\text{NH}}$), 6.44 (br, 1H, ArH), 6.73 (br, 1H, ArH), 6.89 (br, 1H, ArH), 7.02 (br, 2H, ArH), 7.12 (br, 2H, ArH), 7.46 (br, 2H, ArH) ppm. $^{13}\text{C NMR}$ (C_6D_6 , 400 MHz): $\delta=0.01$, 115.4, 115.8, 117.2, 127.3, 127.5,

128.9, 129.9, 142.4, 143.0, 148.1 ppm. GC-MS: m/z calcd. for $C_{15}H_{18}NSi$: 241.10, found. 241.1 (M^+).

Synthesis of $CpTiCl_2(N\text{-}(biphenyl\text{-}3\text{-}yl)SiMe_3)$ (**30**):

A solution of **29** (250 mg, 1.03 mmol) in diethyl ether (20 mL) was cooled to $-37^\circ C$ and $n\text{-BuLi}$ (1.6 M in hexane, 0.65 mL, 1.03 mmol) was added. The reaction mixture was stirred at room temperature for 2 h, and then all volatiles were removed under reduced pressure to get the Li salt of **29** which was re-dissolved in toluene (20 mL). The solution was added to a toluene solution containing trichloro(cyclopentadienyl)titanium (IV) (227 mg, 1.03 mmol) at $-37^\circ C$ and the resulting reaction mixture was allowed to stir at room temperature for 12 h. Finally the reaction mixture was filtered through celite and solvent was removed under reduced pressure to get the crude product. Which was crystallized from n -pentane to get a pure form of **30** (150 mg, 35%) as an orange colored solid. 1H NMR (C_6D_6 , 400 MHz): $\delta=0.31$ (s, 9H, $Si(CH_3)_3$), 5.83 (s, 4H, cp), 6.37 (1H, ArH), 6.92 (s, 2H, ArH), 7.02 (s, 2H, ArH), 7.07-7.09 (m, 2H, ArH), 7.36 (s, 2H, ArH) ppm. ^{13}C NMR (C_6D_6 , 400 MHz): $\delta= 2.1$, 120.7, 122.1, 122.5, 123.4, 127.2, 129.0, 129.1, 140.6, 141.9, 159.5 ppm. **Elemental anal.** calcd. for $C_{20}H_{23}Cl_2NSiTi$. C 56.61, H 5.46, N 3.30; found. C 56.78, H 5.59, N 3.34.

Synthesis of $Cp^*TiCl_2(N\text{-}(biphenyl\text{-}3\text{-}yl)SiMe_3)$ (**31**):

A solution of **29** (250 mg, 1.03 mmol) in diethyl ether (20 mL) was cooled to $-37^\circ C$ and $n\text{-BuLi}$ (1.6 M in hexane, 0.65 mL, 1.03 mmol) was added slowly. The resulting reaction mixture was stirred for 2 h at room temperature. Then the solvent was removed under reduced pressure to get the Li salt of **29**, which was re-dissolved in toluene (15 mL). This solution was added to a toluene solution containing trichloro(pentamethylcyclopentadienyl)titanium (IV) (300 mg, 1.03 mmol) at $-37^\circ C$ and the resulting reaction mixture was allowed to stir at room temperature for 12h. It was then filtered through celite and the solvent was removed under reduced pressure. The crude product was crystallized from n -pentane to get pure form of **31** (300 mg, 58%) as red colored solid. 1H NMR (C_6D_6 , 400 MHz): $\delta=0.30$ (s, 9H, $Si(CH_3)_3$), 1.72 (s, 15H, cp*), 6.87 (s, 1H, ArH), 7.05-7.07 (2H, ArH), 7.16 (3H, ArH), 7.44 (s, 1H, ArH), 7.58 (s, 2H, ArH) ppm. ^{13}C NMR (C_6D_6 , 400 MHz): $\delta= 3.2$, 12.9, 123.1, 125.0, 125.1, 127.0, 128.9, 129.2, 131.4, 141.0, 141.6, 153.0 ppm.

Synthesis of Biphenyl-3-yl-methylamine (**32**):

3-Bromo-N-methyl aniline (1.0 g, 5.37 mmol) and phenyl boronic acid (720 mg, 5.9 mmol) were dissolved in toluene (25 mL) and ethanol (15 mL) and stirred for 10 min. To this solution were added Na₂CO₃ (1.4 g, 13.59 mmol), tetrakis(triphenylphosphine)palladium(0) (30 mg, 0.025 mmol) and water (5 mL). The resulting reaction mixture was degassed and heated to reflux for 20 h. After this time the solvents were removed under reduced pressure and the residue was diluted with water. The aq. layer was extracted with ethyl acetate (2 x 40 mL). The combined organic layers were washed with water (25 mL), brine solution (25 mL) and finally dried over Na₂SO₄. All volatiles were removed under reduced pressure. The resulting crude product was purified by column chromatography (60-120 silica gel) eluting with ethyl acetate in petroleum ether (2:8) to obtain **32** (760 mg, 75%) as an oily product. ¹H NMR (CDCl₃, 250 MHz): δ=2.72 (s, 3H, N-CH₃), 3.64 (br, 1H, NH), 6.43-6.47 (dddd, 1H, J_{HH}=2.5 Hz, ArH), 6.64-6.66 (t, 1H, J_{HH}=2.5 Hz, ArH), 6.76-6.80 (m, 1H, ArH), 7.07-7.10 (t, 1H, ArH), 7.13-7.29 (m, 3H, ArH), 7.40-7.44 (m, 2H, ArH) ppm. ¹³C NMR (CDCl₃, 250 MHz): δ=31.2, 111.6, 111.9, 116.8, 127.5, 127.6, 129.0, 130.0, 142.2, 142.8, 155.0 ppm. GC-MS: *m/z* calcd. for C₁₃H₁₃N: 183.10, found. *m/z* 183.10.

Synthesis of Cp*TiCl₂[N-(biphenyl-3-yl)Me] (**33**):

N-Biphen-3-yl-N-methylamine (**32**, 100 mg, 0.546 mmol) was dissolved in diethyl ether (15 mL) cooled to -37°C and n-BuLi (1.6 M in n-hexane, 0.36 mL, 0.54 mmol) was added slowly. The resulting reaction mixture was allowed to stir at room temperature for 3h, then the diethyl ether was removed under reduced pressure and the residue was re-dissolved in toluene (15 mL), cooled to -37°C, and this solution was slowly added to trichloro(pentamethylcyclopentadienyl) titanium(IV) (0.158 mg, 0.54 mmol) in toluene (15 mL). The mixture was stirred at room temperature for 12 h. Then filtered through celite and the filtrate was removed under reduced pressure. The resulting crude material was stripped off in *n*-pentane to get pure **33** (100 mg, 40%) as a red colored powder. ¹H NMR (C₆D₆, 250 MHz): δ=1.80 (s, 15H, cp*), 3.41 (s, 3H, N-CH₃), 6.81-6.86 (tt, 1H, J_{HH}=2.5 Hz, ArH), 7.18-7.29 (m, 4H, ArH), 7.47-7.48 (d, 1H, J_{HH}=2.5 Hz, ArH), 7.62-7.66 (m, 2H, ArH) ppm. ¹³C NMR (C₆D₆, 250 MHz): δ=12.8, 40.7, 119.5, 121.0, 123.0, 127.6, 127.8, 129.3, 129.5, 130.8, 141.6, 142.2, 155.0 ppm. **Elemental anal.** calcd. for C₂₃H₂₇Cl₂NTi: C 63.32, H 6.24, N 3.21; Found. C 63.39, H 6.63, N 2.98.

Synthesis of CpTiCl₂[N-(biphenyl-3-yl)Me] (**34**):

N-Biphen-3-yl-N-methylamine (**32**, 300 mg, 1.63 mmol) was dissolved in diethyl ether (25 mL), the solution was cooled to -37°C and n-BuLi (1.6 M in n-hexane, 0.77 mL, 1.63 mmol)

was added slowly. The resulting reaction mixture was allowed to stir at room temperature for 3h. Then the diethyl ether was removed under reduced pressure and the residue was re-dissolved in toluene (25 mL) and cooled to -37°C , then slowly added to a solution of trichloro(cyclopentadienyl) titanium(IV) (0.36 mg, 1.63 mmol) in toluene (25 mL). The mixture was stirred at room temperature for 12 h. Then filtered through celite, the all volatiles were removed under reduced pressure. The resulting crude material was stripped off in *n*-pentane to get pure **34** (250 mg, 40%) as an orange color powder. $^1\text{H NMR}$ (C_6D_6 , 400 MHz): $\delta=4.08$ (s, 3H, N- CH_3), 6.01(s, 4H, cp), 6.42-6.43 (m, 1H, ArH), 6.98-7.03(m, 2H, ArH), 7.15-7.2 (m, 4H, ArH), 7.36-7.37 (m, 2H, ArH) ppm. $^{13}\text{C NMR}$ (C_6D_6 , 400 MHz): $\delta= 50.4$, 119.2, 121.0, 121.5, 124.8, 127.3, 127.8, 129.0, 129.6, 140.4, 142.6, 162.6 ppm. **Elemental anal.** calcd. for $\text{C}_{18}\text{H}_{17}\text{Cl}_2\text{NTi}$: C 59.05, H 4.68, N 3.83; found. C 58.96, H 4.70, N 3.76; Crystals suitable for single-crystal X-ray analysis were obtained via re-crystallization from toluene/pentane.

Synthesis of ethane-1,2-diyl bis(4-methylbenzenesulfonate) (**35**):

To a solution of p-toluenesulfonyl chloride (1.0 g, 5.24 mmol) and ethylene glycol (0.16 g/ 0.15 mL, 2.61 mmol) in CH_2Cl_2 (20 mL) was added triethylamine (1.58 g/ 2.1 mL, 15.6 mmol) at 0°C and the resulting reaction mixture was stirred at room temperature for 12 h. Then the organic layer was diluted with CH_2Cl_2 (20 mL) and washed with sat. NaHCO_3 solution (20 mL), water (20 mL) and brine solution (20 mL). The combined organic layers were dried over Na_2SO_4 and the solvent was removed *in vacuo*. The resulting crude material was purified by column chromatography (60- 120 silica) eluting with ethyl acetate in chloroform (2 : 8), **35** was isolated as a white solid (500 mg, 51%). $^1\text{H NMR}$ (CDCl_3 , 600 MHz): $\delta = 7.729$ -7.743 (d, 2H, $J_{\text{HH}}=8.4\text{Hz}$, ArH), 7.349-7.336 (d, 2H, $J_{\text{HH}}=7.8\text{Hz}$, ArH), 4.18 (s, 2H), 2.46 (s, 3H, Ar- CH_3) ppm. $^{13}\text{C NMR}$ (CDCl_3 , 600 MHz): $\delta = 145.4$, 132.3 , 130.1, 128.0, 66.83 , 21.7 ppm. **IR** (neat, $4000 - 400 \text{ cm}^{-1}$) $\nu^- = 3373$, 2926, 1930, 1690, 1589, 1483, 1446, 1409, 1356, 1299, 1173, 1091, 1023, 911, 808, 759, 659 cm^{-1} .

Synthesis of N,N¹-bis(6-(2-(diethylboryl)phenyl)pyrid-2-yl)benzene-1,2-diamine: (**36**)

A mixture of tris(*tert*-butyl) phosphine (21 mg, 0.103 mmol) and palladium(II) acetate (70 mg, 0.31 mmol) in toluene (25 mL) was stirred for 10 min. To this reaction mixture, **9** (500 mg, 2.1 mmol), 1,2-dibromo benzene (0.29 g, 1.26 mmol) and sodium *tert*-butoxide (600 mg, 6.25 mmol) were added under an inert atmosphere and the mixture was heated to 100°C for 12 h. Then it was quenched with saturated NaHCO_3 solution (10 mL) and extracted with ethyl acetate (2x 25 mL). The combined organic layers were washed with water (20 mL), brine

solution (20 mL) and dried over Na₂SO₄. The solvent was removed in *vacuo* and the resulting crude material was purified by column chromatography (60-120 silica) eluting with ethyl acetate in petroleum ether (2: 8), to obtain the **36** (300 mg, 52%) as white solid. ¹H NMR (CDCl₃, 600 MHz): δ=0.35-0.32 (t, 6H, *J*_{HH}=7.2 Hz, *J*_{HH}=7.8 Hz, B(CH₂CH₃)₂), 0.74-0.70 (m, 2H, B(CH₂CH₃)₂), 0.91-0.86 (m, 2H, B(CH₂CH₃)₂), 6.69-6.67 (d, 1H, *J*_{HH}=12 Hz, ArH), 7.26-7.23 (ddd, 1H), 7.37-7.31 (m, 3H), 7.42 (br, 1H, Ar-NH), 7.46-7.45 (m, 1H, ArH), 7.52-7.50 (d, 1H, *J*_{HH}=7.2 Hz, ArH), 7.72-7.69 (t, 1H, *J*_{HH}=8.4 Hz, ArH), 7.74-7.72 (d, 1H, *J*_{HH}=7.8 Hz, ArH) ppm. ¹³C NMR (CDCl₃, 600MHz): δ=10.0, 14.6, 106.3, 107.9, 121.0, 125.2, 125.3, 127.3, 129.1, 129.8, 133.9, 136.9, 140.6, 153.2, 157.7 ppm. HR-MS (ESI) calcd. for C₃₆H₄₀B₂N₄: 550.344, found: 521.30 [M-C₂H₅]⁺, 493.16 [M-C₄H₁₀]⁺. IR (neat, 4000 – 400 cm⁻¹) ν⁻ = 3369, 2934, 2858, 2804, 1619, 1569, 1480, 1443, 1380, 1293, 1163, 1099, 1031, 907, 872, 798, 751 cm⁻¹.

Synthesis of N, N¹-bis(6-(2-(diethylboryl)phenyl)pyridi-2-yl)-4-methylbenzene-1,2-diamine (37): A solution of tris(*tert*-butyl)phosphine (22 mg, 0.108 mmol) and palladium(II) acetate (74 mg, 0.33 mmol) in toluene (30 mL) was stirred for 10 min., then **9** (500 mg, 2.1 mmol), 3,4-dibromo toluene (0.315 g, 1.26 mmol) and sodium *tert*-butoxide (600 mg, 6.3 mmol) were added under an inert atmosphere and the mixture was heated to 100°C for 12 h. After this time, the mixture was quenched with saturated NaHCO₃ solution (20 mL) and extracted with ethyl acetate (2 x 25 mL). The combined organic layers were washed with water (20 mL), brine solution (20 mL) and dried over Na₂SO₄, the solvent was removed in *vacuo* and the resulting crude material was purified by column chromatography (60-120 silica) eluting with ethyl acetate in petroleum ether (2:8) to obtain **37** (280 mg, 47%) as a white solid. ¹H NMR (CDCl₃, 600 MHz): δ =0.35-0.30 (s, 12H, B(CH₂CH₃)₂), 0.73-0.68 (m, 4H, B(CH₂CH₃)₂), 0.91-0.84 (m, 4H, B(CH₂CH₃)₂), 2.41 (s, 3H, Ar-CH₃), 6.57-6.56 (d, 1H, *J*_{HH}=8.4 Hz, ArH), 6.70-6.69 (d, 1H, *J*_{HH}=8.4 Hz, ArH), 7.12-7.11(d, 1H, *J*_{HH}=8.4 Hz, ArH), 7.25-7.22 (t, 2H, *J*_{HH}=6 Hz, *J*_{HH}=12 Hz, ArH), 7.33-7.28 (m, 4H, ArH), 7.37-7.34 (t, 2H, *J*_{HH}=6 Hz, ArH), 7.41 (br, 1H, Ar-NH), 7.52-7.50 (t, 2H, *J*_{HH}=6 Hz, ArH), 7.73-7.65 (m, 4H, ArH) ppm. ¹³C NMR (CDCl₃, 600MHz): δ =163.6, 157.7, 157.5, 153.7, 153.0, 140.6-140.5 (d), 138.0, 136.95- 136.9 (d), 134.2, 130.8, 129.8-129.7(d), 129.0, 127.9, 126.1, 125.2, 121.0, 107.7, 107.4, 106.2, 106.0, 21.3, 14.5, 10.0-9.9(d) ppm. HRMS (ESI positive): calcd. for C₃₇H₄₂B₂N₄ +Na 587.349, found: 587.349. IR (neat, 4000 – 400 cm⁻¹) ν⁻ = 3369, 2934, 2860, 2807, 1618, 1570, 1524, 1477, 1443, 1380, 1296, 1163, 1122, 1031, 903, 873, 807, 749,654 cm⁻¹.

Synthesis of N, N¹-bis(6-(2-(diethylboryl)phenyl)pyrid-2-yl)ethane-1,2-diamine (38):

To NaH (60 wt-% in mineral oil, 0.33 g, 8.4 mmol), DMF (10 mL) was added and the suspension was cooled to 0°C. **9** (1.0 g, 4.2 mmol) dissolved in DMF (5 mL) was slowly added, and the mixture was heated to 80°C for 2 h. Then, **35** (1.0 g, 2.7 mmol) was added portion wise (4 portions) over 60 minutes at 75°C and the reaction was allowed to continue for another 1 h at the same temp. Then the mixture was cooled to room temperature and ice water (5 mL) was added slowly and the mixture was extracted with ethyl acetate (2x30 mL). The combined organic layers were washed with water (3x25 mL), brine (25 mL) and dried over Na₂SO₄, then all volatiles were removed *in vacuo*. The crude product was purified by column chromatography eluting with ethyl acetate in petroleum ether (3:7) to obtained **38** (310 mg, 41%) as a white solid. ¹H NMR (CDCl₃, 600 MHz): δ=0.37-0.34 (t, 6H, *J*_{HH}=7.8 Hz, *J*_{HH}=7.8 Hz, B(CH₂CH₃)₂), 0.73-0.67 (m, 2H, B(CH₂CH₃)₂), 0.93-0.86 (m, 2H, B(CH₂CH₃)₂), 3.67-3.66 (t, 2H, *J*_{HH}=3 Hz, *J*_{HH}=3 Hz, -NH-CH₂-CH₂-NH-), 5.99 (br, 1H, Ar-NH), 6.51-6.50 (d, 1H, *J*_{HH}=6 Hz, ArH), 7.23-7.23 (d, 1H, *J*_{HH}=3.6 Hz, ArH), 7.25-7.24 (d, 1H, *J*_{HH}=6 Hz, ArH), 7.38-7.36 (t, 1H, *J*_{HH}=7.2 Hz, ArH), 7.52-7.51 (d, 1H, *J*_{HH}=7.2 Hz, ArH), 7.75-7.72 (m, 2H, ArH) ppm. ¹³C NMR (CDCl₃, 600 MHz): δ =10.0, 14.5, 42.7, 102.8, 105.8, 121.0, 125.2, 129.0, 129.7, 137.1, 140.8, 154.7, 157.4 ppm. HR-MS (ESI positive) calcd. for C₃₂H₄₀B₂N₄ +Na: 525.334, found: 525.335. IR (neat, 4000 – 400 cm⁻¹) ν⁻ =3416, 3051, 2936, 2856, 2807, 1617, 1572, 1517, 1472, 1445, 1384, 1289, 1228, 1163, 1088, 1039, 943, 903, 848, 800, 750, 655 cm⁻¹.

Synthesis of 2-Bromo-N-(6-(2-(diethylboryl)phenyl)pyrid-2-yl) acetamide (39)

A solution of bromoacetyl bromide (0.084 g, 0.417 mmol) in dichloromethane (10 mL) was cooled to 0°C and **9** (100 mg, 0.42 mmol), dimethylaminopyridine (0.076 g, 0.63 mmol) were dissolved in 5 mL of dichloromethane each and these reagents were added to the reaction mixture at 0° C over 10 min. The reaction was continued for another 3 h at room temperature and its progress was monitored by thin layer chromatography (TLC). Once the reaction was completed, the reaction mass was quenched with ice water (5 mL) and extracted with CH₂Cl₂ (25 mL). The combined organic layers were washed with sat. NaHCO₃ solution (30 mL), water (30 mL), and brine solution (30mL), and dried over Na₂SO₄. The solvent was evaporated and the crude product was purified by column chromatography by eluting with 2-3% ethyl acetate in petroleum ether **39** (120 mg, 80%) was obtained as a white solid. ¹H NMR (CDCl₃, 250 MHz): δ= 0.3-0.36 (t, 6H, *J*_{HH}=7.5 Hz, B(CH₂CH₃)₂), 0.83-1.1 (m, 2H, B(CH₂CH₃)₂), 4.11 (s, 2H, -CH₂-Br), 7.26-7.33 (ddd, 1H, *J*_{HH}=2.5 Hz, ArH), 7.4-7.46 (ddd, 1H, *J*_{HH}=2.5 Hz, ArH), 7.54-7.57 (d, 1H, *J*_{HH}=7.5 Hz, ArH), 7.68-7.72 (dd, 1H, *J*_{HH}=2.5 Hz,

ArH), 7.77-7.81 (d, 1H, $J_{\text{HH}}=10$ Hz, ArH), 7.95-8.02 (t, 1H, $J_{\text{HH}}=7.5$ Hz, ArH), 8.27-8.31 (dd, 1H, $J_{\text{HH}}=2.5$ Hz, ArH), 9.53 (br, 1H, Ar-NH) ppm. ^{13}C NMR (CDCl_3 , 250 MHz): $\delta=10.0$, 15.0, 29.0, 112.0, 113.4, 121.6, 125.9, 129.3, 130.8, 136.6, 141.9, 147.5, 158.1, 164.8 ppm.

2-(tert-Butylamino)-N-(6-(2-(diethylboryl) phenyl)pyridin-2-yl)acetamide (40):

To a solution of **39** (120 mg, 0.335 mmol) in CH_2Cl_2 (20 mL) was added tert-butylamine (122 mg, 1.67 mmol). The mixture was stirred at room temperature for 16 h, then all volatiles were removed under reduced pressure and the resulting crude material was purified by column chromatography (60-120 silica) by eluting with 2-4% ethyl acetate in petroleum ether to yield **40** (100 mg, 85%) as a white solid. ^1H NMR (CDCl_3 , 250 MHz): $\delta=0.33$ -0.39 (t, 6H, $J_{\text{HH}}=7.5$ Hz, $\text{B}(\text{CH}_2\text{CH}_3)_2$), 0.9-1.09 (m, 4H, $\text{B}(\text{CH}_2\text{CH}_3)_2$), 1.25 (s, 9H, tert.butyl), 1.6 (br, 1H, tert-butyl-NH), 3.53 (s, 2H), 7.28-7.34 (t, 1H, $J_{\text{HH}}=7.5$ Hz, ArH), 7.41-7.47 (t, 1H, $J_{\text{HH}}=7.5$ Hz, ArH), 7.57-7.6 (d, 1H, $J_{\text{HH}}=7.5$ Hz, ArH), 7.65-7.68 (d, 1H, $J_{\text{HH}}=7.5$ Hz, ArH), 7.79-7.82 (d, 1H, $J_{\text{HH}}=7.5$ Hz, ArH), 7.93-7.99 (t, 1H, $J_{\text{HH}}=7.5$ Hz, ArH), 8.45-8.48 (d, 1H, $J_{\text{HH}}=7.5$ Hz, ArH), 10.83 (br, 1H, Ar-NH) ppm. ^{13}C NMR (CDCl_3 , 250 MHz): $\delta=9.6$, 13.35, 28.7, 47.3, 51.5, 111.6, 112.0, 120.9, 125.2, 128.8, 128.9, 136.4, 141.1, 147.9, 157.3, 172.4 ppm.

Synthesis of N-tert-Butyl-N¹-(6-(2-(diethylboryl) phenyl)pyridin-2-yl)ethane-1,2-diamine (41):

To a solution of **40** (100 mg, 0.285 mmol) in THF (20 mL) was added LiAlH_4 slowly at 0°C , then the reaction mixture was stirred for 2 h at room temperature. It was then quenched with ice and extracted with ethyl acetate (2x15 mL). The combined organic layers were washed with brine solution (25 mL), dried over Na_2SO_4 and all volatiles were removed *in vacuo* and the resulting crude material was purified by column chromatography (60-120 silica) eluting with 1-2% methanol in chloroform. **41** (70 mg, 72%) was obtained as a white solid. ^1H NMR (CDCl_3 , 250 MHz): $\delta=0.33$ -0.40 (t, 6H, $J_{\text{HH}}=7.5$ Hz, $\text{B}(\text{CH}_2\text{CH}_3)_2$), 0.74-0.94 (m, 4H, $\text{B}(\text{CH}_2\text{CH}_3)_2$), 1.18 (s, 9H, tert-butyl), 2.91-2.95 (t, 2H, $J_{\text{HH}}=5$ Hz, tert.butyl-NH- CH_2 -), 1.45 (br, 1H, tert-butyl-NH), 3.30-3.37 (q, 2H, $J_{\text{HH}}=5$ Hz, $J_{\text{HH}}=7.5$ Hz, $J_{\text{HH}}=5$ Hz, Ar-NH- CH_2 -), 6.38-6.41 (d, 1H, $J_{\text{HH}}=7.5$ Hz, ArH), 6.39 (br, 1H, Ar-NH), 7.13-7.16 (d, 1H, $J_{\text{HH}}=7.5$ Hz, ArH), 7.21-7.27 (ddd, 1H, $J_{\text{HH}}=1.25$ Hz, ArH), 7.33-7.4 (ddd, 1H, $J_{\text{HH}}=1$ Hz, ArH), 7.53-7.56 (d, 1H, $J_{\text{HH}}=7.5$ Hz, ArH), 7.63-7.74 (m, 2H, ArH) ppm. ^{13}C NMR (CDCl_3 , 250 MHz): $\delta=10.2$, 14.1, 29.3, 41.1, 43.3, 51.2, 103.4, 104.9, 121.1, 125.3, 129.2, 129.7, 137.6, 140.5, 155.0, 157.3 ppm. HRMS(ESI positive) calcd. for $\text{C}_{21}\text{H}_{32}\text{BN}_3$: 337.27, found: 323.3 [M- CH_2].

Synthesis of 2-(Adamantylamino)-N-(6-(2-(diethylboryl)phenyl)pyrid-2-yl)acetamide (42): To a solution of **39** (900 mg, 2.5 mmol) in CH₂Cl₂ (40 mL) was added adamantylamine (1.13 g, 7.52 mmol). The mixture was stirred at room temperature for 16 h, then all volatiles were removed under reduced pressure and the remaining crude material was purified by column chromatography (60-120 silica) eluting with 2-4% ethyl acetate in petroleum ether. **42** (1 g, 93%) was obtained as a white solid. ¹H NMR (CDCl₃, 250 MHz): δ=0.31-0.37 (t, 6H, J_{HH}=7.5 Hz, B(CH₂CH₃)₂), 0.91-1.08 (m, 2H, B(CH₂CH₃)₂), 1.56 (br, 1H, Ad-NH), 1.67 (s, 6H, Ad-CH₂), 1.72 (s, 6H, Ad-CH₂), 2.12 (s, 3H, Ad-CH), 3.52 (s, 2H, Ad-NH-CH₂-), 7.24-7.28 (ddd, 1H, J_{HH}=2.5 Hz, ArH), 7.37-7.44 (ddd, 1H, J_{HH}=2.5 Hz, ArH), 7.54-7.57 (d, 1H, J_{HH}=7.5 Hz, ArH), 7.61-7.65 (dd, 1H, J_{HH}=2.5 Hz, ArH), 7.76-7.79 (d, 1H, J_{HH}=7.5 Hz, ArH), 7.9-7.96 (t, 1H, J_{HH}=7.5 Hz, ArH), 8.41-8.45 (dd, 1H, J_{HH}=2.5 Hz, ArH), 10.82 (br, 1H, Ar-NH) ppm.

Synthesis of N-Adamantyl-N¹-(6-(2-(diethylboryl)phenyl)pyrid-2-yl)ethane-1,2-diamine (43): A solution of **42** (1 g, 2.33 mmol) in THF (40 mL) was cooled to 0°C, LiAlH₄ was added and the reaction mixture was stirred for 2 h at room temperature. Then it was quenched with ice and extracted with ethyl acetate (2x 50 mL). The combined organic layers were washed with brine solution (50 mL), dried over Na₂SO₄ and the solvent was evaporated. The resulting crude material was purified by column chromatography (60-120 silica) eluting with 1-2 % methanol in chloroform. **43** (750 mg, 77%) was obtained as a white solid. ¹H NMR (CDCl₃, 250 MHz): δ=0.33-0.39 (t, 6H, J_{HH}=7.5 Hz, B(CH₂CH₃)₂), 0.77-0.94 (m, 4H, B(CH₂CH₃)₂), 1.68 (s, 12H, Ad-CH₂), 2.10 (s, 3H, Ad-CH-), 2.94-2.98 (t, 2H, J_{HH}=5 Hz), 3.29-3.26 (q, 2H), 6.37-6.40 (d, 1H, ArH), 6.38 (br, 1H, Ar-NH), 7.12-7.15 (dd, 1H, J_{HH}=0.75 Hz, ArH), 7.20-7.26 (ddd, 1H, J_{HH}=1.25 Hz, ArH), 7.33-7.39 (ddd, 1H, J_{HH}=1 Hz, ArH), 7.52-7.56 (d, 1H, J_{HH}=7.25 Hz, ArH), 7.62-7.72 (m, 2H, ArH) ppm. ¹³C NMR (CDCl₃, 250 MHz): δ=10.3, 14.0, 30.0, 37.1, 39.1, 43.3, 43.8, 50.9, 103.39, 104.8, 121.0, 125.3, 129.2, 129.7, 137.7, 140.5, 155.0, 157.2 ppm. HRMS (ESI positive) calcd. for C₂₇H₃₈BN₃: 415.33, found: 415.30.

General Procedure for Homopolymerizations: The homopolymerization of styrene, NBE or COE was carried out in Schlenk tubes and all preparations were carried out in a glove box. The freshly distilled monomer and a defined amount of MAO were dissolved in toluene in a Schlenk tube. After the mixture was stirred for 5 minutes it was quickly transferred to the indicated temperature while a defined amount of catalyst in toluene was added. Polymerizations were quenched by addition of 10 mL of methanol. The resulting mixture was

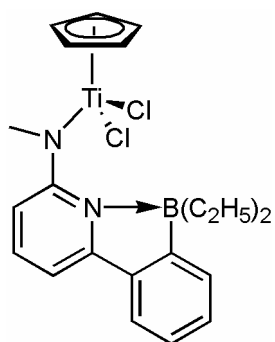
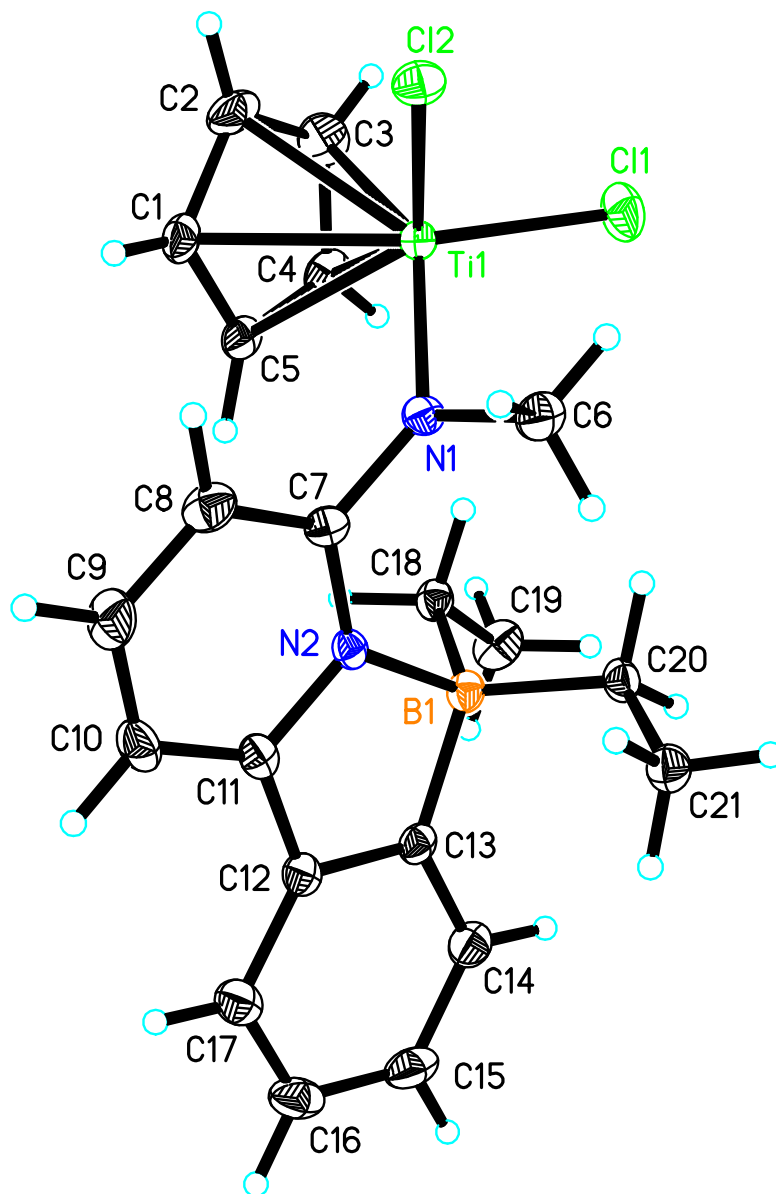
added to a stirred solution of acidic methanol (200 mL including 20 mL of conc. HCl). The polymer was collected by filtration, washed with methanol (3 x 200 mL), and then dried *in vacuo* at 40°C for 24 hours.

General Procedure for Ethylene Homo-/Copolymerization: Polymerizations were carried out in a 500 mL Büchi glass autoclave, equipped with a motor stirrer, external temperature control jacket and pressure gauge. The reactor was heated up to 80°C *in vacuo* for 2 h before starting an experiment.

Procedure A: 235 mL of deoxygenated toluene were poured into the reactor and brought to the desired temperature, and a prescribed amount of monomer (CPE/COE/NBE) and 2.0 M toluene solution of MAO was introduced into the reactor followed by 5 mL toluene solution of prescribed catalyst. Polymerization was started by pressurizing the reactor with ethylene (4 bar). Polymerizations were stopped by closing the ethylene valve and introducing methanol (20 mL) into the reactor. The obtained poly(ethylene) was stirred for 6 h in 20 vol.-% of methanolic HCl (200 mL) to remove any aluminum oxide. Then the polymer was filtered off, washed with methanol and dried *in vacuo* at 50°C for 12 h.

Procedure B: 235 mL of deoxygenated toluene were poured into the reactor and prescribed amount of monomer (CPE/COE/NBE), 2.0 M toluene solution of MAO was introduced into the reactor followed by a 5 mL toluene solution of prescribed catalyst and heated to desired temperature and the was started by pressurizing the reactor with ethylene (2 bar). Polymerizations were stopped by closing the ethylene valve and introducing methanol (20 mL) into the reactor. The obtained poly(ethylene) was stirred for 6 h in 20 vol.-% of methanolic HCl (200 mL) to remove any aluminum oxide. Then the polymer was filtered off, washed with methanol and dried *in vacuo* at 50°C for 12 h.

X-ray structure data for Catalysts 22, 23, 27 and 34

5.1 *Crystal structure of complex 22:*

22

Appendix

Table 1. Crystal data and structure refinement for catalyst **22**.

Identification code	Complex 22
Empirical formula	C ₂₁ H ₂₅ B Cl ₂ N ₂ Ti
Formula weight	435.04
Temperature	100(2) K
Wavelength	0.71073 Å
Crystal system, space group	monoclinic, P2(1)/n
Unit cell dimensions	a = 10.9979(11) Å alpha = 90 deg. b = 16.1318(19) Å beta=106.79(6) deg c = 12.3324(11) Å gamma =90 deg.
Volume	2094.6(4) Å ³
Z, Calculated density	4, 1.380 Mg/m ³
Absorption coefficient	0.672 mm ⁻¹
F(000)	904
Crystal size	0.22 x 0.19 x 0.08 mm
Theta range for data collection	2.14 to 28.57 deg.
Limiting indices	-14<=h<=14, -21<=k<=21, -14<=l<=16
Reflections collected / unique	19850 / 5240 [R(int) = 0.0584]
Completeness to theta = 28.57°	97.9 %
Max. and min. transmission	0.9482 and 0.8662
Refinement method	Full-matrix least-squares on F ²
Data / restraints / parameters	5240 / 0 / 247
Goodness-of-fit on F ²	1.047
Final R indices [I>2sigma(I)]	R1 = 0.0418, wR2 = 0.0741
R indices (all data)	R1 = 0.0792, wR2 = 0.0804
Largest diff. peak and hole	0.403 and -0.291 e.Å ⁻³

Appendix

Table 2. Atomic coordinates ($\times 10^4$) and equivalent isotropic displacement parameters ($\text{\AA}^2 \times 10^3$) for catalyst **22**.

U (eq) is defined as one third of the trace of the orthogonalized U^{ij} tensor.

	x	y	z	U(eq)
Ti(1)	6570(1)	305(1)	3511(1)	15(1)
Cl(1)	6500(1)	1566(1)	4289(1)	28(1)
Cl(2)	7611(1)	-496(1)	5010(1)	21(1)
N(1)	7799(2)	380(1)	2717(1)	16(1)
B(1)	7609(2)	1559(1)	607(2)	16(1)
C(1)	5391(2)	-774(1)	2405(2)	21(1)
N(2)	7956(1)	539(1)	830(1)	14(1)
C(2)	4869(2)	-630(2)	3302(2)	27(1)
C(3)	4377(2)	178(2)	3188(2)	29(1)
C(4)	4581(2)	533(1)	2218(2)	24(1)
C(5)	5204(2)	-55(1)	1732(2)	18(1)
C(6)	9040(2)	617(1)	3529(2)	22(1)
C(7)	7969(2)	35(1)	1717(2)	15(1)
C(8)	8187(2)	-804(1)	1674(2)	23(1)
C(9)	8389(2)	-1154(1)	718(2)	27(1)
C(10)	8376(2)	-650(1)	-182(2)	22(1)
C(11)	8170(2)	194(1)	-111(2)	16(1)
C(12)	8158(2)	822(1)	-963(2)	17(1)
C(13)	7885(2)	1602(1)	-602(2)	16(1)
C(14)	7917(2)	2274(1)	-1305(2)	22(1)
C(15)	8186(2)	2151(2)	-2328(2)	26(1)
C(16)	8429(2)	1366(2)	-2672(2)	26(1)
C(17)	8424(2)	691(1)	-1991(2)	23(1)
C(18)	6127(2)	1672(1)	559(2)	17(1)
C(19)	5538(2)	2506(1)	75(2)	26(1)
C(20)	8538(2)	2159(1)	1530(2)	18(1)
C(21)	9955(2)	2093(1)	1647(2)	21(1)

Appendix

Table 3. Bond lengths [Å] and angles [deg] for catalyst **22**.

Ti(1)-N(1)	1.8891(16)
Ti(1)-Cl(1)	2.2601(7)
Ti(1)-Cl(2)	2.2739(6)
Ti(1)-C(4)	2.334(2)
Ti(1)-C(3)	2.337(2)
Ti(1)-C(5)	2.3459(19)
Ti(1)-C(1)	2.355(2)
Ti(1)-C(2)	2.358(2)
N(1)-C(7)	1.413(2)
N(1)-C(6)	1.490(2)
B(1)-C(13)	1.607(3)
B(1)-C(20)	1.613(3)
B(1)-C(18)	1.624(3)
B(1)-N(2)	1.694(3)
C(1)-C(2)	1.404(3)
C(1)-C(5)	1.406(3)
C(1)-H(1)	0.9500
N(2)-C(7)	1.360(2)
N(2)-C(11)	1.368(2)
C(2)-C(3)	1.403(3)
C(2)-H(2)	0.9500
C(3)-C(4)	1.402(3)
C(3)-H(3)	0.9500
C(4)-C(5)	1.402(3)
C(4)-H(4)	0.9500
C(5)-H(5)	0.9500
C(6)-H(6A)	0.9800
C(6)-H(6B)	0.9800
C(6)-H(6C)	0.9800
C(7)-C(8)	1.379(3)
C(8)-C(9)	1.381(3)
C(8)-H(8)	0.9500
C(9)-C(10)	1.372(3)
C(9)-H(9)	0.9500
C(10)-C(11)	1.387(3)
C(10)-H(10)	0.9500
C(11)-C(12)	1.457(3)
C(12)-C(13)	1.395(3)
C(12)-C(17)	1.397(3)
C(13)-C(14)	1.395(3)
C(14)-C(15)	1.391(3)
C(14)-H(14)	0.9500
C(15)-C(16)	1.387(3)
C(15)-H(15)	0.9500
C(16)-C(17)	1.377(3)
C(16)-H(16)	0.9500
C(17)-H(17)	0.9500
C(18)-C(19)	1.537(3)

Appendix

C(18)-H(18A)	0.9900
C(18)-H(18B)	0.9900
C(19)-H(19A)	0.9800
C(19)-H(19B)	0.9800
C(19)-H(19C)	0.9800
C(20)-C(21)	1.527(3)
C(20)-H(20A)	0.9900
C(20)-H(20B)	0.9900
C(21)-H(21A)	0.9800
C(21)-H(21B)	0.9800
C(21)-H(21C)	0.9800
N(1)-Ti(1)-Cl(1)	106.22(5)
N(1)-Ti(1)-Cl(2)	100.95(5)
Cl(1)-Ti(1)-Cl(2)	103.71(2)
N(1)-Ti(1)-C(4)	107.78(7)
Cl(1)-Ti(1)-C(4)	90.49(6)
Cl(2)-Ti(1)-C(4)	142.88(6)
N(1)-Ti(1)-C(3)	140.83(7)
Cl(1)-Ti(1)-C(3)	89.52(6)
Cl(2)-Ti(1)-C(3)	109.96(6)
C(4)-Ti(1)-C(3)	34.93(8)
N(1)-Ti(1)-C(5)	83.78(7)
Cl(1)-Ti(1)-C(5)	121.95(5)
Cl(2)-Ti(1)-C(5)	130.95(6)
C(4)-Ti(1)-C(5)	34.87(7)
C(3)-Ti(1)-C(5)	57.91(7)
N(1)-Ti(1)-C(1)	95.96(7)
Cl(1)-Ti(1)-C(1)	146.16(6)
Cl(2)-Ti(1)-C(1)	96.58(5)
C(4)-Ti(1)-C(1)	58.02(7)
C(3)-Ti(1)-C(1)	57.89(8)
C(5)-Ti(1)-C(1)	34.81(7)
N(1)-Ti(1)-C(2)	130.40(8)
Cl(1)-Ti(1)-C(2)	119.97(6)
Cl(2)-Ti(1)-C(2)	85.58(6)
C(4)-Ti(1)-C(2)	57.93(8)
C(3)-Ti(1)-C(2)	34.78(8)
C(5)-Ti(1)-C(2)	57.73(7)
C(1)-Ti(1)-C(2)	34.66(7)
C(7)-N(1)-C(6)	111.17(15)
C(7)-N(1)-Ti(1)	136.20(13)
C(6)-N(1)-Ti(1)	108.79(12)
C(13)-B(1)-C(20)	112.23(17)
C(13)-B(1)-C(18)	114.70(16)
C(20)-B(1)-C(18)	112.53(17)
C(13)-B(1)-N(2)	95.60(15)
C(20)-B(1)-N(2)	113.63(16)
C(18)-B(1)-N(2)	106.95(15)
C(2)-C(1)-C(5)	107.8(2)
C(2)-C(1)-Ti(1)	72.76(12)

Appendix

C(5)-C(1)-Ti(1)	72.23(11)
C(2)-C(1)-H(1)	126.1
C(5)-C(1)-H(1)	126.1
Ti(1)-C(1)-H(1)	120.7
C(7)-N(2)-C(11)	118.35(17)
C(7)-N(2)-B(1)	131.34(16)
C(11)-N(2)-B(1)	110.15(15)
C(3)-C(2)-C(1)	108.0(2)
C(3)-C(2)-Ti(1)	71.79(12)
C(1)-C(2)-Ti(1)	72.58(12)
C(3)-C(2)-H(2)	126.0
C(1)-C(2)-H(2)	126.0
Ti(1)-C(2)-H(2)	121.4
C(4)-C(3)-C(2)	108.2(2)
C(4)-C(3)-Ti(1)	72.42(12)
C(2)-C(3)-Ti(1)	73.42(12)
C(4)-C(3)-H(3)	125.9
C(2)-C(3)-H(3)	125.9
Ti(1)-C(3)-H(3)	120.1
C(3)-C(4)-C(5)	107.9(2)
C(3)-C(4)-Ti(1)	72.65(12)
C(5)-C(4)-Ti(1)	73.04(11)
C(3)-C(4)-H(4)	126.1
C(5)-C(4)-H(4)	126.1
Ti(1)-C(4)-H(4)	120.1
C(4)-C(5)-C(1)	108.15(18)
C(4)-C(5)-Ti(1)	72.10(11)
C(1)-C(5)-Ti(1)	72.96(11)
C(4)-C(5)-H(5)	125.9
C(1)-C(5)-H(5)	125.9
Ti(1)-C(5)-H(5)	120.8
N(1)-C(6)-H(6A)	109.5
N(1)-C(6)-H(6B)	109.5
H(6A)-C(6)-H(6B)	109.5
N(1)-C(6)-H(6C)	109.5
H(6A)-C(6)-H(6C)	109.5
H(6B)-C(6)-H(6C)	109.5
N(2)-C(7)-C(8)	121.12(18)
N(2)-C(7)-N(1)	119.59(17)
C(8)-C(7)-N(1)	119.25(18)
C(7)-C(8)-C(9)	120.5(2)
C(7)-C(8)-H(8)	119.8
C(9)-C(8)-H(8)	119.8
C(10)-C(9)-C(8)	118.8(2)
C(10)-C(9)-H(9)	120.6
C(8)-C(9)-H(9)	120.6
C(9)-C(10)-C(11)	119.6(2)
C(9)-C(10)-H(10)	120.2
C(11)-C(10)-H(10)	120.2
N(2)-C(11)-C(10)	121.66(19)
N(2)-C(11)-C(12)	111.08(17)

Appendix

C(10)-C(11)-C(12)	127.26(18)
C(13)-C(12)-C(17)	123.2(2)
C(13)-C(12)-C(11)	110.81(17)
C(17)-C(12)-C(11)	125.98(19)
C(12)-C(13)-C(14)	117.10(18)
C(12)-C(13)-B(1)	111.94(17)
C(14)-C(13)-B(1)	130.94(19)
C(15)-C(14)-C(13)	120.2(2)
C(15)-C(14)-H(14)	119.9
C(13)-C(14)-H(14)	119.9
C(16)-C(15)-C(14)	121.2(2)
C(16)-C(15)-H(15)	119.4
C(14)-C(15)-H(15)	119.4
C(17)-C(16)-C(15)	120.0(2)
C(17)-C(16)-H(16)	120.0
C(15)-C(16)-H(16)	120.0
C(16)-C(17)-C(12)	118.2(2)
C(16)-C(17)-H(17)	120.9
C(12)-C(17)-H(17)	120.9
C(19)-C(18)-B(1)	114.71(17)
C(19)-C(18)-H(18A)	108.6
B(1)-C(18)-H(18A)	108.6
C(19)-C(18)-H(18B)	108.6
B(1)-C(18)-H(18B)	108.6
H(18A)-C(18)-H(18B)	107.6
C(18)-C(19)-H(19A)	109.5
C(18)-C(19)-H(19B)	109.5
H(19A)-C(19)-H(19B)	109.5
C(18)-C(19)-H(19C)	109.5
H(19A)-C(19)-H(19C)	109.5
H(19B)-C(19)-H(19C)	109.5
C(21)-C(20)-B(1)	116.52(17)
C(21)-C(20)-H(20A)	108.2
B(1)-C(20)-H(20A)	108.2
C(21)-C(20)-H(20B)	108.2
B(1)-C(20)-H(20B)	108.2
H(20A)-C(20)-H(20B)	107.3
C(20)-C(21)-H(21A)	109.5
C(20)-C(21)-H(21B)	109.5
H(21A)-C(21)-H(21B)	109.5
C(20)-C(21)-H(21C)	109.5
H(21A)-C(21)-H(21C)	109.5
H(21B)-C(21)-H(21C)	109.5

Appendix

Table 4. Anisotropic displacement parameters ($\text{\AA}^2 \times 10^3$) for catalyst **22**. The anisotropic displacement factor exponent takes the form: $-2 \pi^2 [h^2 a^{*2} U_{11} + \dots + 2 h k a^* b^* U_{12}]$

	U11	U22	U33	U23	U13	U12
Ti(1)	16(1)	15(1)	15(1)	-1(1)	4(1)	-1(1)
Cl(1)	36(1)	18(1)	29(1)	6(1)	7(1)	3(1)
Cl(2)	21(1)	23(1)	20(1)	5(1)	6(1)	2(1)
N(1)	14(1)	19(1)	13(1)	1(1)	2(1)	-1(1)
B(1)	18(1)	12(1)	16(1)	1(1)	3(1)	1(1)
C(1)	20(1)	19(1)	20(1)	-2(1)	0(1)	6(1)
N(2)	12(1)	15(1)	13(1)	-2(1)	2(1)	0(1)
C(2)	20(1)	34(1)	25(1)	5(1)	4(1)	-13(1)
C(3)	17(1)	40(2)	33(1)	-8(1)	11(1)	-6(1)
C(4)	16(1)	24(1)	28(1)	3(1)	1(1)	-1(1)
C(5)	14(1)	21(1)	16(1)	1(1)	-1(1)	-5(1)
C(6)	15(1)	30(1)	18(1)	2(1)	0(1)	-7(1)
C(7)	11(1)	18(1)	17(1)	2(1)	4(1)	1(1)
C(8)	25(1)	17(1)	28(1)	7(1)	9(1)	4(1)
C(9)	31(1)	15(1)	36(1)	-2(1)	12(1)	5(1)
C(10)	21(1)	23(1)	25(1)	-8(1)	9(1)	2(1)
C(11)	10(1)	20(1)	17(1)	-4(1)	(1)	0(1)
C(12)	12(1)	22(1)	16(1)	-3(1)	1(1)	-3(1)
C(13)	13(1)	18(1)	16(1)	0(1)	1(1)	-3(1)
C(14)	22(1)	22(1)	22(1)	1(1)	4(1)	-3(1)
C(15)	23(1)	34(1)	21(1)	8(1)	5(1)	-7(1)
C(16)	19(1)	43(2)	17(1)	-1(1)	5(1)	-5(1)
C(17)	18(1)	31(1)	19(1)	-5(1)	4(1)	-3(1)
C(18)	19(1)	15(1)	17(1)	1(1)	3(1)	0(1)
C(19)	22(1)	21(1)	35(1)	5(1)	8(1)	4(1)
C(20)	22(1)	14(1)	17(1)	-2(1)	5(1)	0(1)
C(21)	22(1)	21(1)	20(1)	-1(1)	5(1)	-2(1)

Appendix

Table 5. Hydrogen coordinates ($\times 10^4$) and isotropic displacement parameters ($\text{\AA}^2 \times 10^3$) for catalyst **22**.

	x	y	z	U(eq)
H(1)	5797	-1269	2277	25
H(2)	4853	-1013	3883	32
H(3)	3974	440	3683	35
H(4)	4340	1075	1938	28
H(5)	5457	19	1064	22
H(6A)	9578	124	3735	34
H(6B)	8895	857	4211	34
H(6C)	9462	1026	3174	34
H(8)	8198	-1144	2305	27
H(9)	8535	-1733	685	32
H(10)	8507	-878	-849	27
H(14)	7754	2817	-1085	27
H(15)	8204	2614	-2800	31
H(16)	8599	1293	-3379	32
H(17)	8598	150	-2213	28
H(18A)	5630	1220	92	21
H(18B)	6050	1611	1335	21
H(19A)	6013	2959	538	39
H(19B)	4651	2526	85	39
H(19C)	5576	2565	-705	39
H(20A)	8271	2739	1333	21
H(20B)	8413	2041	2278	21
H(21A)	10249	1529	1880	32
H(21B)	10424	2488	2219	32
H(21C)	10103	2218	918	32

Table 6. Torsion angles [deg] for catalyst **22**.

Cl(1)-Ti(1)-N(1)-C(7)	-146.16(18)
Cl(2)-Ti(1)-N(1)-C(7)	105.92(18)
C(4)-Ti(1)-N(1)-C(7)	-50.3(2)
C(3)-Ti(1)-N(1)-C(7)	-36.1(3)
C(5)-Ti(1)-N(1)-C(7)	-24.65(19)
C(1)-Ti(1)-N(1)-C(7)	8.0(2)
C(2)-Ti(1)-N(1)-C(7)	12.4(2)
Cl(1)-Ti(1)-N(1)-C(6)	58.89(13)
Cl(2)-Ti(1)-N(1)-C(6)	-49.02(13)
C(4)-Ti(1)-N(1)-C(6)	154.79(13)
C(3)-Ti(1)-N(1)-C(6)	168.97(14)
C(5)-Ti(1)-N(1)-C(6)	-179.60(13)
C(1)-Ti(1)-N(1)-C(6)	-146.93(13)
C(2)-Ti(1)-N(1)-C(6)	-142.55(13)
N(1)-Ti(1)-C(1)-C(2)	174.13(13)
Cl(1)-Ti(1)-C(1)-C(2)	-54.57(17)
Cl(2)-Ti(1)-C(1)-C(2)	72.34(13)

Appendix

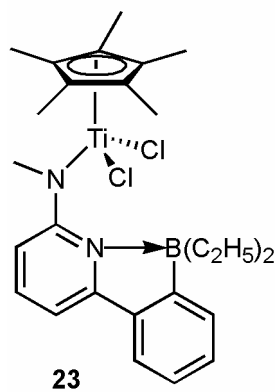
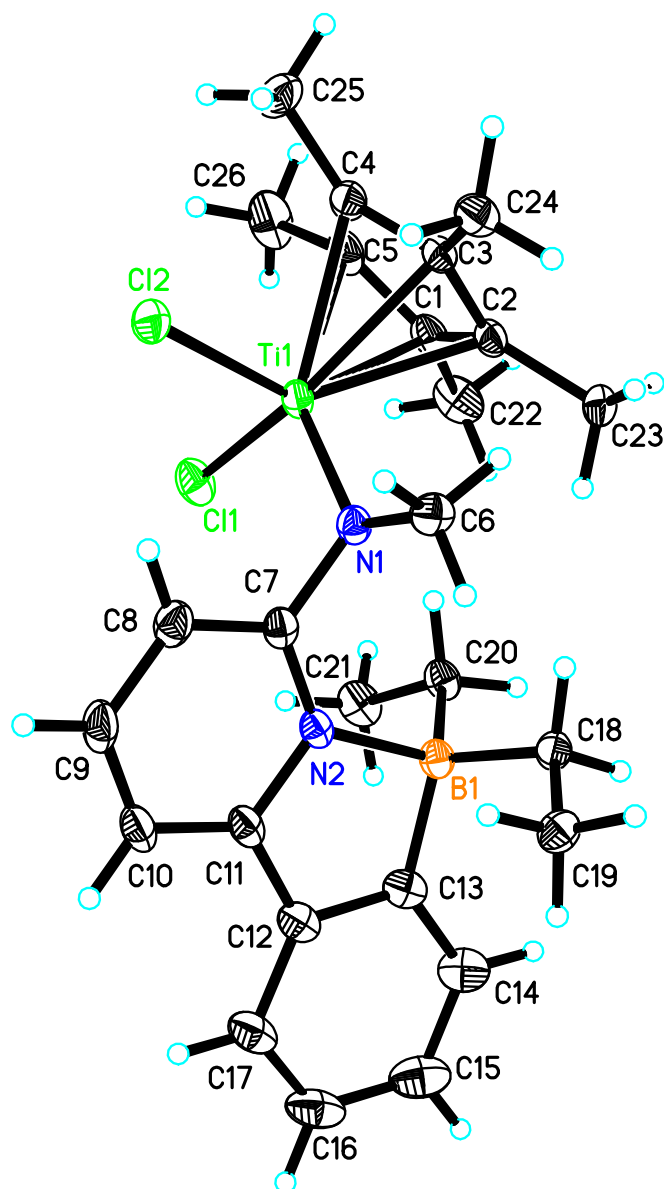
C(4)-Ti(1)-C(1)-C(2)	-78.61(14)
C(3)-Ti(1)-C(1)-C(2)	-37.13(13)
C(5)-Ti(1)-C(1)-C(2)	-115.82(19)
N(1)-Ti(1)-C(1)-C(5)	-70.05(13)
Cl(1)-Ti(1)-C(1)-C(5)	61.26(16)
Cl(2)-Ti(1)-C(1)-C(5)	-171.84(11)
C(4)-Ti(1)-C(1)-C(5)	37.21(12)
C(3)-Ti(1)-C(1)-C(5)	78.69(13)
C(2)-Ti(1)-C(1)-C(5)	115.82(19)
C(13)-B(1)-N(2)-C(7)	178.45(18)
C(20)-B(1)-N(2)-C(7)	61.2(3)
C(18)-B(1)-N(2)-C(7)	-63.6(2)
C(13)-B(1)-N(2)-C(11)	-6.33(18)
C(20)-B(1)-N(2)-C(11)	-123.58(17)
C(18)-B(1)-N(2)-C(11)	111.62(17)
C(5)-C(1)-C(2)-C(3)	-0.7(2)
Ti(1)-C(1)-C(2)-C(3)	63.51(15)
C(5)-C(1)-C(2)-Ti(1)	-64.20(13)
N(1)-Ti(1)-C(2)-C(3)	-124.02(14)
Cl(1)-Ti(1)-C(2)-C(3)	32.08(15)
Cl(2)-Ti(1)-C(2)-C(3)	135.37(13)
C(4)-Ti(1)-C(2)-C(3)	-37.46(13)
C(5)-Ti(1)-C(2)-C(3)	-78.91(14)
C(1)-Ti(1)-C(2)-C(3)	-116.33(19)
N(1)-Ti(1)-C(2)-C(1)	-7.68(17)
Cl(1)-Ti(1)-C(2)-C(1)	148.42(11)
Cl(2)-Ti(1)-C(2)-C(1)	-108.30(13)
C(4)-Ti(1)-C(2)-C(1)	78.88(13)
C(3)-Ti(1)-C(2)-C(1)	116.33(19)
C(5)-Ti(1)-C(2)-C(1)	37.42(12)
C(1)-C(2)-C(3)-C(4)	0.5(2)
Ti(1)-C(2)-C(3)-C(4)	64.56(15)
C(1)-C(2)-C(3)-Ti(1)	-64.02(14)
N(1)-Ti(1)-C(3)-C(4)	-24.0(2)
Cl(1)-Ti(1)-C(3)-C(4)	91.55(13)
Cl(2)-Ti(1)-C(3)-C(4)	-164.02(12)
C(5)-Ti(1)-C(3)-C(4)	-37.49(13)
C(1)-Ti(1)-C(3)-C(4)	-78.84(14)
C(2)-Ti(1)-C(3)-C(4)	-115.84(19)
N(1)-Ti(1)-C(3)-C(2)	91.80(17)
Cl(1)-Ti(1)-C(3)-C(2)	-152.61(13)
Cl(2)-Ti(1)-C(3)-C(2)	-48.18(14)
C(4)-Ti(1)-C(3)-C(2)	115.84(19)
C(5)-Ti(1)-C(3)-C(2)	78.35(14)
C(1)-Ti(1)-C(3)-C(2)	37.00(12)
C(2)-C(3)-C(4)-C(5)	-0.2(2)
Ti(1)-C(3)-C(4)-C(5)	65.04(14)
C(2)-C(3)-C(4)-Ti(1)	-65.22(15)
N(1)-Ti(1)-C(4)-C(3)	164.32(13)
Cl(1)-Ti(1)-C(4)-C(3)	-88.45(13)
Cl(2)-Ti(1)-C(4)-C(3)	25.38(18)

Appendix

C(5)-Ti(1)-C(4)-C(3)	115.58(19)
C(1)-Ti(1)-C(4)-C(3)	78.44(14)
C(2)-Ti(1)-C(4)-C(3)	37.29(13)
N(1)-Ti(1)-C(4)-C(5)	48.74(14)
Cl(1)-Ti(1)-C(4)-C(5)	155.97(12)
Cl(2)-Ti(1)-C(4)-C(5)	-90.20(14)
C(3)-Ti(1)-C(4)-C(5)	-115.58(19)
C(1)-Ti(1)-C(4)-C(5)	-37.15(12)
C(2)-Ti(1)-C(4)-C(5)	-78.29(14)
C(3)-C(4)-C(5)-C(1)	-0.2(2)
Ti(1)-C(4)-C(5)-C(1)	64.54(13)
C(3)-C(4)-C(5)-Ti(1)	-64.78(14)
C(2)-C(1)-C(5)-C(4)	0.6(2)
Ti(1)-C(1)-C(5)-C(4)	-63.97(14)
C(2)-C(1)-C(5)-Ti(1)	64.55(14)
N(1)-Ti(1)-C(5)-C(4)	-133.94(13)
Cl(1)-Ti(1)-C(5)-C(4)	-28.68(14)
Cl(2)-Ti(1)-C(5)-C(4)	126.95(11)
C(3)-Ti(1)-C(5)-C(4)	37.56(13)
C(1)-Ti(1)-C(5)-C(4)	116.19(18)
C(2)-Ti(1)-C(5)-C(4)	78.93(14)
N(1)-Ti(1)-C(5)-C(1)	109.87(13)
Cl(1)-Ti(1)-C(5)-C(1)	-144.87(11)
Cl(2)-Ti(1)-C(5)-C(1)	10.76(15)
C(4)-Ti(1)-C(5)-C(1)	-116.19(18)
C(3)-Ti(1)-C(5)-C(1)	-78.63(13)
C(2)-Ti(1)-C(5)-C(1)	-37.26(12)
C(11)-N(2)-C(7)-C(8)	-0.2(3)
B(1)-N(2)-C(7)-C(8)	174.70(18)
C(11)-N(2)-C(7)-N(1)	177.59(16)
B(1)-N(2)-C(7)-N(1)	-7.5(3)
C(6)-N(1)-C(7)-N(2)	-90.2(2)
Ti(1)-N(1)-C(7)-N(2)	115.2(2)
C(6)-N(1)-C(7)-C(8)	87.6(2)
Ti(1)-N(1)-C(7)-C(8)	-66.9(3)
N(2)-C(7)-C(8)-C(9)	-0.5(3)
N(1)-C(7)-C(8)-C(9)	-178.28(18)
C(7)-C(8)-C(9)-C(10)	0.4(3)
C(8)-C(9)-C(10)-C(11)	0.4(3)
C(7)-N(2)-C(11)-C(10)	1.0(3)
B(1)-N(2)-C(11)-C(10)	-174.92(17)
C(7)-N(2)-C(11)-C(12)	-178.42(16)
B(1)-N(2)-C(11)-C(12)	5.7(2)
C(9)-C(10)-C(11)-N(2)	-1.1(3)
C(9)-C(10)-C(11)-C(12)	178.20(19)
N(2)-C(11)-C(12)-C(13)	-2.2(2)
C(10)-C(11)-C(12)-C(13)	178.44(19)
N(2)-C(11)-C(12)-C(17)	175.59(18)
C(10)-C(11)-C(12)-C(17)	-3.8(3)
C(17)-C(12)-C(13)-C(14)	-1.6(3)
C(11)-C(12)-C(13)-C(14)	176.25(17)

Appendix

C(17)-C(12)-C(13)-B(1)	179.63(18)
C(11)-C(12)-C(13)-B(1)	-2.5(2)
C(20)-B(1)-C(13)-C(12)	23.43(18)
C(18)-B(1)-C(13)-C(12)	-106.5(2)
N(2)-B(1)-C(13)-C(12)	5.06(19)
C(20)-B(1)-C(13)-C(14)	-55.1(3)
C(18)-B(1)-C(13)-C(14)	4.9(3)
N(2)-B(1)-C(13)-C(14)	-173.49(19)
C(12)-C(13)-C(14)-C(15)	3(3)
B(1)-C(13)-C(14)-C(15)	79.78(19)
C(13)-C(14)-C(15)-C(16)	-0.1(3)
C(14)-C(15)-C(16)-C(17)	-0.9(3)
C(15)-C(16)-C(17)-C(12)	6(3)
C(13)-C(12)-C(17)-C(16)	6(3)
C(11)-C(12)-C(17)-C(16)	-176.87(19)
C(13)-B(1)-C(18)-C(19)	-60.9(2)
C(20)-B(1)-C(18)-C(19)	69.0(2)
N(2)-B(1)-C(18)-C(19)	-165.56(16)
C(13)-B(1)-C(20)-C(21)	-49.4(2)
C(18)-B(1)-C(20)-C(21)	179.44(17)
N(2)-B(1)-C(20)-C(21)	57.7(2)

5.2 *Crystal structure of complex 23*

23

Table 1. Crystal data and structure refinement for catalyst **23**.

Identification code	Catalyst 23
Empirical formula	C ₂₆ H ₃₅ B Cl ₂ N ₂ Ti
Formula weight	505.17
Temperature	100(2) K
Wavelength	0.71073 Å
Crystal system, space group	triclinic, p-1
Unit cell dimensions	a = 9.2538(4) Å alpha = 77.233(2) deg. b = 11.5135(5) Å beta = 81.007(2) deg. c = 12.7779(6) Å gamma = 72.946(2) deg.
Volume	1263.24(10) Å ³
Z, Calculated density	2, 1.328 Mg/m ³
Absorption coefficient	0.567 mm ⁻¹
F(000)	532
Crystal size	0.36 x 0.20 x 0.10 mm
Theta range for data collection	1.64 to 28.49 deg.
Limiting indices	-12 ≤ h ≤ 12, -15 ≤ k ≤ 15, -17 ≤ l ≤ 17
Reflections collected / unique	44991 / 6331 [R(int) = 0.0242]
Completeness to theta = 28.49°	98.8 %
Max. and min. transmission	0.9444 and 0.8240
Refinement method	Full-matrix least-squares on F ²
Data / restraints / parameters	6331 / 0 / 297
Goodness-of-fit on F ²	1.039
Final R indices [I > 2σ(I)]	R1 = 0.0274, wR2 = 0.0712
R indices (all data)	R1 = 0.0360, wR2 = 0.0742
Largest diff. peak and hole	0.362 and -0.257 e.Å ⁻³

Appendix

Table 2. Atomic coordinates ($\times 10^4$) and equivalent isotropic displacement parameters ($\text{\AA}^2 \times 10^3$) for catalyst **23**.

U(eq) is defined as one third of the trace of the orthogonalized Uij tensor.

	x	y	z	U(eq)
Ti(1)	1778(1)	936(1)	2471(1)	17(1)
Cl(1)	4287(1)	446(1)	1927(1)	26(1)
Cl(2)	1646(1)	-663(1)	3877(1)	26(1)
N(1)	1408(1)	2256(1)	3261(1)	18(1)
C(1)	1156(2)	1598(1)	668(1)	23(1)
B(1)	3035(2)	4411(1)	2478(1)	18(1)
N(2)	3323(1)	3184(1)	3492(1)	17(1)
C(2)	-110(1)	2206(1)	1326(1)	20(1)
C(3)	-724(1)	1285(1)	2017(1)	20(1)
C(4)	138(2)	113(1)	1765(1)	24(1)
C(5)	1281(2)	310(1)	932(1)	26(1)
C(6)	-70(1)	2874(1)	3789(1)	22(1)
C(7)	2609(1)	2274(1)	3826(1)	18(1)
C(8)	2977(2)	1393(1)	4750(1)	25(1)
C(9)	4116(2)	1415(1)	5327(1)	29(1)
C(10)	4868(2)	2316(1)	4978(1)	25(1)
C(11)	4452(1)	3199(1)	4064(1)	20(1)
C(12)	5074(1)	4245(1)	3604(1)	22(1)
C(13)	4322(1)	4966(1)	2715(1)	22(1)
C(14)	4759(2)	6034(1)	2212(1)	30(1)
C(15)	5904(2)	6344(2)	2582(1)	35(1)
C(16)	6648(2)	5595(2)	3458(1)	34(1)
C(17)	6231(1)	4542(1)	3985(1)	28(1)
C(18)	1357(1)	5340(1)	2660(1)	20(1)
C(19)	990(2)	5819(1)	3725(1)	23(1)
C(20)	3350(1)	3962(1)	1330(1)	21(1)
C(21)	4998(2)	3364(1)	961(1)	27(1)
C(22)	2073(2)	2225(2)	-230(1)	33(1)
C(23)	-751(2)	3583(1)	1177(1)	25(1)
C(24)	-2093(2)	1445(1)	2829(1)	26(1)
C(25)	-260(2)	-1077(1)	2222(1)	38(1)
C(26)	2405(2)	682(2)	407(1)	40(1)

Table 3. Bond lengths [\AA] and angles [deg] for catalyst **23**.

Ti(1)-N(1)	1.9259(10)
Ti(1)-Cl(1)	2.2571(4)
Ti(1)-Cl(2)	2.2868(4)
Ti(1)-C(1)	2.3670(12)
Ti(1)-C(3)	2.3724(12)
Ti(1)-C(4)	2.3795(13)
Ti(1)-C(2)	2.3842(12)
Ti(1)-C(5)	2.3874(12)
N(1)-C(7)	1.4242(15)

Appendix

N(1)-C(6)	1.4779(15)
C(1)-C(5)	1.4196(19)
C(1)-C(2)	1.4288(17)
C(1)-C(22)	1.4991(19)
B(1)-C(13)	1.6012(18)
B(1)-C(20)	1.6172(17)
B(1)-C(18)	1.6226(18)
B(1)-N(2)	1.6800(16)
N(2)-C(7)	1.3555(15)
N(2)-C(11)	1.3708(15)
C(2)-C(3)	1.4169(17)
C(2)-C(23)	1.5015(17)
C(3)-C(4)	1.4286(17)
C(3)-C(24)	1.5005(18)
C(4)-C(5)	1.409(2)
C(4)-C(25)	1.4935(19)
C(5)-C(26)	1.5034(18)
C(6)-H(6A)	0.9800
C(6)-H(6B)	0.9800
C(6)-H(6C)	0.9800
C(7)-C(8)	1.3900(16)
C(8)-C(9)	1.3871(19)
C(8)-H(8)	0.9500
C(9)-C(10)	1.371(2)
C(9)-H(9)	0.9500
C(10)-C(11)	1.3897(17)
C(10)-H(10)	0.9500
C(11)-C(12)	1.4547(18)
C(12)-C(17)	1.3973(18)
C(12)-C(13)	1.3983(18)
C(13)-C(14)	1.3962(18)
C(14)-C(15)	1.388(2)
C(14)-H(14)	0.9500
C(15)-C(16)	1.391(2)
C(15)-H(15)	0.9500
C(16)-C(17)	1.380(2)
C(16)-H(16)	0.9500
C(17)-H(17)	0.9500
C(18)-C(19)	1.5337(16)
C(18)-H(18A)	0.9900
C(18)-H(18B)	0.9900
C(19)-H(19A)	0.9800
C(19)-H(19B)	0.9800
C(19)-H(19C)	0.9800
C(20)-C(21)	1.5254(17)
C(20)-H(20A)	0.9900
C(20)-H(20B)	0.9900
C(21)-H(21A)	0.9800
C(21)-H(21B)	0.9800
C(21)-H(21C)	0.9800
C(22)-H(22A)	0.9800

Appendix

C(22)-H(22B)	0.9800
C(22)-H(22C)	0.9800
C(23)-H(23A)	0.9800
C(23)-H(23B)	0.9800
C(23)-H(23C)	0.9800
C(24)-H(24A)	0.9800
C(24)-H(24B)	0.9800
C(24)-H(24C)	0.9800
C(25)-H(25A)	0.9800
C(25)-H(25B)	0.9800
C(25)-H(25C)	0.9800
C(26)-H(26A)	0.9800
C(26)-H(26B)	0.9800
C(26)-H(26C)	0.9800
N(1)-Ti(1)-Cl(1)	106.26(3)
N(1)-Ti(1)-Cl(2)	99.61(3)
Cl(1)-Ti(1)-Cl(2)	101.225(14)
N(1)-Ti(1)-C(1)	114.27(4)
Cl(1)-Ti(1)-C(1)	91.63(3)
Cl(2)-Ti(1)-C(1)	138.69(3)
N(1)-Ti(1)-C(3)	98.72(4)
Cl(1)-Ti(1)-C(3)	146.99(3)
Cl(2)-Ti(1)-C(3)	95.38(3)
C(1)-Ti(1)-C(3)	58.02(4)
N(1)-Ti(1)-C(4)	132.85(4)
Cl(1)-Ti(1)-C(4)	119.70(3)
Cl(2)-Ti(1)-C(4)	82.17(3)
C(1)-Ti(1)-C(4)	57.70(5)
C(3)-Ti(1)-C(4)	34.99(4)
N(1)-Ti(1)-C(2)	89.30(4)
Cl(1)-Ti(1)-C(2)	123.39(3)
Cl(2)-Ti(1)-C(2)	129.96(3)
C(1)-Ti(1)-C(2)	35.00(4)
C(3)-Ti(1)-C(2)	34.66(4)
C(4)-Ti(1)-C(2)	57.74(4)
N(1)-Ti(1)-C(5)	146.68(4)
Cl(1)-Ti(1)-C(5)	90.16(3)
Cl(2)-Ti(1)-C(5)	105.45(4)
C(1)-Ti(1)-C(5)	34.74(5)
C(3)-Ti(1)-C(5)	57.78(4)
C(4)-Ti(1)-C(5)	34.39(5)
C(2)-Ti(1)-C(5)	57.75(4)
C(7)-N(1)-C(6)	109.85(9)
C(7)-N(1)-Ti(1)	117.28(7)
C(6)-N(1)-Ti(1)	126.24(8)
C(5)-C(1)-C(2)	108.00(11)
C(5)-C(1)-C(22)	125.96(12)
C(2)-C(1)-C(22)	125.70(12)
C(5)-C(1)-Ti(1)	73.42(7)
C(2)-C(1)-Ti(1)	73.16(7)

Appendix

C(22)-C(1)-Ti(1)	124.50(9)
C(13)-B(1)-C(20)	114.05(10)
C(13)-B(1)-C(18)	111.15(10)
C(20)-B(1)-C(18)	112.98(10)
C(13)-B(1)-N(2)	96.29(9)
C(20)-B(1)-N(2)	110.40(9)
C(18)-B(1)-N(2)	110.81(9)
C(7)-N(2)-C(11)	118.77(10)
C(7)-N(2)-B(1)	131.14(9)
C(11)-N(2)-B(1)	110.04(9)
C(3)-C(2)-C(1)	107.74(11)
C(3)-C(2)-C(23)	127.78(11)
C(1)-C(2)-C(23)	124.03(11)
C(3)-C(2)-Ti(1)	72.21(7)
C(1)-C(2)-Ti(1)	71.84(7)
C(23)-C(2)-Ti(1)	127.52(8)
C(2)-C(3)-C(4)	107.85(11)
C(2)-C(3)-C(24)	128.71(11)
C(4)-C(3)-C(24)	123.31(11)
C(2)-C(3)-Ti(1)	73.13(7)
C(4)-C(3)-Ti(1)	72.78(7)
C(24)-C(3)-Ti(1)	123.01(8)
C(5)-C(4)-C(3)	108.25(11)
C(5)-C(4)-C(25)	126.84(12)
C(3)-C(4)-C(25)	124.48(13)
C(5)-C(4)-Ti(1)	73.11(7)
C(3)-C(4)-Ti(1)	72.23(7)
C(25)-C(4)-Ti(1)	126.34(9)
C(4)-C(5)-C(1)	108.13(11)
C(4)-C(5)-C(26)	125.21(13)
C(1)-C(5)-C(26)	126.65(14)
C(4)-C(5)-Ti(1)	72.50(7)
C(1)-C(5)-Ti(1)	71.84(7)
C(26)-C(5)-Ti(1)	122.55(9)
N(1)-C(6)-H(6A)	109.5
N(1)-C(6)-H(6B)	109.5
H(6A)-C(6)-H(6B)	109.5
N(1)-C(6)-H(6C)	109.5
H(6A)-C(6)-H(6C)	109.5
H(6B)-C(6)-H(6C)	109.5
N(2)-C(7)-C(8)	120.79(11)
N(2)-C(7)-N(1)	119.85(10)
C(8)-C(7)-N(1)	119.27(11)
C(9)-C(8)-C(7)	120.14(13)
C(9)-C(8)-H(8)	119.9
C(7)-C(8)-H(8)	119.9
C(10)-C(9)-C(8)	119.30(12)
C(10)-C(9)-H(9)	120.4
C(8)-C(9)-H(9)	120.4
C(9)-C(10)-C(11)	119.15(12)
C(9)-C(10)-H(10)	120.4

Appendix

C(11)-C(10)-H(10)	120.4
N(2)-C(11)-C(10)	121.83(12)
N(2)-C(11)-C(12)	111.35(10)
C(10)-C(11)-C(12)	126.80(11)
C(17)-C(12)-C(13)	122.94(13)
C(17)-C(12)-C(11)	126.51(12)
C(13)-C(12)-C(11)	110.53(11)
C(14)-C(13)-C(12)	117.07(12)
C(14)-C(13)-B(1)	131.11(12)
C(12)-C(13)-B(1)	111.79(11)
C(15)-C(14)-C(13)	120.71(14)
C(15)-C(14)-H(14)	119.6
C(13)-C(14)-H(14)	119.6
C(14)-C(15)-C(16)	120.76(14)
C(14)-C(15)-H(15)	119.6
C(16)-C(15)-H(15)	119.6
C(17)-C(16)-C(15)	120.15(13)
C(17)-C(16)-H(16)	119.9
C(15)-C(16)-H(16)	119.9
C(16)-C(17)-C(12)	118.34(14)
C(16)-C(17)-H(17)	120.8
C(12)-C(17)-H(17)	120.8
C(19)-C(18)-B(1)	115.79(10)
C(19)-C(18)-H(18A)	108.3
B(1)-C(18)-H(18A)	108.3
C(19)-C(18)-H(18B)	108.3
B(1)-C(18)-H(18B)	108.3
H(18A)-C(18)-H(18B)	107.4
C(18)-C(19)-H(19A)	109.5
C(18)-C(19)-H(19B)	109.5
H(19A)-C(19)-H(19B)	109.5
C(18)-C(19)-H(19C)	109.5
H(19A)-C(19)-H(19C)	109.5
H(19B)-C(19)-H(19C)	109.5
C(21)-C(20)-B(1)	116.66(10)
C(21)-C(20)-H(20A)	108.1
B(1)-C(20)-H(20A)	108.1
C(21)-C(20)-H(20B)	108.1
B(1)-C(20)-H(20B)	108.1
H(20A)-C(20)-H(20B)	107.3
C(20)-C(21)-H(21A)	109.5
C(20)-C(21)-H(21B)	109.5
H(21A)-C(21)-H(21B)	109.5
C(20)-C(21)-H(21C)	109.5
H(21A)-C(21)-H(21C)	109.5
H(21B)-C(21)-H(21C)	109.5
C(1)-C(22)-H(22A)	109.5
C(1)-C(22)-H(22B)	109.5
H(22A)-C(22)-H(22B)	109.5
C(1)-C(22)-H(22C)	109.5
H(22A)-C(22)-H(22C)	109.5

Appendix

H(22B)-C(22)-H(22C)	109.5
C(2)-C(23)-H(23A)	109.5
C(2)-C(23)-H(23B)	109.5
H(23A)-C(23)-H(23B)	109.5
C(2)-C(23)-H(23C)	109.5
H(23A)-C(23)-H(23C)	109.5
H(23B)-C(23)-H(23C)	109.5
C(3)-C(24)-H(24A)	109.5
C(3)-C(24)-H(24B)	109.5
H(24A)-C(24)-H(24B)	109.5
C(3)-C(24)-H(24C)	109.5
H(24A)-C(24)-H(24C)	109.5
H(24B)-C(24)-H(24C)	109.5
C(4)-C(25)-H(25A)	109.5
C(4)-C(25)-H(25B)	109.5
H(25A)-C(25)-H(25B)	109.5
C(4)-C(25)-H(25C)	109.5
H(25A)-C(25)-H(25C)	109.5
H(25B)-C(25)-H(25C)	109.5
C(5)-C(26)-H(26A)	109.5
C(5)-C(26)-H(26B)	109.5
H(26A)-C(26)-H(26B)	109.5
C(5)-C(26)-H(26C)	109.5
H(26A)-C(26)-H(26C)	109.5
H(26B)-C(26)-H(26C)	109.5

Appendix

Table 4. Anisotropic displacement parameters ($\text{\AA}^2 \times 10^3$) for catalyst **23**.

The anisotropic displacement factor exponent takes the form: $-2 \pi^2 [h^2 a^{*2} U11 + \dots + 2 h k a^* b^* U12]$

	U11	U22	U33	U23	U13	U12
Ti(1)	17(1)	17(1)	16(1)	-5(1)	-5(1)	1(1)
Cl(1)	19(1)	32(1)	25(1)	-10(1)	-3(1)	1(1)
Cl(2)	32(1)	22(1)	24(1)	1(1)	-11(1)	-7(1)
N(1)	18(1)	17(1)	17(1)	-4(1)	-3(1)	-2(1)
C(1)	24(1)	30(1)	16(1)	-5(1)	-7(1)	-3(1)
B(1)	19(1)	20(1)	15(1)	-2(1)	-2(1)	-4(1)
N(2)	15(1)	19(1)	15(1)	-6(1)	-2(1)	0(1)
C(2)	21(1)	20(1)	19(1)	-3(1)	-9(1)	-2(1)
C(3)	20(1)	19(1)	22(1)	-4(1)	-8(1)	-3(1)
C(4)	31(1)	19(1)	25(1)	-6(1)	-14(1)	-3(1)
C(5)	28(1)	28(1)	22(1)	-11(1)	-12(1)	3(1)
C(6)	20(1)	23(1)	25(1)	-10(1)	2(1)	-5(1)
C(7)	20(1)	18(1)	16(1)	-6(1)	-2(1)	0(1)
C(8)	35(1)	19(1)	19(1)	-3(1)	-7(1)	-4(1)
C(9)	39(1)	22(1)	20(1)	-4(1)	-13(1)	3(1)
C(10)	25(1)	27(1)	23(1)	-10(1)	-11(1)	5(1)
C(11)	15(1)	24(1)	18(1)	-10(1)	-3(1)	3(1)
C(12)	15(1)	29(1)	22(1)	-13(1)	1(1)	-2(1)
C(13)	19(1)	28(1)	20(1)	-9(1)	2(1)	-7(1)
C(14)	32(1)	36(1)	25(1)	-7(1)	3(1)	-16(1)
C(15)	34(1)	43(1)	36(1)	-17(1)	12(1)	-23(1)
C(16)	19(1)	48(1)	41(1)	-27(1)	6(1)	-13(1)
C(17)	16(1)	40(1)	31(1)	-20(1)	-1(1)	-2(1)
C(18)	20(1)	17(1)	20(1)	-3(1)	-3(1)	-3(1)
C(19)	23(1)	21(1)	24(1)	-7(1)	1(1)	-4(1)
C(20)	21(1)	25(1)	15(1)	-3(1)	-3(1)	-4(1)
C(21)	24(1)	36(1)	20(1)	-10(1)	1(1)	-5(1)
C(22)	34(1)	49(1)	17(1)	-7(1)	-2(1)	-13(1)
C(23)	28(1)	18(1)	29(1)	-1(1)	-13(1)	-3(1)
C(24)	22(1)	28(1)	29(1)	-4(1)	-4(1)	-8(1)
C(25)	59(1)	20(1)	42(1)	-3(1)	-26(1)	-12(1)
C(26)	42(1)	41(1)	36(1)	-25(1)	-14(1)	11(1)

Appendix

Table 5. Hydrogen coordinates ($\times 10^4$) and isotropic displacement parameters ($\text{\AA}^2 \times 10^3$) for catalyst **23**.

	X	Y	Z	U(eq)
H(6A)	-342	2315	4438	34
H(6B)	-853	3088	3290	34
H(6C)	5	3627	3987	34
H(8)	2446	775	4986	30
H(9)	4374	813	5957	34
H(10)	5663	2337	5356	30
H(14)	4268	6553	1610	36
H(15)	6184	7077	2233	42
H(16)	7444	5809	3694	40
H(17)	6720	4032	4591	33
H(18A)	1244	6060	2059	23
H(18B)	594	4907	2617	23
H(19A)	1140	5117	4330	34
H(19B)	-69	6317	3782	34
H(19C)	1664	6329	3746	34
H(20A)	2754	3365	1366	25
H(20B)	2955	4688	772	25
H(21A)	5584	3975	833	41
H(21B)	5042	3066	293	41
H(21C)	5428	2668	1521	41
H(22A)	3088	1666	-343	49
H(22B)	2162	2979	-42	49
H(22C)	1569	2438	-893	49
H(23A)	-1666	3782	1678	38
H(23B)	-1011	3911	435	38
H(23C)	6	3956	1322	38
H(24A)	-2585	2328	2802	39
H(24B)	-1780	1064	3552	39
H(24C)	-2810	1046	2662	39
H(25A)	-1036	-1152	1818	57
H(25B)	-654	-1092	2981	57
H(25C)	649	-1769	2166	57
H(26A)	2773	-1408	959	61
H(26B)	3263	-372	29	61
H(26C)	1911	-913	-111	61

Appendix

Table 6. Torsion angles [deg] for catalyst **23**.

Cl(1)-Ti(1)-N(1)-C(7)	-30.71(9)
Cl(2)-Ti(1)-N(1)-C(7)	74.06(8)
C(1)-Ti(1)-N(1)-C(7)	-130.16(8)
C(3)-Ti(1)-N(1)-C(7)	171.08(8)
C(4)-Ti(1)-N(1)-C(7)	162.25(8)
C(2)-Ti(1)-N(1)-C(7)	-155.44(8)
C(5)-Ti(1)-N(1)-C(7)	-147.39(9)
Cl(1)-Ti(1)-N(1)-C(6)	-179.10(9)
Cl(2)-Ti(1)-N(1)-C(6)	-74.33(9)
C(1)-Ti(1)-N(1)-C(6)	81.45(10)
C(3)-Ti(1)-N(1)-C(6)	22.69(10)
C(4)-Ti(1)-N(1)-C(6)	13.86(12)
C(2)-Ti(1)-N(1)-C(6)	56.17(10)
C(5)-Ti(1)-N(1)-C(6)	64.22(13)
N(1)-Ti(1)-C(1)-C(5)	-163.40(8)
Cl(1)-Ti(1)-C(1)-C(5)	87.92(8)
Cl(2)-Ti(1)-C(1)-C(5)	-21.19(10)
C(3)-Ti(1)-C(1)-C(5)	-78.30(8)
C(4)-Ti(1)-C(1)-C(5)	-36.71(8)
C(2)-Ti(1)-C(1)-C(5)	-115.28(11)
N(1)-Ti(1)-C(1)-C(2)	-48.13(8)
Cl(1)-Ti(1)-C(1)-C(2)	-156.80(7)
Cl(2)-Ti(1)-C(1)-C(2)	94.08(8)
C(3)-Ti(1)-C(1)-C(2)	36.97(7)
C(4)-Ti(1)-C(1)-C(2)	78.56(8)
C(5)-Ti(1)-C(1)-C(2)	115.28(11)
N(1)-Ti(1)-C(1)-C(22)	74.00(12)
Cl(1)-Ti(1)-C(1)-C(22)	-34.67(11)
Cl(2)-Ti(1)-C(1)-C(22)	-143.79(10)
C(3)-Ti(1)-C(1)-C(22)	159.10(13)
C(4)-Ti(1)-C(1)-C(22)	-159.31(13)
C(2)-Ti(1)-C(1)-C(22)	122.13(15)
C(5)-Ti(1)-C(1)-C(22)	-122.60(15)
C(13)-B(1)-N(2)-C(7)	178.29(11)
C(20)-B(1)-N(2)-C(7)	-63.12(15)
C(18)-B(1)-N(2)-C(7)	62.81(15)
C(13)-B(1)-N(2)-C(11)	0.97(11)
C(20)-B(1)-N(2)-C(11)	119.55(10)
C(18)-B(1)-N(2)-C(11)	-114.51(10)
C(5)-C(1)-C(2)-C(3)	1.94(14)
C(22)-C(1)-C(2)-C(3)	175.51(12)
Ti(1)-C(1)-C(2)-C(3)	-63.74(8)
C(5)-C(1)-C(2)-C(23)	-170.83(11)
C(22)-C(1)-C(2)-C(23)	2.75(19)
Ti(1)-C(1)-C(2)-C(23)	123.50(11)
C(5)-C(1)-C(2)-Ti(1)	65.68(9)
C(22)-C(1)-C(2)-Ti(1)	-120.75(13)
N(1)-Ti(1)-C(2)-C(3)	-106.53(7)
Cl(1)-Ti(1)-C(2)-C(3)	144.36(6)

Appendix

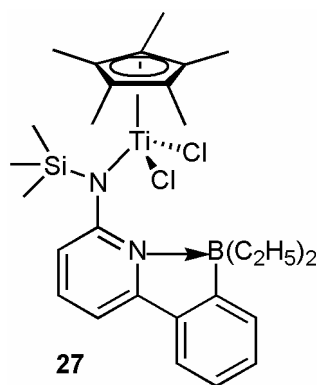
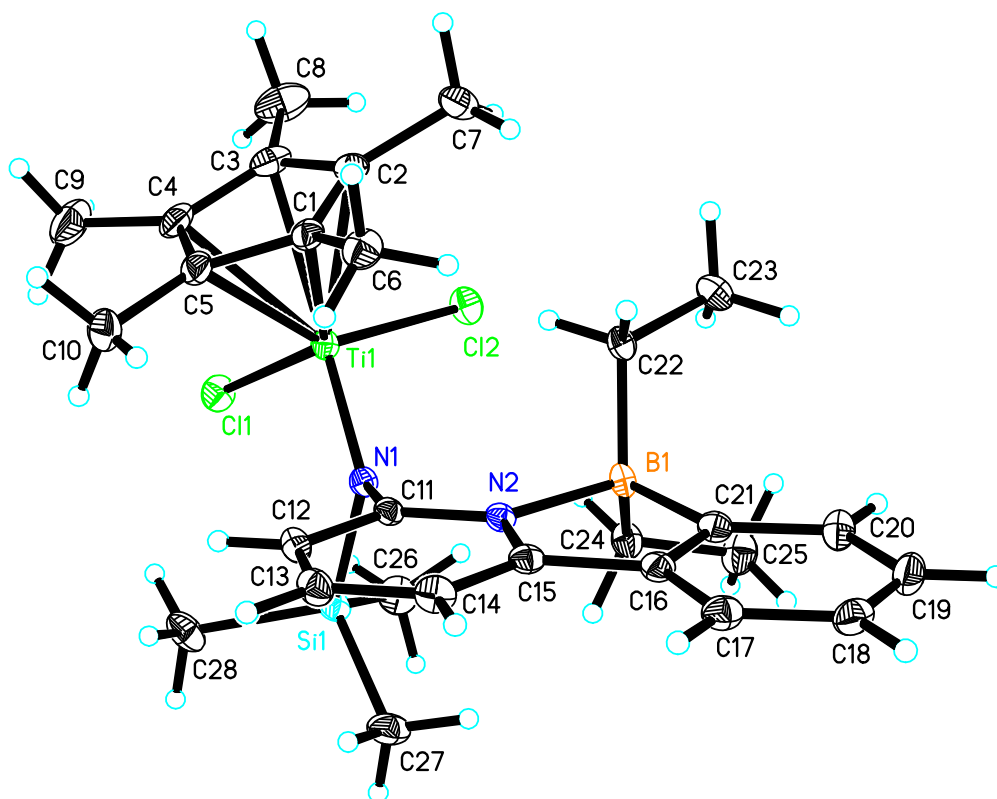
Cl(2)-Ti(1)-C(2)-C(3)	-4.56(8)
C(1)-Ti(1)-C(2)-C(3)	116.23(10)
C(4)-Ti(1)-C(2)-C(3)	37.77(7)
C(5)-Ti(1)-C(2)-C(3)	78.69(8)
N(1)-Ti(1)-C(2)-C(1)	137.24(8)
Cl(1)-Ti(1)-C(2)-C(1)	28.14(8)
Cl(2)-Ti(1)-C(2)-C(1)	-120.79(7)
C(3)-Ti(1)-C(2)-C(1)	-116.23(10)
C(4)-Ti(1)-C(2)-C(1)	-78.46(8)
C(5)-Ti(1)-C(2)-C(1)	-37.54(8)
N(1)-Ti(1)-C(2)-C(23)	17.86(11)
Cl(1)-Ti(1)-C(2)-C(23)	-91.25(11)
Cl(2)-Ti(1)-C(2)-C(23)	119.83(10)
C(1)-Ti(1)-C(2)-C(23)	-119.39(14)
C(3)-Ti(1)-C(2)-C(23)	124.39(14)
C(4)-Ti(1)-C(2)-C(23)	162.15(13)
C(5)-Ti(1)-C(2)-C(23)	-156.93(13)
C(1)-C(2)-C(3)-C(4)	-1.49(13)
C(23)-C(2)-C(3)-C(4)	170.91(11)
Ti(1)-C(2)-C(3)-C(4)	-64.99(8)
C(1)-C(2)-C(3)-C(24)	-177.40(12)
C(23)-C(2)-C(3)-C(24)	-5.0(2)
Ti(1)-C(2)-C(3)-C(24)	119.11(13)
C(1)-C(2)-C(3)-Ti(1)	63.50(8)
C(23)-C(2)-C(3)-Ti(1)	-124.10(12)
N(1)-Ti(1)-C(3)-C(2)	75.89(7)
Cl(1)-Ti(1)-C(3)-C(2)	-63.25(9)
Cl(2)-Ti(1)-C(3)-C(2)	176.49(6)
C(1)-Ti(1)-C(3)-C(2)	-37.34(7)
C(4)-Ti(1)-C(3)-C(2)	-115.43(10)
C(5)-Ti(1)-C(3)-C(2)	-78.62(8)
N(1)-Ti(1)-C(3)-C(4)	-168.68(7)
Cl(1)-Ti(1)-C(3)-C(4)	52.18(10)
Cl(2)-Ti(1)-C(3)-C(4)	-68.08(7)
C(1)-Ti(1)-C(3)-C(4)	78.09(8)
C(2)-Ti(1)-C(3)-C(4)	115.43(10)
C(5)-Ti(1)-C(3)-C(4)	36.81(7)
N(1)-Ti(1)-C(3)-C(24)	-49.72(10)
Cl(1)-Ti(1)-C(3)-C(24)	171.14(7)
Cl(2)-Ti(1)-C(3)-C(24)	50.88(10)
C(1)-Ti(1)-C(3)-C(24)	-162.95(12)
C(4)-Ti(1)-C(3)-C(24)	118.96(13)
C(2)-Ti(1)-C(3)-C(24)	-125.61(13)
C(5)-Ti(1)-C(3)-C(24)	155.78(12)
C(2)-C(3)-C(4)-C(5)	0.49(14)
C(24)-C(3)-C(4)-C(5)	176.67(11)
Ti(1)-C(3)-C(4)-C(5)	-64.73(9)
C(2)-C(3)-C(4)-C(25)	-172.44(12)
C(24)-C(3)-C(4)-C(25)	3.73(19)
Ti(1)-C(3)-C(4)-C(25)	122.33(12)
C(2)-C(3)-C(4)-Ti(1)	65.22(8)

Appendix

C(24)-C(3)-C(4)-Ti(1)	-118.60(11)
N(1)-Ti(1)-C(4)-C(5)	131.51(8)
Cl(1)-Ti(1)-C(4)-C(5)	-34.13(8)
Cl(2)-Ti(1)-C(4)-C(5)	-132.63(7)
C(1)-Ti(1)-C(4)-C(5)	37.10(7)
C(3)-Ti(1)-C(4)-C(5)	116.17(11)
C(2)-Ti(1)-C(4)-C(5)	78.77(8)
N(1)-Ti(1)-C(4)-C(3)	15.34(10)
Cl(1)-Ti(1)-C(4)-C(3)	-150.30(6)
Cl(2)-Ti(1)-C(4)-C(3)	111.20(7)
C(1)-Ti(1)-C(4)-C(3)	-79.07(8)
C(2)-Ti(1)-C(4)-C(3)	-37.40(7)
C(5)-Ti(1)-C(4)-C(3)	-116.17(11)
N(1)-Ti(1)-C(4)-C(25)	-104.81(13)
Cl(1)-Ti(1)-C(4)-C(25)	89.55(13)
Cl(2)-Ti(1)-C(4)-C(25)	-8.95(12)
C(1)-Ti(1)-C(4)-C(25)	160.78(14)
C(3)-Ti(1)-C(4)-C(25)	-120.15(16)
C(2)-Ti(1)-C(4)-C(25)	-157.55(14)
C(5)-Ti(1)-C(4)-C(25)	123.68(16)
C(3)-C(4)-C(5)-C(1)	0.71(14)
C(25)-C(4)-C(5)-C(1)	173.43(12)
Ti(1)-C(4)-C(5)-C(1)	-63.45(9)
C(3)-C(4)-C(5)-C(26)	-177.94(12)
C(25)-C(4)-C(5)-C(26)	-5.2(2)
Ti(1)-C(4)-C(5)-C(26)	117.91(13)
C(3)-C(4)-C(5)-Ti(1)	64.16(8)
C(25)-C(4)-C(5)-Ti(1)	-123.12(13)
C(2)-C(1)-C(5)-C(4)	-1.63(14)
C(22)-C(1)-C(5)-C(4)	-175.19(12)
Ti(1)-C(1)-C(5)-C(4)	63.87(9)
C(2)-C(1)-C(5)-C(26)	176.99(12)
C(22)-C(1)-C(5)-C(26)	3.4(2)
Ti(1)-C(1)-C(5)-C(26)	-117.50(13)
C(2)-C(1)-C(5)-Ti(1)	-65.51(8)
C(22)-C(1)-C(5)-Ti(1)	120.94(13)
N(1)-Ti(1)-C(5)-C(4)	-88.24(11)
Cl(1)-Ti(1)-C(5)-C(4)	150.83(7)
Cl(2)-Ti(1)-C(5)-C(4)	49.13(7)
C(1)-Ti(1)-C(5)-C(4)	-116.53(11)
C(3)-Ti(1)-C(5)-C(4)	-37.47(7)
C(2)-Ti(1)-C(5)-C(4)	-78.71(8)
N(1)-Ti(1)-C(5)-C(1)	28.30(13)
Cl(1)-Ti(1)-C(5)-C(1)	-92.64(7)
Cl(2)-Ti(1)-C(5)-C(1)	165.67(7)
C(3)-Ti(1)-C(5)-C(1)	79.06(8)
C(4)-Ti(1)-C(5)-C(1)	116.53(11)
C(2)-Ti(1)-C(5)-C(1)	37.82(7)
N(1)-Ti(1)-C(5)-C(26)	150.70(11)
Cl(1)-Ti(1)-C(5)-C(26)	29.77(13)
Cl(2)-Ti(1)-C(5)-C(26)	-71.93(13)

Appendix

C(1)-Ti(1)-C(5)-C(26)	122.40(16)
C(3)-Ti(1)-C(5)-C(26)	-158.54(14)
C(4)-Ti(1)-C(5)-C(26)	-121.06(16)
C(2)-Ti(1)-C(5)-C(26)	160.23(15)
C(11)-N(2)-C(7)-C(8)	2.08(16)
B(1)-N(2)-C(7)-C(8)	-175.05(11)
C(11)-N(2)-C(7)-N(1)	178.51(10)
B(1)-N(2)-C(7)-N(1)	1.38(17)
C(6)-N(1)-C(7)-N(2)	-94.89(12)
Ti(1)-N(1)-C(7)-N(2)	111.82(10)
C(6)-N(1)-C(7)-C(8)	81.60(13)
Ti(1)-N(1)-C(7)-C(8)	-71.69(12)
N(2)-C(7)-C(8)-C(9)	-1.89(18)
N(1)-C(7)-C(8)-C(9)	-178.34(11)
C(7)-C(8)-C(9)-C(10)	0.27(19)
C(8)-C(9)-C(10)-C(11)	1.07(19)
C(7)-N(2)-C(11)-C(10)	-0.71(16)
B(1)-N(2)-C(11)-C(10)	176.98(10)
C(7)-N(2)-C(11)-C(12)	-179.11(9)
B(1)-N(2)-C(11)-C(12)	-1.41(12)
C(9)-C(10)-C(11)-N(2)	-0.87(18)
C(9)-C(10)-C(11)-C(12)	177.26(11)
N(2)-C(11)-C(12)-C(17)	179.80(11)
C(10)-C(11)-C(12)-C(17)	1.50(19)
N(2)-C(11)-C(12)-C(13)	1.29(13)
C(10)-C(11)-C(12)-C(13)	-177.01(11)
C(17)-C(12)-C(13)-C(14)	-0.88(18)
C(11)-C(12)-C(13)-C(14)	177.70(11)
C(17)-C(12)-C(13)-B(1)	-179.15(11)
C(11)-C(12)-C(13)-B(1)	-0.57(13)
C(20)-B(1)-C(13)-C(14)	66.17(17)
C(18)-B(1)-C(13)-C(14)	-62.96(17)
N(2)-B(1)-C(13)-C(14)	-178.16(13)
C(20)-B(1)-C(13)-C(12)	-115.88(11)
C(18)-B(1)-C(13)-C(12)	114.99(11)
N(2)-B(1)-C(13)-C(12)	-0.21(11)
C(12)-C(13)-C(14)-C(15)	0.66(19)
B(1)-C(13)-C(14)-C(15)	178.53(13)
C(13)-C(14)-C(15)-C(16)	0.4(2)
C(14)-C(15)-C(16)-C(17)	-1.3(2)
C(15)-C(16)-C(17)-C(12)	1.09(19)
C(13)-C(12)-C(17)-C(16)	0.01(18)
C(11)-C(12)-C(17)-C(16)	-178.34(11)
C(13)-B(1)-C(18)-C(19)	-49.38(14)
C(20)-B(1)-C(18)-C(19)	-179.07(10)
N(2)-B(1)-C(18)-C(19)	56.44(13)
C(13)-B(1)-C(20)-C(21)	36.74(15)
C(18)-B(1)-C(20)-C(21)	164.94(11)
N(2)-B(1)-C(20)-C(21)	-70.35(13)

5.3 *Crystal structure of complex 27*

Appendix

Table 1. Crystal data and structure refinement for catalyst **27**.

Identification code	Catalyst 27
Empirical formula	C ₂₈ H ₄₁ B Cl ₂ N ₂ Si Ti
Formula weight	563.33
Temperature	100(2) K
Wavelength	0.71073 Å
Crystal system, space group	monoclinic, P2(1)/c
Unit cell dimensions	a = 9.2509(4) Å alpha = 90 deg. b = 15.4881(6) Å beta = 98.239(3) deg. c = 20.6554(10) Å gamma = 90 deg.
Volume	2928.9(2) Å ³
Z, Calculated density	4, 1.277 Mg/m ³
Absorption coefficient	0.535 mm ⁻¹
F(000)	1192
Crystal size	0.22 x 0.16 x 0.14 mm
Theta range for data collection	1.65 to 28.38 deg.
Limiting indices	-12 ≤ h ≤ 12, -20 ≤ k ≤ 20, -27 ≤ l ≤ 24
Reflections collected / unique	51448 / 7311 [R(int) = 0.0452]
Completeness to theta = 28.38°	99.4 %
Max. and min. transmission	0.7454 and 0.7160
Refinement method	Full-matrix least-squares on F ²
Data / restraints / parameters	7311 / 0 / 326
Goodness-of-fit on F ²	1.049
Final R indices [I > 2σ(I)]	R1 = 0.0355, wR2 = 0.0749
R indices (all data)	R1 = 0.0581, wR2 = 0.0798
Largest diff. peak and hole	0.392 and -0.391 e.Å ⁻³

Appendix

Table 2. Atomic coordinates ($\times 10^4$) and equivalent isotropic displacement parameters ($\text{\AA}^2 \times 10^3$) for catalyst **27**.

U(eq) is defined as one third of the trace of the orthogonalized Uij tensor.

	x	y	z	U(eq)
Ti(1)	3988(1)	8664(1)	1776(1)	13(1)
Cl(1)	6238(1)	8784(1)	1467(1)	20(1)
Cl(2)	3701(1)	10075(1)	2018(1)	19(1)
Si(1)	6227(1)	8030(1)	3038(1)	15(1)
B(1)	2162(2)	8784(1)	3584(1)	14(1)
N(1)	4348(1)	8092(1)	2615(1)	12(1)
C(1)	1752(2)	7905(1)	1392(1)	16(1)
N(2)	2605(1)	7780(1)	3350(1)	12(1)
C(2)	1631(2)	8761(1)	1142(1)	17(1)
C(3)	2683(2)	8872(1)	715(1)	21(1)
C(4)	3456(2)	8084(1)	695(1)	22(1)
C(5)	2892(2)	7492(1)	1117(1)	18(1)
C(6)	681(2)	7474(1)	1767(1)	20(1)
C(7)	454(2)	9400(1)	1233(1)	25(1)
C(8)	2915(2)	9676(1)	341(1)	35(1)
C(9)	4523(2)	7863(2)	246(1)	35(1)
C(10)	3299(2)	6553(1)	1160(1)	28(1)
C(11)	3478(2)	7508(1)	2915(1)	12(1)
C(12)	3616(2)	6624(1)	2793(1)	16(1)
C(13)	2867(2)	6023(1)	3106(1)	17(1)
C(14)	1981(2)	6300(1)	3546(1)	17(1)
C(15)	1878(2)	7176(1)	3667(1)	13(1)
C(16)	1065(2)	7575(1)	4141(1)	14(1)
C(17)	249(2)	7139(1)	4557(1)	17(1)
C(18)	-436(2)	7614(1)	4990(1)	19(1)
C(19)	-315(2)	8509(1)	5001(1)	22(1)
C(20)	491(2)	8932(1)	4580(1)	19(1)
C(21)	1222(2)	8477(1)	4141(1)	15(1)
C(22)	1096(2)	9171(1)	2959(1)	14(1)
C(23)	624(2)	10112(1)	3023(1)	21(1)
C(24)	3617(2)	9348(1)	3830(1)	17(1)
C(25)	3426(2)	10094(1)	4301(1)	23(1)
C(26)	7023(2)	9130(1)	3155(1)	23(1)
C(27)	6209(2)	7511(1)	3850(1)	23(1)
C(28)	7379(2)	7300(1)	2607(1)	23(1)

Appendix

Table 3. Bond lengths [Å] and angles [deg] for catalyst **27**.

Ti(1)-N(1)	1.9319(14)
Ti(1)-Cl(2)	2.2653(5)
Ti(1)-Cl(1)	2.2715(5)
Ti(1)-C(3)	2.3680(18)
Ti(1)-C(2)	2.3815(17)
Ti(1)-C(4)	2.3920(18)
Ti(1)-C(5)	2.4042(17)
Ti(1)-C(1)	2.4124(16)
Si(1)-N(1)	1.8327(14)
Si(1)-C(26)	1.8584(18)
Si(1)-C(27)	1.8622(19)
Si(1)-C(28)	1.8655(18)
B(1)-C(21)	1.609(3)
B(1)-C(22)	1.623(2)
B(1)-C(24)	1.624(2)
B(1)-N(2)	1.697(2)
N(1)-C(11)	1.412(2)
C(1)-C(5)	1.420(2)
C(1)-C(2)	1.422(2)
C(1)-C(6)	1.498(2)
N(2)-C(11)	1.358(2)
N(2)-C(15)	1.372(2)
C(2)-C(3)	1.415(3)
C(2)-C(7)	1.503(2)
C(3)-C(4)	1.419(3)
C(3)-C(8)	1.497(3)
C(4)-C(5)	1.415(3)
C(4)-C(9)	1.488(3)
C(5)-C(10)	1.503(2)
C(6)-H(6A)	0.9800
C(6)-H(6B)	0.9800
C(6)-H(6C)	0.9800
C(7)-H(7A)	0.9800
C(7)-H(7B)	0.9800
C(7)-H(7C)	0.9800
C(8)-H(8A)	0.9800
C(8)-H(8B)	0.9800
C(8)-H(8C)	0.9800
C(9)-H(9A)	0.9800
C(9)-H(9B)	0.9800
C(9)-H(9C)	0.9800
C(10)-H(10A)	0.9800
C(10)-H(10B)	0.9800
C(10)-H(10C)	0.9800
C(11)-C(12)	1.402(2)
C(12)-C(13)	1.375(2)
C(12)-H(12)	0.9500
C(13)-C(14)	1.376(2)

Appendix

C(13)-H(13)	0.9500
C(14)-C(15)	1.386(2)
C(14)-H(14)	0.9500
C(15)-C(16)	1.456(2)
C(16)-C(17)	1.396(2)
C(16)-C(21)	1.404(2)
C(17)-C(18)	1.381(2)
C(17)-H(17)	0.9500
C(18)-C(19)	1.390(2)
C(18)-H(18)	0.9500
C(19)-C(20)	1.389(3)
C(19)-H(19)	0.9500
C(20)-C(21)	1.398(2)
C(20)-H(20)	0.9500
C(22)-C(23)	1.532(2)
C(22)-H(22A)	0.9900
C(22)-H(22B)	0.9900
C(23)-H(23A)	0.9800
C(23)-H(23B)	0.9800
C(23)-H(23C)	0.9800
C(24)-C(25)	1.536(2)
C(24)-H(24A)	0.9900
C(24)-H(24B)	0.9900
C(25)-H(25A)	0.9800
C(25)-H(25B)	0.9800
C(25)-H(25C)	0.9800
C(26)-H(26A)	0.9800
C(26)-H(26B)	0.9800
C(26)-H(26C)	0.9800
C(27)-H(27A)	0.9800
C(27)-H(27B)	0.9800
C(27)-H(27C)	0.9800
C(28)-H(28A)	0.9800
C(28)-H(28B)	0.9800
C(28)-H(28C)	0.9800
N(1)-Ti(1)-Cl(2)	104.77(4)
N(1)-Ti(1)-Cl(1)	104.02(4)
Cl(2)-Ti(1)-Cl(1)	97.121(18)
N(1)-Ti(1)-C(3)	153.16(6)
Cl(2)-Ti(1)-C(3)	90.73(5)
Cl(1)-Ti(1)-C(3)	95.43(5)
N(1)-Ti(1)-C(2)	123.30(6)
Cl(2)-Ti(1)-C(2)	86.20(4)
Cl(1)-Ti(1)-C(2)	130.09(5)
C(3)-Ti(1)-C(2)	34.65(6)
N(1)-Ti(1)-C(4)	130.62(6)
Cl(2)-Ti(1)-C(4)	123.61(5)
Cl(1)-Ti(1)-C(4)	80.92(5)
C(3)-Ti(1)-C(4)	34.68(6)
C(2)-Ti(1)-C(4)	57.38(6)

Appendix

N(1)-Ti(1)-C(5)	99.59(6)
Cl(2)-Ti(1)-C(5)	143.13(4)
Cl(1)-Ti(1)-C(5)	103.39(4)
C(3)-Ti(1)-C(5)	57.38(6)
C(2)-Ti(1)-C(5)	57.17(6)
C(4)-Ti(1)-C(5)	34.31(6)
N(1)-Ti(1)-C(1)	95.80(6)
Cl(2)-Ti(1)-C(1)	114.90(4)
Cl(1)-Ti(1)-C(1)	136.44(4)
C(3)-Ti(1)-C(1)	57.51(6)
C(2)-Ti(1)-C(1)	34.51(5)
C(4)-Ti(1)-C(1)	57.19(6)
C(5)-Ti(1)-C(1)	34.28(6)
N(1)-Si(1)-C(26)	110.16(7)
N(1)-Si(1)-C(27)	108.82(7)
C(26)-Si(1)-C(27)	109.46(9)
N(1)-Si(1)-C(28)	111.84(8)
C(26)-Si(1)-C(28)	112.00(9)
C(27)-Si(1)-C(28)	104.36(8)
C(21)-B(1)-C(22)	110.40(14)
C(21)-B(1)-C(24)	116.44(15)
C(22)-B(1)-C(24)	115.54(14)
C(21)-B(1)-N(2)	96.35(12)
C(22)-B(1)-N(2)	104.80(13)
C(24)-B(1)-N(2)	111.01(12)
C(11)-N(1)-Si(1)	108.53(10)
C(11)-N(1)-Ti(1)	130.65(11)
Si(1)-N(1)-Ti(1)	118.84(7)
C(5)-C(1)-C(2)	107.36(15)
C(5)-C(1)-C(6)	126.24(15)
C(2)-C(1)-C(6)	125.39(15)
C(5)-C(1)-Ti(1)	72.54(9)
C(2)-C(1)-Ti(1)	71.56(9)
C(6)-C(1)-Ti(1)	130.25(12)
C(11)-N(2)-C(15)	118.87(13)
C(11)-N(2)-B(1)	131.66(13)
C(15)-N(2)-B(1)	109.45(13)
C(3)-C(2)-C(1)	108.34(15)
C(3)-C(2)-C(7)	124.99(16)
C(1)-C(2)-C(7)	126.11(16)
C(3)-C(2)-Ti(1)	72.15(10)
C(1)-C(2)-Ti(1)	73.93(9)
C(7)-C(2)-Ti(1)	126.55(12)
C(2)-C(3)-C(4)	107.95(16)
C(2)-C(3)-C(8)	125.86(18)
C(4)-C(3)-C(8)	126.18(18)
C(2)-C(3)-Ti(1)	73.20(10)
C(4)-C(3)-Ti(1)	73.58(10)
C(8)-C(3)-Ti(1)	119.96(13)
C(5)-C(4)-C(3)	107.90(16)
C(5)-C(4)-C(9)	124.84(18)

Appendix

C(3)-C(4)-C(9)	126.74(19)
C(5)-C(4)-Ti(1)	73.32(10)
C(3)-C(4)-Ti(1)	71.73(10)
C(9)-C(4)-Ti(1)	127.05(13)
C(4)-C(5)-C(1)	108.44(15)
C(4)-C(5)-C(10)	123.56(17)
C(1)-C(5)-C(10)	127.27(17)
C(4)-C(5)-Ti(1)	72.37(10)
C(1)-C(5)-Ti(1)	73.18(9)
C(10)-C(5)-Ti(1)	128.00(12)
C(1)-C(6)-H(6A)	109.5
C(1)-C(6)-H(6B)	109.5
H(6A)-C(6)-H(6B)	109.5
C(1)-C(6)-H(6C)	109.5
H(6A)-C(6)-H(6C)	109.5
H(6B)-C(6)-H(6C)	109.5
C(2)-C(7)-H(7A)	109.5
C(2)-C(7)-H(7B)	109.5
H(7A)-C(7)-H(7B)	109.5
C(2)-C(7)-H(7C)	109.5
H(7A)-C(7)-H(7C)	109.5
H(7B)-C(7)-H(7C)	109.5
C(3)-C(8)-H(8A)	109.5
C(3)-C(8)-H(8B)	109.5
H(8A)-C(8)-H(8B)	109.5
C(3)-C(8)-H(8C)	109.5
H(8A)-C(8)-H(8C)	109.5
H(8B)-C(8)-H(8C)	109.5
C(4)-C(9)-H(9A)	109.5
C(4)-C(9)-H(9B)	109.5
H(9A)-C(9)-H(9B)	109.5
C(4)-C(9)-H(9C)	109.5
H(9A)-C(9)-H(9C)	109.5
H(9B)-C(9)-H(9C)	109.5
C(5)-C(10)-H(10A)	109.5
C(5)-C(10)-H(10B)	109.5
H(10A)-C(10)-H(10B)	109.5
C(5)-C(10)-H(10C)	109.5
H(10A)-C(10)-H(10C)	109.5
H(10B)-C(10)-H(10C)	109.5
N(2)-C(11)-C(12)	120.00(15)
N(2)-C(11)-N(1)	121.44(13)
C(12)-C(11)-N(1)	118.39(15)
C(13)-C(12)-C(11)	120.75(16)
C(13)-C(12)-H(12)	119.6
C(11)-C(12)-H(12)	119.6
C(12)-C(13)-C(14)	119.21(15)
C(12)-C(13)-H(13)	120.4
C(14)-C(13)-H(13)	120.4
C(13)-C(14)-C(15)	119.10(15)
C(13)-C(14)-H(14)	120.5

Appendix

C(15)-C(14)-H(14)	120.5
N(2)-C(15)-C(14)	122.05(15)
N(2)-C(15)-C(16)	111.60(13)
C(14)-C(15)-C(16)	126.32(15)
C(17)-C(16)-C(21)	123.17(16)
C(17)-C(16)-C(15)	125.86(15)
C(21)-C(16)-C(15)	110.95(15)
C(18)-C(17)-C(16)	118.67(16)
C(18)-C(17)-H(17)	120.7
C(16)-C(17)-H(17)	120.7
C(17)-C(18)-C(19)	119.84(17)
C(17)-C(18)-H(18)	120.1
C(19)-C(18)-H(18)	120.1
C(20)-C(19)-C(18)	120.70(17)
C(20)-C(19)-H(19)	119.6
C(18)-C(19)-H(19)	119.6
C(19)-C(20)-C(21)	121.41(16)
C(19)-C(20)-H(20)	119.3
C(21)-C(20)-H(20)	119.3
C(20)-C(21)-C(16)	116.20(16)
C(20)-C(21)-B(1)	132.47(15)
C(16)-C(21)-B(1)	111.21(14)
C(23)-C(22)-B(1)	115.52(14)
C(23)-C(22)-H(22A)	108.4
B(1)-C(22)-H(22A)	108.4
C(23)-C(22)-H(22B)	108.4
B(1)-C(22)-H(22B)	108.4
H(22A)-C(22)-H(22B)	107.5
C(22)-C(23)-H(23A)	109.5
C(22)-C(23)-H(23B)	109.5
H(23A)-C(23)-H(23B)	109.5
C(22)-C(23)-H(23C)	109.5
H(23A)-C(23)-H(23C)	109.5
H(23B)-C(23)-H(23C)	109.5
C(25)-C(24)-B(1)	115.88(14)
C(25)-C(24)-H(24A)	108.3
B(1)-C(24)-H(24A)	108.3
C(25)-C(24)-H(24B)	108.3
B(1)-C(24)-H(24B)	108.3
H(24A)-C(24)-H(24B)	107.4
C(24)-C(25)-H(25A)	109.5
C(24)-C(25)-H(25B)	109.5
H(25A)-C(25)-H(25B)	109.5
C(24)-C(25)-H(25C)	109.5
H(25A)-C(25)-H(25C)	109.5
H(25B)-C(25)-H(25C)	109.5
Si(1)-C(26)-H(26A)	109.5
Si(1)-C(26)-H(26B)	109.5
H(26A)-C(26)-H(26B)	109.5
Si(1)-C(26)-H(26C)	109.5
H(26A)-C(26)-H(26C)	109.5

Appendix

H(26B)-C(26)-H(26C)	109.5
Si(1)-C(27)-H(27A)	109.5
Si(1)-C(27)-H(27B)	109.5
H(27A)-C(27)-H(27B)	109.5
Si(1)-C(27)-H(27C)	109.5
H(27A)-C(27)-H(27C)	109.5
H(27B)-C(27)-H(27C)	109.5
Si(1)-C(28)-H(28A)	109.5
Si(1)-C(28)-H(28B)	109.5
H(28A)-C(28)-H(28B)	109.5
Si(1)-C(28)-H(28C)	109.5
H(28A)-C(28)-H(28C)	109.5
H(28B)-C(28)-H(28C)	109.5

Table 4. Anisotropic displacement parameters ($\text{\AA}^2 \times 10^3$) for catalyst **27**.

The anisotropic displacement factor exponent takes the form: $-2 \pi^2 [h^2 a^{*2} U_{11} + \dots + 2 h k a^* b^* U_{12}]$.

	U11	U22	U33	U23	U13	U12
Ti(1)	12(1)	13(1)	13(1)	0(1)	3(1)	-1(1)
Cl(1)	15(1)	24(1)	21(1)	-1(1)	6(1)	-3(1)
Cl(2)	20(1)	13(1)	25(1)	0(1)	6(1)	-1(1)
Si(1)	10(1)	18(1)	19(1)	2(1)	3(1)	0(1)
B(1)	13(1)	12(1)	17(1)	-3(1)	5(1)	1(1)
N(1)	10(1)	14(1)	14(1)	0(1)	3(1)	0(1)
C(1)	13(1)	19(1)	14(1)	-4(1)	-1(1)	-1(1)
N(2)	9(1)	13(1)	13(1)	1(1)	1(1)	0(1)
C(2)	15(1)	21(1)	14(1)	-1(1)	-2(1)	0(1)
C(3)	20(1)	29(1)	13(1)	2(1)	-2(1)	-4(1)
C(4)	16(1)	35(1)	13(1)	-8(1)	1(1)	-2(1)
C(5)	16(1)	22(1)	16(1)	-6(1)	0(1)	1(1)
C(6)	18(1)	22(1)	21(1)	-3(1)	2(1)	-5(1)
C(7)	21(1)	26(1)	26(1)	-1(1)	-3(1)	7(1)
C(8)	41(1)	40(1)	22(1)	11(1)	1(1)	-11(1)
C(9)	24(1)	62(1)	22(1)	-14(1)	7(1)	-2(1)
C(10)	33(1)	23(1)	27(1)	-11(1)	-3(1)	8(1)
C(11)	10(1)	13(1)	13(1)	1(1)	1(1)	1(1)
C(12)	14(1)	14(1)	18(1)	-2(1)	3(1)	2(1)
C(13)	19(1)	11(1)	21(1)	-1(1)	2(1)	1(1)
C(14)	17(1)	15(1)	19(1)	3(1)	3(1)	-3(1)
C(15)	10(1)	16(1)	14(1)	2(1)	0(1)	-1(1)
C(16)	10(1)	19(1)	14(1)	0(1)	0(1)	0(1)
C(17)	14(1)	20(1)	17(1)	2(1)	0(1)	-1(1)
C(18)	13(1)	30(1)	14(1)	4(1)	3(1)	-2(1)
C(19)	19(1)	30(1)	17(1)	-4(1)	6(1)	2(1)
C(20)	18(1)	20(1)	19(1)	-3(1)	6(1)	0(1)
C(21)	12(1)	18(1)	15(1)	-1(1)	0(1)	0(1)
C(22)	11(1)	16(1)	17(1)	0(1)	5(1)	1(1)
C(23)	20(1)	16(1)	25(1)	2(1)	2(1)	4(1)
C(24)	14(1)	17(1)	21(1)	-3(1)	4(1)	-1(1)

Appendix

C(25)	21(1)	24(1)	24(1)	-8(1)	4(1)	-6(1)
C(26)	15(1)	26(1)	28(1)	-2(1)	3(1)	-6(1)
C(27)	15(1)	31(1)	22(1)	7(1)	1(1)	3(1)
C(28)	16(1)	22(1)	33(1)	5(1)	9(1)	5(1)

Table 5. Hydrogen coordinates ($\times 10^4$) and isotropic displacement parameters ($\text{\AA}^2 \times 10^3$) for catalyst **27**.

	x	y	z	U(eq)
H(6A)	444	7864	2110	31
H(6B)	1111	6942	1966	31
H(6C)	-211	7336	1469	31
H(7A)	890	9971	1326	37
H(7B)	-40	9218	1599	37
H(7C)	-256	9427	833	37
H(8A)	2302	9657	-87	52
H(8B)	3944	9716	279	52
H(8C)	2652	10181	585	52
H(9A)	5287	7489	474	53
H(9B)	4966	8394	106	53
H(9C)	4019	7560	-138	53
H(10A)	3062	6285	728	43
H(10B)	2751	6263	1470	43
H(10C)	4348	6496	1311	43
H(12)	4233	6437	2490	19
H(13)	2961	5425	3020	20
H(14)	1448	5895	3764	20
H(17)	167	6528	4542	21
H(18)	-989	7330	5281	23
H(19)	-788	8834	5299	26
H(20)	547	9545	4591	23
H(22A)	1601	9123	2569	17
H(22B)	208	8808	2880	17
H(23A)	141	10174	3413	31
H(23B)	-57	10276	2634	31
H(23C)	1484	10488	3063	31
H(24A)	4378	8954	4047	21
H(24B)	3982	9590	3440	21
H(25A)	2678	10492	4092	35
H(25B)	4354	10402	4408	35
H(25C)	3125	9862	4702	35
H(26A)	7515	9279	2780	35
H(26B)	7732	9143	3556	35
H(26C)	6244	9548	3191	35
H(27A)	5549	7830	4095	34
H(27B)	7198	7516	4095	34
H(27C)	5871	6913	3788	34
H(28A)	6913	6732	2547	35
H(28B)	8345	7239	2868	35
H(28C)	7485	7545	2179	35

Appendix

Table 6. Torsion angles [deg] for catalyst **27**.

C(26)-Si(1)-N(1)-C(11)	-138.00(11)
C(27)-Si(1)-N(1)-C(11)	-17.99(13)
C(28)-Si(1)-N(1)-C(11)	96.76(12)
C(26)-Si(1)-N(1)-Ti(1)	56.35(11)
C(27)-Si(1)-N(1)-Ti(1)	176.35(8)
C(28)-Si(1)-N(1)-Ti(1)	-68.89(10)
Cl(2)-Ti(1)-N(1)-C(11)	111.03(13)
Cl(1)-Ti(1)-N(1)-C(11)	-147.55(13)
C(3)-Ti(1)-N(1)-C(11)	-12.3(2)
C(2)-Ti(1)-N(1)-C(11)	15.80(16)
C(4)-Ti(1)-N(1)-C(11)	-57.56(16)
C(5)-Ti(1)-N(1)-C(11)	-41.04(14)
C(1)-Ti(1)-N(1)-C(11)	-6.64(14)
Cl(2)-Ti(1)-N(1)-Si(1)	-87.01(7)
Cl(1)-Ti(1)-N(1)-Si(1)	14.41(8)
C(3)-Ti(1)-N(1)-Si(1)	149.61(11)
C(2)-Ti(1)-N(1)-Si(1)	177.76(7)
C(4)-Ti(1)-N(1)-Si(1)	104.40(9)
C(5)-Ti(1)-N(1)-Si(1)	120.92(8)
C(1)-Ti(1)-N(1)-Si(1)	155.32(8)
N(1)-Ti(1)-C(1)-C(5)	-98.52(11)
Cl(2)-Ti(1)-C(1)-C(5)	152.23(9)
Cl(1)-Ti(1)-C(1)-C(5)	18.88(13)
C(3)-Ti(1)-C(1)-C(5)	78.43(11)
C(2)-Ti(1)-C(1)-C(5)	115.76(15)
C(4)-Ti(1)-C(1)-C(5)	36.97(10)
N(1)-Ti(1)-C(1)-C(2)	145.71(10)
Cl(2)-Ti(1)-C(1)-C(2)	36.46(11)
Cl(1)-Ti(1)-C(1)-C(2)	-96.89(10)
C(3)-Ti(1)-C(1)-C(2)	-37.33(10)
C(4)-Ti(1)-C(1)-C(2)	-78.80(11)
C(5)-Ti(1)-C(1)-C(2)	-115.76(15)
N(1)-Ti(1)-C(1)-C(6)	24.55(15)
Cl(2)-Ti(1)-C(1)-C(6)	-84.70(15)
Cl(1)-Ti(1)-C(1)-C(6)	141.95(13)
C(3)-Ti(1)-C(1)-C(6)	-158.50(17)
C(2)-Ti(1)-C(1)-C(6)	-121.16(19)
C(4)-Ti(1)-C(1)-C(6)	160.04(17)
C(5)-Ti(1)-C(1)-C(6)	123.07(19)
C(21)-B(1)-N(2)-C(11)	-175.48(15)
C(22)-B(1)-N(2)-C(11)	71.43(19)
C(24)-B(1)-N(2)-C(11)	-54.0(2)
C(21)-B(1)-N(2)-C(15)	6.29(15)
C(22)-B(1)-N(2)-C(15)	-106.80(14)
C(24)-B(1)-N(2)-C(15)	127.80(15)
C(5)-C(1)-C(2)-C(3)	0.26(19)
C(6)-C(1)-C(2)-C(3)	-168.79(16)
Ti(1)-C(1)-C(2)-C(3)	64.44(12)

Appendix

C(5)-C(1)-C(2)-C(7)	171.97(16)
C(6)-C(1)-C(2)-C(7)	2.9(3)
Ti(1)-C(1)-C(2)-C(7)	-123.85(17)
C(5)-C(1)-C(2)-Ti(1)	-64.18(11)
C(6)-C(1)-C(2)-Ti(1)	126.77(17)
N(1)-Ti(1)-C(2)-C(3)	-158.00(10)
Cl(2)-Ti(1)-C(2)-C(3)	96.81(10)
Cl(1)-Ti(1)-C(2)-C(3)	0.69(12)
C(4)-Ti(1)-C(2)-C(3)	-37.71(10)
C(5)-Ti(1)-C(2)-C(3)	-78.76(11)
C(1)-Ti(1)-C(2)-C(3)	-115.89(15)
N(1)-Ti(1)-C(2)-C(1)	-42.11(12)
Cl(2)-Ti(1)-C(2)-C(1)	-147.30(10)
Cl(1)-Ti(1)-C(2)-C(1)	116.59(9)
C(3)-Ti(1)-C(2)-C(1)	115.89(15)
C(4)-Ti(1)-C(2)-C(1)	78.18(11)
C(5)-Ti(1)-C(2)-C(1)	37.13(10)
N(1)-Ti(1)-C(2)-C(7)	81.26(16)
Cl(2)-Ti(1)-C(2)-C(7)	-23.94(15)
Cl(1)-Ti(1)-C(2)-C(7)	-120.05(14)
C(3)-Ti(1)-C(2)-C(7)	-120.7(2)
C(4)-Ti(1)-C(2)-C(7)	-158.45(18)
C(5)-Ti(1)-C(2)-C(7)	160.50(18)
C(1)-Ti(1)-C(2)-C(7)	123.4(2)
C(1)-C(2)-C(3)-C(4)	0.31(19)
C(7)-C(2)-C(3)-C(4)	-171.52(16)
Ti(1)-C(2)-C(3)-C(4)	65.91(12)
C(1)-C(2)-C(3)-C(8)	179.22(17)
C(7)-C(2)-C(3)-C(8)	7.4(3)
Ti(1)-C(2)-C(3)-C(8)	-115.18(18)
C(1)-C(2)-C(3)-Ti(1)	-65.60(12)
C(7)-C(2)-C(3)-Ti(1)	122.57(17)
N(1)-Ti(1)-C(3)-C(2)	43.90(18)
Cl(2)-Ti(1)-C(3)-C(2)	-82.24(10)
Cl(1)-Ti(1)-C(3)-C(2)	-179.47(9)
C(4)-Ti(1)-C(3)-C(2)	115.12(15)
C(5)-Ti(1)-C(3)-C(2)	78.11(11)
C(1)-Ti(1)-C(3)-C(2)	37.17(9)
N(1)-Ti(1)-C(3)-C(4)	-71.22(18)
Cl(2)-Ti(1)-C(3)-C(4)	162.64(10)
Cl(1)-Ti(1)-C(3)-C(4)	65.41(10)
C(2)-Ti(1)-C(3)-C(4)	-115.12(15)
C(5)-Ti(1)-C(3)-C(4)	-37.02(10)
C(1)-Ti(1)-C(3)-C(4)	-77.95(11)
N(1)-Ti(1)-C(3)-C(8)	166.06(14)
Cl(2)-Ti(1)-C(3)-C(8)	39.91(16)
Cl(1)-Ti(1)-C(3)-C(8)	-57.31(16)
C(2)-Ti(1)-C(3)-C(8)	122.2(2)
C(4)-Ti(1)-C(3)-C(8)	-122.7(2)
C(5)-Ti(1)-C(3)-C(8)	-159.74(18)
C(1)-Ti(1)-C(3)-C(8)	159.33(18)

Appendix

C(2)-C(3)-C(4)-C(5)	-0.8(2)
C(8)-C(3)-C(4)-C(5)	-179.66(17)
Ti(1)-C(3)-C(4)-C(5)	64.90(12)
C(2)-C(3)-C(4)-C(9)	171.29(17)
C(8)-C(3)-C(4)-C(9)	-7.6(3)
Ti(1)-C(3)-C(4)-C(9)	-123.06(18)
C(2)-C(3)-C(4)-Ti(1)	-65.65(12)
C(8)-C(3)-C(4)-Ti(1)	115.44(18)
N(1)-Ti(1)-C(4)-C(5)	29.83(13)
Cl(2)-Ti(1)-C(4)-C(5)	-136.90(9)
Cl(1)-Ti(1)-C(4)-C(5)	130.55(10)
C(3)-Ti(1)-C(4)-C(5)	-115.90(15)
C(2)-Ti(1)-C(4)-C(5)	-78.22(11)
C(1)-Ti(1)-C(4)-C(5)	-36.93(10)
N(1)-Ti(1)-C(4)-C(3)	145.73(10)
Cl(2)-Ti(1)-C(4)-C(3)	-21.00(12)
Cl(1)-Ti(1)-C(4)-C(3)	-113.55(10)
C(2)-Ti(1)-C(4)-C(3)	37.68(10)
C(5)-Ti(1)-C(4)-C(3)	115.90(15)
C(1)-Ti(1)-C(4)-C(3)	78.97(11)
N(1)-Ti(1)-C(4)-C(9)	-91.58(19)
Cl(2)-Ti(1)-C(4)-C(9)	101.70(17)
Cl(1)-Ti(1)-C(4)-C(9)	9.15(17)
C(3)-Ti(1)-C(4)-C(9)	122.7(2)
C(2)-Ti(1)-C(4)-C(9)	160.4(2)
C(5)-Ti(1)-C(4)-C(9)	-121.4(2)
C(1)-Ti(1)-C(4)-C(9)	-158.3(2)
C(3)-C(4)-C(5)-C(1)	0.92(19)
C(9)-C(4)-C(5)-C(1)	-171.31(16)
Ti(1)-C(4)-C(5)-C(1)	64.78(12)
C(3)-C(4)-C(5)-C(10)	171.79(16)
C(9)-C(4)-C(5)-C(10)	-0.5(3)
Ti(1)-C(4)-C(5)-C(10)	-124.36(17)
C(3)-C(4)-C(5)-Ti(1)	-63.85(12)
C(9)-C(4)-C(5)-Ti(1)	123.91(18)
C(2)-C(1)-C(5)-C(4)	-0.73(19)
C(6)-C(1)-C(5)-C(4)	168.20(16)
Ti(1)-C(1)-C(5)-C(4)	-64.26(12)
C(2)-C(1)-C(5)-C(10)	-171.16(17)
C(6)-C(1)-C(5)-C(10)	-2.2(3)
Ti(1)-C(1)-C(5)-C(10)	125.31(18)
C(2)-C(1)-C(5)-Ti(1)	63.53(11)
C(6)-C(1)-C(5)-Ti(1)	-127.54(17)
N(1)-Ti(1)-C(5)-C(4)	-157.49(10)
Cl(2)-Ti(1)-C(5)-C(4)	71.51(13)
Cl(1)-Ti(1)-C(5)-C(4)	-50.47(10)
C(3)-Ti(1)-C(5)-C(4)	37.43(10)
C(2)-Ti(1)-C(5)-C(4)	78.90(11)
C(1)-Ti(1)-C(5)-C(4)	116.29(15)
N(1)-Ti(1)-C(5)-C(1)	86.23(11)
Cl(2)-Ti(1)-C(5)-C(1)	-44.77(14)

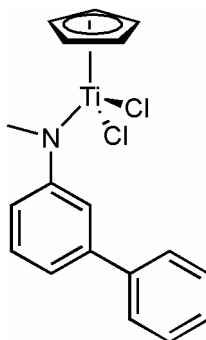
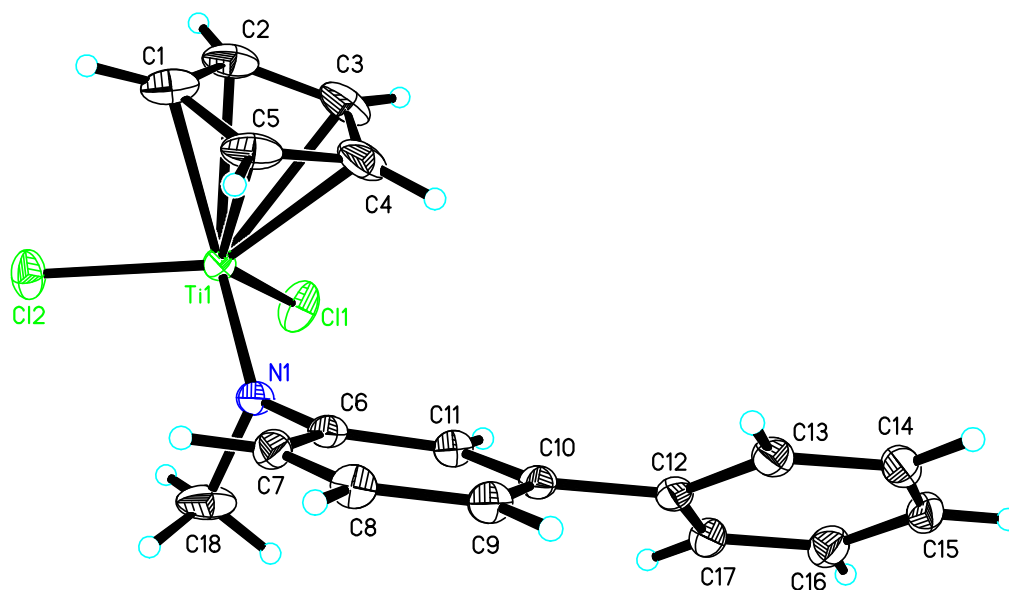
Appendix

Cl(1)-Ti(1)-C(5)-C(1)	-166.75(9)
C(3)-Ti(1)-C(5)-C(1)	-78.86(11)
C(2)-Ti(1)-C(5)-C(1)	-37.39(10)
C(4)-Ti(1)-C(5)-C(1)	-116.29(15)
N(1)-Ti(1)-C(5)-C(10)	-38.29(18)
Cl(2)-Ti(1)-C(5)-C(10)	-169.29(13)
Cl(1)-Ti(1)-C(5)-C(10)	68.73(17)
C(3)-Ti(1)-C(5)-C(10)	156.62(19)
C(2)-Ti(1)-C(5)-C(10)	-161.9(2)
C(4)-Ti(1)-C(5)-C(10)	119.2(2)
C(1)-Ti(1)-C(5)-C(10)	-124.5(2)
C(15)-N(2)-C(11)-C(12)	0.5(2)
B(1)-N(2)-C(11)-C(12)	-177.57(15)
C(15)-N(2)-C(11)-N(1)	-174.60(14)
B(1)-N(2)-C(11)-N(1)	7.3(2)
Si(1)-N(1)-C(11)-N(2)	100.58(15)
Ti(1)-N(1)-C(11)-N(2)	-96.05(18)
Si(1)-N(1)-C(11)-C(12)	-74.62(16)
Ti(1)-N(1)-C(11)-C(12)	88.76(17)
N(2)-C(11)-C(12)-C(13)	0.4(2)
N(1)-C(11)-C(12)-C(13)	175.65(15)
C(11)-C(12)-C(13)-C(14)	-0.3(3)
C(12)-C(13)-C(14)-C(15)	-0.7(2)
C(11)-N(2)-C(15)-C(14)	-1.5(2)
B(1)-N(2)-C(15)-C(14)	176.96(15)
C(11)-N(2)-C(15)-C(16)	176.59(14)
B(1)-N(2)-C(15)-C(16)	-4.92(17)
C(13)-C(14)-C(15)-N(2)	1.6(2)
C(13)-C(14)-C(15)-C(16)	-176.22(16)
N(2)-C(15)-C(16)-C(17)	-177.96(15)
C(14)-C(15)-C(16)-C(17)	0.1(3)
N(2)-C(15)-C(16)-C(21)	0.98(19)
C(14)-C(15)-C(16)-C(21)	179.01(16)
C(21)-C(16)-C(17)-C(18)	-0.2(2)
C(15)-C(16)-C(17)-C(18)	178.65(16)
C(16)-C(17)-C(18)-C(19)	0.6(2)
C(17)-C(18)-C(19)-C(20)	-0.1(3)
C(18)-C(19)-C(20)-C(21)	-1.0(3)
C(19)-C(20)-C(21)-C(16)	1.3(2)
C(19)-C(20)-C(21)-B(1)	176.98(17)
C(17)-C(16)-C(21)-C(20)	-0.8(2)
C(15)-C(16)-C(21)-C(20)	-179.77(14)
C(17)-C(16)-C(21)-B(1)	-177.34(15)
C(15)-C(16)-C(21)-B(1)	3.68(19)
C(22)-B(1)-C(21)-C(20)	-73.1(2)
C(24)-B(1)-C(21)-C(20)	61.2(2)
N(2)-B(1)-C(21)-C(20)	178.46(17)
C(22)-B(1)-C(21)-C(16)	102.66(15)
C(24)-B(1)-C(21)-C(16)	-123.01(15)
N(2)-B(1)-C(21)-C(16)	-5.74(16)
C(21)-B(1)-C(22)-C(23)	81.81(17)

Appendix

C(24)-B(1)-C(22)-C(23)	-53.0(2)
N(2)-B(1)-C(22)-C(23)	-175.46(13)
C(21)-B(1)-C(24)-C(25)	-47.2(2)
C(22)-B(1)-C(24)-C(25)	84.8(2)
N(2)-B(1)-C(24)-C(25)	-156.09(14)

5.4 Crystal structure of complex 34



34

Appendix

Table 1. Crystal data and structure refinement for catalyst **34**.

Identification code	Catalyst 34
Empirical formula	C ₁₈ H ₁₇ Cl ₂ N Ti
Formula weight	366.13
Temperature	100(2) K
Wavelength	0.71073 Å
Crystal system, space group	orthorhombic, P b c a
Unit cell dimensions	a = 13.2542(12) Å alpha = 90 deg. b = 11.6665(9) Å beta = 90 deg. c = 21.732(2) Å gamma = 90 deg.
Volume	3360.3(5) Å ³
Z, Calculated density	8, 1.447 Mg/m ³
Absorption coefficient	0.822 mm ⁻¹
F(000)	1504
Crystal size	0.41 x 0.32 x 0.09 mm
Theta range for data collection	1.87 to 28.44 deg.
Limiting indices	-17<=h<=17, -15<=k<=14, -28<=l<=28
Reflections collected / unique	27226 / 4148 [R(int) = 0.0289]
Completeness to theta =28.44°	98.0 %
Max. and min. transmission	0.9267 and 0.7292
Refinement method	Full-matrix least-squares on F ²
Data / restraints / parameters	4148 / 0 / 200
Goodness-of-fit on F ²	1.045
Final R indices [I>2sigma(I)]	R1 = 0.0278, wR2 = 0.0673
R indices (all data)	R1 = 0.0403, wR2 = 0.0715
Largest diff. peak and hole	0.356 and -0.304 e.Å ⁻³

Appendix

Table 2. Atomic coordinates ($\times 10^4$) and equivalent isotropic displacement parameters ($\text{\AA}^2 \times 10^3$) for catalyst **34**.

U(eq) is defined as one third of the trace of the orthogonalized Uij tensor.

	x	y	z	U(eq)
Ti(1)	681(1)	3402(1)	3136(1)	14(1)
Cl(1)	1674(1)	2119(1)	2631(1)	28(1)
Cl(2)	-431(1)	3895(1)	2380(1)	25(1)
N(1)	-17(1)	2483(1)	3702(1)	16(1)
C(1)	752(1)	5367(1)	3372(1)	29(1)
C(2)	1657(1)	5074(1)	3072(1)	28(1)
C(3)	2184(1)	4298(2)	3446(1)	32(1)
C(4)	1599(1)	4098(2)	3977(1)	29(1)
C(5)	713(1)	4755(1)	3930(1)	27(1)
C(6)	-86(1)	2345(1)	4356(1)	16(1)
C(7)	-877(1)	2835(1)	4685(1)	18(1)
C(8)	-918(1)	2680(1)	5321(1)	19(1)
C(9)	-175(1)	2052(1)	5624(1)	18(1)
C(10)	620(1)	1555(1)	5296(1)	16(1)
C(11)	647(1)	1702(1)	4656(1)	17(1)
C(12)	1438(1)	914(1)	5615(1)	17(1)
C(13)	1768(1)	1257(1)	6198(1)	19(1)
C(14)	2536(1)	675(1)	6497(1)	23(1)
C(15)	2986(1)	-269(1)	6220(1)	24(1)
C(16)	2669(1)	-621(1)	5641(1)	23(1)
C(17)	1898(1)	-30(1)	5340(1)	20(1)
C(18)	-582(1)	1587(1)	3365(1)	31(1)

Appendix

Table 3. Bond lengths [Å] and angles [deg] for catalyst **34**.

Ti(1)-N(1)	1.8750(12)
Ti(1)-Cl(1)	2.2759(5)
Ti(1)-Cl(2)	2.2810(4)
Ti(1)-C(5)	2.3384(15)
Ti(1)-C(4)	2.3400(15)
Ti(1)-C(2)	2.3446(16)
Ti(1)-C(3)	2.3489(16)
Ti(1)-C(1)	2.3505(16)
N(1)-C(6)	1.4327(17)
N(1)-C(18)	1.4803(18)
C(1)-C(2)	1.407(2)
C(1)-C(5)	1.409(2)
C(1)-H(1)	0.9500
C(2)-C(3)	1.404(3)
C(2)-H(2)	0.9500
C(3)-C(4)	1.409(2)
C(3)-H(3)	0.9500
C(4)-C(5)	1.406(3)
C(4)-H(4)	0.9500
C(5)-H(5)	0.9500
C(6)-C(11)	1.390(2)
C(6)-C(7)	1.393(2)
C(7)-C(8)	1.3942(19)
C(7)-H(7)	0.9500
C(8)-C(9)	1.391(2)
C(8)-H(8)	0.9500
C(9)-C(10)	1.398(2)
C(9)-H(9)	0.9500
C(10)-C(11)	1.4032(19)
C(10)-C(12)	1.4880(19)
C(11)-H(11)	0.9500
C(12)-C(17)	1.394(2)
C(12)-C(13)	1.3978(19)
C(13)-C(14)	1.386(2)
C(13)-H(13)	0.9500
C(14)-C(15)	1.389(2)
C(14)-H(14)	0.9500
C(15)-C(16)	1.388(2)
C(15)-H(15)	0.9500
C(16)-C(17)	1.395(2)
C(16)-H(16)	0.9500
C(17)-H(17)	0.9500
C(18)-H(18A)	0.9800
C(18)-H(18B)	0.9800
C(18)-H(18C)	0.9800
N(1)-Ti(1)-Cl(1)	103.02(4)
N(1)-Ti(1)-Cl(2)	107.34(4)
Cl(1)-Ti(1)-Cl(2)	101.055(18)

Appendix

N(1)-Ti(1)-C(5)	84.90(5)
Cl(1)-Ti(1)-C(5)	142.12(5)
Cl(2)-Ti(1)-C(5)	111.92(5)
N(1)-Ti(1)-C(4)	86.74(5)
Cl(1)-Ti(1)-C(4)	107.69(5)
Cl(2)-Ti(1)-C(4)	144.19(5)
C(5)-Ti(1)-C(4)	34.98(6)
N(1)-Ti(1)-C(2)	141.91(5)
Cl(1)-Ti(1)-C(2)	101.48(4)
Cl(2)-Ti(1)-C(2)	95.95(5)
C(5)-Ti(1)-C(2)	58.19(5)
C(4)-Ti(1)-C(2)	58.08(6)
N(1)-Ti(1)-C(3)	119.00(6)
Cl(1)-Ti(1)-C(3)	86.59(5)
Cl(2)-Ti(1)-C(3)	129.98(5)
C(5)-Ti(1)-C(3)	58.17(6)
C(4)-Ti(1)-C(3)	34.97(6)
C(2)-Ti(1)-C(3)	34.80(6)
N(1)-Ti(1)-C(1)	115.77(5)
Cl(1)-Ti(1)-C(1)	136.32(4)
Cl(2)-Ti(1)-C(1)	86.40(5)
C(5)-Ti(1)-C(1)	34.97(6)
C(4)-Ti(1)-C(1)	58.05(6)
C(2)-Ti(1)-C(1)	34.88(6)
C(3)-Ti(1)-C(1)	57.95(6)
C(6)-N(1)-C(18)	112.27(11)
C(6)-N(1)-Ti(1)	138.24(9)
C(18)-N(1)-Ti(1)	109.19(9)
C(2)-C(1)-C(5)	107.91(16)
C(2)-C(1)-Ti(1)	72.33(9)
C(5)-C(1)-Ti(1)	72.04(9)
C(2)-C(1)-H(1)	126.0
C(5)-C(1)-H(1)	126.0
Ti(1)-C(1)-H(1)	121.3
C(3)-C(2)-C(1)	108.18(15)
C(3)-C(2)-Ti(1)	72.77(9)
C(1)-C(2)-Ti(1)	72.79(9)
C(3)-C(2)-H(2)	125.9
C(1)-C(2)-H(2)	125.9
Ti(1)-C(2)-H(2)	120.3
C(2)-C(3)-C(4)	107.90(16)
C(2)-C(3)-Ti(1)	72.43(9)
C(4)-C(3)-Ti(1)	72.17(9)
C(2)-C(3)-H(3)	126.0
C(4)-C(3)-H(3)	126.0
Ti(1)-C(3)-H(3)	121.1
C(5)-C(4)-C(3)	108.10(15)
C(5)-C(4)-Ti(1)	72.45(9)
C(3)-C(4)-Ti(1)	72.86(9)
C(5)-C(4)-H(4)	125.9
C(3)-C(4)-H(4)	125.9

Appendix

Ti(1)-C(4)-H(4)	120.5
C(4)-C(5)-C(1)	107.89(14)
C(4)-C(5)-Ti(1)	72.57(9)
C(1)-C(5)-Ti(1)	72.98(9)
C(4)-C(5)-H(5)	126.1
C(1)-C(5)-H(5)	126.1
Ti(1)-C(5)-H(5)	120.2
C(11)-C(6)-C(7)	120.40(13)
C(11)-C(6)-N(1)	118.80(12)
C(7)-C(6)-N(1)	120.80(13)
C(6)-C(7)-C(8)	119.03(13)
C(6)-C(7)-H(7)	120.5
C(8)-C(7)-H(7)	120.5
C(9)-C(8)-C(7)	120.66(13)
C(9)-C(8)-H(8)	119.7
C(7)-C(8)-H(8)	119.7
C(8)-C(9)-C(10)	120.70(13)
C(8)-C(9)-H(9)	119.7
C(10)-C(9)-H(9)	119.7
C(9)-C(10)-C(11)	118.28(13)
C(9)-C(10)-C(12)	121.41(13)
C(11)-C(10)-C(12)	120.29(13)
C(6)-C(11)-C(10)	120.92(13)
C(6)-C(11)-H(11)	119.5
C(10)-C(11)-H(11)	119.5
C(17)-C(12)-C(13)	118.47(13)
C(17)-C(12)-C(10)	121.13(13)
C(13)-C(12)-C(10)	120.39(13)
C(14)-C(13)-C(12)	120.98(14)
C(14)-C(13)-H(13)	119.5
C(12)-C(13)-H(13)	119.5
C(13)-C(14)-C(15)	120.03(14)
C(13)-C(14)-H(14)	120.0
C(15)-C(14)-H(14)	120.0
C(16)-C(15)-C(14)	119.84(14)
C(16)-C(15)-H(15)	120.1
C(14)-C(15)-H(15)	120.1
C(15)-C(16)-C(17)	119.96(15)
C(15)-C(16)-H(16)	120.0
C(17)-C(16)-H(16)	120.0
C(12)-C(17)-C(16)	120.72(14)
C(12)-C(17)-H(17)	119.6
C(16)-C(17)-H(17)	119.6
N(1)-C(18)-H(18A)	109.5
N(1)-C(18)-H(18B)	109.5
H(18A)-C(18)-H(18B)	109.5
N(1)-C(18)-H(18C)	109.5
H(18A)-C(18)-H(18C)	109.5
H(18B)-C(18)-H(18C)	109.5

Appendix

Table 4. Anisotropic displacement parameters ($\text{\AA}^2 \times 10^3$) for catalyst **34**.

The anisotropic displacement factor exponent takes the form: $-2 \pi^2 [h^2 a^{*2} U_{11} + \dots + 2 h k a^* b^* U_{12}$

	U11	U22	U33	U23	U13	U12
Ti(1)	15(1)	16(1)	12(1)	1(1)	1(1)	-1(1)
Cl(1)	33(1)	29(1)	24(1)	1(1)	6(1)	14(1)
Cl(2)	21(1)	37(1)	18(1)	7(1)	-1(1)	4(1)
N(1)	20(1)	17(1)	13(1)	0(1)	0(1)	-3(1)
C(1)	38(1)	18(1)	30(1)	-3(1)	7(1)	-8(1)
C(2)	33(1)	27(1)	25(1)	-1(1)	8(1)	-14(1)
C(3)	20(1)	42(1)	33(1)	-4(1)	-1(1)	-13(1)
C(4)	30(1)	37(1)	20(1)	-1(1)	-6(1)	-16(1)
C(5)	36(1)	24(1)	22(1)	-8(1)	9(1)	-13(1)
C(6)	19(1)	16(1)	14(1)	0(1)	0(1)	-5(1)
C(7)	20(1)	16(1)	19(1)	0(1)	-2(1)	0(1)
C(8)	19(1)	20(1)	19(1)	-3(1)	3(1)	0(1)
C(9)	23(1)	20(1)	12(1)	-2(1)	1(1)	-3(1)
C(10)	18(1)	14(1)	16(1)	0(1)	-1(1)	-3(1)
C(11)	19(1)	17(1)	15(1)	-1(1)	2(1)	-1(1)
C(12)	17(1)	19(1)	15(1)	4(1)	1(1)	-4(1)
C(13)	20(1)	23(1)	15(1)	1(1)	1(1)	-5(1)
C(14)	20(1)	33(1)	15(1)	5(1)	-1(1)	-8(1)
C(15)	17(1)	30(1)	24(1)	11(1)	-2(1)	-4(1)
C(16)	22(1)	22(1)	26(1)	4(1)	2(1)	2(1)
C(17)	21(1)	21(1)	17(1)	2(1)	-1(1)	-2(1)
C(18)	48(1)	28(1)	15(1)	-4(1)	1(1)	-21(1)

Table 5. Hydrogen coordinates ($\times 10^4$) and isotropic displacement parameters ($\text{\AA}^2 \times 10^3$) for catalyst **34**.

	x	y	z	U(eq)
H(1)	256	5886	3224	34
H(2)	1874	5353	2683	34
H(3)	2823	3967	3358	38
H(4)	1773	3605	4308	35
H(5)	182	4781	4223	33
H(7)	-1382	3269	4480	22
H(8)	-1457	3005	5550	23
H(9)	-209	1961	6058	22
H(11)	1173	1357	4424	20
H(13)	1460	1897	6392	23
H(14)	2756	921	6891	27
H(15)	3509	-671	6426	29
H(16)	2977	-1265	5450	28
H(17)	1685	-273	4944	24
H(18A)	-336	829	3488	46
H(18B)	-481	1688	2921	46
H(18C)	-1302	1650	3461	46

Appendix

Table 6. Torsion angles [deg] for catalyst **34**.

Cl(1)-Ti(1)-N(1)-C(6)	114.88(14)
Cl(2)-Ti(1)-N(1)-C(6)	-138.96(14)
C(5)-Ti(1)-N(1)-C(6)	-27.56(15)
C(4)-Ti(1)-N(1)-C(6)	7.46(15)
C(2)-Ti(1)-N(1)-C(6)	-13.9(2)
C(3)-Ti(1)-N(1)-C(6)	21.53(17)
C(1)-Ti(1)-N(1)-C(6)	-44.50(16)
Cl(1)-Ti(1)-N(1)-C(18)	-58.17(11)
Cl(2)-Ti(1)-N(1)-C(18)	48.00(11)
C(5)-Ti(1)-N(1)-C(18)	159.39(11)
C(4)-Ti(1)-N(1)-C(18)	-165.58(11)
C(2)-Ti(1)-N(1)-C(18)	173.06(11)
C(3)-Ti(1)-N(1)-C(18)	-151.51(11)
C(1)-Ti(1)-N(1)-C(18)	142.45(11)
N(1)-Ti(1)-C(1)-C(2)	146.69(10)
Cl(1)-Ti(1)-C(1)-C(2)	-3.52(13)
Cl(2)-Ti(1)-C(1)-C(2)	-105.78(10)
C(5)-Ti(1)-C(1)-C(2)	116.27(15)
C(4)-Ti(1)-C(1)-C(2)	78.75(11)
C(3)-Ti(1)-C(1)-C(2)	37.25(10)
N(1)-Ti(1)-C(1)-C(5)	30.42(12)
Cl(1)-Ti(1)-C(1)-C(5)	-119.79(9)
Cl(2)-Ti(1)-C(1)-C(5)	137.95(10)
C(4)-Ti(1)-C(1)-C(5)	-37.52(10)
C(2)-Ti(1)-C(1)-C(5)	-116.27(15)
C(3)-Ti(1)-C(1)-C(5)	-79.02(11)
C(5)-C(1)-C(2)-C(3)	-0.95(18)
Ti(1)-C(1)-C(2)-C(3)	-64.65(11)
C(5)-C(1)-C(2)-Ti(1)	63.70(11)
N(1)-Ti(1)-C(2)-C(3)	62.69(14)
Cl(1)-Ti(1)-C(2)-C(3)	-66.50(10)
Cl(2)-Ti(1)-C(2)-C(3)	-169.09(9)
C(5)-Ti(1)-C(2)-C(3)	78.76(11)
C(4)-Ti(1)-C(2)-C(3)	37.31(10)
C(1)-Ti(1)-C(2)-C(3)	115.98(14)
N(1)-Ti(1)-C(2)-C(1)	-53.29(15)
Cl(1)-Ti(1)-C(2)-C(1)	177.52(9)
Cl(2)-Ti(1)-C(2)-C(1)	74.93(10)
C(5)-Ti(1)-C(2)-C(1)	-37.22(10)
C(4)-Ti(1)-C(2)-C(1)	-78.66(11)
C(3)-Ti(1)-C(2)-C(1)	-115.98(14)
C(1)-C(2)-C(3)-C(4)	0.76(18)
Ti(1)-C(2)-C(3)-C(4)	-63.91(11)
C(1)-C(2)-C(3)-Ti(1)	64.66(11)
N(1)-Ti(1)-C(3)-C(2)	-141.20(9)
Cl(1)-Ti(1)-C(3)-C(2)	115.80(10)

Appendix

Cl(2)-Ti(1)-C(3)-C(2)	14.22(12)
C(5)-Ti(1)-C(3)-C(2)	-78.82(11)
C(4)-Ti(1)-C(3)-C(2)	-116.14(16)
C(1)-Ti(1)-C(3)-C(2)	-37.34(10)
N(1)-Ti(1)-C(3)-C(4)	-25.06(13)
Cl(1)-Ti(1)-C(3)-C(4)	-128.06(11)
Cl(2)-Ti(1)-C(3)-C(4)	130.37(10)
C(5)-Ti(1)-C(3)-C(4)	37.33(10)
C(2)-Ti(1)-C(3)-C(4)	116.14(16)
C(1)-Ti(1)-C(3)-C(4)	78.80(11)
C(2)-C(3)-C(4)-C(5)	-0.27(18)
Ti(1)-C(3)-C(4)-C(5)	-64.35(11)
C(2)-C(3)-C(4)-Ti(1)	64.08(11)
N(1)-Ti(1)-C(4)-C(5)	-85.76(10)
Cl(1)-Ti(1)-C(4)-C(5)	171.60(8)
Cl(2)-Ti(1)-C(4)-C(5)	29.78(13)
C(2)-Ti(1)-C(4)-C(5)	78.88(10)
C(3)-Ti(1)-C(4)-C(5)	116.01(15)
C(1)-Ti(1)-C(4)-C(5)	37.52(9)
N(1)-Ti(1)-C(4)-C(3)	158.22(11)
Cl(1)-Ti(1)-C(4)-C(3)	55.59(11)
Cl(2)-Ti(1)-C(4)-C(3)	-86.23(13)
C(5)-Ti(1)-C(4)-C(3)	-116.01(15)
C(2)-Ti(1)-C(4)-C(3)	-37.13(11)
C(1)-Ti(1)-C(4)-C(3)	-78.50(11)
C(3)-C(4)-C(5)-C(1)	-0.31(18)
Ti(1)-C(4)-C(5)-C(1)	-64.94(11)
C(3)-C(4)-C(5)-Ti(1)	64.62(11)
C(2)-C(1)-C(5)-C(4)	0.78(18)
Ti(1)-C(1)-C(5)-C(4)	64.67(11)
C(2)-C(1)-C(5)-Ti(1)	-63.89(11)
N(1)-Ti(1)-C(5)-C(4)	91.60(10)
Cl(1)-Ti(1)-C(5)-C(4)	-13.09(13)
Cl(2)-Ti(1)-C(5)-C(4)	-161.74(8)
C(2)-Ti(1)-C(5)-C(4)	-78.53(10)
C(3)-Ti(1)-C(5)-C(4)	-37.32(10)
C(1)-Ti(1)-C(5)-C(4)	-115.64(14)
N(1)-Ti(1)-C(5)-C(1)	-152.75(11)
Cl(1)-Ti(1)-C(5)-C(1)	102.55(11)
Cl(2)-Ti(1)-C(5)-C(1)	-46.10(11)
C(4)-Ti(1)-C(5)-C(1)	115.64(14)
C(2)-Ti(1)-C(5)-C(1)	37.12(10)
C(3)-Ti(1)-C(5)-C(1)	78.33(11)
C(18)-N(1)-C(6)-C(11)	91.54(16)
Ti(1)-N(1)-C(6)-C(11)	-81.36(18)
C(18)-N(1)-C(6)-C(7)	-87.84(17)
Ti(1)-N(1)-C(6)-C(7)	99.26(17)
C(11)-C(6)-C(7)-C(8)	0.6(2)
N(1)-C(6)-C(7)-C(8)	179.96(13)
C(6)-C(7)-C(8)-C(9)	0.5(2)
C(7)-C(8)-C(9)-C(10)	-0.7(2)

Appendix

C(8)-C(9)-C(10)-C(11)	-0.2(2)
C(8)-C(9)-C(10)-C(12)	177.94(13)
C(7)-C(6)-C(11)-C(10)	-1.5(2)
N(1)-C(6)-C(11)-C(10)	179.10(12)
C(9)-C(10)-C(11)-C(6)	1.3(2)
C(12)-C(10)-C(11)-C(6)	-176.87(13)
C(9)-C(10)-C(12)-C(17)	146.18(14)
C(11)-C(10)-C(12)-C(17)	-35.7(2)
C(9)-C(10)-C(12)-C(13)	-34.3(2)
C(11)-C(10)-C(12)-C(13)	143.78(14)
C(17)-C(12)-C(13)-C(14)	0.2(2)
C(10)-C(12)-C(13)-C(14)	-179.32(13)
C(12)-C(13)-C(14)-C(15)	-0.5(2)
C(13)-C(14)-C(15)-C(16)	0.5(2)
C(14)-C(15)-C(16)-C(17)	-0.2(2)
C(13)-C(12)-C(17)-C(16)	0.2(2)
C(10)-C(12)-C(17)-C(16)	179.65(13)
C(15)-C(16)-C(17)-C(12)	-0.2(2)

Appendix

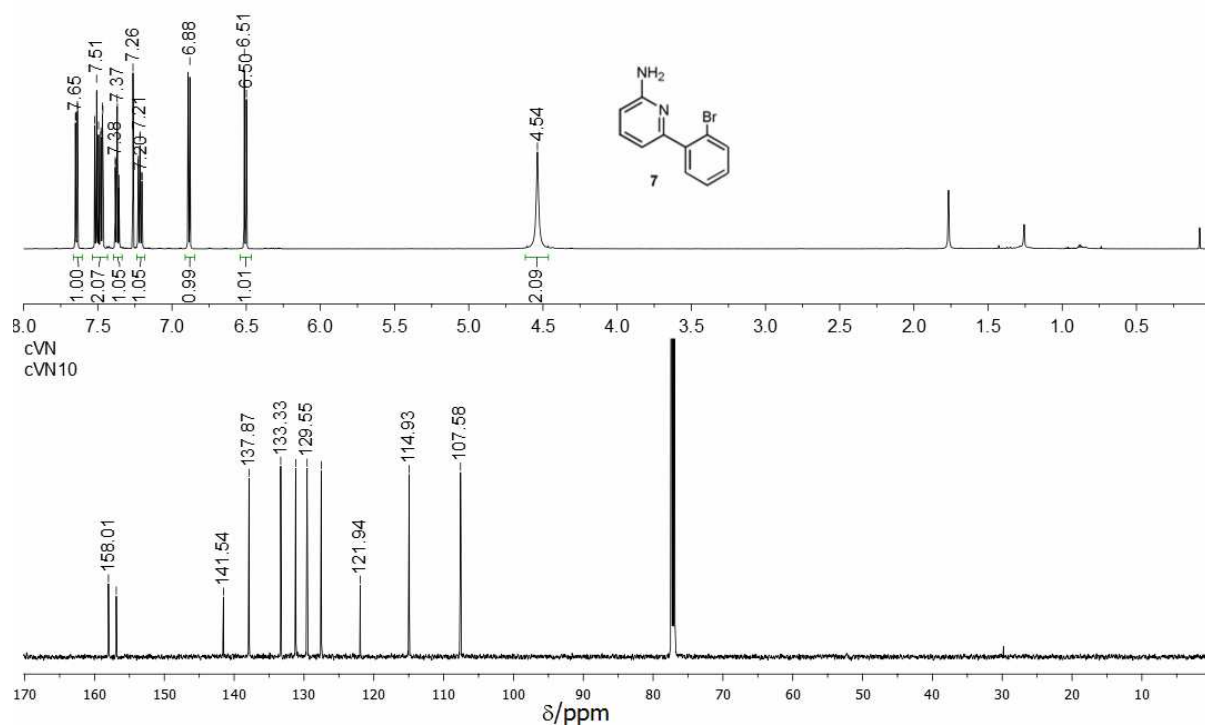


Figure 5.1. ^1H and ^{13}C NMR spectra of **7** in CDCl_3 at 298 K.

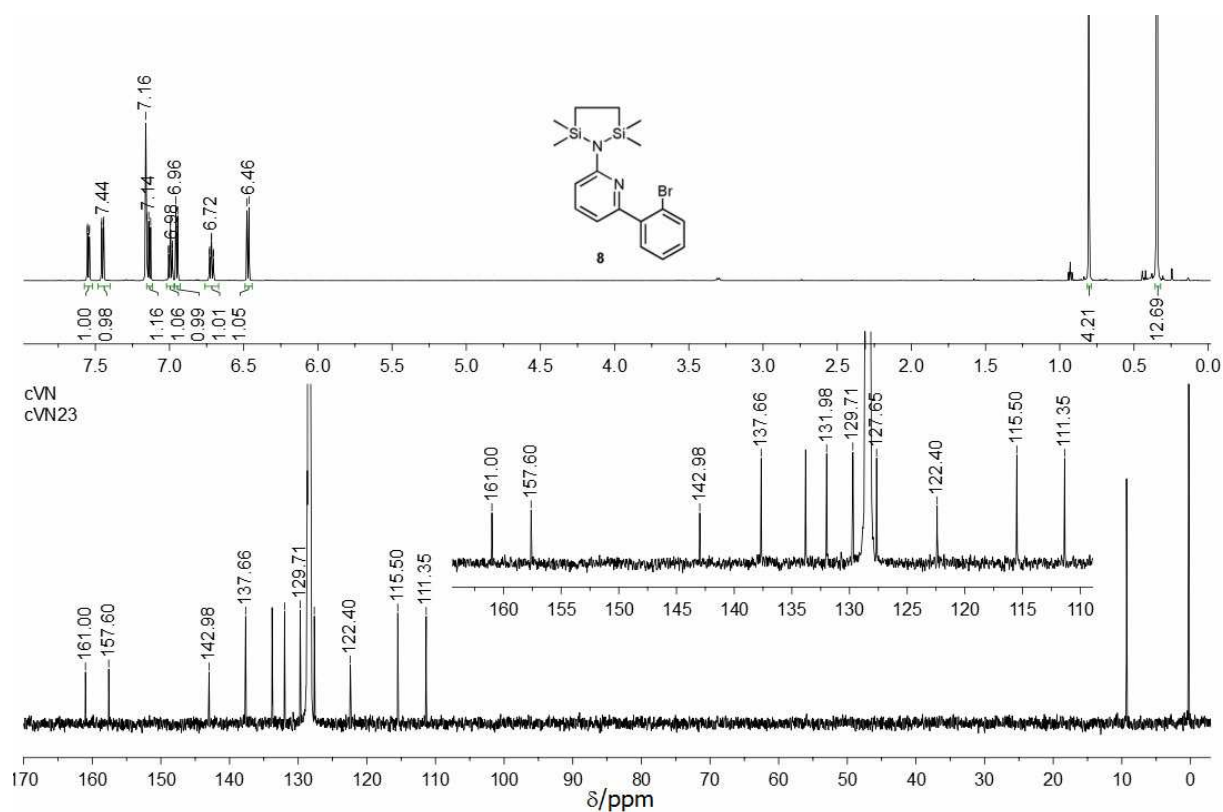


Figure 5.2. ^1H and ^{13}C NMR spectra of **8** in C_6D_6 at 298 K.

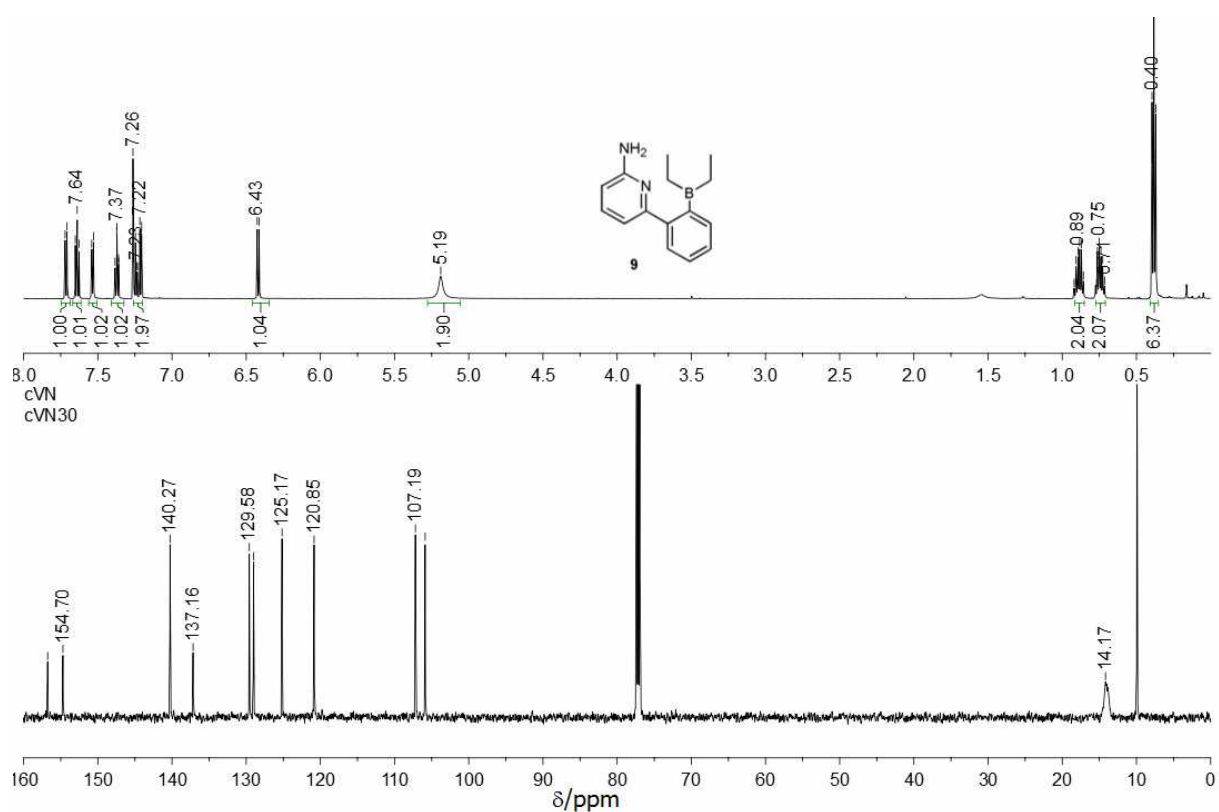


Figure 5.3. ^1H and ^{13}C NMR spectra of **9** in CDCl_3 at 298 K.

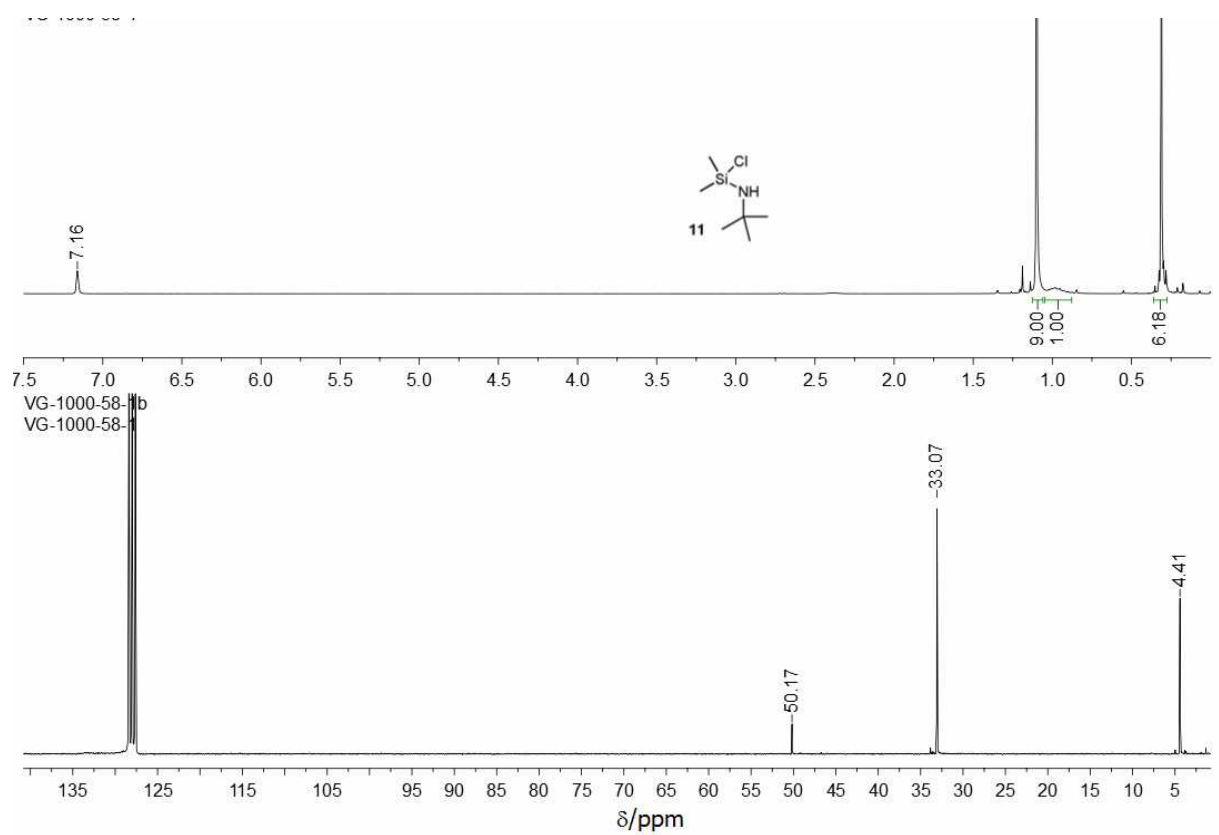


Figure 5.4. ^1H and ^{13}C NMR spectra of **11** in C_6D_6 at 298 K.

Appendix

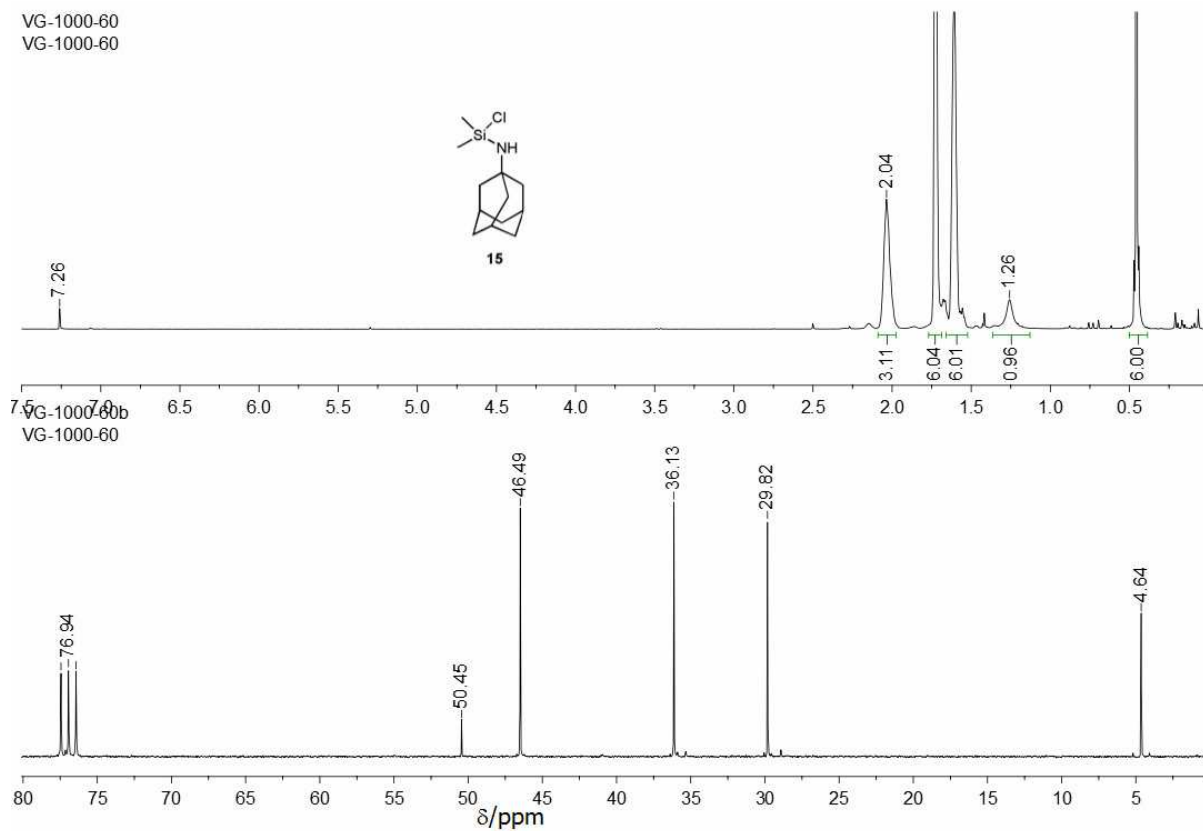


Figure 5.5. ^1H and ^{13}C NMR spectra of **15** in CDCl_3 at 298 K.

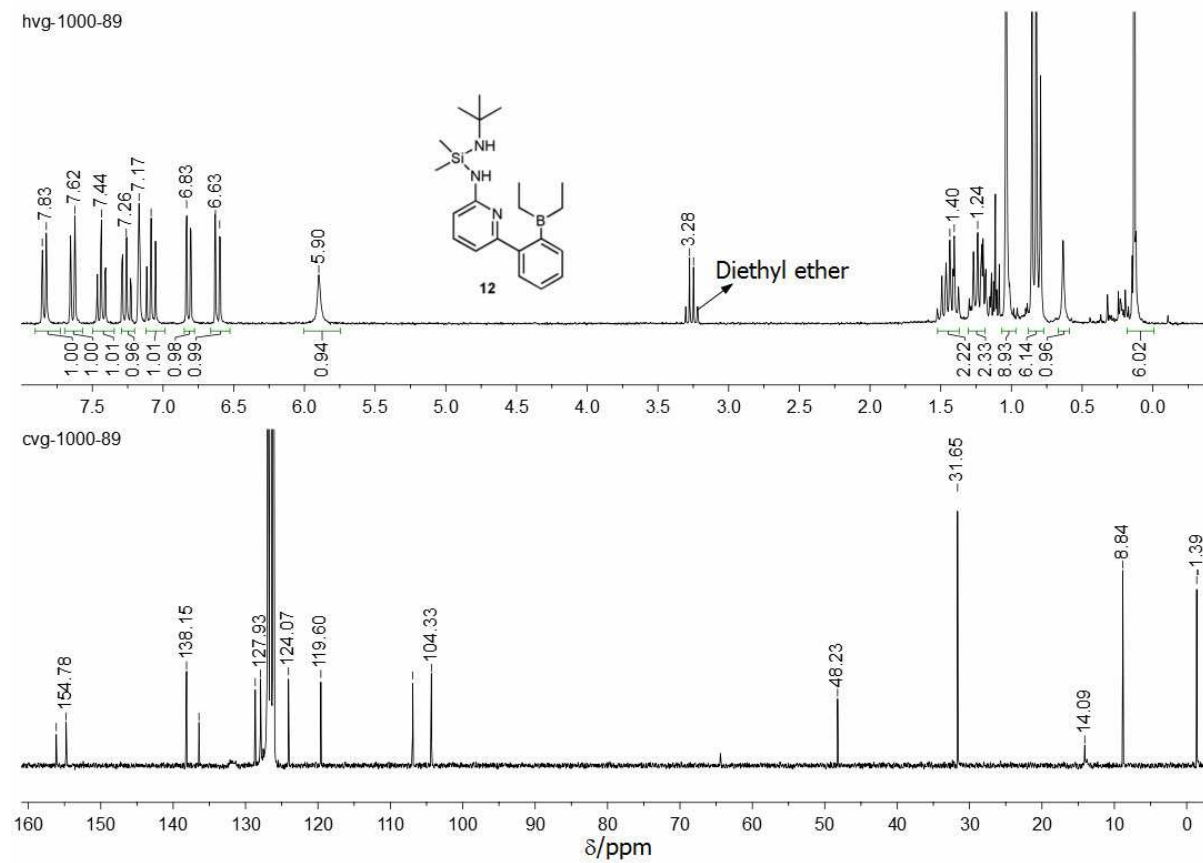


Figure 5.6. ^1H and ^{13}C NMR spectra of **12** in C_6D_6 at 298 K.

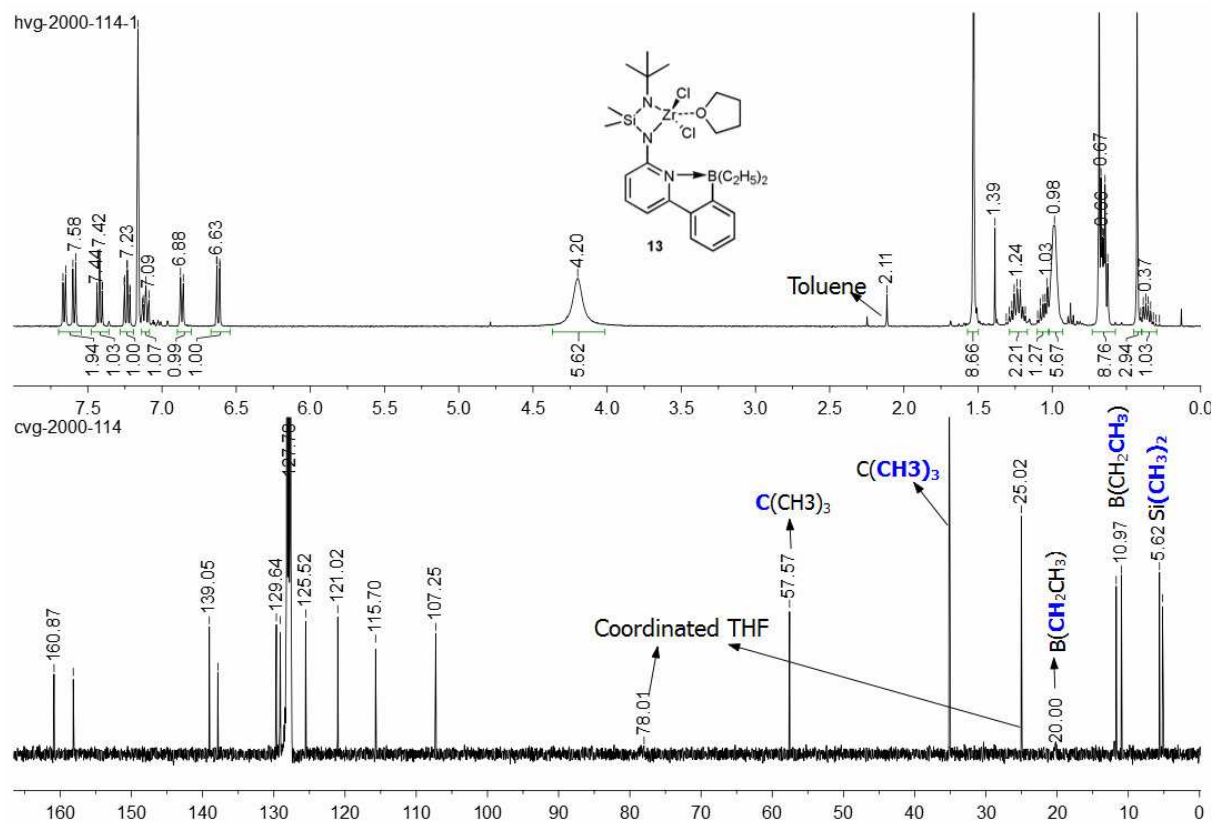


Figure 5.7. ^1H and ^{13}C NMR spectra of **13** in C_6D_6 at 298 K.

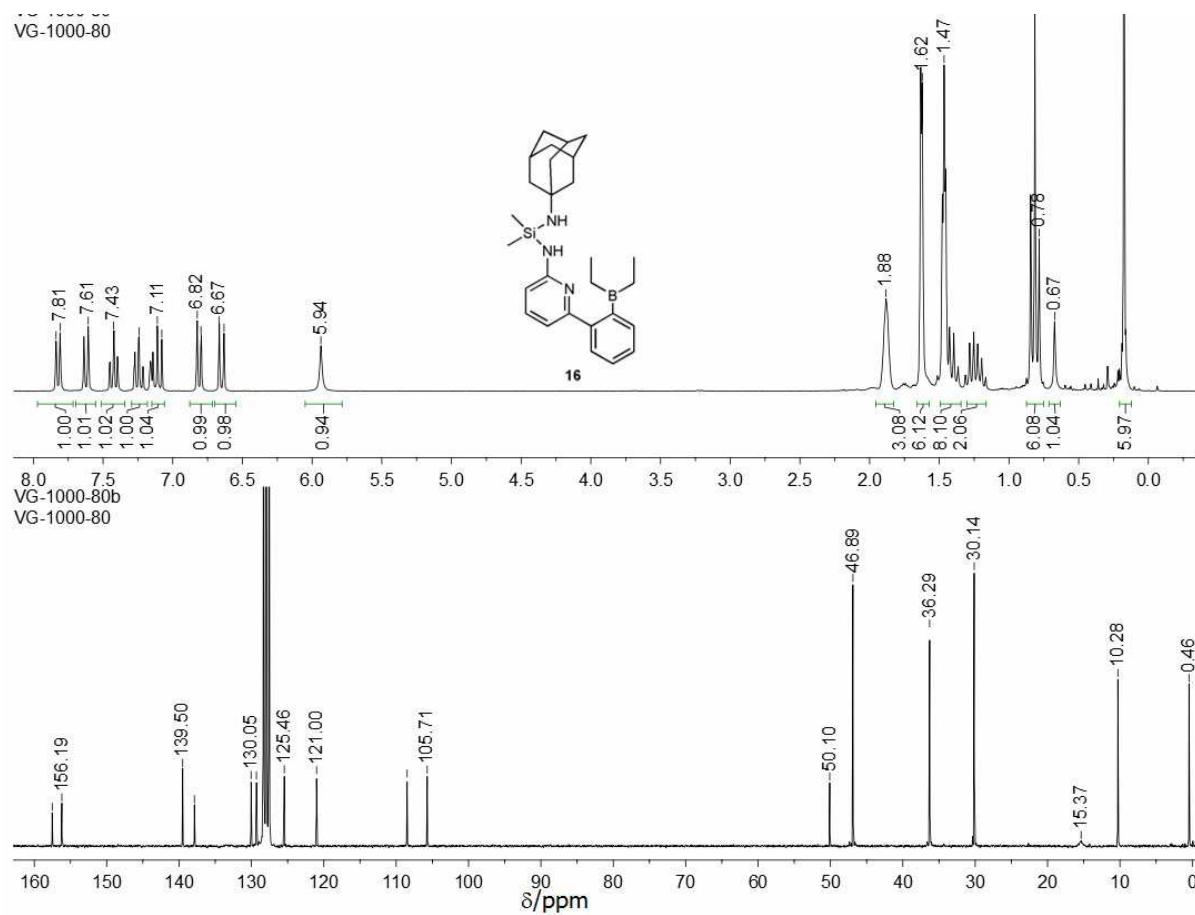


Figure 5.8. ^1H and ^{13}C NMR spectra of **16** in C_6D_6 at 298 K.

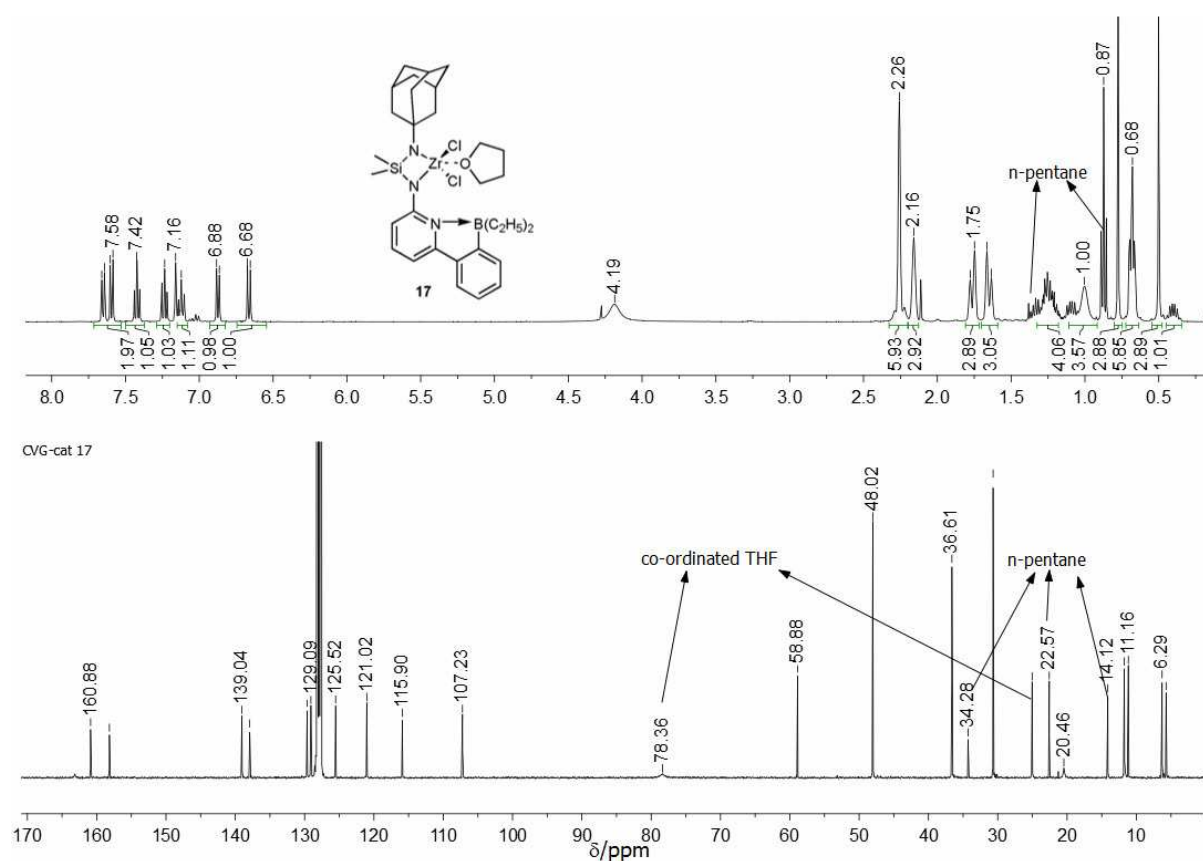


Figure 5.9. ^1H and ^{13}C NMR spectra of **17** in C_6D_6 at 298 K.

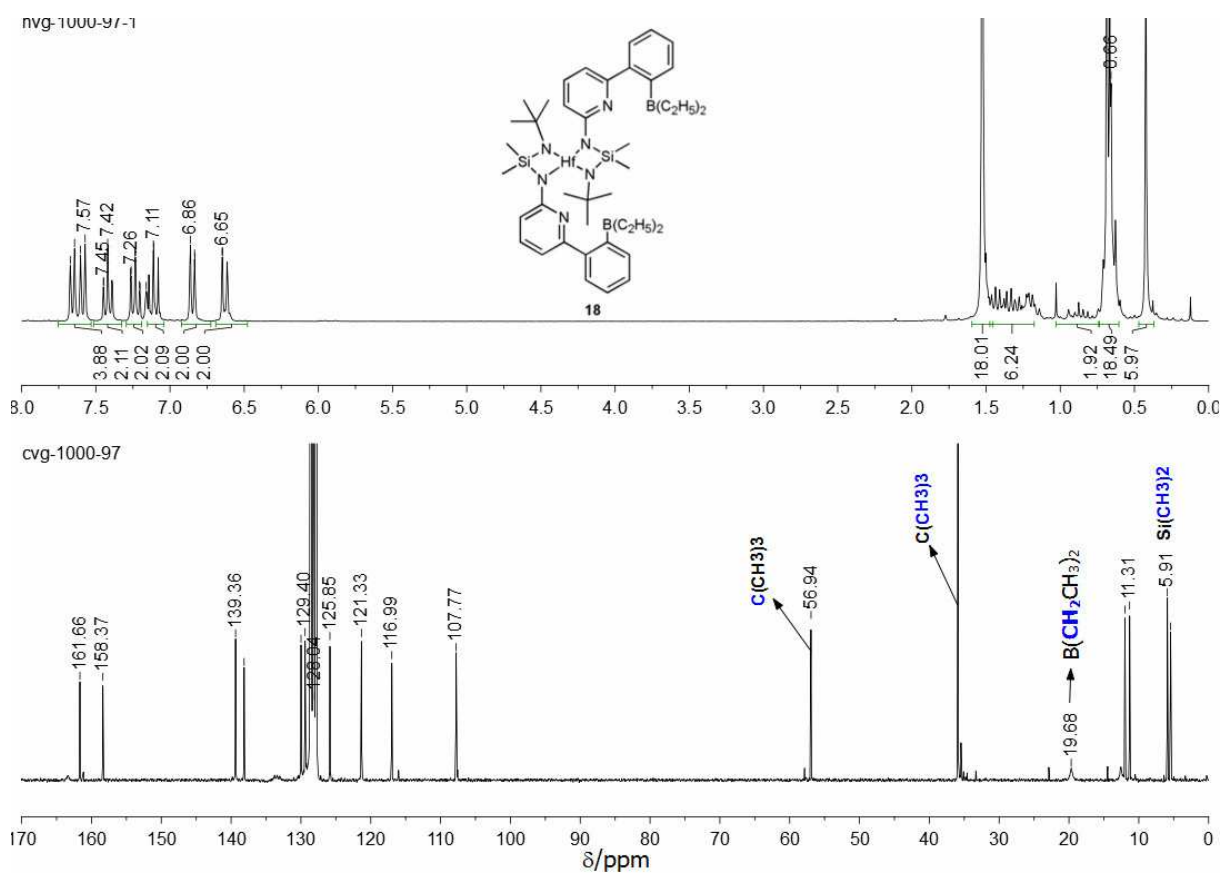


Figure 5.10. ^1H and ^{13}C NMR spectra of **18** in C_6D_6 at 298 K.

Appendix

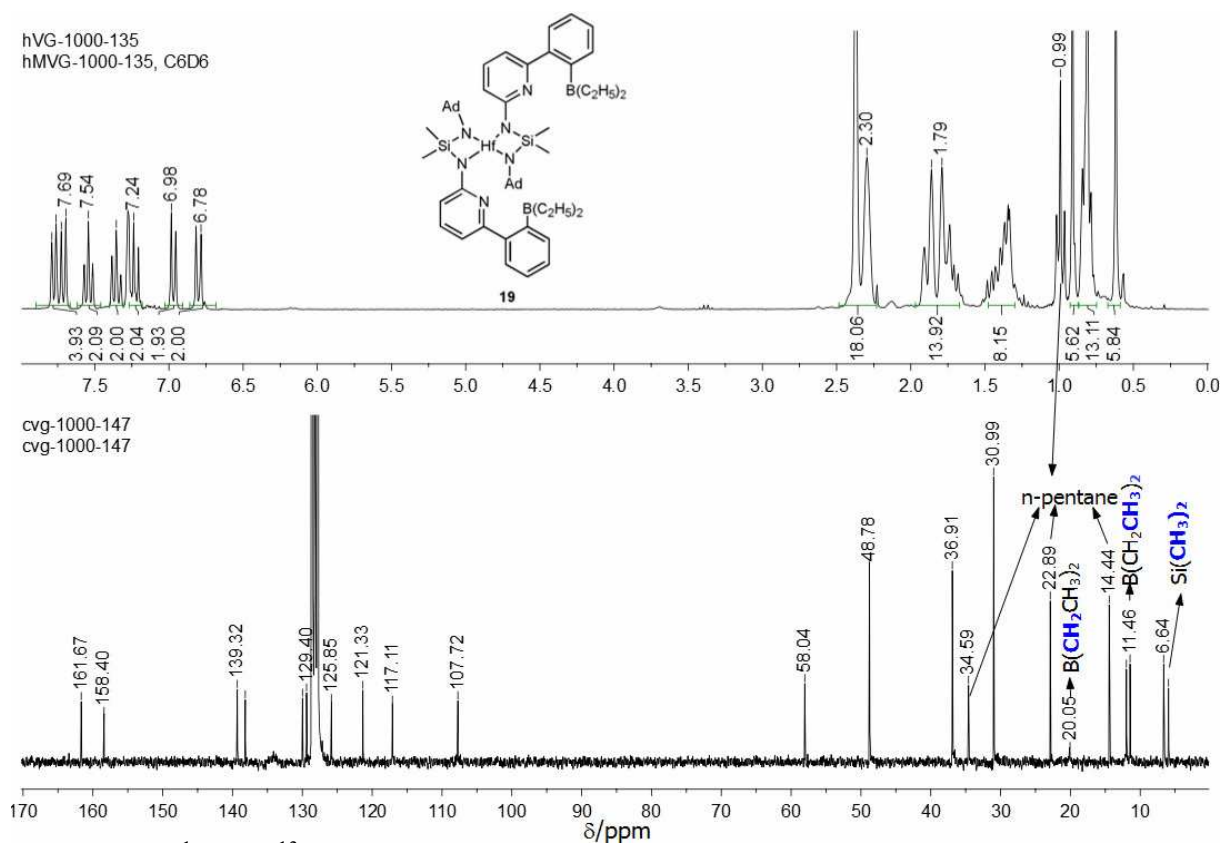


Figure 5.11. ^1H and ^{13}C NMR spectra of **19** in C_6D_6 at 298 K.

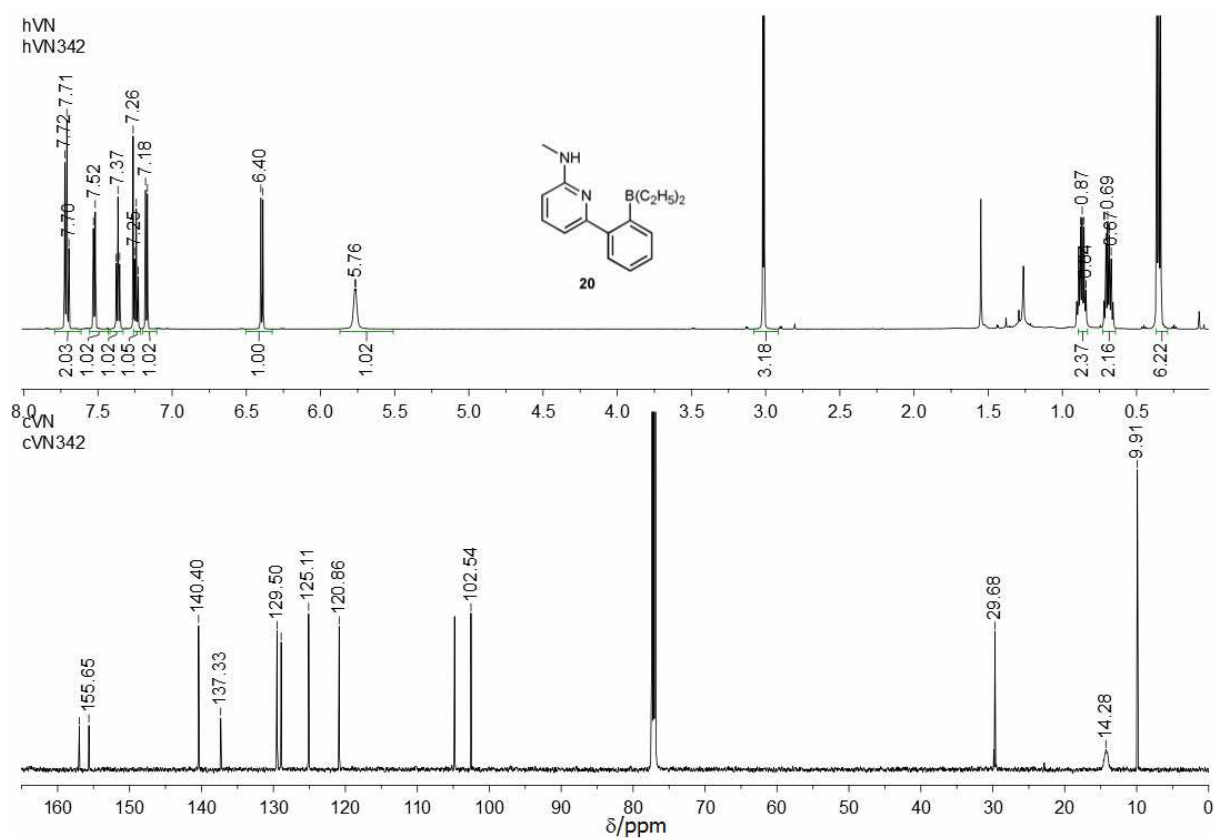


Figure 5.12. ^1H and ^{13}C NMR spectra of **20** in CDCl_3 at 298 K.

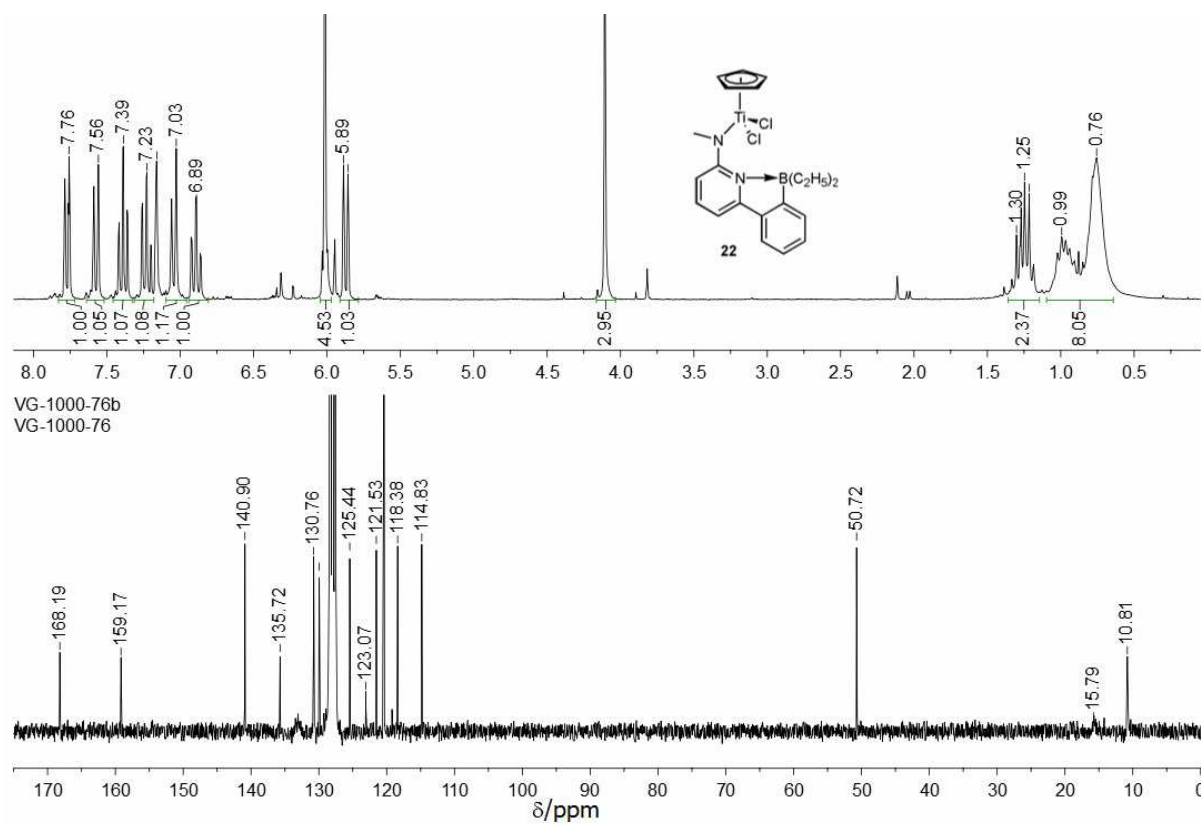


Figure 5.13. ^1H and ^{13}C NMR spectra of **22** in C_6D_6 at 298 K.

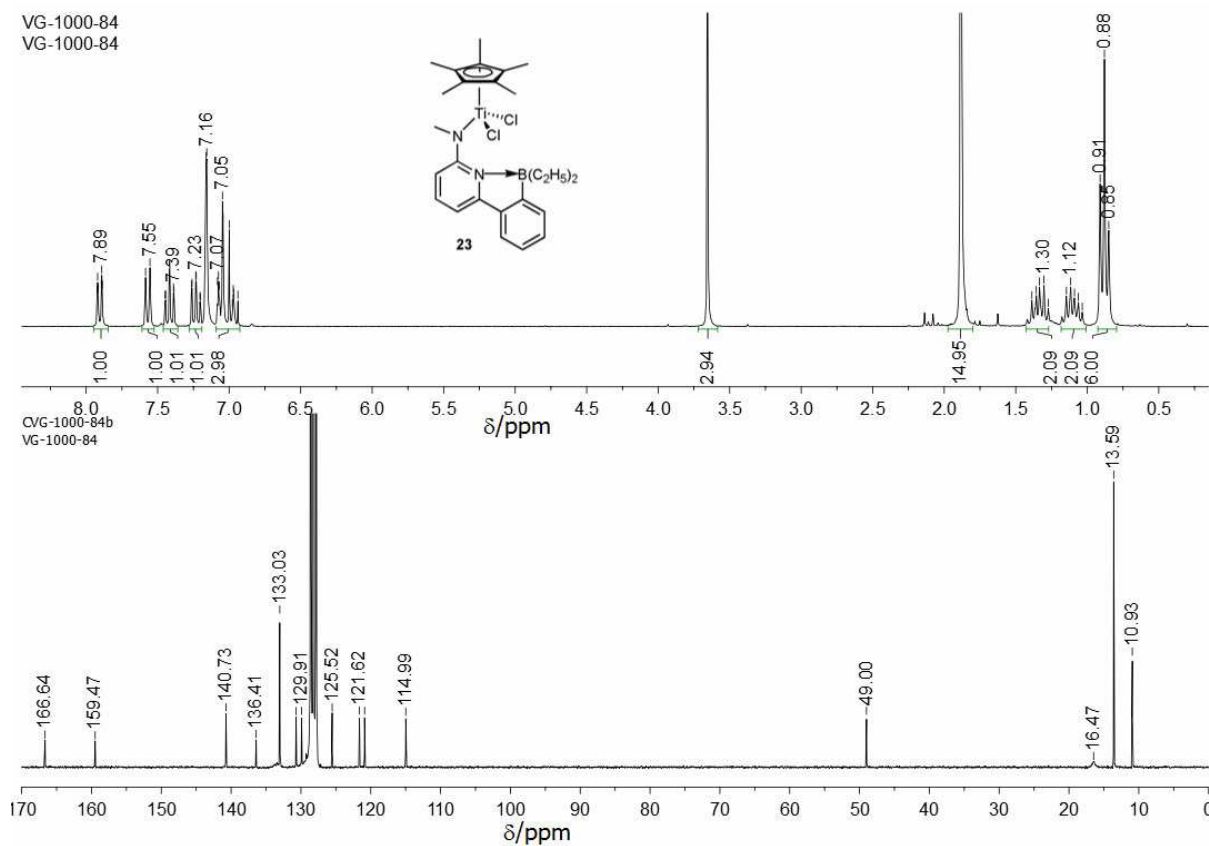


Figure 5.14. ^1H and ^{13}C NMR spectra of **23** in C_6D_6 at 298 K.

Appendix

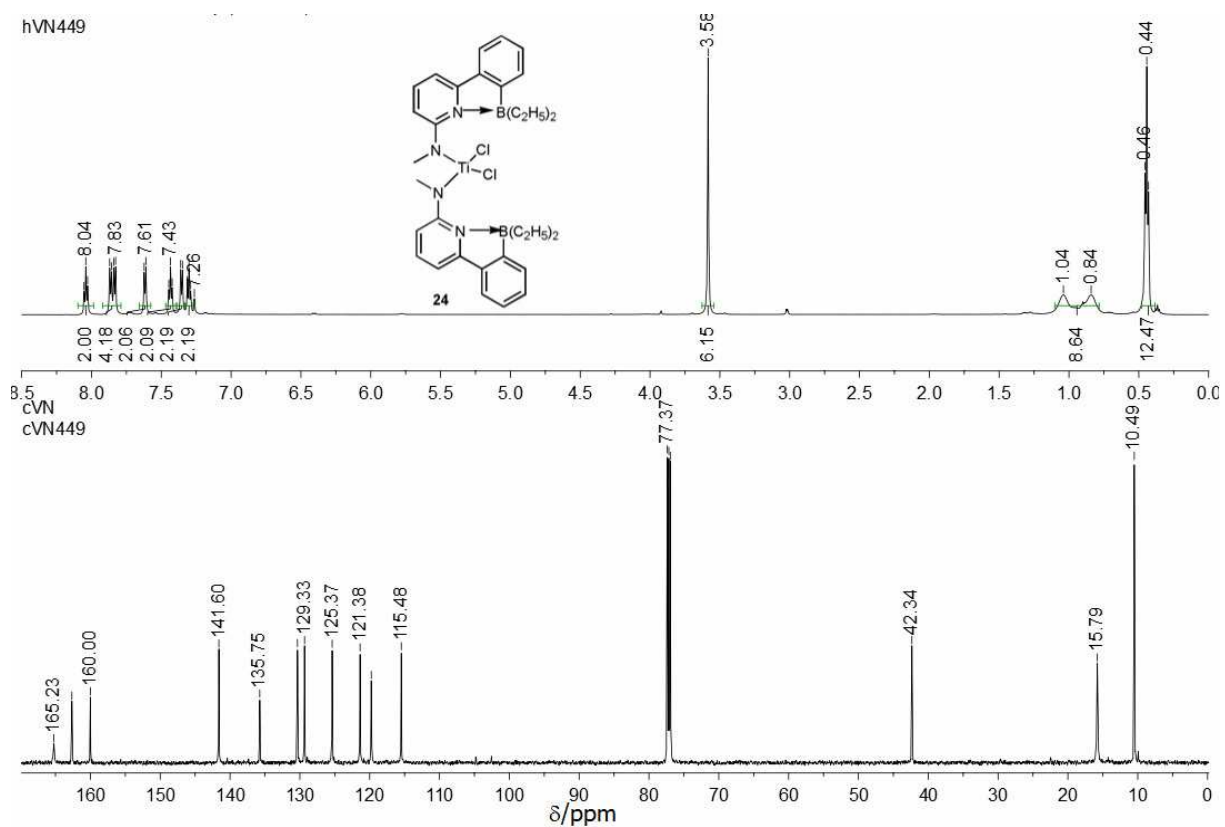


Figure 5.15. ^1H and ^{13}C NMR spectra of **24** in CDCl_3 at 298 K.

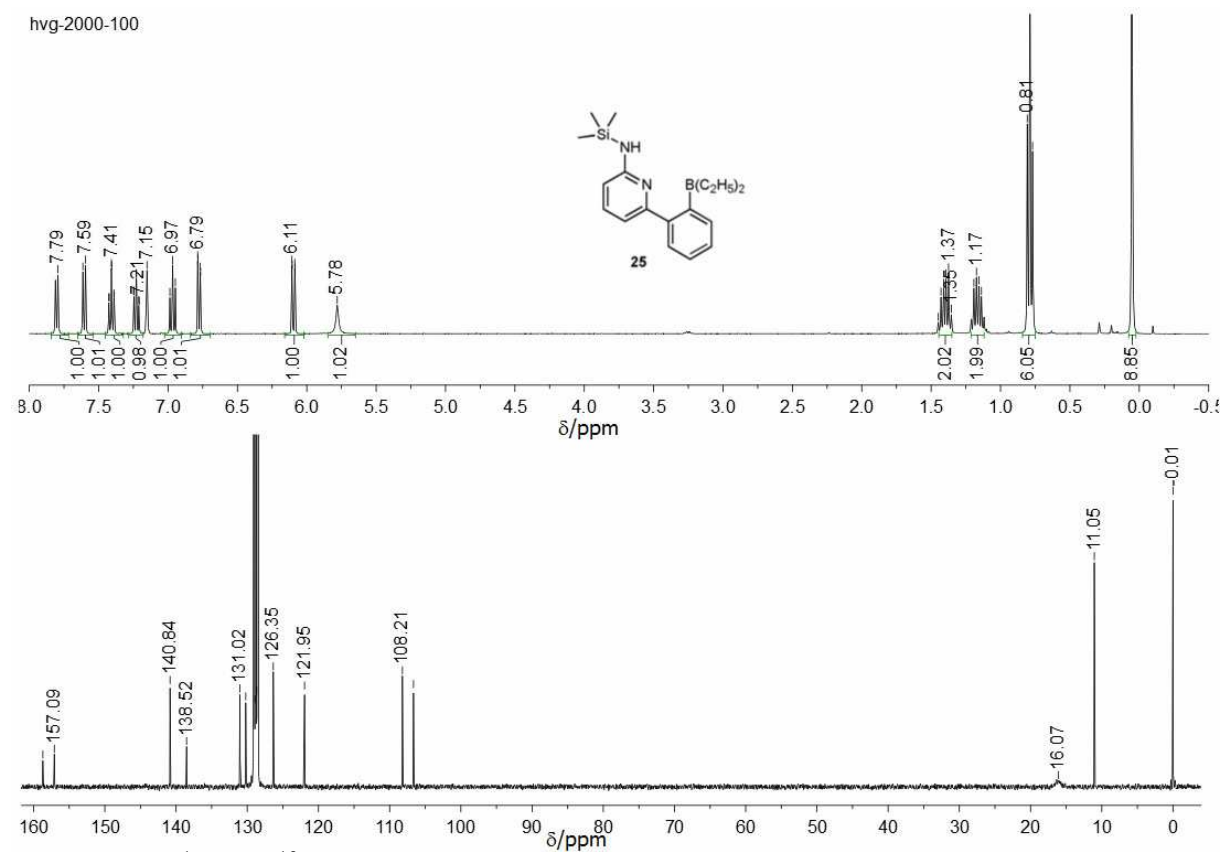


Figure 5.16. ^1H and ^{13}C NMR spectra of **25** in C_6D_6 at 298 K.

Appendix

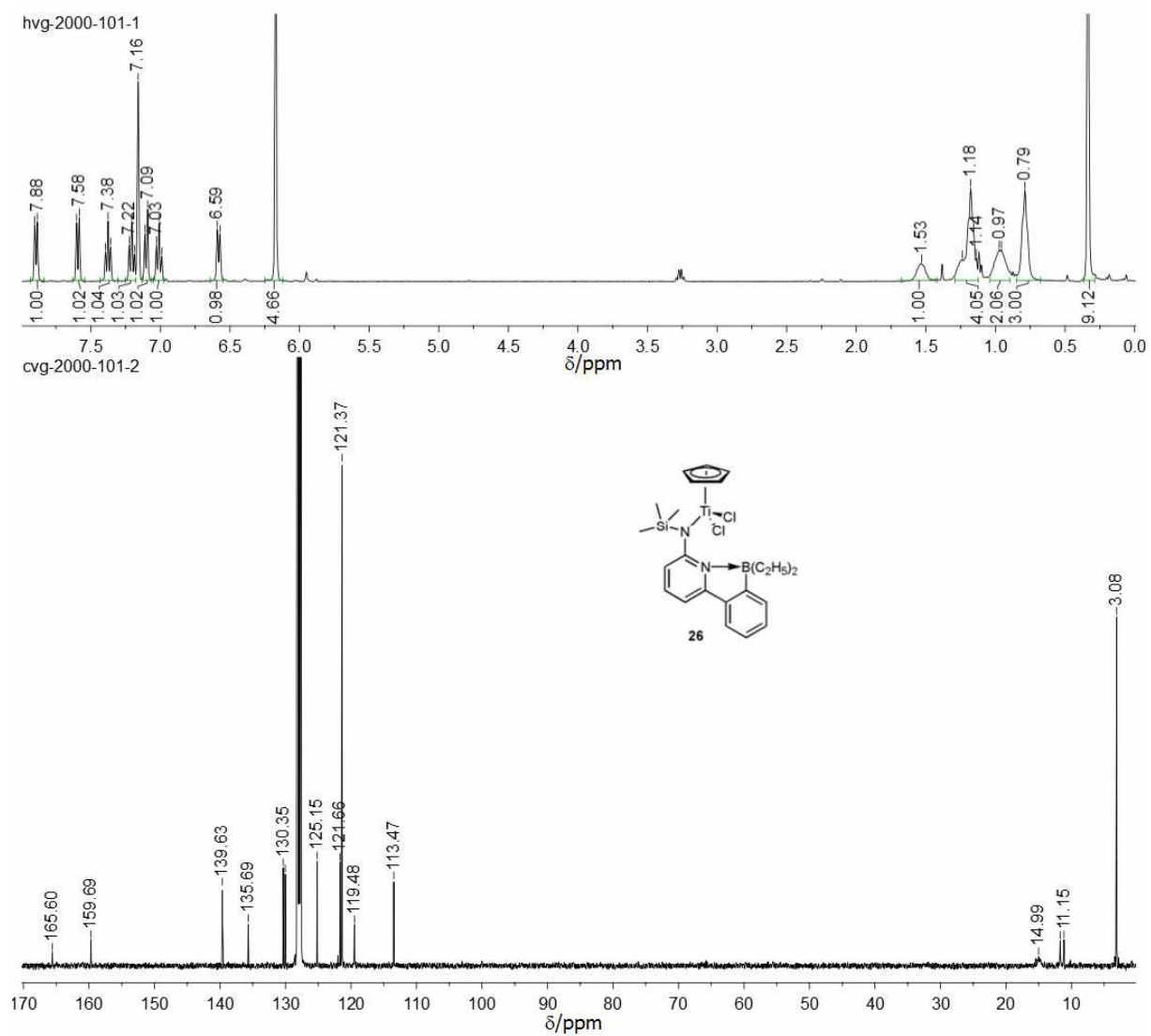


Figure 5.17. ^1H and ^{13}C NMR spectra of **26** in C_6D_6 at 298 K.

Appendix

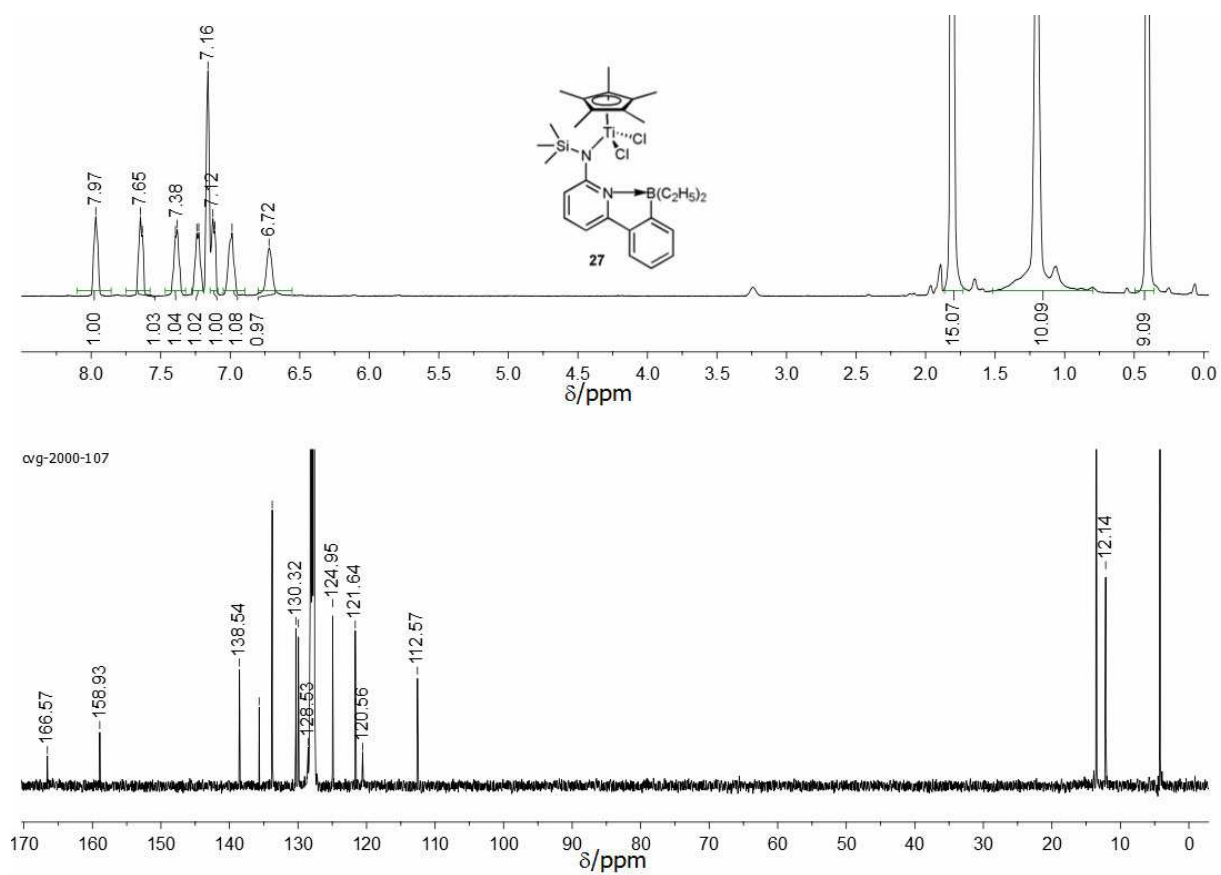


Figure 5.18. ^1H and ^{13}C NMR spectra of **27** in C_6D_6 at 298 K.

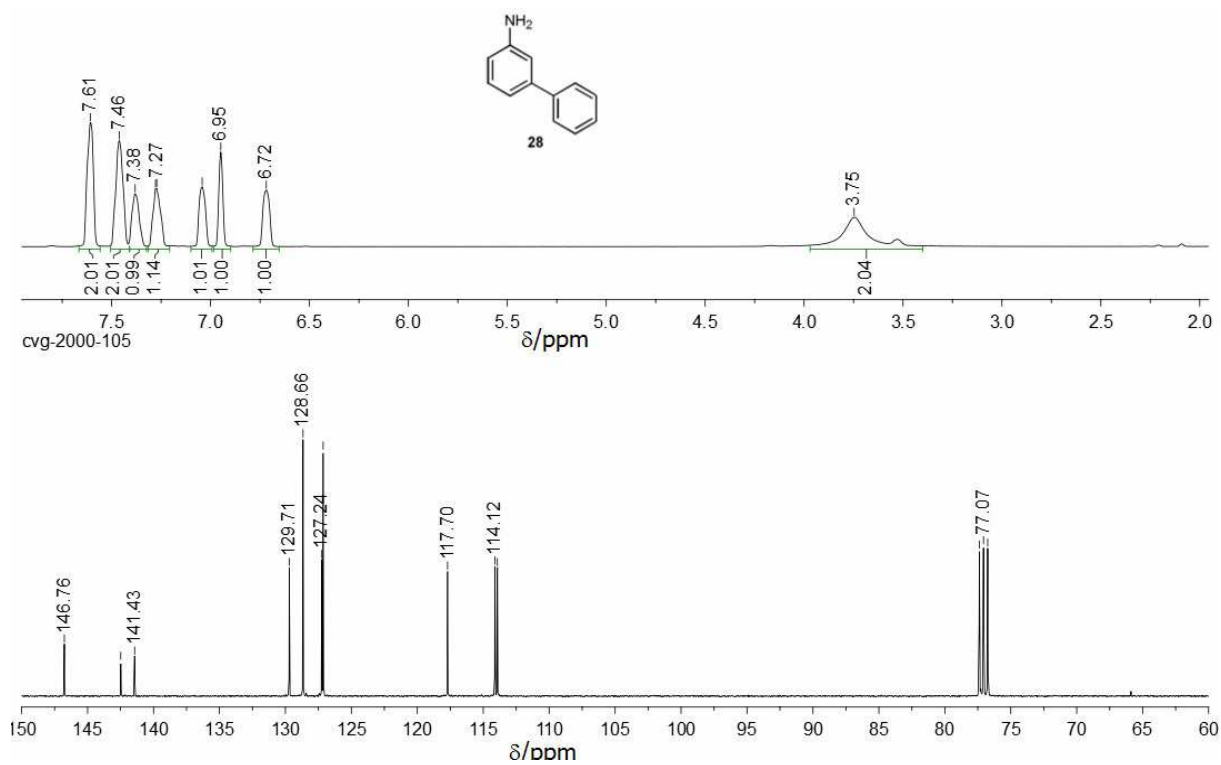


Figure 5.19. ^1H and ^{13}C NMR spectra of **28** in CDCl_3 at 298 K.

Appendix

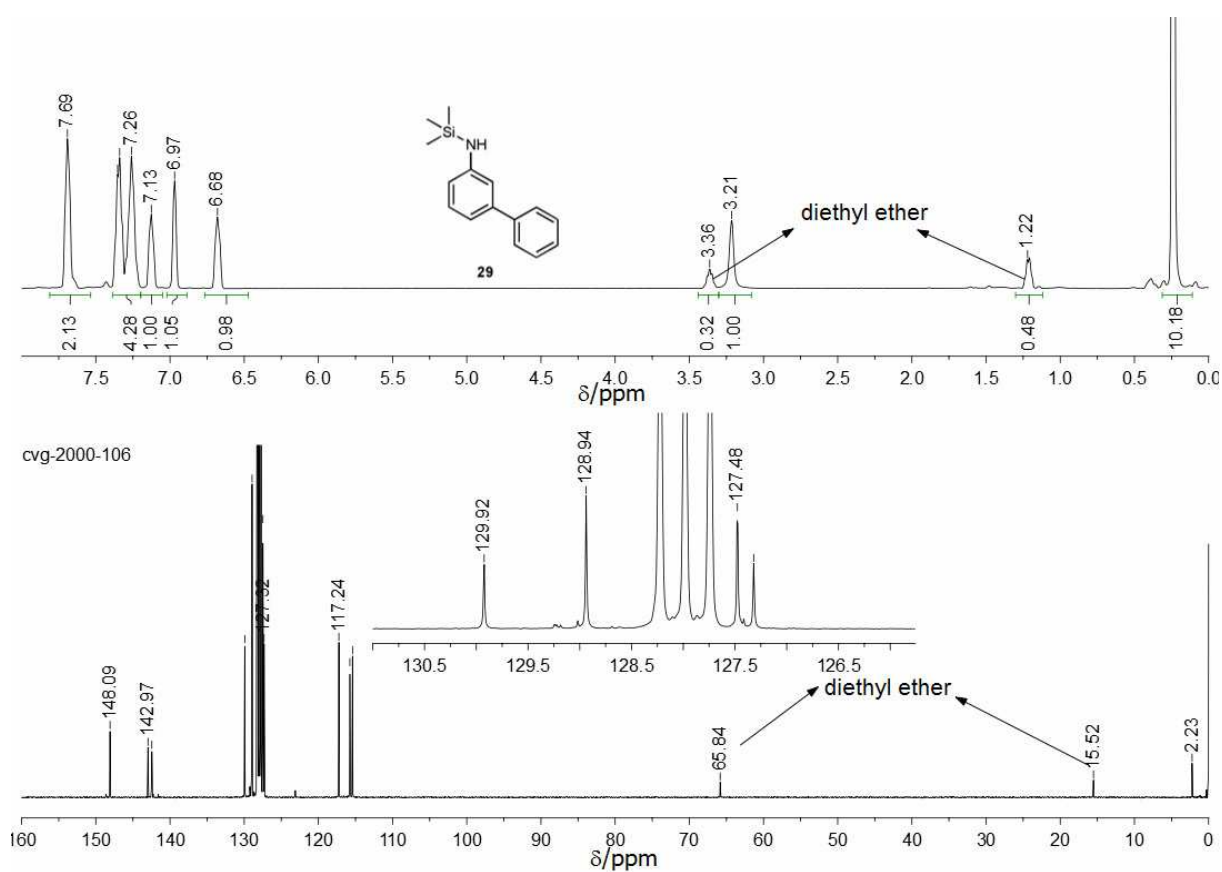


Figure 5.20. ^1H and ^{13}C NMR spectra of **29** in C_6D_6 at 298 K.

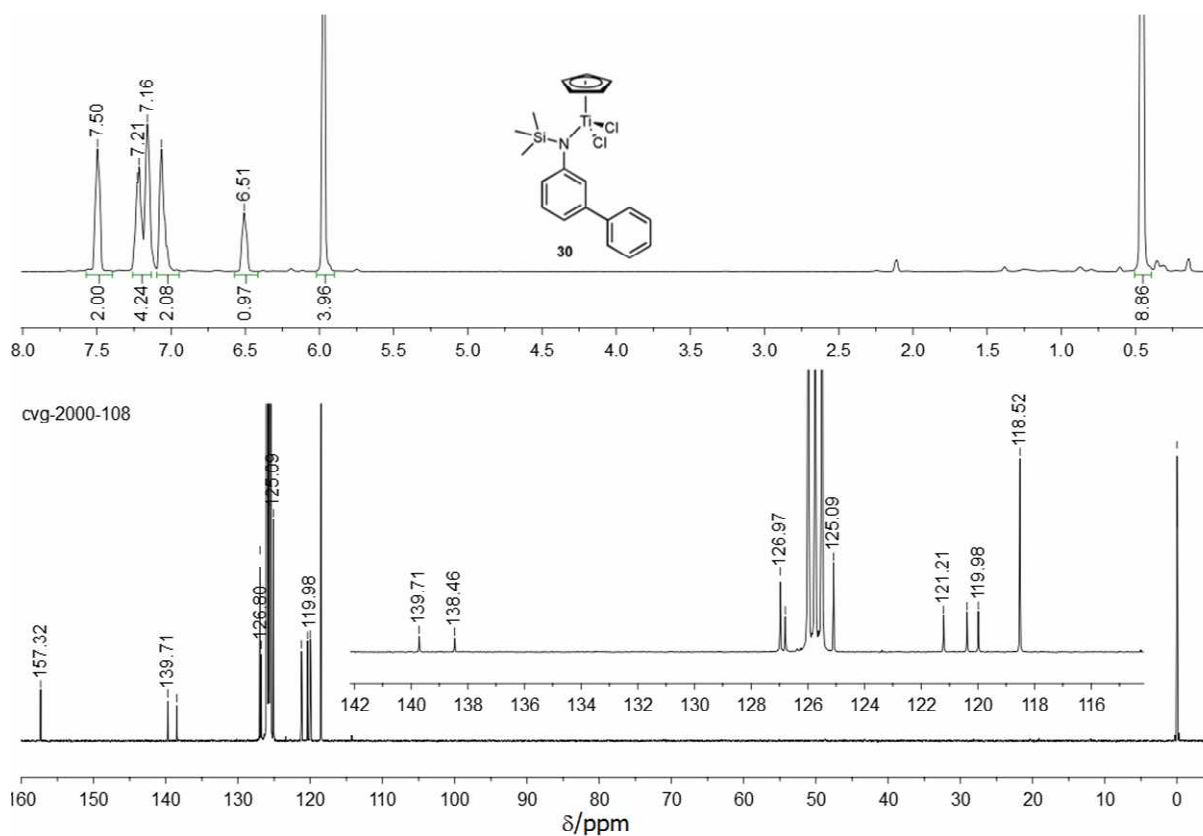


Figure 5.21. ^1H and ^{13}C NMR spectra of **30** in C_6D_6 at 298 K.

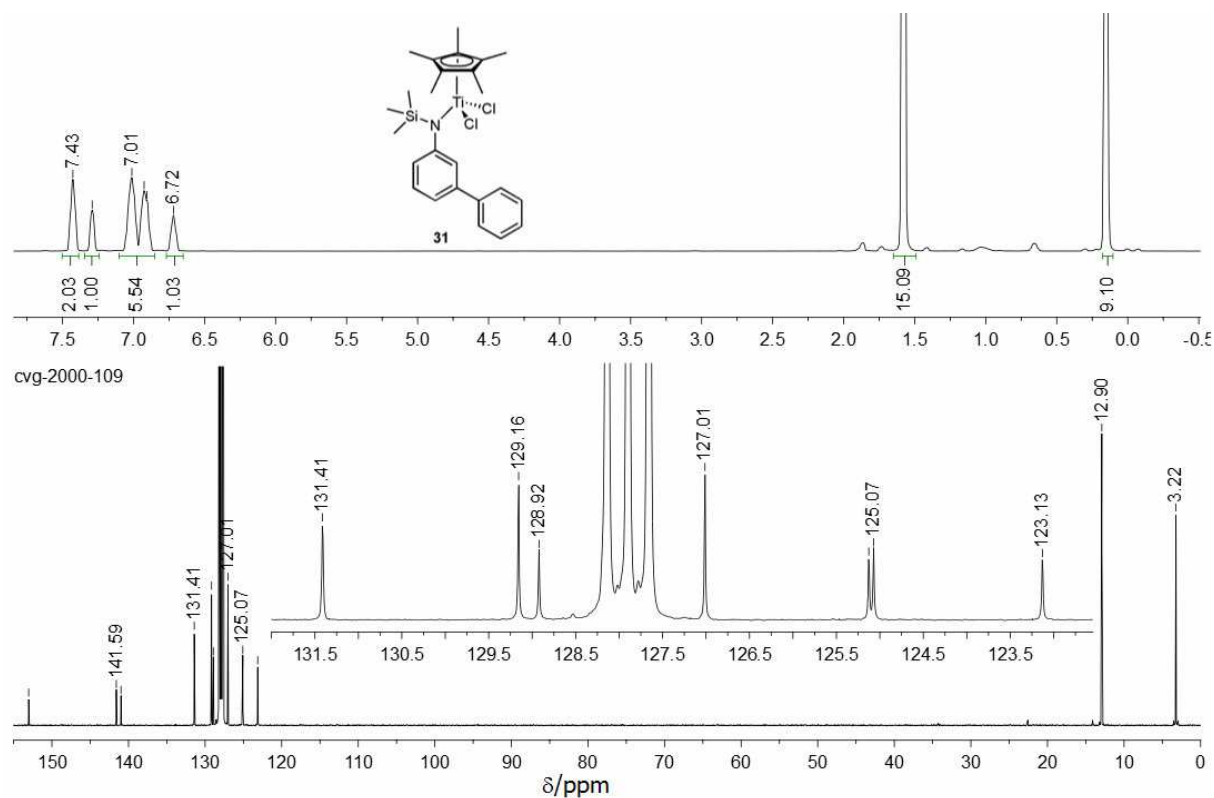


Figure 5.22. ^1H and ^{13}C NMR spectra of **31** in C_6D_6 at 298 K.

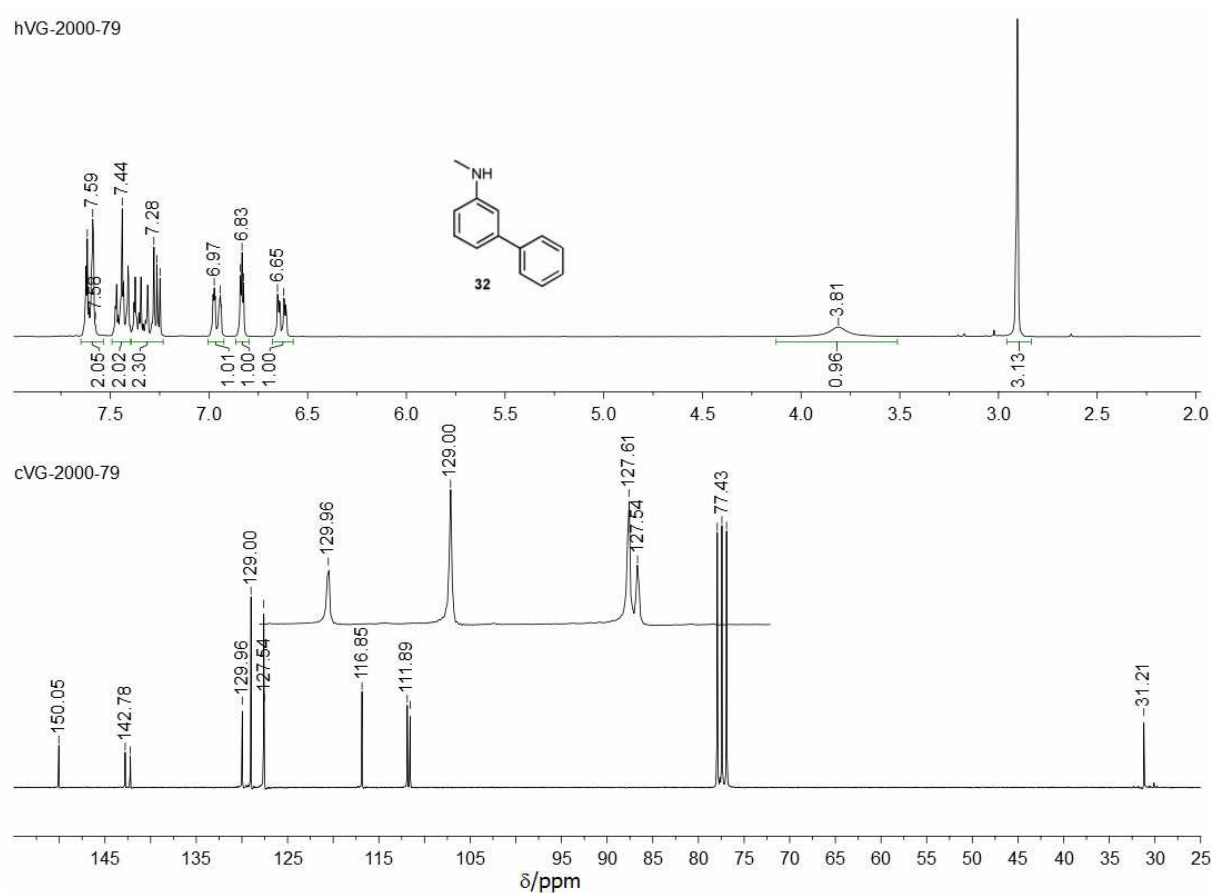


Figure 5.23. ^1H and ^{13}C NMR spectra of **32** in CDCl_3 at 298 K.

Appendix

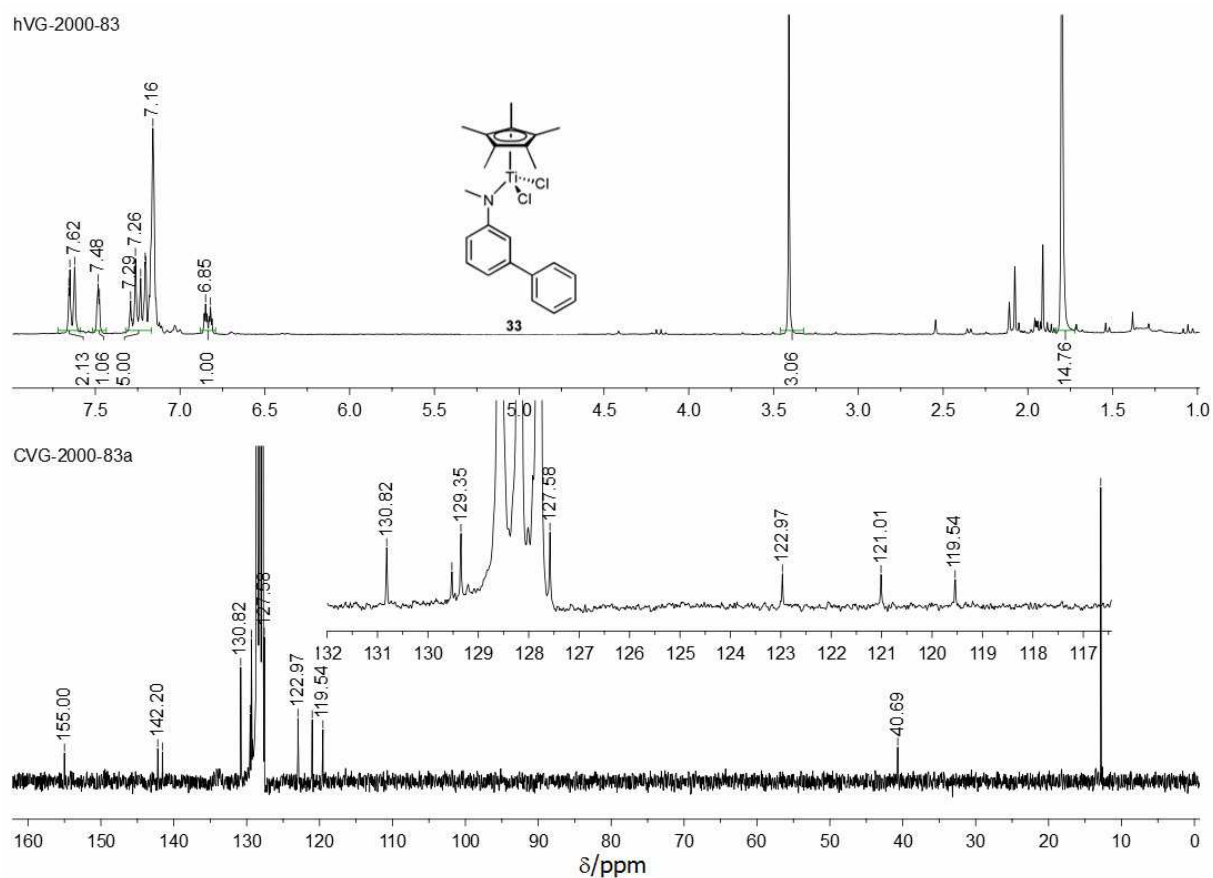


Figure 5.24. ^1H and ^{13}C NMR spectra of **33** in C_6D_6 at 298 K.

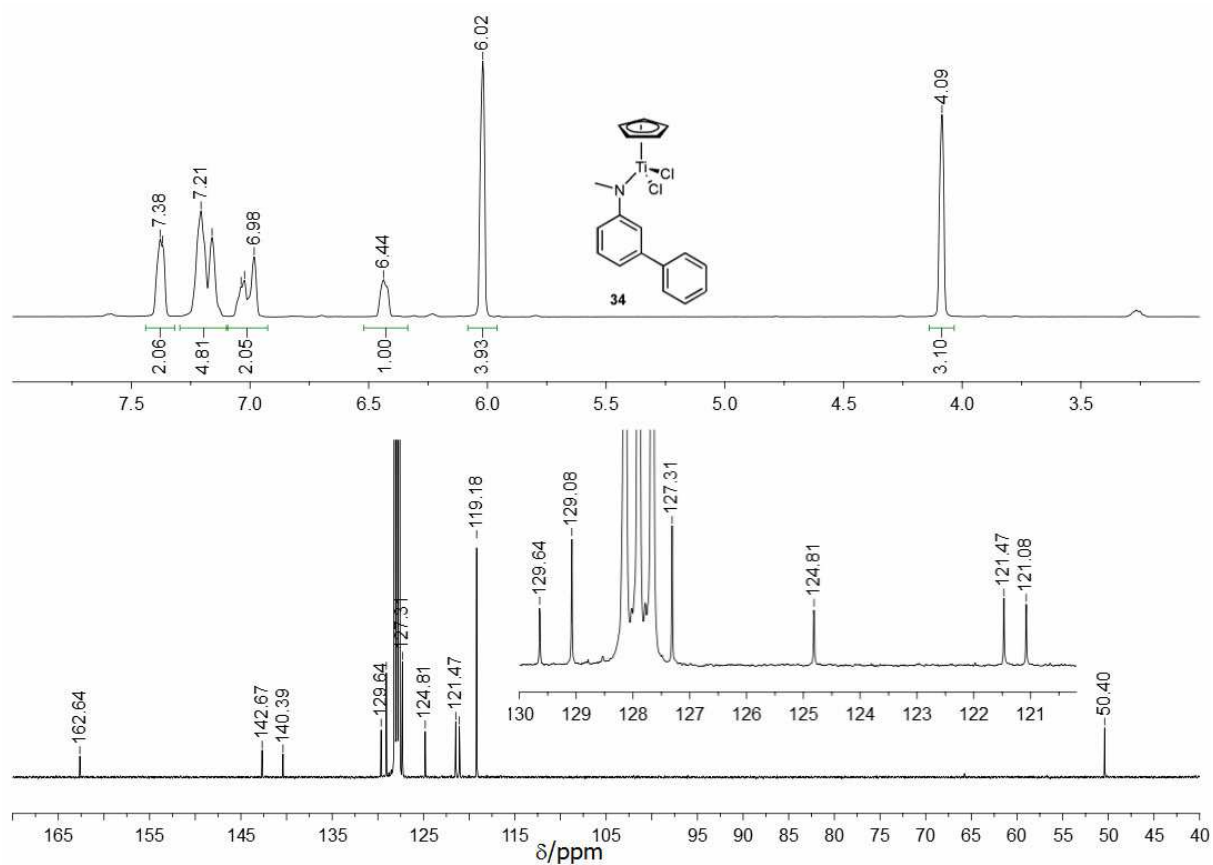


Figure 5.25. ^1H and ^{13}C NMR spectra of **34** in C_6D_6 at 298 K.

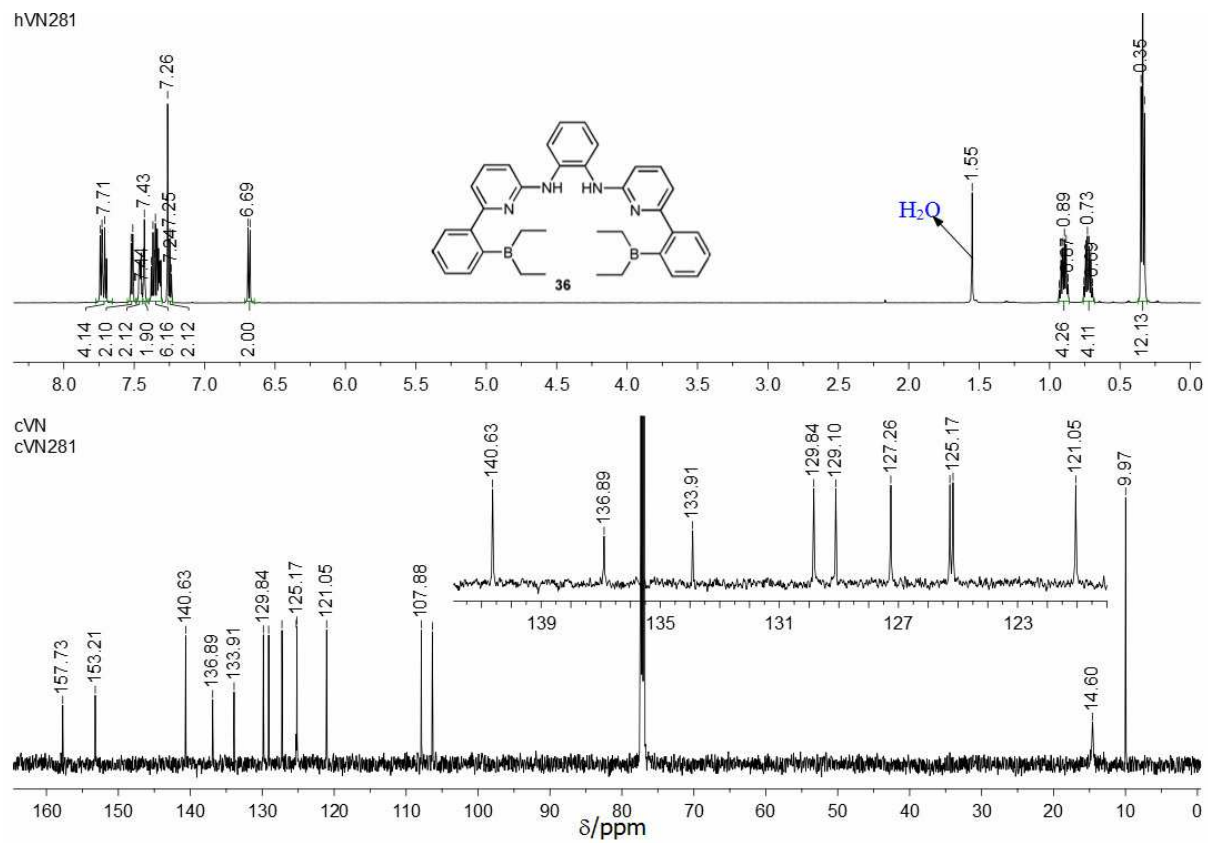


Figure 5.26. ^1H and ^{13}C NMR spectra of **36** in CDCl_3 at 298 K.

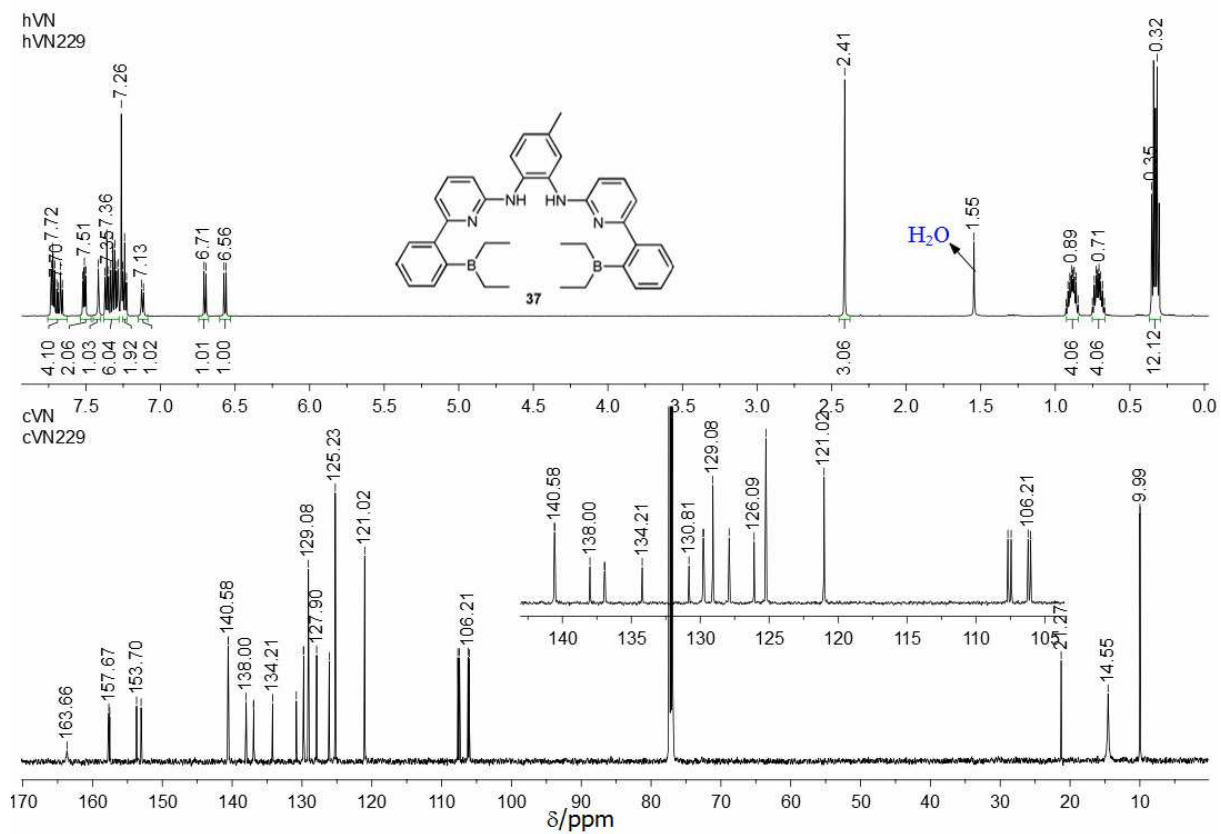


Figure 5.27. ^1H and ^{13}C NMR spectra of **37** in CDCl_3 at 298 K.

Appendix

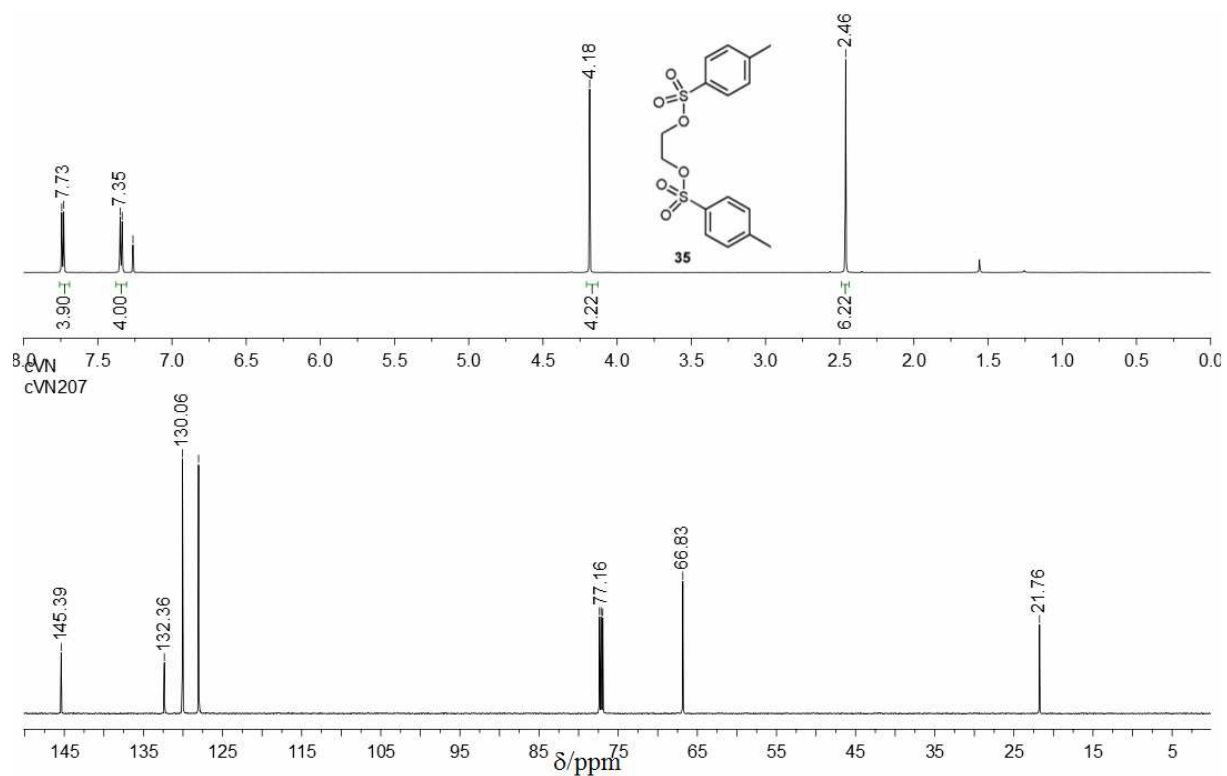


Figure 5.28. ^1H and ^{13}C NMR spectra of **35** in CDCl_3 at 298 K.

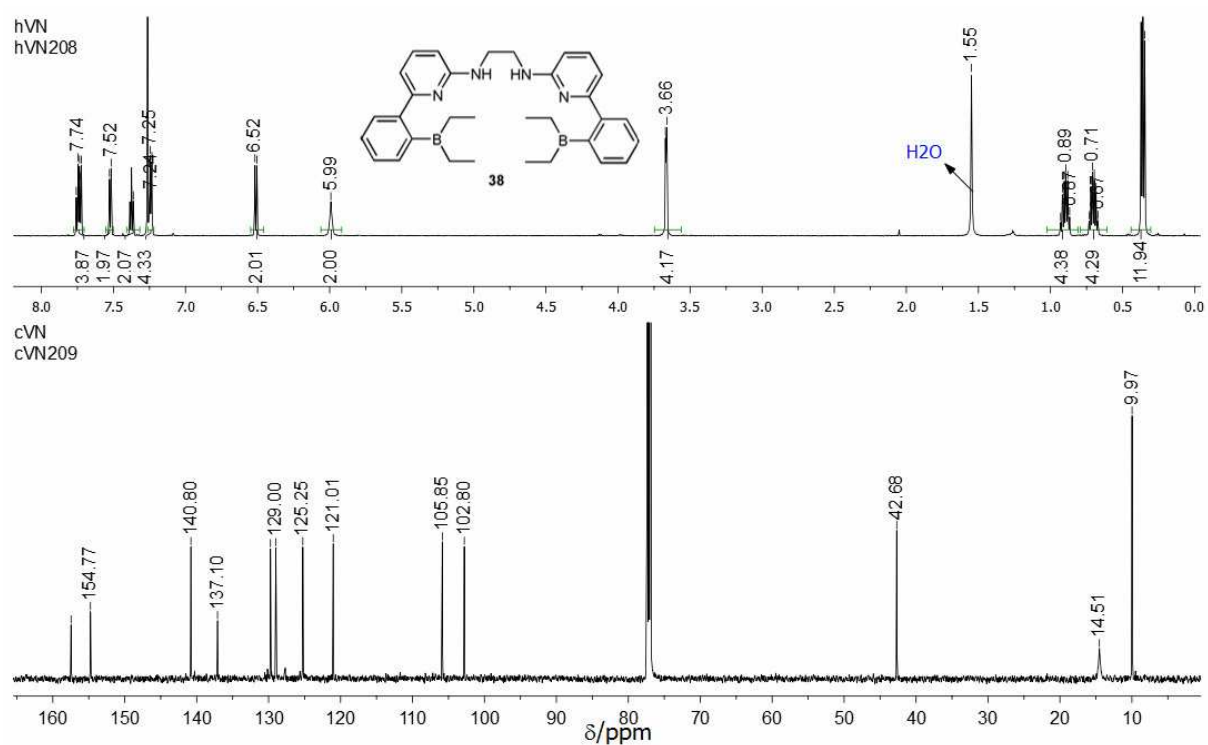


Figure 5.29. ^1H and ^{13}C NMR spectra of **38** in CDCl_3 at 298 K.

Appendix

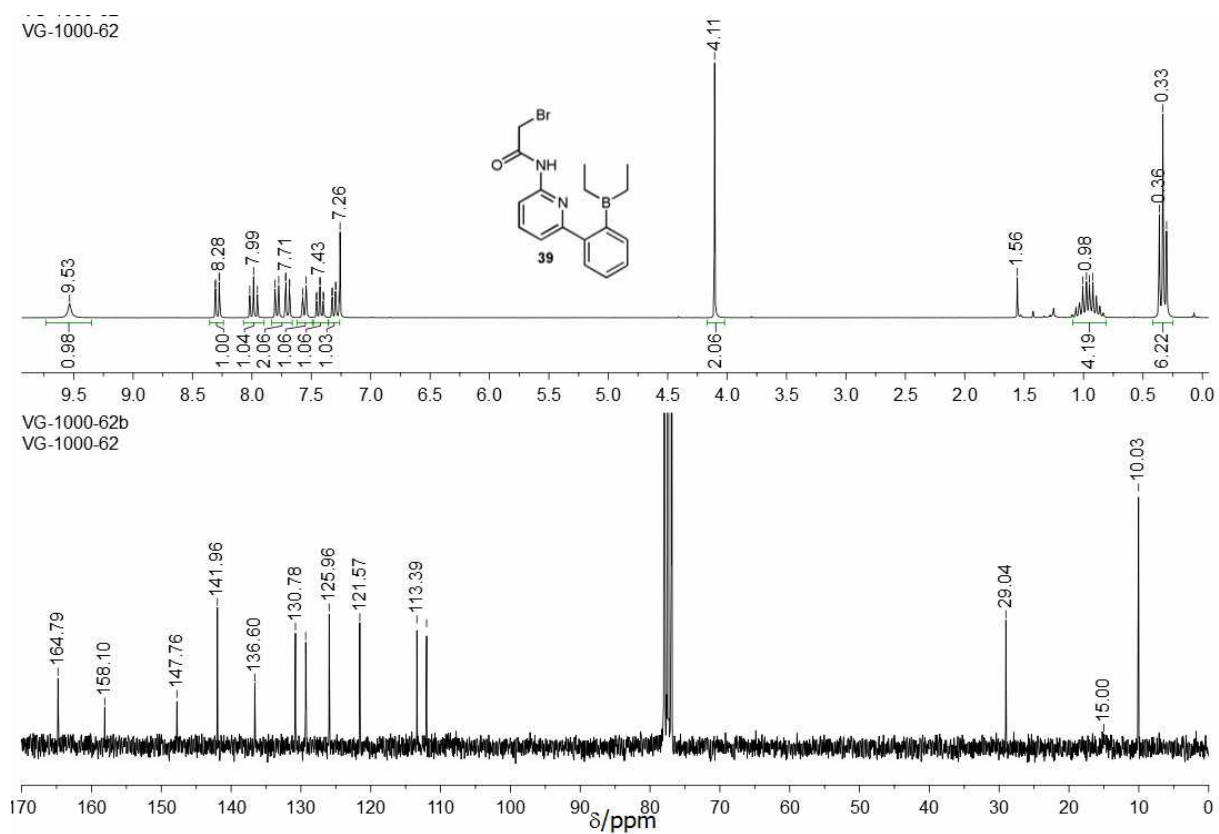


Figure 5.30. ^1H and ^{13}C NMR spectra of **39** in CDCl_3 at 298 K.

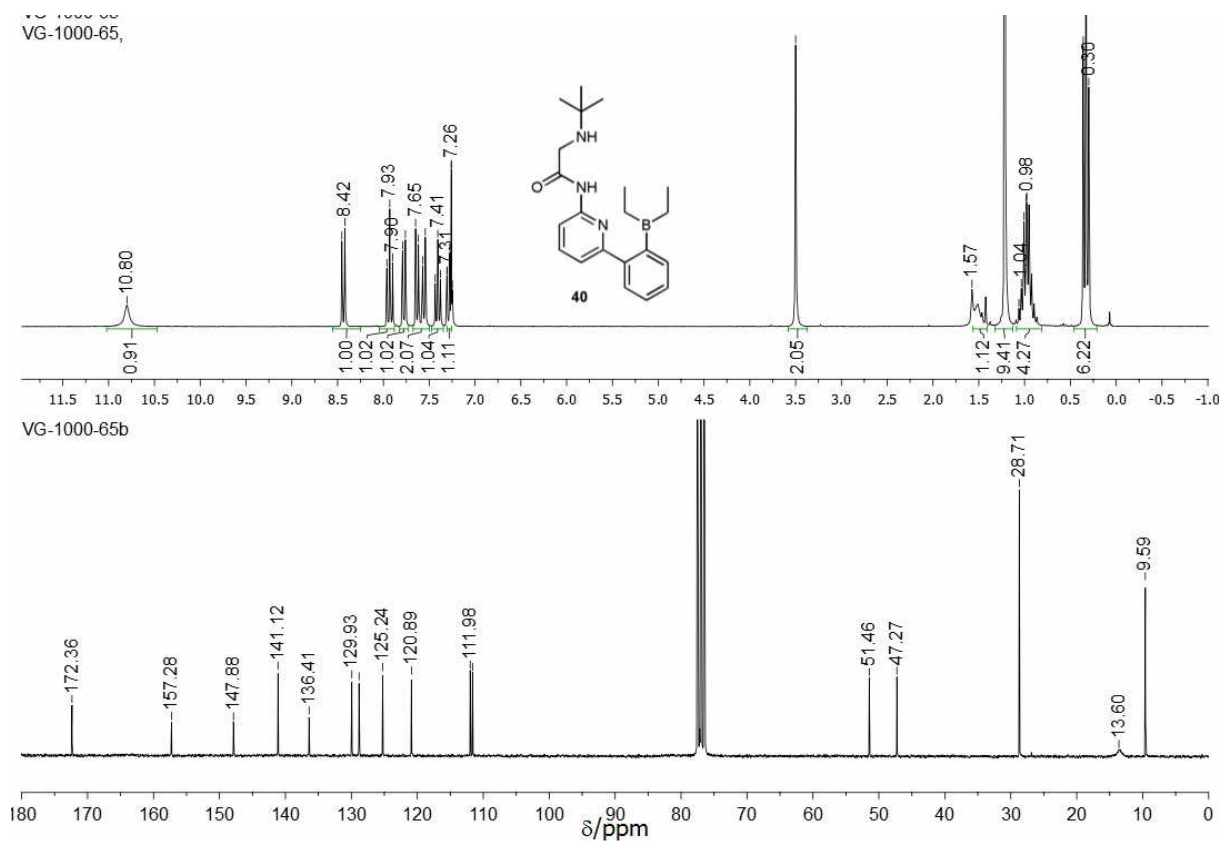


Figure 5.31. ^1H and ^{13}C NMR spectra of **40** in CDCl_3 at 298 K.

Appendix

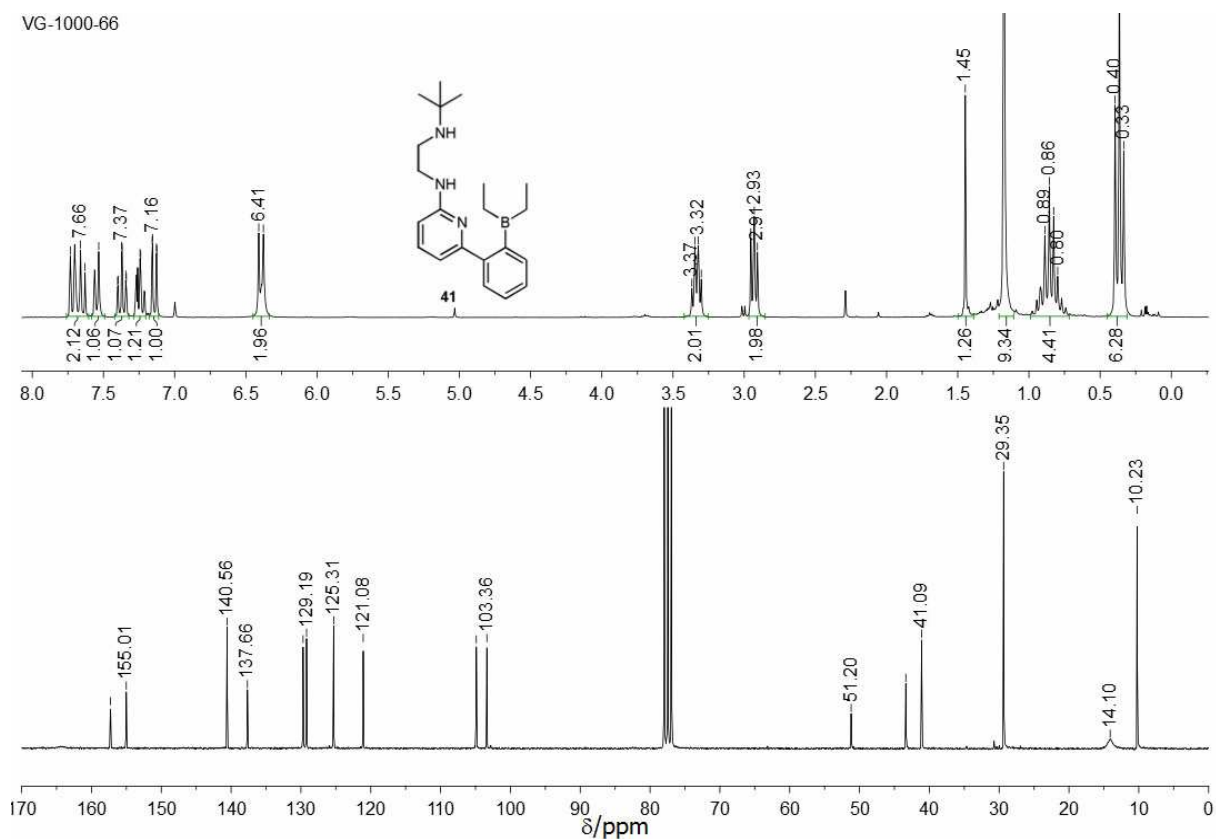


Figure 5.32. ^1H and ^{13}C NMR spectra of **41** in CDCl_3 at 298 K.

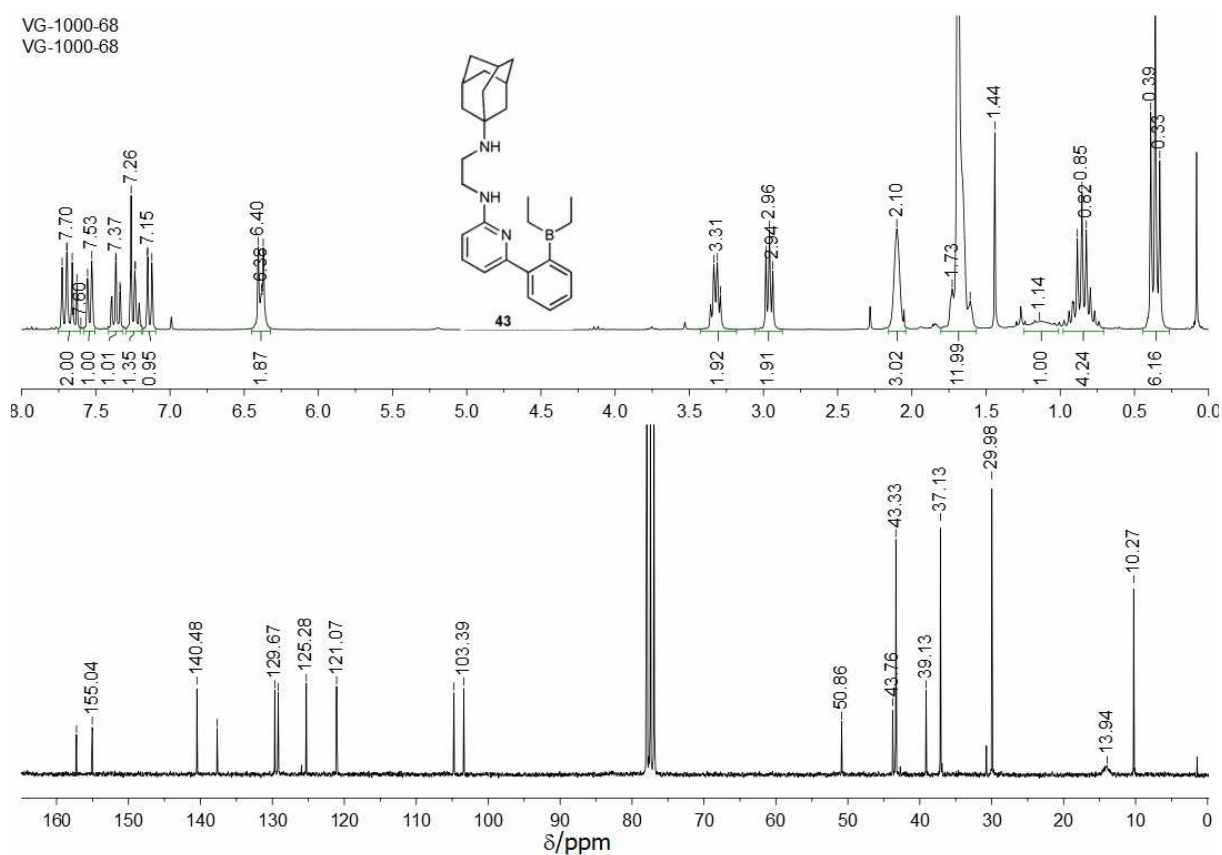


Figure 5.33. ^1H and ^{13}C NMR spectra of **43** in CDCl_3 at 298 K.

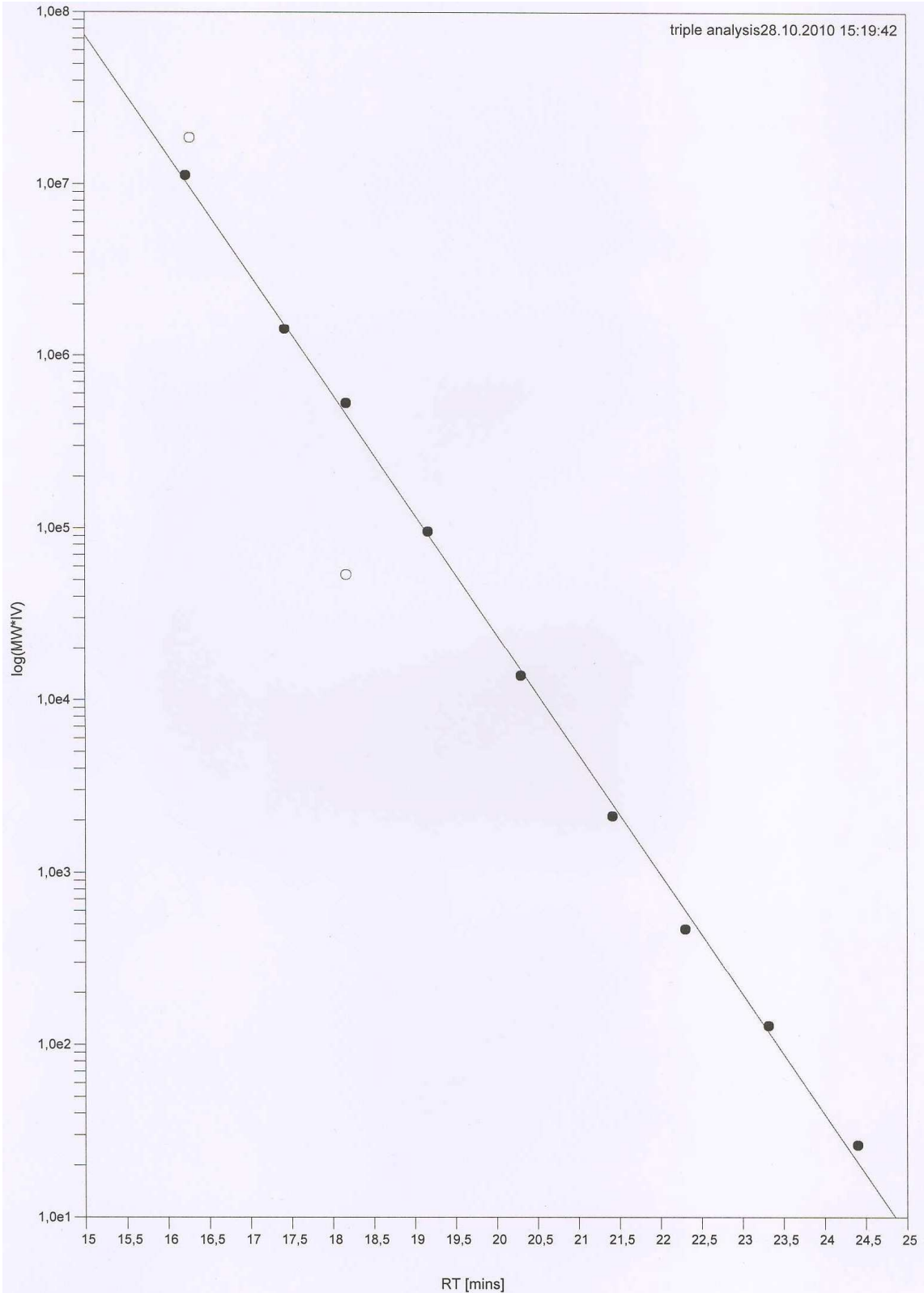


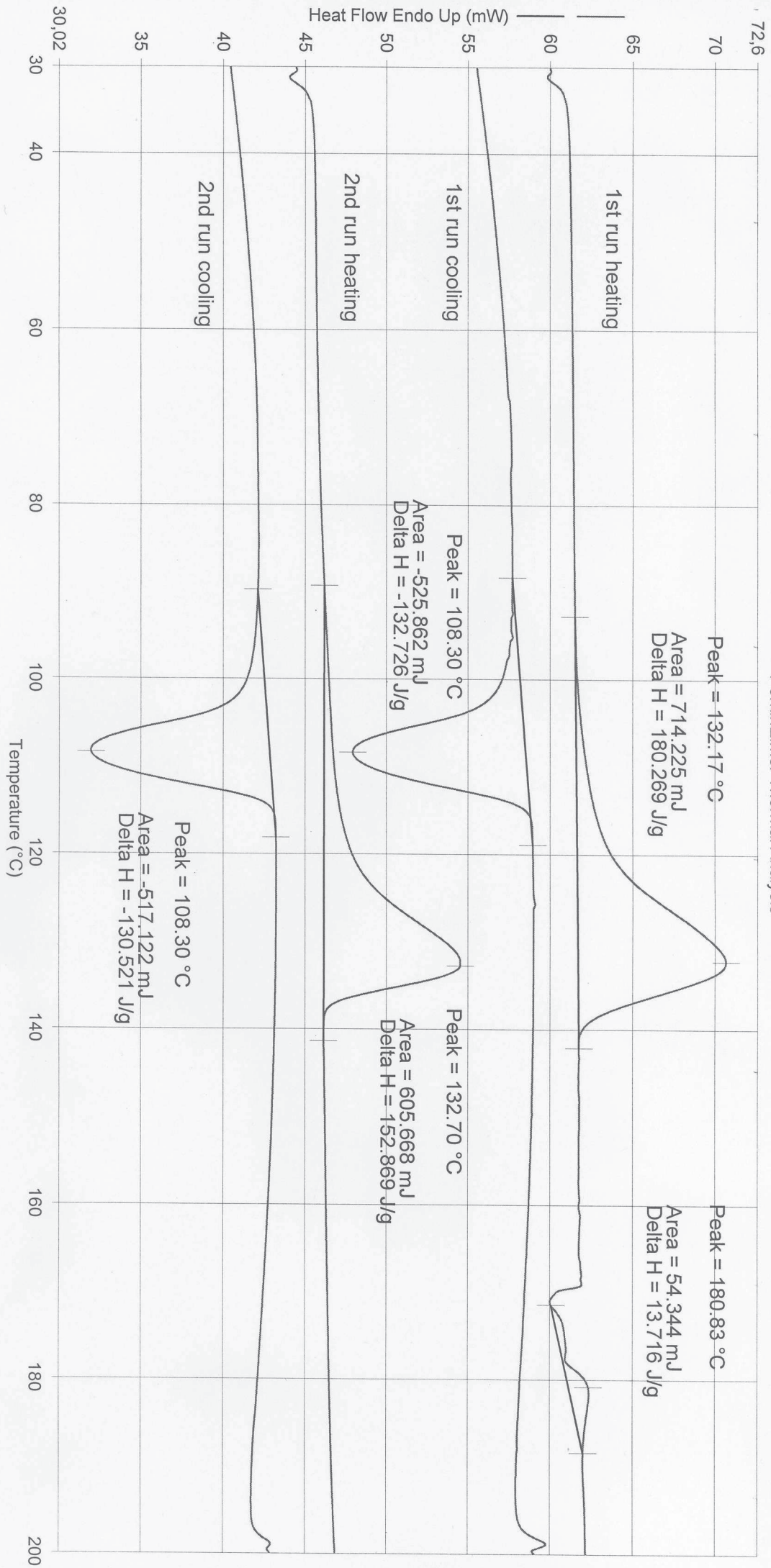
Figure 5.34. High temperature GPC calibration curve.

DSCs of Polyethylene

Operator ID: Schweizer
Sample ID: 2000-139
Sample Weight: 3.962 mg
Comment:

Cat. 13 derived PE at 50°C.

PerkinElmer Thermal Analysis



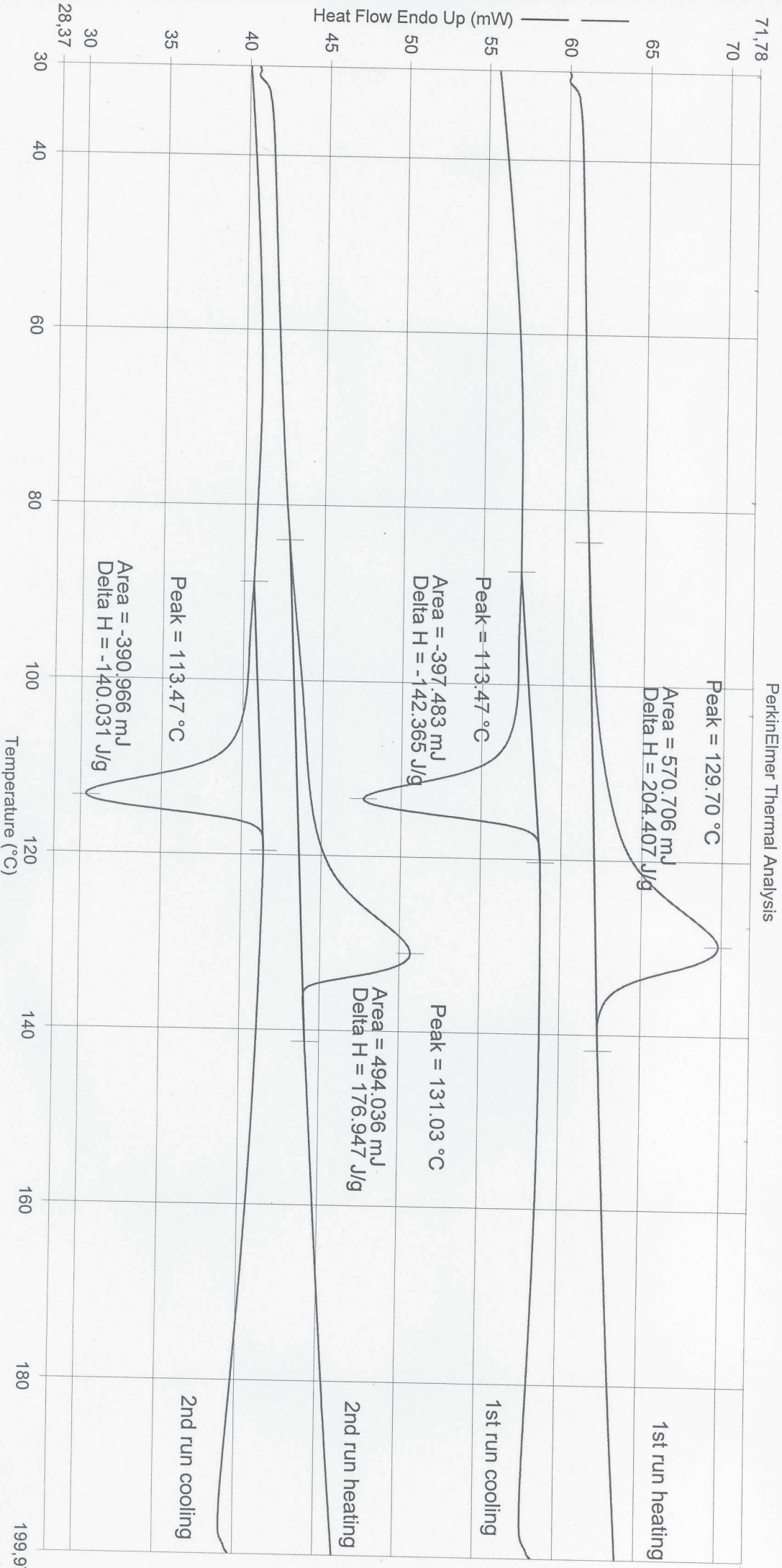
- 1) Hold for 1.0 min at 30.00°C
- 2) Heat from 30.00°C to 200.00°C at 10.00°C/min
- 3) Hold for 1.0 min at 200.00°C
- 4) Cool from 200.00°C to 30.00°C at 10.00°C/min

- 5) Hold for 1.0 min at 30.00°C
- 6) Heat from 30.00°C to 200.00°C at 10.00°C/min
- 7) Hold for 1.0 min at 200.00°C
- 8) Cool from 200.00°C to 30.00°C at 10.00°C/min

Operator ID: Schweizer
Sample ID: 2000-140
Sample Weight: 2.792 mg
Comment:

Cat. 13 derived PE at 65°C.

PerkinElmer Thermal Analysis

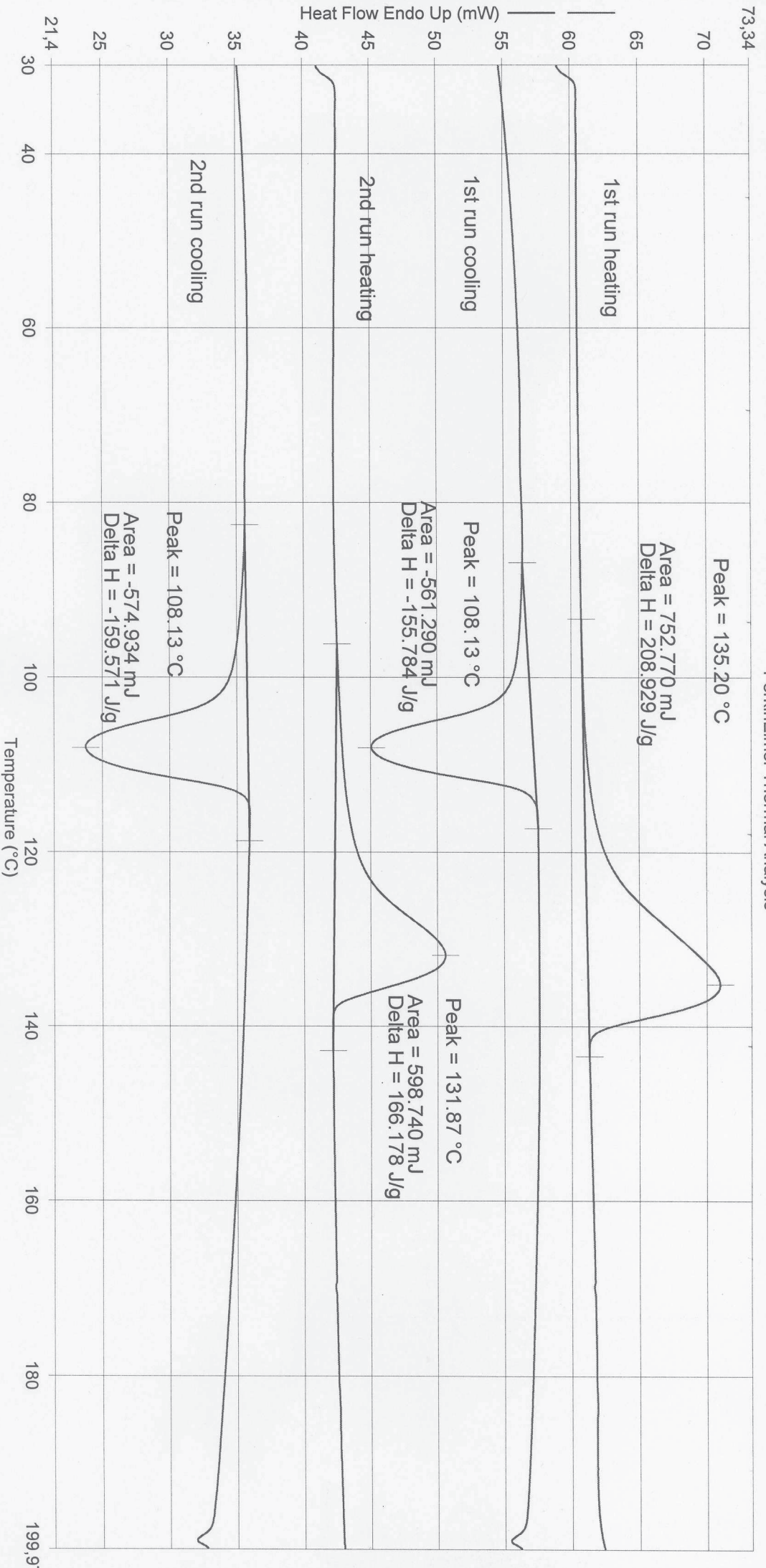


- 1) Hold for 1.0 min at 30.00°C
- 2) Heat from 30.00°C to 200.00°C at 10.00°C/min
- 3) Hold for 1.0 min at 200.00°C
- 4) Cool from 200.00°C to 30.00°C at 10.00°C/min

- 5) Hold for 1.0 min at 30.00°C
- 6) Heat from 30.00°C to 200.00°C at 10.00°C/min
- 7) Hold for 1.0 min at 200.00°C
- 8) Cool from 200.00°C to 30.00°C at 10.00°C/min

Operator ID: Schweizer
Sample ID: 2000-170
Sample Weight: 3.603 mg
Comment: Cat. 13 deviated PE at 90°C.

PerkinElmer Thermal Analysis



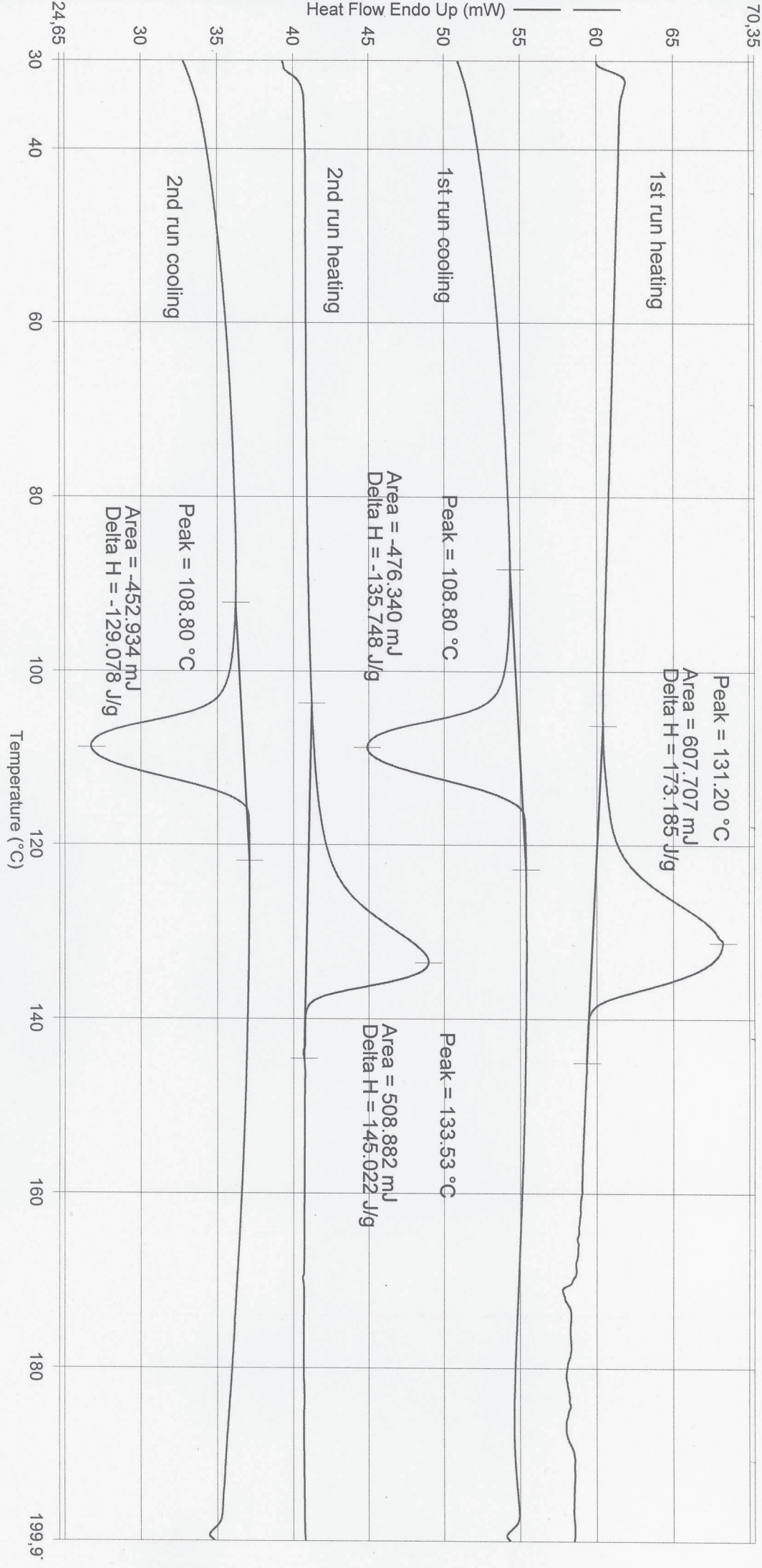
- 1) Hold for 1.0 min at 30.00°C
- 2) Heat from 30.00°C to 200.00°C at 10.00°C/min
- 3) Hold for 1.0 min at 200.00°C
- 4) Cool from 200.00°C to 30.00°C at 10.00°C/min

- 5) Hold for 1.0 min at 30.00°C
- 6) Heat from 30.00°C to 200.00°C at 10.00°C/min
- 7) Hold for 1.0 min at 200.00°C
- 8) Cool from 200.00°C to 30.00°C at 10.00°C/min

28.10.2011 14:42:41

Operator ID: Schweizer
Sample ID: 2000-165
Sample Weight: 3.509 mg
Comment: *Cat. 17 derived PE at 58°C*

PerkinElmer Thermal Analysis

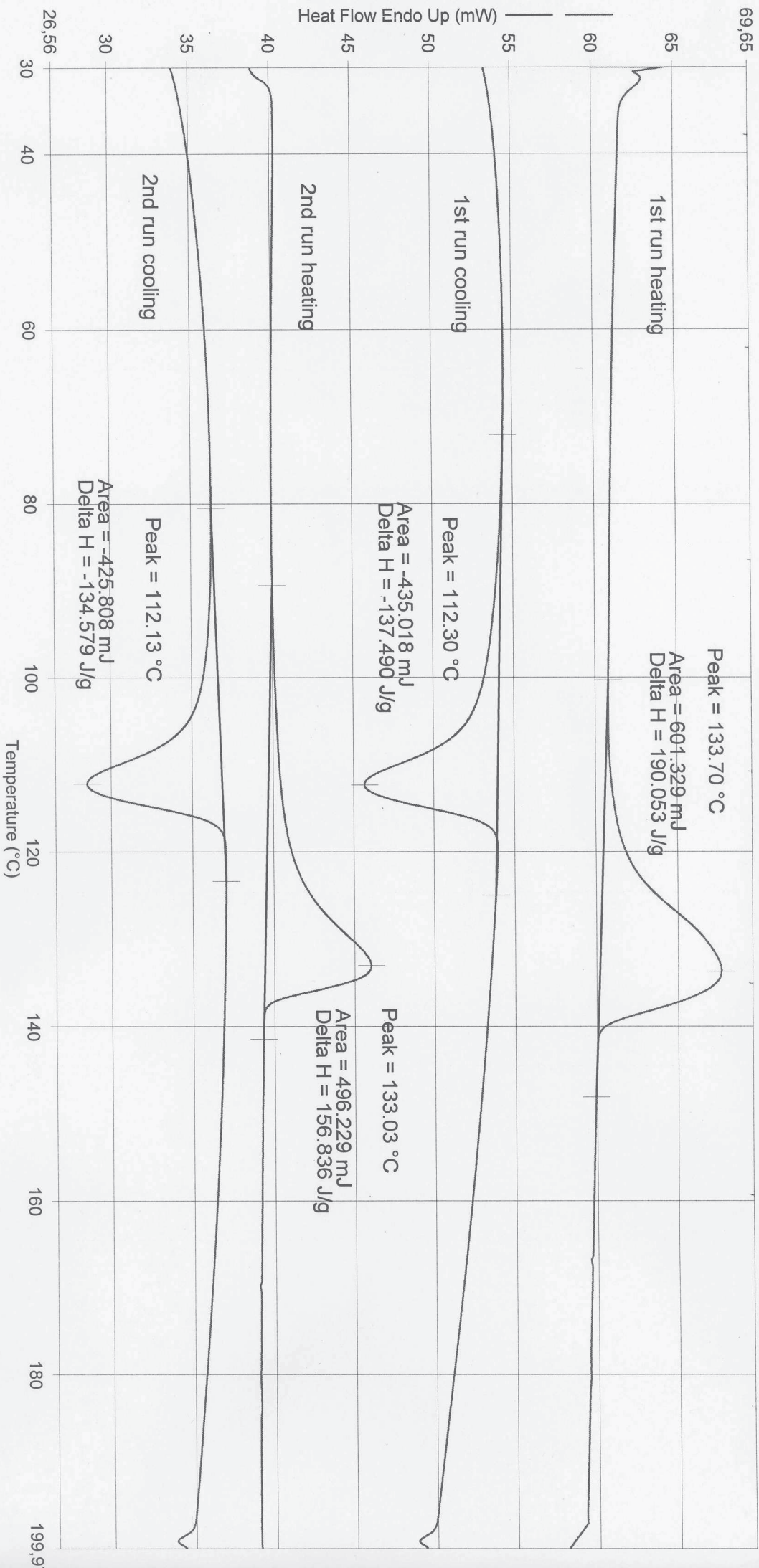


- 1) Hold for 1.0 min at 30.00°C
- 2) Heat from 30.00°C to 200.00°C at 10.00°C/min
- 3) Hold for 1.0 min at 200.00°C
- 4) Cool from 200.00°C to 30.00°C at 10.00°C/min

- 5) Hold for 1.0 min at 30.00°C
- 6) Heat from 30.00°C to 200.00°C at 10.00°C/min
- 7) Hold for 1.0 min at 200.00°C
- 8) Cool from 200.00°C to 30.00°C at 10.00°C/min

Cat. 77 derived PE at 65°C

PerkinElmer Thermal Analysis



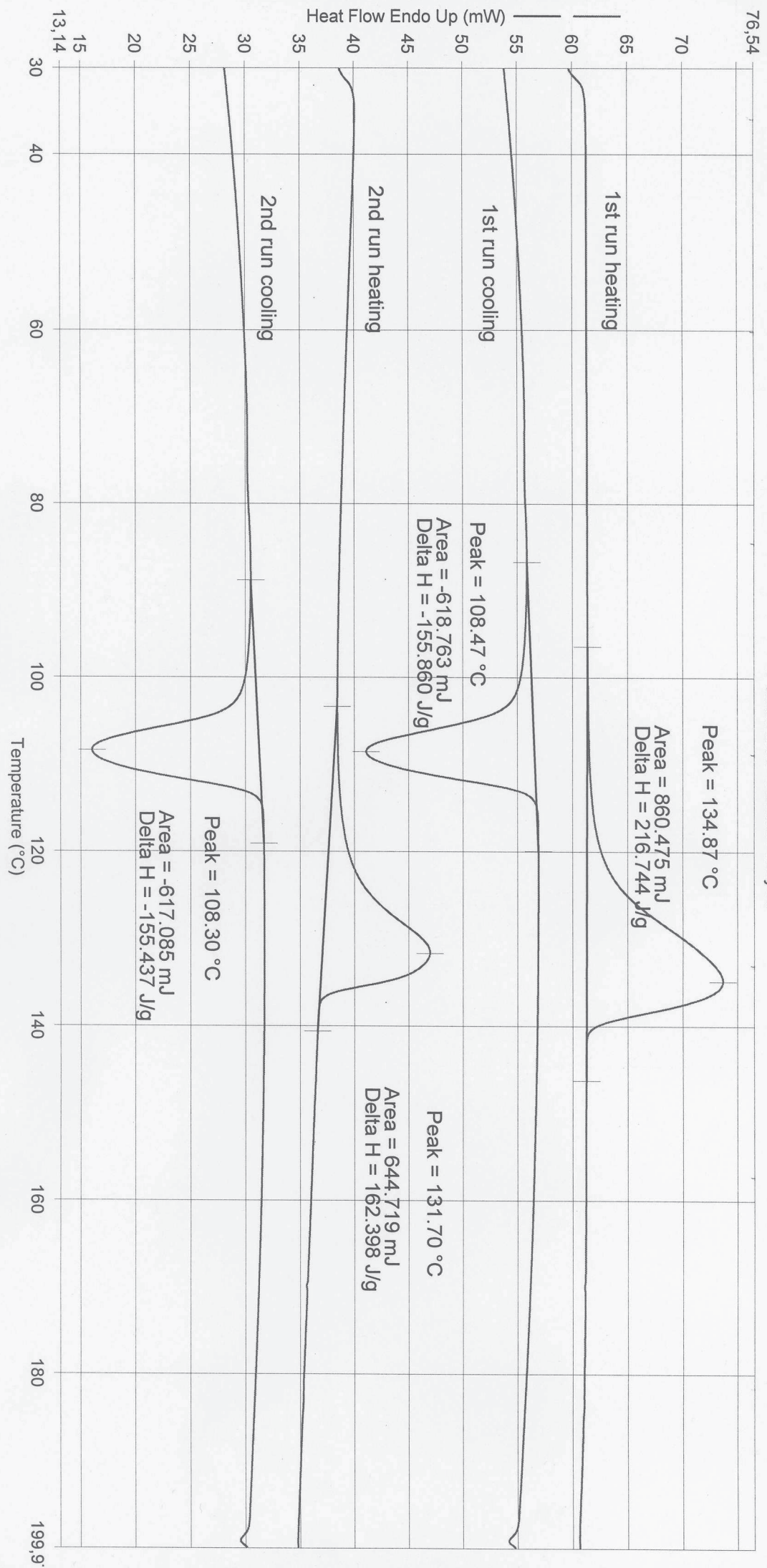
- 1) Hold for 1.0 min at 30.00°C
- 2) Heat from 30.00°C to 200.00°C at 10.00°C/min
- 3) Hold for 1.0 min at 200.00°C
- 4) Cool from 200.00°C to 30.00°C at 10.00°C/min

- 5) Hold for 1.0 min at 30.00°C
- 6) Heat from 30.00°C to 200.00°C at 10.00°C/min
- 7) Hold for 1.0 min at 200.00°C
- 8) Cool from 200.00°C to 30.00°C at 10.00°C/min

Operator ID: Schweizer
Sample ID: 2000-173
Sample Weight: 3.970 mg
Comment:

Cat. 17 derived PE at 90°C.

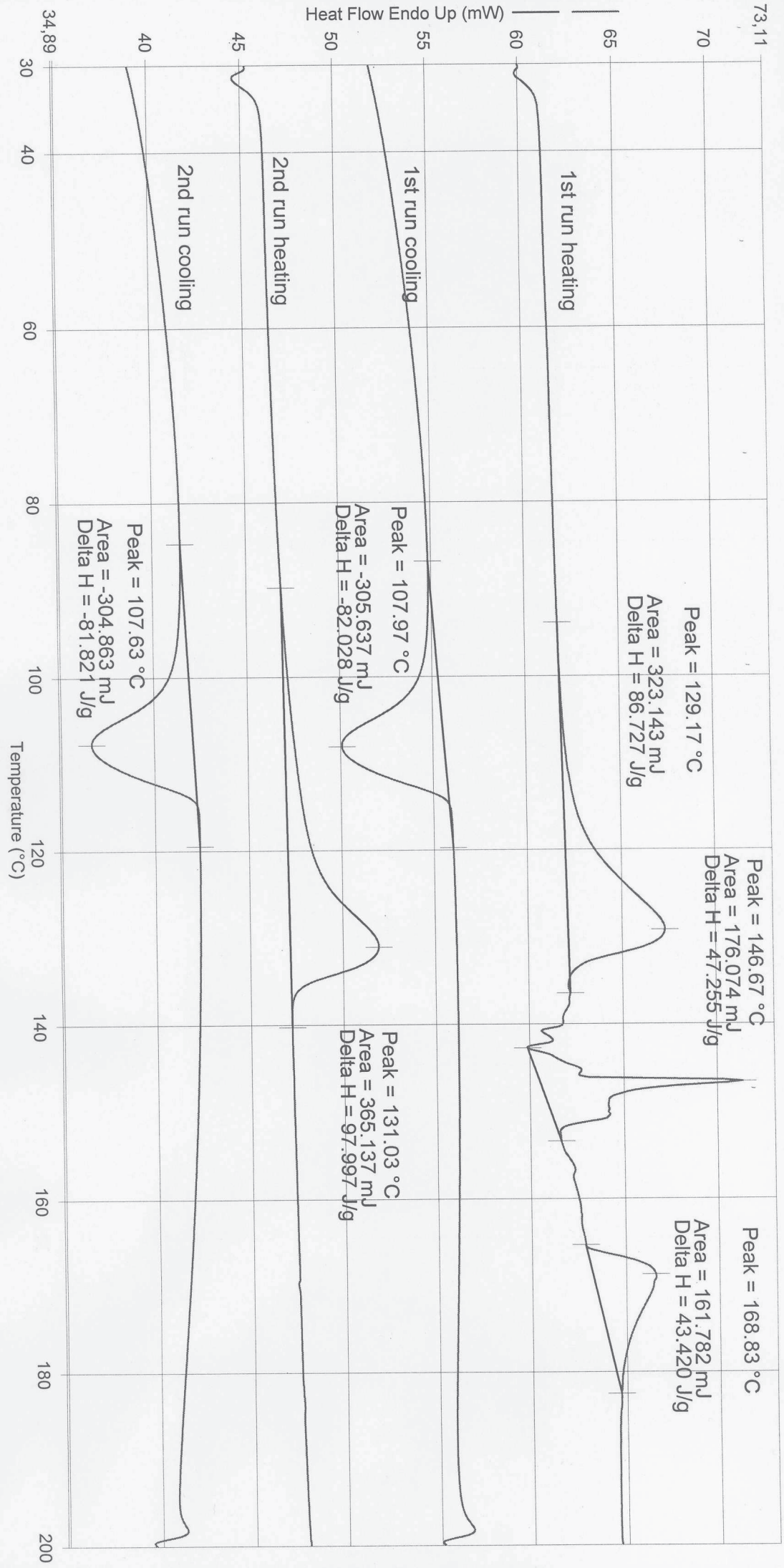
PerkinElmer Thermal Analysis



- 1) Hold for 1.0 min at 30.00°C
- 2) Heat from 30.00°C to 200.00°C at 10.00°C/min
- 3) Hold for 1.0 min at 200.00°C
- 4) Cool from 200.00°C to 30.00°C at 10.00°C/min

- 5) Hold for 1.0 min at 30.00°C
- 6) Heat from 30.00°C to 200.00°C at 10.00°C/min
- 7) Hold for 1.0 min at 200.00°C
- 8) Cool from 200.00°C to 30.00°C at 10.00°C/min

Cat. 27 derived PE at 65°C

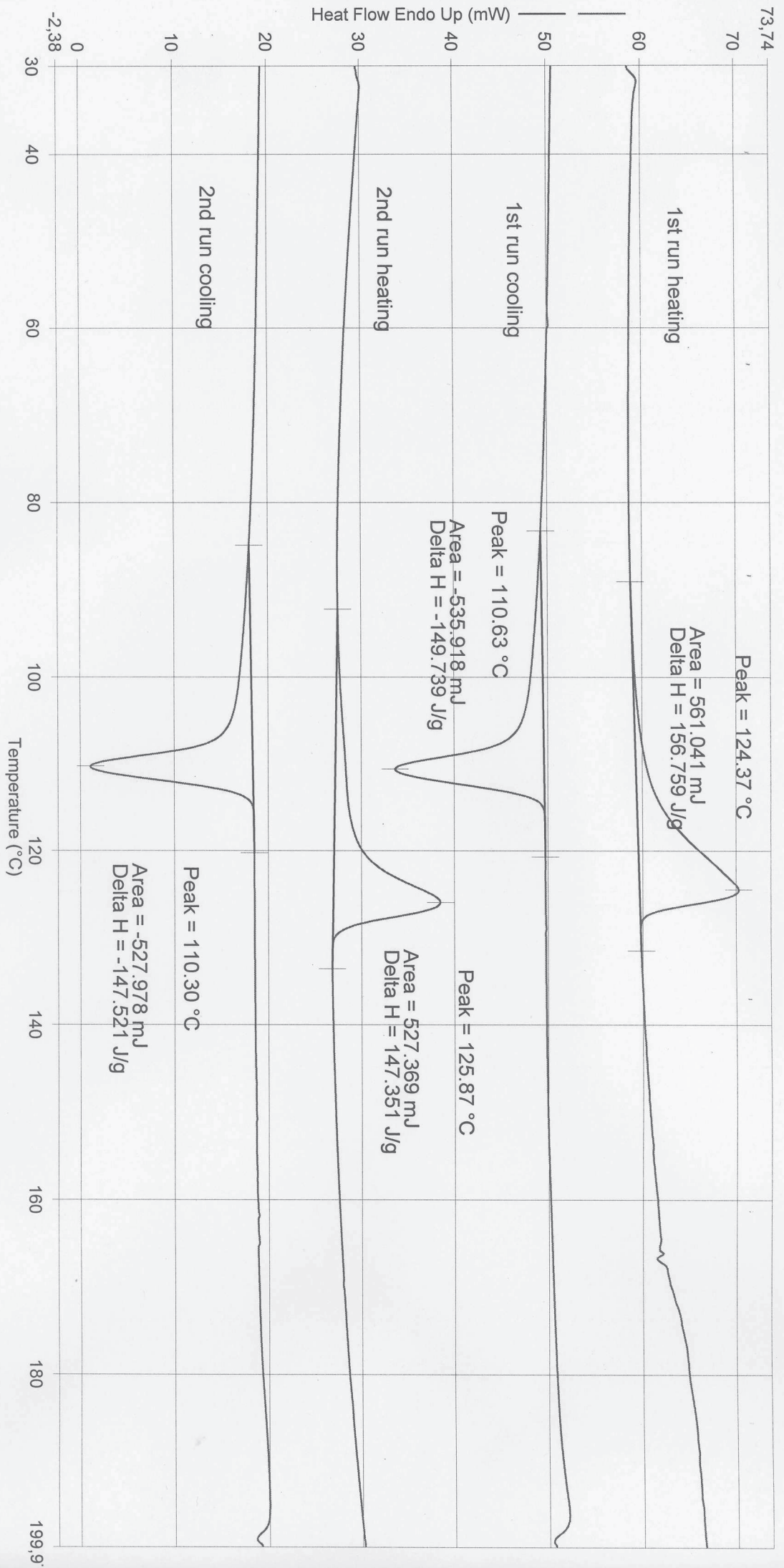


- 1) Hold for 1.0 min at 30.00°C
- 2) Heat from 30.00°C to 200.00°C at 10.00°C/min
- 3) Hold for 1.0 min at 200.00°C
- 4) Cool from 200.00°C to 30.00°C at 10.00°C/min

- 5) Hold for 1.0 min at 30.00°C
- 6) Heat from 30.00°C to 200.00°C at 10.00°C/min
- 7) Hold for 1.0 min at 200.00°C
- 8) Cool from 200.00°C to 30.00°C at 10.00°C/min

Operator ID: Schweizer
Sample ID: 2000-177
Sample Weight: 3.579 mg
Comment:

cat. 27 derived PE at 90°C

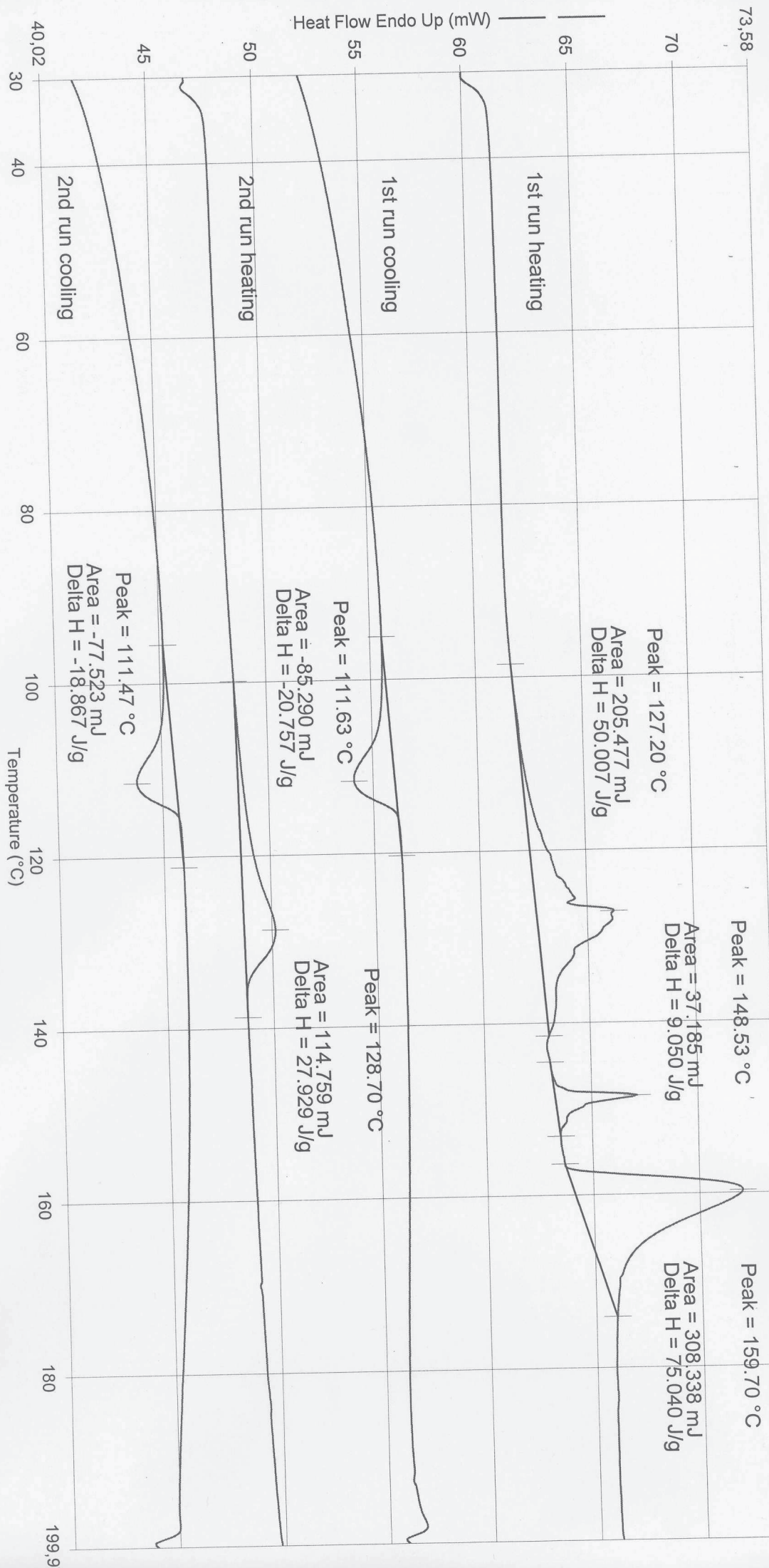


- 1) Hold for 1.0 min at 30.00°C
- 2) Heat from 30.00°C to 200.00°C at 10.00°C/min
- 3) Hold for 1.0 min at 200.00°C
- 4) Cool from 200.00°C to 30.00°C at 10.00°C/min

- 5) Hold for 1.0 min at 30.00°C
- 6) Heat from 30.00°C to 200.00°C at 10.00°C/min
- 7) Hold for 1.0 min at 200.00°C
- 8) Cool from 200.00°C to 30.00°C at 10.00°C/min

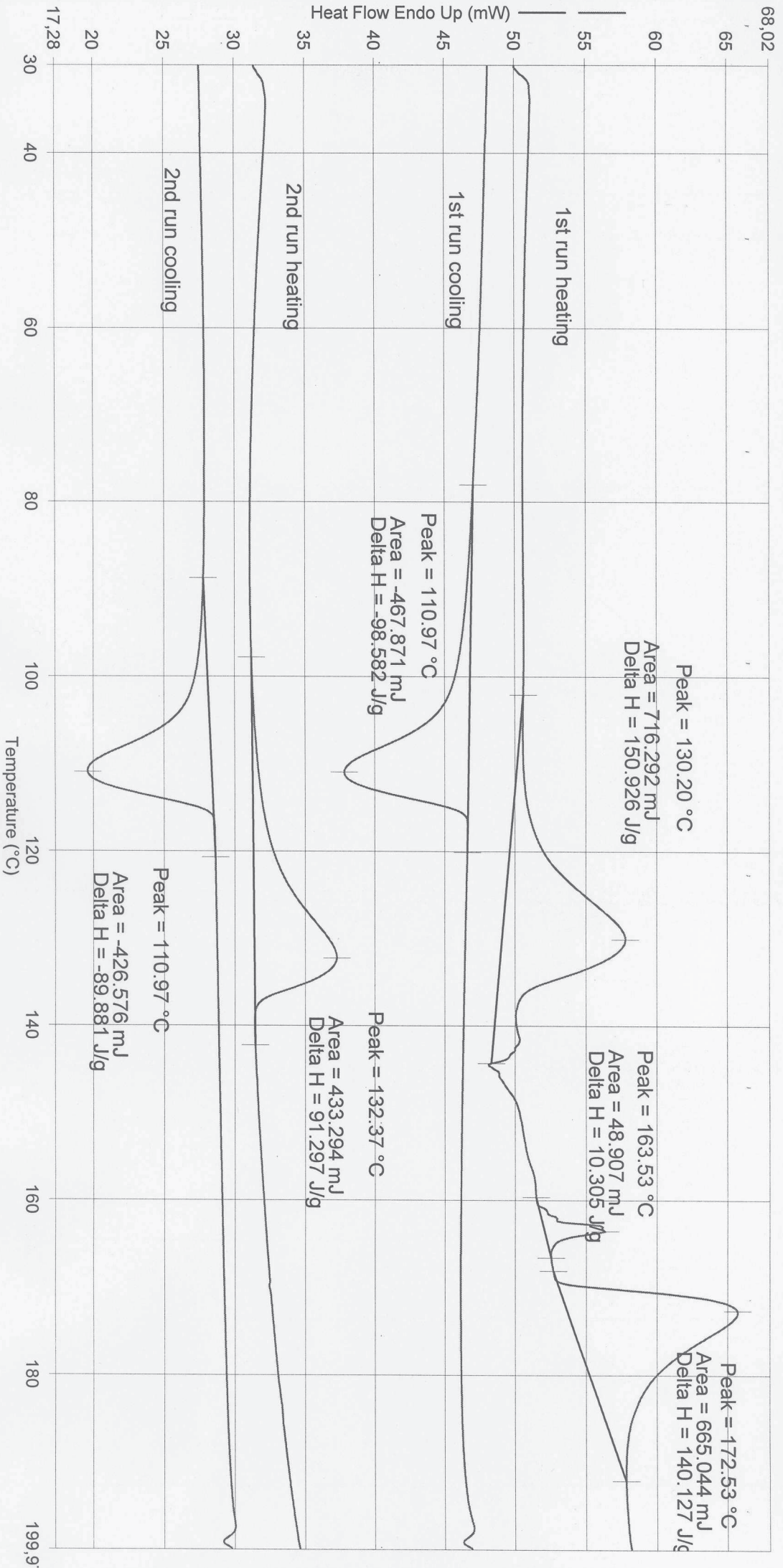
03.11.2011 09:50:58

Filename: C:\Program Files\Pyris\Data...2000_137.dsd
 Operator ID: Schweizer
 Sample ID: 2000-137
 Sample Weight: 4.109 mg
 Comment: Cat. 23 derived PE 50°C



- 1) Hold for 1.0 min at 30.00°C
- 2) Heat from 30.00°C to 200.00°C at 10.00°C/min
- 3) Hold for 1.0 min at 200.00°C
- 4) Cool from 200.00°C to 30.00°C at 10.00°C/min
- 5) Hold for 1.0 min at 30.00°C
- 6) Heat from 30.00°C to 200.00°C at 10.00°C/min
- 7) Hold for 1.0 min at 200.00°C
- 8) Cool from 200.00°C to 30.00°C at 10.00°C/min

cat. 23 devined PE at 90°C

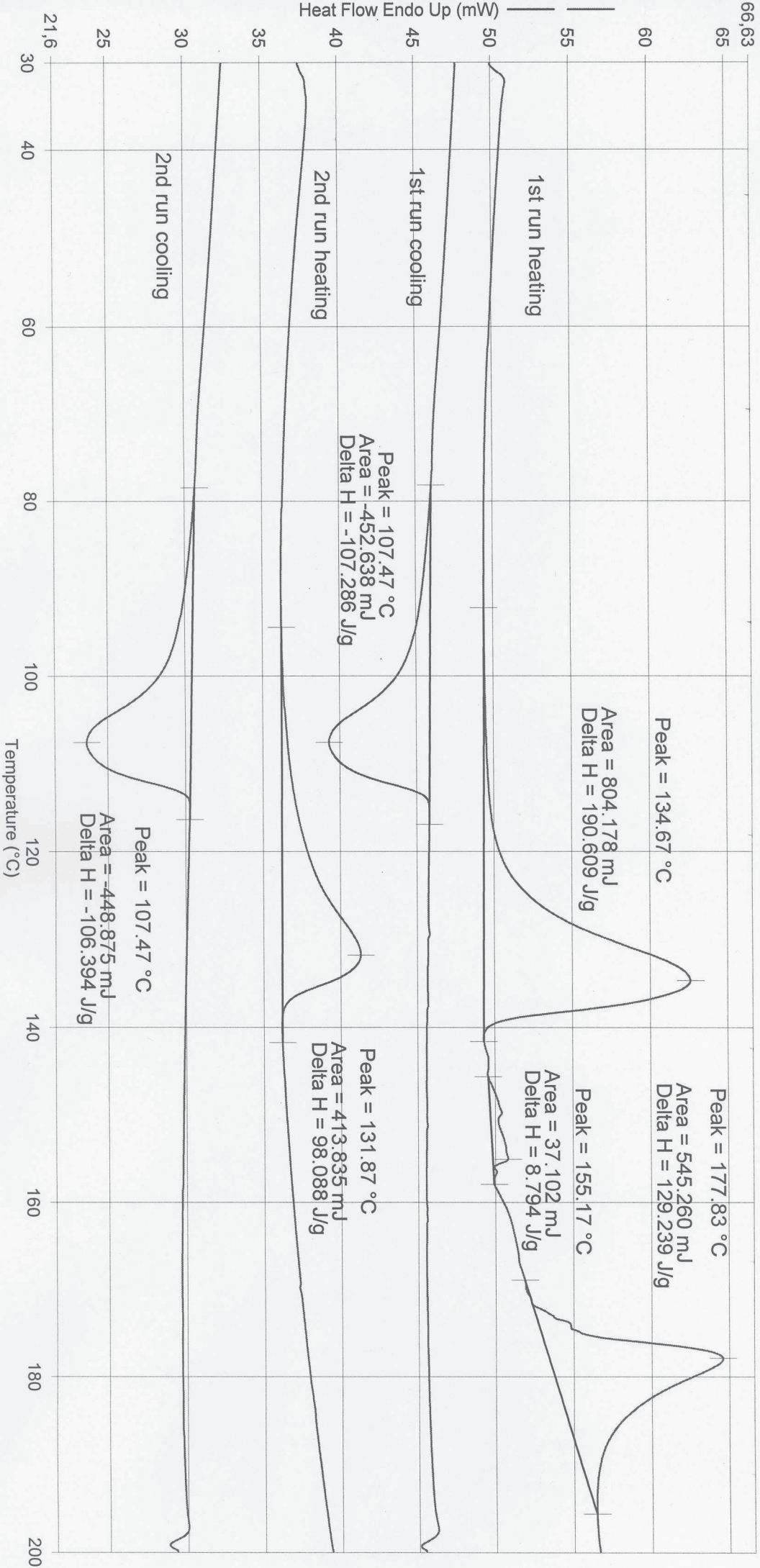


- 1) Hold for 1.0 min at 30.00°C
- 2) Heat from 30.00°C to 200.00°C at 10.00°C/min
- 3) Hold for 1.0 min at 200.00°C
- 4) Cool from 200.00°C to 30.00°C at 10.00°C/min

- 5) Hold for 1.0 min at 30.00°C
- 6) Heat from 30.00°C to 200.00°C at 10.00°C/min
- 7) Hold for 1.0 min at 200.00°C
- 8) Cool from 200.00°C to 30.00°C at 10.00°C/min

Filename: C:\Program Files\TGA\TGAData\...
 Operator ID: Schweizer
 Sample ID: 2000-180
 Sample Weight: 4.219 mg
 Comment: *Cat. 22 derived PE 56C*

PerkinElmer Thermal Analysis



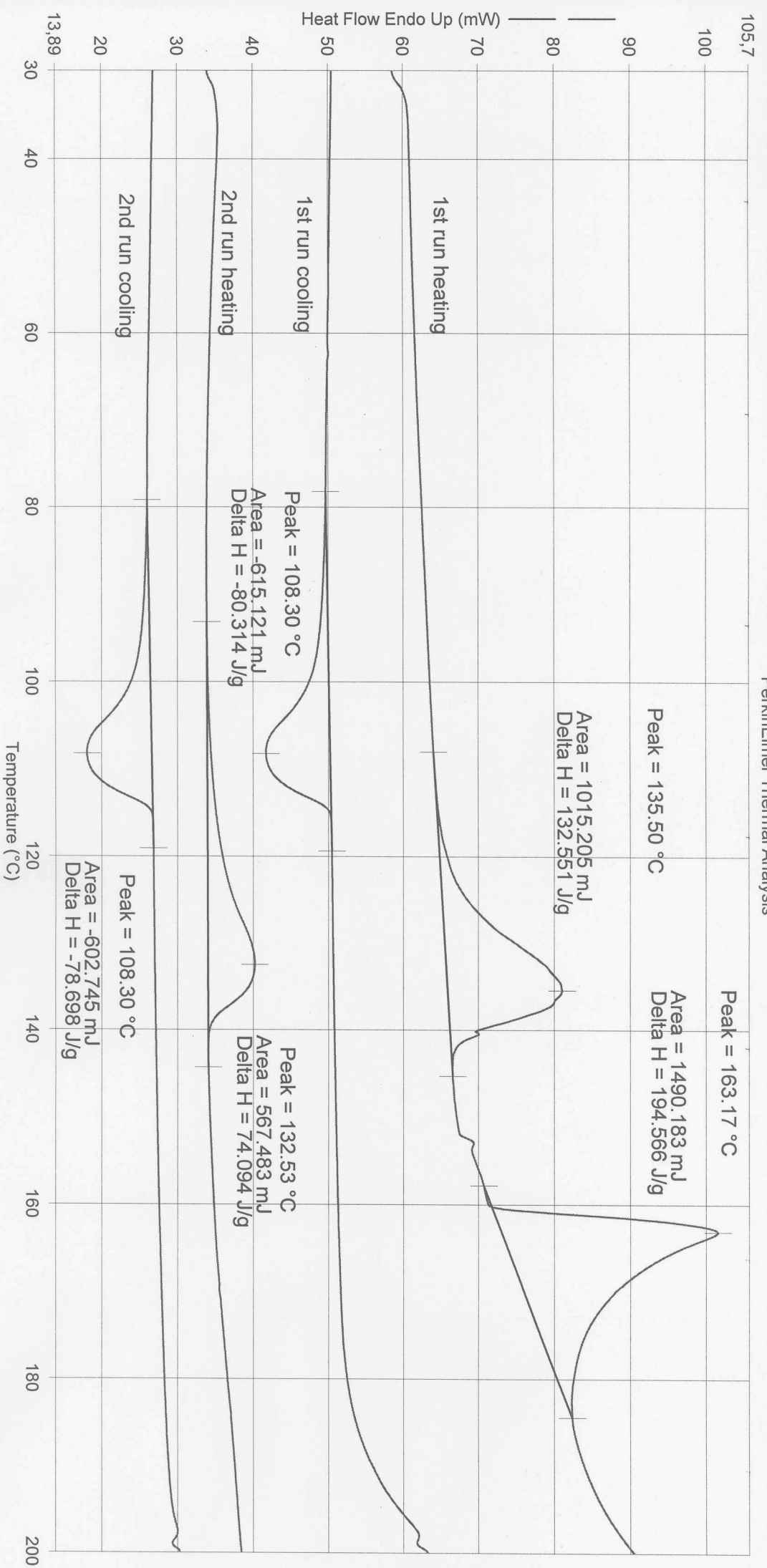
- 1) Hold for 1.0 min at 30.00°C
- 2) Heat from 30.00°C to 200.00°C at 10.00°C/min
- 3) Hold for 1.0 min at 200.00°C
- 4) Cool from 200.00°C to 30.00°C at 10.00°C/min

- 5) Hold for 1.0 min at 30.00°C
- 6) Heat from 30.00°C to 200.00°C at 10.00°C/min
- 7) Hold for 1.0 min at 200.00°C
- 8) Cool from 200.00°C to 30.00°C at 10.00°C/min

Operator ID: Schweizer
Sample ID: 2000-181
Sample Weight: 7.659 mg
Comment:

cat. aa derived Pc at 65°C.

PerkinElmer Thermal Analysis



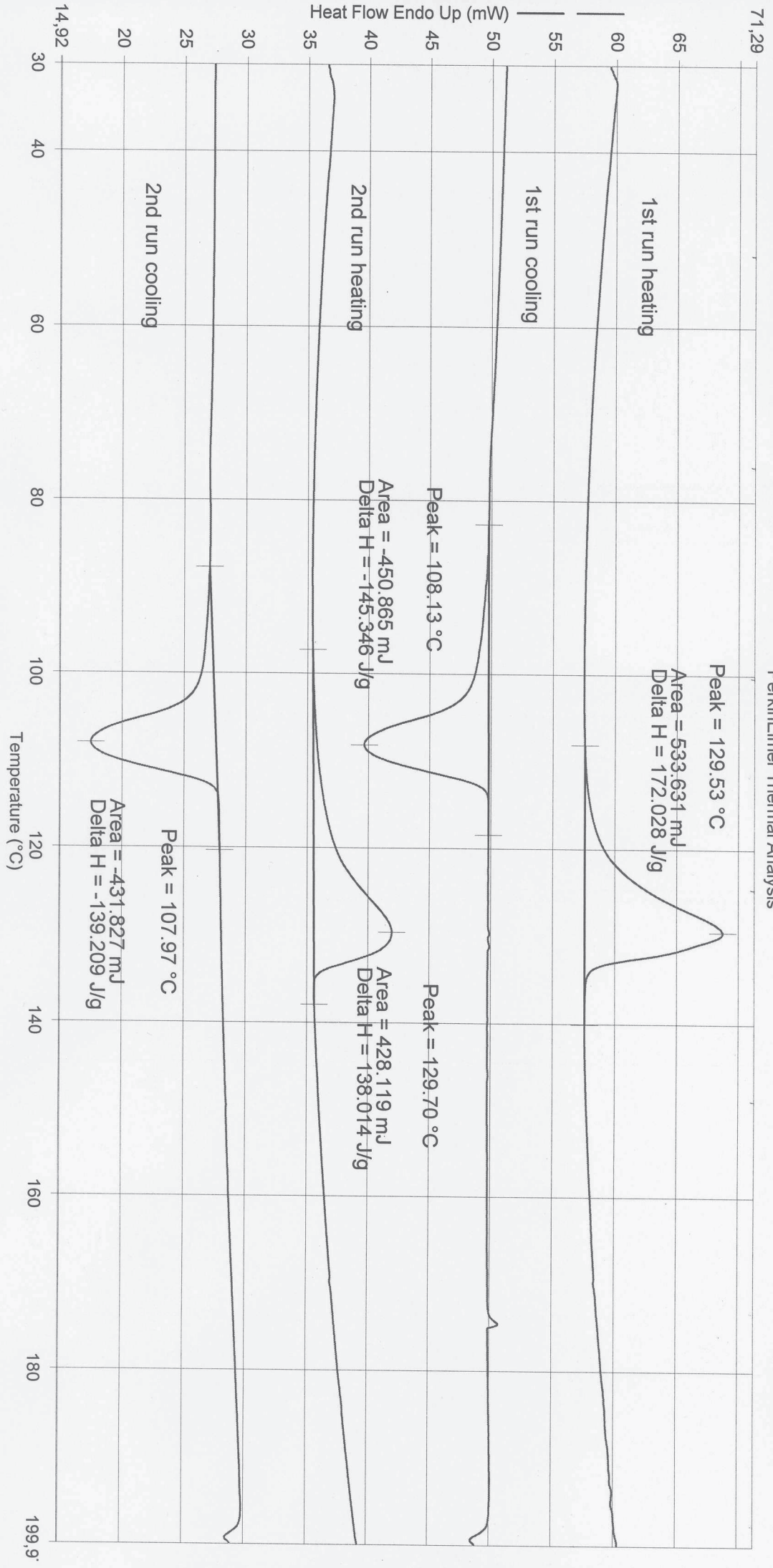
- 1) Hold for 1.0 min at 30.00°C
- 2) Heat from 30.00°C to 200.00°C at 10.00°C/min
- 3) Hold for 1.0 min at 200.00°C
- 4) Cool from 200.00°C to 30.00°C at 10.00°C/min

- 5) Hold for 1.0 min at 30.00°C
- 6) Heat from 30.00°C to 200.00°C at 10.00°C/min
- 7) Hold for 1.0 min at 200.00°C
- 8) Cool from 200.00°C to 30.00°C at 10.00°C/min

Operator ID: Schweizer
Sample ID: 2000-182
Sample Weight: 3.102 mg
Comment:

cat. 22 derived PE at 90°C.

PerkinElmer Thermal Analysis



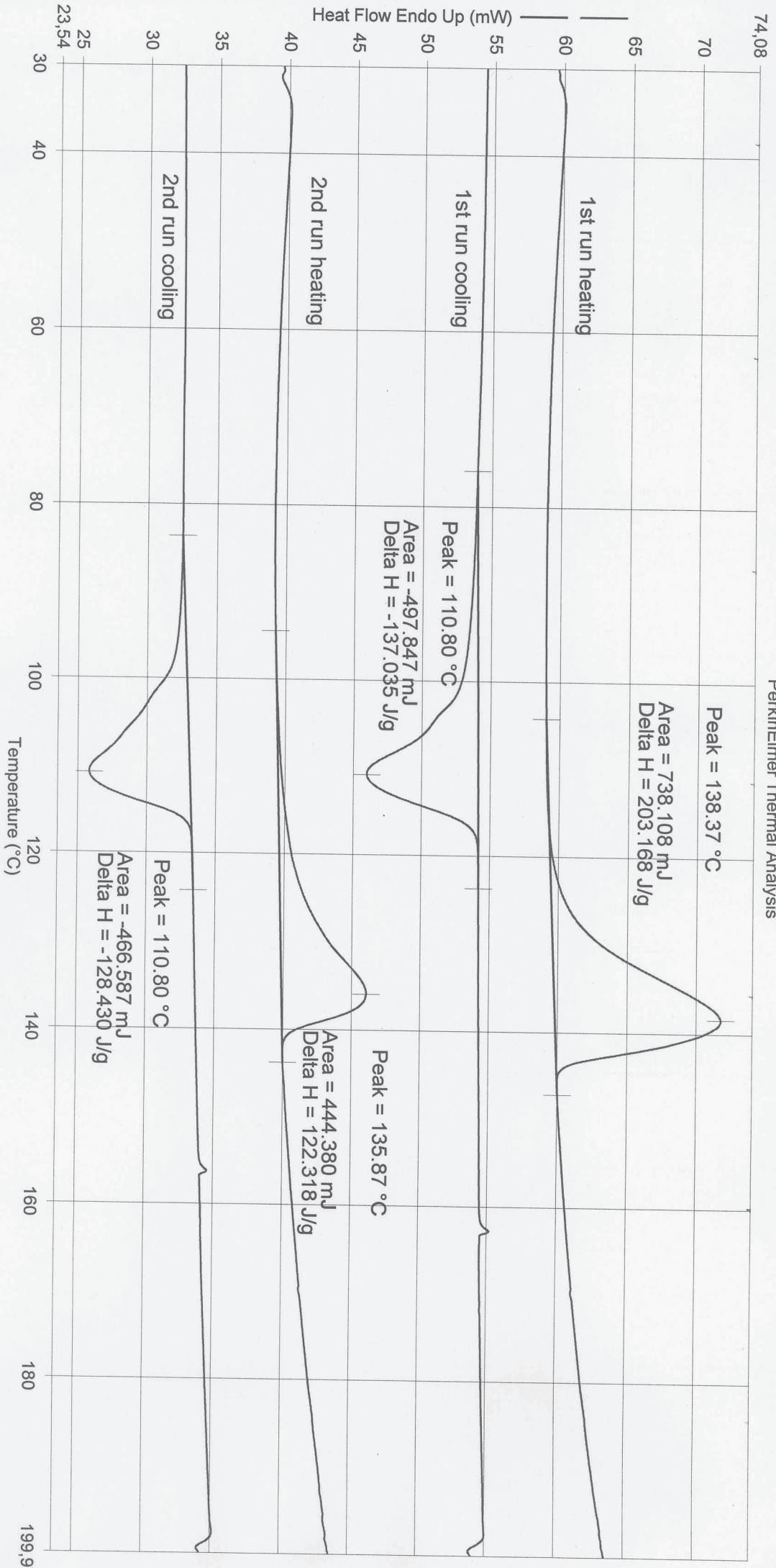
- 1) Hold for 1.0 min at 30.00°C
- 2) Heat from 30.00°C to 200.00°C at 10.00°C/min
- 3) Hold for 1.0 min at 200.00°C
- 4) Cool from 200.00°C to 30.00°C at 10.00°C/min

- 5) Hold for 1.0 min at 30.00°C
- 6) Heat from 30.00°C to 200.00°C at 10.00°C/min
- 7) Hold for 1.0 min at 200.00°C
- 8) Cool from 200.00°C to 30.00°C at 10.00°C/min

Operator ID: Schweizer
Sample ID: 3000-14
Sample Weight: 3.633 mg
Comment:

Cat. 94 derived PE at 50°C.

PerkinElmer Thermal Analysis

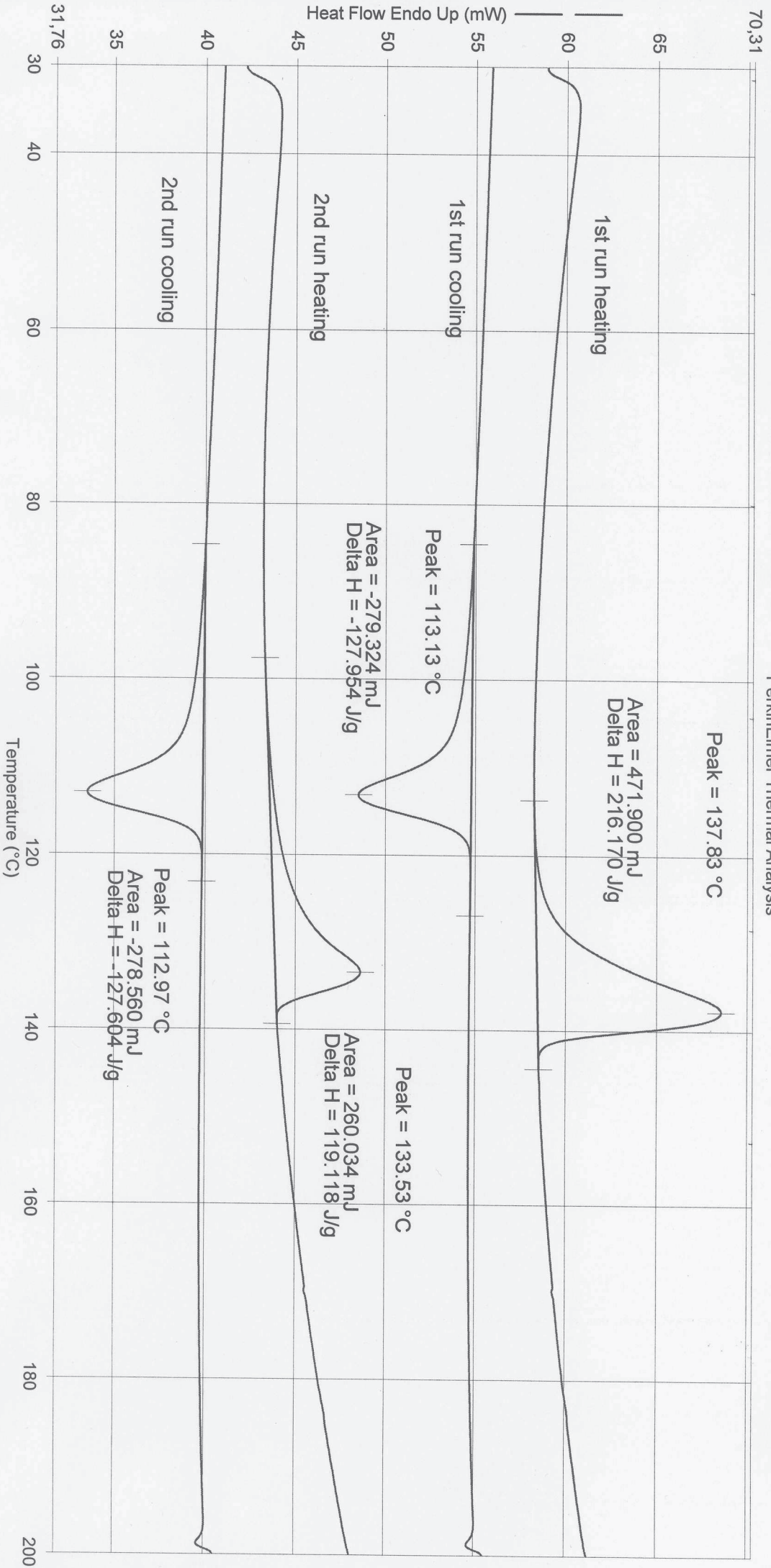


- 1) Hold for 1.0 min at 30.00°C
- 2) Heat from 30.00°C to 200.00°C at 10.00°C/min
- 3) Hold for 1.0 min at 200.00°C
- 4) Cool from 200.00°C to 30.00°C at 10.00°C/min

- 5) Hold for 1.0 min at 30.00°C
- 6) Heat from 30.00°C to 200.00°C at 10.00°C/min
- 7) Hold for 1.0 min at 200.00°C
- 8) Cool from 200.00°C to 30.00°C at 10.00°C/min

Operator ID: Schweizer
 Sample ID: 3000-13
 Sample Weight: 2.183 mg
 Comment: Cat. 24 derived PE at 65°C.

PerkinElmer Thermal Analysis



- 1) Hold for 1.0 min at 30.00°C
- 2) Heat from 30.00°C to 200.00°C at 10.00°C/min
- 3) Hold for 1.0 min at 200.00°C
- 4) Cool from 200.00°C to 30.00°C at 10.00°C/min

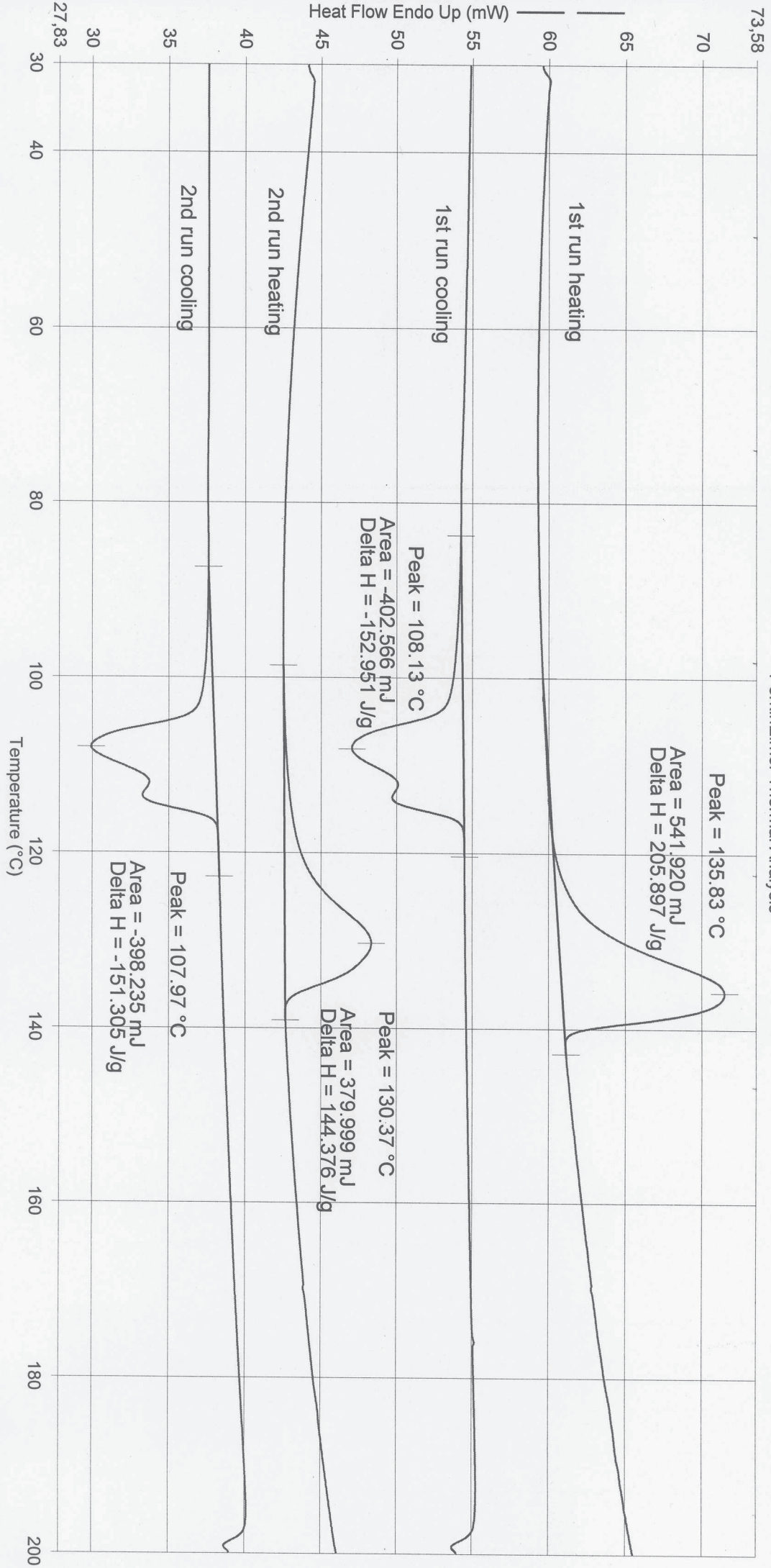
- 5) Hold for 1.0 min at 30.00°C
- 6) Heat from 30.00°C to 200.00°C at 10.00°C/min
- 7) Hold for 1.0 min at 200.00°C
- 8) Cool from 200.00°C to 30.00°C at 10.00°C/min

05.12.2011 16:31:48

Operator ID: Schweizer
Sample ID: 3000-19
Sample Weight: 2.632 mg
Comment:

cat. 24 derived PE at 90°C, 45bar ethylene.

PerkinElmer Thermal Analysis



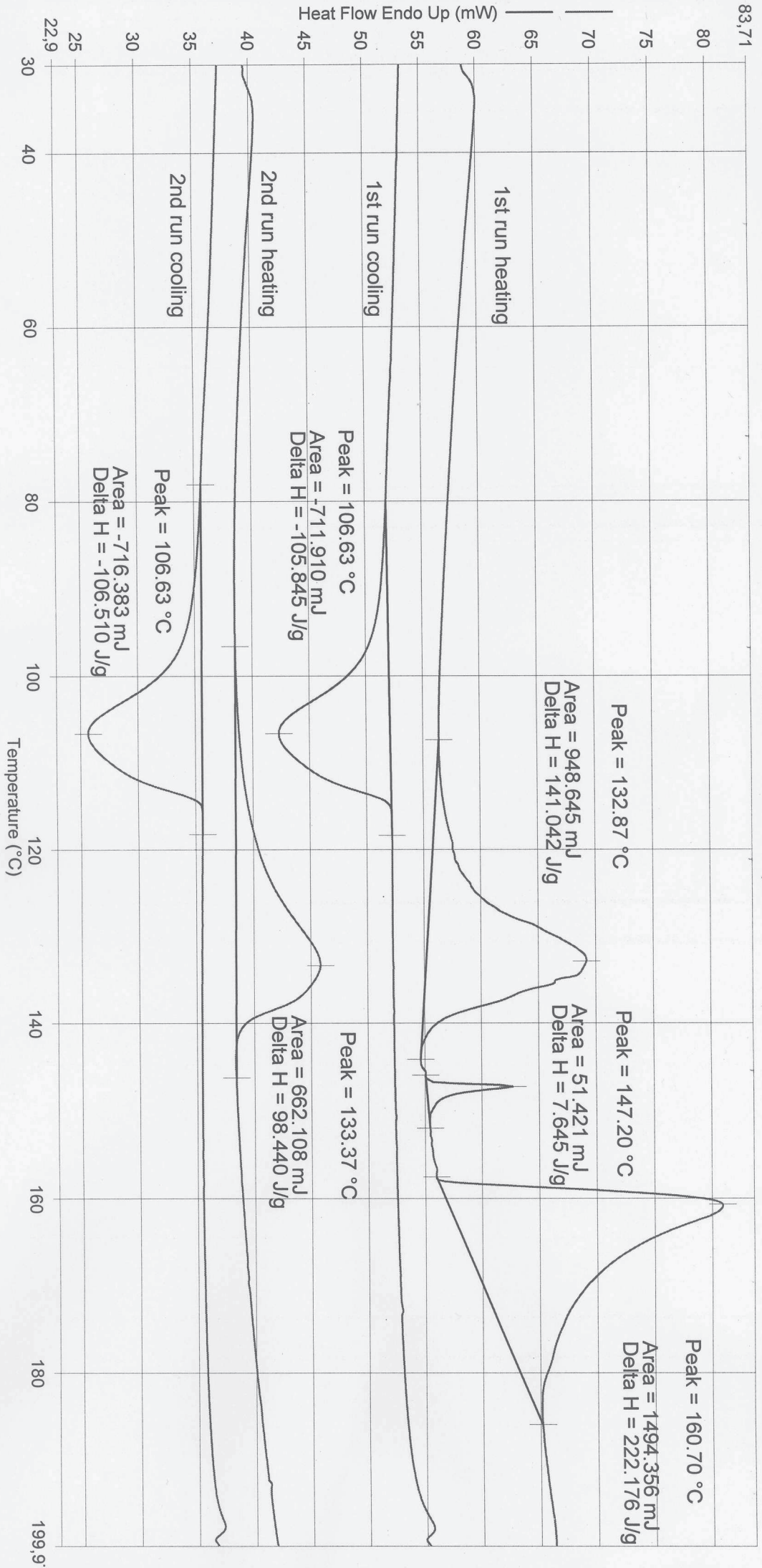
- 1) Hold for 1.0 min at 30.00°C
- 2) Heat from 30.00°C to 200.00°C at 10.00°C/min
- 3) Hold for 1.0 min at 200.00°C
- 4) Cool from 200.00°C to 30.00°C at 10.00°C/min

- 5) Hold for 1.0 min at 30.00°C
- 6) Heat from 30.00°C to 200.00°C at 10.00°C/min
- 7) Hold for 1.0 min at 200.00°C
- 8) Cool from 200.00°C to 30.00°C at 10.00°C/min

Operator ID: Schweizer
 Sample ID: 3000-186
 Sample Weight: 6.726 mg
 Comment:

cat. 26 derived PE at 65°C

PerkinElmer Thermal Analysis



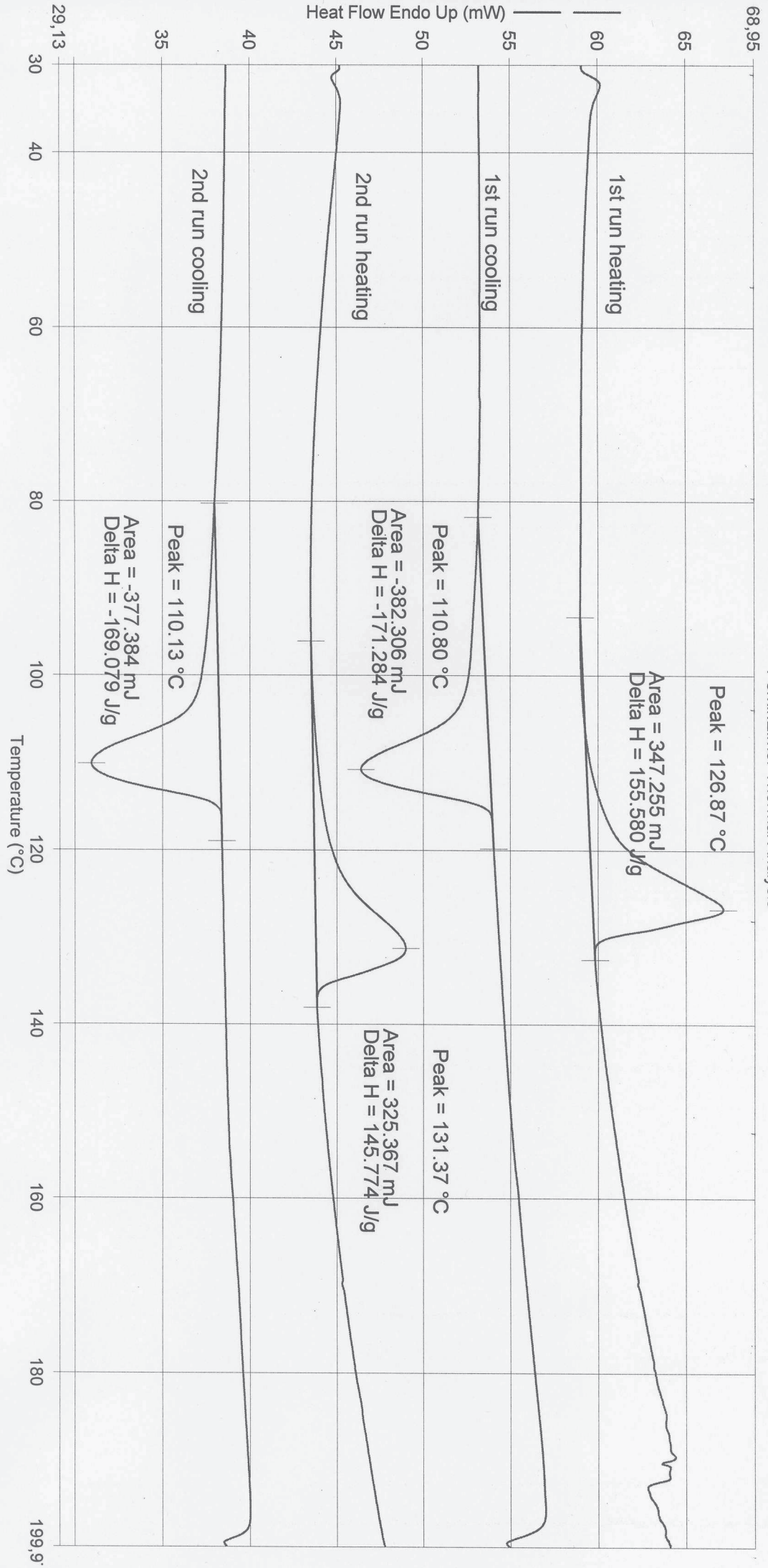
- 1) Hold for 1.0 min at 30.00°C
- 2) Heat from 30.00°C to 200.00°C at 10.00°C/min
- 3) Hold for 1.0 min at 200.00°C
- 4) Cool from 200.00°C to 30.00°C at 10.00°C/min

- 5) Hold for 1.0 min at 30.00°C
- 6) Heat from 30.00°C to 200.00°C at 10.00°C/min
- 7) Hold for 1.0 min at 200.00°C
- 8) Cool from 200.00°C to 30.00°C at 10.00°C/min

Operator ID: Schweizer
Sample ID: 3000-192
Sample Weight: 2.232 mg
Comment:

Cat. 26 derived PE at 90°C.

PerkinElmer Thermal Analysis



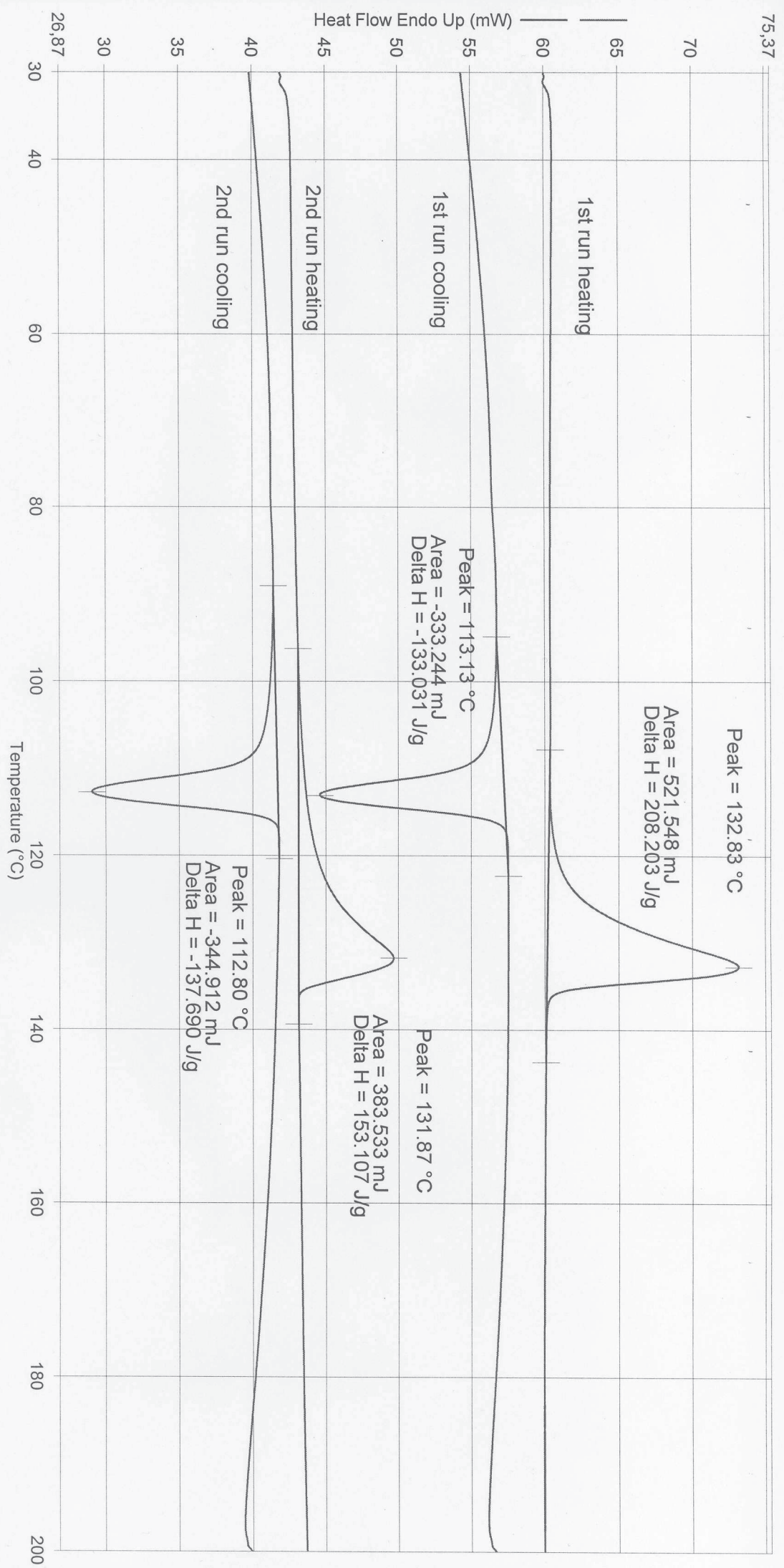
- 1) Hold for 1.0 min at 30.00°C
- 2) Heat from 30.00°C to 200.00°C at 10.00°C/min
- 3) Hold for 1.0 min at 200.00°C
- 4) Cool from 200.00°C to 30.00°C at 10.00°C/min

- 5) Hold for 1.0 min at 30.00°C
- 6) Heat from 30.00°C to 200.00°C at 10.00°C/min
- 7) Hold for 1.0 min at 200.00°C
- 8) Cool from 200.00°C to 30.00°C at 10.00°C/min

08.12.2011 09:42:00

DSCs of poly(E-*co*-CPE)

Cat. 13 derived Polyethylene in the presence of 2vvl-% CPE at 50°C



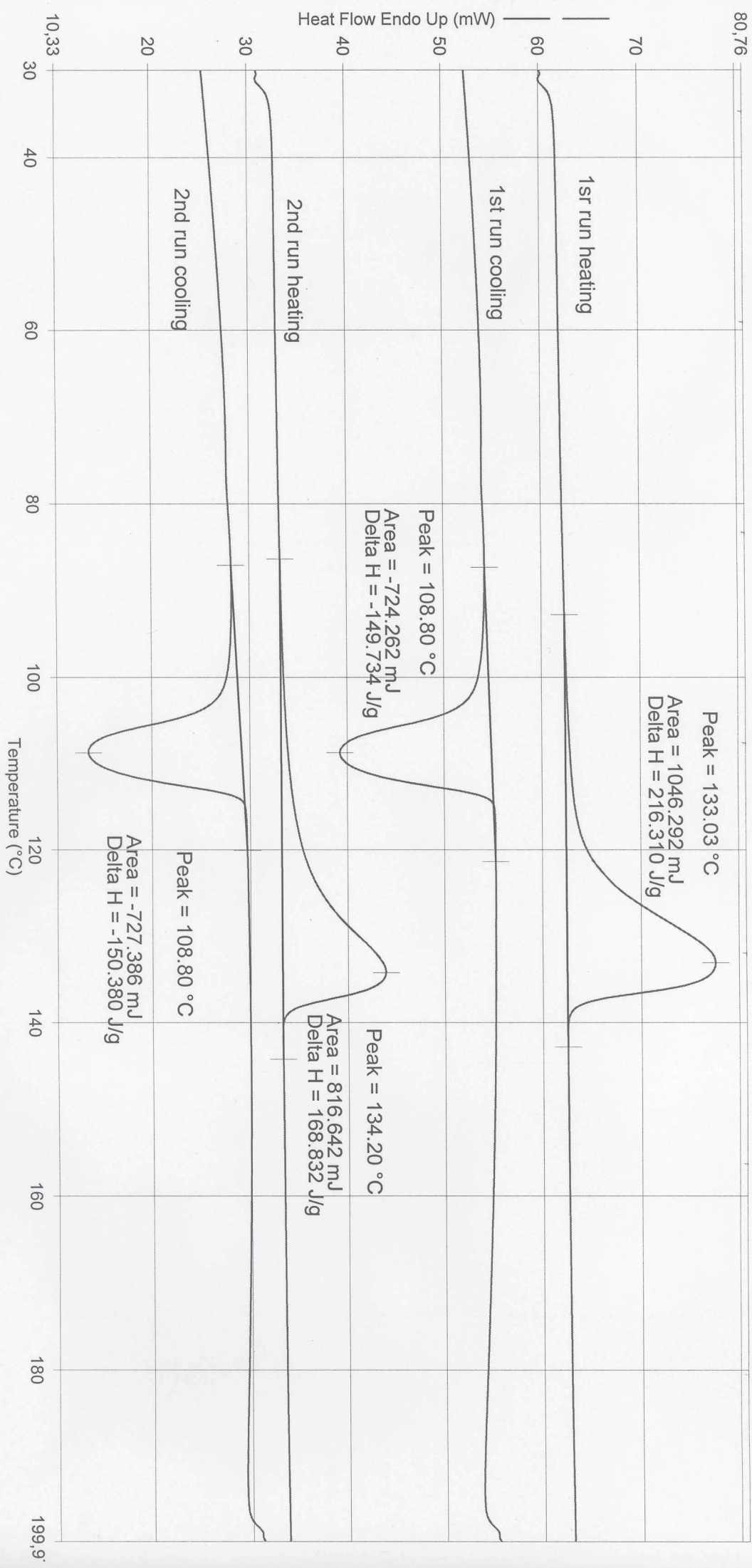
- 1) Hold for 1.0 min at 30.00°C
- 2) Heat from 30.00°C to 200.00°C at 10.00°C/min
- 3) Hold for 1.0 min at 200.00°C
- 4) Cool from 200.00°C to 30.00°C at 10.00°C/min

- 5) Hold for 1.0 min at 30.00°C
- 6) Heat from 30.00°C to 200.00°C at 10.00°C/min
- 7) Hold for 1.0 min at 200.00°C
- 8) Cool from 200.00°C to 30.00°C at 10.00°C/min

Filename: C:\Tlogram\resv\y15\data\...
 Operator ID: Schweizer
 Sample ID: 2000-145
 Sample Weight: 4.837 mg
 Comment:

Cat. 13 derived Polyethylene in the presence of 5-vol-% of CPE at 50°C.

PerkinElmer Thermal Analysis

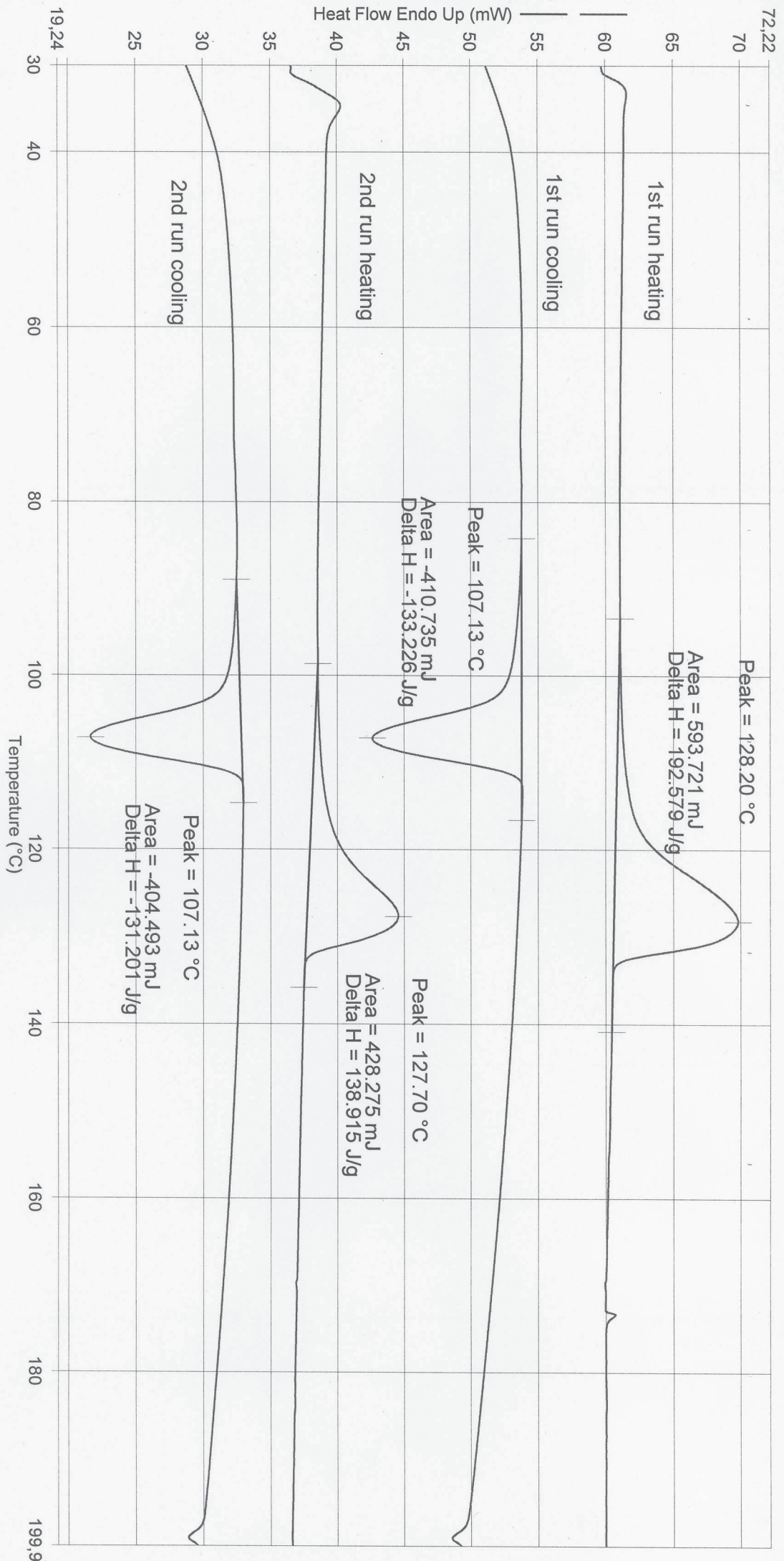


- 1) Hold for 1.0 min at 30.00°C
- 2) Heat from 30.00°C to 200.00°C at 10.00°C/min
- 3) Hold for 1.0 min at 200.00°C
- 4) Cool from 200.00°C to 30.00°C at 10.00°C/min

- 5) Hold for 1.0 min at 30.00°C
- 6) Heat from 30.00°C to 200.00°C at 10.00°C/min
- 7) Hold for 1.0 min at 200.00°C
- 8) Cool from 200.00°C to 30.00°C at 10.00°C/min

01.09.2011 16:14:23

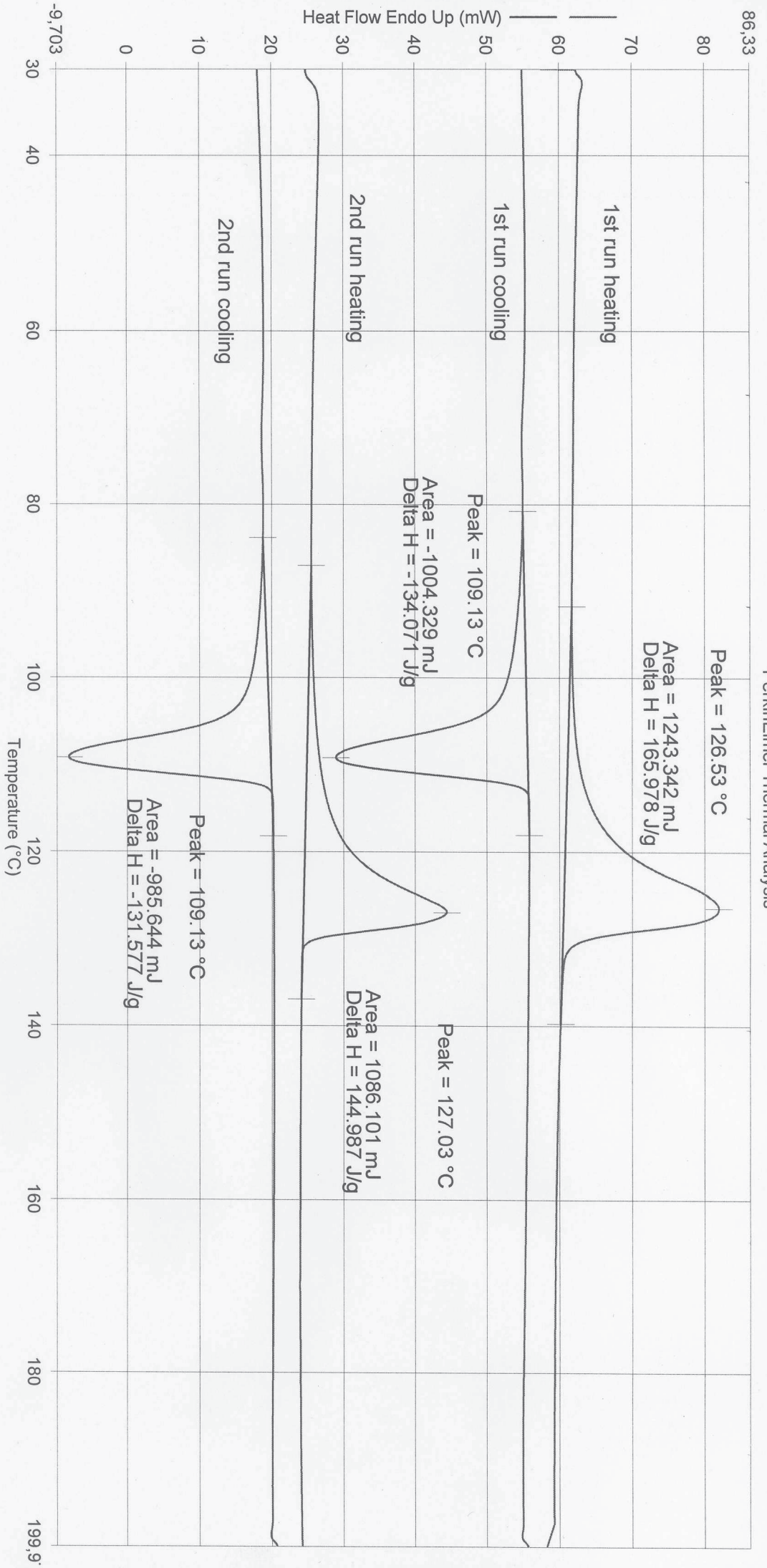
Operator ID: Schweizer
 Sample ID: 2000-168
 Sample Weight: 3.083 mg
 Comment: *Cat. 73 derived Polyethylene in the presence of 20 vol-% of CPE at 50°C.*



- 1) Hold for 1.0 min at 30.00°C
- 2) Heat from 30.00°C to 200.00°C at 10.00°C/min
- 3) Hold for 1.0 min at 200.00°C
- 4) Cool from 200.00°C to 30.00°C at 10.00°C/min
- 5) Hold for 1.0 min at 30.00°C
- 6) Heat from 30.00°C to 200.00°C at 10.00°C/min
- 7) Hold for 1.0 min at 200.00°C
- 8) Cool from 200.00°C to 30.00°C at 10.00°C/min

Operator ID: Schweizer
 Sample ID: 2000-169
 Sample Weight: 7.491 mg
 Comment: Cat. 13 derived Poly(E-co-CPE) in the presence of 40 vol-% of CPE at 50°C.

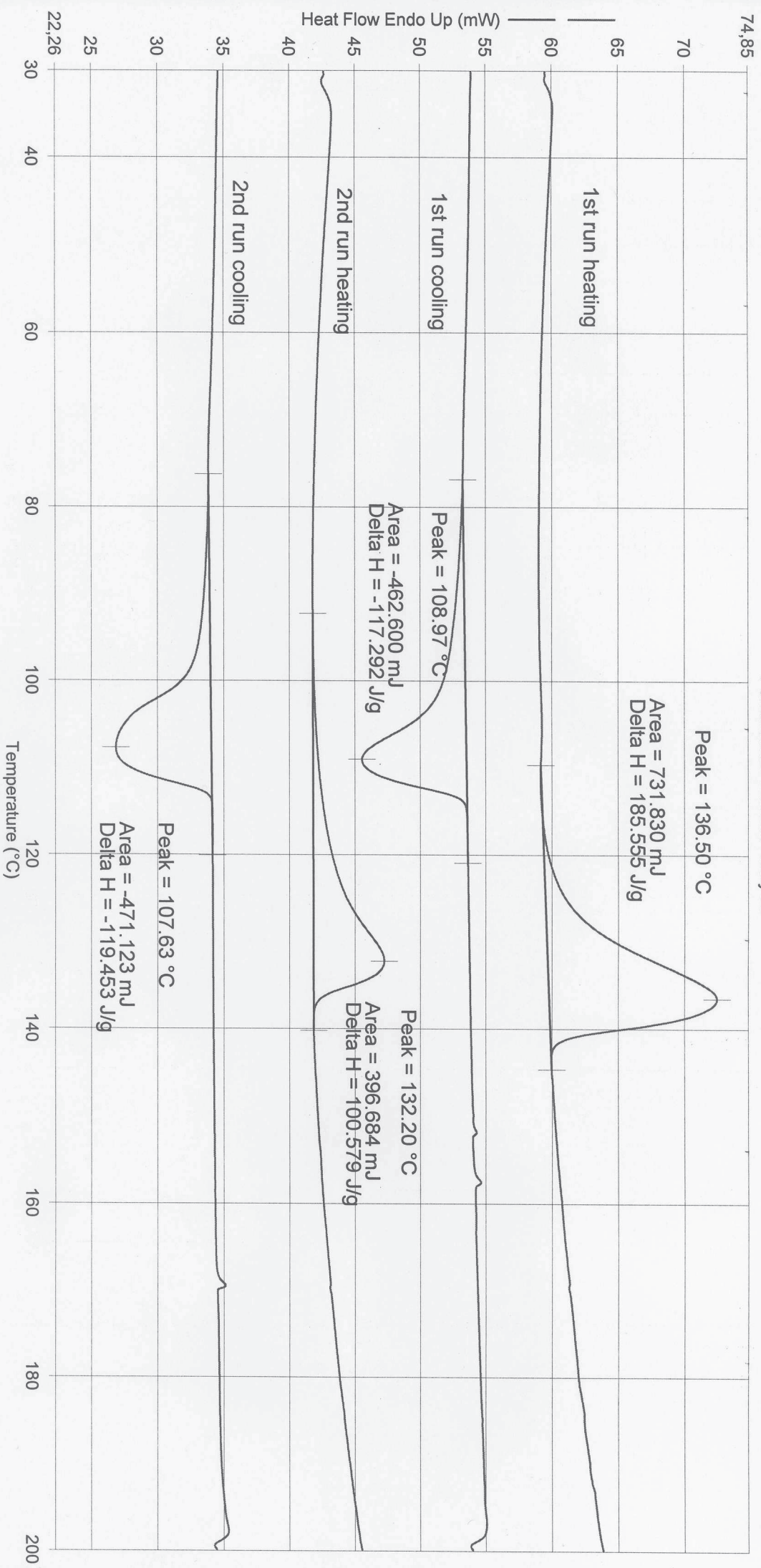
PerkinElmer Thermal Analysis



- 1) Hold for 1.0 min at 30.00°C
- 2) Heat from 30.00°C to 200.00°C at 10.00°C/min
- 3) Hold for 1.0 min at 200.00°C
- 4) Cool from 200.00°C to 30.00°C at 10.00°C/min
- 5) Hold for 1.0 min at 30.00°C
- 6) Heat from 30.00°C to 200.00°C at 10.00°C/min
- 7) Hold for 1.0 min at 200.00°C
- 8) Cool from 200.00°C to 30.00°C at 10.00°C/min

Operator ID: Schweizer
 Sample ID: 3000-20
 Sample Weight: 3.944 mg
 Comment: *Cat. #1 derived Polyethylene in the presence of 10 wt-% dPE at 58°C.*

PerkinElmer Thermal Analysis

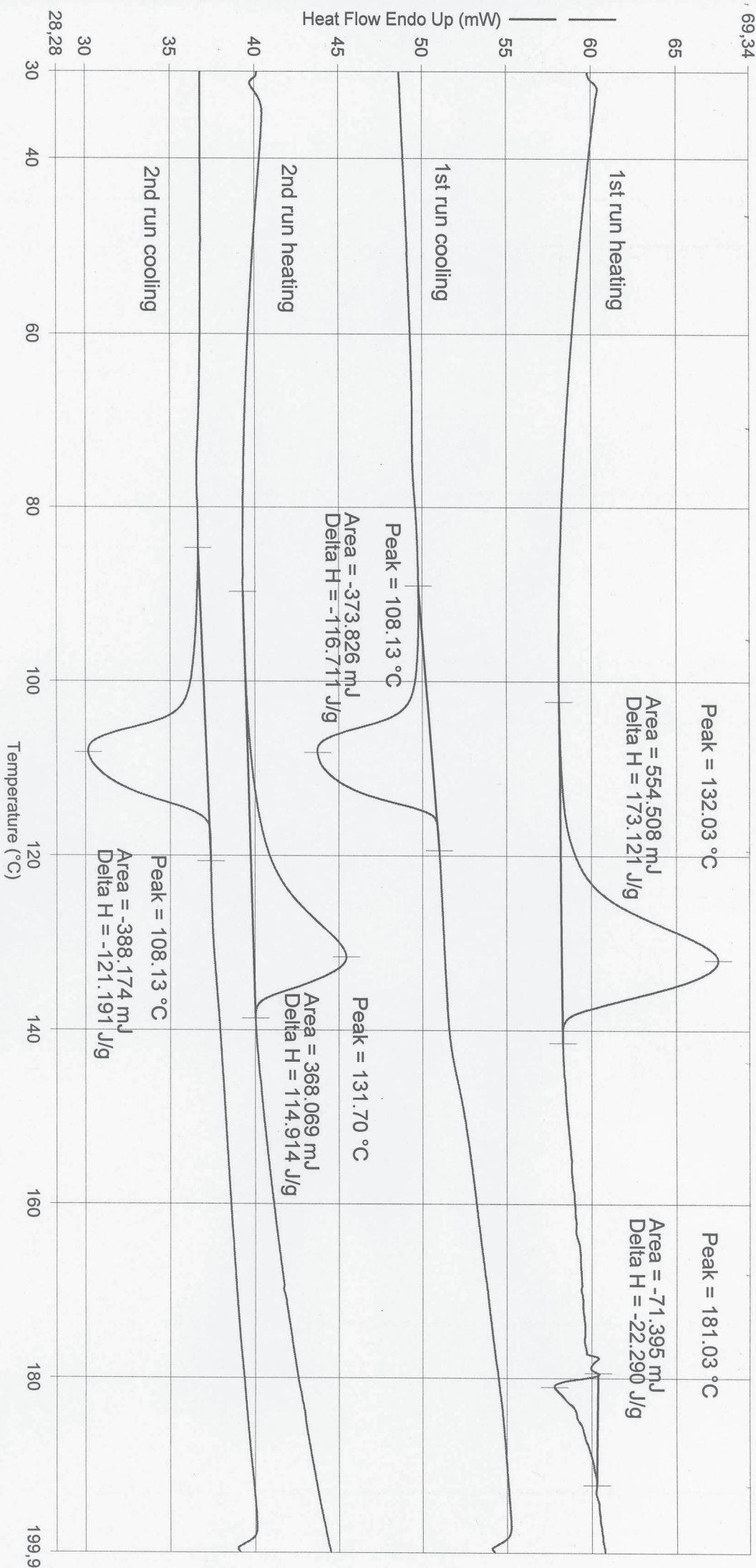


- 1) Hold for 1.0 min at 30.00°C
- 2) Heat from 30.00°C to 200.00°C at 10.00°C/min
- 3) Hold for 1.0 min at 200.00°C
- 4) Cool from 200.00°C to 30.00°C at 10.00°C/min
- 5) Hold for 1.0 min at 30.00°C
- 6) Heat from 30.00°C to 200.00°C at 10.00°C/min
- 7) Hold for 1.0 min at 200.00°C
- 8) Cool from 200.00°C to 30.00°C at 10.00°C/min

Operator ID: Schwelzer
 Sample ID: 3000-22
 Sample Weight: 3.203 mg
 Comment: Cat. #4

derived Polyethylene in the presence of 10 wt-% CPE at 70°C.

PerkinElmer Thermal Analysis



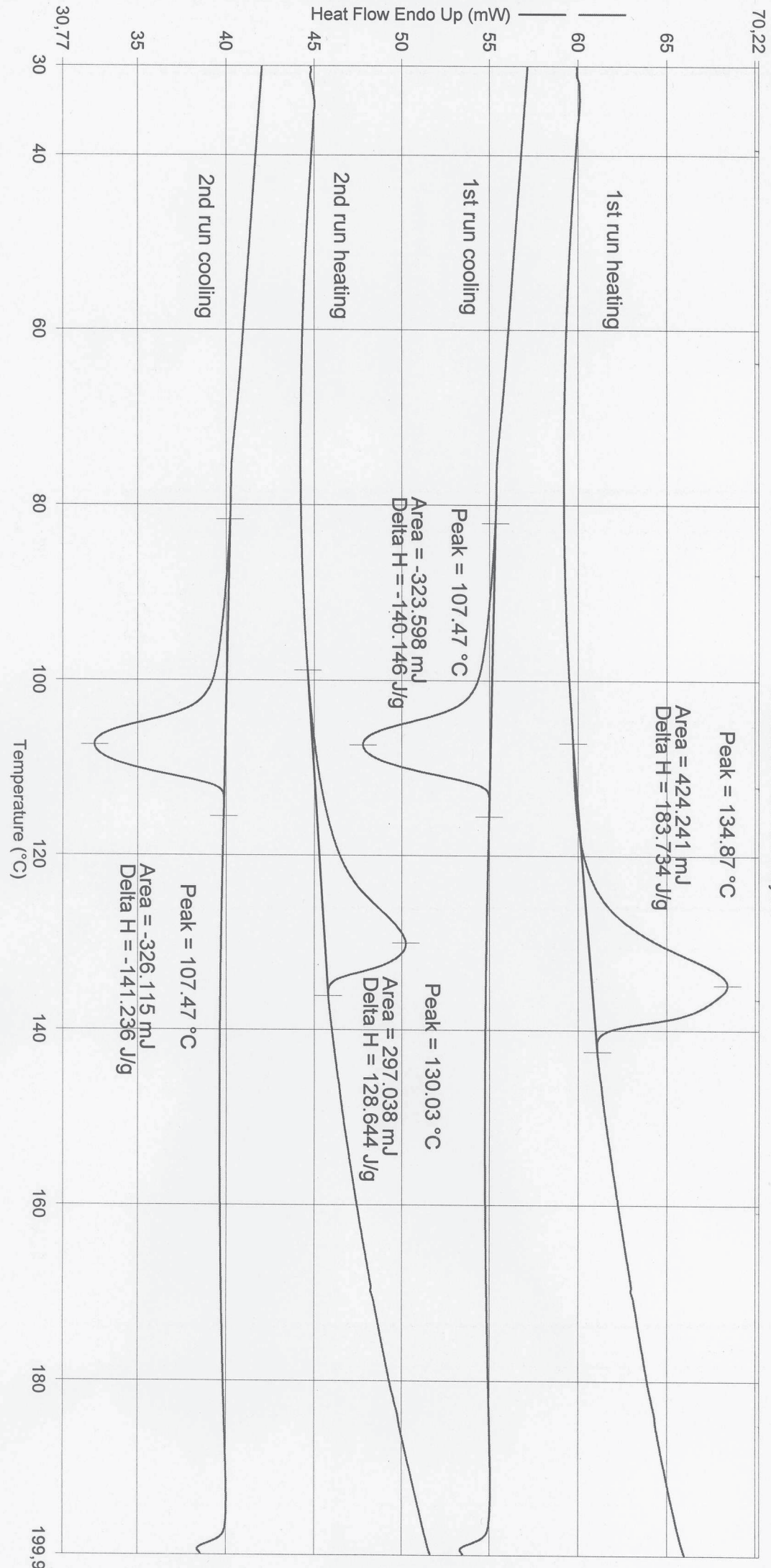
- 1) Hold for 1.0 min at 30.00°C
- 2) Heat from 30.00°C to 200.00°C at 10.00°C/min
- 3) Hold for 1.0 min at 200.00°C
- 4) Cool from 200.00°C to 30.00°C at 10.00°C/min

- 5) Hold for 1.0 min at 30.00°C
- 6) Heat from 30.00°C to 200.00°C at 10.00°C/min
- 7) Hold for 1.0 min at 200.00°C
- 8) Cool from 200.00°C to 30.00°C at 10.00°C/min

07.12.2011 13:33:44

Operator ID: Schweizer
Sample ID: 3000-21
Sample Weight: 2.309 mg
Comment: *cat. 211 derived Polyethylene in the presence of 25 vol-% of CPE at 50°C.*

PerkinElmer Thermal Analysis



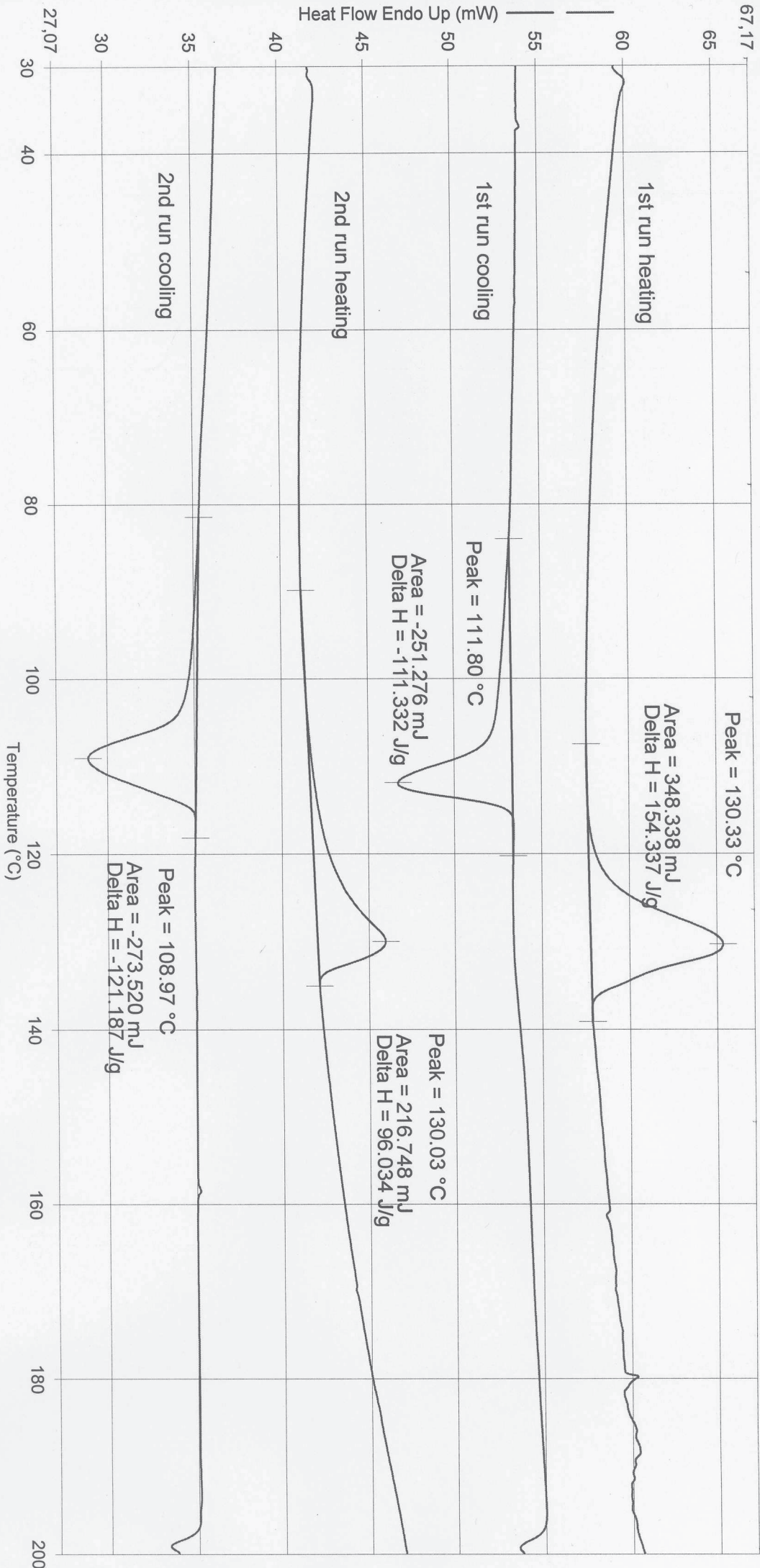
- 1) Hold for 1.0 min at 30.00°C
- 2) Heat from 30.00°C to 200.00°C at 10.00°C/min
- 3) Hold for 1.0 min at 200.00°C
- 4) Cool from 200.00°C to 30.00°C at 10.00°C/min

- 5) Hold for 1.0 min at 30.00°C
- 6) Heat from 30.00°C to 200.00°C at 10.00°C/min
- 7) Hold for 1.0 min at 200.00°C
- 8) Cool from 200.00°C to 30.00°C at 10.00°C/min

07.12.2011 13:20:42

Operator ID: Schweizer
 Sample ID: 3000-27
 Sample Weight: 2.257 mg
 Comment: *Cat. 24 derived Polyethylene in the presence of 25 wt-% of CPE at 78°C.*

PerkinElmer Thermal Analysis



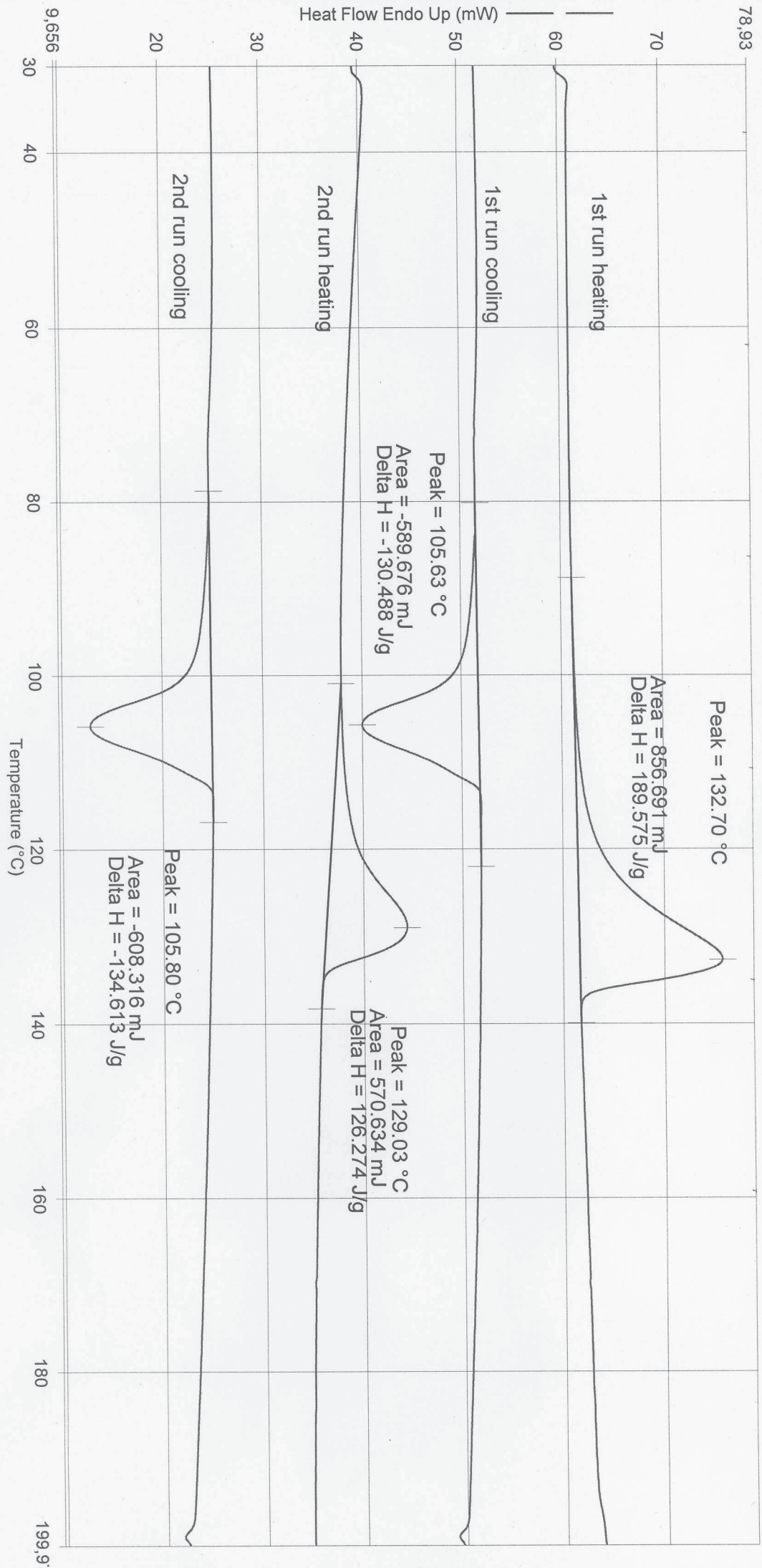
- 1) Hold for 1.0 min at 30.00°C
- 2) Heat from 30.00°C to 200.00°C at 10.00°C/min
- 3) Hold for 1.0 min at 200.00°C
- 4) Cool from 200.00°C to 30.00°C at 10.00°C/min

- 5) Hold for 1.0 min at 30.00°C
- 6) Heat from 30.00°C to 200.00°C at 10.00°C/min
- 7) Hold for 1.0 min at 200.00°C
- 8) Cool from 200.00°C to 30.00°C at 10.00°C/min

Operator ID: Schweizer
Sample ID: 2000-152
Sample Weight: 4.519 mg
Comment:

Cat. 23 deviled Polyethylene in the presence of 2 wt% of CPE at 50°C.

PerkinElmer Thermal Analysis



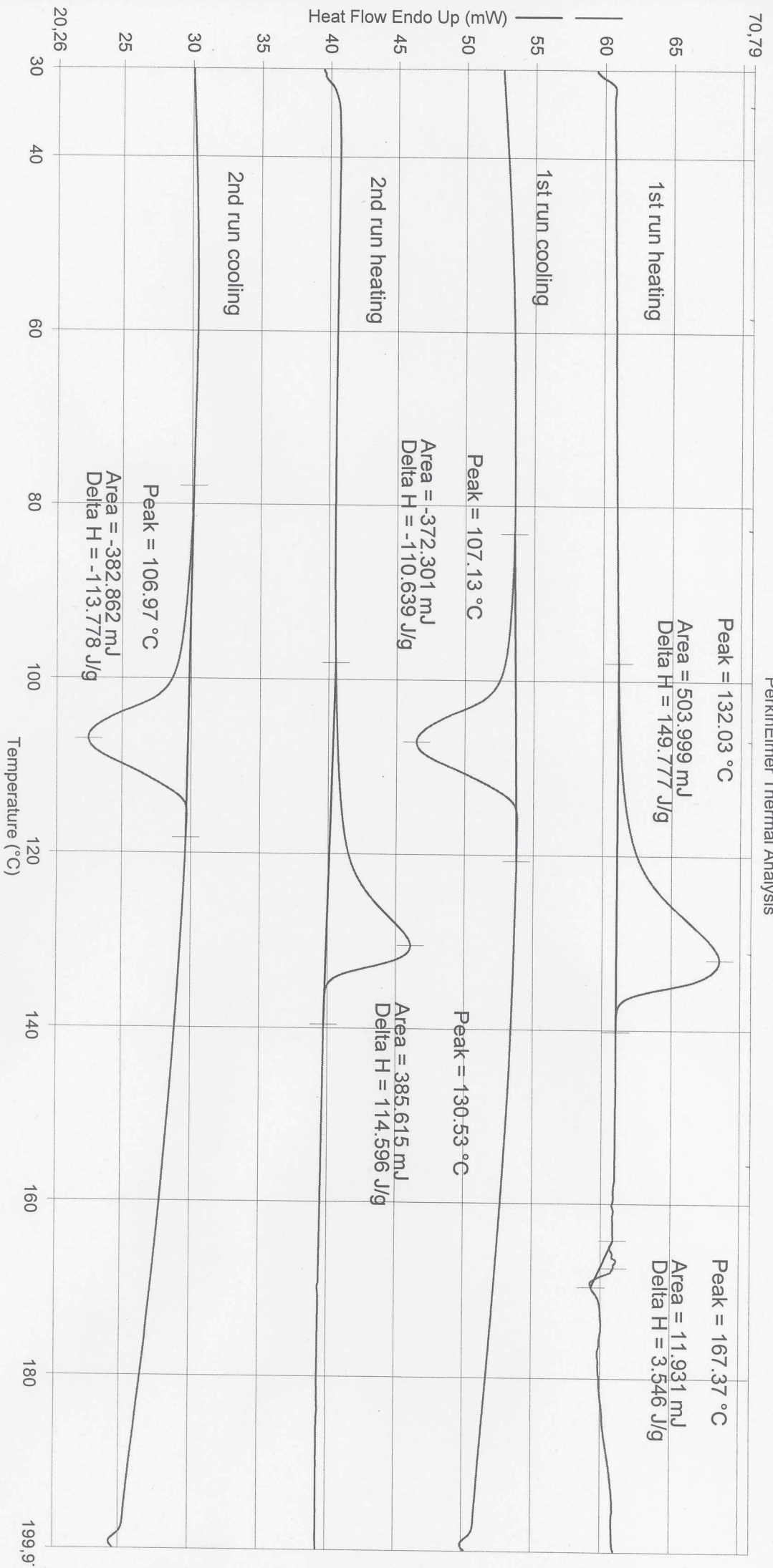
- 1) Hold for 1.0 min at 30.00°C
- 2) Heat from 30.00°C to 200.00°C at 10.00°C/min
- 3) Hold for 1.0 min at 200.00°C
- 4) Cool from 200.00°C to 30.00°C at 10.00°C/min

- 5) Hold for 1.0 min at 30.00°C
- 6) Heat from 30.00°C to 200.00°C at 10.00°C/min
- 7) Hold for 1.0 min at 200.00°C
- 8) Cool from 200.00°C to 30.00°C at 10.00°C/min

Operator ID: Schweizer
Sample ID: 2000-153
Sample Weight: 3.365 mg
Comment: Cat. 23

derived Polyethylene in the presence of 200-1% of CPE at 70°C.

PerkinElmer Thermal Analysis



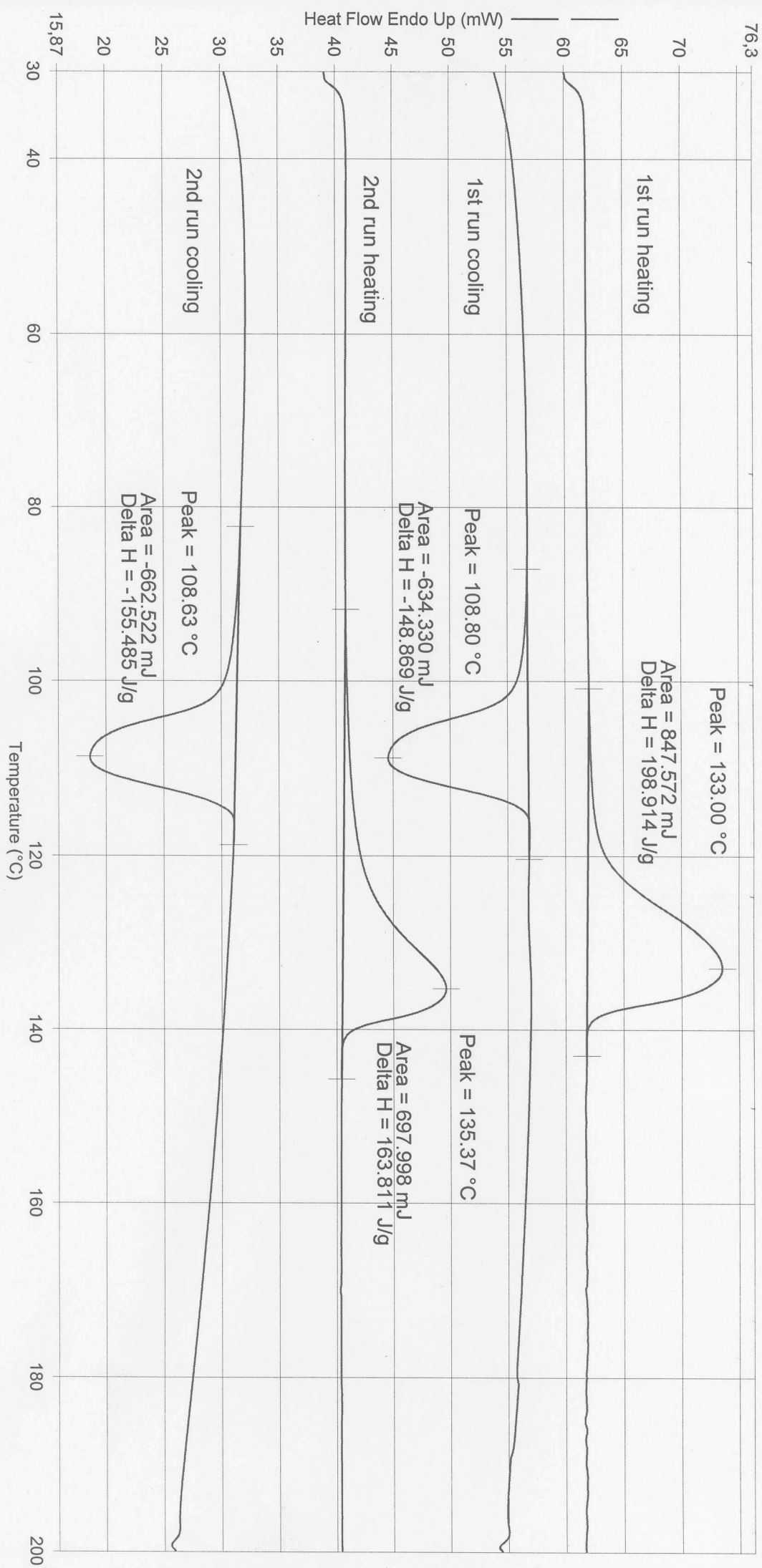
- 1) Hold for 1.0 min at 30.00°C
- 2) Heat from 30.00°C to 200.00°C at 10.00°C/min
- 3) Hold for 1.0 min at 200.00°C
- 4) Cool from 200.00°C to 30.00°C at 10.00°C/min

- 5) Hold for 1.0 min at 30.00°C
- 6) Heat from 30.00°C to 200.00°C at 10.00°C/min
- 7) Hold for 1.0 min at 200.00°C
- 8) Cool from 200.00°C to 30.00°C at 10.00°C/min

24.10.2011 12:52:00

Operator ID: Schweizer
 Sample ID: 2000-166
 Sample Weight: 4.261 mg
 Comment: Cat. 77 derived Polyethylene in the presence of 2 wt-% of PPE at 70°C

PerkinElmer Thermal Analysis

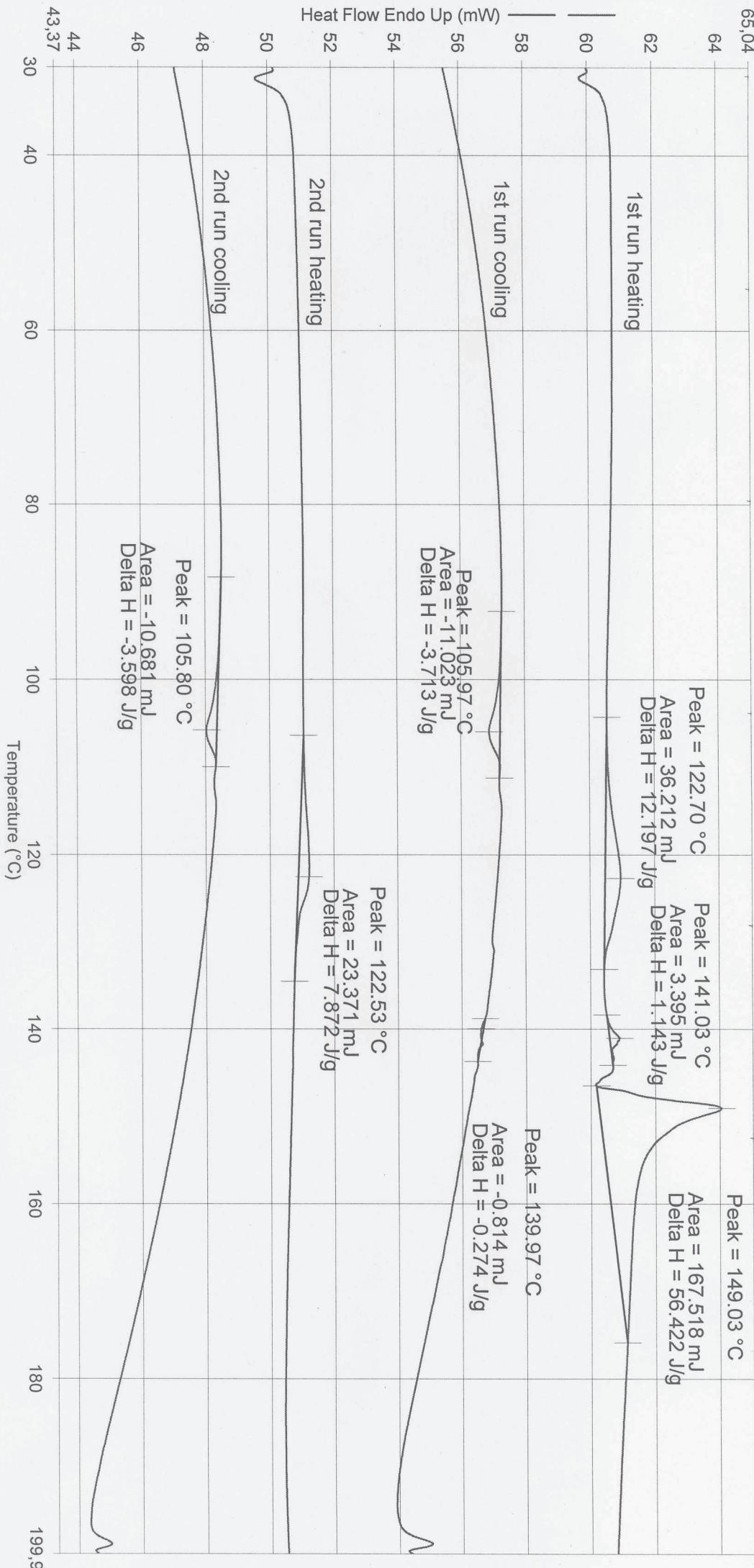


- 1) Hold for 1.0 min at 30.00°C
- 2) Heat from 30.00°C to 200.00°C at 10.00°C/min
- 3) Hold for 1.0 min at 200.00°C
- 4) Cool from 200.00°C to 30.00°C at 10.00°C/min
- 5) Hold for 1.0 min at 30.00°C
- 6) Heat from 30.00°C to 200.00°C at 10.00°C/min
- 7) Hold for 1.0 min at 200.00°C
- 8) Cool from 200.00°C to 30.00°C at 10.00°C/min

DSCs of poly(E-*co*-NBE)

Operator ID: Schweizer
 Sample ID: 2000-148
 Sample Weight: 2.969 mg
 Comment: cat. 13 derived poly(E-co-NBE) at 50°C, 4 bar E, cat: MAO; NBE (1:2000; 20,000)

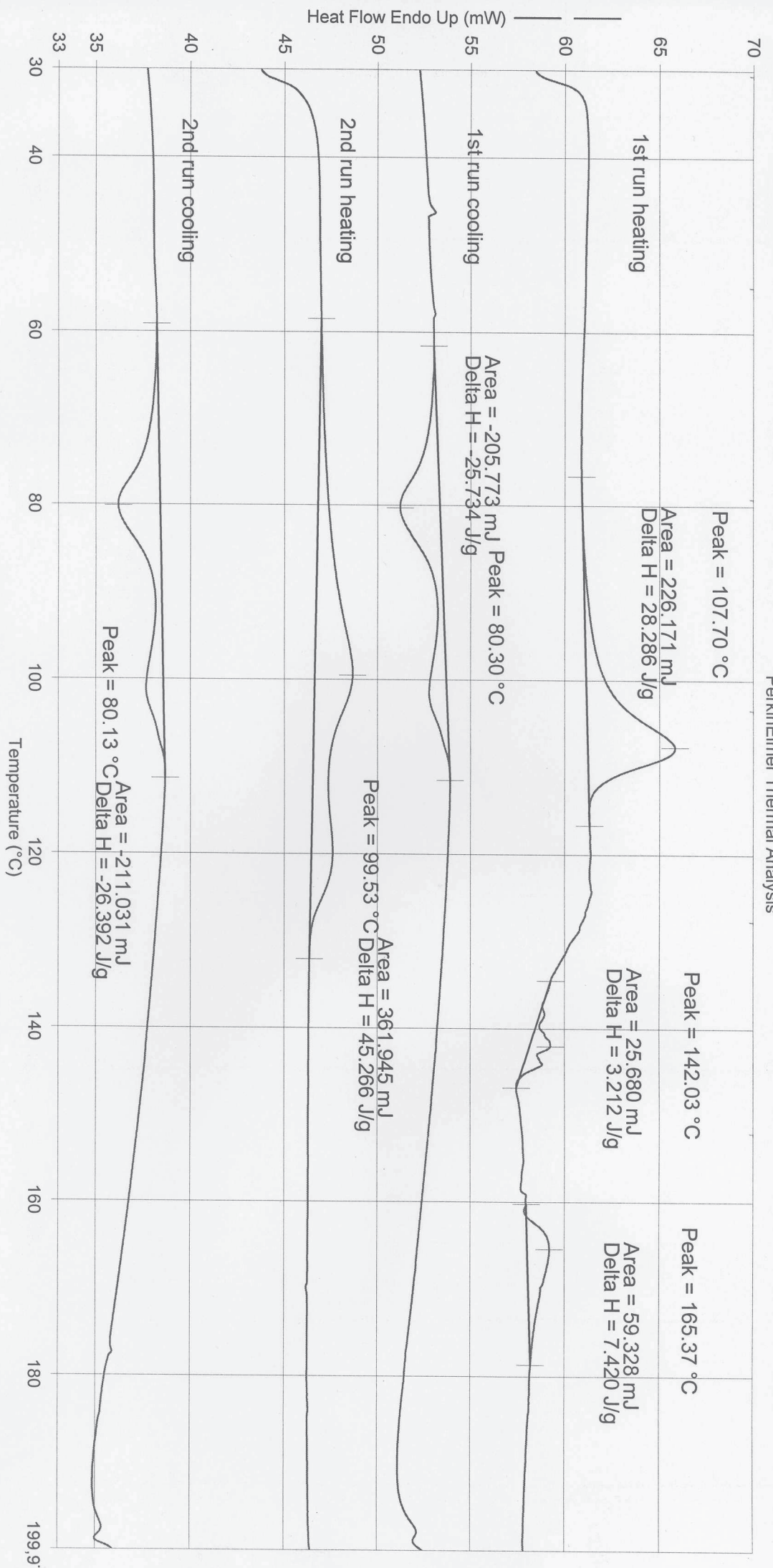
PerkinElmer Thermal Analysis



- 1) Hold for 1.0 min at 30.00°C
- 2) Heat from 30.00°C to 200.00°C at 10.00°C/min
- 3) Hold for 1.0 min at 200.00°C
- 4) Cool from 200.00°C to 30.00°C at 10.00°C/min
- 5) Hold for 1.0 min at 30.00°C
- 6) Heat from 30.00°C to 200.00°C at 10.00°C/min
- 7) Hold for 1.0 min at 200.00°C
- 8) Cool from 200.00°C to 30.00°C at 10.00°C/min

Operator ID: Schweizer
 Sample ID: 2000-161
 Sample Weight: 7.996 mg
 Comment: Cat. 13 dev. seed (poly (E-co-NBE) at 70°C, 4 bar E, cat. into NBE (1:2000, 120,000))

PerkinElmer Thermal Analysis



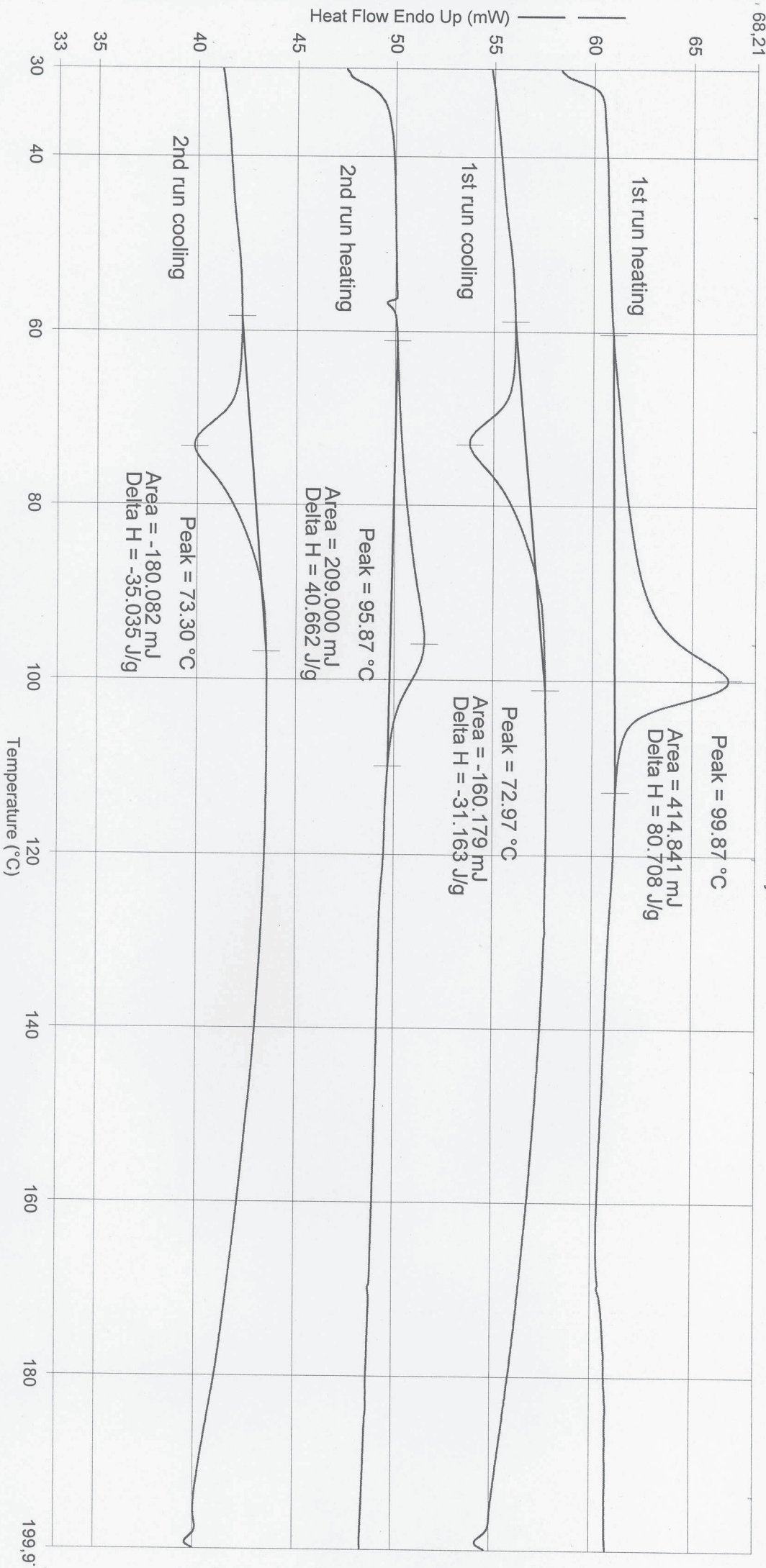
- 1) Hold for 1.0 min at 30.00°C
- 2) Heat from 30.00°C to 200.00°C at 10.00°C/min
- 3) Hold for 1.0 min at 200.00°C
- 4) Cool from 200.00°C to 30.00°C at 10.00°C/min

- 5) Hold for 1.0 min at 30.00°C
- 6) Heat from 30.00°C to 200.00°C at 10.00°C/min
- 7) Hold for 1.0 min at 200.00°C
- 8) Cool from 200.00°C to 30.00°C at 10.00°C/min

26.10.2011 17:11:47

Operator ID: Schweizer
 Sample ID: 2000-171
 Sample Weight: 5.140 mg
 Comment: Cat. 73 derived poly(E-co-NBE) at 90°C, 4 bar E, cat: MAO; NBE (1:2000:20,000)

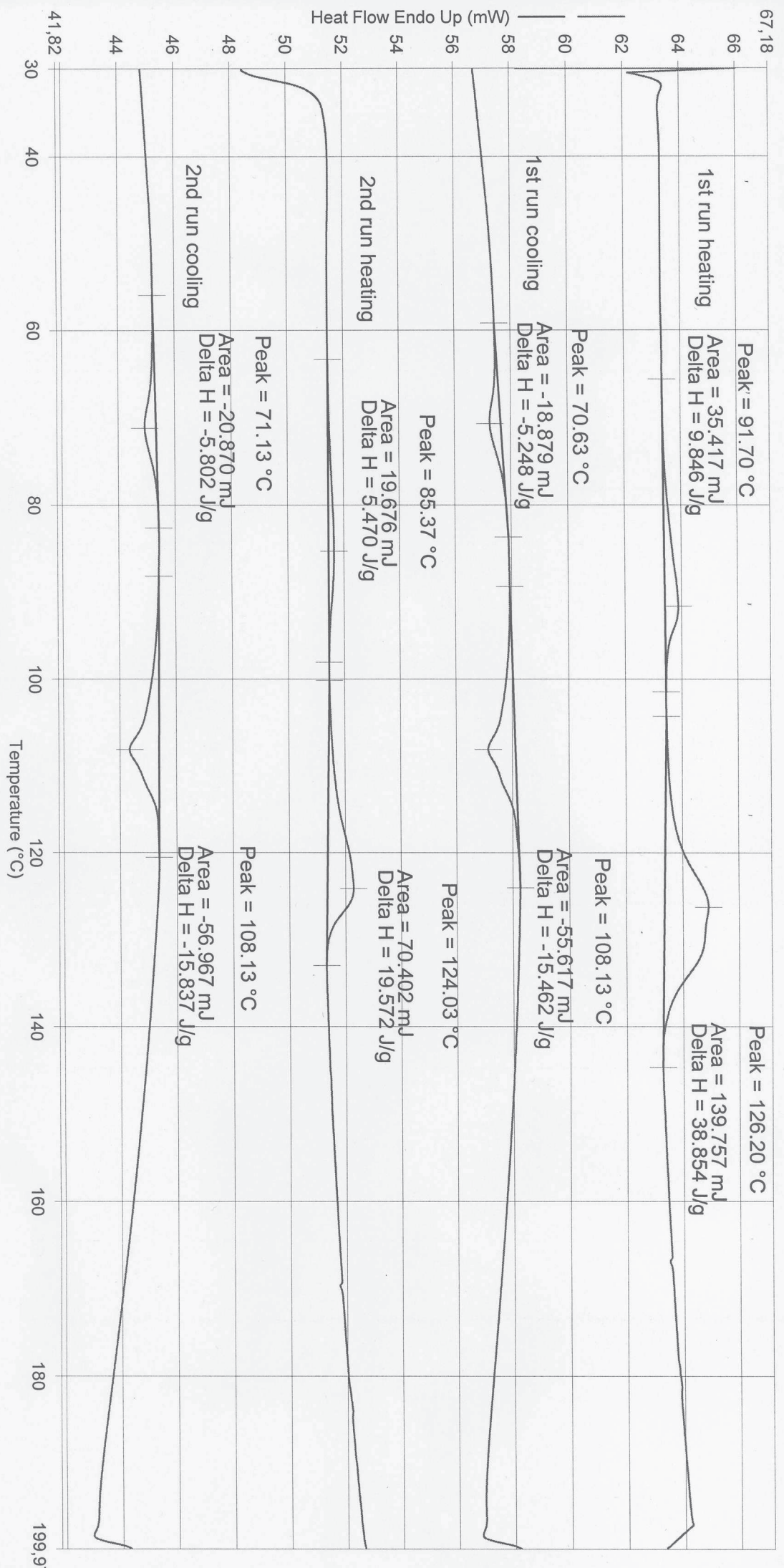
68.21
 PerkinElmer Thermal Analysis



- 1) Hold for 1.0 min at 30.00°C
- 2) Heat from 30.00°C to 200.00°C at 10.00°C/min
- 3) Hold for 1.0 min at 200.00°C
- 4) Cool from 200.00°C to 30.00°C at 10.00°C/min
- 5) Hold for 1.0 min at 30.00°C
- 6) Heat from 30.00°C to 200.00°C at 10.00°C/min
- 7) Hold for 1.0 min at 200.00°C
- 8) Cool from 200.00°C to 30.00°C at 10.00°C/min

28.10.2011 14:49:06

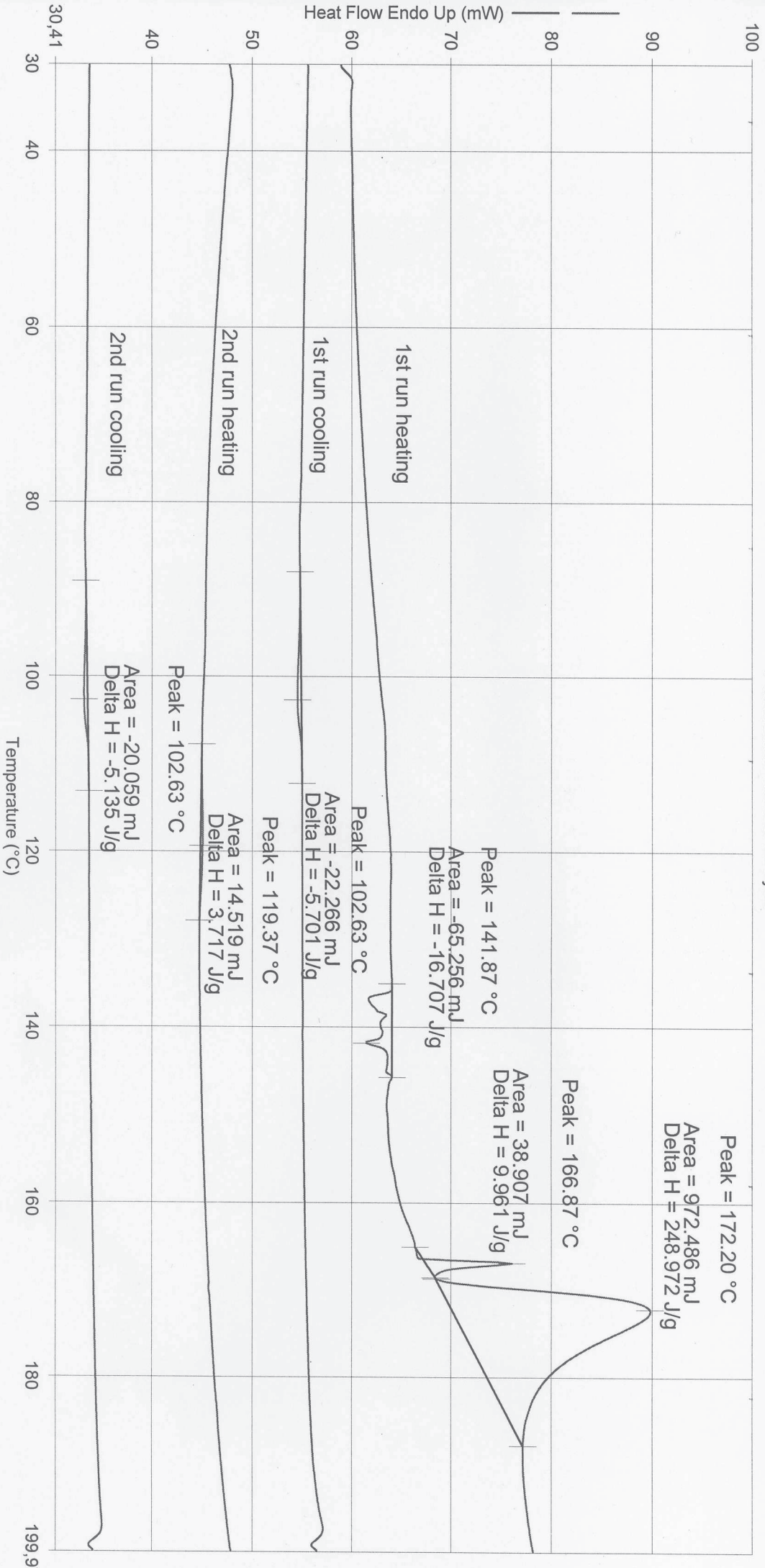
Operator ID: Schweizer
 Sample ID: 2000-174
 Sample Weight: 3.597 mg
 Comment: Cat. 13 derived Poly(e-co-NBE) at 110°C, 4 bar e, cat:IMAD;NBE (1:2000:20,000)



- 1) Hold for 1.0 min at 30.00°C
- 2) Heat from 30.00°C to 200.00°C at 10.00°C/min
- 3) Hold for 1.0 min at 200.00°C
- 4) Cool from 200.00°C to 30.00°C at 10.00°C/min
- 5) Hold for 1.0 min at 30.00°C
- 6) Heat from 30.00°C to 200.00°C at 10.00°C/min
- 7) Hold for 1.0 min at 200.00°C
- 8) Cool from 200.00°C to 30.00°C at 10.00°C/min

Operator ID: Schweizer
 Sample ID: 2000-179
 Sample Weight: 3.906 mg
 Comment: Cat: 17 derived poly(E-co-NBE) at 50°C, 4bar E, Cat: MAO: NBE (1:3000:30,000)

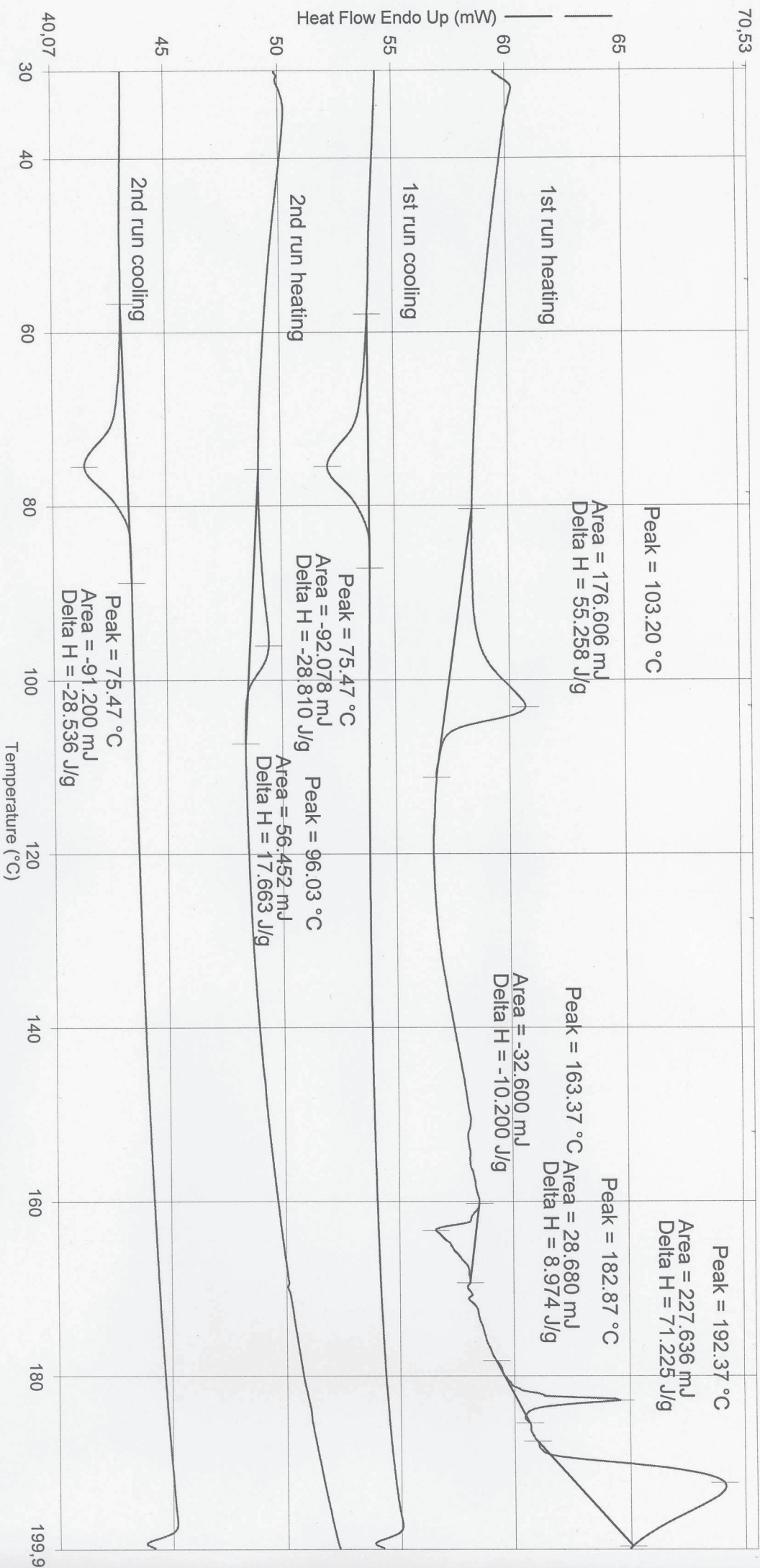
PerkinElmer Thermal Analysis



- 1) Hold for 1.0 min at 30.00°C
- 2) Heat from 30.00°C to 200.00°C at 10.00°C/min
- 3) Hold for 1.0 min at 200.00°C
- 4) Cool from 200.00°C to 30.00°C at 10.00°C/min
- 5) Hold for 1.0 min at 30.00°C
- 6) Heat from 30.00°C to 200.00°C at 10.00°C/min
- 7) Hold for 1.0 min at 200.00°C
- 8) Cool from 200.00°C to 30.00°C at 10.00°C/min

derived Poly(E-co-NBE) at JSC, 4 have, cat: M1A0; NBE (1:2000; 80,000)

PerkinElmer Thermal Analysis

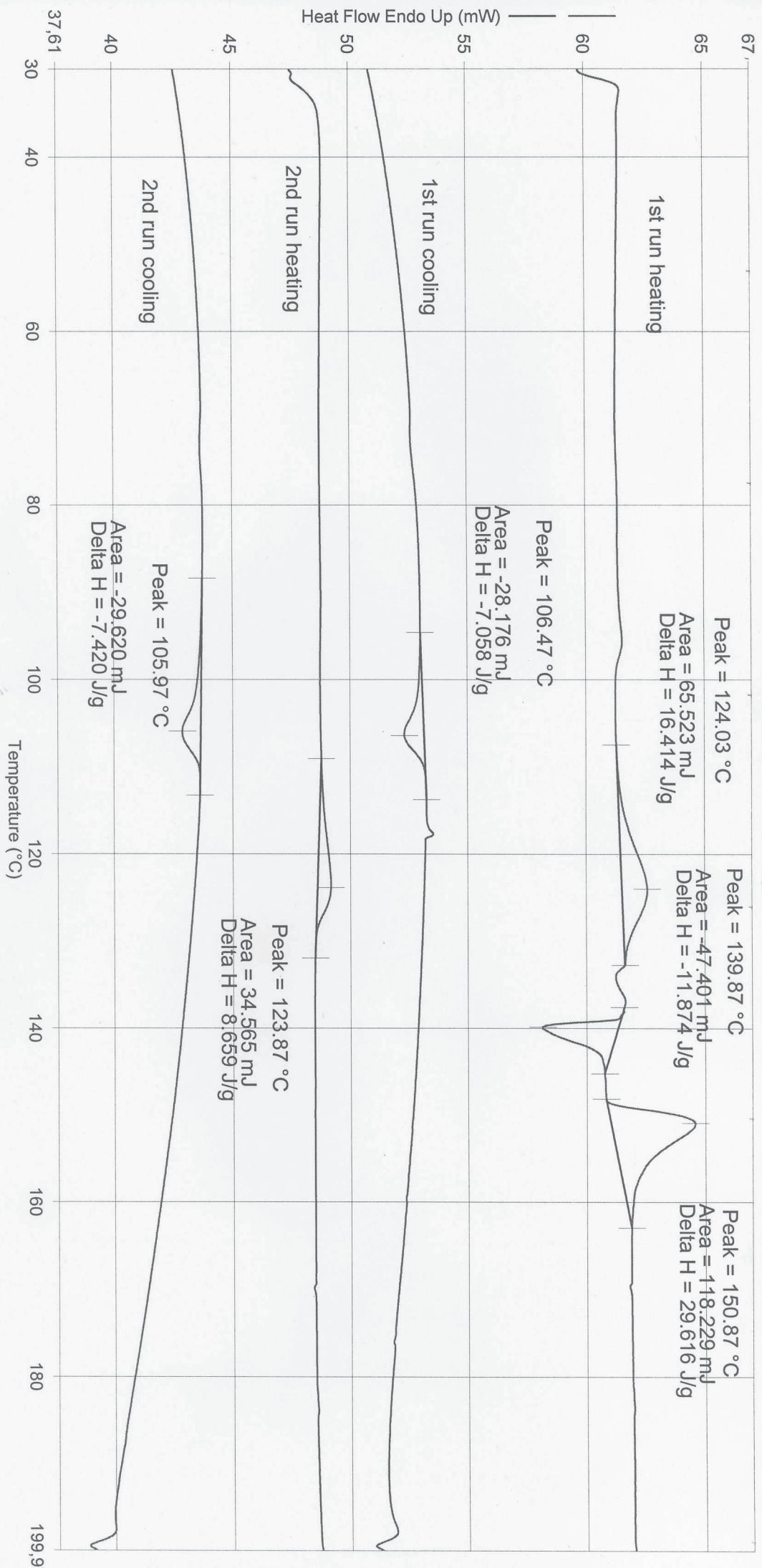


- 1) Hold for 1.0 min at 30.00°C
- 2) Heat from 30.00°C to 200.00°C at 10.00°C/min
- 3) Hold for 1.0 min at 200.00°C
- 4) Cool from 200.00°C to 30.00°C at 10.00°C/min

- 5) Hold for 1.0 min at 30.00°C
- 6) Heat from 30.00°C to 200.00°C at 10.00°C/min
- 7) Hold for 1.0 min at 200.00°C
- 8) Cool from 200.00°C to 30.00°C at 10.00°C/min

Operator ID: Schweizer
 Sample ID: 2000-172
 Sample Weight: 3.992 mg
 Comment: Cat. 17 deviced poly(E-co-NBE) at 90°C, 4 bar E ; cat: MAD: NBE (1: 2000: 20,000)

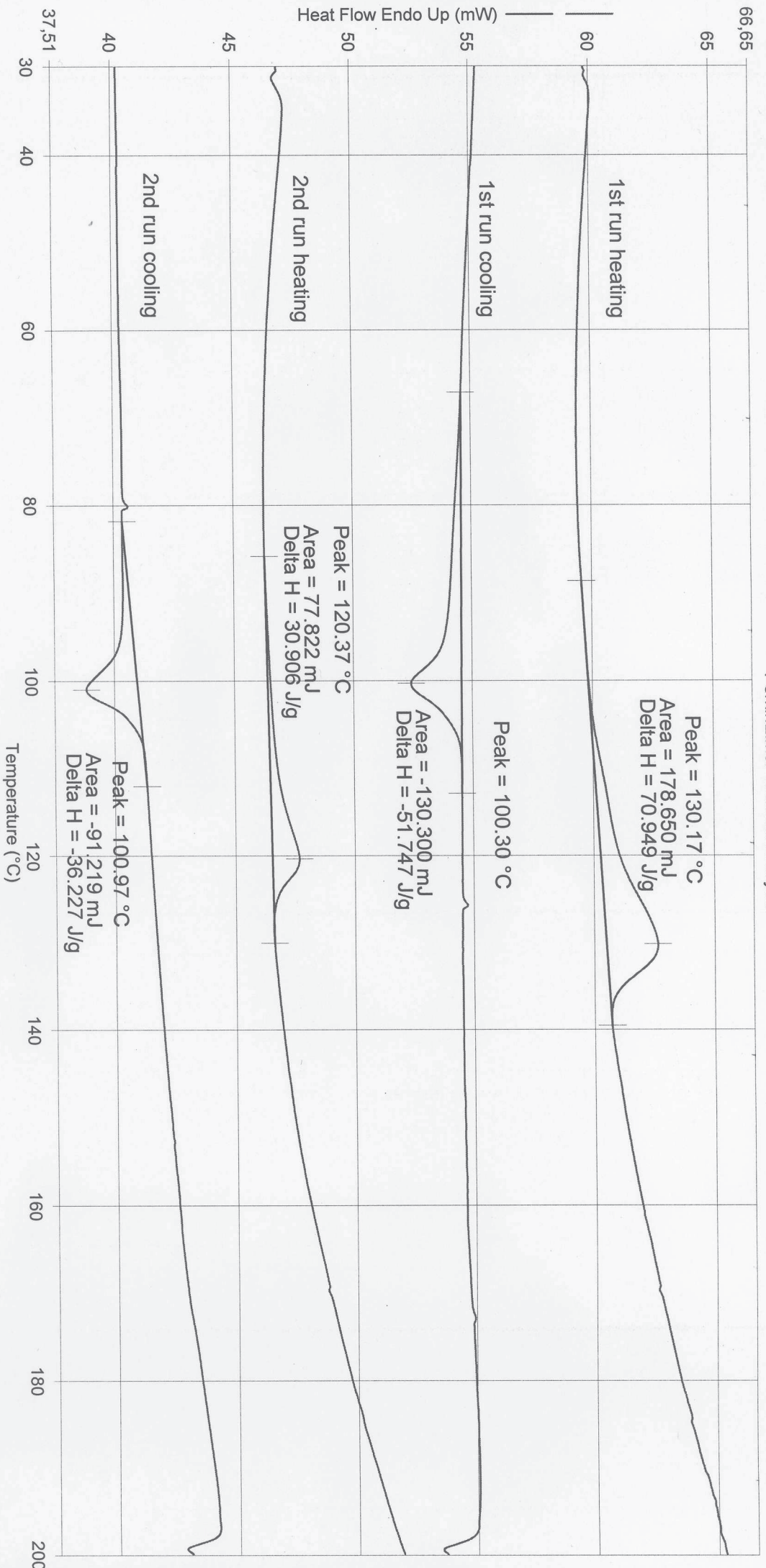
PerkinElmer Thermal Analysis



- 1) Hold for 1.0 min at 30.00°C
- 2) Heat from 30.00°C to 200.00°C at 10.00°C/min
- 3) Hold for 1.0 min at 200.00°C
- 4) Cool from 200.00°C to 30.00°C at 10.00°C/min
- 5) Hold for 1.0 min at 30.00°C
- 6) Heat from 30.00°C to 200.00°C at 10.00°C/min
- 7) Hold for 1.0 min at 200.00°C
- 8) Cool from 200.00°C to 30.00°C at 10.00°C/min

Operator ID: Schwelzer
 Sample ID: 3000-15
 Sample Weight: 2.518 mg
 Comment: *Cat. 24 derived Poly(E-co-NBE) at 50C; 4 bar E; cat: MAD: NBE (1: 2000; 20: 1000)*

PerkinElmer Thermal Analysis

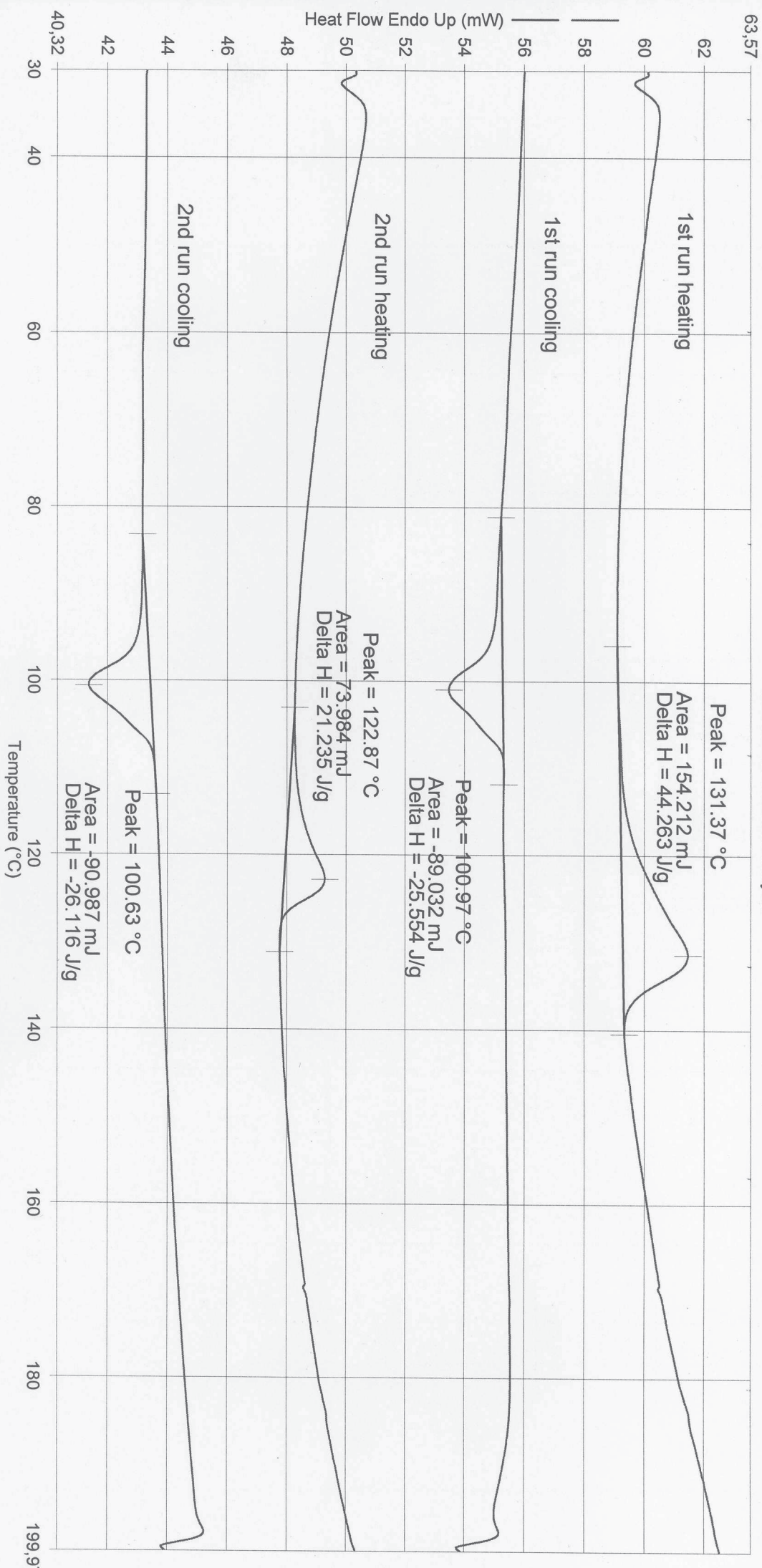


- 1) Hold for 1.0 min at 30.00°C
- 2) Heat from 30.00°C to 200.00°C at 10.00°C/min
- 3) Hold for 1.0 min at 200.00°C
- 4) Cool from 200.00°C to 30.00°C at 10.00°C/min

- 5) Hold for 1.0 min at 30.00°C
- 6) Heat from 30.00°C to 200.00°C at 10.00°C/min
- 7) Hold for 1.0 min at 200.00°C
- 8) Cool from 200.00°C to 30.00°C at 10.00°C/min

Operator ID: Schweizer
 Sample ID: 3000-17
 Sample Weight: 3.484 mg
 Comment: Cat. 24 derived poly(E-co-NBE) at 70°C, 4 bar E; cat: mAD; NBE (1:2000; 20,000)

PerkinElmer Thermal Analysis

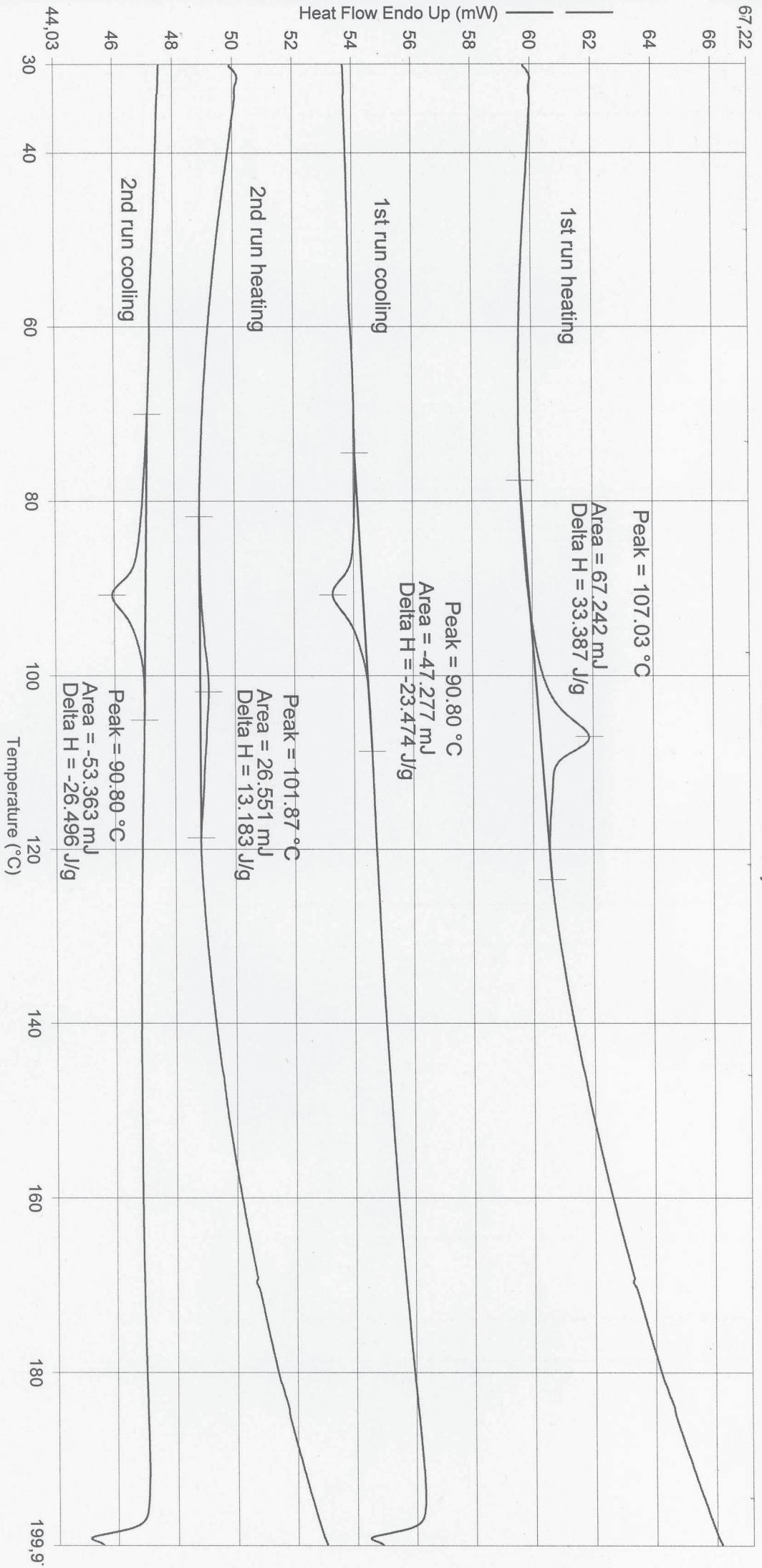


- 1) Hold for 1.0 min at 30.00°C
- 2) Heat from 30.00°C to 200.00°C at 10.00°C/min
- 3) Hold for 1.0 min at 200.00°C
- 4) Cool from 200.00°C to 30.00°C at 10.00°C/min
- 5) Hold for 1.0 min at 30.00°C
- 6) Heat from 30.00°C to 200.00°C at 10.00°C/min
- 7) Hold for 1.0 min at 200.00°C
- 8) Cool from 200.00°C to 30.00°C at 10.00°C/min

06.12.2011 14:03:00

Operator ID: Schweizer
 Sample ID: 3000-12
 Sample Weight: 2.014 mg
 Comment: Cat. 26 derived Poly(E-co-NBE) at qdc, 4 bar E; Cat: MAO: NBE (1: 8000: 20,000)

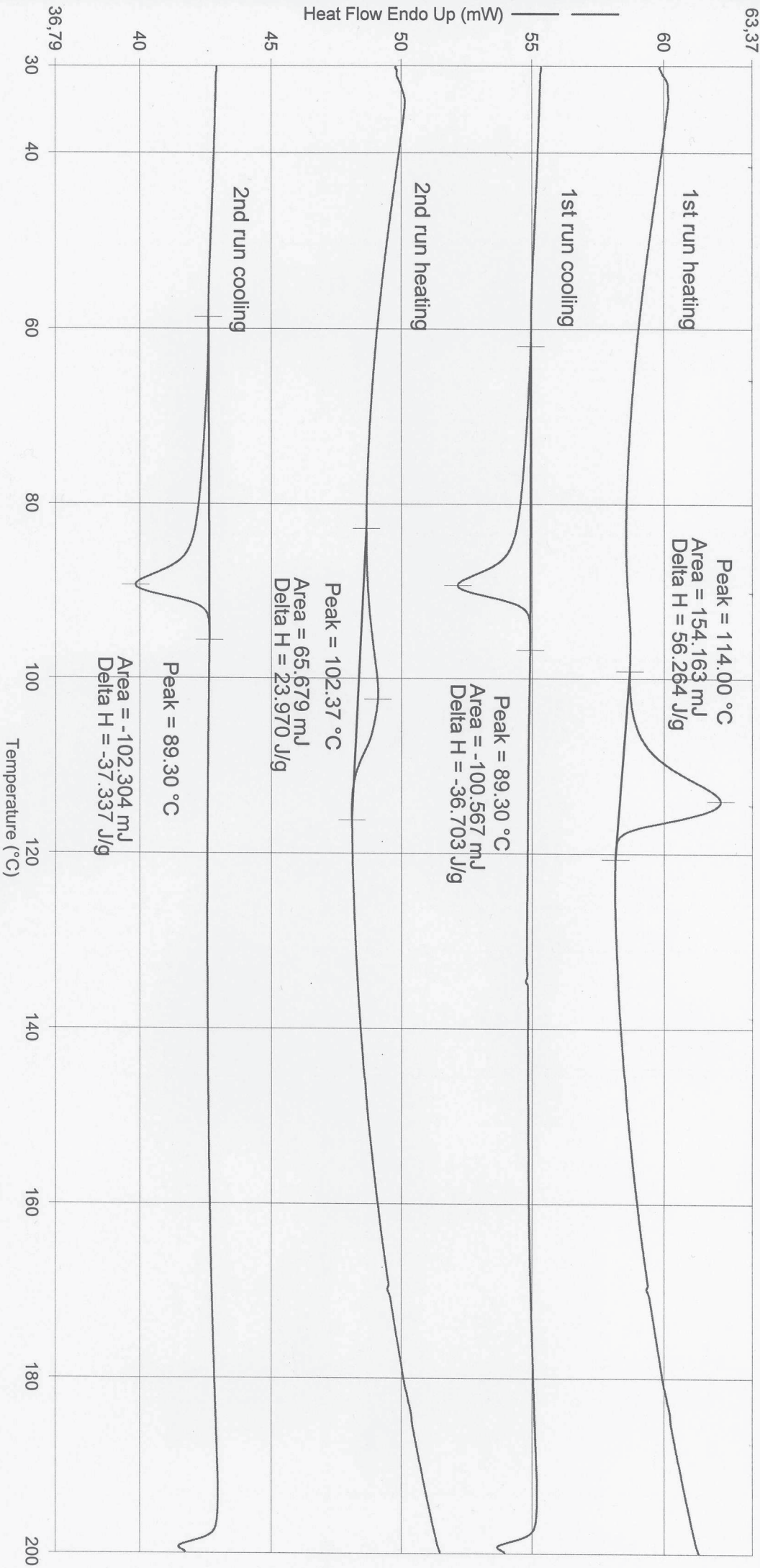
PerkinElmer Thermal Analysis



- 1) Hold for 1.0 min at 30.00°C
- 2) Heat from 30.00°C to 200.00°C at 10.00°C/min
- 3) Hold for 1.0 min at 200.00°C
- 4) Cool from 200.00°C to 30.00°C at 10.00°C/min
- 5) Hold for 1.0 min at 30.00°C
- 6) Heat from 30.00°C to 200.00°C at 10.00°C/min
- 7) Hold for 1.0 min at 200.00°C
- 8) Cool from 200.00°C to 30.00°C at 10.00°C/min

Operator ID: Schweizer
 Sample ID: 3000-11
 Sample Weight: 2.740 mg
 Comment: Cat: 26 derived Poly(E-co-NBE) at 50% UBAVE ; cat: MAO: NBE (1:2000:20,000)

PerkinElmer Thermal Analysis



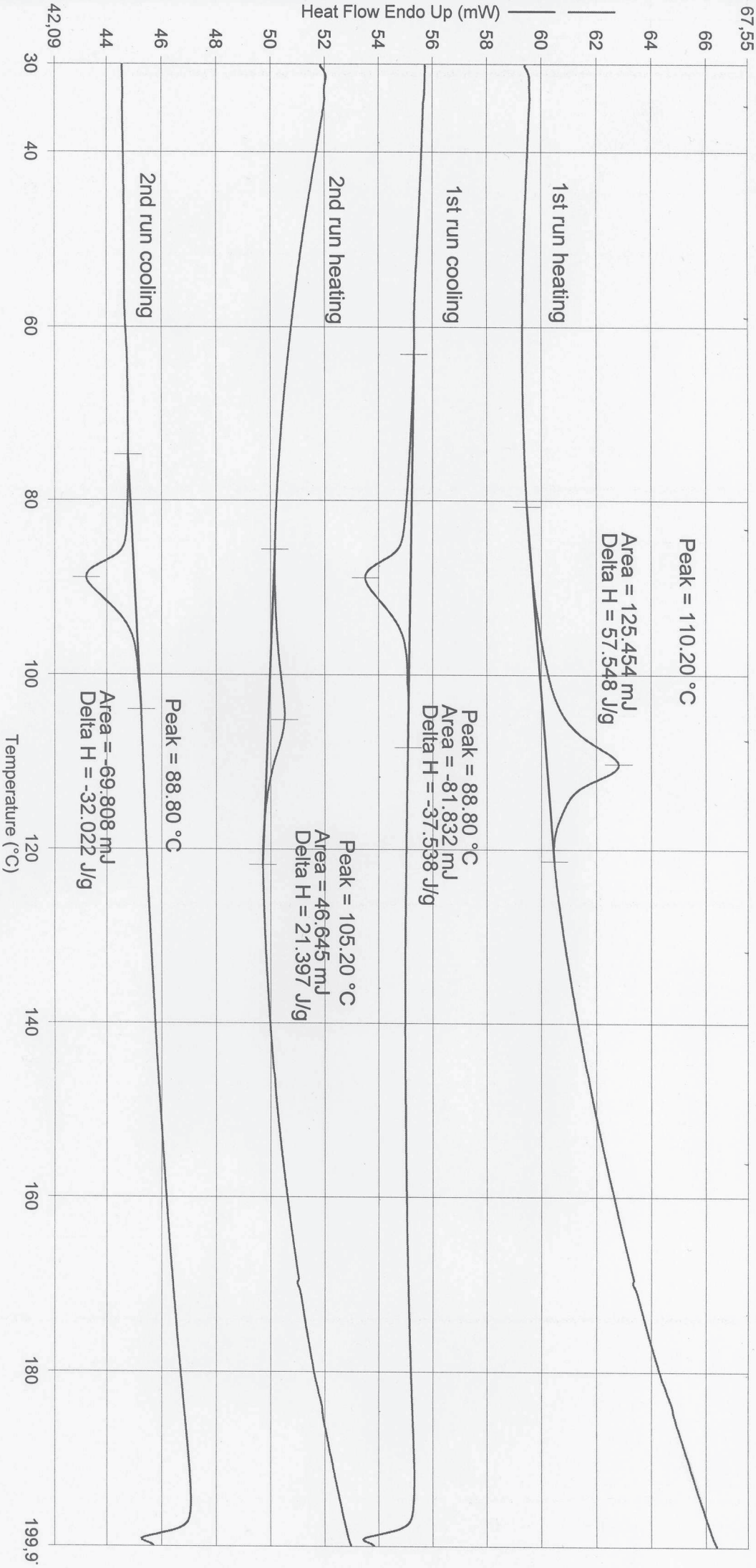
- 1) Hold for 1.0 min at 30.00°C
- 2) Heat from 30.00°C to 200.00°C at 10.00°C/min
- 3) Hold for 1.0 min at 200.00°C
- 4) Cool from 200.00°C to 30.00°C at 10.00°C/min

- 5) Hold for 1.0 min at 30.00°C
- 6) Heat from 30.00°C to 200.00°C at 10.00°C/min
- 7) Hold for 1.0 min at 200.00°C
- 8) Cool from 200.00°C to 30.00°C at 10.00°C/min

05.12.2011 14:33:34

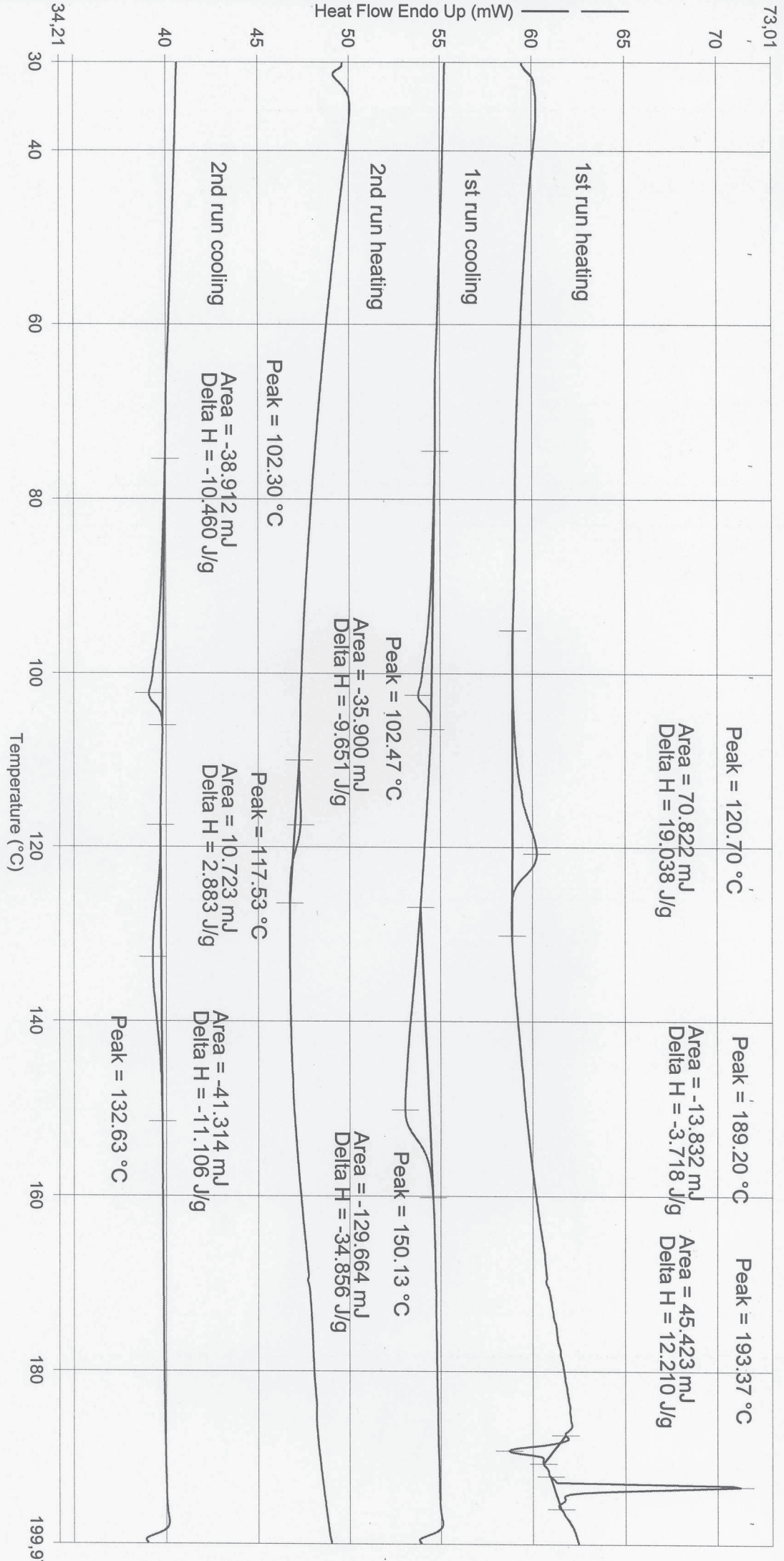
Operator ID: Schweizer
 Sample ID: 3000-10
 Sample Weight: 2.180 mg
 Comment: Cat. 26 devived Poly(E-co-NBE) at 78C, 4 bar E; cat: MAO; NBE (1:2000:20,000)

PerkinElmer Thermal Analysis



- 1) Hold for 1.0 min at 30.00°C
- 2) Heat from 30.00°C to 200.00°C at 10.00°C/min
- 3) Hold for 1.0 min at 200.00°C
- 4) Cool from 200.00°C to 30.00°C at 10.00°C/min
- 5) Hold for 1.0 min at 30.00°C
- 6) Heat from 30.00°C to 200.00°C at 10.00°C/min
- 7) Hold for 1.0 min at 200.00°C
- 8) Cool from 200.00°C to 30.00°C at 10.00°C/min

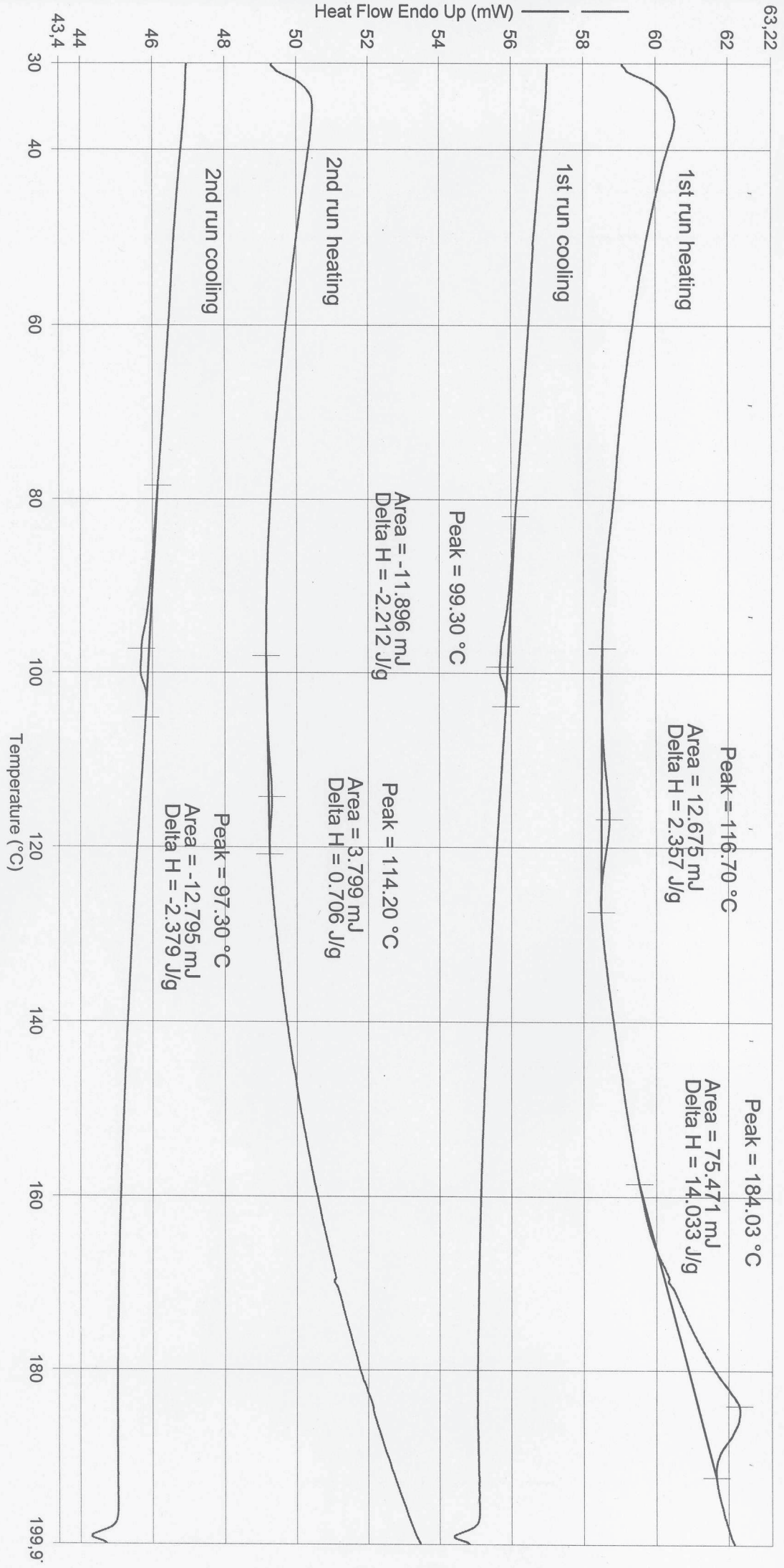
Operator ID: Schweizer
 Sample ID: 3000-9
 Sample Weight: 3.720 mg
 Comment: Cat. 27 derived Poly(E-co-NBE) at 70°C, 4 bar E; cat: MA0; NBE (1: 2000; 20000)



- 1) Hold for 1.0 min at 30.00°C
- 2) Heat from 30.00°C to 200.00°C at 10.00°C/min
- 3) Hold for 1.0 min at 200.00°C
- 4) Cool from 200.00°C to 30.00°C at 10.00°C/min
- 5) Hold for 1.0 min at 30.00°C
- 6) Heat from 30.00°C to 200.00°C at 10.00°C/min
- 7) Hold for 1.0 min at 200.00°C
- 8) Cool from 200.00°C to 30.00°C at 10.00°C/min

02.12.2011 17:59:16

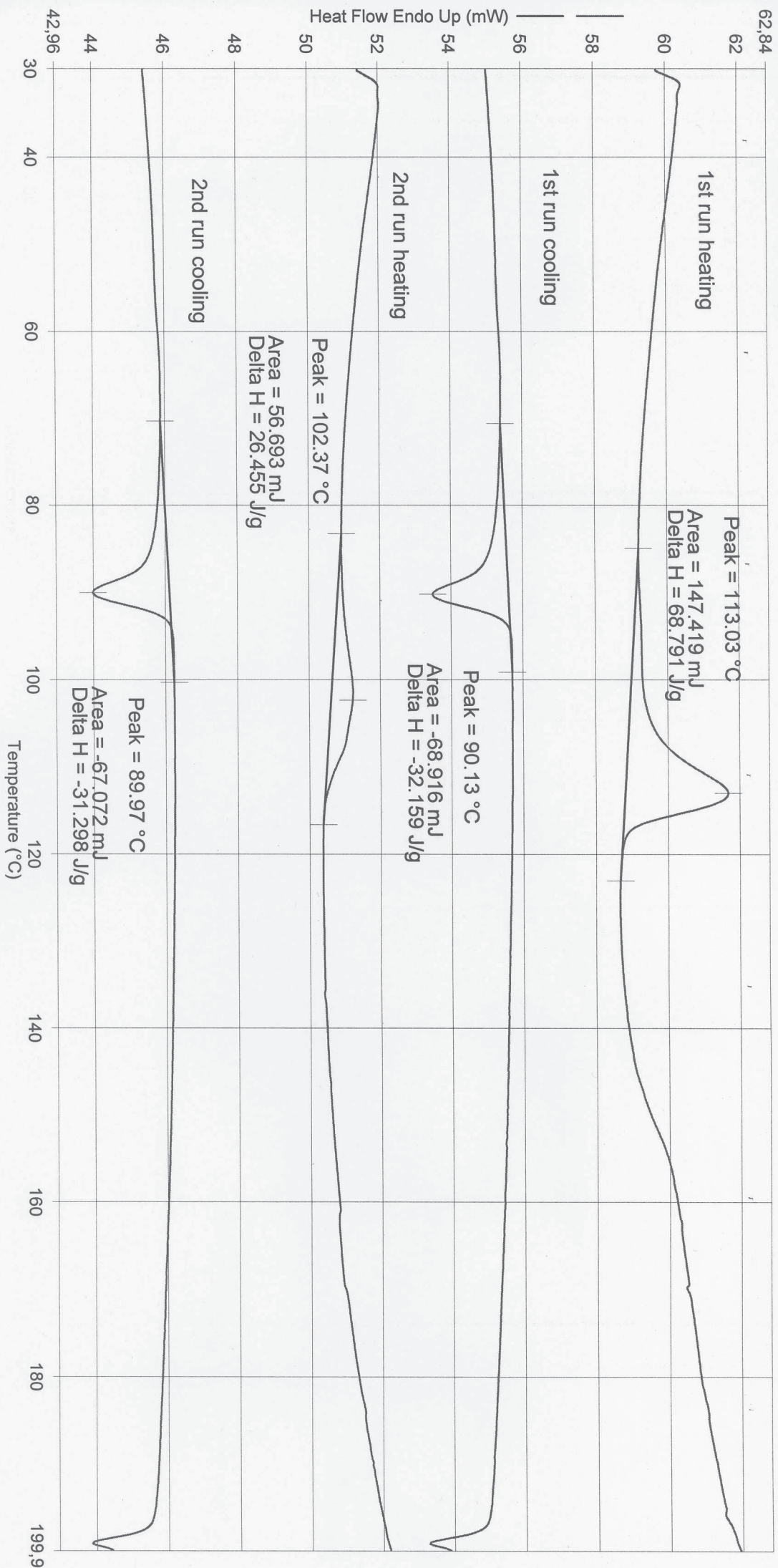
Operator ID: Schweizer
 Sample ID: 3000-8
 Sample Weight: 5.378 mg
 Comment: Cat. 97 derived poly(E-co-NBE) at 50°C, 4 bar E; cat: MAPI-NBE (1: 2000; 20,000)



- 1) Hold for 1.0 min at 30.00°C
- 2) Heat from 30.00°C to 200.00°C at 10.00°C/min
- 3) Hold for 1.0 min at 200.00°C
- 4) Cool from 200.00°C to 30.00°C at 10.00°C/min
- 5) Hold for 1.0 min at 30.00°C
- 6) Heat from 30.00°C to 200.00°C at 10.00°C/min
- 7) Hold for 1.0 min at 200.00°C
- 8) Cool from 200.00°C to 30.00°C at 10.00°C/min

02.12.2011 16:56:22

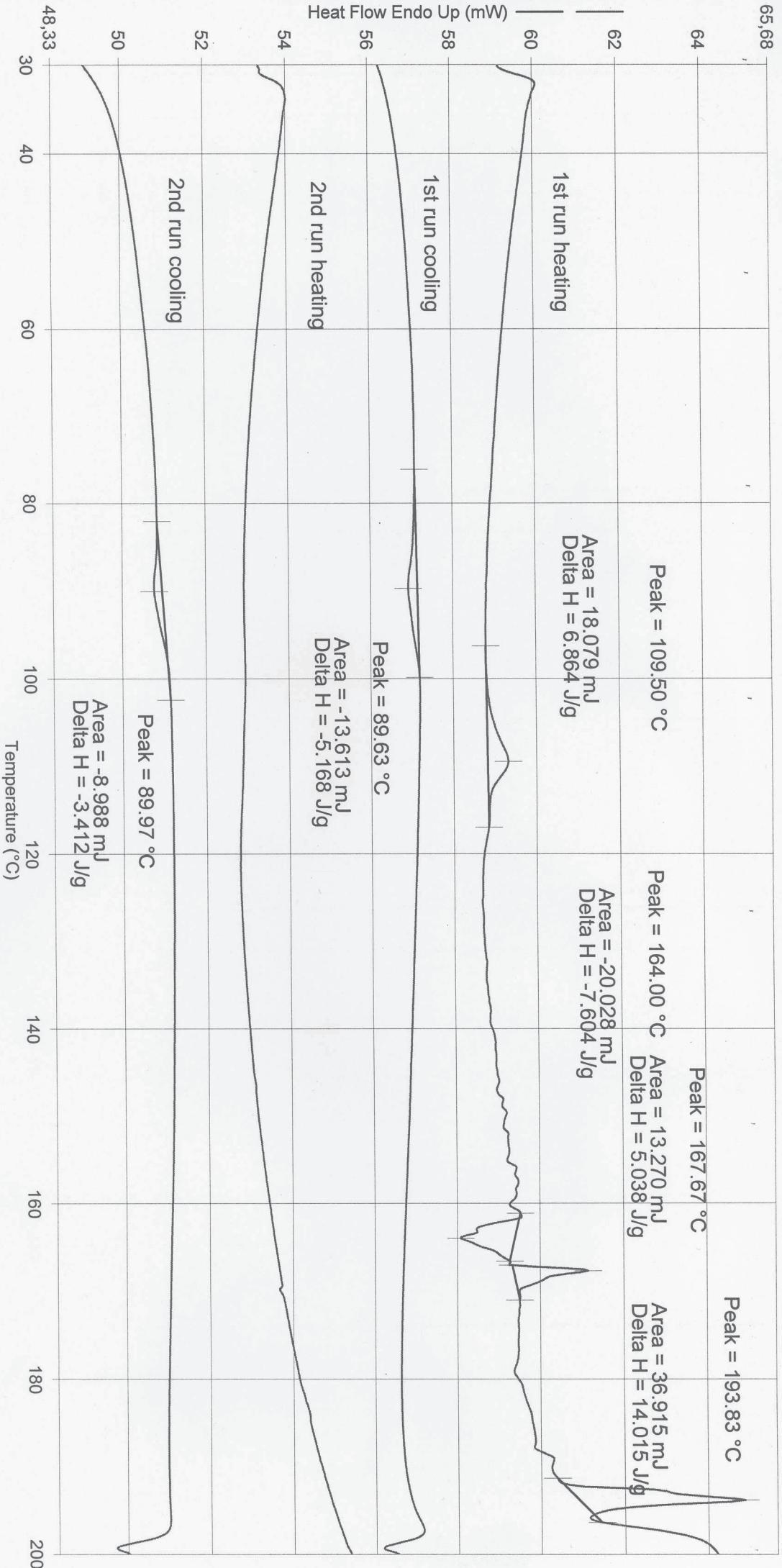
Operator ID: Schweizer
 Sample ID: 3000-7
 Sample Weight: 2.143 mg
 Comment: *Cdf 9a deviced Poly(E-co-NBE) at 58C / 4 bar E ; Cat: MAD ; NBE (71.2000: 20.000)*



- 1) Hold for 1.0 min at 30.00°C
- 2) Heat from 30.00°C to 200.00°C at 10.00°C/min
- 3) Hold for 1.0 min at 200.00°C
- 4) Cool from 200.00°C to 30.00°C at 10.00°C/min
- 5) Hold for 1.0 min at 30.00°C
- 6) Heat from 30.00°C to 200.00°C at 10.00°C/min
- 7) Hold for 1.0 min at 200.00°C
- 8) Cool from 200.00°C to 30.00°C at 10.00°C/min

02.12.2011 16:48:59

Operator ID: Schweizer
 Sample ID: 3000-5
 Sample Weight: 2.634 mg
 Comment: Cat. 22 derived Poly(E-co-NBE) at 70°C, 14 bar E; cat: MAD: NBE (1: 2000; 20000)

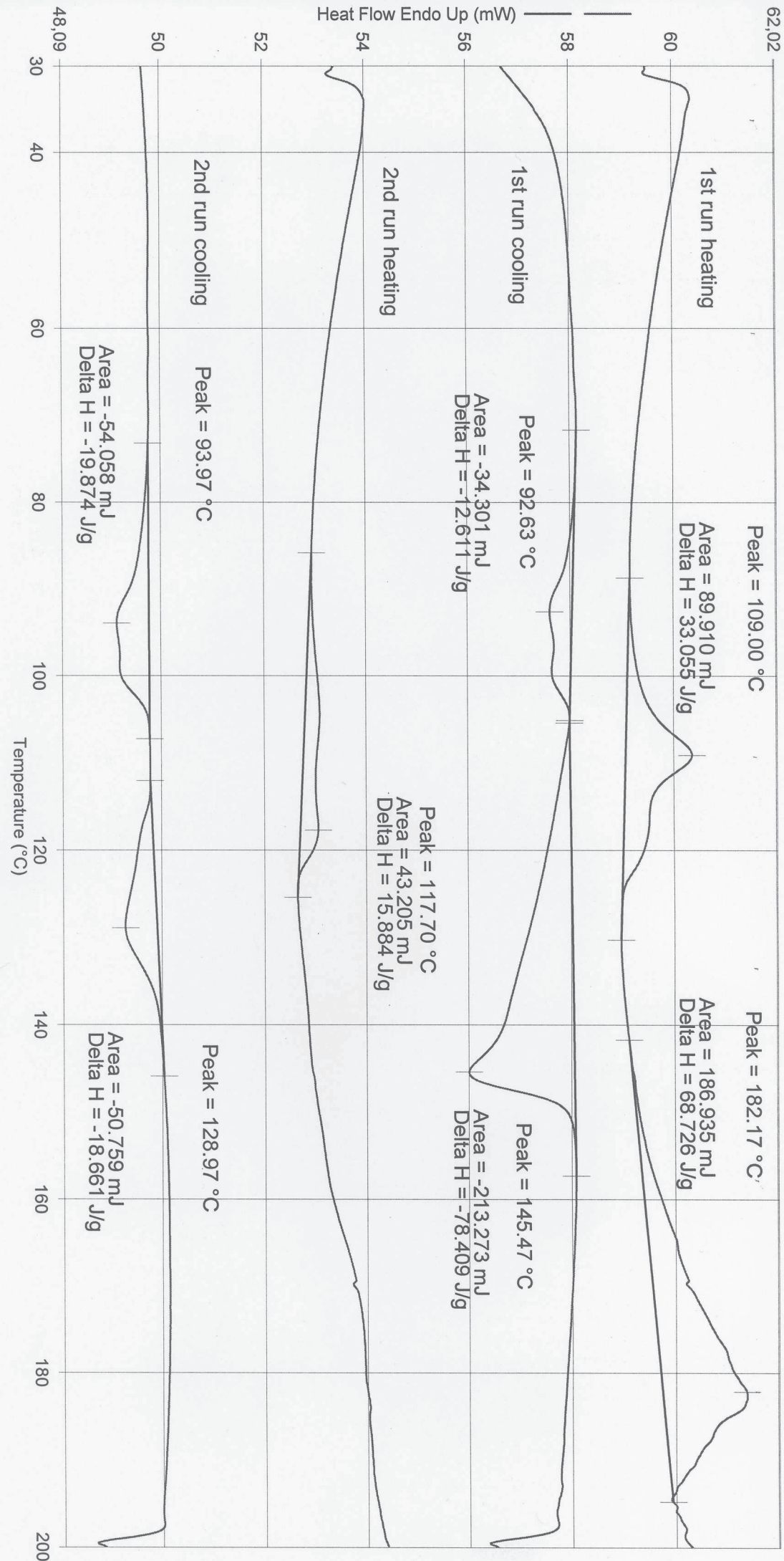


- 1) Hold for 1.0 min at 30.00°C
- 2) Heat from 30.00°C to 200.00°C at 10.00°C/min
- 3) Hold for 1.0 min at 200.00°C
- 4) Cool from 200.00°C to 30.00°C at 10.00°C/min

- 5) Hold for 1.0 min at 30.00°C
- 6) Heat from 30.00°C to 200.00°C at 10.00°C/min
- 7) Hold for 1.0 min at 200.00°C
- 8) Cool from 200.00°C to 30.00°C at 10.00°C/min

01.12.2011 18:10:57

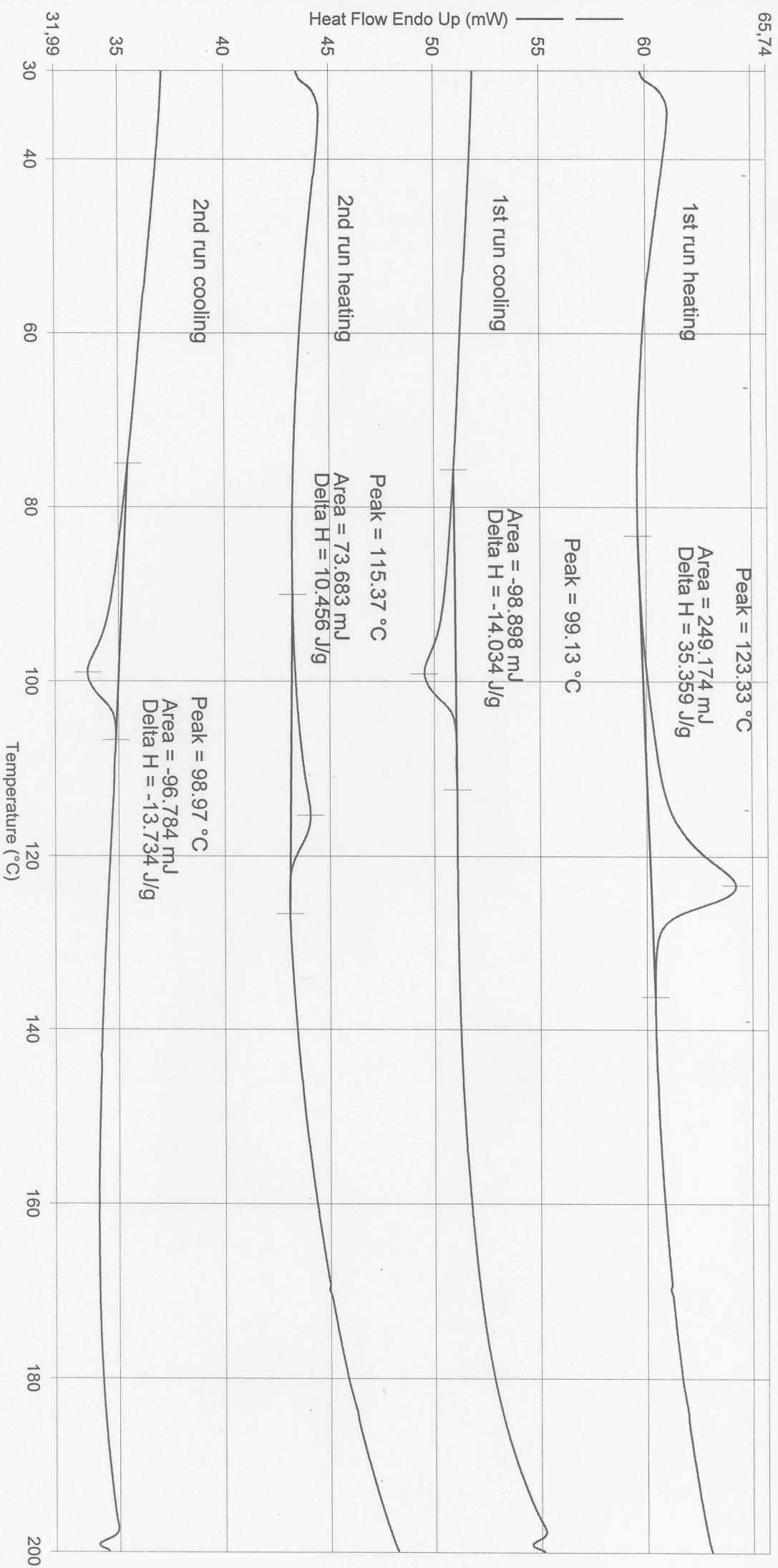
Operator ID: Schweizer
 Sample ID: 3000-6
 Sample Weight: 2.720 mg
 Comment: cat. 22 derived Poly(E-co-NBE) at 90°C, 4 bar E; cat: MAD: NBE (1:2000: 20/1000)



- 1) Hold for 1.0 min at 30.00°C
- 2) Heat from 30.00°C to 200.00°C at 10.00°C/min
- 3) Hold for 1.0 min at 200.00°C
- 4) Cool from 200.00°C to 30.00°C at 10.00°C/min
- 5) Hold for 1.0 min at 30.00°C
- 6) Heat from 30.00°C to 200.00°C at 10.00°C/min
- 7) Hold for 1.0 min at 200.00°C
- 8) Cool from 200.00°C to 30.00°C at 10.00°C/min

01.12.2011 18:19:04

Operator ID: Schweizer
 Sample ID: 2000-184
 Sample Weight: 7.047 mg
 Comment: Cat. 23 derived poly(E-co-NBE) at 70°C, 4 bar E; cat: MAD: NBE (-1: 2000: 20,000)



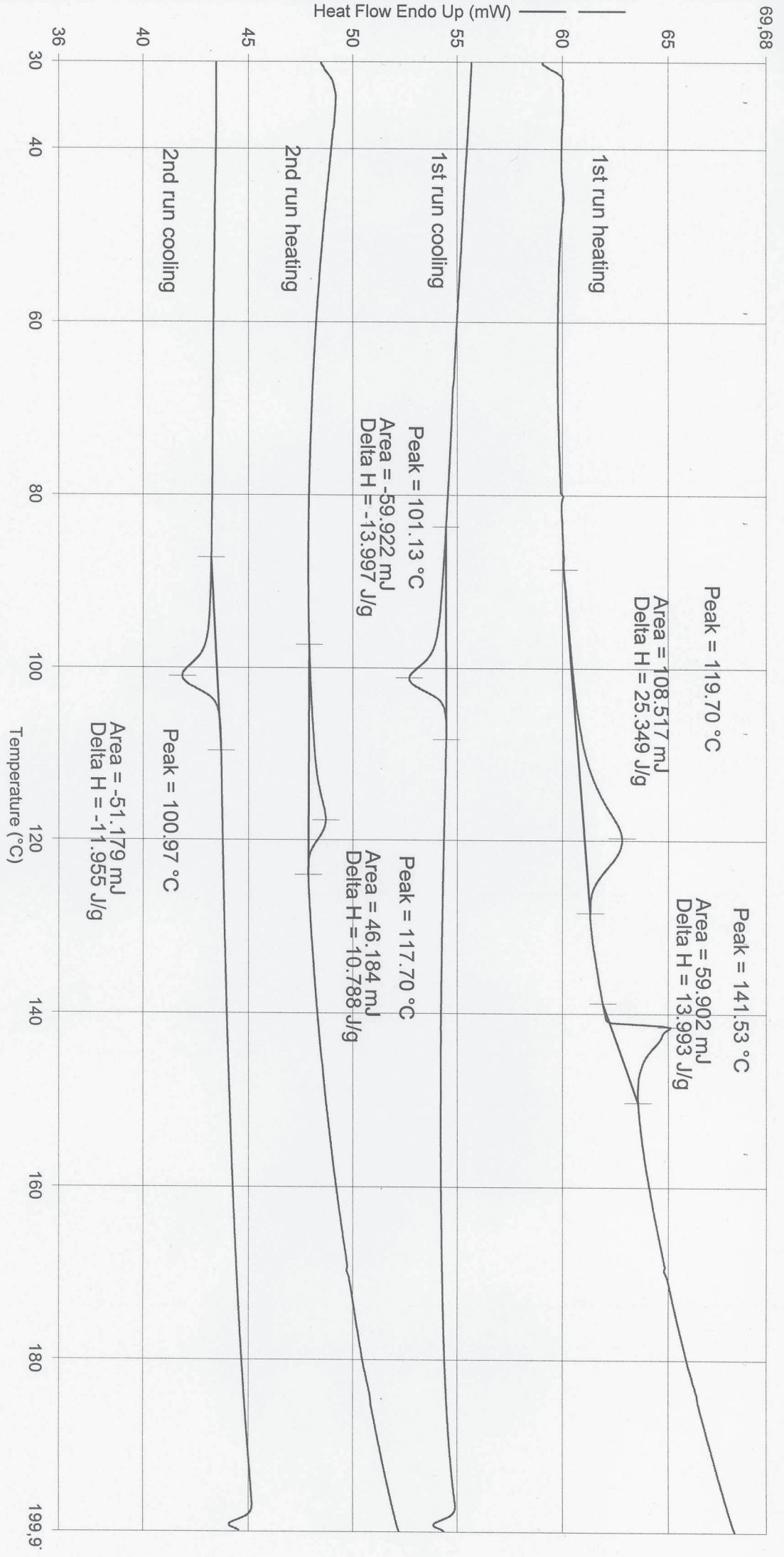
- 1) Hold for 1.0 min at 30.00°C
- 2) Heat from 30.00°C to 200.00°C at 10.00°C/min
- 3) Hold for 1.0 min at 200.00°C
- 4) Cool from 200.00°C to 30.00°C at 10.00°C/min

- 5) Hold for 1.0 min at 30.00°C
- 6) Heat from 30.00°C to 200.00°C at 10.00°C/min
- 7) Hold for 1.0 min at 200.00°C
- 8) Cool from 200.00°C to 30.00°C at 10.00°C/min

04.11.2011 13:25:48

Operator ID: Schweizer
 Sample ID: 2000-183
 Sample Weight: 4.281 mg
 Comment: Cat. 23

derived poly(E-co-NBE) at 50°C, 4 bar E; Cat: MAD: NBE (1:2000:20,000)



- 1) Hold for 1.0 min at 30.00°C
- 2) Heat from 30.00°C to 200.00°C at 10.00°C/min
- 3) Hold for 1.0 min at 200.00°C
- 4) Cool from 200.00°C to 30.00°C at 10.00°C/min

- 5) Hold for 1.0 min at 30.00°C
- 6) Heat from 30.00°C to 200.00°C at 10.00°C/min
- 7) Hold for 1.0 min at 200.00°C
- 8) Cool from 200.00°C to 30.00°C at 10.00°C/min

04.11.2011 13:20:22